NAVY ELECTRONICS LABORATORY
LIBRARY

27025

AD 200 782

NTIS ae
DDC-IR-10May66

DATE 6/16/55 NEL NO. 1
UNCLASSIFIED
CNR Navac Msg dtd 7 Sept 54
AUTH.
L. Smith/4223
SIGNATURE & CODE

U/C

DATE 4-15-54 NEL NO. 1
CONFIDENTIAL
RECLASSIFIED TO S/C
AUTH. N.R.L. Ltr. dtd. 21 Dec 54
L. Marshall 4223
SIGNATURE & CODE

BEST AVAILABLE COPY

# SUMMARY TECHNICAL REPORT
# OF THE
# NATIONAL DEFENSE RESEARCH COMMITTEE

This document contains information affecting the national defense of the United States within the meaning of the Espionage Act, 50 U.S.C., 31 and 32, as amended. Its transmission or the revelation of its contents in any manner to an unauthorized person is prohibited by law.

This volume is classified RESTRICTED in accordance with security regulations of the War and Navy Departments because certain chapters contain material which was RESTRICTED at the date of printing. Other chapters may have had a lower classification or none. The reader is advised to consult the War and Navy agencies listed on the reverse of this page for the current classification of any material.

UNCLASSIFIED
~~RESTRICTED~~

Manuscript and illustrations for this volume were prepared for publication by the Summary Reports Group of the Columbia University Division of War Research under contract OEMsr-1131 with the Office of Scientific Research and Development. This volume was printed and bound by the Columbia University Press.

Distribution of the Summary Technical Report of NDRC has been made by the War and Navy Departments. Inquiries concerning the availability and distribution of the Summary Technical Report volumes and microfilmed and other reference material should be addressed to the War Department Library, Room 1A-522, The Pentagon, Washington 25, D. C., or to the Office of Naval Research, Navy Department, Attention: Reports and Documents Section, Washington 25, D. C.

Copy No.
**316**

This volume, like the seventy others of the Summary Technical Report of NDRC, has been written, edited, and printed under great pressure. Inevitably there are errors which have slipped past Division readers and proofreaders. There may be errors of fact not known at time of printing. The author has not been able to follow through his writing to the final page proof.

Please report errors to:

JOINT RESEARCH AND DEVELOPMENT BOARD
PROGRAMS DIVISION (STR ERRATA)
WASHINGTON 25, D. C.

A master errata sheet will be compiled from these reports and sent to recipients of the volume. Your help will make this book more useful to other readers and will be of great value in preparing any revisions.

RESTRICTED
UNCLASSIFIED

SUMMARY TECHNICAL REPORT OF DIVISION 6, NDRC

VOLUME 7

# PRINCIPLES AND APPLICATIONS OF UNDERWATER SOUND

OFFICE OF SCIENTIFIC RESEARCH AND DEVELOPMENT
VANNEVAR BUSH, DIRECTOR

NATIONAL DEFENSE RESEARCH COMMITTEE
JAMES B. CONANT, CHAIRMAN

DIVISION 6
JOHN T. TATE, CHIEF

---

WASHINGTON, D. C., 1946

UNCLASSIFIED

# NATIONAL DEFENSE RESEARCH COMMITTEE

James B. Conant, *Chairman*
Richard C. Tolman, *Vice Chairman*

| | |
|---|---|
| Roger Adams | Army Representative[1] |
| Frank B. Jewett | Navy Representative[2] |
| Karl T. Compton | Commissioner of Patents[3] |

Irvin Stewart, *Executive Secretary*

[1]*Army Representatives in order of service:*

Maj. Gen. G. V. Strong
Maj. Gen. R. C. Moore
Maj. Gen. C. C. Williams
Brig. Gen. W. A. Wood, Jr.
Col. L. A. Denson
Col. P. R. Faymonville
Brig. Gen. E. A. Regnier
Col. M. M. Irvine
Col. E. A. Routheau

[2]*Navy Representatives in order of service:*

Rear Adm. H. G. Bowen
Capt. Lybrand P. Smith
Rear Adm. J. A. Furer
Rear Adm. A. H. Van Keuren
Commodore H. A. Schade

[3]*Commissioners of Patents in order of Service:*

Conway P. Coe
Casper W. Ooms

## *NOTES ON THE ORGANIZATION OF NDRC*

The duties of the National Defense Research Committee were (1) to recommend to the Director of OSRD suitable projects and research programs on the instrumentalities of warfare, together with contract facilities for carrying out these projects and programs, and (2) to administer the technical and scientific work of the contracts. More specifically, NDRC functioned by initiating research projects on requests from the Army or the Navy, or on requests from an allied government transmitted through the Liaison Office of OSRD, or on its own considered initiative as a result of the experience of its members. Proposals prepared by the Division, Panel, or Committee for research contracts for performance of the work involved in such projects were first reviewed by NDRC, and if approved, recommended to the Director of OSRD. Upon approval of a proposal by the Director, a contract permitting maximum flexibility of scientific effort was arranged. The business aspects of the contract, including such matters as materials, clearances, vouchers, patents, priorities, legal matters, and administration of patent matters were handled by the Executive Secretary of OSRD.

Originally NDRC administered its work through five divisions, each headed by one of the NDRC members. These were:

Division A—Armor and Ordnance
Division B—Bombs, Fuels, Gases, & Chemical Problems
Division C—Communication and Transportation
Division D—Detection, Controls, and Instruments
Division E—Patents and Inventions

In a reorganization in the fall of 1942, twenty-three administrative divisions, panels, or committees were created, each with a chief selected on the basis of his outstanding work in the particular field. The NDRC members then became a reviewing and advisory group to the Director of OSRD. The final organization was as follows:

Division 1—Ballistic Research
Division 2—Effects of Impact and Explosion
Division 3—Rocket Ordnance
Division 4—Ordnance Accessories
Division 5—New Missiles
Division 6—Sub-Surface Warfare
Division 7—Fire Control
Division 8—Explosives
Division 9—Chemistry
Division 10—Absorbents and Aerosols
Division 11—Chemical Engineering
Division 12—Transportation
Division 13—Electrical Communication
Division 14—Radar
Division 15—Radio Coordination
Division 16—Optics and Camouflage
Division 17—Physics
Division 18—War Metallurgy
Division 19—Miscellaneous
Applied Mathematics Panel
Applied Psychology Panel
Committee on Propagation
Tropical Deterioration Administrative Committee



RESTRICTED

# NDRC FOREWORD

As events of the years preceding 1940 revealed more and more clearly the seriousness of the world situation, many scientists in this country came to realize the need of organizing scientific research for service in a national emergency. Recommendations which they made to the White House were given careful and sympathetic attention, and as a result the National Defense Research Committee [NDRC] was formed by Executive Order of the President in the summer of 1940. The members of NDRC, appointed by the President, were instructed to supplement the work of the Army and the Navy in the development of the instrumentalities of war. A year later, upon the establishment of the office of Scientific Research and Development [OSRD], NDRC became one of its units.

The Summary Technical Report of NDRC is a conscientious effort on the part of NDRC to summarize and evaluate its work and to present it in a useful and permanent form. It comprises some seventy volumes broken into groups corresponding to the NDRC Divisions, Panels, and Committees.

The Summary Technical Report of each Division, Panel, or Committee is an integral survey of the work of that group. The first volume of each group's report contains a summary of the report, stating the problems presented and the philosophy of attacking them and summarizing the results of the research, development, and training activities undertaken. Some volumes may be "state of the art" treatises covering subjects to which various research groups have contributed information. Others may contain descriptions of devices developed in the laboratories. A master index of all these divisional, panel, and committee reports which together constitute the Summary Technical Report of NDRC is contained in a separate volume, which also includes the index of a microfilm record of pertinent technical laboratory reports and reference material.

Some of the NDRC-sponsored researches which had been declassified by the end of 1945 were of sufficient popular interest that it was found desirable to report them in the form of monographs, such as the series on radar by Division 14 and the monograph on sampling inspection by the Applied Mathematics Panel. Since the material treated in them is not duplicated in the Summary Technical Report of NDRC, the monographs are an important part of the story of these aspects of NDRC research.

In contrast to the information on radar, which is of widespread interest and much of which is released to the public, the research on subsurface warfare is largely classified and is of general interest to a more restricted group. As a consequence, the report of Division 6 is found almost entirely in its Summary Technical Report, which runs to over twenty volumes. The extent of the work of a Division cannot therefore be judged solely by the number of volumes devoted to it in the Summary Technical Report of NDRC; account must be taken of the monographs and available reports published elsewhere.

Any great cooperative endeavor must stand or fall with the will and integrity of the men engaged in it. This fact held true for NDRC from its inception, and for Division 6 under the leadership of Dr. John T. Tate. To Dr. Tate and the men who worked with him—some as members of Division 6, some as representatives of the Division's contractors—belongs the sincere gratitude of the Nation for a difficult and often dangerous job well done. Their efforts contributed significantly to the outcome of our naval operations during the war and richly deserved the warm response they received from the Navy. In addition, their contributions to the knowledge of the ocean and to the art of oceanographic research will assuredly speed peacetime investigations in this field and bring rich benefits to all mankind.

The Summary Technical Report of Division 6, prepared under the direction of the Division Chief and authorized by him for publication, not only presents the methods and results of widely varied research and development programs but is essentially a record of the unstinted loyal cooperation of able men linked in a common effort to contribute to the defense of their Nation. To them all we extend our deep appreciation.

VANNEVAR BUSH, Director
*Office of Scientific Research and Development*

J. B. CONANT, Chairman
*National Defense Research Committee*

# FOREWORD

THE ASSURED way of effecting improvement in any art is through a broadening of the base of fundamental knowledge of all the factors upon which the art rests. In his statement to the Navy of the plan of organization and of the objectives of Division 6, Dr. F. B. Jewett emphasized this fact and recommended as a first objective "the most complete investigation possible of all the factors and phenomena involved in the accurate detection of submerged or partially submerged submarines and in antisubmarine devices." In this statement he had particularly in mind phenomena in the field of underwater sound. Consequently, Division 6 promptly extended and intensified the research program in the physics of underwater acoustics already begun under NDRC contract with the Woods Hole Oceanographic Institution, and, in addition, assigned to their San Diego laboratory, organized under contract with the University of California, a principal responsibility for the systematic study of all phases of underwater acoustics. All of the Division's laboratories which were concerned with the development of underwater-sound equipment contributed much to these studies. In this connection special mention should be made of the Underwater Sound Reference Laboratories, whose development of basic standards of measurement and of methods of calibration of transducers (described in Volumes 10 and 11 of Division 6) was essential to the program.

To coordinate and review the entire research program of the Division in the field of underwater acoustics, there was soon established in the headquarters office of the Division a section of the Columbia University "Special Studies Group" which came to be known as the "Sonar Analysis Group." The function of this group was to assist in the analysis of data being accumulated by Woods Hole, San Diego, and other laboratories, to assess their significance in relation to the development and design of sonar gear, and to present their conclusions to other groups in the NDRC and to groups in the Navy interested in such matters. Quite promptly the interest of the Navy led to its very active participation, in fact, to actual sharing in the operations of the Sonar Analysis Group.

Because of their fundamental importance, the results of this research program have been rather completely summarized in four volumes (Volumes 6A, 7, 8, and 9 of Division 6) of the Summary Report Series. Volume 6A, "Oceanography," deals with the physical properties of the medium. Volume 7, the present one, may be regarded as a general text on underwater acoustics, while Volumes 8 and 9 deal with certain more specific aspects of the subject.

The responsibility for preparing this report was undertaken by Dr. Carl Eckart, Associate Director of the San Diego Laboratory. In this he has had the assistance of a number of persons who have been in one way or another closely associated with this research program. The Division appreciates the efforts of those who have participated in the preparation of this report and particularly recognized its obligations to the Navy which made it possible for Dr. Eckart to prepare most of this material after responsibility for operating the San Diego Laboratory had been transferred to the Navy.

The institutions principally involved in these researches have already been mentioned. For over four years it was peculiarly a group effort, and no attempt will be made to name the large number of individual scientists who contributed. The names of those who ably directed various groups sharing in this research program are Carl Eckart, C. O'D. Iselin, V. O. Knudsen, G. P. Harnwell, W. V. Houston, and Lyman Spitzer. Dr. H. Sverdrup, Director of the Scripps Institution, was appointed Consultant to the Division. He and his staff contributed significantly.

As is true of the Division's program as a whole, this research activity secured most effective support from the Navy, at first from Rear Admirals S. M. Robinson and A. H. Van Keuren, and later following changes in Navy assignments, from Vice-Admiral E. L. Cochrane and Rear Admiral J. A. Furer. More detailed and most helpful liaison was provided by Captain Rawson Bennett, Jr., Commander Roger Revelle, Commander J. C. Myers and others in the Bureau of Ships and Commander Burwell of the Office of the Coordinator of Research and Development. In addition, the Sonar Analysis Group, in particular, maintained close contact with the Operations Research Group in the Office of the Commander-in-Chief. This, supplementing other liaison, facilitated prompt application of research results to operations.

JOHN T. TATE
Chief, Division 6

# PREFACE

In 1940 the National Defense Research Committee appointed a Subcommittee on the Submarine Problem. One of the recommendations of this subcommittee was the establishment, at San Diego, of a laboratory responsible for "a broad research program covering the fundamentals of every aspect of the problem." San Diego was chosen because of its proximity to deep water, and because of the number of days per year that would be favorable to research at sea. This recommendation resulted in the organization, in 1941, of such a laboratory by the University of California. It was located in the buildings of the U. S. Navy Radio and Sound Laboratory and became known as the University of California Division of War Research [UCDWR].

UCDWR continued its activities until July 1946, and received many additional assignments. Other NDRC organizations, notably the Columbia University Division of War Research, the Sonar Analysis Group, and the Woods Hole Oceanographic Institution, as well as various Naval shore activities, and vessels of the Fleet, also participated in the "broad research program." The urgencies of World War II somewhat limited the broadness and thoroughness of this research, but a continually expanding subdivision of UCDWR -eventually known as the Sonar Data Division —was actively engaged in the accumulation of scientific data on underwater sound for nearly five years. When, in the normal course of reconversion, OSRD ceased to support this work, the Bureau of Ships assumed the contract.

This Summary Technical Report attempts to cover the scientific work of all the above named organizations. It was prepared by the Sonar Data Division of UCDWR, and, as this was the largest of the associated research groups, it is inevitable that its contributions occupy a large part of the report. An effort has been made to cover the field completely and to include the work of the other groups in adequate detail, but the editor is conscious that this ideal has not always been achieved.

The operations of the Sonar Data Division were a good example of cooperative scientific effort. Many of the advantages of free individualistic research were unavoidably lost because of the necessity for concentrated attacks on constantly shifting objectives, but without exception each member of the staff contributed as generously to the group effort as he would have to his personal research. The normal desire for signed publications was cheerfully sacrificed to the anonymity of classified reports, so that, in retrospect, it is very difficult to give due credit for individual achievement. The constantly changing assignments, and the number of people engaged in different phases of the same urgent problem, prevented the association of single names with most of the important conclusions. It is therefore essential to include in this preface a brief account of the staff of the Sonar Data Division of UCDWR.

The first Director of UCDWR was Dr. V. O. Knudsen, who was assisted by Dr. K. S. Van Dyke, Mr. L. J. Sivian, and Dr. H. E. Hartig in organizing the work. During 1942, the three first named were transferred to other war activities, and the directorship was assumed by Dr. G. P. Harnwell. The laboratory was divided into three major parts: the Sonar Training Division, led by Dr. Hartig; the Sonar Devices Division, led by Dr. F. N. D. Kurie, and the Sonar Data Division, led by the undersigned and later by Dr. R. H. Fleming. While all three divisions took some part in the broad research program, the Sonar Data Division had the primary responsibility for it.

Some of the earliest experimental work was that on reverberation, under the leadership of Dr. C. F. Eyring. This group later expanded its activities under the joint leadership of Drs. R. J. Christensen and R. W. Raitt, to include the experiments on the transmission of 24-kc sound and on the properties of wakes. Other members of this group, who have made major contributions to the work reported in the present volume, are Messrs. R. R. Carhart, G. E. Duvall, T. H. Schafer, M. J. Sheehy. The onerous task of conducting the extensive experiments at sea was largely under the leadership of Messrs. N. Most and J. D. Frautschy. Dr. W. R. Rayton also did much work at sea, as well as in cooperation with Mr. R. C. Fisher in developing the periodmeter with which the records reproduced in Chapter 5 were obtained.

Other early experimental work was on background noise and on the attenuation of sound, under the leadership of Mr. F. A. Everest, Dr. R. W. Young and Mr. H. T. O'Neil. Under the joint leadership of the first two, the activities of this group expanded to include all phases of low-frequency underwater sound. Major contributions to this phase of the work were made by Messrs. A. R. Champion, T. F.

Johnston, T. McMillian, L. Sepmeyer, and G. P. Welch. The first three spent much time at sea.

The Oceanographic Section was organized in 1941 under the direction of Dr. H. U. Sverdrup of Scripps Institution of Oceanography. Other members of that Institution joined UCDWR at the same time. This section was later headed by Dr. R. H. Fleming, who was assisted by Dr. R. D. Russell; the studies of bottom sediments were carried on under the direction of Drs. F. P. Shepard and K. O. Emery; the biological aspects of underwater noise were studied by Dr. M. W. Johnson; Mr. F. C. LaFond was in charge of the analysis of thermal data. The photographs of internal waves (Chapter 4) were made at the University of Iowa by Mr. W. H. Munk of the Oceanographic Section, Professor Hunter Rouse, and Dr. J. S. McNown of the Iowa Institute of Research, University of Iowa. Later experiments on internal waves in the sea were performed by Dr. W. C. Ufford.

The work on the propagation of explosive sound was planned by Dr. W. R. Smyth, and carried on under the leadership of Dr. R. A. Peterson, by Dr. B. G. Eaton, Mr. T. F. Johnston, and Dr. R. W. Raitt.

Psycho-acoustic studies were carried on by Dr. A. M. Small, assisted by Mr. R. S. Gales, and Mr. L. J. Goldberg. The work of this group and other groups would have been impossible had it not been for the excellent recording facilities designed and largely constructed by Mr. L. Sepmeyer. These include a radio link for making high-fidelity phonograph recordings, in the shore laboratory, of underwater sounds picked up at sea.

Other groups of the UCDWR staff made essential contributions by designing and constructing equipment, or by contributing services and facilities. These include the Transducer Design Group, the Calibration Group, the Circuit Laboratory, the Marine Facilities Group, and the Photographic Laboratory.

It is scarcely possible to make adequate acknowledgment of the numerous and varied contributions made by personnel of the U. S. Navy. The USS *Jasper* (PY-13) was an essential part of the laboratory throughout its existence; it was later joined by the YP-267 (ex-*Democracy*) and YAG-6 (ex-*Enchantress*). The able and willing cooperation of the officers and men of these vessels, as well as of the civilian-manned *E. W. Scripps*, made possible the experiments at sea. For many experiments, the above vessels were joined by others, made available by various commands of the U. S. Fleet. Especially to be commended is the effective manner in which the officers of many of these visiting vessels responded to the strange and incomprehensible requests of the civilian scientists. The complex operations were greatly facilitated by the liaison officers, notably by Dr. Roger Revelle, Comdr. (USNR), stationed at the Bureau of Ships in Washington, and by Dr. L. P. Delsasso, Comdr. (USNR), stationed at San Diego.

In preparing the manuscript of this report, the undersigned was ably assisted by Mr. C. E. Behrens. In most cases, first drafts of sections were written by those actively concerned in the original work. These drafts were then edited into a coherent whole, but it is feared that some degree of repetitiousness and incoherence remains. The line-drawings were prepared by Mrs. Florence Clarkson Welch and Miss Carolyn Wilhelm, and the photographic material, by Messrs. A. E. Handley and C. M. Johnson.

Dr. Lyman Spitzer, Jr., and other members of the Sonar Analysis Group made the manuscripts of other Summary Technical Reports (Volumes 8 and 9) available in advance of publication. These were consulted freely in preparing many chapters.

Portions of the final manuscript were read by Dr. Spitzer, Dr. Revelle, Dr. Edward Gerjuoy, and Mr. John Major, Lieut. (USNR), as well as by members of the Sonar Data Division. Their criticisms and suggestions have been most helpful. The Summary Reports Group of NDRC gave generous assistance on all matters relating to publication.

The editor wishes to record his personal appreciation of the cordial manner in which all of those named, and many others, extended their help to him.

CARL ECKART
Editor

RESTRICTED

# CONTENTS

## *PART I*
## *BASIC PRINCIPLES OF UNDERWATER SOUND*


| CHAPTER | | PAGE |
|---|---|---|
| 1 | Theory of an Ideal Medium | 1 |
| 2 | The Refraction of Sound | 10 |
| 3 | The Transmission of Sound in the Sea | 22 |
| 4 | The Oceanography of Sound Conditions | 68 |
| 5 | Echoes, Scattering and Reverberation | 82 |
| 6 | Wakes | 115 |


## *PART II*
## *ECHO RANGING*


| | | |
|---|---|---|
| 7 | The Acoustic Output of Sonars | 135 |
| 8 | Target Strength and Echo Level | 153 |
| 9 | Maximum Echo Ranges When Background Noise is Limiting | 175 |
| 10 | Maximum Echo Ranges When Reverberation is Limiting | 192 |
| 11 | Miscellaneous Echo Ranging Applications | 200 |


## *PART III*
## *LISTENING*


| | | |
|---|---|---|
| 12 | The Acoustic Output of Ships and Submarines | 223 |
| 13 | Background Noise | 243 |
| 14 | Hearing and Recognition | 255 |
| 15 | Sonic and Supersonic Listening | 266 |
| | List of Symbols Used | 279 |
| | Bibliography | 281 |
| | Contract Numbers | 286 |
| | Project Numbers | 287 |
| | Index | 289 |

# *PART I*

# *BASIC PRINCIPLES OF UNDERWATER SOUND*

Chapter 1

# THEORY OF AN IDEAL MEDIUM

## 1.1 INTRODUCTION

### 1.1.1 Objectives

THE GENERAL purpose of this book is to discuss the factors that limit the performance of underwater sound apparatus. These can be divided into three groups, according to their cause.

1. Those originating in the sea;
2. Those originating in the electrical and mechanical parts of the gear;
3. Those originating in the operator who uses the gear.

The factors that originate in the sea itself are the principal subject matter of this book.

It is assumed that the reader has had college courses in sound, electricity, and mathematics. While it will be helpful if the reader has a thorough knowledge of sound and acoustics, the discussion has everywhere been kept at as elementary a level as possible, with a minimum use of mathematics. One or more of the standard textbooks on sound should be available for reference (see bibliography). All these books deal with acoustic phenomena as they are observed in relatively confined regions, such as the air in a room or the water in a tank. In the open air and open sea, other phenomena become dominant and often obscure the simple relations that are observed in the laboratory.

There are various reasons for this. Some effects increase with the distance to which the sound is propagated, while others remain relatively constant. The temperature differences in a small tank of water can be reduced by stirring to the point where they are negligible; in the ocean, temperature differences produce large effects over long distances. Again, the water in a tank can be assumed not to move or change its temperature during an experiment; waves and ripples on the surface can be eliminated to a considerable extent. None of these simplifying conditions can be enforced in the sea, and the principal purpose of this book is to discuss the manner in which these dynamic properties of the ocean influence the propagation of sound and cause it to differ from propagation in an ideal static medium.

However, in order to furnish a standard of comparison, this first chapter will review the generation and transmission of sound in an ideal medium.

## 1.2 LARGE AND SMALL SOURCES IN AN IDEAL MEDIUM

### 1.2.1 Intensity and Pressure Level

When a body of any shape whatsoever vibrates harmonically in an ideal fluid of infinite extent, longitudinal waves are propagated outwards, and during the transmission of the waves the fluid is condensed and rarefied cyclically with the frequency of vibration. The root-mean-square (rms) departure from the average hydrostatic pressure is called the *sound pressure*. The *sound field* is completely described if the sound pressure at every point is specified. In the case of simple sound fields the flow of sound energy at a given point can be calculated if the sound pressure only at that point is known.

When points on the surface of the vibrating body move in a more complicated manner, so that the assumption of simple harmonic motion with a definite frequency cannot be made, the above remarks are in need of some modification. The motion of the medium at a given point is then a sort of delayed average of the motions of all the points on the vibrating object. The sound field is not completely specified unless this motion of the medium is given at each point. For some purposes, it is still sufficient to specify only the rms pressure; for others, additional information about the motion of the medium is required, but it is rarely necessary or possible to describe it completely. Usually it is sufficient to know how the sound energy is distributed among the various frequencies of vibration—to know the "power spectrum" of the sound.

#### DEFINITIONS OF INTENSITY

Intensity is defined in various ways:

*Energy Density (W).* Energy density at a point is the quantity of energy in a unit volume of the medium about the point. In any sound field the energy density is given by

$$W = \frac{p^2}{\rho c^2}, \tag{1}$$

where $p$ = the rms sound pressure at the point,
$\rho$ = the density of the medium, and
$c$ = the velocity of sound in that medium.

If $p$ is measured in dynes/cm², $\rho$ in grams/cm³, and $c$ in cm/sec, then $W$ will be measured in ergs/cm³.

*Energy Flow* ($F$). Energy flow at a point in the sound field is the quantity of energy passing in one second through a unit area containing the point and normal to the direction of the flow. The calculation of the energy flow is, in general, not simple. In the simplest unidirectional sound fields it is given by

$$F = \frac{p^2}{\rho c} = cW. \tag{2}$$

With $p$, $\rho$, and $c$ measured in cgs units as before, energy flow $F$ will be in ergs/(sec)(cm²). In some applications of sound it is convenient to express the energy flow in watts/yd² rather than in cgs units; the pressure, however, is still measured in dynes per sq cm. Using the appropriate values for the density of sea water and the velocity of sound in the ocean, the energy flow in these units is given by

$$F = (5.57 \times 10^{-9})p^2 \text{ (watt/yd}^2\text{)}. \tag{3}$$

*Intensity* ($I$). For many practical purposes a third definition of sound intensity may be used,

$$I = p^2 \text{ (dynes}^2\text{/cm}^4\text{)}. \tag{4}$$

This unit is convenient because, while energy flow and energy are difficult to measure, the sound pressure $p$ is easily measured. This definition of intensity will be used in this book. Where it becomes necessary to discuss the energy flow, this will be indicated explicitly.

### Sound Level ($L$)

The values of $p$ encountered in practice range from about $10^{-4}$ to $10^5$ dynes/cm², hence the *decibel* system is used to specify sound intensities. The *pressure level* of sound, or simply the *sound level*, $L$, in decibels, is defined by the equation

$$L = 10 \log I = 20 \log p \text{ (db)}. \tag{5}$$

The logarithm is to the base 10.

### Other Units of Sound Intensity and Pressure

Two units of pressure are in common use. These are 1 dyne/cm² and 0.0002 dyne/cm². The latter unit is almost invariably used in dealing with airborne sound. Both units have been used in dealing with underwater sound, but the dyne/cm² is preferred by the Navy. However, it is sometimes necessary to convert from one system of units to the other.

Let $p$ and $p'$ be the numbers expressing the same pressure in the two units. Then

$$p \text{ dynes/cm}^2 = p' \text{ (0.0002 dyne/cm}^2\text{)} \tag{6}$$

or

$$p' = 5{,}000p.$$

In the same way, let $L$ and $L'$ be the levels in the two cases. Then

$$\begin{aligned} L' &= 20 \log p' = 20 \log (5{,}000p), \\ &= 20 \log p + 74, \\ &= L + 74. \end{aligned} \tag{7}$$

In this book the dyne/cm² will be used only for underwater sound. In keeping with international practice, the unit 0.0002 dyne/cm² will be used for airborne sound.

It is unfortunate that no name has been given this latter unit, so that it is necessary to use such cumbersome phrases as "pressure in units of 0.0002 dyne per square centimeter," and "the sound level in decibels above 0.0002 dyne per square centimeter." To avoid such interruptions to the reader's train of thought, the simpler phrases "pressure" and "sound level" will be used throughout; unless specifically indicated in footnotes, the unit will be the dyne/cm² for underwater sound and 0.0002 dyne/cm² for airborne sound. The relation among the several units is shown graphically in Figure 1.

## 2.2 Large and Small Sound Sources

The character of the sound field is determined in the first instance by the source of the sound. In the ocean the sound sources that come into consideration differ widely. Hulls of ships are large sources emitting noise with a complicated spectrum; sound projectors are moderately large sources emitting relatively pure tones or sound of controlled frequency bands; minute air bubbles may be secondary sources of sound. It is important to characterize all of them.

Any source can be considered to be divided into elemental areas, each of which acts as a point source of sound. If the linear dimensions of the source are small compared to the wavelength of the sound, the differences in the distances from a remote point in the sound field to any two elemental areas on the source are small compared to the wavelength, so that all

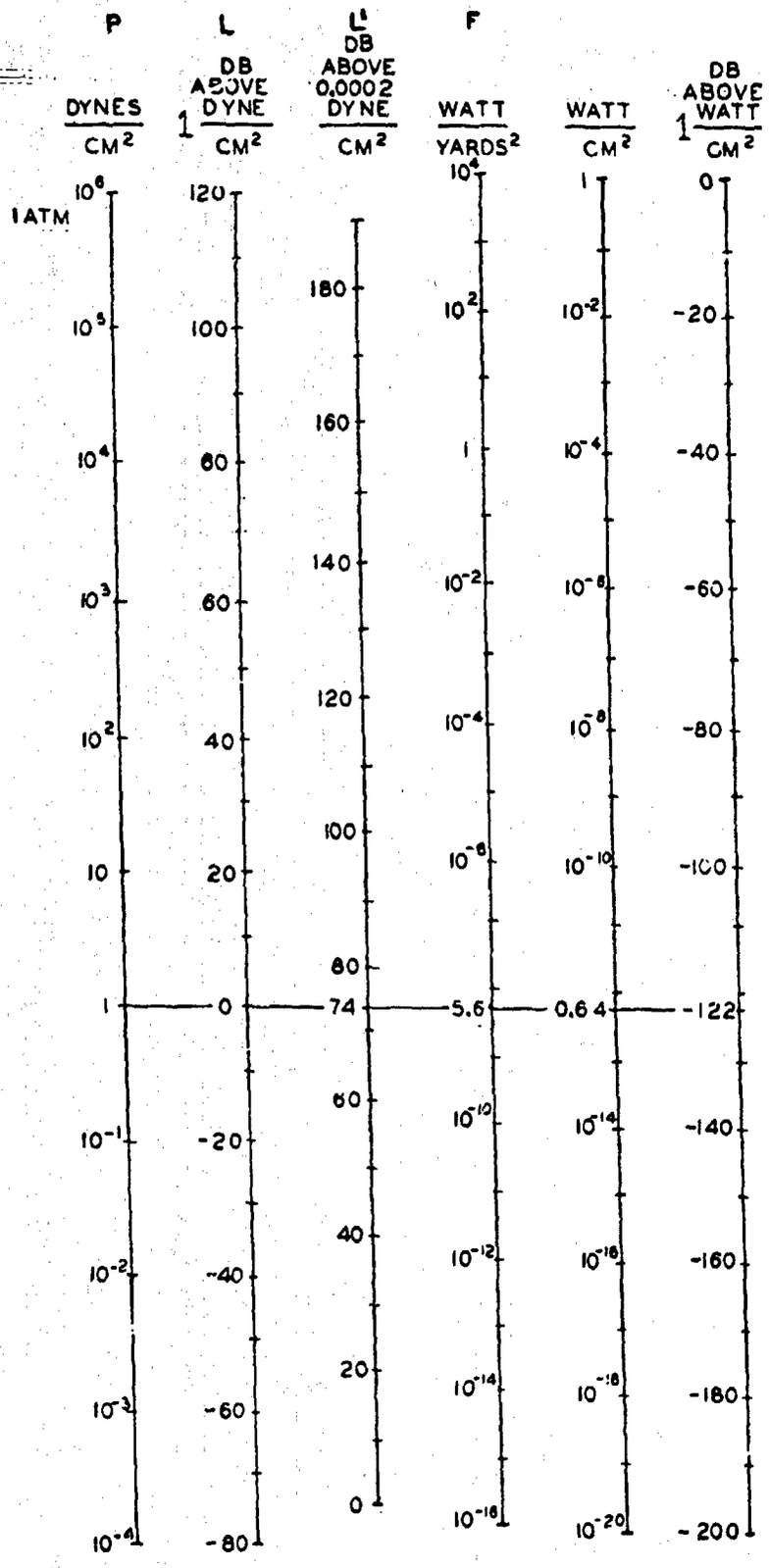


FIGURE 1. Comparison of units for underwater sound.

pressures arrive at the remote point substantially at the same time; the delayed average mentioned above is then a simple sum and the pressures from each of the elementary areas add. The sound, moreover, is radiated uniformly in all directions. In this case the source can be called small.

If a source of simple harmonic waves is large compared to one wavelength, the waves from the various elementary areas will not all arrive at a given point at the same time. Hence there will be interference effects, and the intensity radiated in some directions will be greater than in others.

If the source is large, for example a ship, but emits noise rather than single frequency sound, the more obvious interference effects largely disappear. However, the intensity radiated in some directions will still be different from that in others. In this case, complications in measurement can occur because some parts of the source are nearer the point of measurement than others. Usually these complications disappear when the distance to the nearest point of the source is more than four or five times its largest dimension.

## 1.2.3 The Inverse Square Law—Small Sources

If a very small radially pulsating sphere is imagined placed in the medium, its pulsations spread out spherically and affect the whole space occupied by the medium. The power (total energy per second) transmitted through any concentric spherical surface is constant, and since the surface area is $4\pi r^2$, where $r$ is the distance (in yards) of the wave front from the source, the energy flow can be expressed by the equation

$$F = \frac{P}{(4\pi r^2)}, \tag{8}$$

where $F$ is the energy flow in watts/yd$^2$ at a distance $r$ from the source and $P$ the total power radiated by the source. This can also be expressed in terms of the intensity as follows.

Equations (3) and (4) apply in this simple case, and thus

$$F = (5.57 \times 10^9)p^2 = 5.57 \times 10^9 I$$
$$= \frac{P}{4\pi r^2} \text{ (watts/yd}^2\text{)}. \tag{9}$$

Define $I_1$ so that

$$(5.57 \times 10^9) I_1 = \frac{P}{4\pi}, \tag{10}$$

then

$$I = \frac{I_1}{r^2}, \tag{11}$$

and $I_1$ can also be defined as the intensity at a point 1 yd from the center of the sphere.*

In the decibel system, equation (11) becomes

$$L = L_1 - 20 \log r, \tag{12}$$

where $L = 10 \log I$ is the sound level at range $r$ and $L_1 = 10 \log I_1$ is the level at unit range. The quantity $L_1$ is called the *source level*.

Since graphical methods of presenting data are commonly used, it is important to become familiar with the appearance of the foregoing equations when

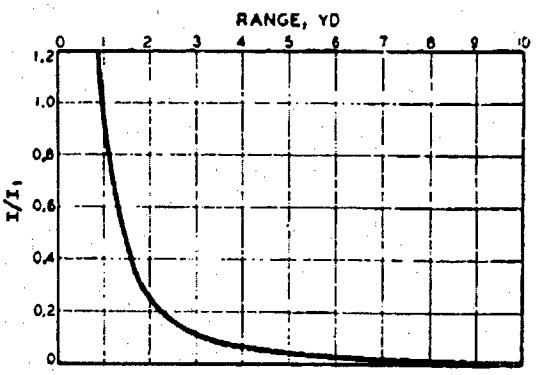


FIGURE 2. Graph of $I/I_1$ as a function of range. Ordinates are the relative intensity; abscissas are the range in yards.

they are plotted in different ways. The inverse square law, equations (11) and (12), can be presented graphically in various ways. In Figure 2 the abscissa is proportional to $r$, and the ordinate is $I/I_1 (= 1/r^2)$. This mode of presentation is not useful because the graph approaches too closely to the horizontal axis to be visible beyond about 10 yards.

This objection is overcome by plotting

$$L - L_1 = 10 \log \left(\frac{I}{I_1}\right) = -20 \log r \tag{13}$$

as ordinate against $r$ as abscissa. Such a graph is shown in Figure 3; the expansion of the scale for small values of $I/I_1$ into large negative values of $L - L_1$

* Equation (11) can also be expressed by the equation
$pr = \text{const}$
and is sometimes called the *PD* law (*P* for pressure, *D* for distance).

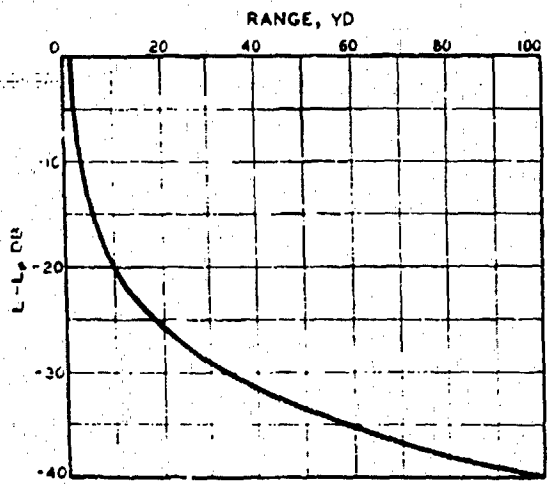


FIGURE 3. Graph of $L - L_1$ as a function of range. Ordinates are sound level, in decibels, above the source level; abscissas are range in yards.

makes such a graph useful over a wider interval of ranges.

A third type of graph also uses $L - L_1$ as ordinate, but plots $\log r$ instead of $r$ as abscissa. Figure 4 is the graph of equation (12) plotted in this way. This has

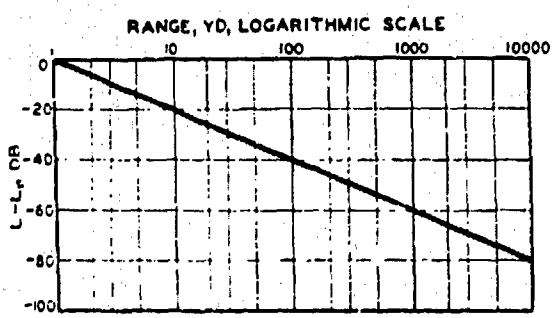


FIGURE 4. Graph of $L - L_1$ as a function of range, the range being plotted on a logarithmic scale.

two advantages: a much greater interval of ranges can be presented, and the graph of the inverse square law is a straight line.

## 1.2.4 The Inverse Square Law—Large Sources

A large source does not radiate sound energy equally in all directions; however, the intensity ratios at two remote points on a straight line through the source can still be calculated from the inverse square law. We may say that a large source is equivalent to an imaginary small source which radiates the same intensity in a given direction as the large source. If in equation (9) $I_1$ were given a different value for each direction, this equation would still hold for large sources at great distances. This is not true for points close to the source. Figure 5 illustrates this schematically. The solid graph represents the actual sound

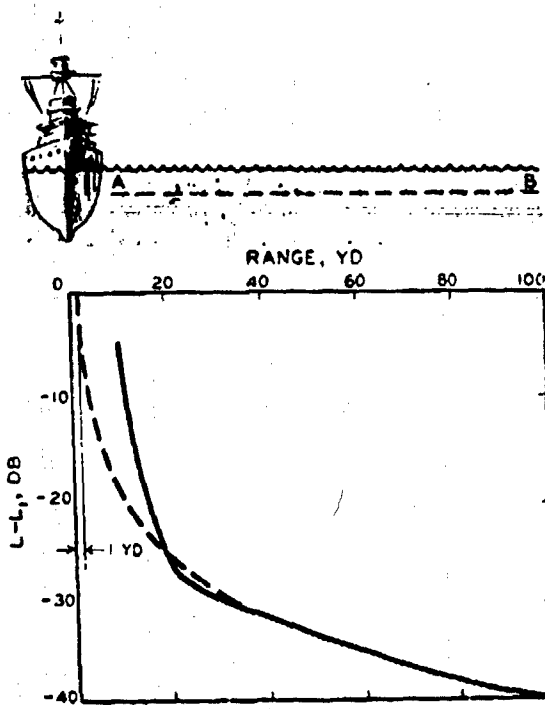


FIGURE 5. Schematic diagram illustrating departures from inverse square law with a large source. The hydrophone is supposed to have been carried along the line $AB$, and the solid graph shows the sound level that might have been observed. The dotted graph of the inverse square law shows that, at long ranges, the observed level is the same as would have been produced by an imaginary small source at the center of the ship. The actual level nowhere reaches the value $L_1$ and cannot, in the nature of things, be extended inside the ship.

level in decibels along the line $AB$, while the dotted graph is the curve of equation (12). At great distances the two graphs coincide very closely; at short distances marked departures occur.

## 1.2.5 Directivity and Beam Patterns

Instead of assigning a different value to the source intensity for each direction, one can designate the intensity at 1 yd in an arbitrary direction as the source intensity. The intensity in any other direction can then be obtained by multiplying by an appropriate

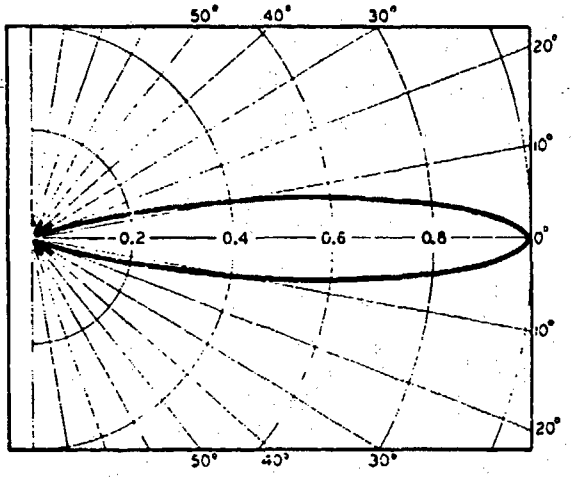


FIGURE 6. Beam pattern of a projector. Radius represents the value of $b$. Note the difficulty of showing the side lobes.

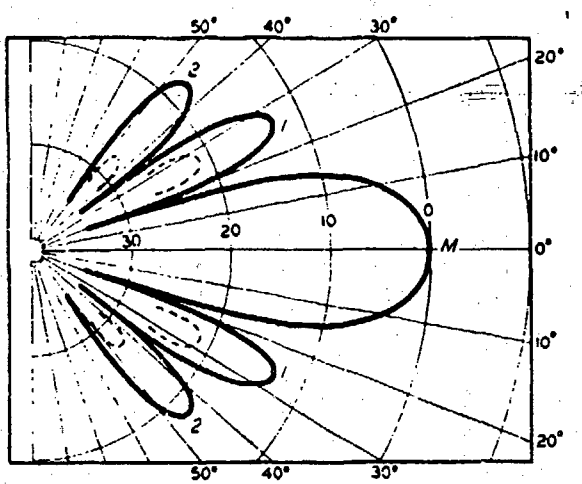


FIGURE 7. Beam pattern of Figure 6, with the ratio of $I_1(\theta)$, $I_a$ expressed in decibels. $M$ is the main "lobe"; the side lobes are marked 1 and 2. The dotted curves show the result of lobe suppression.

factor determined by the direction. In the case of a projector that concentrates most of its sound energy in a beam, the value of the intensity at 1 yd from the source in the direction of the axis of the beam is considered to be the source intensity. Call it $I_a$ and let the intensity at 1 yd from the source in a direction making an angle $\theta$ with the axis of the beam be $I_1(\theta)$, and the ratio of the latter to $I_a$ be $b(\theta)$, i.e.,

$$b(\theta) = \frac{I_1(\theta)}{I_a}, \tag{14}$$

then equation (11) becomes

$$I = \frac{I_a b(\theta)}{r^2}. \tag{15}$$

In converting to the decibel system, let $L_a = 10 \log I_a$; $L_a$ is called the axial source level. Since $b(\theta)$ is usually a proper fraction, its logarithm is usually negative and represents a reduction in sound level. To avoid confusion in the use of signs, it is better to express this reduction as a positive number and subtract it than to add it as a negative number. It is therefore defined as $B = -10 \log b(\theta)$, and thus equation (15) converted to decibels becomes

$$L = L_a - B - 20 \log r. \tag{16}$$

The quantity $B$ is called the *beam pattern* or *directivity function* and, by converting equation (14) to decibels, is defined by

$$B = L_a - L_1. \tag{17}$$

It will be found useful in many equations. Equation (16) is convenient because $L_a$ is a constant, $B$ depends on direction but not on range, and the term 20 log $r$ depends only on range. At all points on the axis $B = 0$, since $b(0)$ is unity.

Figures 6 and 7 show polar graphs of the functions $b(\theta)$ and $B(\theta)$ for the same projector. They have been calculated theoretically for a vibrating rectangular plate, the side of which is about four wavelengths long. Figure 6, the graph of $b$, shows clearly that most of the sound is projected in directions which make angles less than 10° with the perpendicular to the plate. However, the very weak radiation at greater angles is of importance in some cases. Consequently, the graph of $B$ (Figure 7) is useful, since the decibel scale emphasizes these small intensities.

The maxima $M$, 1, 2, and others not shown are usually called "lobes." $M$ is the main lobe. In order that sonar bearings be accurate, it is desirable to have the main lobe narrow. The side lobes 1 and 2 are, for many purposes, detrimental, and the design of modern projectors lays emphasis on their suppression. With modern designs, the maxima of all side lobes are usually more than 20 db below that on the main lobe.

Graphs like these are drawn for projectors from actual measurements of sound level in different directions. They are called "directivity patterns."

## 13 ACTUAL MEDIUM: TRANSMISSION LOSS AND TRANSMISSION ANOMALY

### 131 The Ocean Is Not an Ideal Acoustic Medium

The ocean, considered as a medium for the transmission of sound, is far different from the ideal one

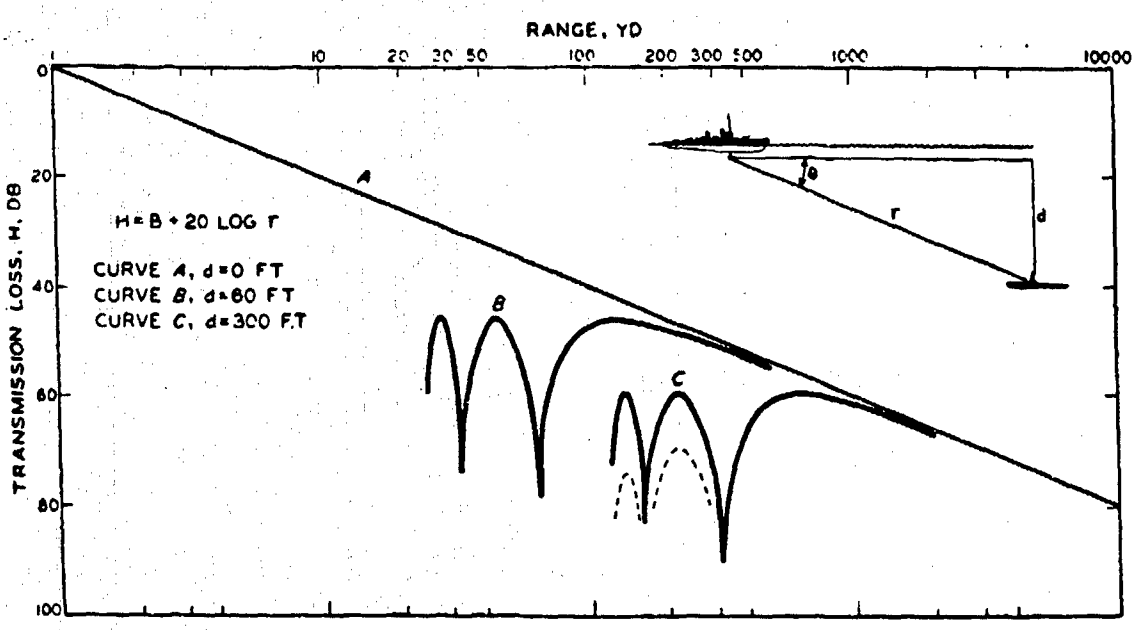


FIGURE 8. Graphs of equation $H = B + 20 \log r$. Sketch at upper right shows applicability of the equation to echo ranging.

presupposed in the previous section. It is not infinite in extent, being bounded by the bottom and the surface. It is not homogeneous; the upper layers are usually warmer than the lower ones and near large rivers may be less saline. For both reasons the water will be less dense in the upper layers. The temperature and salinity may change also in a horizontal direction. Thus a sound wave propagated through the ocean will be distorted from the spherical shape characteristic of a small source in an ideal medium.

Other less obvious acoustic properties of the ocean contribute to making the calculation of sound intensity difficult. As a sound wave travels outward from a source in the sea, some of the energy is converted into heat by friction because of the viscosity of the water. This process is called absorption. Another portion of the energy goes into the production of secondary wavelets which travel in directions other than that of the primary wave. This is the phenomenon called scattering. A more general term, embracing both absorption and scattering, is attenuation.

Even such a brief résumé of the acoustic characteristics of the ocean indicates that the transmission of sound through it is a very complex process and that an experimental study of the individual aspects of the process is difficult. But it is possible to measure the total transmission loss and to observe how it deviates from the inverse square loss, equation (12), of the ideal medium. Experiments have been carried out in which one ship carries a sound projector and a second ship a hydrophone that receives the transmitted sound and measures its sound level. The study of these measurements has led to some useful conclusions.

### 1.3.2 Transmission Loss

In these experiments the axial source level $L_a$ is kept constant and the sound level $L$ is measured at the receiving ship. Usually the source ship is in motion and the receiver stationary. The distance $r$ between the two vessels can be measured by noting the difference in arrival time of the sound and a simultaneously emitted radio signal.

The difference

$$H = L_a - L \tag{18}$$

is the loss in intensity level suffered by the sound in being transmitted from one ship to the other and is usually called the *transmission loss*. Except for sign, this is the same quantity as that plotted in Figures 3 and 4.

In the ideal medium assumed in Section 1.2, the transmission loss at a point on the axis of the beam would be $20 \log r$; at points not on the axis, $H$ would be equal to $B + 20 \log r$, according to equation (16). Figure 8 shows graphs of $H = B + 20 \log r$, the values of $B$ having been taken from Figure 7. The sketch at the upper right shows the applicability of the results to echo ranging. A surface vessel is presumed to be ranging for possible targets at a depth $d$ beneath the sound projector. The strength of the echo received

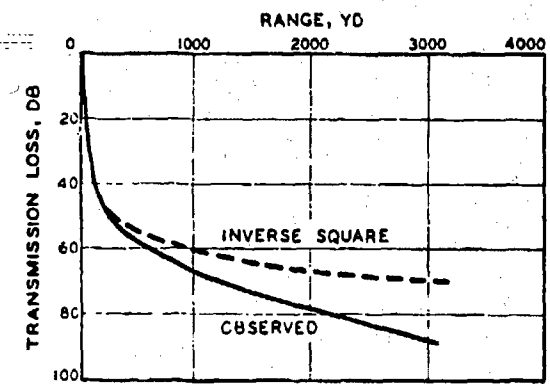


FIGURE 9. Comparison of transmission loss observed in an experiment with that calculated from the inverse square law.

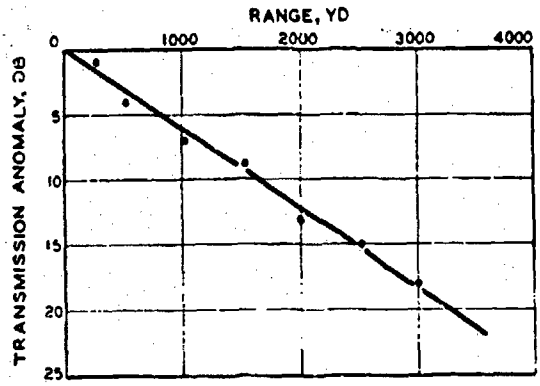


FIGURE 10. The same experimental data as Figure 9, plotted as transmission anomaly.

depends on the sound level which reaches the target and this decreases as the transmission loss $H$ increases. Because the target is submerged beneath the projector, only that sound will reach it which is emitted at an angle $\theta$ with the axis of the projector. As the surface vessel runs in on the target, this angle will increase, causing $B$ to change.

If the depth of the target were $d = 0$, $\theta$ and $B$ would be zero at all ranges. Consequently, the transmission loss $H$ would be simply 20 log $r$. This is plotted as curve $A$. Curves $B$ and $C$ are plotted for the cases $d = 60$ and 300 ft, respectively. The minima of transmission loss are caused by the lobes of the beam pattern of Figure 7. These minima all have the same value in decibels for the case illustrated in the diagram; with lobe suppression, the minima at short range, i.e., large values of $\theta$, are less pronounced and occur at larger values of $H$ than those at longer ranges. They are shown by the dotted curve for $d = 300$ ft.

### 1.3.3 Transmission Anomaly

Experiment shows that equation (16) does not accurately represent the actual transmission loss. The difference between the observed value of $H$ and that calculated from equation (16) is thus a measure of the departure of the ocean from an ideal medium; this departure might be called the *transmission anomaly*.

It is sometimes difficult to isolate the effects of the beam pattern from the other causes of the transmission loss; consequently, a more practicable definition of transmission anomaly is the difference between the observed transmission loss and the transmission loss calculated from the inverse square law alone without taking into account the directivity effect; the latter is thus included in the transmission anomaly defined by

$$A = H - 20 \log r. \tag{19}$$

whence the sound level can be calculated from the equation

$$L = L_a - A - 20 \log r. \tag{20}$$

The usefulness of this concept of transmission anomaly is illustrated by Figures 9 and 10. These are based on experimental data obtained under special conditions. The solid curve of Figure 9 is a graph of observed transmission loss $H$ and for comparison, the transmission loss calculated from the inverse square law is also plotted as a dotted curve. The difference between the two does not seem very great, and would hardly be noticed if the dotted curve were omitted. Yet the difference is very important in echo ranging. Thus, suppose the echo from a certain submarine can just be detected by a certain sonar when the transmission loss is 70 db. If the inverse square law were valid, it could then be detected at 3,000 yd, but under the actual transmission conditions it could not be detected beyond 1,250 yd, unless some other factor happened to be especially favorable at moderate ranges. Thus a graph like Figure 9 does not sufficiently emphasize the importance of relatively small departures from the inverse square law.

On a graph like Figure 10, the graph of the inverse square law can be omitted, since it coincides with the horizontal axis at the top of the graph. The increasing departure from the inverse square law, as range increases, is immediately apparent. Moreover, a very simple law is also obvious: the transmission anomaly is proportional to range. This law is not valid under

all conditions; it will be discussed in detail in Chapter 3. When it is valid, one may express the transmission anomaly by the simple equation

$$A = ar. \tag{21}$$

The coefficient $a$, is called the *attenuation coefficient*. In the example, it has the value $6 \times 10^{-3}$ db/yd.

## 1.3.4 Causes of Transmission Anomaly

Defined in this way, it is seen that the transmission anomaly measures the difference in the transmission loss of sound from an actual source in the ocean and that of sound transmitted to the same range by a small source in an ideal medium. It may be helpful to summarize the components of the transmission anomaly:

1. The effect of *directivity*, discussed in Section 1.2.
2. Variations in temperature and salinity cause changes in density; together with increasing hydrostatic pressure with depth these result in variation of the velocity of the sound and consequent *refraction* of the sound rays. This is discussed in the following chapter.
3. The conversion of sound energy into heat energy, due to the viscosity of the water, called *absorption*.
4. The *scattering* of sound by the surface, the bottom, and by obstacles in the body of the sea. It is advisable to distinguish between specular reflection, as from the surface and the bottom, and the diffuse reflections ordinarily designated by the term *scattering*. This is discussed in Chapter 5.
5. Other factors about which little is known may contribute to the transmission anomaly.

## Chapter 2

# THE REFRACTION OF SOUND

## 2.1 THE VELOCITY OF SOUND IN THE SEA

### 2.1.1 Refraction of Sound Rays

IN SECTION 1.3 the refraction of sound in the sea was mentioned as a contributing cause of the transmission anomaly. In a homogeneous medium, sound would travel in straight lines. As in the analogous case of light, sound rays are curved if the velocity of propagation is not the same at all points. If a plane wave passes obliquely from a medium of lower to one of higher velocity, one part of the wave will travel faster than the other and the ray will be bent toward the medium of lower velocity. The ordinary laws of geometrical optics can be applied to the refraction of sound, although they are strictly true only for sound of very high frequency, and ignore such phenomena as scattering, diffraction, reflection, and absorption. These cannot always be ignored, but it is simplest to omit them from a first discussion.

According to ray theory, the power transmitted in a beam bounded by a tube of adjacent rays will then remain constant, but if the beam is bent the variation in the intensity, i.e., in the amount of power transmitted through a unit area, may be different from the variation that would occur if the rays remained straight. (See Figure 16A, B, C.) In order to calculate intensity, it is necessary, among other things, to know the shape of the sound rays and this in turn can be calculated from a graph of velocity of sound at different points.

It should be said immediately that this ray theory does not agree in all respects with experiments on the transmission of sound. The agreement is close enough, however, to make an acquaintance with the theory essential to an understanding of the principles that have been deduced from the experiments.

### 2.1.2 Influence of Temperature, Salinity, and Pressure on the Velocity of Sound

The velocity of a sound at a given point in any medium is determined by the pressure and the density of the medium at that point. In the ocean, the pressure increases with depth, and the density will vary if the temperature and salinity change. Of these three factors, temperature is by far the most important in affecting the velocity of sound.

Standard conditions of temperature, pressure, and salinity are conventionally chosen as 32°F, one atmosphere pressure, and a saline content of 35 g/kg of sea water. Under these conditions, sound travels with a speed of 4,742.4 ft/sec, or about $1.44 \times 10^5$ cm/sec.

The velocity increases with the temperature at a variable rate; Figure 1 shows the variation with temperature for various salinities. Changes of 20°F,

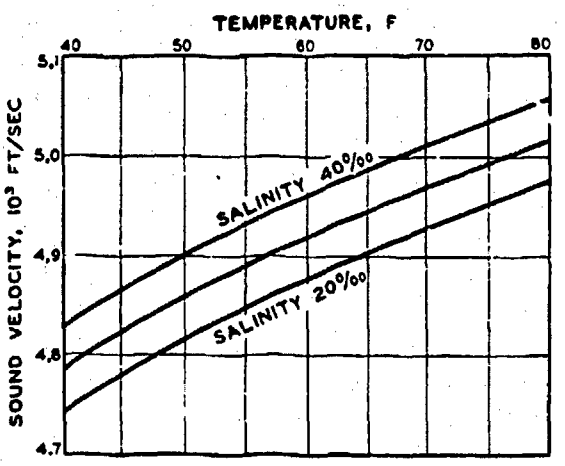


FIGURE 1. Variation of the velocity of sound in the sea with temperature and depth. The symbol 0/00 represents parts per thousand.

in the upper layer of the ocean are not uncommon. An increase in salinity of one part in a thousand increases the velocity of sound 4.27 ft/sec; but salinity is comparatively constant except at the mouths of large rivers and thus in most cases its effect can be neglected.

Increase of pressure with depth causes an increase in the speed of sound of 1.82 ft/sec per 100 ft of depth. It is obvious that the pressure effect will be important only if both the temperature and the salinity are constant. This is illustrated in Figure 4B, in which the solid line shows how the temperature varies with depth in a particular case and the dotted line indicates the change in the velocity of sound with depth corresponding to this temperature distribution. The salinity effect is negligible. The effect of

pressure on the velocity of sound is evident in the upper 180 ft: while in this layer the temperature is constant, the velocity graph shows a slight increase in the velocity with depth. Elsewhere the velocity curve is seen to parallel the temperature curve quite closely.

At greater depths, temperature and salinity change only slightly, and the pressure effect dominates. The average temperature decreases with depth,[1a] as shown in Figure 2, and down to a depth of about 2,500 ft this decrease is sufficiently great to neutralize the effect of the increasing salinity and pressure, so that the velocity of sound also decreases. At greater depths, the pressure effect begins to outweigh the temperature effect, and the sound velocity is seen to increase with depth. This minimum velocity at great depths has interesting acoustic consequences and will be mentioned again. (See Section 2.3.3.)

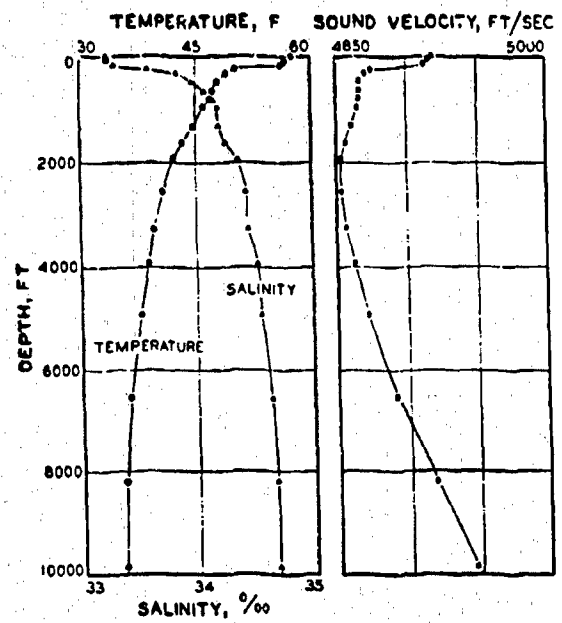


FIGURE 2. Variation of temperature, salinity, and sound velocity with depth in the ocean.

## 2.1.3 The Bathythermograph

The temperature of the sea is measured with specially constructed thermometers, with thermopiles, and with bathythermographs. The last mentioned is generally preferred: it is rugged and of convenient size, and can be used while the vessel is underway. Moreover, the bathythermograph draws a graph showing the temperature as a function of depth and does this automatically as it is lowered from a vessel. Thermometers are less convenient, since they usually show only the temperature at the greatest depth to which they were lowered.

The construction of the bathythermograph is shown in Figure 3. As the instrument is lowered, a stylus is moved by the thermal expansion or contraction of a

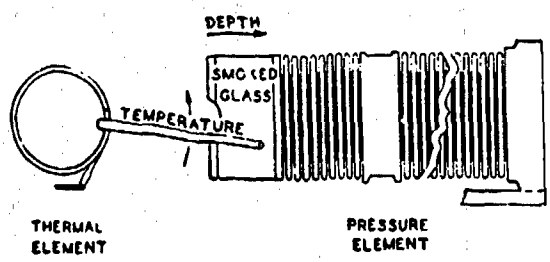


FIGURE 3. Construction of the bathythermograph.

liquid in the copper thermometer tube. The increasing hydrostatic pressure compresses a bellows, which draws a smoked slide horizontally while the temperature stylus moves in a vertical arc. The temperature

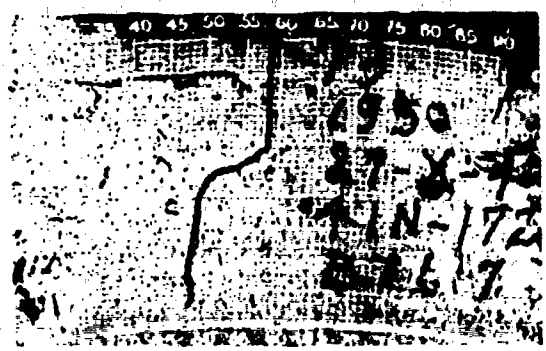

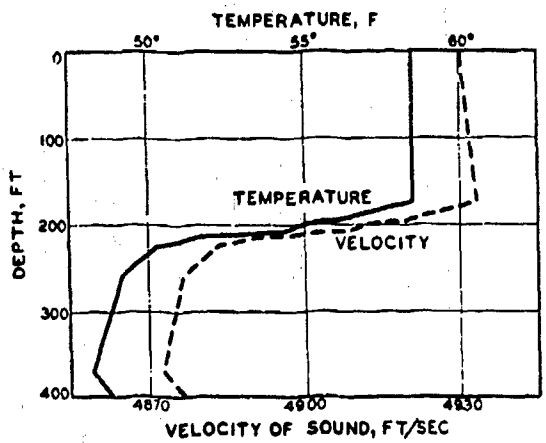


FIGURE 4. (*Top*) Typical bathythermograph slide with coordinate grid superposed; (*bottom*) the corresponding temperature-depth graph of the slide (solid curve), with the velocity of sound corresponding to this distribution (dotted curve).

and depth are thus recorded simultaneously on the slide. Figure 4A shows a typical slide with a coordinate grid superposed; Figure 4B is the temperature-depth graph made from the trace on the slide. The graph of the velocity corresponding to this particular temperature-depth distribution has been referred to above. Such temperature-depth graphs are called bathythermograms.

## 2.14 Horizontal and Vertical Temperature Changes

In considering the refraction of sound in the sea, it can often be assumed that only the variation of temperature in a vertical direction is significant. This is equivalent to considering the ocean as consisting of strata, in any one of which the same temperature exists over a large horizontal distance. Compared with the vertical variation of temperature, the horizontal variations actually observed are very small.[7] Changes in temperature over a *horizontal* distance of 100 ft are rarely as much as 0.5°F, and usually less than 0.1°F. They also are not systematic. Over a *vertical* distance of 100 ft the temperature may vary as much as 10°F, as Figure 4 shows. This has been established in various ways. Simultaneous bathythermograph lowerings have been made from two ships separated by several thousand yards. The two traces were similar, but significant quantitative differences were observed. Even when lowerings are made simultaneously from the bow and stern of the same ship, the traces are not identical. Recording thermometers have been mounted on a submarine, and their records show quite conclusively that there are horizontal temperature differences over distances as small as 10 yd. The magnitude of these differences increases with distance but not in a systematic manner.

## 2.15 Terminology for the Description of Bathythermograms

### General Terms

Twelve typical bathythermograms are exhibited in Figure 5. These illustrate the variable character of the temperature distribution in the surface layers of the sea. This diversity makes it difficult to develop a terminology for describing the temperature conditions near the surface. Certain oceanographic terms have been adopted, and in the analysis of sound transmission data (Chapter 3) specialized systems have been used for describing the general characteristics of the temperature-depth distribution. These will be discussed presently.

All these systems distinguish sharply between temperature differences and temperature gradients, although this distinction is sometimes obscured in conversation. The temperature difference is obviously

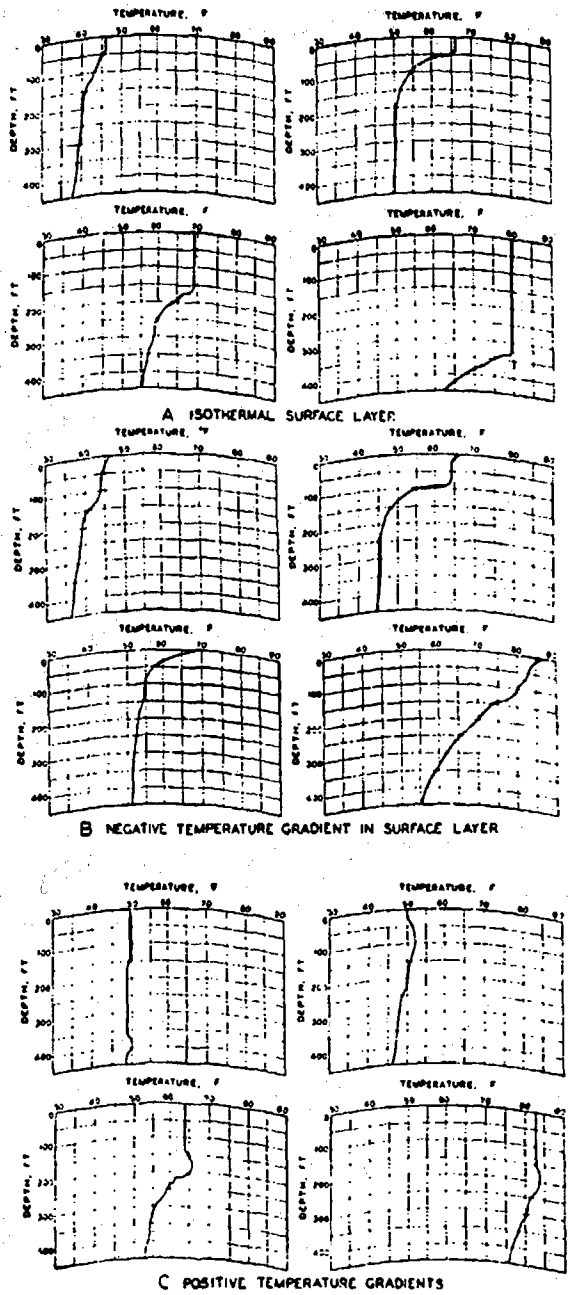


FIGURE 5. Typical bathythermograms corresponding to various gradients.

the difference between the temperature at two points and is measured in degrees Fahrenheit. The vertical temperature gradient is the rate at which the temperature changes with depth and is measured in degrees Fahrenheit per foot. It is also the slope of the trace on the bathythermogram.

Examination of Figure 5 shows that the temperature depth curve can usually be subdivided into segments having different temperature gradients. *Negative gradients* describe conditions in a layer where the temperature decreases with increasing depth, *positive gradients* describe layers in which the temperature increases with depth. The term *isothermal* is applied to layers in which the temperature is uniform. A layer where the temperature decreases very rapidly, particularly if it is immediately beneath an isothermal layer or a layer of smaller gradient, is commonly called a *thermocline*. It is sometimes convenient to use the term *permanent thermocline* to describe the decrease in temperature (Section 2.1.2) which always occurs at great depths.

### A Code for Describing Temperature Differences near the Surface of the Sea

As mentioned above, specialized systems have been devised for describing the general characteristics of the temperature distribution in the sea. One such system, used at San Diego, is a code constructed as follows: Let $T$ = the temperature at the surface and $D$ = the depth at which some specified temperature decrease occurs according to the following tabulation

$D_1$ = depth at which the temperature is $T - 0.1$°F.
$D_2$ = depth at which the temperature is $T - 0.3$°F.
$D_3$ = depth at which the temperature is $T - 1.0$°F.
$D_4$ = depth at which the temperature is $T - 5.0$°F.
$D_5$ = depth at which the temperature is $T - 10.0$°F.

The bathythermogram is then described adequately for some purposes by the five depths, $D_1$, $D_2$, $D_3$, $D_4$, and $D_5$.

In order to enable the use of single digits for the respective values of the $D$'s the following code numbers are used:

Code digit 0: $0 \text{ ft} < D < 5$ ft.
Code digit 1: $5 \text{ ft} < D < 10$ ft
Code digit 2: $10 \text{ ft} < D < 20$ ft.
Code digit 3: $20 \text{ ft} < D < 40$ ft.
Code digit 4: $40 \text{ ft} < D < 80$ ft.
Code digit 5: $80 \text{ ft} < D < 160$ ft.
Code digit 6: $160 \text{ ft} < D < 320$ ft.
Code digit 7: $320 \text{ ft} < D$.
Code digit 8: Unassigned.
Code digit 9: $D >$ greatest depth reached by the bathythermograph.

If the temperature at any depth is greater than the temperature at some smaller depth, the symbol is POS.

The surface temperature $T$ is coded by taking $T/10$ to the nearest whole number.

The symbol for any bathythermograph slide is a numeral consisting, in general, of six digits and a decimal point, e.g., 12345.6. Reading from left to right, the first digit is the code for $D_1$, the second for $D_2$, etc. The digit to the right of the decimal point is the code for $T$.

As examples of the code system, the upper right-hand bathythermogram of Figure 5, showing an isothermal layer, has the code symbol 34445.7; the one immediately below it, 77777.8. The two bathythermograms on the left have code symbols 01359.5 and 00023.7, top and bottom respectively.

## 2.1.6 Direct Measurement of Sound Velocity

Instead of measuring the temperature, it is possible to measure the velocity of sound directly with an

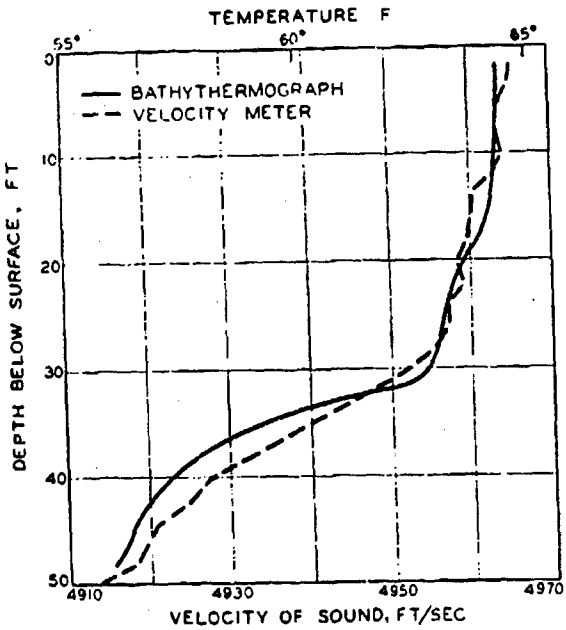


FIGURE 6. Records of bathythermograph and velocity meter taken simultaneously. The two instruments were lashed together and lowered at the same time.

instrument developed by the U.S. Navy Radio and Sound Laboratory [USNRSL].[3] This device essentially measures the time required for sound to travel

from a projector to a hydrophone rigidly mounted about a foot away. It can be lowered into the sea on a cable through which it is also supplied with power.

This velocity meter is sensitive to small changes in the velocity of sound occurring in a few feet, which the bathythermograph fails to detect because of the time lag in its thermometer. An example of the record of a velocity meter is shown in Figure 6, together with the record obtained from a bathythermograph which was lashed to it and lowered on the same line. The two records agree within the limits of experimental error; both instruments contribute to this error.

## 2.2 RAY THEORY

### 2.2.1 Snell's Law of Refraction

The velocity of sound at each point in the sea being known, it is theoretically possible to calculate the sound rays, or paths, along which the sound travels. If the simplifying assumption can be made that the ocean is stratified, so that the temperature at all points having the same depth is the same, the calculation becomes quite simple.

Detailed explanations of the computational methods are contained in several reports,[4,5] and only a summary of the method will be presented here. It is based on Snell's law*, which is illustrated by Figure 7, for an especially simple case of three layers or

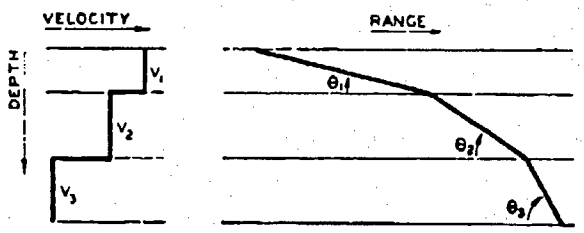


FIGURE 7. Diagram illustrating Snell's law. $V_1/\cos\theta_1 = V_2/\cos\theta_2 = V_3/\cos\theta_3$.

strata, in each of which the sound velocity is constant. Consider a plane wave passing through these three layers; then Snell's law is

$$\frac{V_1}{\cos\theta_1} = \frac{V_2}{\cos\theta_2} = \frac{V_3}{\cos\theta_3}, \qquad (1)$$

where $V_1$ and $\theta_1$ are the velocity and inclination of the ray in the first layer, and so on.

* Snell's law of refraction is discussed in all textbooks of physics as it applies to light rays. It is applicable, without change, to sound rays.[6]

The ray in each layer is a segment of a straight line; but if the layers are imagined to become thinner, the ray approaches a smooth curve. However, at each point along the ray the relation between the inclination of the ray and the velocity of sound is still given by equation (1).

### 2.2.2 Rays in a Constant Gradient

A somewhat less simple case is that of a constant gradient, which is illustrated in Figure 8. The gradient cannot remain constant indefinitely, since if it did, and the medium were of infinite extent, the sound velocity would ultimately become zero or negative, which is impossible. However, the depth at which the velocity would become zero is a convenient geometrical fiction and is used in constructing Figure 8.

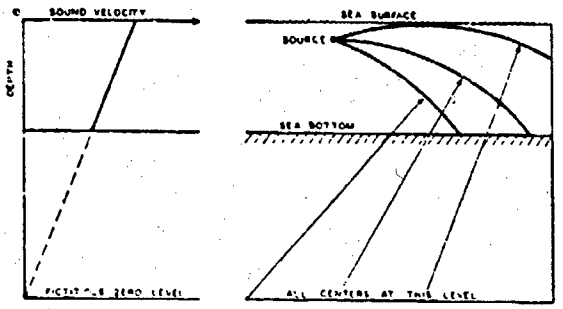


FIGURE 8. Diagram illustrating the curvature of rays in a medium of constant velocity gradient.

It can be shown that where the velocity gradient is constant the rays are circular. All these circles do not have the same radius but all their centers are at the fictitious level mentioned above. In the case of positive gradients, this level is above the ray, which consequently curves upward. With negative gradients, the zero level is below the ray, and it curves downward as in Figure 8. The figure shows clearly that the radius of curvature of the ray depends on the angle at which it leaves the source. It should be noted that all rays leaving the source at steep angles have large radii, i.e., small curvature. Thus refraction has little effect on steeply inclined rays.

In actual cases the curvature of all rays is small and their radii are correspondingly large. Consider, for example, the isothermal layer shown in Figure 4. In this layer the velocity increases with depth as a result of the increase in pressure; the gradient is

$a = 0.182$ ft/sec/ft increase in depth. Following through the discussion given above, it can be shown that the radii are all greater than 270,000 ft. This is equivalent to saying that a ray starting in a horizontal direction from a projector located in this layer will be bent upward 51 ft in traversing 1 mile in a horizontal direction.

To illustrate the bending of a ray in a layer with a negative velocity gradient, consider the layer extending from 180 to 230 ft in Figure 1B. It is seen that in this 50-ft layer the temperature decreases 8°F; the sound is passing through a region of negative gradient and consequently the ray is bent downward. From the velocity curve the value of the gradient $a$ is $(4{,}920 - 4{,}870) \div 50 = 1$ ft/sec/ft of depth. It follows that the radius is 4,900 ft. The curvature of the ray in this layer is therefore much greater than in the isothermal layer.

### 2.2.3 Rays in a Composite Gradient

This construction can be generalized to the case of two layers, in each of which the velocity gradient is constant, as shown in Figure 9. The radius for the portion $AB$ of the ray is determined as though the second layer were not present. The radius for the

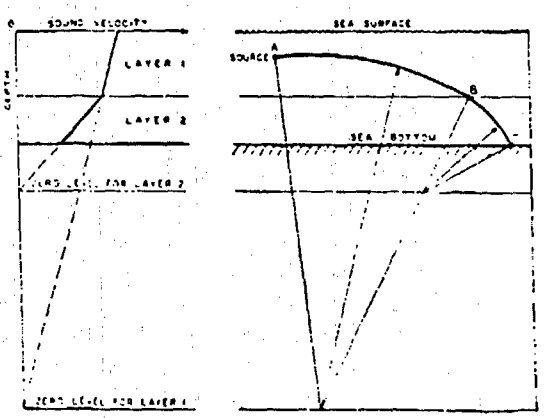


FIGURE 9. Diagram illustrating curvature of rays in a composite gradient.

portion $BC$ is determined as though the first layer were absent, and the center is fixed so that $BC$ joins smoothly on to $AB$.

Since most velocity distributions can be approximated by a series of such layers (see Figure 4), an approximate ray construction can be carried out in this way. Practical complications arise from the fact that the centers of the circular rays usually fall beyond the limits of the drawing board. Moreover, it is desirable to use a large vertical scale and a small horizontal scale for such diagrams. This distortion converts the circles into ellipses. Methods for coping with these complications have been devised.[4,5]

It is also possible to construct a mechanical device which, once it has been set up for a given velocity distribution, will plot many rays in a relatively short time.[6]

## 2.3 TYPICAL RAY DIAGRAMS

### 2.3.1 Marked Downward Refraction

A ray diagram for typical conditions of sharp downward refraction is shown in Figure 10. It should always be borne in mind that the curvature of the rays is very much exaggerated because of the neces-

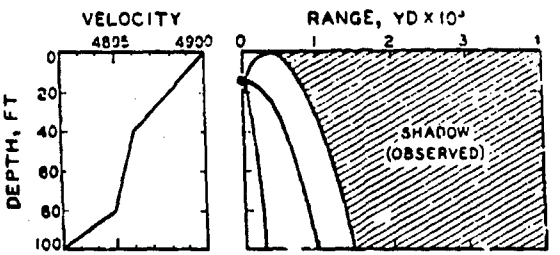


FIGURE 10. Ray diagram with a sharp downward refraction.

sary contraction of the horizontal scale. In Figure 10 the ratio of horizontal to vertical scale is 75. Figure 11 shows a portion of the same diagram drawn on an undistorted scale.

The contracted horizontal scale also exaggerates the inclination of the rays with the horizontal. This is shown in Figure 12, the numbers being the true angles in degrees and the lines showing the angles as plotted on the diagram. The part of the beam above the axis is considered to have positive inclination; the part below the axis, negative inclination. In the case of a directional transducer, nearly all the energy is concentrated in a cone of about 10 degrees opening. Hence a judicious selection of rays with initial inclinations of between 5 and 6 degrees on either side of the axis will provide a sufficiently complete picture of the paths followed by the sound rays.

The velocity-depth graph of Figure 10 shows three layers in which the velocity gradient is con-

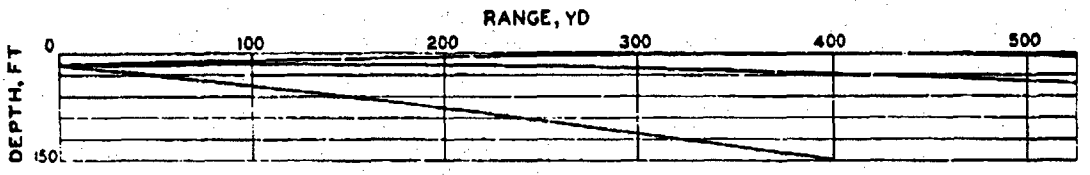


FIGURE 11. Diagram of part of Figure 10 drawn with undistorted scale.

stant. The projector is at a depth of 16 ft. Three rays are drawn.

1. The ray that leaves the projector at −6 degrees, and which may be considered as the lower boundary of the main lobe of the projected beam of sound. The

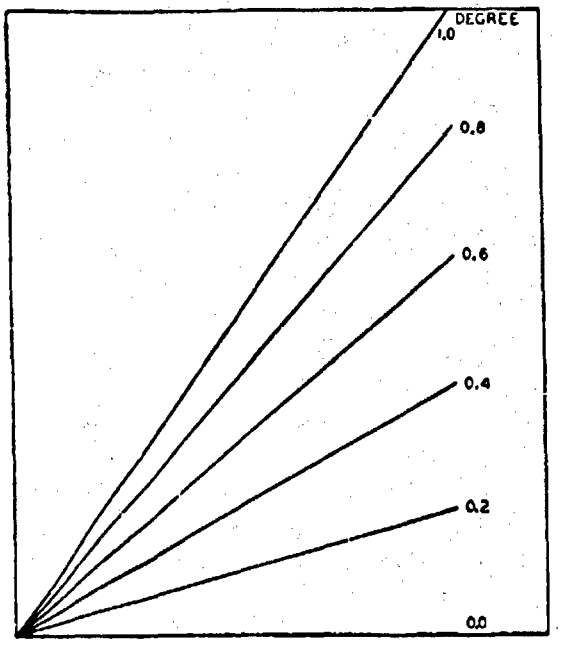


FIGURE 12. Diagram showing how the inclination of the rays is distorted in the conventional ray diagram.

dimensions of the figure do not permit the inclusion of the +6 degree (upper bounding) ray.

2. The ray leaving the projector horizontally—the axial or zero degree ray. This ray is shown bent sharply downward.

3. The ray leaving the projector at +1.4 degrees; this angle was chosen because this ray is tangent to the surface. These three rays are also shown on Figure 11 with an undistorted horizontal scale.

The most striking feature of this ray diagram is that all the sound is confined to a very limited region and that beyond about 500 yd from the projector the surface casts a shadow. The explanation of this shadow is as follows. The outer rays of the upper half of the sound beam fall on the surface and are reflected there. A ray of a certain critical inclination is refracted downward so that its inclination when it reaches the surface will be zero. All rays with inclinations greater than this critical value are reflected back by the surface inside the region bounded by the ray tangent to the surface.

A ray with less initial inclination will not reach the surface but will curve down inside the critical ray; the 0-degree ray illustrates this. The critical ray in the present example is the 1.4-degree ray. It bounds the direct sound field and for this reason is called the "limiting ray."

Except for sound scattered or diffracted from the direct sound field, the shadow should be a region of silence. This picture is approximately a true one; observations made under conditions of strong downward refraction show a sharp drop of from 30 to 40 db in the sound level near the range indicated by the limiting ray. Experimental measurements of the transmission of sound under conditions like these are discussed in Chapter 3.

### 2.3.2 Isothermal Layer and Thermocline

Another common type of thermal distribution is the kind shown in Figure 4. This shows an isothermal layer at the surface, below which there occurs a sharp negative gradient. In the isothermal layer, the velocity gradient is positive because of the pressure effect; this is shown in Figure 4B. About 90 per cent of all the bathythermograph records from all over the world show this type of thermal structure. The sound velocity graph and ray diagram corresponding to this example are shown in Figure 13.

The theory again predicts a shadow, limited by the ray which is horizontal at the level of maximum velocity. The rays above the limiting ray are refracted upward and are ultimately reflected at the surface. Those below the limiting ray enter the thermocline and are there refracted downward. The sound beam is split along the limiting ray into an upper and lower section; hence the term "split-beam pattern" is commonly applied to this type of ray diagram.

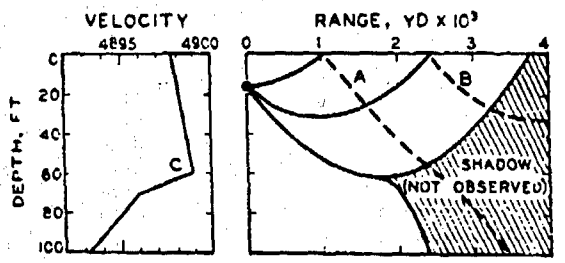


FIGURE 13. Ray diagram for the case of an isothermal surface layer. Dotted curves represent rays reflected from the surface into the theoretical shadow.

As in the previous case, one would expect the shadow beyond the limiting ray to be a region of relative silence. Actually the shadow in Figure 13 differs from that in Figure 10 in that it is penetrated by surface-reflected rays such as those designated by *A* and *B*. Since the surface reflects approximately all of the incident sound energy, it is obvious that the shadow in Figure 13 will not be as complete as the one in Figure 10. Also, in the sound velocity graph, the corner at the point *C* of maximum velocity is actually rounded instead of being sharp as shown. When this rounding is properly introduced into the theory, the "shadow" is found to be actually a region into which few direct rays, rather than none at all, penetrate.

Experiments show that there is no noticeable shadow under these conditions. The intensity at a given depth is found to decrease gradually with increasing range and shows no abrupt drop as the limiting ray is crossed. The decrease of intensity is more rapid below the split point than above. A more detailed discussion of transmission under conditions such as these is given in Chapter 3. This decrease in intensity in this region is known as the *layer effect* and will be discussed further in Section 2.1.

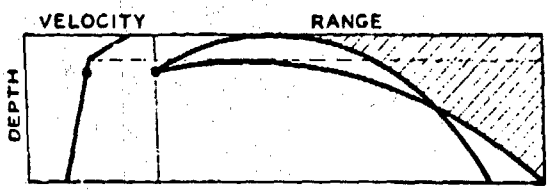


FIGURE 14. Diagram showing sound field bounded by two limiting rays.

### 2.2.3 Crossing Rays and Sound Channels

Other thermal structures result in the sound field conditions illustrated by the ray diagrams shown in Figures 14 and 15. Figure 14 illustrates the case where two limiting rays bound the field. Figure 15 shows a velocity distribution resulting in what is called a *sound channel*. All rays leaving the projector between the two rays *A* and *B* are alternately refracted up and down. They are consequently confined to a certain layer, to which the above term is applied. The transmission loss in sound channels is exceptionally low, and long echo ranges are possible.

In the open sea sound channels are rare and transitory in the upper layers, since the thermal conditions causing them are unstable (see Chapter 4). Near the mouths of large rivers, where salinity conditions cause changes in sound velocity, it is possible to have stable sound channels in the surface layers.

At great depths, where the temperature is nearly constant, the pressure effect causes the sound velocity to increase with depth, and there is a permanent sound channel, as described in Section 2.1.2 and Figure 2. Experiments with the transmission of sound in the deep sound channel are discussed in Section 3.1.

## 2.4 SOUND INTENSITY AND RAY DIAGRAMS

### 2.4.1 Ray Divergence and Intensity

The effects of refraction have thus far been presented in a black-and-white picture of silent shadows and regions of direct or reflected sound. This was the earliest form of theory on which echo-range predictions were based, and gave better results than no theory at all. However, it has since been learned that the shadows are not silent and that there are marked variations of intensity within the field of direct sound.

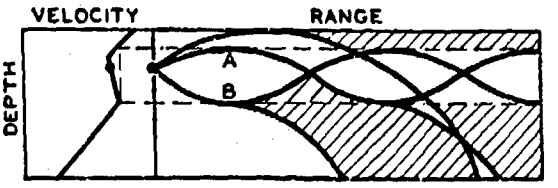


FIGURE 15. Diagram illustrating the formation of a sound channel.

Even before this experimental knowledge was obtained, attempts had been made to elaborate the ray theory to enable the calculation of intensity changes in the direct field. This intermediate theory is still useful for some purposes even though it also

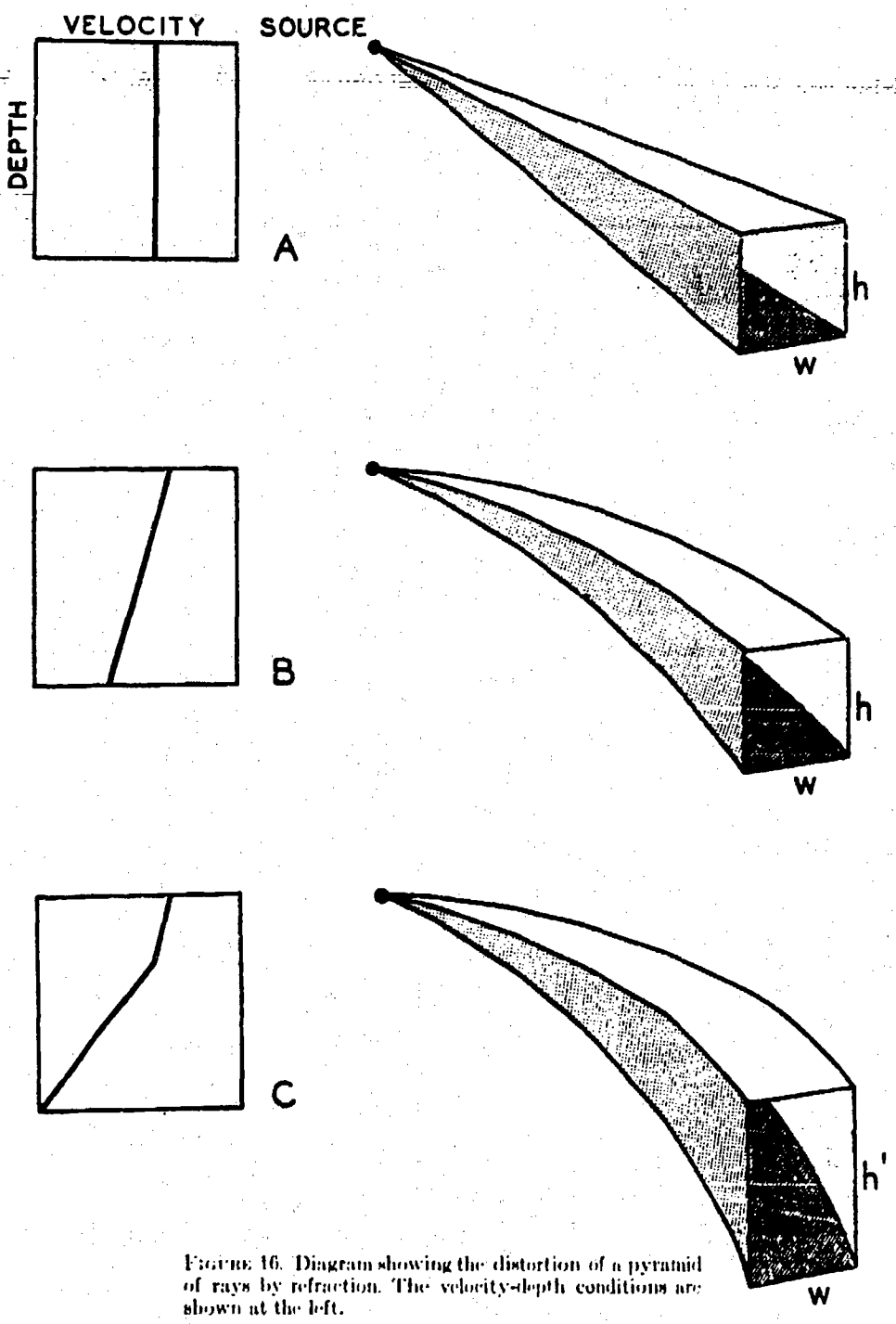


FIGURE 16. Diagram showing the distortion of a pyramid of rays by refraction. The velocity-depth conditions are shown at the left.

predicts completely silent shadows that are not observed.

The general idea of this theory is to consider pyramids or cones of rays, the vertices of which are at the source of sound. Figure 16A shows such a pyramid of straight rays. Neglecting losses caused by absorption and scattering, all of the power radiated into this pyramid by the projector will remain inside the

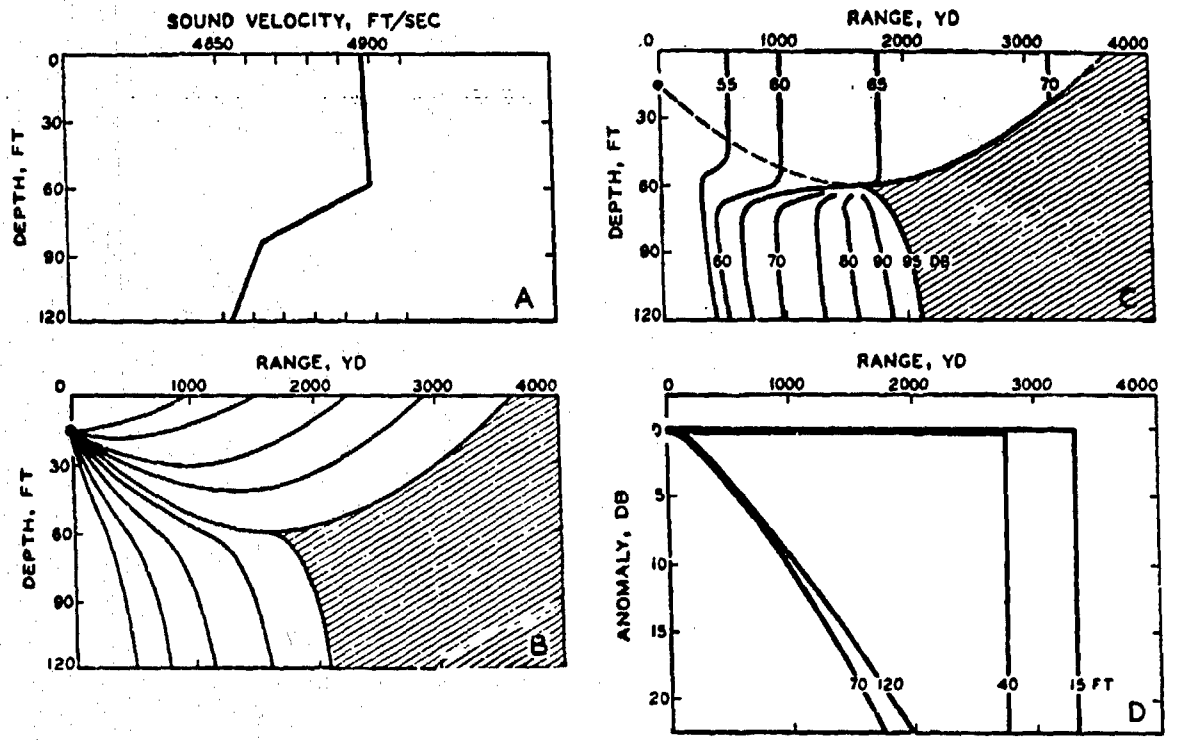


FIGURE 17. Diagram illustrating the calculation of theoretical intensities for typical ray diagram. (A) Bathythermogram, (B) ray diagram, (C) intensity contours, (D) anomaly graph for several depths.

pyramid as it travels outward. The energy flow (power per unit area) is consequently inversely proportional to the cross section of the pyramid. As the cross section increases, the energy flow, or intensity will decrease. Since the cross section increases as the square of the range $r$, the intensity will decrease according to the inverse square law discussed in Section 1.2:

$$I = \frac{I_1}{r^2}. \tag{2}$$

Figure 16B shows the same pyramid as refracted by a constant-velocity gradient. The cross section of the pyramid at any range is seen to be approximately the same as at the same range in Figure 16A. The two may be considered equal in a practical calculation. Consequently, in a layer of constant velocity gradient the intensity also follows the inverse square law.

Figure 16C shows two layers with different gradients. The rays diverge abruptly as they enter the lower layer, increasing the cross section of the pyramid; this results in a decrease of the intensity. The horizontal spread $w$ in $C$ is the same as in $A$; the cross-sectional areas of the two pyramids are therefore in the ratio of the heights $h'/h$. It follows that the intensity $I$ in Figure 16C is given by

$$I = \left(\frac{I_1}{r^2}\right)\left(\frac{h}{h'}\right). \tag{3}$$

Converting this to decibels, we have

$$L = S - 20 \log r - 10 \log \left(\frac{h'}{h}\right), \tag{4}$$

and the transmission loss is

$$H = 20 \log r + 10 \log \left(\frac{h'}{h}\right). \tag{5}$$

The second term is the transmission anomaly due to refraction. Hence this theory predicts that the transmission anomaly should be

$$A = 10 \log \left(\frac{h'}{h}\right). \tag{6}$$

### 2.4.2 Theoretical Intensities for Typical Ray Diagrams

The calculation of the transmission anomaly $A$, using equation (6), can be carried out for various

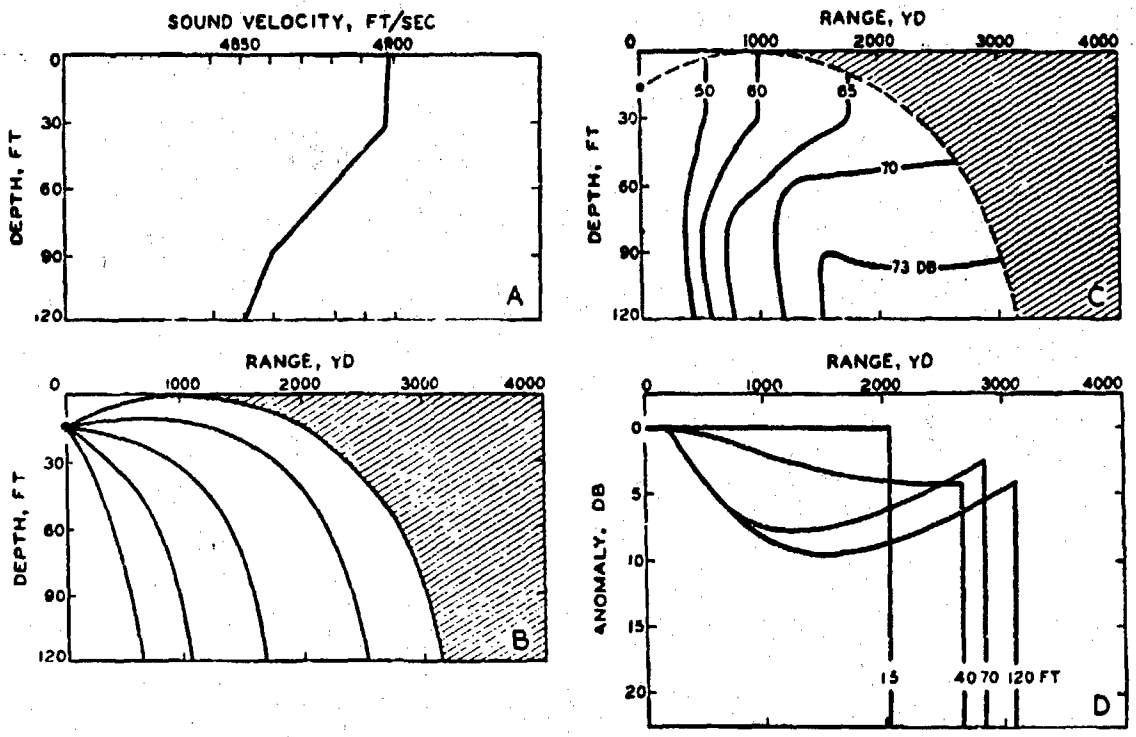


FIGURE 18. Same as Figure 17 for a case of downward refraction.

points in the sound field, once a sufficient number of rays have been plotted. At a given point, the value of $h$ is given by

$$h = r\Delta\theta, \tag{7}$$

where $r$ is the range to the point and $\Delta\theta$ is the angular separation between adjacent rays as they leave the projector. The value of $h'$ can be approximated with sufficient accuracy for practical purposes by measuring the vertical displacement between the two adjacent rays at the depth and range of the point under consideration, provided the value of $\Delta\theta$ has been chosen sufficiently small.

The results of such calculations can be presented graphically in various ways, as illustrated in Figures 17 and 18. Figure 17A is a typical bathythermogram showing an isothermal layer and thermocline. The corresponding ray diagram is shown as B. Figure 17C shows a series of contours on which the sound level is constant. They are identified by the values of transmission loss in db. Above the thermocline they represent the loss calculated from the inverse square law. It is seen that, above the thermocline, these contours are, in general, farther from the projector than they are below the thermocline, and also, that they are more widely spaced above than below. Throughout the whole shadow (shaded area) the calculated intensity is zero, and the transmission loss is consequently infinite.

A second method of presenting the results is shown by Figure 17D. The transmission anomaly was calculated for various points. Holding the depth of the point constant (say at 70 ft) and allowing its distance from the source to vary, one obtains a series of values that can be plotted as a curve (see curve marked 70 ft on Figure 17D). These graphs are smooth curves when the depth is greater than that of the thermocline. When the point is above the thermocline, however, the transmission anomaly is practically zero until the point reaches the shadow zone, when it suddenly becomes infinite.

This discontinuous change in the transmission anomaly is partly due to the approximate velocity-depth curve used in the calculation (see above). If these approximations were eliminated from the calculation, the change at the shadow boundary would not be so abrupt, and the curves would not drop so far. No calculations on this point have been made, partly because the available thermal data is not accurate enough to yield definite results. These theoretical values of the transmission anomaly will be compared with the observed values in Chapter 3.

THE LAYER EFFECT

The very marked increase in the transmission anomaly in the thermocline has important operational implications. From Figure 17C it appears that if at a range of, say, 1,000 yd a hydrophone is lowered to a depth of 75 to 80 ft, it will enter a region where the sound transmission was poorer by nearly 10 db than it is 20 to 25 ft higher. The sudden increase of the transmission loss in the thermocline is called the *layer effect*. The importance of the layer effect is enhanced by the great prevalence of this type of thermal pattern in the ocean all over the world. It will be further discussed in Chapter 3.

Figure 18 shows corresponding diagrams for a case of downward refraction. They will be compared with experiment in Chapter 3.

## 2.4.3 Preview

At this stage it would appear logical that we consider next the contributions of absorption and scattering to the transmission anomaly. Equally urgent, however, is a more intimate acquaintance with the nature of the ocean, the medium through which the sound travels.

Because of the complexity of the subject, it was decided that at this point it would be more advantageous to introduce the experimental study of transmission. This is therefore done in Chapter 3. Following this discussion, the essentials of oceanography pertaining to sound transmission are presented in Chapter 4. A detailed discussion of scattering and absorption will be found in Chapter 5.

## Chapter 3

# THE TRANSMISSION OF SOUND IN THE SEA

THE VARIOUS factors that contribute to produce the transmission anomaly, as summarized in Section 1.3.4, have all been investigated experimentally to a greater or lesser extent. The variability in the transmission loss was first observed in actual echo-ranging operations at sea. In certain areas, the ranges achieved in the afternoon of clear, relatively calm days were found to be less than those obtained in the mornings. Numerous explanations were advanced, but the true reason was discovered by the Woods Hole Oceanographic Institution as the result of experiments performed in cooperation with the U. S. Navy. The effect was found to be caused by the heating of the upper layers of the ocean by the sun. This observation resulted in the theoretical investigations described in the preceding chapter. The conclusions based on this theory were in their turn subjected to rigorous experimental investigation, and it is with these experiments that the present chapter deals, together with the attempts to determine the role played by the other factors mentioned.

Most of the experimental work was done using sound of supersonic frequencies, generated by standard sonar projectors. More recently, however, the transmission of sounds of sonic frequencies has been investigated to some extent, and promises to provide a fruitful field for extensive research. For certain phases of the research program, sound produced by underwater explosions was found to be ideally suited, for reasons that will become clear in the following paragraphs. These three kinds of experiments will all be considered in this chapter, the experiments with explosive sound being discussed first.

## 3.1 THE SOUND OF UNDERWATER EXPLOSIONS

The suitability of explosive sounds for investigating some features of sound propagation is well known to acoustic engineers. In making a preliminary survey of a room that is to be acoustically treated, they often use a handclap as the experimental sound. The shortness of the duration of the original sound makes it readily possible to hear echoes distinctly and to estimate their relative intensity. In geophysical and underwater sound investigations, blasting caps and other explosives are generally employed. While the sound produced by a blasting cap exploding under water is not quite so simple as that of a handclap, it does have some of the characteristics of the latter, as well as much greater intensity.

### 3.1.1 The Explosion Bubble and Its Oscillation

The explosion suddenly creates a relatively small bubble of gas at a very high temperature and pressure. The pressure is imparted to the water and is radiated as a sound wave of extraordinary intensity — a "shock" wave, which, because of the enormous pressure, differs from ordinary sound waves in some particulars. A shock wave bears a similar relation to an ordinary sound wave as that of a large breaker on a beach to an ordinary water wave. One effect, due to the high pressure, is that the shock wave has a higher velocity than ordinary sound waves; however, at reasonable distances, its velocity begins to approach the normal value.

The gas bubble created by the explosion expands and sets the surrounding water in motion. The expansion continues even after the pressure in the bubble has become much less than the normal hydrostatic pressure. This is because of the inertia of the water. The bubble finally ceases to expand and begins to contract; again the inertia of the water

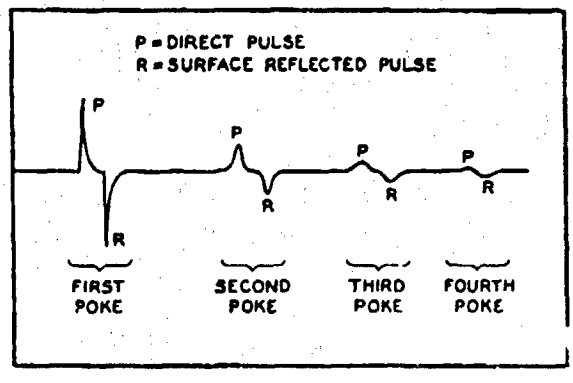


FIGURE 1. Diagram of oscillogram of underwater explosion, showing direct and surface-reflected pulses of consecutive "pokes."

causes the equilibrium point to be passed, and the contraction continues until the pressure in the bubble has become very great. During this high-pressure phase, intense sound is again radiated. The mechanism is similar to the familiar water hammer when a faucet is turned off too suddenly.

The alternate expansion and contraction is repeated a number of times, resulting in well-separated pulses or "pokes" of sound; these are shown diagrammatically in Figure 1. The time intervals between the pokes depend on the hydrostatic pressure at the place of the explosion, but obviously not on the distance from the explosion or on the depth of the hydrophone. The dependence on the hydrostatic pressure is shown in Figure 2.[9]

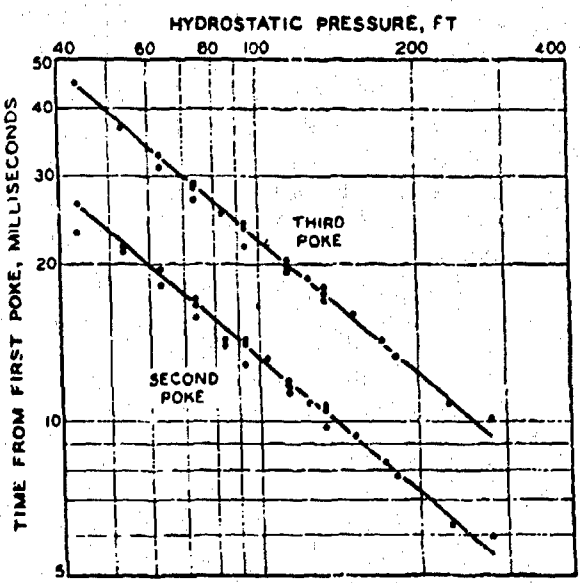


FIGURE 2. Dependence of time interval between pokes on the hydrostatic pressure at the point of explosion.

## 3.1.2 The Reflection of Sound at the Sea Surface

The immediate result of the experiments with explosive sound was to emphasize the importance of the ocean surface in the study of sound transmission in the sea. This importance rests upon the fact that sound reflected from the surface interferes with that traveling directly.

### TIME DELAY OF THE REFLECTED PULSE

Figure 1 shows each of the pokes to consist of two peaks, the first of which corresponds to a wave of compression, the second to a wave of rarefaction. These peaks are easily seen in the oscillograms of Figure 3, each of which is the record of the first poke only. The oscillograms show a variable time interval between the positive and negative peaks; this time interval depends on the distance from the explosion to the hydrophone and on the depth of both the hydrophone and the explosion.

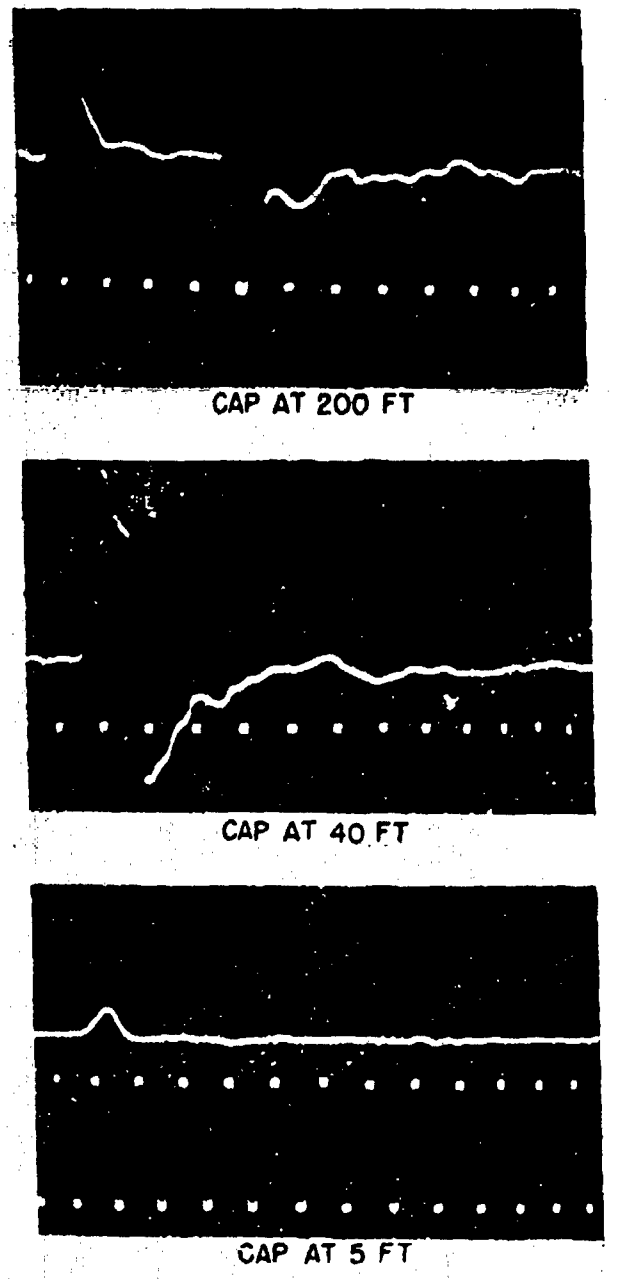


FIGURE 3. Oscillograms showing variation of time interval between direct and reflected pulses.

It has been found that the separation of positive and negative peaks can be calculated quite accurately on the assumption that the positive peak represents sound that travels directly from the explosion to the hydrophone, while the negative one is the echo from the surface. The geometry of this calculation is shown by Figure 4. The direct sound travels over the distance $EH$, while the surface echo travels the distance $ER + RH = IH$. Thus, both the time and direction of arrival of the echo is the same as if it originated at the

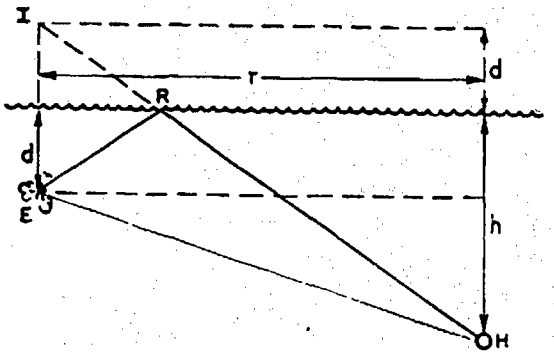


FIGURE 4. Diagram of sound travel. The explosion occurs at $E$, $d$ ft beneath the surface. The sound will travel via the hydrophone $H$, located $h$ ft below the surface, either directly via $EH$, or by reflection from the surface, via $ERH$. In the latter case the travel distance is equal to $IRH$, where $I$ is the image of $E$.

mirror image $I$ of the actual explosion. The reflected sound travels farther than the direct sound by the distance $III - EH$. From Figure 4,

$$(EH)^2 = r^2 + (h-d)^2,$$
$$= r^2 + h^2 - 2hd + d^2;$$
$$(III)^2 = r^2 + (h+d)^2,$$
$$= r^2 + h^2 + 2hd + d^2.$$

Subtracting one equation from the other, one finds

$$(III)^2 - (EH)^2 = 4hd,$$

or

$$III - EH = \frac{4hd}{(III + EH)}. \qquad (1)$$

If $r$ is much greater than either $h$ or $d$, as is often the case, $III + EH$ is very nearly equal to $2r$. Hence, approximately,

$$III - EH = \frac{2hd}{r}. \qquad (2)$$

The time delay $\Delta t$ in the arrival of the echo is given by

$$\Delta t = \frac{(III - EH)}{c},$$
$$= \frac{2hd}{rc}, \qquad (3)$$

where $c$ is the velocity of sound. This law is compared with experiment in Figure 5.[9]

These considerations leave no doubt that the negative pulse is the echo reflected from the surface. Theoretical considerations lead to the prediction that the echo of a compression pulse from the air-water surface should be a rarefaction, and the oscillograms show that this is actually the case.[1a,2a,6a]

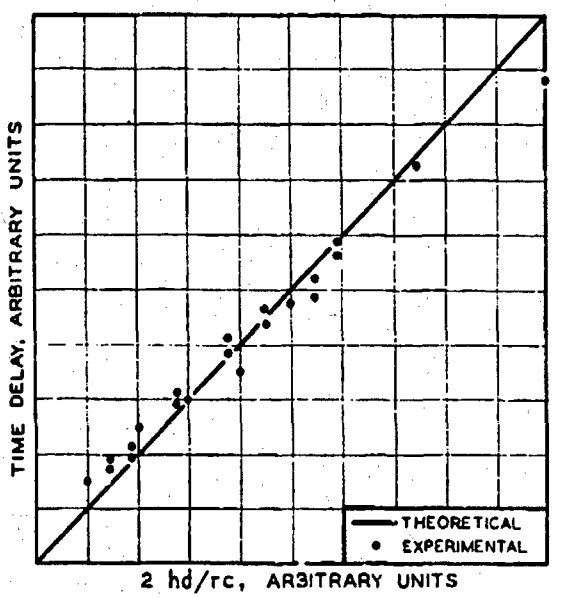


FIGURE 5. Comparison of theoretical and observed time delay between direct and surface-reflected pulses of explosive sound.

## INTERFERENCE OF DIRECT AND SURFACE-REFLECTED RAYS—THE IMAGE EFFECT

These oscillograms of Figure 3 also show the phenomenon of interference in a very instructive manner. When the explosion occurred at a depth of 200 ft, the direct and reflected pulses were well separated in time. At 40 ft, however, the negative (reflected) pulse arrived before the positive (direct) pulse had ended; and when the charge was exploded at a 5-ft depth the two pulses arrived almost simultaneously. In this last instance,

the compression is almost completely canceled by the rarefaction. This interference between the direct and reflected sound is called the *image effect*. It will be discussed further in Section 3.3.2, at which time the quantitative aspects will be considered.

### 3.1.3 Modification of the Image Effect by Refraction

The manner in which refraction modifies the image effect is very conveniently investigated with explosive sound. The case of simple downward refraction is illustrated by Figure 6. As the shadow boundary is approached, the rays of the direct and reflected sound reaching a given point coincide more and more

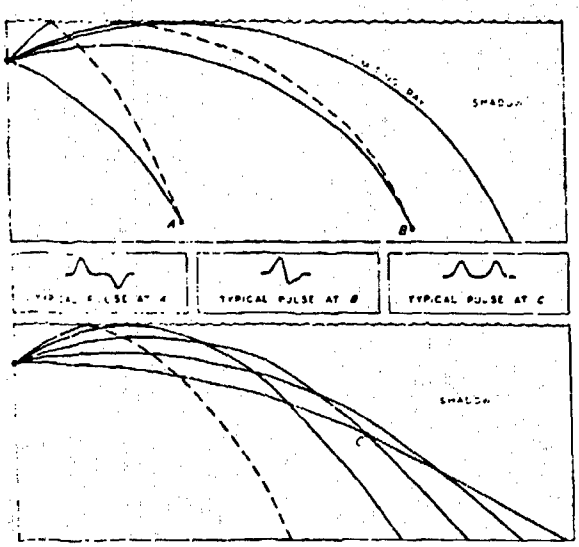


FIGURE 6. Diagram showing the modification of the image effect by refraction.

closely. At points near the shadow boundary (*B* in the diagram), the time delay of the surface echo approaches zero. In the absence of refraction, this would not occur until very great ranges are reached. This reduction of the time delay by downward refraction occurs at all ranges but is small at short ranges. The reduction in time delay has been observed in experiments with explosive sound, and the data used in Figure 5 have been selected to exclude conditions under which it is appreciable.

Even more complicated effects are possible, as shown in the bottom diagram of Figure 6. In this case the rays cross, and there are two direct rays reaching some points such as *C*. Moreover, no reflected rays reach such points. Consequently, the

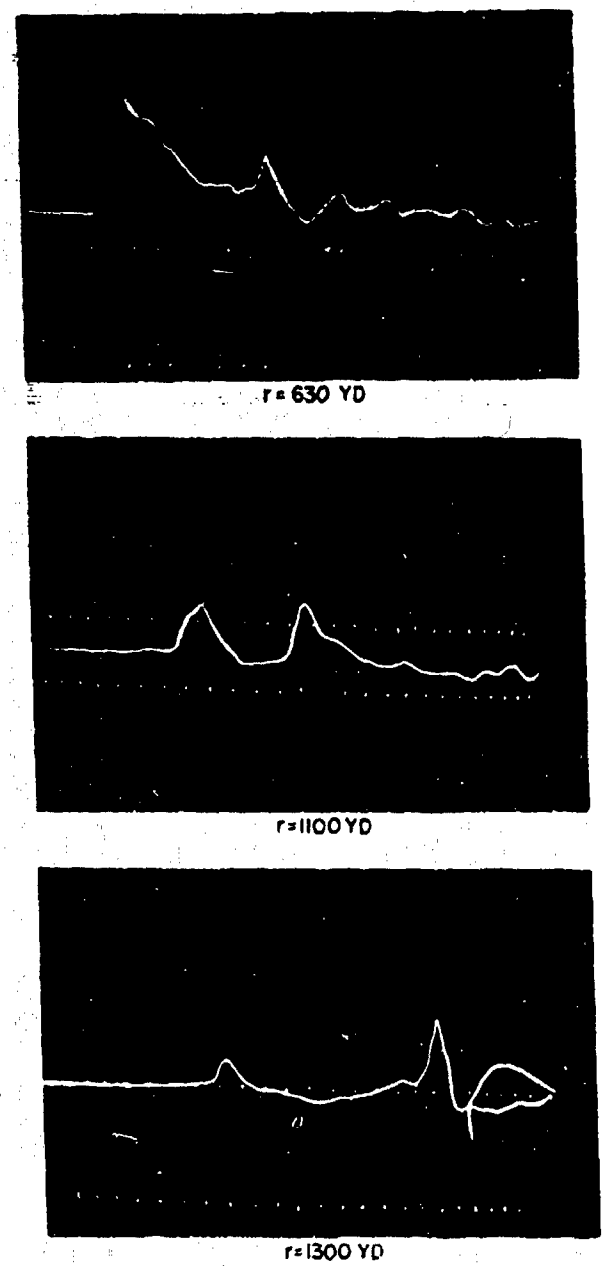


FIGURE 7. Oscillograms showing multiple path effects in explosions.

received sound consists of two positive peaks and no negative one. This has been experimentally observed (see Figure 7).

### 3.1.4 The Intensity of the Direct Sound

The study of the direct-sound pulses has resulted in a verification of the intensity theory developed in

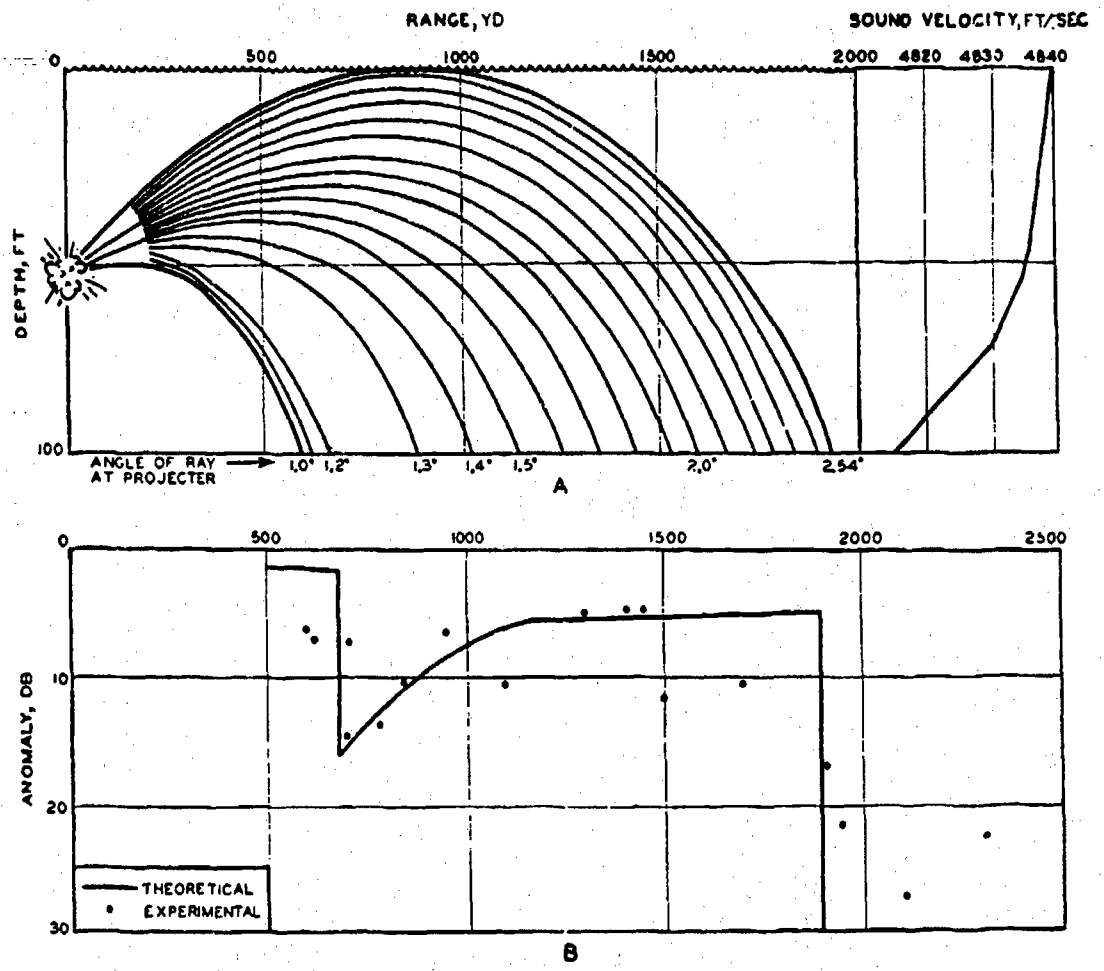


FIGURE 8. Experimental data showing effect of refraction on transmission of explosive sound. (A) Bathythermogram and ray diagram. (B) Graph of calculated transmission anomaly and measured values. The dip in the anomaly curve at 600 yd is due to the spreading of the rays by refraction: note that there is a markedly greater spread between the 1.2° ray and 1.3° ray than between the rays to the left and right. The rays incline more than 1.4° tend to converge slightly, with a corresponding decrease in the transmission loss. Beyond the 2.54° ray is the shadow, and here the transmission anomaly experiences an increase.

Section 2.4.2. The intensity was measured by noting the maximum value attained by the pressure during the positive peak of direct sound, and this measured intensity was then compared with the theoretical intensity as calculated from the bathythermogram shown in Figure 8A. The bathythermogram shows that during the experiments there were three more or less distinct layers, in each of which the temperature gradient was negative and nearly constant. The explosion occurred near the top of the second layer, while the hydrophone was deep in the third layer. From this data, a detailed ray diagram was carefully constructed, rays leaving the source being plotted at intervals of 0.1°. It will be noted that the 1.0°, 1.1°, and 1.2° rays are quite close together and have their vertices in the second layer. The 1.3° ray is the first of the plotted rays which penetrate the top layer, where the gradient is smaller. Consequently, there is a marked divergence of this ray from the previous three. The rays leaving the explosion at steeper angles all penetrate the first layer, and their divergence diminishes with increasing angle but remains greater than that of the rays whose vertices are in the second layer.

These peculiarities of the ray diagram result in the anomaly graph shown in Figure 8B, which has a marked dip between 600 and 700 yd and then rises out to the shadow boundary at about 2,000 yd. The experimental points scatter considerably but confirm the general trend between 600 and 1,500 yd. Between 1,500 yd and the shadow boundary at 1,900 yd, the observed values are too low. Beyond the

shadow boundary, theory predicts that there should be no sound, but, experimentally, some was detected.

It may be concluded that the ray theory of intensities is valid except near the shadow boundary. The reasons for the departures in this region are not simple, but one major factor is undoubtedly the difficulty of distinguishing the direct and surface-reflected pulses. Their overlapping and partial cancellation can be invoked to explain the low observed values in the 1,500 to 1,900-yd region, but it cannot explain the weak sound that is observed beyond the shadow boundary.

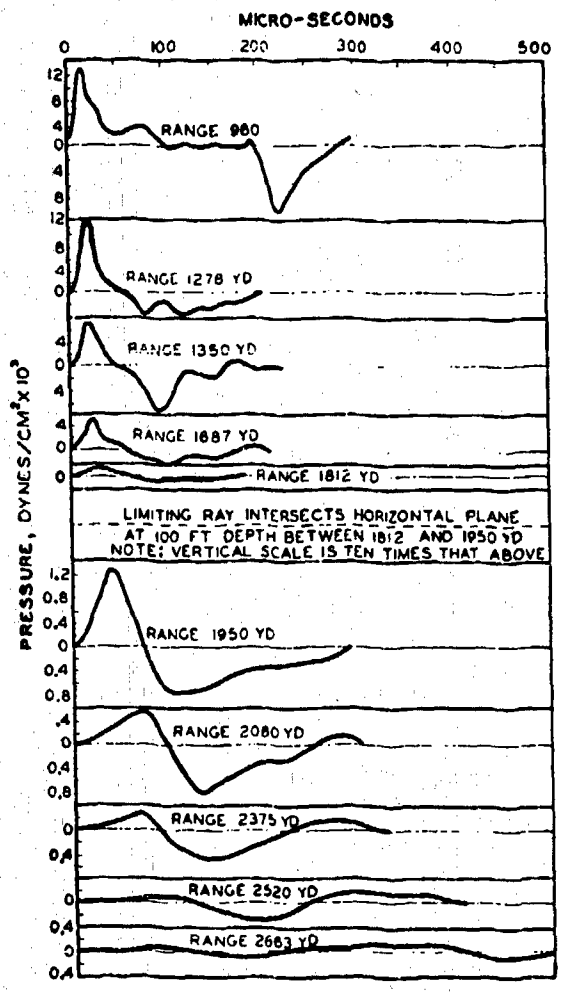


FIGURE 9. Oscillograms made at increasing distances from the explosions.

## 3.1.5 The Sound in the Acoustic Shadow

Figure 9 shows a series of oscillograms made at increasing distances from the explosions. At shorter ranges it is easily possible to distinguish the direct compressional pulse from the reflected rarefaction. As the shadow boundary is approached, this becomes more difficult and the maximum pressure diminishes rapidly. Moreover, there is an increase in the time elapsing between the first perceptible increase in pressure and the attainment of the maximum value.

Both these effects become more pronounced beyond the shadow boundary, and the disturbance tends to become oscillatory, with several maxima and minima. The time between successive maxima appears to increase with range, approaching 300 microseconds.

No complete explanation of these phenomena has been given. Since they are similar to others that will be described below, a discussion of proposed explanations will be given in Section 3.2.3.

## 3.1.6 Explosions in the Permanent Sound Channel

The transmission of the sound of explosions occurring at great depth has been investigated by the Woods Hole Oceanographic Institution. Such sounds have been heard at great distances: the explosion of ½ lb of TNT was heard at a distance of more than 800 miles, and that of a blasting cap at a distance of 75 miles. These remarkable results are a consequence of the permanent sound channel that has been described in Chapter 2.

When both the sound source and hydrophone are at depths near the minimum of the velocity, there are many rays joining them. A few of these have been plotted schematically in Figure 10 for the velocity distribution shown at the right. Several different kinds of rays can be distinguished. Those which are roughly sinusoidal and do not reach either the surface or bottom are called the *sound channel* [*SC*] *rays*. Those which are reflected at the surface but are refracted upward before reaching the bottom are called *RSR rays*. Those reflected at both surface and bottom are the *R rays*. The horizontal ray at the minimum sound velocity is called the *axis* of the channel.

The times required to traverse the different ray paths will not all be equal, with the result that a single pressure pulse of the original wave will cause a large number of "arrivals" at the hydrophone. This is the same phenomenon as shown on Figure 7 but, under the conditions being discussed, as many as 100 arrivals have been distinguished (see Figure 11).

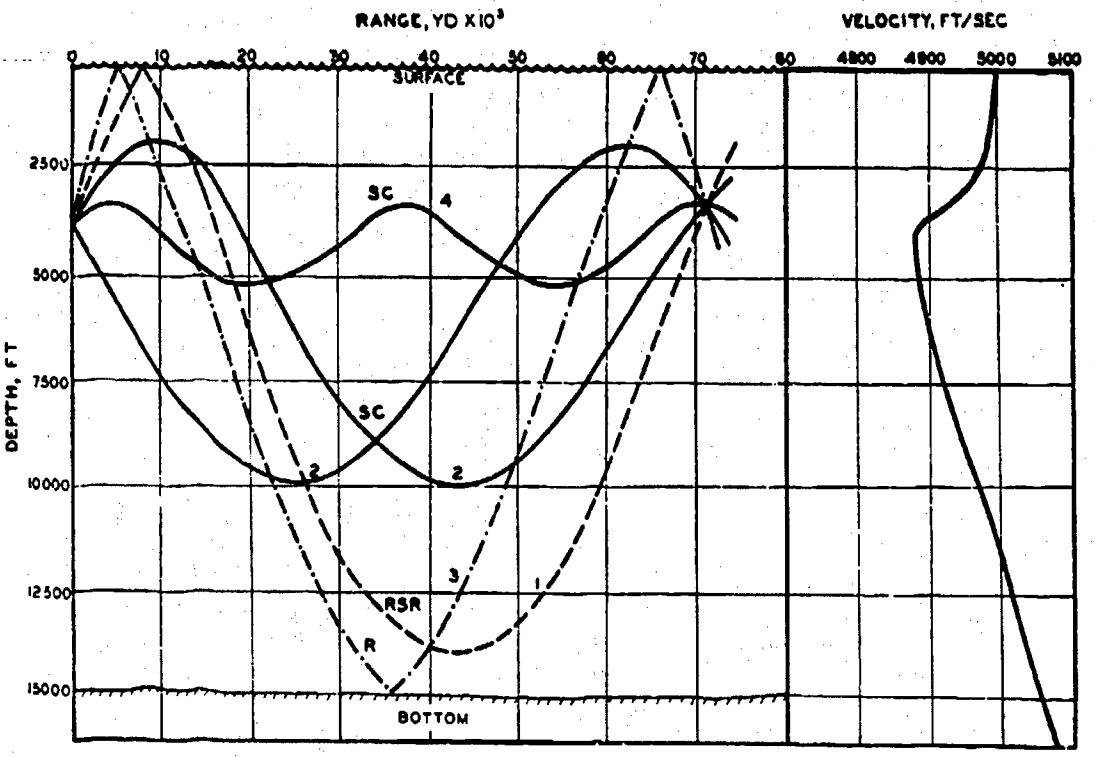


FIGURE 10. Graph of several possible ray paths in deep sound channel.

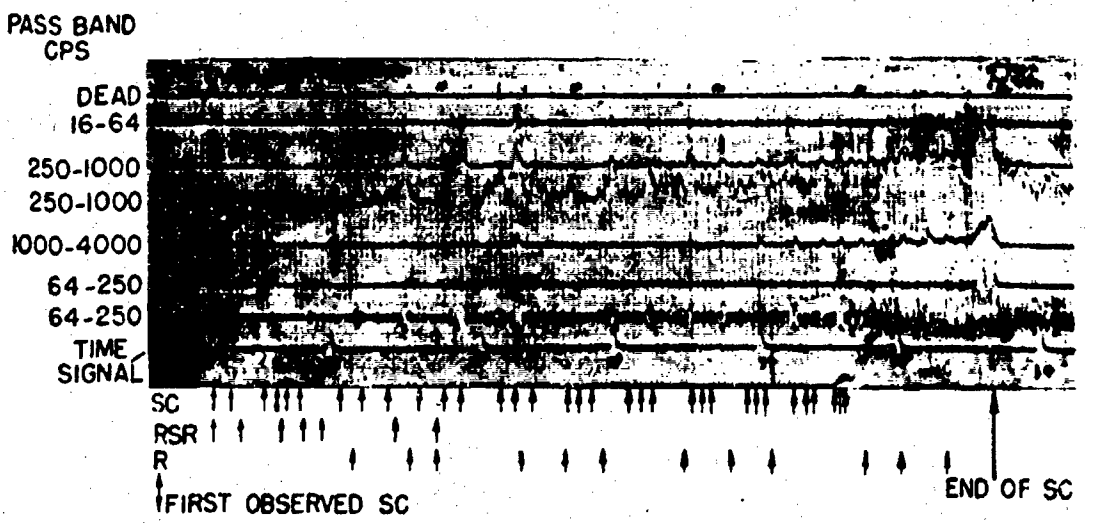


FIGURE 11. Oscillograms of sound transmitted in the deep sound channel. The arrival times of the sound, via several paths, are indicated by the arrows.

The first sound to arrive will be that which has deviated farthest from the axis of the channel and thus has spent most of its time in regions of high velocity. It will arrive via that ray which has crossed the channel axis the smallest number of times. The second arrival makes one more crossing, the third, two more. In Figure 10 the rays are numbered roughly in the order of arrival; sound traversing the two rays numbered 2 will arrive practically simultaneously.

These remarks apply separately to the SC, RSR, and R rays; in general, the SC sounds arrive first, then the RSR and finally the R sounds. The first SC arrivals are weak and separated by long intervals; subsequent arrivals increase in intensity, and the intervals decrease, the whole resulting in a final crescendo followed by an abrupt termination of the sound. This can be followed on Figure 11 by noting the arrivals indicated by the upper row of arrows.

The RSR sounds have the same kind of time pattern, but do not show the crescendo of intensity. The R sounds have the reverse pattern. The early R arrivals are strong and separated by short intervals, and show a diminuendo of intensity and a slowing tempo. The earliest R's sometimes come in before the SC's but continue to arrive after the SC's have terminated.

The possibility of using this technique for long-range signaling has been considered, and particularly for the location of airmen forced down at sea.

### 3.1.7 Summary

To sum up, the study of explosive sounds shows:

1. The signal received at a given point in the deep ocean will consist of sound that has been reflected from the surface, in addition to that which travels directly from the projector to the hydrophone. At the surface the incident sound experiences a phase shift of half a cycle on reflection, or, in other words, a wave of compression is reflected as a rarefaction. The surface-reflected sound, therefore, tends to interfere with the direct sound.

2. The measured sound intensity of the direct rays compares quite accurately with the intensity calculated from refraction theory, except in the region near the shadow boundary, and in the shadow itself.

3. The deep sound channel to be expected below the permanent thermocline actually does exist and may be a useful channel of communication.

## 3.2 THE TRANSMISSION OF SUPERSONIC HORIZONTAL BEAMS

### 3.2.1 Description of the Experiments

#### Experimental Procedure

While experiments with explosive sound were instructive and provided important contributions to the knowledge of the transmission of underwater sound in general, the behavior of sound of the frequencies and intensities currently used in echo ranging was naturally of more immediate interest.

An extensive program of experiments was undertaken in 1943 by the University of California in cooperation with the U. S. Navy Electronics Laboratory [NEL], formerly U. S. Navy Radio and Sound Laboratory [USNRSL]. Two vessels were used in the work. One carried a standard echo-ranging projector which transmitted 24 kc signals. The other vessel was equipped with hydrophones that could be lowered to any depth less than about 500 ft, and with oscillographs; the latter provided a permanent record of the experiment. The distance between the two vessels was measured by transmitting radio signals simultaneously with the sound signals and recording the difference in their arrival times at the receiving ship. Knowing the velocity of sound, an accurate measure of this distance was obtained.

The simplest experiments were performed as follows. The receiving vessel was allowed to drift, and the transmitting vessel ran on a straight course, opening or closing the range. During the whole of the run, the sound beam was directed at the receiving vessel by using pelorus bearings from the bridge, which were repeated in the sound room. The receiving vessel suspended its hydrophones at depths which were kept fixed during the experiment. The oscillograms of the received sound were developed ashore and measured. The results were expressed as transmission anomaly.

Early experiments of this sort had been performed by the Naval Research Laboratory [NRL][16] but were difficult to interpret and did not receive the recognition that they merited.

#### Treatment of Data

Data obtained on two typical runs are shown in Figures 12 and 13. In each case, two hydrophones were used, one at a depth of 300 ft, the other at a depth of 50 or 30 ft. During the period covered by Figure 12, the temperature gradient in the upper 100 ft averaged about 0.03° F/ft, and the temperature decrease began at the surface. During the period covered by Figure 13, the upper 200 ft of the ocean was isothermal, and a very rapid decrease of several degrees (a thermocline) occurred just below this depth. The differences between the two figures show

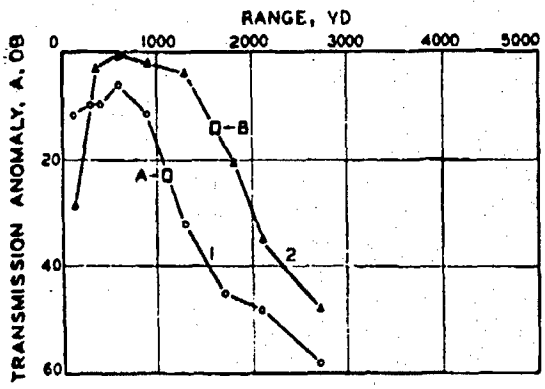


FIGURE 12. Observed transmission anomaly of a single run. Negative gradient at surface curve 1 shows the level with a shallow hydrophone (50 ft), curve 2, those with a deep hydrophone (300 ft). The squares *A* and *B* indicate the range at which the limiting ray crossed the horizontal at the depth of the hydrophone.

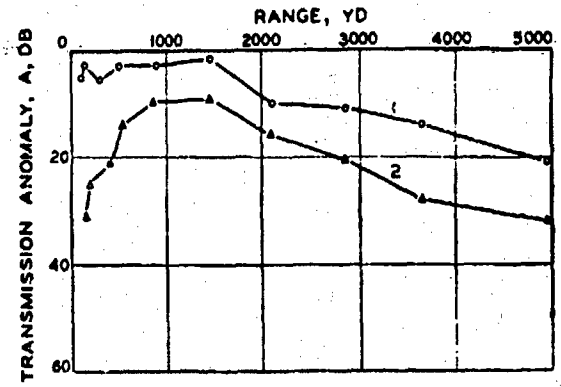


FIGURE 13. Observed transmission anomaly of a single run—isothermal layer 200 ft deep at the surface. Curve 1 shows the levels with a shallow hydrophone (30 ft), curve 2 those with a deep hydrophone (300 ft). The greater anomaly in the second case indicates layer effect.

clearly that the temperature distribution affects the transmission loss.

Too much reliance cannot be placed on the results of any single experiment; the variability of the ocean as a medium of sound transmission is so great that the next experiment may give quite different values.

Consequently, the procedure was to make a number of experiments under similar thermal conditions and to average the experimental measurements at a given range. These average values were then studied first, with a view to determining general principles.

The next step was the study of the departures of single individual values. It was recognized that these departures from the averages were often as important, from a practical point of view, as the averages themselves.

In this section, the emphasis will be on average results and general principles. The discussion of the departures of single experiments from the average will be postponed to Section 3.5.

## 3.2.2 Major Factors Influencing Transmission from a Shallow Projector

The general objective of the study of the transmission records was to establish the effects caused by the changing conditions in the sea. When these changes are numerous and complex, as they are in the upper layers of the ocean, this is difficult to do unless a good theory is available. As was mentioned at the beginning of this chapter, the early discoveries led to the general conclusion that the changeability of underwater sound transmission should be ascribed chiefly to the temperature distribution.

The ray theory, discussed in Chapter 2, was used as a guide in the interpretation of the data. It has been mentioned that this theory does not account adequately for all the facts in the transmission of explosive sounds and this is true to an even greater degree for supersonic sound. However, some of its predictions have been verified in a satisfactory manner and it has served a useful purpose in the analysis of the data.

In the succeeding paragraphs we shall summarize the major results of the experimental study of the transmission of sound in the sea in the form of conclusions that have been definitely established. These conclusions will be compared qualitatively with the ray theory. We shall then, in Section 3.2.3, proceed to a more detailed, quantitative comparison of ray theory and experiment.

### The Dependence of Transmission on $D_2$

*Conclusion 1. The transmission of supersonic sound is very strongly dependent on the depth at which the first appreciable decrease of temperature occurs.*

With present bathythermographs, the smallest temperature difference that can be established with certainty is about 0.3° F. Hence this depth will be $D_2$, according to the bathythermogram code system described in Section 2.1.5.

*General Features of the Anomaly Curves.* Conclusion 1 is established by the data shown in Figure 14. All these data were obtained with the hydrophone at about the same depth as the projector, about 16 ft

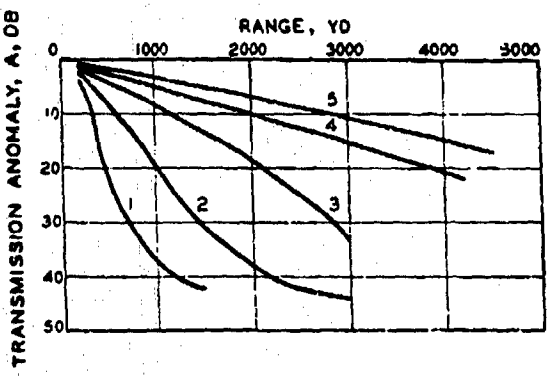


FIGURE 14. Average transmission anomaly under various oceanographic conditions: Curve 1—0 ft < $D_2$ < 5 ft; Curve 2—5 ft < $D_2$ < 20 ft; Curve 3—20 ft < $D_2$ < 40 ft; Curve 4—40 ft < $D_2$ < 80 ft; Curve 5—80 ft < $D_2$ < 300 ft.

below the surface. This fact is important, for reasons that will become clear presently.

The experiments were classified into five groups according to the values of $D_2$. For each group the values of the transmission anomaly at given ranges were averaged, yielding the five curves of Figure 14.

These curves show very clearly the progressive increase in the transmission anomaly as $D_2$ increases. Considering the curves individually, it is seen that in all cases the transmission anomaly increases with range. The significance of the differences between the curves will be more easily comprehended if the reader will refer to Figures 10, 17, and 18, Chapter 2.

*Isothermal Layer Present.* Curves 4 and 5 of Figure 14 show the transmission anomaly when $D_2$ is greater than 40 ft. The corresponding typical ray diagrams for these conditions are represented by the ones in Figure 17, Chapter 2. A hydrophone at 16 ft depth would be in the theoretical direct sound field out to quite long ranges. Under these conditions the anomaly graph is practically a straight line, and this linear relation continues to be valid from 10,000 to 15,000 yd.

In a general way, this linear increase of the anomaly with range is observed in the graphs of individual measurements, such as curve 1 on Figure 13, as well as of averaged ones; but the graphs of individual measurements often show maxima and minima that are as yet unexplained.

*Negative Surface Gradients Present.* When $D_2$ is less than 20 ft, the transmission-anomaly graphs are curved and drop rapidly to a value of about 40 db for the anomaly; this is shown by curves 1 and 2 on Figure 14. This condition is illustrated by the bathythermograms and the ray diagrams in Figures 10 and 18, Chapter 2. It is seen that a hydrophone at 16 ft depth would be in the shadow at very short ranges.

The anomaly curves show a tendency to become horizontal at longer ranges. While it is difficult to measure such large values of the transmission anomaly at long ranges, because of the interference from various sources of noise, there is reason to believe that this tendency is real.

This description of the average curves again applies in a qualitative way to the curves of individual experiments, such as curve 1 on Figure 12.

## DEPENDENCE OF TRANSMISSION ON DEPTH OF HYDROPHONE

The second conclusion based on experiment is the following:

*Conclusion 2. The transmission of supersonic sound from a directional projector mounted on a surface vessel is very strongly dependent on the depth of the hydrophone receiving the sound.*

This conclusion is established by the data of Figures 15 and 16, which show curves of average transmission anomaly measured with hydrophones at different depths. Thermal patterns were of various kinds, but $D_2$ in all cases was less than 30 ft. In these figures, curve 1 applies to the shallow hydrophone, curve 2 to the deeper one. In both figures it is seen that lowering the hydrophone improves the transmission, because curve 2 lies above curve 1 in each case. Reference to Figure 10 or 18 of Chapter 2 will show that this is in general agreement with the ray theory. When $D_2$ is small, the negative gradient near the surface will be large, and the sound rays are bent down in a marked manner. At medium or short ranges the sound beam may be expected to pass below a shallow hydrophone, whereas a deep hydrophone will be in the beam.

An exception to this may occur at very short ranges, however; the sound beam may pass above the deeper hydrophone while it strikes the shallower one, the beam not having yet been bent downward appreciably at these short ranges. That this occurs is borne out by the data of Figure 16, where curve 2 is seen to cross below curve 1 at about a 400 yd range; that is to say, at this range the transmission to the shallower hydrophone is better.

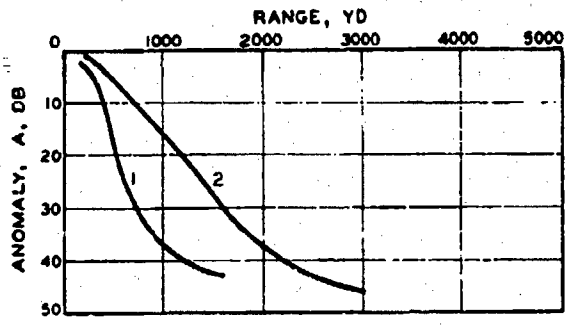


FIGURE 15. Average transmission anomaly—dependence on hydrophone depth $D_2 < 5$ ft. Curve 1—depth of hydrophone < 25 ft; Curve 2—Depth of hydrophone 50 to 100 ft.

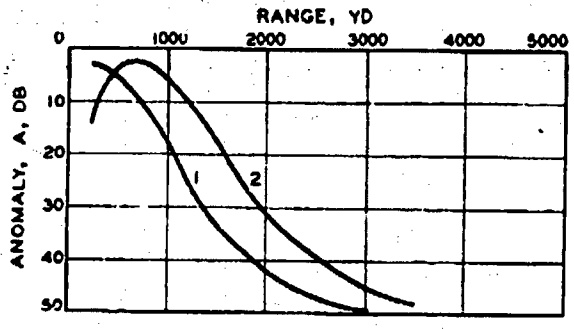


FIGURE 16. Average transmission anomaly—dependence on hydrophone depth, $5 \text{ ft} < D_2 < 30$ ft. Curve 1—depth of hydrophone $\leqslant 100$ ft; Curve 2—depth of hydrophone $\geqslant 200$ ft.

### DEPENDENCE OF TRANSMISSION ON THE DEPTH AT WHICH A THERMOCLINE OCCURS

The relation of transmission to hydrophone depth is completely reversed when $D_2$ is greater than 40 ft. Under these conditions there is usually a more or less marked thermocline just below the depth $D_2$. The following conclusion has been found to apply to this case.

*Conclusion 3. If there is a sharp thermocline, the depth at which it occurs influences the transmission.*

The experimental data are shown in Figure 17. Conclusion 3 is closely related to conclusion 2, and Figure 17 is a confirmation of both conclusions 2 and 3. The anomaly curve for the deeper hydrophone is in this case below that for the shallower one.

Figure 17 of Chapter 2 is a typical illustration of the case when $D_2$ is greater than 40 ft. It appears from a study of this ray diagram that the experimental data again provide a qualitative confirmation of the theory based on ray acoustics. The beam splits at the depth where the sound has the maximum velocity, and, while the shadow zone predicted by the theory is not observed, there is a greater loss in transmission below this depth, as shown by Figure 17. This experimentally observed layer effect is important even though it is not so great as that predicted in Section 2.4.

## 3.2.3 Comparison of Ray Theory and Experiment—Strong Negative Gradients

The experimental results of transmission experiments will now be compared in more detail with those predicted by ray theory.

### THE LIMITING RANGE

The transmission anomaly curves predicted by ray theory were shown in Figure 18 of Chapter 2. They show relatively small values out to the range of the shadow boundary, but at that range the curve drops suddenly to infinity. The range to the shadow boundary is called the *limiting range*, $r_{\text{lim}}$.

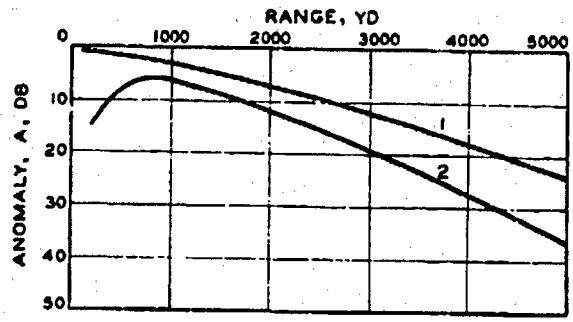


FIGURE 17. Average transmission anomaly—dependence on depth of hydrophone $D_2 \geqslant 40$ ft. Curve 1—hydrophone *above* thermocline; Curve 2—hydrophone *below* thermocline.

The observed transmission anomaly curves such as those shown in Figure 12, while they are quite different in shape, also show relatively small values of the anomaly at short ranges, followed by a rapid but continuous drop to about 40 or 50 db. Investigation led to the following important fourth conclusion:

*Conclusion 4. When negative temperature gradients exist, the rapid drop in the observed curves occurs at about the predicted limiting range.*

This conclusion was first established by marking the predicted limiting range on a large number of experimental curves and noting that it always falls on the steeply sloping part of the curve. Figure 12

illustrates this procedure; the limiting ranges are indicated by the squares marked *A* and *B*.

It will be recalled that experiments with explosives (Section 3.1.5) exhibited a similar effect, a rapid diminution of the maximum pressure near the shadow boundary.

### The Predicted Limiting Range and $r_{40}$

A more objective method than the one mentioned above was then sought. This was accomplished by defining a range that could be determined experimentally and compared directly with the limiting range. Several definitions were tried with more or less success. The method finally adopted (more or less arbitrarily) was to find the range at which the received sound level was 40 db less than that received at 100 yd. This range is called $r_{40}$ and has been found to be a very useful empirical concept. It is very approximately equal to the range at which the transmission loss is 80 db. This follows, since the transmission loss at 100 yd can be calculated fairly accurately from the inverse square law: $H = 20 \log r = 20 \log 100 = 40$ db. Hence the level at 100 yd is 40 db below that at 1 yd, and the level at $r_{40}$ is $40 + 40 = 80$ db below that at 1 yd.

The experimental results expressed in terms of $r_{40}$ are compared with ray theory in Figure 18, in which

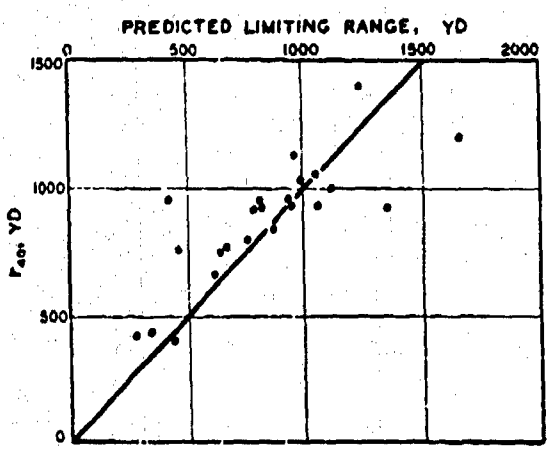


FIGURE 18. Comparison between $r_{40}$ and predicted limiting range.

the values of $r_{40}$ are plotted against the predicted limiting range. If theory and experiment agreed absolutely, the points representing $r_{40}$ would all lie on the 45-degree line through the origin, shown in the figure. While the points scatter considerably, there is evidence of a tendency for them to cluster about the 45-degree line, sufficient to justify the conclusion that this is not accidental. The ray theory is thus not verified in detail, but does give a qualitative account of the facts.

### The Inadequacy of the Ray Theory

There has been much speculation about the reasons for the differences between the ray theory and experiment, and some efforts have been made to construct a more adequate theory. A brief summary of these efforts will be instructive.

*Effect of Diffraction.* The failure to observe the sharply bounded, silent shadow predicted by the ray theory has been discussed by Pekeris.[10,11] It is well known that, even in the case of light, shadow boundaries are not sharp. Light is diffracted around the edges of obstacles and does not travel along rays. As explained in all textbooks on physics, these diffraction effects increase with the wavelength of the disturbance, so that the ray theory becomes less and less correct as the wavelength increases. The wavelength of 24-kc sound in sea water is several inches and much longer than the wavelength of light, so that considerable diffraction of sound may be expected. Pekeris has made calculations which show that the predicted effect due to diffraction is large enough to explain why the transmission anomaly curve has a gradual slope as it crosses the limiting range, instead of dropping to infinity, as seen in Figure 18 of Chapter 2. However, the quantitative agreement between this diffraction theory and the measurements is not exact. Further experiments designed specially to check the theory would be of interest.

*Effect of Scattering.* Another possible explanation of the sound observed in the shadow is the scattering by obstacles suspended in the sea. The scattering of light by dust particles, snowflakes, etc., in the atmosphere is a familiar phenomenon and is known to be responsible for the many changes in the color of the sky and in the visibility of objects. The scattering of sound corresponding to this is known to occur in the sea. It is probable that this is the explanation for the upward curvature, at longer ranges, of curves 1 and 2 on Figure 14. No final conclusion on this topic has been reached, but some interesting calculations are presented in Chapter 5.

*The Effect of Thermal Microstructure in the Sea.* A final reason for departures from the calculations is found in their approximate nature. In making them,

it is assumed that the temperature at a given depth is the same at all points of the ocean, in other words, that the horizontal temperature gradient is zero. It is true that the horizontal gradient is very much smaller than the vertical gradient but it is not zero. The study of this thermal microstructure and its effect on the transmission of sound has not yet yielded any conclusion (Chapter 2).

### 3.2.4 Comparison of Ray Theory and Experiment—Weak Gradients

The inadequacy of the ray theory to explain sound transmission becomes still more pronounced when thermal conditions in the ocean are characterized by weak gradients or an isothermal layer near the surface, below which a more or less well-defined thermocline exists. As these conditions are the ones most commonly encountered over the greatest part of the ocean and much of the time in all regions (see Chapter 4), it is of special importance to study in greater detail the sound conditions associated with these thermal patterns.

The anomaly curves predicted for this case by ray theory are shown in Figure 17 of Chapter 2. If the hydrophone depth is nearly the same as the projector depth, with the latter located in the mixed layer, the theoretical transmission anomaly is zero out to the limiting range and then suddenly increases to infinity. If the hydrophone is at greater depths, the ray theory predicts a rapid increase in the transmission anomaly beginning at very short ranges.

The experimental anomaly curves 4 and 5 of Figure 14 and those in Figure 17 (Section 3.2.2) show that the actual behavior of sound is entirely different. These curves are approximately straight lines passing through the origin, and the anomaly increases with range. (The departures from the straight line at short ranges are caused by the beam pattern, and will be ignored in the following discussion.)

The linear relationship between the transmission anomaly $A$ and the range $r$ is an important one, for it leads to the introduction of the concept of the *attenuation coefficient*.

#### The Attenuation Coefficient

The anomaly curves have equations of the form

$$A = ar \qquad (4)$$

where $a$ is an empirical number. It is the attenuation coefficient just mentioned; the equation (4) shows that it denotes the rate at which the transmission anomaly increases with the range. It is, therefore, measured in decibels per yard.

The information concerning the attenuation coefficient that has been obtained from a systematic study of available transmission records is summed up in the following paragraphs.[12]

#### The Dependence of $a$ on the Depth of the Layer

The depth to the bottom of the mixed layer varies from day to day and from place to place. It has been found that, on the average, the value of $a$ is determined by this depth, which we shall denote by $d$. On any one occasion, however, there are departures from this law. Both these facts are illustrated by Figures 19 and 20, in which $a$ (in units of $10^{-3}$ db/yd) is plotted against $1/d$. The dots represent values of $a$ obtained from single experiments. The squares are the averages of all measurements for which $1/d$ had a value within 0.025 $ft^{-1}$ of the plotted abscissas. The general increase of the attenuation coefficient as $1/d$ increases, that is, as the layer becomes shallower, is apparent.

A similar result would have been obtained if $d$ had been replaced by $D_2$, defined above. The two quantities $d$ and $D_2$ are roughly proportional.

#### The Dependence of $a$ on the Depth of the Hydrophone

Another factor affecting the value of $a$ is the layer effect, which has been defined and explained before. The source was at 16-ft depth in the mixed layer above the thermocline in each of the experiments. The hydrophone was at various depths. Those experiments in which it was above the thermocline are included in Figure 19, while Figure 20 is based on those in which it was below the thermocline.

Comparison of the two graphs shows some evidence for the existence of a layer effect under conditions of weak surface gradients. The equations of the straight lines, obtained by a least squares solution to fit the squares, are, for the hydrophone *above* the thermocline,

$$a = 10^{-3}\left(2.5 + \frac{170}{d}\right) \text{db/yd},$$

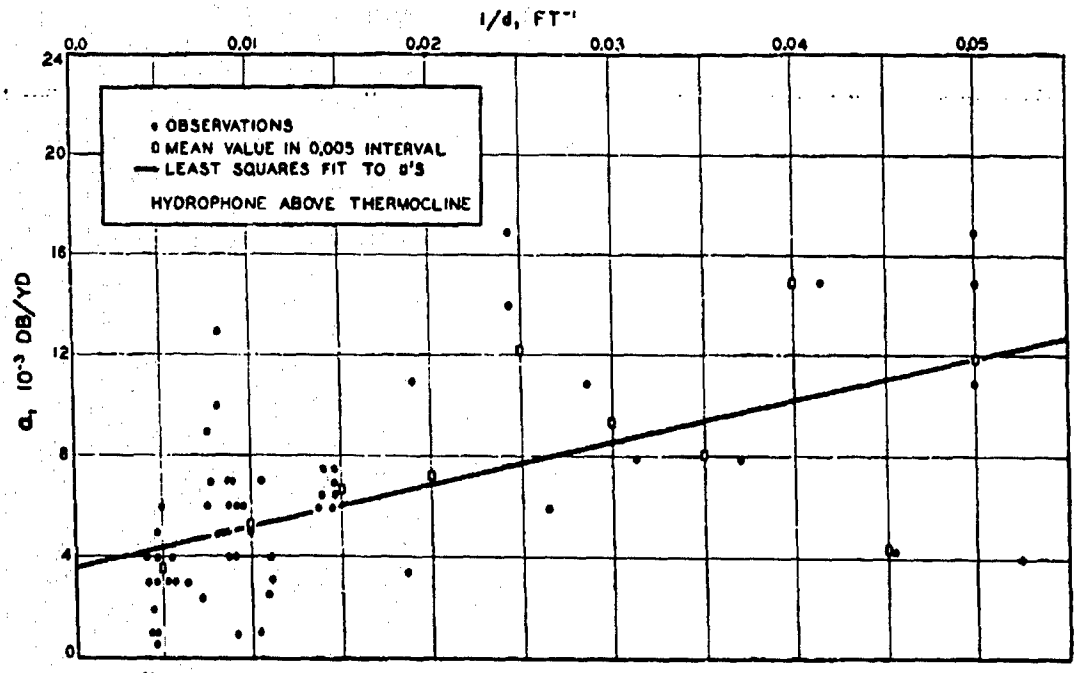


FIGURE 19. Attenuation coefficient—dependence on the depth $d$ of the isothermal layer.

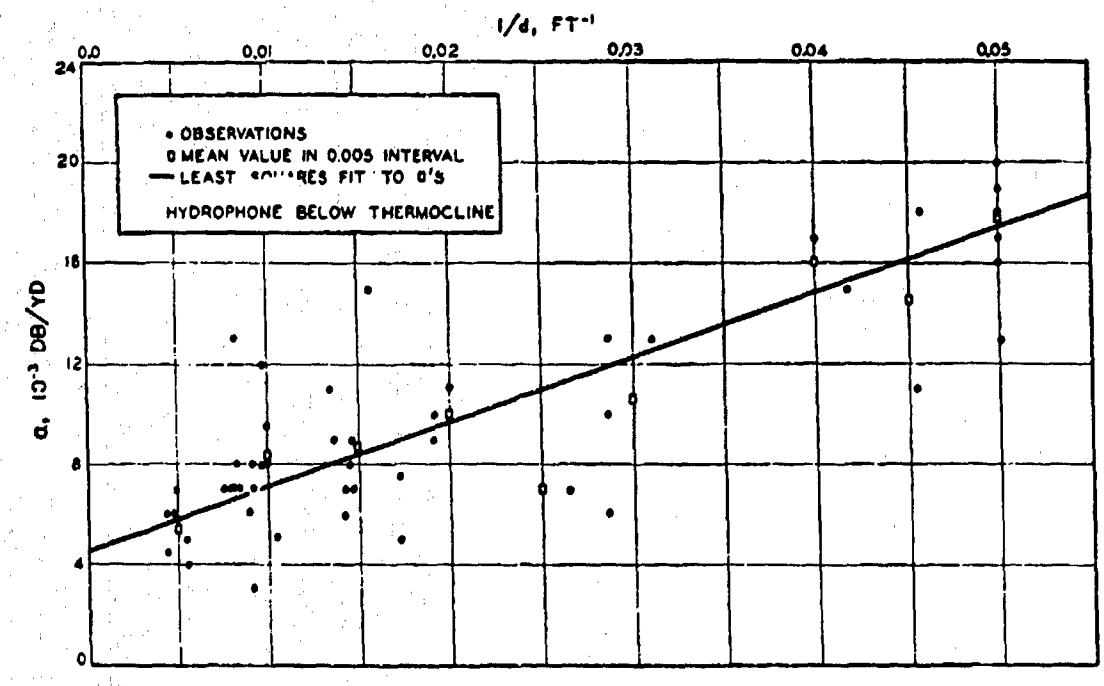


FIGURE 20. Attenuation coefficient—dependence on the depth $d$ of the isothermal layer.

and for the hydrophone *below* the thermocline,

$$a = 10^{-3}\left(4.5 + \frac{260}{d}\right) \text{db/yd.}$$

The depth $d$ is in feet.

The scatter of the dots makes it obvious that these equations give the correct value of the attenuation coefficient only on the average, and that they will probably be in error on any one occasion. The probable error on a single occasion is about $2 \times 10^{-3}$ db/yd. This large error is not caused by faulty experimentation but by unexplained changes in the acoustic state of the sea. This topic will be discussed in greater detail in Section 3.4.

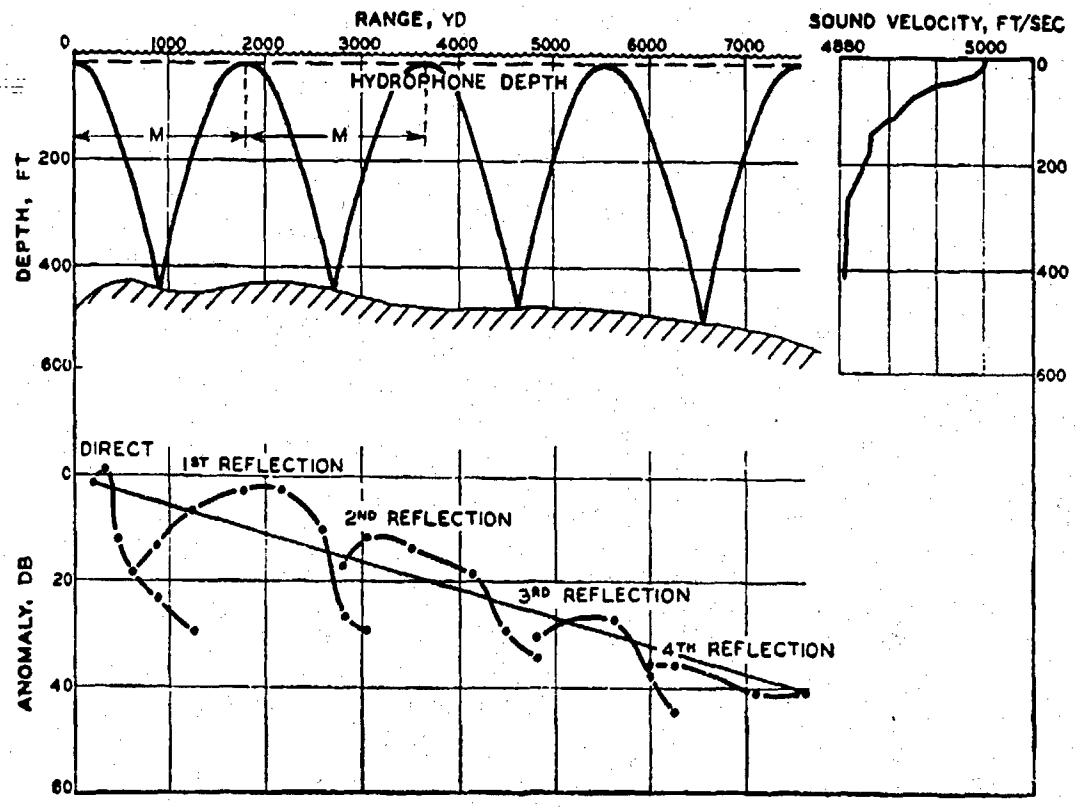


FIGURE 21. Successive refraction and reflection of a sound ray in shallow water with negative surface gradients. Lower figure shows observed transmission anomaly corresponding to this condition. $M$ is the horizontal distance between successive arches of the ray. This figure illustrates the oscillograms of Figure 23.

## 3.2.5 Reflection from the Bottom

The transmission-anomaly curves discussed so far have been plotted from data in which the sound received at the hydrophone arrived either directly from the projector or by reflection from the surface. These curves will be different if the receiver records sound that has been reflected by the ocean bottom.

When the sound beam is refracted downward it will eventually strike the bottom of the ocean, where some of its energy will be absorbed or scattered and the remainder will be reflected. The reflected beam (the echo from the bottom) will rise toward the surface but will be refracted downward once more. Figure 21 shows a ray leaving the projector in a horizontal direction and being successively refracted and reflected in a series of arches, or bounces.

In deep water the bottom echoes can be ignored when short pulses are transmitted, since the time delay between the reception of the direct sound and the bottom echo is then so great that the two pulses are well separated and neither interferes with the measurement of the other. If long pulses are used, the direct signal pulse and the bottom echo pulse may overlap in time. During the period when both pulses are being received, they will interfere, and the resultant amplitude may be either greater or less during the periods when only one is coming in.

In shallow water this interference will occur with short pings also, for in this case the difference in the arrival times of direct signal and bottom echo may easily be less than the duration of the signal pulse.

### Interference of Direct Signal and Bottom Echo

The phenomenon of interference is of considerable importance in underwater sound transmission. It has already been introduced in connection with explosive sound (Section 3.1) and will be encountered in other places (Section 3.3). Hence a digression on its theory appears warranted at this place.

For simplicity, suppose the amplitude of the signals received by direct transmission and by bottom reflection are both equal to $V$. These received signals will be alternating voltages, and, because of the difference in travel time of the two signals in the water, the two voltages will not be in phase. Let the phase difference be $\phi$; then the two signals can be

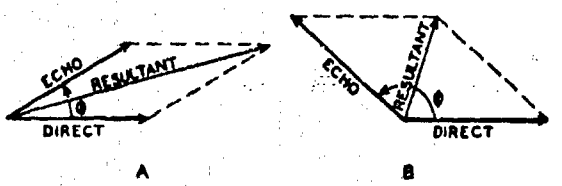


FIGURE 22. Diagram showing the resultant amplitude of the direct pulse and bottom echo for variable phase difference $\theta$.

represented graphically by vectors, as in Figure 22A and B, or analytically by

$$\begin{aligned} \text{Direct} &= V \cos 2\pi ft \\ \text{Echo} &= V \cos (2\pi ft + \phi). \end{aligned} \tag{5}$$

During the period when both are being received, the resultant voltage will be the vector sum of the two, as shown in Figure 22.

Considering the phase angle of the direct signal to be zero degrees for simplicity and applying the cosine law of trigonometry to the triangles of this figure one obtains the following equation:

$$\begin{aligned} (\text{Resultant})^2 &= V^2 + 2V^2 \cos \phi + V^2, \\ &= 2V^2 (1 + \cos \phi), \\ &= 4V^2 \cos^2 (\tfrac{1}{2}\phi), \end{aligned} \tag{6}$$

whence the resultant amplitude is $2V \cos (\frac{1}{2}\phi)$.

If $\phi = 0°$, this amplitude will be $2V$; if $\phi = 180°$, the amplitude will be zero; for intermediate values of $\phi$, the amplitude will vary between zero and $2V$.

These interference effects are shown very clearly in the oscillograms of Figure 23, which are the records of successive pings received at various ranges. The first pulse of the 2,600 yd sequence shows the case when the direct signal and the bottom echo arrive at the hydrophone in phase, $\phi = 0°$. This type of pulse has been called the "transformer" type. The third pulse of this sequence is an example of the direct signal and bottom echo arriving out of phase—the amplitude diminishes, and a "spool" type of pulse results. If the phase difference were precisely 180°, there would be an extreme spool pulse. For intermediate values of $\phi$, there will be a graded series of pulse shapes; various types can be observed on the oscillograms, some of which are more complicated than can be explained by the simple theory outlined above.

### Successive Bottom Reflections

The effect of the bottom on transmission measurements can be followed on Figure 23 or even more closely on the anomaly graph that forms the lower part of Figure 21, and which is based on the former. At ranges less than 600 yd, only the intensity of the directly transmitted sound was measured; comparison with the top diagram of Figure 21 shows that this is about the range where the beam strikes the bottom. From 600 to 1,200 yd, both the direct sound and the bottom echo could be measured separately. The intensity of the direct sound diminished in a manner that could have been predicted from the bathythermogram and the principles outlined above.

The part of the anomaly curve that pertains to bottom-echo intensity rises out to about 2,000 yd; the upper diagram shows that the reflected beam approaches most closely to the surface at about this range. Beyond this, the curve drops again out to 3,000 yd; at about this range a second echo, which has been reflected twice from the bottom, becomes measurable. Its rise, decline, and ultimate replacement by a third and a fourth echo are clearly shown on the graph. This succession of events can be followed quite easily on the complete oscillographic record of the experiment. The small sections of this record which are reproduced as Figure 23 necessarily lack the continuity which is the essential element in establishing the interpretation.

### Effect of Bottom Topography

The effect of bottom topography is illustrated schematically in Figure 24 for a sloping bottom. Some measurements have been made that confirm this figure in a general way, but none has been made in as great detail as those on which Figure 21 is based. The ray diagram again shows the successive refraction and reflection of the ray which leaves the projector horizontally. Because of the slope of the bottom, it will be reflected at less of an angle with the horizontal than its angle of incidence; consequently, it will be bent downward before reaching the level of the projector. This is repeated at each reflection, with the result that the tops of the successive arches are at increasing depths. If the hydrophone is near the surface, the main part of the reflected sound beam will not reach it. Consequently, even though some bottom echoes may be detected, their intensity will be very much less than if the bottom had been horizontal.

A sloping bottom may therefore increase the intensity of sound received at a given range by a shallow hydrophone, but the increase will be less than that due to a flat bottom.

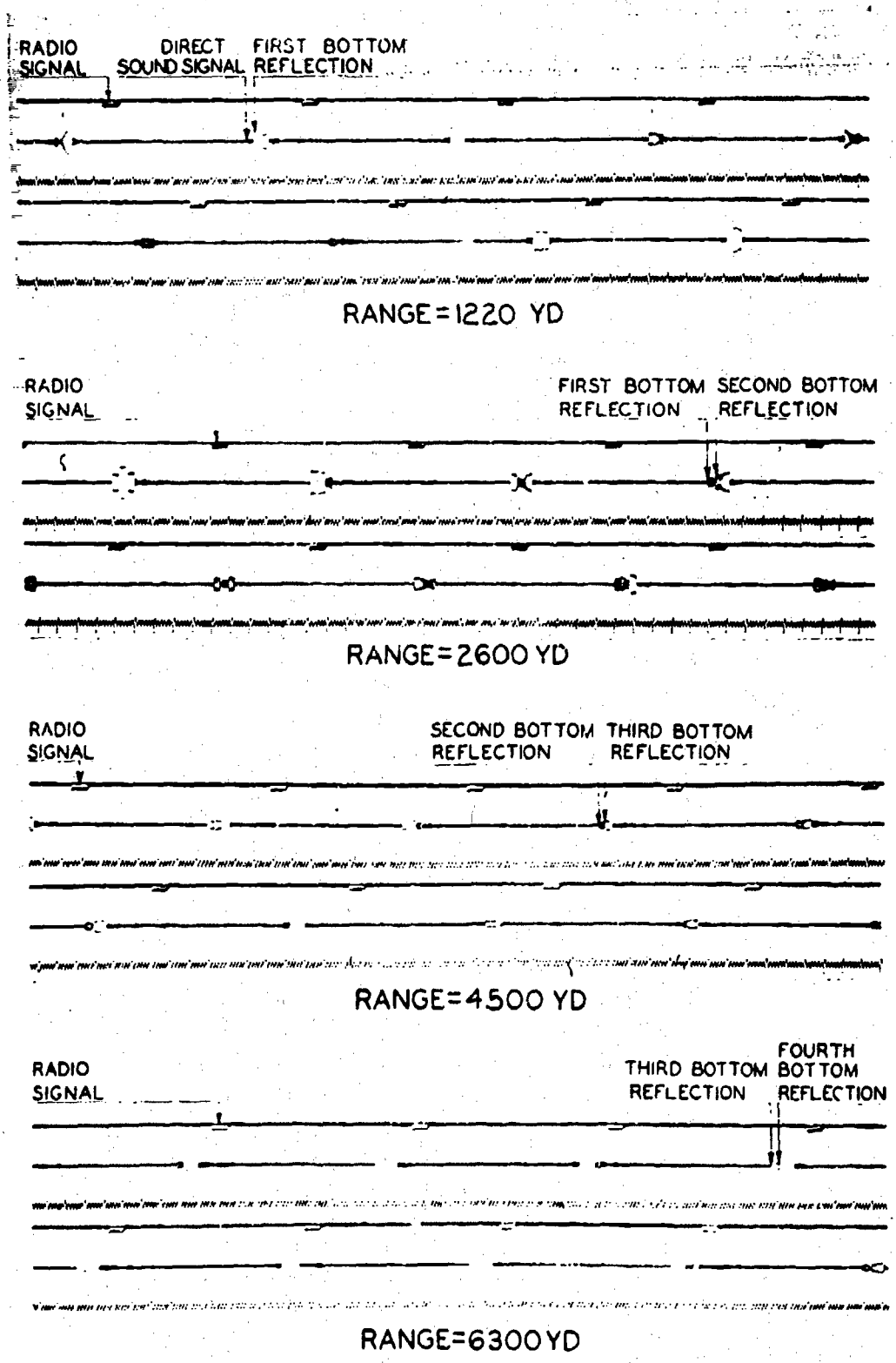


FIG. 10.23. Oscillograms showing successive bottom reflection in shallow (80 fathom) water. The lower half of each strip follows the upper half immediately.

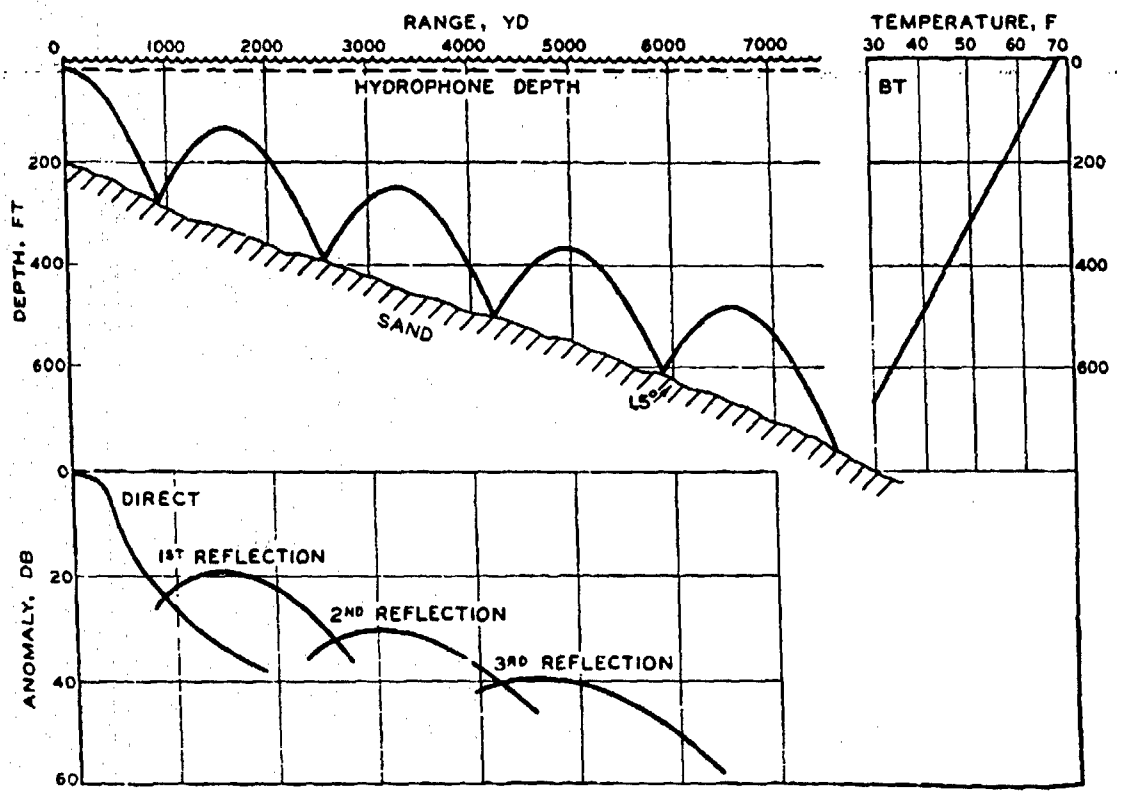


FIGURE 24. Schematic figure of successive bottom reflections over sloping bottom with negative temperature gradients.

### THE INFLUENCE OF OCEAN DEPTH ON TRANSMISSION

From this discussion, certain general conclusions can be drawn concerning the influence of water depth on transmission over a flat bottom. It has been tacitly assumed that the projector is directional and emits a well-defined horizontal beam of sound. These conclusions will need modification below, when transmission from nondirectional sources is considered. Even in the case of directional beams, these theoretical conclusions are oversimplified and must be applied with caution to actual conditions. The experimental results that are presented in the next section will indicate the nature of the complications to be expected.

The fundamental parameter is $M$, the distance between successive arches in the ray diagram of Figure 21. This distance will increase with increasing water depth and decrease with increasing downward refraction. When there is only slight downward refraction or upward refraction, $M$ will be very large or even undefined; the conclusions are completely inapplicable to such cases. A mathematical formula for $M$ can be derived, and appears to be very useful in correlating the data on transmission in shallow water. This work is still in progress as this is being written.

With some reservations, therefore, the following conclusions can be accepted.

1. When the range of the hydrophone from the projector is less than about $\frac{1}{2} M$, the transmission is the same as in very deep water.

2. When the range is greater than about $\frac{1}{2} M$, the transmission will be as good or better than that in deep water. The amount of the improvement will depend on the strength of the bottom echo, i.e., on the reflection coefficient of the bottom.

3. As the range increases, a large number of bottom reflections is needed to bring the sound to the hydrophone, and the transmission loss increases. Theoretically, the transmission anomaly should be roughly proportional to the number of reflections, i.e., to the ratio $r/M$, where $r$ is the range. This is indicated in Figure 21 by the straight line; there will be periodic departures from this law, as can be seen in the figure.

4. With extreme temperature gradients in water of moderate depths, these maxima and minima may

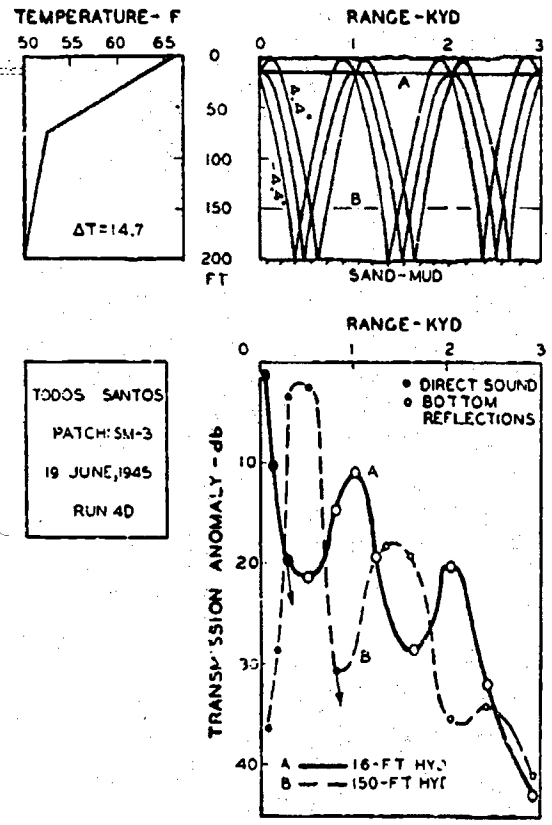


FIGURE 25. Transmission of 24-kc sound over sand-mud with strong downward refraction, showing direct and bottom-reflected sound.

become very pronounced. This can be seen from Figure 25.

## 3.2.6 Transmission in Shallow Water

### FACTORS AFFECTING THE TRANSMISSION

The transmission of sound in shallow water is affected by many more factors than in deep water. This makes the experimental study much more difficult, since it is often uncertain whether a given change is caused by one or another of the factors. The results discussed in this section are therefore more complicated and less certain than those presented for deep water.

The various factors affecting shallow-water transmission include

1. The flatness of the bottom (topography).
2. The depth of the water.
3. The kind of material forming the bottom (bottom character).
4. Thermal gradients:
   a. In the surface layers.
   b. In the deep layers.
5. State of the sea surface.

The first two of these have already been sufficiently treated in the previous section; the others will now be discussed.

### DEPENDENCE ON BOTTOM CHARACTER AND SURFACE GRADIENTS

The range $r_{40}$, defined above in Section 3.2.3, is a convenient parameter to use in the discussion. A large value of $r_{40}$ means good transmission and a small value poor transmission. Figure 26 summarizes the dependence of $r_{40}$ on the factors listed above as

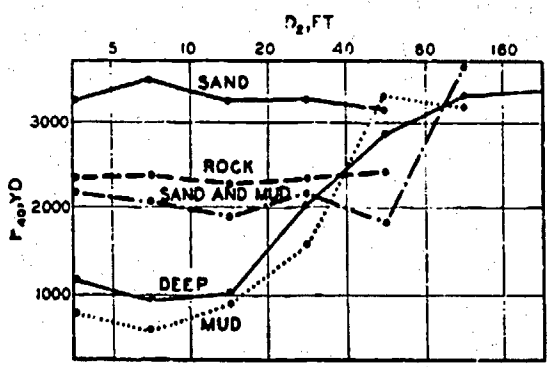


FIGURE 26. Dependence of $r_{40}$ on bottom character and the thermal gradients in the surface layers. The latter are indicated by the magnitude of $D_2$. The curve for the deep water is included for comparison.

3 and 4a, the variable $D_2$ being the depth at which the temperature is 0.3°F less than at the surface (see Section 3.2.2). For comparison, a graph for deep water has been included.

In constructing these graphs from the experimental data, some attempt has been made to allow for the influence of the other factors, such as the state of the sea surface and the thermal gradients at greater depths. It cannot be hoped that this attempt has been completely successful, but it is believed that the plotted values of $r_{40}$ are usually within 500 yd of their proper relative positions. The absolute values may be in error by even greater amounts, but the shapes of the curves are probably reasonably accurate.

It is seen that transmission over *sand* bottoms is very good, indicating that sand reflects a large fraction of the incident sound. The value of $r_{40}$ is practically independent of the gradient in the sur-

face layers, which may be rather surprising in view of the conclusions at the end of the previous section Several reasons, however, can be advanced for this fact. The spacing of the ray arches will be more strongly determined by the gradients in the deeper layers than by those in the upper layers. Moreover, the previous discussion was based largely on the ray that leaves the projector horizontally; the projector used in these experiments has a beam whose half width is about 6 degrees. Consequently other rays must be considered, including some that are reflected by the sea surface as well as by the bottom. It is possible that an adequate explanation of the observations could be worked out along these lines.

*Rock* bottoms behave very much like *sand* bottoms, but the transmission is not so good as over *sand*. *Sand and mud* is shown to be very similar to *rock*. It is interesting to note the sudden increase in $r_{40}$ when $D_2$ is greater than 80 ft. While this point is based on very meager data, it is in accord with the conclusion that the transmission in shallow water should never be worse than that in deep water. The two points on the *rock* and on the *sand and mud* curves which apparently do not conform to this principle may be affected by the experimental errors discussed above.

The curve for shallow water with a *mud* bottom coincides, within experimental error, with that for deep water. It will be concluded from this that *mud* does not reflect an appreciable amount of sound.

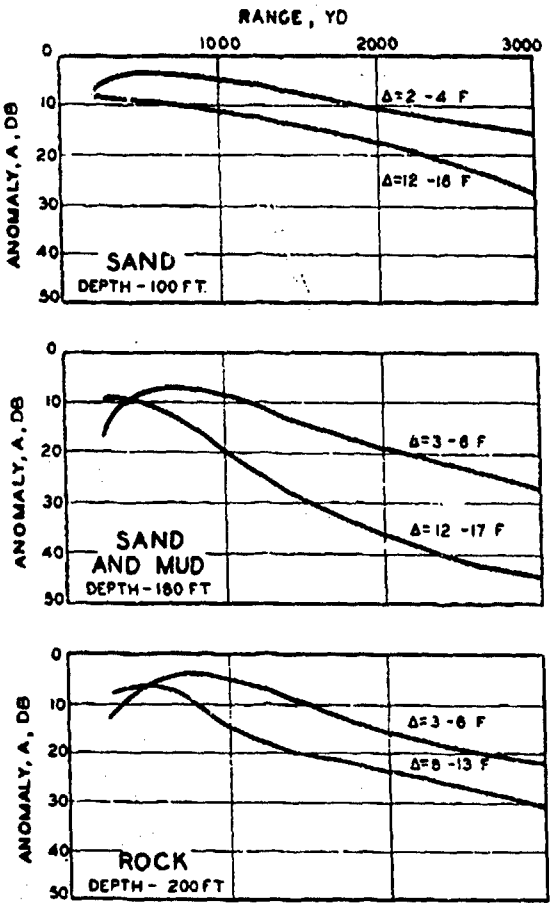


FIGURE 27. Dependence of transmission anomaly on bottom character and Δ, the temperature difference between the surface and a depth of 150 ft. If the water depth is less than 150 ft, Δ denotes the temperature difference between the surface and the bottom.

## EFFECT OF DEEP GRADIENTS

The evidence for a strong dependence of transmission on the temperature gradient in deeper layers is good, although somewhat unsystematic; it is given in Figure 27. As a measure of the deep gradient, the temperature difference Δ between the surface and 150 ft was chosen; in the event water depth was less than 150 ft, the temperature difference between surface and bottom was used instead. Each pair of graphs refers to a single bottom character, and the two graphs show the average anomaly as a function of range for small and large values of Δ. The averages extend over data for various values of the sea and wind force, but some residual effects of these variables may be present. However, the differences shown are undoubtedly real and caused by the deep temperature gradients. They are in qualitative agreement with the conclusions of the previous section. The maxima associated with successive bottom reflections appeared on some (though not all) of the individual curves, but have been lost in the process of averaging. The large anomaly at short ranges is due to the great depth of the hydrophone used in these experiments; this may also be responsible for the lack of prominence of the reflection maxima.

As indicated above, there is some evidence that transmission in shallow water is worse when the sea surface is rough than when it is smooth. This effect, however, is not so great as was once supposed.[14,15] It so happened that most of the data for smooth surfaces were taken when Δ had small values, and most of that for rough surfaces when Δ had large values. Thus much of the observed effect was actually caused by the variation in Δ and was erroneously ascribed to changes in the sea surface. This incident is recorded as an illustration of the errors of interpretation that can occur during the study of a

complex set of causes. However, experiments have now been performed on days when the wind force changed, with corresponding change in the sea surface, but no change occurred in Δ. They show that there is a definite effect of the kind described, whose magnitude appears to be different for various bottom types.

Work in progress as this is written appears to be systematizing the results on transmission in shallow water and promises to yield a satisfactory account of the major phenomena.

### 3.2.7 Transmission of 60-kc Sound in the Sea

While most of the experimental work on the transmission of supersonic sound from one ship to another has been done with 24-kc sound, a fairly adequate amount of work has also been done at 60 kc.

Figure 28 shows the results of an experiment in which pulses of 24- and 60-kc sound were emitted simultaneously from the same projector. This projector was designed so that the 60-kc beam was of about the same width as the 24-kc beam used in the work described in the previous section; it was much narrower than the 24-kc beam associated with it because of dependence of the beam pattern on frequency.

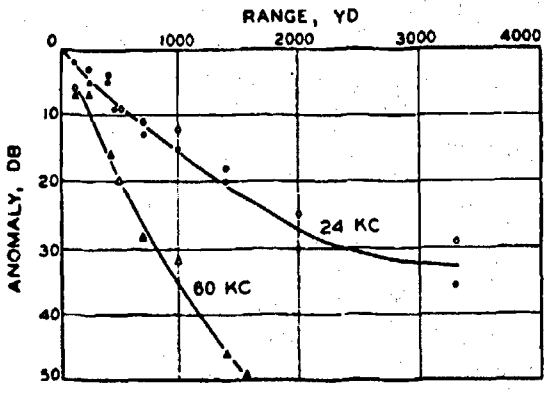


FIGURE 28. Simultaneous transmission of 24-kc and 60-kc signals. Single experiment. Slight negative surface gradient, marked thermocline at 50 ft (gradient 1 F per foot for 5 ft). Hydrophone depth 16 ft.

The two signals were received by a single hydrophone but recorded separately, after being separated with filters. As a check, the 24-kc signals were also received by a second hydrophone. Both the hydrophones and the projector were at a depth of 16 ft. By these means it was possible to measure the transmission anomaly for 24- and 60-kc sound under identical thermal conditions. At the beginning of the experiment shown by Figure 28, there was a constant negative gradient of about 0.015°F/ft in the upper 50 ft of the ocean. From 50 to 55 ft there was a marked thermocline, in which the gradient was 1.0°F/ft, and beneath this the temperature decreased more slowly. It is possible that these conditions changed, both with time during the experiment, and also from point to point over the path traveled by the sound beam.

Results shown by Figure 28 and similar graphs leave no doubt that the transmission of 24-kc sound is better than that of 60-kc sound. The difference is greatest when there is no marked downward refraction.

The average of a large number of transmission experiments with 60-kc sound and a shallow hydrophone is shown on Figure 29. This figure is directly comparable with Figure 14, the five curves of the latter corresponding to the five sets of plotted points on the former. Only two curves have been drawn on Figure 29; the upper is to be compared with the curves 3, 4, and 5 of Figure 14 and lies well below all three. The lower curve corresponds to curves 1 and 2 of Figure 14; it lies between them at all except the shortest ranges. It should be noted that the special projector was used for the 60-kc work in order to make certain that the differences between Figure 14

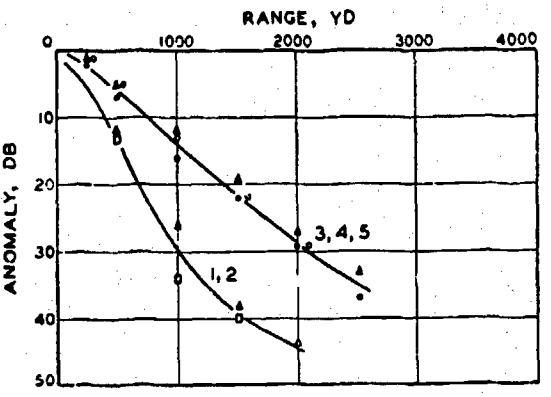


FIGURE 29. Average transmission of 60-kc sound for various oceanographic conditions. Shallow hydrophone. Numbering of curves corresponds to that of Figure 14.

□ 0 ft < $D_2$ < 5 ft
△ 5 ft < $D_2$ < 20 ft
● 20 ft < $D_2$ < 40 ft
⊙ 40 ft < $D_2$ < 80 ft
▲ 80 ft < $D_2$ < 300 ft

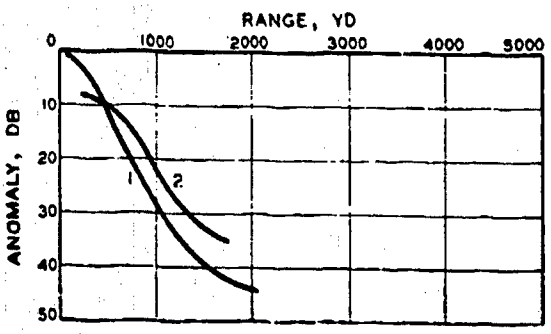


FIGURE 30. Dependence of transmission anomaly on hydrophone depth for 60-kc sound. Negative surface gradients $D_2 < 5$ ft. Curve 1—shallow hydrophone; Curve 2—deep hydrophone. Compare with Figure 15 for 24-kc sound.

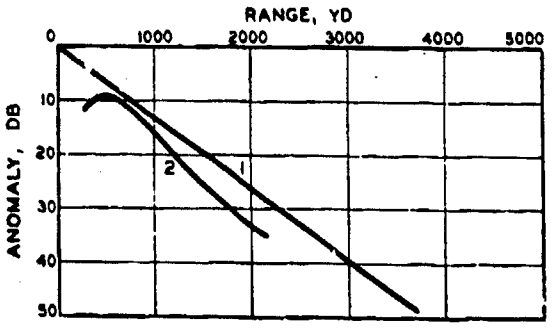


FIGURE 31. Dependence of average transmission anomaly on hydrophone depth for 60-kc sound. Isothermal surface layer. $D_2 < 40$ ft. Curve 1—hydrophone above thermocline; Curve 2—hydrophone below thermocline. Compare with Figure 17 for 24-kc sound.

and Figure 29 were not due to beam-pattern effects.

It may be concluded that the transition from good to bad transmission conditions is more abrupt at 60 kc than at 24 kc, and that good conditions at 60 kc are quantitatively equivalent to fairly poor conditions at 24 kc.

In the same way, Figures 30 and 31 should be roughly comparable to Figures 15 and 17. There are slight differences in the thermal conditions and hydrophone depths used in separating the data into classes before averaging. It is thought that this does not appreciably affect the comparison. It is seen that the dependence of transmission anomaly on hydrophone depth is qualitatively the same at 60 kc and at 24 kc. Under conditions of marked downward refraction, the effect may possibly be somewhat smaller at 60 kc. Under good thermal conditions, the average attenuation coefficients at 60 kc are $13.5 \times 10^{-3}$ db/yd for hydrophones above the thermocline, and $16.5 \times 10^{-3}$ db/yd for hydrophones below the thermocline. The corresponding values for 24-kc sound are 4.0 and $6.7 \times 10^{-3}$ db/yd. Within the limits of error, the layer effect (difference between the two coefficients) is the same at the two frequencies.

## 3.28 Transmission of 24-kc Sound When Both Projector and Hydrophone Are Deep

The study of the transmission of supersonic sound at greater depths will probably yield information concerning the causes of various phenomena. Specifically, if both source and receiver are deep enough, the time delay between the direct and surface-reflected sound is great enough to resolve the two pulses and thus to obtain more information on each.

Experiments with deep projectors transmitting 24-kc sound were carried out in the summer of 1945.[20] The projector was lowered to depths of 150 ft, 300 ft, 500 ft, and 1,000 ft. In addition, a few runs were made with the source at 16 ft for comparison. The signals were received on three hydrophones: one always at 16 ft, a second at the projector depth, and a third at some other of the stated depths.

Oceanographic conditions during the experiments were such as to produce negative gradients near the surface. The thermal structure at depths greater than 400 ft could not be determined with the bathythermographs available at the time.

A small amount of data was accumulated, but the completion of the project was deferred by the pressure of more urgent work and by the need of a more suitable transducer. The available data appear to warrant some tentative conclusions.

In Figure 32 are shown average anomaly curves for three projector depths, 150 ft, 300 ft, and 1,000 ft. The hydrophone was at the same depth as the projector. These curves are not intended to provide the complete information obtained but merely to illustrate the conclusions that have been drawn from a study of all data.

1. Down to a depth of 300 ft, transmission improves as the projector is lowered. At 150-ft depth, Figure 32 shows that the anomaly increases 26 db out to 2,000 yd, whereas at 300-ft depth the anomaly has increased only 7 db at the same range; at 1,000-ft depth the increase is about 5 db, very nearly equal, considering experimental error, to the increase at 300 ft.

The results agree with deductions from ray theory. The shadow boundary extends to greater ranges at greater depths (see Figure 17 of Chapter 2), and one

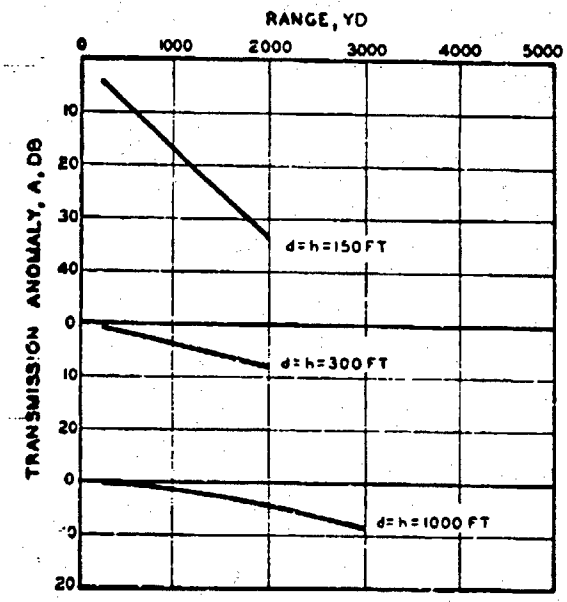


FIG. 32. Average transmission of sound using deep projector. Projector depth = $d$; hydrophone depth = $h$.

might expect better transmission at greater depths. Moreover, one might expect that this improvement would gradually cease as the projector was lowered still more, since the refraction effect would tend to become constant for all practical ranges as the projector depth increased.

2. The anomaly graphs are seen to be linear and thus are similar to curves 4 and 5 of Figure 14, which represent transmission conditions near the surface where there exists a deep isothermal surface layer.

This also is to be expected, for below the main thermocline the gradients are weak (see Figure 2 of Chapter 2). At depths of 500 ft or more it is very probable that the refraction of the sound beam contributes less to the transmission loss at all ranges than does absorption, and thus the attenuation would approach a minimal value. However, this minimal attenuation is still much larger than can be explained by theory. This subject is discussed in detail in Section 3.4.

3. In some cases the direct signal is weaker than the surface-reflected pulse. The reason for this is not known; it may possibly be attributable to refraction effects similar to those described in Section 3.1.4 in connection with explosive sound.

4. The direct signal appears to fluctuate less at short ranges when the projector is deep. This is not true at long ranges, nor was any improvement noted in the case of the surface-reflected signal. This point will be discussed in Section 3.5.

## 3.3 THE TRANSMISSION OF SONIC FREQUENCIES

### 3.3.1 Description of the Experiments

The transmission of underwater sound of sonic frequencies was not studied experimentally in a systematic manner until January 1945. In late 1943, plans for the cooperative program of the University of California and the U. S. Navy Radio and Sound Laboratory had been extended to include this phase of the general problem of transmission. Delays were occasioned by the outfitting of additional vessels and the building of a suitable sound source of high intensity, as well as other equipment.

In general, the experiments were similar to those with supersonic sound, already described. The technique of simultaneous transmission of several frequencies was extended, provision being made for the simultaneous use of 0.2, 0.6, 1.8, 7.5, and 22.5 kc. The supersonic frequency of 22.5 kc was included to facilitate comparison with the 24-kc experiments previously carried out. It was possible to record all five of these frequencies oscillographically on a single strip of paper. Alternatively, any one or more of the frequencies could be omitted and the remainder received on several hydrophones each, thus enabling the observer to compare simultaneous measurements at any particular frequency. However, the maximum number of simultaneous records was limited to five.

The logging of such complex operations presented formidable problems which were overcome by the use of various automatic recording devices. After the program was well under way, data were accumulated at such a rate that the available office staff was barely able to cope with the routine aspects of its analysis. The possibility of constructing special computing machines to facilitate this work was considered but has not been put into effect at the date of this writing.

As a result of these experiments, it has been found that two major qualitative differences exist between the transmission of horizontal supersonic beams and the transmission of the spherical waves of lower frequencies. In the first place, the *image effect*, the general nature of which has already been discussed in connection with explosive sound, assumes a much greater importance in the transmission of sonic frequencies than in that of supersonic. In the second place, much more sound is *reflected from*

*the bottom* even in deep water, since the sources of sonic sound are relatively nondirectional.

## 3.3.2 Theory of the Surface-Image Effect

The phenomenon called the "image effect," as encountered in the study of explosive sounds, was described in Section 3.1: The waves that are transmitted directly arrive at a slightly earlier time than the waves that have been reflected by the surface. The sound emitted by a projector, however, differs essentially from that of an explosion: the latter consists of a single compression, whereas the former is a sinusoidal wave train and consists of an alternation of compressions and rarefactions. This introduces interference, which is, in principle, similar to that described in Section 3.2.5 in connection with the bottom echo. We shall proceed to calculate the effect of the interference of the surface reflection on the transmission anomaly.

### The Image Effect and the Transmission Anomaly

The pressure in the direct wave is given by the equation

$$p_1 = P \cos 2\pi f t, \tag{7}$$

where $P$ = the amplitude of the pressure variation,
$f$ = the frequency of the sound,
$t$ = the time

The pressure $p_2$ in the wave reflected from the surface will be given by an equation similar to equation (7). However, the sound reflected from the surface will be delayed by a time interval $\Delta t$. Moreover, the amplitude of the wave will be different after reflection: if the surface reflects the fraction $\mu$ of the sound energy incident on it, the amplitude of the reflected wave will be $\mu P$. (The fraction $\mu$ is known as the *effective reflection coefficient* of the surface.) Finally, the wave suffers a change of phase when reflected from the surface, as was shown by the explosion experiments described above. This reverses the sign of the equation. Thus the pressure in the reflected wave will be given by

$$p_2 = -\mu P \cos 2\pi f (t - \Delta t). \tag{8}$$

The resultant intensity $I$ of the direct and reflected waves can be calculated by the methods described in Section 3.2 that led to equation (6); a generalization of equation (6) is

$$I = P^2 (1 - 2\mu \cos 2\pi f \Delta t + \mu^2). \tag{9}$$

Equation (9) can be put into a more convenient form by using the expression for $\Delta t$ derived in equation (3),

$$\Delta t = \frac{2hd}{rc} \tag{3}$$

and by introducing a parameter $R$, defined by

$$R = 4hd\left(\frac{f}{c}\right) = \frac{4hd}{\lambda} \tag{10}$$

where $\lambda$ ($= c/f$) is the wavelength of the sound, in the same units as $h$ and $d$.

Multiplying equation (3) by $f$ and using equation (10),

$$f\Delta t = \frac{2fhd}{cr} = \frac{R}{2r}, \tag{11}$$

and substituting this in equation (9), we get

$$\frac{I}{P^2} = 1 - 2\mu \cos\left(\frac{\pi R}{r}\right) + \mu^2 \tag{12}$$

It can be shown that, when this interference between surface echo and direct sound occurs, the mathematical expression for the transmission anomaly is

$$A = -10 \log\left(\frac{I}{P^2}\right),$$
$$= -10 \log\left[1 - 2\mu \cos\left(\frac{\pi R}{r}\right) + \mu^2\right]. \tag{13}$$

Graphs of $A$ as a function of $r/R$ for several values of the surface-reflection coefficient $\mu$ are shown on Figure 33. The curves have been displaced vertically by arbitrary amounts in order to avoid confusing intersections.

It is seen that the curves have alternate maxima and minima; these occur as the cosine takes its extreme values of $\pm 1$ and are given by the equation

$$A = -20 \log (1 \pm \mu) \tag{14}$$

at values of the range

$$r = R, \frac{R}{2}, \frac{R}{3}, \text{ etc.}$$

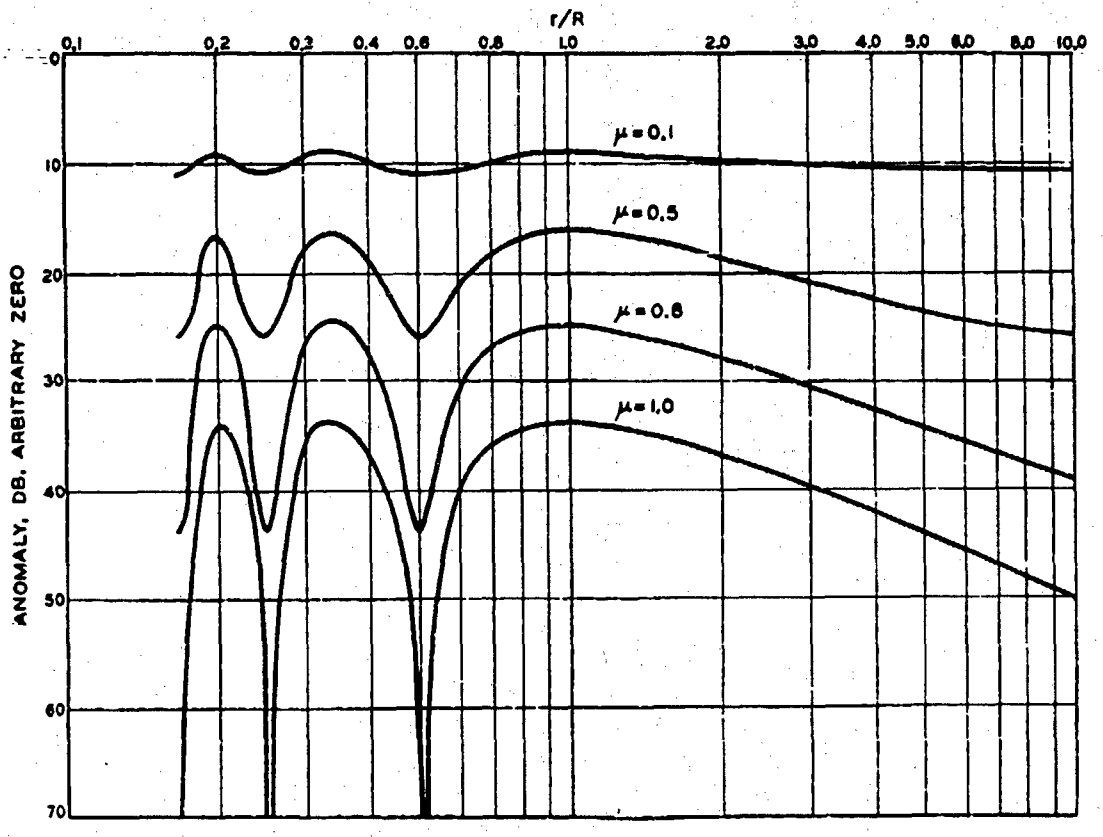


FIGURE 33. The image effect as a function of $r/R$, for various values of the surface-reflection coefficient $\mu$. The curves have been displaced vertically by arbitrary amounts to avoid confusing intersections.

The range to the last maximum is $R$, which, as seen from equation (10), is determined by the depth of projector and hydrophone and varies inversely as the wavelength $\lambda$ of the sound. This particular critical value of the range is called the Lloyd range, after Humphrey Lloyd, who first studied the analogous optical effect, which is generally called the Lloyd mirror effect. (Other names are the image effect, which has been used here, the double-source effect, and the dipole effect.)

### EFFECT OF REFRACTION ON THE IMAGE EFFECT

While it has been assumed that there is no curvature of the sound rays, it may be anticipated that the equations will be valid provided the refraction is not too great. Thus, in the case of downward refraction, it should be sufficient that the Lloyd range be much less than the range to the shadow boundary at the hydrophone depth. Departures will be expected whenever the Lloyd range becomes comparable to the latter.

A more careful consideration of this matter leads to Table 1. In preparing this table, it was assumed that hydrophone and source are both at the depth $d$ ($=h$), and $\Delta T$ is the temperature difference between the surface and the depth $d$ (regardless of sign). The tabulated values $\Delta T$ are the largest for which the above equations should be valid. For convenience, the values of $R$ corresponding to the tabulated values of frequency and depth are also tabulated.

It is seen that, for very low frequencies, the Lloyd range is so short that the equations should be valid for almost any thermal conditions that are apt to occur in the ocean. For frequencies above 5 kc, on the other hand, it is very unlikely that they will ever be applicable without modification except when the projector and hydrophone are at very shallow depths and short ranges.

Figures 34, 35, and 36 show a comparison between this theory and experimental data for 200, 600, and 1,800 c. The arrows indicate the Lloyd range: its increase with frequency is apparent. The curves

TABLE 1. Maximum values of $\Delta T$ for which equation (13) is valid.

| Frequency (c) | $d = h = 16$ ft | | $d = h = 35$ ft | | $d = h = 90$ ft | |
|---|---|---|---|---|---|---|
| | $R$(yds) | $\Delta T$(°F) | $R$(yds) | $\Delta T$(°F) | $R$(yds) | $\Delta T$(°F) |
| 100 | 7 | ..... | 34 | ..... | 225 | 15 |
| 500 | 35 | 20 | 170 | 4 | 1,125 | 0.6 |
| 1,000 | 70 | 5 | 340 | 1 | 2,250 | 0.15 |
| 5,000 | 350 | 0.2 | 1,700 | 1.04 | 11,250 | 0.006 |
| 10,000 | 700 | 0.05 | 3,400 | 0.01 | 22,500 | ..... |
| 24,000 | 1,700 | 0.008 | 8,150 | ..... | 54,000 | ..... |

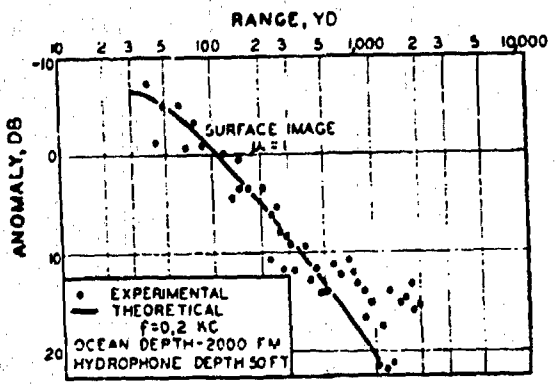


FIGURE 34. Theoretical and observed transmission of sound in deep water. Frequency 0.2 kc.

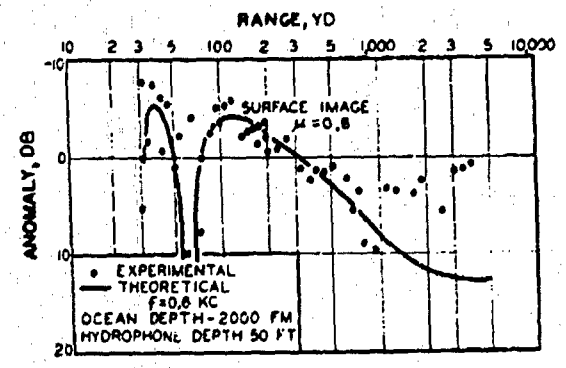


FIGURE 35. Same as Figure 34 for 0.6-kc sound.

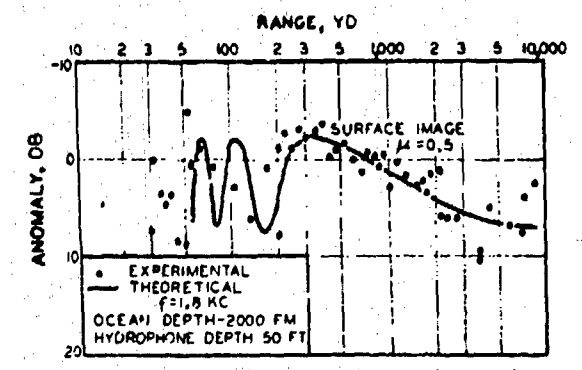


FIGURE 36. Same as Figure 34 for 1.8-kc sound.

have been plotted for values of $\mu$ chosen to give the best fit. In agreement with Table 1, no data for higher frequencies conform to these equations.

The manner in which refraction should modify the image effect is shown by Figure 37.[3] The solid curve has been calculated for the case of downward refraction, projector and hydrophone being at a depth of 20 ft and the range to the shadow boundary being 2,200 yd. For comparison, the dotted curve

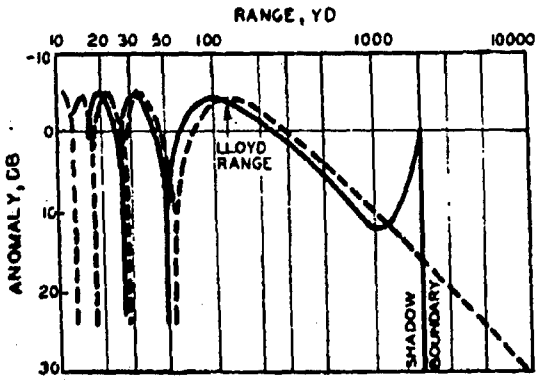


FIGURE 37. Image effect with slight downward refraction. Frequency 1,000 c, $\mu = 1$. The arrow indicates the range of the last maximum.

shows the effect in the absence of refraction. The curves are drawn for $\mu = 1$ and 1,000 c. They show that refraction displaces all the maxima toward shorter ranges and that the sound level should increase at ranges just short of the shadow. This last effect is caused by the diminished time delay of the surface echo (see Figure 5), together with the increased divergence of the reflected rays.

It may be anticipated that this theory will be valid at short ranges, but it is likely that diffraction and other neglected phenomena will greatly modify the anomaly curve near the shadow.

The effect of increased refraction will be to move the shadow boundary toward shorter ranges and to compress the curve still further. The effect of increased frequency will be to move the maxima toward longer ranges, the shadow boundary remaining fixed.

At short ranges, the image effect is modified because the source and its image are not at the same distance from the surface. This and other effects have been investigated theoretically, and partially confirmed by experiments.[4] The data of one experiment are compared with theory in Figure 38.

One point is brought out by this figure: the intensity of the sound is not constant but fluctuates

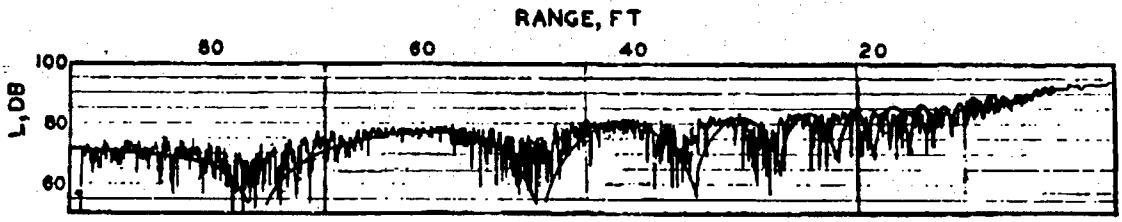


FIGURE 38. Power-level recorder trace showing the image effect at very close ranges. This figure is a photograph of the original trace; the solid curve was drawn in and shows the theoretical image effect. The two are seen to check fairly well.

rapidly in an unpredictable manner. Something of the nature of these fluctuations can be seen in Figure 23, which shows details of the interference between sounds arriving by two paths. The great variability of the complex signals is, in that case, probably caused by a combination of effects that include pitching and rolling of the ship, local irregularities in the bottom topography, and local variations in the velocity of sound. In the case of Figure 38, the changing shape of the sea surface is another cause. Fluctuation of transmission is discussed in detail in Section 3.5.

When these fluctuations become extreme, one is reduced to considering only average values. These average values are not influenced by interference and can be calculated simply by adding the intensities of the sounds arriving by different paths, without regard to the phase relations.

### 3.3.3 Theory of Bottom Reflection

There are many ways in which sound can reach the hydrophone from the projector. A few of the most important of these are shown in Figure 39. They are

| | |
|---|---|
| *PH* | Direct |
| *PSH* | Surface reflected |
| *PBH* | Bottom reflected |
| $PS_1B_1H$<br>$PB_2S_2H$<br>$PS_2B_3S_4H$ | Multiply reflected |

There are additional paths involving several reflections from the bottom as well as several from the surface.

A complete theory of sound transmission would involve a consideration of all the infinite variety of paths, together with their modification by refraction.[5] Fortunately, the sound arriving via most of

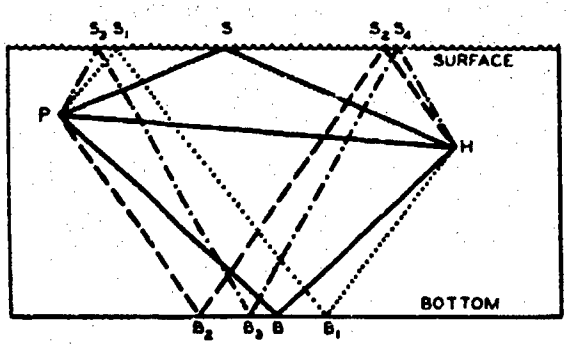


FIGURE 39. Diagram illustrating reflection from the surface and the bottom, and showing some of the rays along which sound may travel between projector and hydrophone.

the paths is usually negligible, so that only a small number of them need be considered at any one time. The problem can be made simpler as follows.

1. If a narrow beam is sent out horizontally in deep water, very little sound will be emitted along rays that reach the bottom at reasonable ranges. If a nondirectional projector sends out a short pulse, the reflected sound traveling along *PBH* may arrive so much later than that going directly via *PH* that the two pulses are easily distinguished. Under either of these circumstances only the two paths, *PH* and *PSH*, need be considered. These are involved in the surface-image effect, which has been discussed in Sections 3.1.2 and 3.3.2.

2. If a projector sends out long pulses, the possibility of distinguishing the direct from the bottom-reflected sound is lost, and under certain conditions, the latter may be the more intense. Thus there will be interference between the two pulses. This effect was discussed in Section 3.2.5.

3. When both hydrophone and projector are near the surface, and the water is very deep, the four paths, *PBH*, $PS_1B_1H$, $PB_2S_2H$, and $PS_2B_3S_4H$, will not differ greatly in length. If, in addition, the

sound frequency is low, the waves arriving by these four paths may interfere, producing effects analogous to but more complex than the surface-image effect. Calculations of the expected effects have been made and receive some confirmation from experimental data.[10,11] In general, however, the fluctuations discussed at the end of the previous section will be so great as to obscure the details of the interference pattern. It is then sufficient to calculate the average intensity resulting from the four paths. This can be done crudely by calculating the intensity of the sound arriving via *PBII* and multiplying it by four. If the water depth is comparable to the horizontal distance between *P* and *H*, a further simplification is possible, for the rays *PB* and *BH* are then inclined so steeply to the horizontal that all refraction effects can be neglected.

With these simplifications, the length of the path is approximately

$$PBH = (r^2 + 4s^2)^{\frac{1}{2}}, \tag{15}$$

where $r = PH$ and $s$ is the depth of the bottom below the projector or hydrophone. (The difference in their depth is neglected.) The total intensity of the bottom-reflected sound arriving over all four paths can then be calculated from the inverse square law to be

$$I = \frac{4I_1\mu^2}{r^2 + 4s^2}, \tag{16}$$

where $I_1$ = intensity at unit distance from the source, $\mu$ being the amplitude-reflection coefficient of the bottom. The transmission loss is therefore

$$H = 10 \log \left(\frac{I_1}{I}\right)$$

$$= 10 \log (s^2 + \tfrac{1}{4}r^2) - 20 \log \mu, \tag{17}$$

and the transmission anomaly is

$$A = H - 10 \log r^2$$

$$= 10 \log \left[\frac{s^2}{r^2} + \frac{1}{4}\right] - 20 \log \mu. \tag{18}$$

The upper curve of Figure 40 shows this equation for $\mu = 1$. If $\mu$ has any other constant value less than unity, the whole curve will be shifted downward without altering its shape. However, there are theoretical reasons for supposing that $\mu$ is not constant,

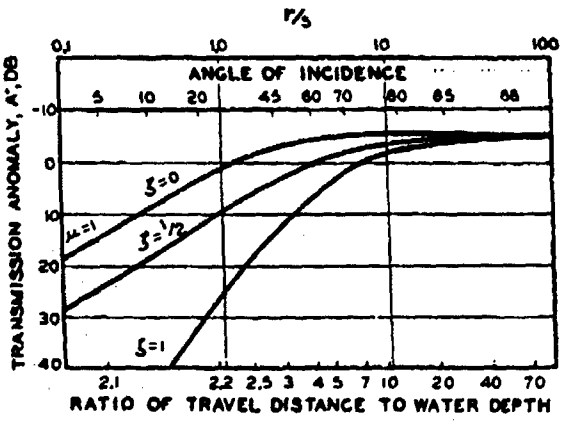


FIGURE 40. Graphs of the equation $a = 10 \log (8^2/r^2 + \frac{1}{4}) - 20 \log \mu$ for various values of $\zeta$. The value of $\mu$ is given by

$$\mu = \frac{1 - \zeta \cos\theta}{1 + \zeta \cos\theta}$$

when $\theta$ is the angle of incidence and is given by $\tan \theta = r/2S$. On the figure both $\theta$ and $r/S$ are indicated as abscissas.

but changes with the angle $\theta$ at which the sound is reflected from the bottom. This angle is given by

$$\tan \theta = \frac{r}{2s}. \tag{19}$$

The value of $\theta$ corresponding to a given value of $r/s$ is shown by the upper scale of Figure 40.

There are no good data on the manner in which the reflection coefficient varies with $\theta$. One equation, based on the concept of acoustic impedance, is

$$\mu = \left[\frac{1 - \zeta \cos\theta}{1 + \zeta \cos\theta}\right] \tag{20}$$

where $\zeta$ is the acoustic impedance of the bottom, measured in units of the acoustic impedance of water.[1b] From equation (20), if $\zeta = 0$, $\mu = 1$; curves of $A$ for $\zeta = \frac{1}{2}$, and $\zeta = 1$, are also shown in Figure 40. Other theoretical equations for $\mu$ would yield curves of slightly different shapes.

### THE EFFECTIVE REFLECTION COEFFICIENT

It would be expected that the effective reflection coefficient $\mu$ would decrease as the sea's surface becomes rougher. This effect, if it exists, is obscured by the large uncertainty in the value of $\mu$ determined by the method of best fit. It would also be expected

that $\mu$ would decrease with increasing frequency. This may be an additional reason why the image effect is not observed at higher frequencies. Two samples of data on this effect are shown in Table 2;

TABLE 2. Distribution of effective reflection coefficients of the sea surface.

| $\mu$ | Number of observed cases | | | | | |
|---|---|---|---|---|---|---|
| | 20 c | | 600 c | | 1,800 c | |
| | W-Sp | Su | W-Sp | Su | W-Sp | Su |
| 1.0 | 7 | 20 | 3 | 20 | 1 | 12 |
| 0.8 | 4 | 0 | 7 | 2 | 3 | 4 |
| 0.5 | 0 | 0 | 16 | 1 | 16 | 0 |
| 0.1 | 0 | 0 | 0 | 0 | 4 | 0 |
| No fit | 3 | 0 | 3 | 0 | 4 | 4 |

one sample taken in winter and spring, the other in the summer. The latter sample, in general, shows higher values of $\mu$, perhaps because the sea surface is smoother in summer.

### 3.3.4 An Example of the Simultaneous Transmission of 0.2- and 22.5-kc Sounds

Figure 41 presents the data obtained during an unusually long transmission experiment, in which

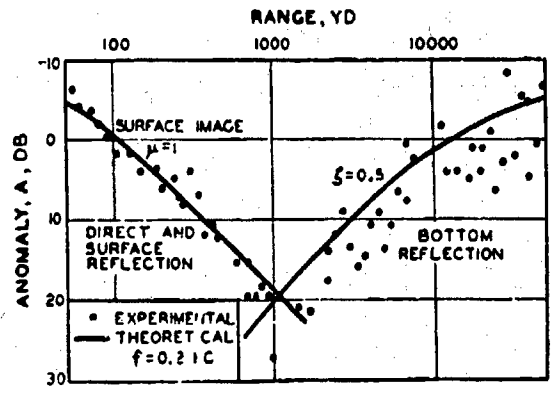


FIGURE 41. Transmission of 200-c sound, for ranges from 60 yd to 60,000 yd. Theoretical curves for direct and surface-reflected sound ($r \leqslant 1{,}000$ yd) and for bottom-reflected sound ($r \geqslant 1{,}000$ yd) are shown. Projector depth = 14 ft. Hydrophone depth = 50 ft. Isothermal surface layer approximately 75 ft deep. Average ocean depth 2,000 fathoms.

the range was opened from 60 yd to more than 60,000 yd. At ranges less than 1,000 yd, the sound was received via the paths *PH* and *PSH*, and its intensity is governed by the equation (18) with $\mu = 1$, as shown by the smooth curve. At ranges greater than 1,000 yd, the sound was received via bottom reflection. This was established by comparing the arrival time with that calculated from the range; the latter was determined by radar or radioacoustic ranging with 22.5-kc sound, or both. The smooth curve for ranges greater than 1,000 yd is taken from Figure 40 for $\zeta = 0.5$; it is probable that $\zeta = 0.6$ would have fitted the data more closely. The irregular fluctuation of the bottom-reflected sound is apparent from the scatter of the experimental points.

The sound frequency was 200 c, the projector depth 14 ft and the hydrophone depth 50 ft. There was an approximately isothermal layer about 75 ft deep at the surface of the sea. The water depth was not constant over the whole range, but averaged about 1,000 fathoms. The 200-c sound received on a hydrophone at 300 ft showed much the same variation with range, although the quantitative agreement with the theory was not so good.

For comparison, Figure 42 shows the transmission of 22.5-kc sound to the 50-ft hydrophone from a projector at 12-ft depth. The data for Figures 41 and

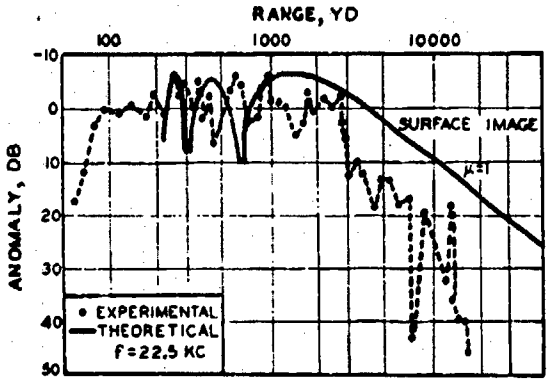


FIGURE 42. Transmission of 22.5-kc sound obtained simultaneously with that of Figure 41. Theoretical curve showing image effect drawn for comparison. Projector depth = 12 ft. Hydrophone depth = 50 ft.

42 were obtained simultaneously. At ranges less than 100 yd, the directivity of the 22.5-kc projector causes a large anomaly. At ranges from 300 to 3,000 yd, the 22.5-kc anomaly is less than the 0.2-kc anomaly and is unusually small compared to the average of the 24-kc runs (see Figure 14). Beyond 3,000 yd,

the anomaly of the 22.5-kc sound increases rapidly, and, because of the directivity of the source, there is no measurable bottom-reflected sound. The graph of the surface-image effect for $\mu = 1$, and neglecting refraction, is included for comparison.

### 3.3.5 The Influence of Hydrophone Depth on the Transmission of Low-Frequency Sound—Layer Effect

The discussion of the average values of the transmission anomaly at low frequencies is simplified by the fact that thermal conditions near the surface do not greatly influence them. In Figures 43 to 48, inclusive, the averages of five to twelve experimental points obtained under similar thermal conditions are plotted with different symbols. The data have been classified according to $D_2$. The expression $d_2 = 2$ indicates that $D_2$ was between 10 and 20 ft; $d_2 = 3$ indicates the range 20 to 40 ft; $d_2 = 4$, 40 to 80 ft; $d_2 = 5$, 80 to 160 ft, and so forth, according to the code described in Section 2.1.5. The averages for these different classes show some differences but they are usually not greater than the sampling error, and when they are greater, they do not appear to be systematic.

It is quite possible that some other classification based on thermal conditions would reveal more systematic differences. The discovery of this method of classification, if it exists, must await further data and analytic work.

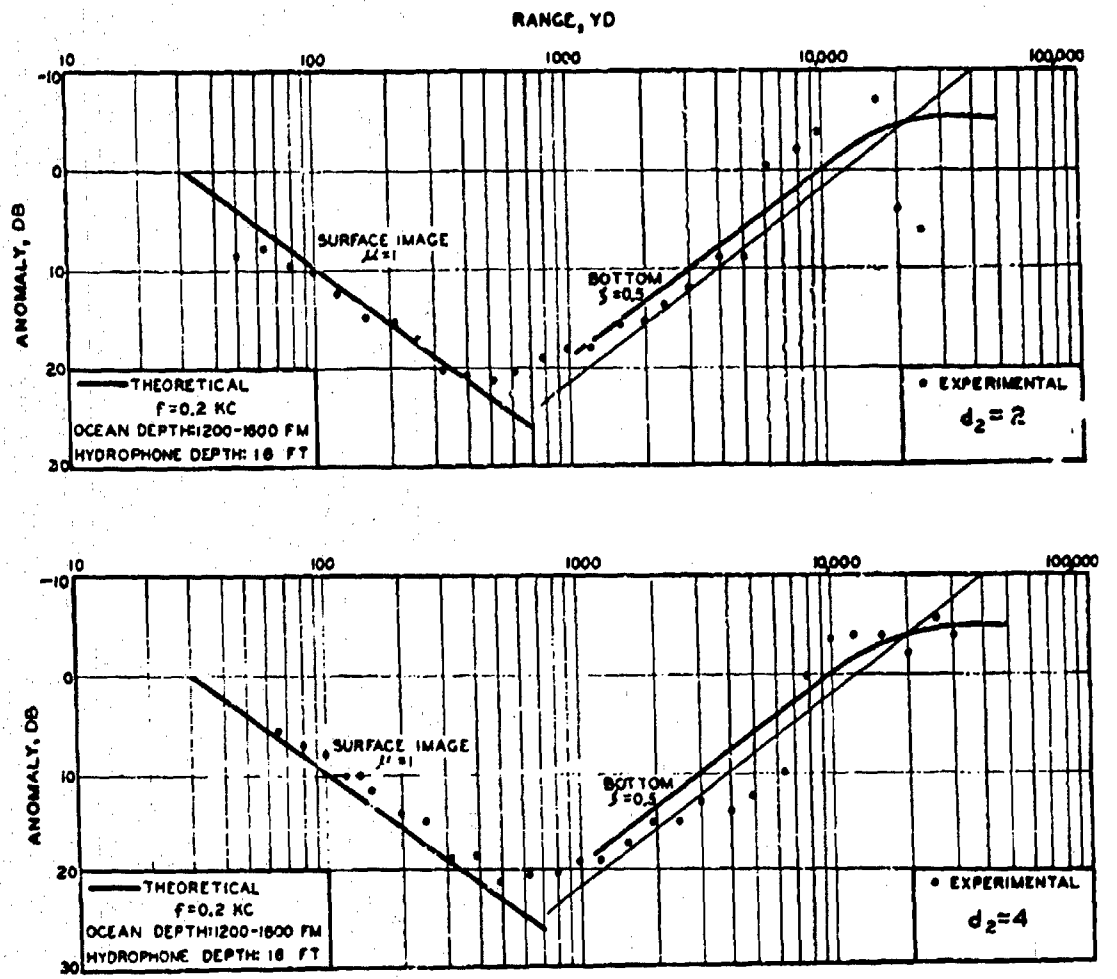


FIGURE 43. Comparison of simple theory with data of an experiment in transmission of 0.2 kc, with shallow hydrophone, for $d_2 = 2$ and $d_2 = 4$. The light solid curve represents constant level.

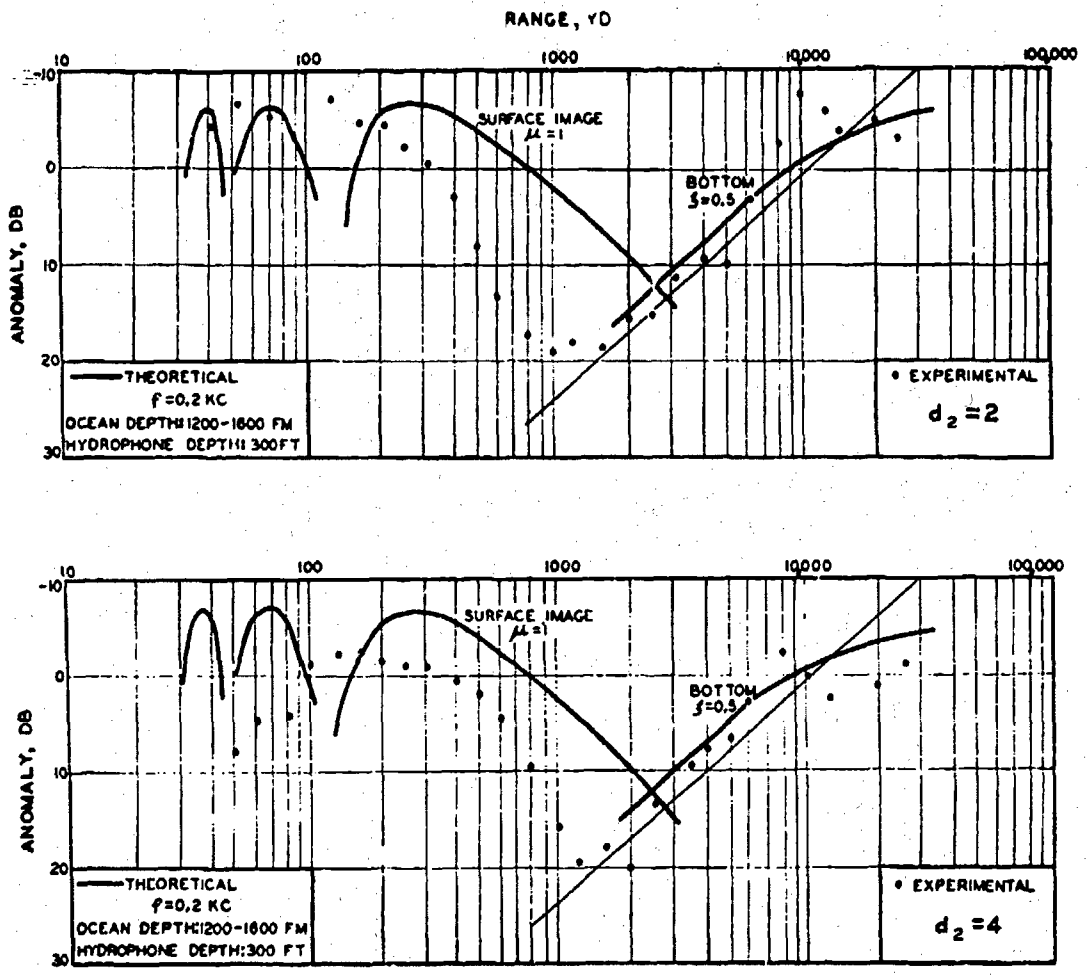


FIGURE 44. Same as Figure 43, but with deep hydrophone.

The data at 0.2, 0.6, and 1.8 kc are adequately explained by the combination of surface and bottom reflection. This is indicated by the solid curves, which represent the theoretical graphs of these effects, neglecting refraction. In every case, the bottom reflection is in fair agreement with the theoretical curve for bottom impedance $\zeta = 0.5$. The data for the 16-ft hydrophone (Figures 43, 45, 47) agree well with the theory of the surface-image effect for reflection coefficients of 0.8 to 1.0. The data for the 300-ft hydrophone (Figures 44, 46, 48) show systematic departures which are, however, precisely of the kind to be expected from the effects of refraction in the deep layers. (See Figure 37.) Some of the average curves even show some of the maxima and minima of the surface-image interference, but they are displaced to ranges shorter than those predicted by the simple theory. (See the broken lines of Figures 46 and 48.)

This general agreement with simple theory is very gratifying, and holds promise for quantitative improvement when the theory has been elaborated to include the effects of refraction.

As of the date of writing, the data on the transmission of 7.5-kc sound do not lend themselves to presentation in summary graphs. There are good indications that these will be intermediate between those presented here for 24- and 60-kc sound, on the one hand, and those for 0.2, 0.6, and 1.8 kc on the other. The values of the transmission anomaly are probably markedly dependent on the depth at which the first perceptible decrease of temperature occurs. There is also some indication that conditions at greater depths have an influence. Bottom-reflected sound is less prominent, since the 7.5-kc projector is somewhat directional. The maxima and minima of the surface-image effect are, to say the least, not obvious.

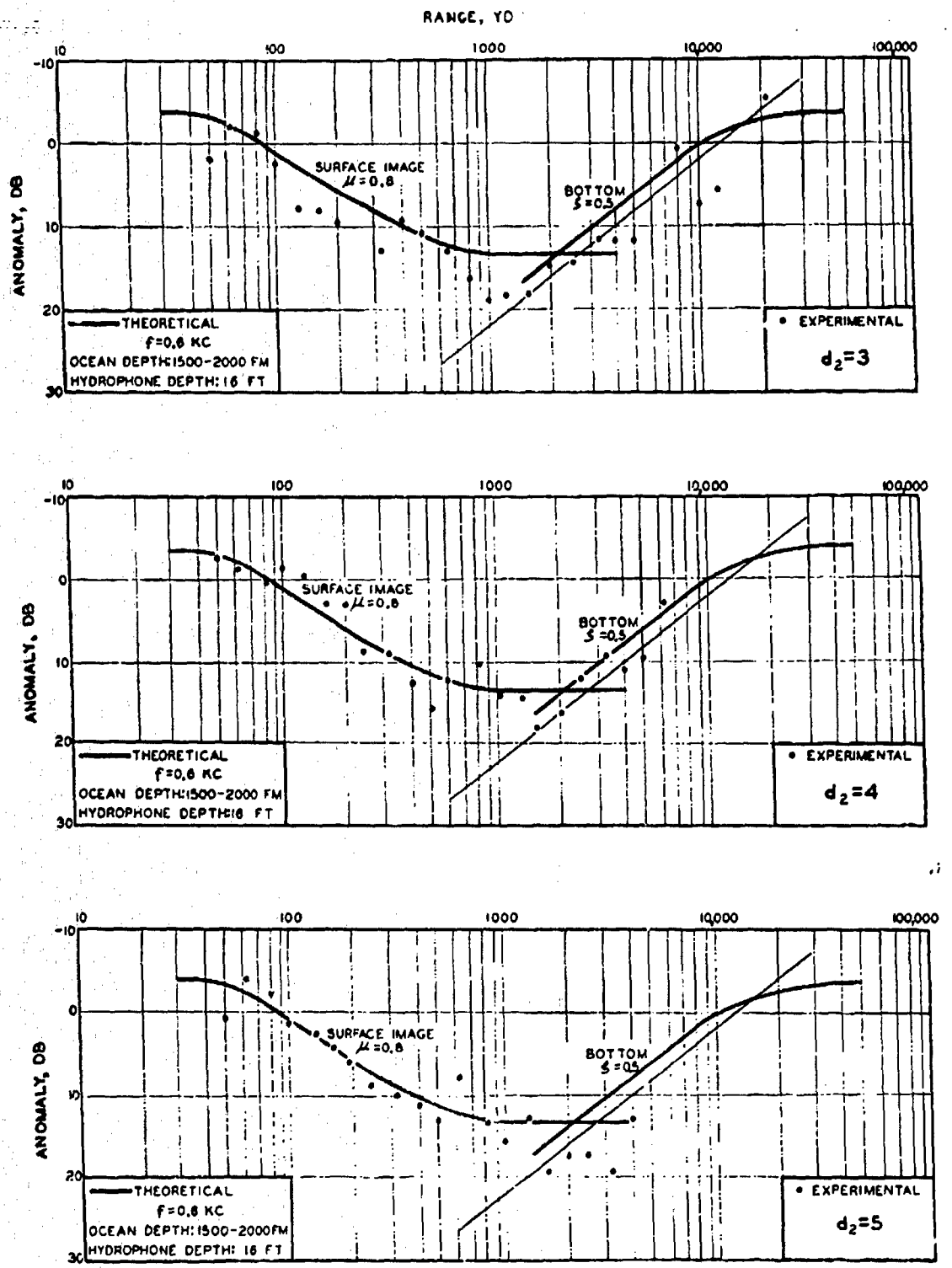


FIGURE 45. Same as Figure 43, for three different thermal conditions, with sound of 0.6 kc, using shallow hydrophone.

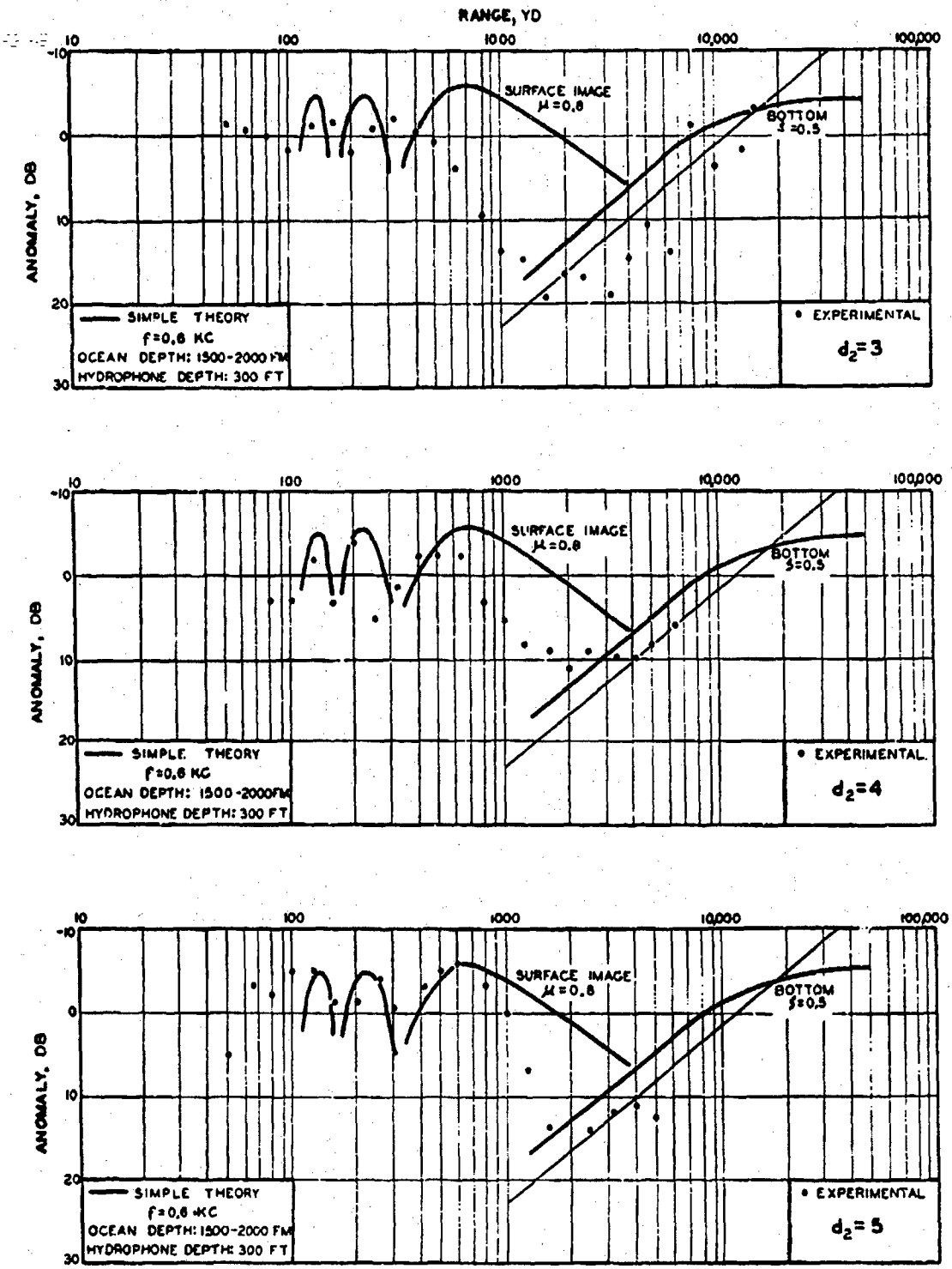


FIGURE 46. Same as Figure 45, but with deep hydrophone.

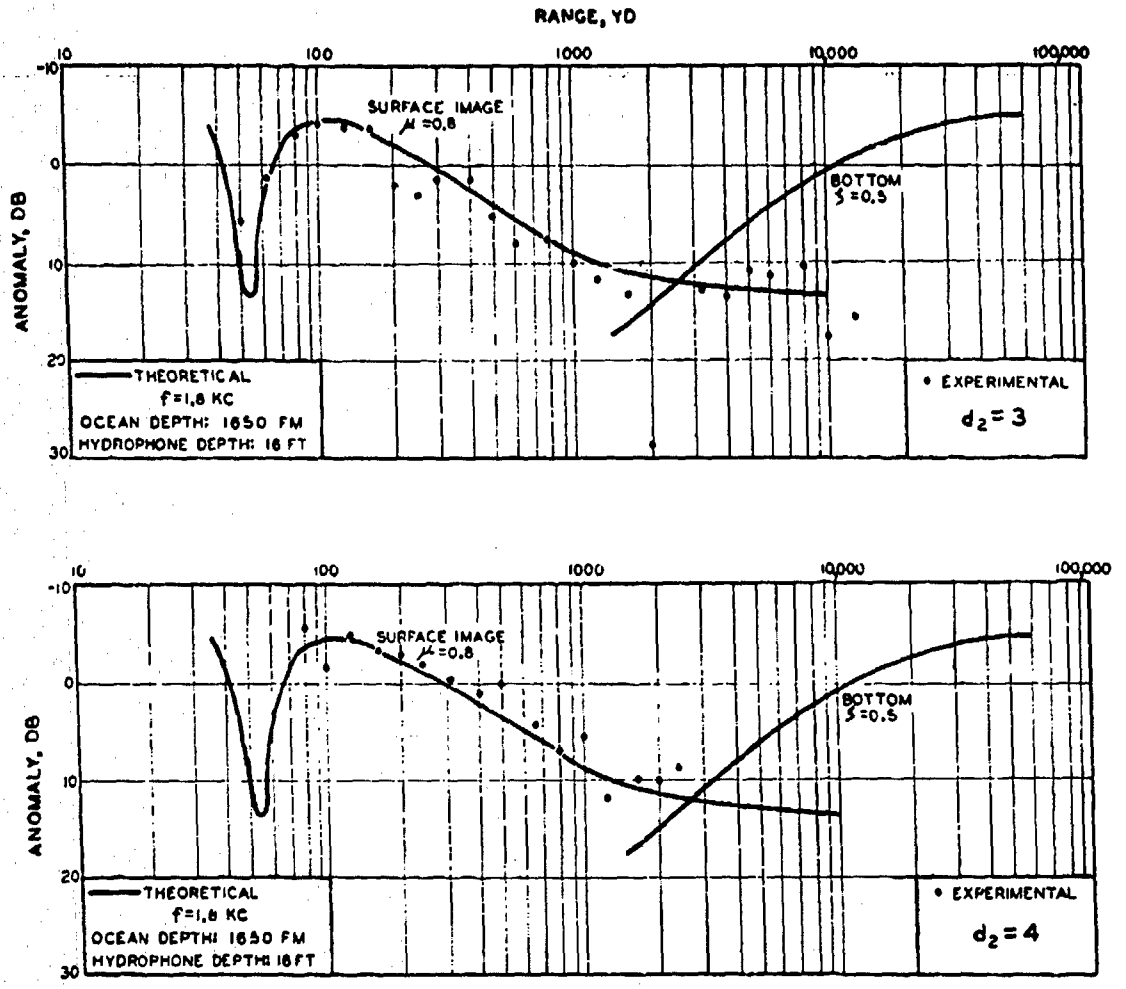


FIGURE 47. Same as Figure 43, with sound of 1.8 kc, using shallow hydrophone.

## 3.4 THE MINIMAL ATTENUATION COEFFICIENT

### 3.4.1 Causes of Attenuation

It has been shown (Section 3.2) that, under the most favorable conditions, the transmission anomaly can be represented by an equation of the form

$$A = ar \qquad (4)$$

where $a$ is an empirical constant called the *attenuation coefficient*. It was shown further that under less favorable conditions this simple equation completely fails to represent the facts.

The physical significance of equation (4) is that energy is removed from the beam in amounts that are proportional to the total energy in the beam. Under favorable conditions, i.e., when there is no refraction and the sound rays are straight, there are two general ways in which this will happen:

1. A certain fraction of the sound energy is converted into heat energy. This is called *absorption*.

2. Another fraction of the sound energy is deflected from its original path by obstacles suspended in the medium and thus is removed from the beam. This is called *scattering*.

Absorption in turn is caused by at least three processes:

1. The *viscosity* of the medium causes sound energy to be converted into heat by internal friction.

2. *Thermal conduction*: some sound energy is converted into heat because sound waves alternately raise and lower the temperature by very small amounts.

3. Suspended particles are set to oscillating by the sound waves and in this process some of the sound energy is dissipated in the form of heat. This is especially the case if the particles are *air bubbles*.

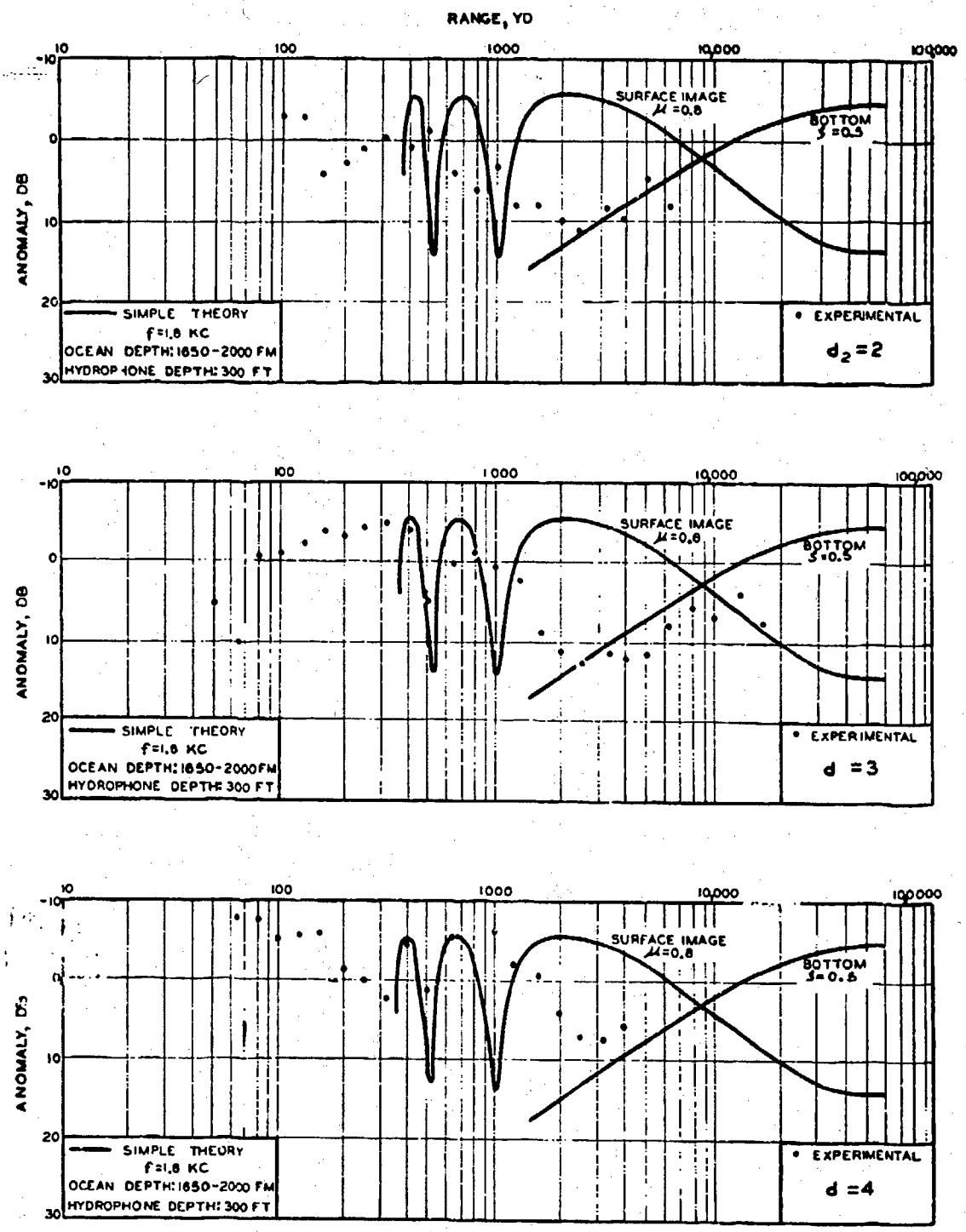


FIGURE 48. Same as Figure 47, but with deep hydrophone.

The effects of scattering cannot be readily isolated from those of absorption, but the theories of scattering and absorption are rather different. These three processes are not all of equal importance in the sea. According to calculation, viscosity is more important than thermal conduction and scattering combined. It is possible that the effect of bubbles is important, but this has not been proved. Because of

the complex mathematics involved in its discussion, no detailed treatment will be given here.[7, 22, 23] (See Section 3.4.2 below.) The attenuation due to scattering will be considered in Chapter 5.

### 3.4.2 The Attenuation Caused by Viscosity

The theory of absorption due to viscosity was first given by Kirchhoff, and is reproduced in most standard textbooks.[2b] The result is that

$$a = \frac{16\pi^2\eta f^2}{3\rho c^3} \log_{10} e \text{ db per unit length,} \quad (21)$$

where $\eta$ = coefficient of viscosity of medium,
$f$ = frequency of sound,
$\rho$ = density of medium,
$c$ = velocity of sound.

Substituting the values of $\eta$, $\rho$, and $c$ appropriate to sea water at 65°F, and expressing $f$ in kc,

$$a = 6.8 f^2 \times 10^{-5} \text{ db/yd.} \quad (22)$$

A similar numerical expression can be obtained for fresh water. Laboratory experiments indicate that, at frequencies above several hundred megacycles, this equation gives the proper order of magnitude of the attenuation coefficient but is in error by a factor of 2 or 3.[19a] A possible explanation of this error has been suggested.[12] At lower frequencies, the observed attenuation is very much greater than that to be expected from viscosity.

This is shown by Figure 49, in which the ratios of the experimental values of $a$ to those given by equation (21) are plotted against the frequency in kilocycles. The dotted curve, for fresh water, is taken from Reference 7. The solid curve is taken from Figure 50. It is seen that for frequencies less than 1,000 kc, all measured attenuations are more than 10 times greater than can be caused by viscosity. In the 10- to 100-kc range, the attenuation in the sea is 40 to 200 times greater than that resulting from viscosity, but is still several hundred times less than would be expected from an extrapolation of the curve for fresh water.

A possible explanation for the large attenuation was proposed by H. F. Willis, who suggested that it could be ascribed to the absorption caused by the suspension of very small air bubbles in the water. Laboratory experiments with ordinary and air-free water do show a difference, but it is not great enough to explain the facts of Figure 49. Further experimental research in this field is urgently needed. Such large discrepancies cannot be ascribed to experimental error, and theoretical speculation appears unable to suggest a completely satisfactory explanation.

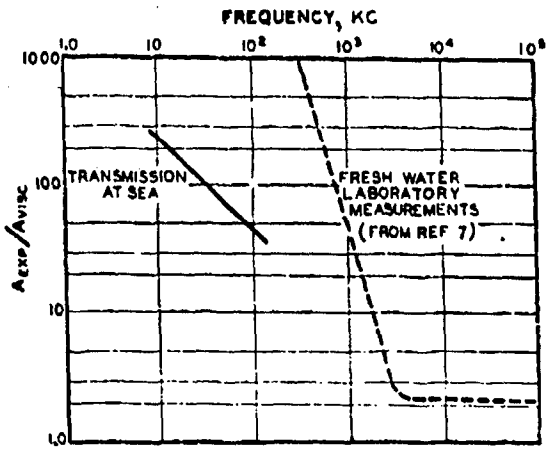


FIGURE 49. Ratio of experimental values of $A$ to those given by equation (21), for both fresh water laboratory measurements and transmission at sea.

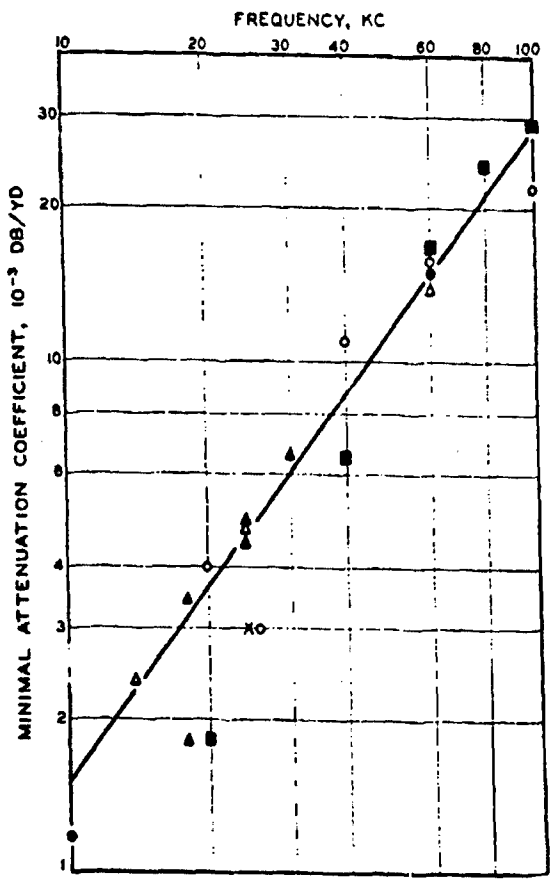


FIGURE 50. Observed values of the minimal attenuation coefficients listed in Table 3 (taken from Reference 12, revised to 1945). The meaning of the symbols is given in Table 3.

## 3.4 3 The Minimal Attenuation Coefficient

### Definition

The attenuation observed in the transmission experiments differs from that caused by viscosity in another important respect. The latter coefficient should be quite independent of thermal gradients, although it might be obscured by the effects of refraction. The values of the observed attenuation, on the contrary, depend markedly on the temperature gradient in the upper layers (see Figure 14) and decrease as the gradients diminish.* In order to have a single definite value for the observed attenuation coefficient, only the values observed when the temperature gradients in the upper layers are small and negative have been considered. For want of a better term, these values have been called the minimal attenuation coefficients and are designated by $a_o$. It is probable that these values approximate the attenuation that would be observed in an isothermal ocean.

* An exception to this rule occurs when both negative and positive gradients are present, forming a sound channel (see Section 2.3.3). The exceptionally low values of the transmission loss under these conditions is adequately explained by refraction theory. They are therefore excluded from consideration in the following paragraphs.

### Observed Values

Observed values of the minimal attenuation coefficients are listed in Table 3 and plotted on Figure 50. The table and figure are taken from a report,[12] revised to 1945. They summarize the measurements made at sea in the frequency range 10 to 100 kc.

Table 3. Minimal attenuation coefficients.

| Freq. (kc) | Minimal atten. coeff. ($10^{-3}$ db/yd) | Location | Method | Experimenters | Figure 50 symbol |
|---|---|---|---|---|---|
| 18 | 1.8 | S. Atlantic and Caribbean | Ship-to-ship | NRL Ref. 16 | Solid triangle |
| 24 | 4.4 | S. Atlantic and Caribbean | Ship-to-ship | NRL Ref. 16 | Solid triangle |
| 30 | 6.5 | S. Atlantic and Caribbean | Ship-to-ship | NRL Ref. 16 | Solid triangle |
| 18 | 3.4 | Off Panama | Ship-to-ship | NRL Ref. 16 | Solid triangle |
| 21 | 4.8 | Off Panama | Ship-to-ship | NRL Ref. 16 | Solid triangle |
| 14 | 2.5 | Off San Diego | Ship-to-ship | UCDWR Ref. 12 and later work | Open triangle |
| 24 | 4.5 | Off San Diego | Ship-to-ship | UCDWR Ref. 12 and later work | Open triangle |
| 56, 60 | 15.0 | Off San Diego | Ship-to-ship | UCDWR Ref. 12 and later work | Open triangle |
| 21 | 4.7 | Off Pt. Conception | Ship-to-ship | UCDWR Ref. 12 and later work | Open triangle |
| 20 | 1.8 | San Diego Harbor | | UCDWR Ref. 17 | Solid Square |
| 40 | 6.5 | San Diego Harbor | | UCDWR Ref. 17 | Solid square |
| 60 | 16.5 | San Diego Harbor | | UCDWR Ref. 17 | Solid square |
| 80 | 24.0 | San Diego Harbor | | UCDWR Ref. 17 | Solid square |
| 100 | 29.5 | San Diego Harbor | | UCDWR Ref. 17 | Solid square |
| 20 | 4 ± 1 | Off San Diego | Vertical pulse | UCDWR Ref. 17 | Open circle |
| 25 | 3 ± 2 | Off San Diego | Vertical pulse | UCDWR Ref. 17 | Open circle |
| 40 | 11 ± 2 | Off San Diego | Vertical pulse | UCDWR Ref. 17 | Open circle |
| 60 | 16 ± 2 | Off San Diego | Vertical pulse | UCDWR Ref. 17 | Open circle |
| 100 | 22 ± 1 | Off San Diego | Vertical pulse | UCDWR Ref. 17 | Open circle |
| 10 | 1.2 | ? | ? | British | Solid circle |
| 60 | 15 | | | | Solid circle |
| 300 | 300 | | | | |
| 24 | 3.0 | Off San Diego | Deep projector and hydrophone | See Sect. 3.2.8 | Cross |

### Vertical Pulsing

The method of ship-to-ship transmission of pulses is rendered difficult by the rarity of suitable thermal conditions in inshore water (see Chapter 4). This difficulty could be overcome by transmitting sound vertically through the ocean, since refraction does not affect vertical sound rays (see Chapter 2) and presumably the transmission anomaly under these conditions will be given by equation (4). However, the shallowness of most inshore waters then materially restricts the distance $r$ that can be achieved between source and receiver.

Other obvious experimental difficulties also arise when transducers are to be operated at very great depths. These have been avoided by using echo-sounding gear and studying the intensity of the bottom echo produced when the sound beam is directed vertically downward.

A somewhat oversimplified theory of echo sounding will be given as a basis for discussing the experiments. If the bottom of the sea were perfectly flat, the echo would appear to come from a virtual image source, located as far below the bottom as the actual source is located above the bottom. If the actual distance from source to bottom is $s$ yd, the transmission loss should be

$$H = 2a_0 s - 20 \log (2s). \tag{23}$$

If the bottom were also a perfect reflector, the difference $L_1 - E$ between the source level $L$ and the level of the echo $E$ would be $H$. However, the bottom is not a perfect reflector, so that the effective source level of the image will be less than $L_1$, say $L_1'$. If $\mu$ ($<1$) is the amplitude-reflection coefficient of the bottom,

$$L_1' = L_1 + 20 \log \mu, \tag{24}$$

and

$$L_1 - E = 2a_0 s - 20 \log \frac{2s}{\mu}. \tag{25}$$

This is a single equation which contains the two unknowns $a_0$ and $\mu$. Both can be determined, provided measurements can be made in water of different depths over bottoms having the same value of $\mu$.

The procedure actually followed was to make a series of measurements over mud bottom, in the hope that this would insure the constancy of the reflection coefficient. As a test of this assumption, the values of

$$A = L_1 - E + 20 \log (2s) \tag{26}$$

were plotted against $2s$. The result is shown in Figure 51. If $\mu$ is constant, the graph for any one frequency should be a straight line, the slope of which is $a_0$ db/yd and the intercept at $s = 0$ is $-20 \log \mu$. It is seen that the points do fall close to the straight lines, but there is a possibility that differences in the

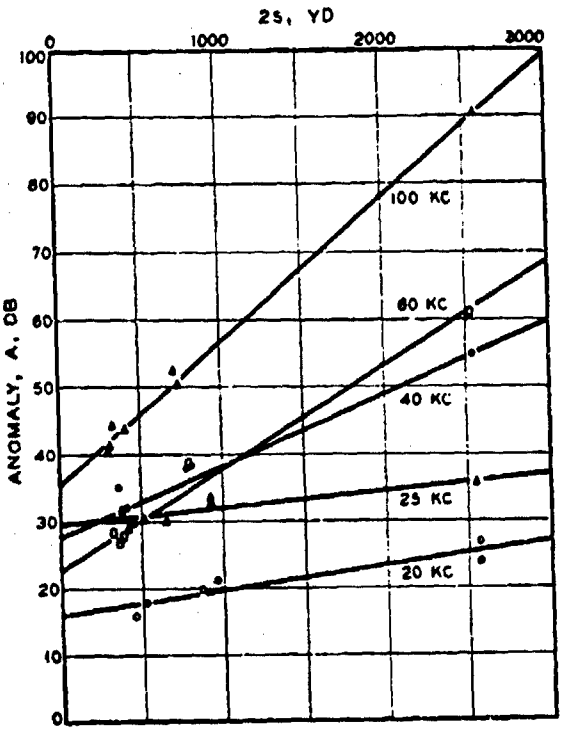


Figure 51. Transmission anomaly at various frequencies as determined by echo-sounding (vertical pulsing) experiments.

reflection coefficient at the various locations have influenced the slope of the lines as drawn. In particular, the 60-kc line does not appear to be in its proper position between those for 40 and 100 kc and there is rather more difference between 20 and 25 kc than might have been expected. These discrepancies may also indicate that the theory outlined above is too simple and that the bottom does not behave like a mirror under these conditions.

The vertical pulsing and the ship-to-ship transmission under good thermal conditions are the principal methods by which values of the minimal attenuation coefficient have been determined. In addition, some measurements have been made in the shallow water of San Diego Harbor by transmitting pulses from the end of a dock to a small boat, which moved along a measured cable. The maximum separation between source and receiver in this case was

about 1,000 yd. The effects of surface and bottom reflection were pronounced in these experiments, and some uncertainty exists as to the necessary corrections.

## 3.5 VARIABILITY OF TRANSMISSION LOSS

### 3.5.1 Changes in Transmission Loss with Time

#### General Remarks

In the preceding sections the general empirical laws governing the transmission of sound *on the average* have been discussed. Experience has shown that *departures from the average* often have an important bearing on many problems, and this is true also of the transmission of underwater sound.

If sound of constant intensity and frequency is transmitted through the sea from one ship and received on another at some fixed distance, the received intensity will not be constant. This is very apparent when the reception is by ear: the loudness of the sound increases and decreases in an easily perceptible but very irregular manner. The same effect is noticed when sound is transmitted several thousand yards through the open air; it is commonly said that the wind "blows the sound away". A similar effect is also known in the transmission of radio waves; this is called "fading."

The cause of this phenomenon is the changing condition of the medium through which the sound is transmitted. Even though the wind does not literally blow the sound away, it does cause changes in the air through which the sound must pass, and these in turn cause changes in the transmission loss. Similar changes occur in the sea, even though the currents are not so strong as the wind. The roll and pitch of the ships, as well as their steady motion, also contribute to change the path of the sound traveling from projector to receiver.

#### Three Kinds of Time Changes in Signals

A cursory examination of typical oscillographic records of sound transmitted through the sea shows the marked variability in the amplitude at a given point even during short periods of time. Some typical oscillograms of signals received during ship-to-ship transmission at various ranges are shown in Figure 52. These are records of short pings (of 100 msec duration) transmitted successively a half-second or a second apart. Once each minute a long signal of 10 sec was transmitted. These long signals are exhibited in the upper strips of A, B, and C of Figure 52; the bottom halves are records of the short 100-msec pings. Strip D is a record of pings received at a range of 13 ft and is included for comparison. At this short range the signals show very little change. The ray diagram at the top shows that the sound recorded in A was received in the direct-sound field, and that recorded in B and C in the shadow zone. The hydrophone was at 16 ft.

It is useful to introduce certain terms to describe the obvious differences in the oscillograms reproduced in Figure 52.

*Distortion.* The amplitude of a short segment of a signal will change during a time less than 0.1 sec; this will be called *distortion.* Distortion is especially noticeable at long ranges, where the amplitude may change by a factor of two or three in 0.05 sec. At moderate ranges this factor is considerably less, and at 13 ft the effect is practically nonexistent.

*Fluctuation.* There are changes in the average amplitudes of successive short pings and of successive short segments of long pings; this will be called *fluctuation.* It is especially apparent at moderate ranges, where there is little distortion. It also occurs at longer ranges, but then it is necessary to average out the distortion before the fluctuation becomes obvious. This average can be found either by inspection or by making a series of measurements and computing it arithmetically.

*Variation.* Although not shown by Figure 52, there are still slower changes in the transmission loss, which become appreciable in 15 or 30 minutes. These become apparent when the average amplitude of a number of pings at one time is compared with that of another set received at a later time. The range should, of course, be constant for both sets. These slow changes are called *variation.* The term variation is also used to designate differences in transmission loss measured under similar thermal conditions on different days.

There is no sharp dividing line between these three effects, but as they affect practical echo ranging and listening in somewhat different ways it is convenient to use the terms.

### 3.5.2 Distortion of Signals

It is thought that this effect is not very important in echo ranging, and consequently it has not been studied in great detail.

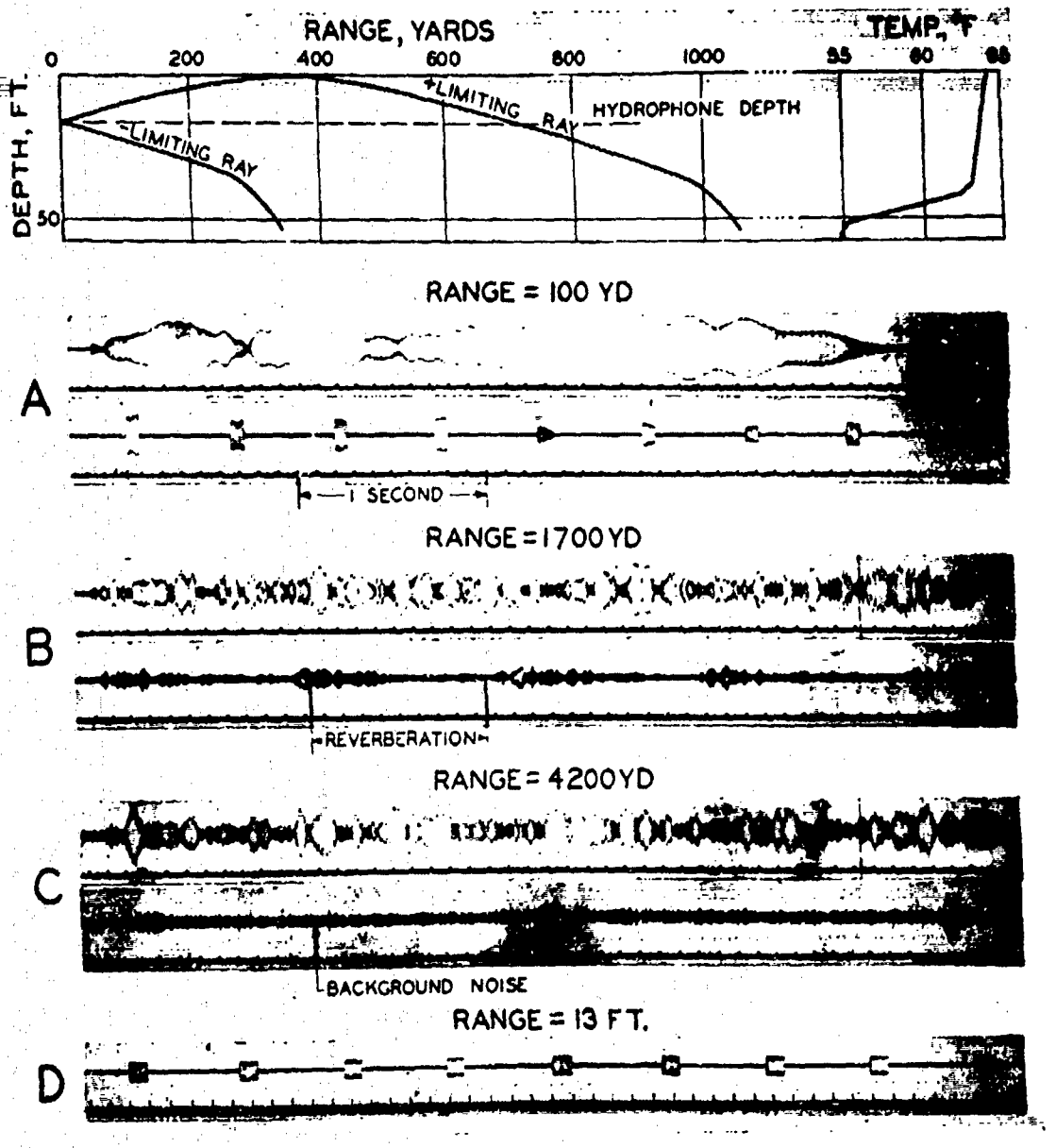


FIGURE 52. Oscillograms of 24-kc signals received at various ranges during ship-to-ship transmission. The upper halves of strips *A*, *B*, and *C* show a long (10-sec) ping; the 100-msec pulses, strip *D* shows pulses received at 13 feet. The bathythermogram and corresponding ray diagram at the top show the sound condition prevailing during the experiment. Projector and hydrophone depth = 16 ft. Reverberation (forward scattering) and background noise are indicated. The increased distortion of the signal at long ranges is clearly seen (UCDWR, San Diego).

As has already been remarked, the distortion is most pronounced at long ranges, where the transmission loss is high and the ray theory predicts a silent shadow. The small amount of sound received at these ranges is probably the result of scattering that occurs in the volume or at the bottom of the sea. The sound travels along one ray until it reaches some suspended obstacle, which becomes a secondary source and reradiates some of the incident sound along other rays.

This explanation is supported by the fact that the distorted oscillograms of Figure 52B and C are very similar in appearance to oscillograms of reverberation, such as Figure 9 of Chapter 5. Reverberation has not yet been discussed but it will be shown to be caused by scattering. Further evidence for the validity of this explanation of the distortion is to be found in the "reverberation tails" indicated on the oscillograms of the pings in Figure 52B. These indicate that

some sound has been en route for a longer time than the rest. This is typical of scattering processes, since the time required to travel from projector to scatterer and thence to receiver depends upon the location of the scatterer. Neglecting refraction, this time will be least when the three are in the same straight line and will increase if the scatterer is out of the direct line.

At extreme ranges, it is probable that not all of the recorded sound originated at the projector. The impossibility of avoiding extraneous noise imposes limitations on measurements of this kind.

### 3.5.3 Fluctuation

Turning our attention to the manner in which successive pings differ from each other, we see from Figure 52 that when pings of about 100-msec duration are projected at intervals of a few seconds with the same amplitude, the average amplitude of one ping will, after transmission, differ from the average amplitude of its neighbors. This effect is very clearly shown by Figure 53A and C, in which the average amplitudes of 100 successive signals, received at ½-sec intervals, are expressed as ratios to the average amplitude of all the 100 signals and are plotted against time. These fluctuations can be dealt with quantitatively by the use of quantities common in statistical procedure. Some of these will be discussed briefly.

#### Standard Deviation

Let the amplitude of the first ping in a set of $N$ pings be $x_1$, that of the second ping $x_2$, and so on to $x_N$. Let the average amplitude of all $N$ pings be $\bar{x}$. The quantity $x_1-\bar{x}$ is called the *deviation* of the first ping, $x_2-\bar{x}$, the deviation of the second ping, and so on. Two other quantities used to describe fluctuation are *variance* of the set and the *standard deviation*.

The *variance* $\gamma$ is computed by squaring the individual deviations and averaging them:

$$\gamma = \frac{1}{N}\left[(x_1-\bar{x})^2+(x_2-\bar{x})^2+\cdots (x_{N-1}-\bar{x}^2)+(x_n-\bar{x})^2\right] \quad (27)$$

The *standard deviation* $\sigma$ is the square root of the variance:

$$\sigma = \gamma^{\frac{1}{2}} \quad (28)$$

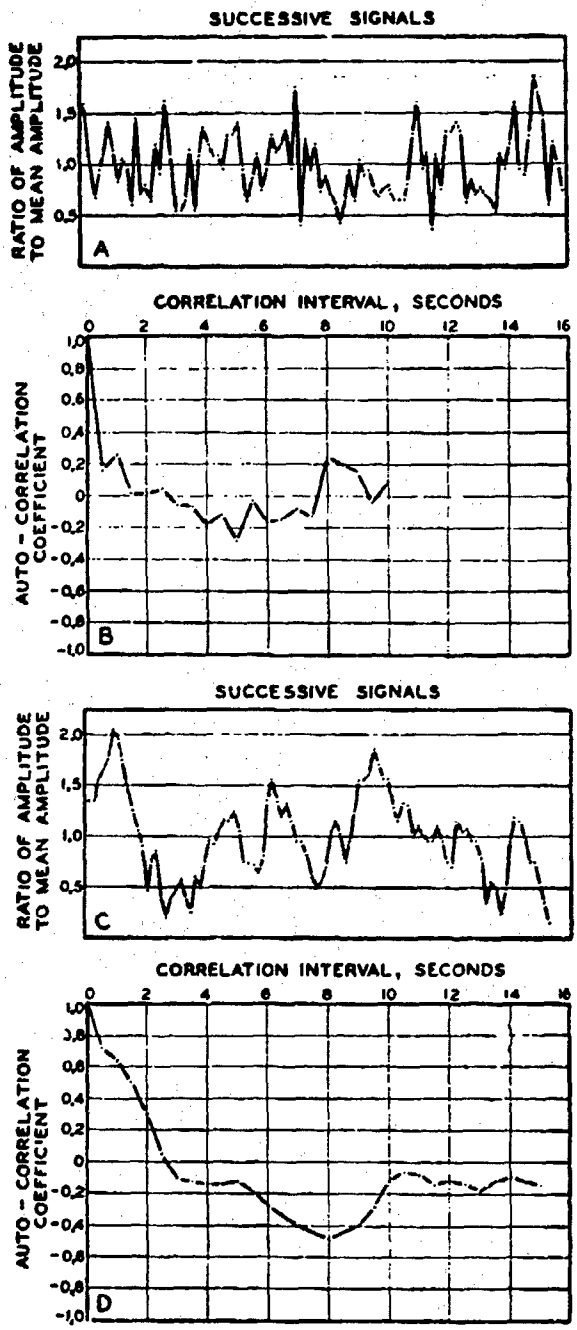


FIGURE 53. Fluctuation of successive signals (24-kc), and the corresponding autocorrelation graphs (see Section 3.5.4). B shows the autocorrelation coefficient for the signals in A; D that for the signals plotted in C. The ratio of the amplitude of each signal to the average amplitude of the signals in the set is plotted.

The standard deviation is often expressed as a per cent of the average $\bar{x}$.

It is convenient to measure the fluctuation of received signals by their standard deviation, using in the calculation a set of $N = 50$ or more, all received within a few minutes. The fluctuation, as measured in this way, ranges from 20 to 70 per cent. Values smaller than 35 per cent or larger than 50 per cent are relatively rare when both projector and receiver are near the surface. The average value of $\sigma$ in a large number of such measurements of fluctuation, for frequencies from 10 to 60 kc, is 43 per cent. There is no significant dependence of the fluctuation on frequency in this range.

### Importance of Fluctuation

For the purpose of plotting graphs like Figures 11 and 12, the effect of fluctuation has been largely eliminated by using the average value of the amplitude, the average being calculated from a set of 5 successive pings. For some practical purposes, the fluctuation can be ignored and eliminated in much the same way. This is true, for example, in most echo-sounding operations. There is then sufficient time to consider several echoes before arriving at a conclusion.

In searching operations, however, a given region can usually be swept only with one ping, the next ping sweeping in another direction. When fluctuation makes the echo especially weak, a target may escape detection, even though it would be detectable if the transmission had been average.

### Use of Medians and Quartiles

In order to deal with problems such as this, neither the average nor the standard deviation is a very useful numerical measure. Statisticians have developed several other concepts for such purposes:

The *median* of a set of numbers $x_n$ is a number such that 50 per cent of the $x_n$ are greater than it, 50 per cent less.

The *upper quartile* is a number such that 25 per cent of the $x_n$ are greater than it, 75 per cent less.

The *lower quartile* is a number such that 75 per cent of the $x_n$ are greater than it, 25 per cent less.

The *upper* and *lower deciles* are similarly defined in terms of the 10 per cent: 90 per cent division of the set.

In this book, a single measurement of transmission loss or anomaly is always the average of the amplitudes of several transmissions, after conversion to db. For some applications it would be preferable to use the median of the amplitudes. For other applications, when failure to achieve transmission of the signal is highly penalized, it would be better to use the lower quartile or decile of the amplitudes in making estimates. In still other cases, e.g., when estimating the chance of being overheard by a distant enemy, the upper quartile or decile should be used.

The general relation between these various measures is shown in Table 4. These values are quoted merely as guides and not as accurate values. This is especially true of the deciles: values for the upper decile as large as 1.95 and as small as 1.42 are not uncommon.

Table 4. Fluctuation in the intensity of transmitted signals.

| | Ratio to average | Decibels above average |
|---|---|---|
| Upper decile | 1.65 | 4.4 |
| Upper quartile | 1.26 | 2.0 |
| Median | 0.97 | −0.2 |
| Lower quartile | 0.63 | −4.0 |
| Lower decile | 0.48 | −6.4 |

Table 4 emphasizes the great fluctuation in the transmission. In order to embrace 80 per cent of the signals, a latitude of more than 10 db must be allowed. Even if only 50 per cent of the signals are to be included, the limits must be 6 db apart.

This applies only to one-way transmission. The fluctuation in the intensity of echoes is probably slightly greater. Thus, on two occasions the fluctuations of transmission and echo intensity were determined within one hour of each other. The transmission fluctuated by 50 and 49 per cent, while the corresponding values for echo intensity were 66 and 69 per cent. A longer series of echo measurements, not made simultaneously with transmission studies, gave an average fluctuation of 40 per cent.

## 3.6.4 Autocorrelation

### The Problem

The standard deviation gives quantitative information concerning the amount of fluctuation; but it is easy to see that the rate at which the signal amplitude changes is also important. A periodicity in the fluctuation may suggest a possible cause of the fluctuation.

Inspection of Figure 53A and C shows that there is a difference in the rate at which the amplitude changes. In A, a high-amplitude signal is as likely to be succeeded by a low one as by another high one; whereas in C, a high-amplitude signal is much more likely to be succeeded by another one above average than by one that is below average. In both cases the signals succeeded one another at ½-sec intervals; hence this indicates a different tempo of the amplitude changes.

The rate at which the signal amplitude fluctuates can be described by calculating a quantity known as the *autocorrelation coefficient.*

### Definition

As before, let $x_n - \bar{x}$ be the deviation of the $n$th signal from the average. The calculation of the autocorrelation coefficient is similar to that of variance; however, instead of squaring the deviation, one computes the product of the deviation of one item with the deviation of another, keeping the separation between the items of a pair constant through the series. In mathematical symbols,

$$\beta_m = \frac{1}{N-m}\Big[(x_1-\bar{x})\,(x_{1+m}-\bar{x}) + (x_2-\bar{x})\,(x_{2+m}-\bar{x}) + \cdots + (x_n-\bar{x})\,(x_{n+m}-\bar{x})\Big], \quad (29)$$

where $m$ may equal 1, 2, 3 · · ·, but has a fixed value throughout a summation.

It is seen that when $m = 0$, equation (29) reduces to equation (27), hence $\beta_0 = \gamma$ is the variance. When $m$ is different from zero, $\beta_m$ is called the *mean displaced product* or the *autocorrelation function.* It is more convenient to use when expressed as a ratio to the variance; this ratio is called the *autocorrelation coefficient.* It is often stated as a per cent. The number $m$ is the *correlation interval.*

It can be shown that the autocorrelation coefficient cannot be greater than 100 per cent. It is 100 per cent if $m = 0$ by definition; moreover, by comparing equations (27) and (29) it is evident that it is 100 per cent if, for all values of $n$, $x_{n+m} = x_n$. Thus, if $\beta_2 = 100$ per cent, $x_n$ and $x_{n+2}$ must be equal for all $n$; this means that the fluctuation is periodic, with a period of 2.

The autocorrelation coefficient can never be less than − 100 per cent. In that case all the pairs of deviations are equal, but opposite in sign. In both these extreme instances the fluctuation is periodic.

In general, the autocorrelation coefficient will be less than 100 per cent for all values of $m$ (except $m = 0$). If it is always zero, the fluctuation is perfectly random. A graph of $\beta_m$ gives information about the departures from periodicity on the one hand, and about the departures from perfect randomness on the other.

### Illustration

Examples of graphs of autocorrelation coefficients are shown in Figure 53B and D. These graphs correspond respectively to the graphs of the amplitude deviations of Figure 53A and C, and illustrate the foregoing remarks. In Figure 53B the values of $\beta_m$ are rarely greater than 20 per cent; this indicates that the fluctuation shown in A is nearly random. In Figure 53D the coefficient remains above 50 per cent for 1½ sec and drops to − 50 per cent at 8 sec. This means that a high signal is followed by high signals for a period of 1½ sec, but after 8 sec it is followed by unusually low signals. There is thus a trace of a 16-sec period in this set of data. In Figure 53A one can see smaller traces of 5-sec and 8-sec periods.

## 3.5.5 Cause of Fluctuation

A number of causes of fluctuation have been suggested and considered. It appears that no one of them is capable of producing all of the known effects.[18] Four possible causes may be listed:

1. Roll and pitch of the projector.
2. Interference between direct sound and surface echo.
3. Interference between sound traveling via many different paths.
4. Focusing and defocusing due to action of local thermal inhomogeneities as lenses.

### Roll and Pitch of the Projector

If cause 1 were dominant, it would be expected that the fluctuations would keep step with the motion of the ship and that fluctuations at different ranges would also keep step. This has not been fully investigated, particularly as the motion of both transmitting and receiving ships must be considered.

While this cause is apparently not dominant, it may explain the traces of long periodic changes indicated by Figure 53C and D.

As the range is increased, the fluctuation becomes more rapid at the range where the effects of reverberation (the "tail") become prominent (see Figure 52B). At all ranges the correlation between signals spaced more than 1.5 sec apart is usually less than 0.5.

If the roll and pitch of the gear were the dominant cause of fluctuation, one would expect sound of sonic frequencies also to show the effect. Figure 54 shows the autocorrelation graph of 5-kc signals at long

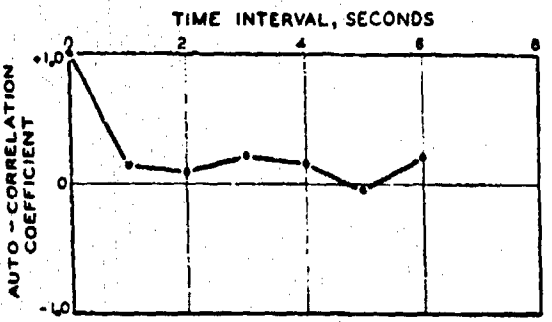


FIGURE 54. Autocorrelation of sonic (5-kc) signals at long range. The fluctuation is seen to be practically random.

range. This figure suggests that for sonic frequencies the fluctuation is practically random, but this conclusion is based on very little data.

Attempts to determine the nature of fluctuation have included experiments in which the signals were received simultaneously on two hydrophones at different depths, and on two hydrophones at the same depth but horizontally separated from 5 to 15 ft. The correlation between such signals becomes less with increasing range and with greater separation of the hydrophones. For ranges greater than about 500 yd and when the hydrophones are at different depths, the coefficient is practically always less than 50 per cent. The significance of these results is not clear.

### Interference Between Direct Sound and Surface Echo

If cause 2 were dominant, the fluctuation would be sharply limited, the upper limit being $1+\mu$ times the average, the lower $1-\mu$, where $\mu$ is the surface-reflection coefficient. Since $\mu$ is necessarily less than unity, the maximum amplitude would be less than twice the average. On some occasions, nearly 10 per cent of the observed amplitudes are more than twice the average. The fluctuations almost never are sharply limited, but show some very large and very small values at long intervals. Thus cause 2 cannot be the only one acting.

However, experiments performed with both projector and hydrophone at a depth of more than 500 ft (Section 3.2.8) make it possible to separate the direct and surface-reflected sound. At short ranges (less than 500 yd), the fluctuation of the direct sound was only 20 per cent, while that of the surface-reflected sound was 50 per cent. This suggests that, although the simple theory of interference is not applicable, surface reflection may be an important factor in fluctuation.

At longer ranges, with deep projector and hydrophone, the fluctuation of both direct and surface-reflected sound is about 50 per cent.

It may also be noted that, in experiments with explosive sound, direct and surface-reflected sound can be separated (Section 3.1.2). In some of these experiments the fluctuation of direct sound was less than 10 per cent.

### Other Causes—Summary

Causes 3 and 4 are not open to these objections, but as yet thermal measurements have shown no reason to expect local variations in the velocity of sound which are large enough to account for the observations.

Probably all these causes act together in proportions that change from day to day.

If causes 2 or 3 were dominant, it would be expected that sounds of different frequency, transmitted simultaneously, would be affected differently. At a time when the transmission of one frequency is poor, that for another would be good. Such simultaneous transmission of many frequencies can be approximated by transmitting "chirp" signals, in which the frequency changes during the transmission. An experiment with chirps in which the frequency changed from 23.5 to 24.5 kc showed about 15 per cent less fluctuation than did single-frequency pings on the same day. This result might be accidental, and further study is needed.

Signals of 16 kc and 24 kc were emitted simultaneously by the same projector and received by the same hydrophone, as well as signals of 24 and 56 kc. The correlation between such pairs of signals averaged 30 per cent. Sets of signals of the same fre-

quency have a standard deviation of about 70 per cent. This suggests that a significant portion of the fluctuation at each frequency is due to a common cause.

## 3.5.6 Variation of Transmission

Mention was made in Section 3.5.1 of slow changes in the transmission loss, which become apparent when the average amplitude of a number of pings at one time is compared with that of another set received at a later time. These slow changes were designated *variation*.

### Treatment of Data

In assembling data for the study of the long-period changes, the following procedure was carried out.

The oscillograms used were those obtained during a single experiment in which the receiving vessel drifted and the transmitting vessel opened or closed the range (see Section 3.2). The amplitude of successive received signals were determined; sets of five nonsuccessive signals were averaged to eliminate some of the fluctuation. Nonsuccessive pings were chosen in order to avoid the possible effects of correlation. These averages were plotted as a function of range. After a large number of such graphs had been accumulated, they were sorted into more or less homogeneous sets, according to the depth of the 0.3°F decrease, $D_2$. From each graph, the value of the transmission anomaly was read at certain ranges, and plotted on a graph like the one shown in Figure 55. This figure is the set of data for values of $D_2$ lying between 10 and 20 ft. The hydrophone depth for most of the points was 16 ft and for all of them less than 40 ft.

Despite the relative homogeneity of the conditions under which the measurements were made, the points scatter very widely. This is the phenomenon which has been called variation. The most convenient method of discussing the variation is by using medians and quartiles, defined above. In Figure 55, the median values at various ranges are connected by the solid curve, the quartile values by dotted curves. The median and quartile values are also given in Table 5, together with the average deviation of the quartiles from the respective medians; this quantity is called the *quartile deviation*. It is indicated on the graph by half the vertical spread between the dotted curves.

Table 5. Variation of the transmission anomaly at various ranges.*

| Range (yd) | Lower quartile (db) | Median (db) | Upper quartile (db) | Quartile deviation (db) |
|---|---|---|---|---|
| 250 | 0 | 2 | 4 | 2 |
| 500 | 2 | 5 | 8 | 3 |
| 1,000 | 12 | 12 | 26 | 7 |
| 1,500 | 26 | 31 | 37 | 5.5 |
| 2,000 | 31 | 38 | 41 | 5 |
| 2,500 | 30 | 39 | 46 | 8 |
| 3,000 | 29 | 38 | 48 | 9.5 |
| 4,000 | 27 | 34 | 48 | 10.5 |
| 5,000 | 24 | 28 | 47 | 11.5 |

*Data from Figure 55.

Similar results are obtained under other conditions. It is seen from Figure 55 and Table 5 that there is a marked increase in the scatter as the range increases.

### The Causes of the Variation

The possible causes of variation are of two kinds: those which originate in the apparatus, and those which originate in the sea. There are many possibilities of the first kind, but most of them have been eliminated by the experimenters and need not be discussed here. The outstanding sources of error that remain are:

1. Uncertainty in the zero of the anomaly scale.
2. Uncertainty in the orientation of the hydrophone.
3. Residual effects of fluctuation, not eliminated by averaging five pings.

All of these sources of error might cause variation; but none will explain the increase in the quartile deviation with increasing range. This is obvious in causes 1 and 2. In the case of fluctuation (cause 3), it follows from the fact that the percentage fluctuation is independent of range.

Concerning the first cause—uncertainty in the zero of the anomaly scale—no attempt has been made to measure the received sound pressure in dynes per square centimeter in the work with supersonic sound. Only changes in sound level are measured. These relative levels are plotted with reference to the level of the sound received at 1 yd from the projector. In practice, the level at 1 yd is not actually measured, but is estimated by extrapolating from a measurement taken at 100 or 200 yd, assuming that $H = 20 \log r$ from 1 yd to this distance. Consequently, all transmission-loss measurements may be too high or too low by the amount of error

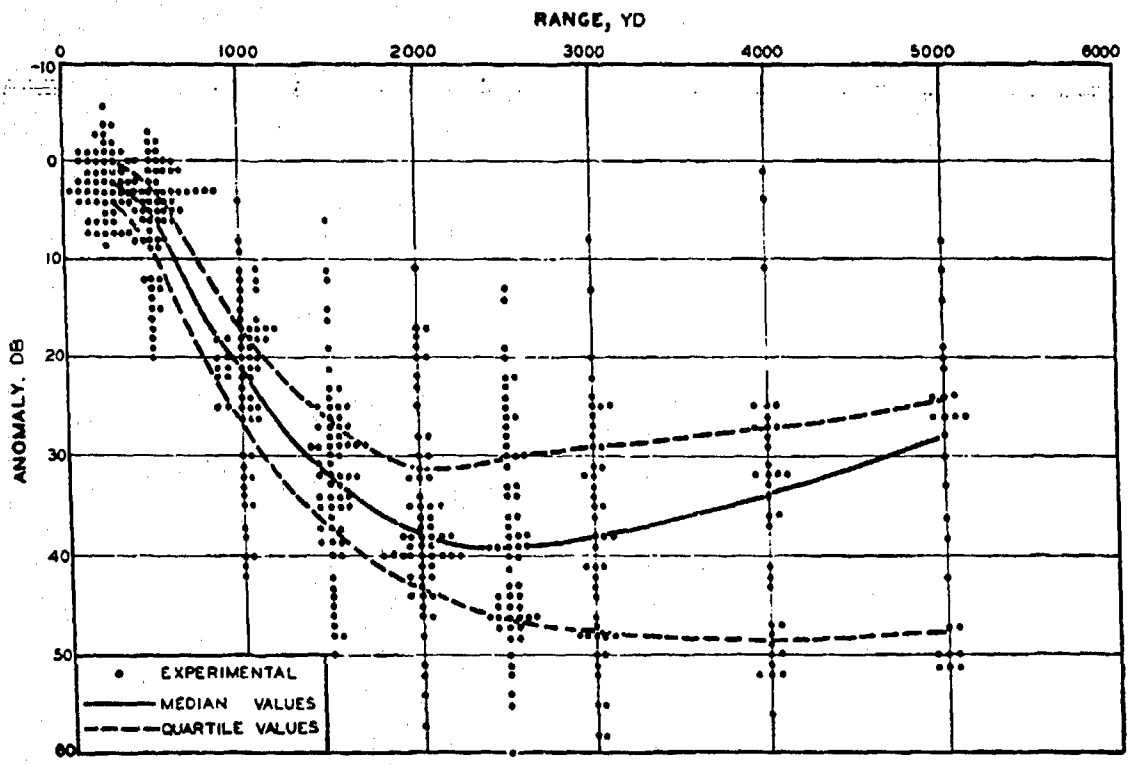


FIGURE 55. Variation of 24-kc sound. Each point represents the average of five nonsuccessive signals received during a single experiment; the median and quartile values at the various selected ranges are connected by lines. Hydrophone depth for most points = 16 ft; for all the points, < 40 ft. 10 ft $< D_2 <$ 20 ft.

involved in this extrapolation. The correction of this error is not easy, although later measurements are less subject to it than the earlier ones. The error may change from day to day and thus contribute to the variation. If this were the only cause of the variation, however, the difference between the upper and lower quartiles would be the same at all ranges.

It follows that the total effect of the three causes listed cannot be greater than the smallest observed variation. From Table 4 this is seen to be $\pm$ 2 db for the difference between quartiles and median at 250 yd. At 3,000 yd this difference is of the order $\pm$ 9 db. Thus it may be concluded that some other cause is operative.

## Chapter 4

# THE OCEANOGRAPHY OF SOUND CONDITIONS

## 4.1 INTRODUCTION

IT HAS BEEN MADE abundantly evident in Chapters 2 and 3 that the transmission of sound in the sea is decidedly influenced by the temperature conditions in the upper layers; in particular, temperature differences of a fraction of 1°F, occurring in the upper 40 or 50 ft of the ocean, can strongly influence sound transmission.

These surface gradients are extremely variable: they change from season to season, from day to day, even from hour to hour, and from place to place. In this respect the ocean is very similar to the atmosphere, and thus there is a close analogy between oceanography, on the one hand, and meteorology and climatology on the other. One may speak of the subsurface weather and of its seasonal and diurnal changes, and of the subsurface climate, the annual and seasonal averages of the components of the weather. The analogy between oceanography and meteorology holds true further in that one of the practical objectives of the oceanography of underwater sound is the forecasting of subsurface weather.

The study of subsurface weather was neglected until its importance for underwater acoustics was recognized. The results of this study are discussed fully in another volume of this series.[1] In the present chapter only a brief summary of the acoustically significant results can be given.

The outstanding characteristic of weather, whether in the air or under the sea, is its changeability. These changes are the outcome of a complex set of processes, which are continuously in action. Sometimes one of these processes may dominate all others; more often, several will exert appreciable influences on the resultant.

There are at least ten or a dozen such processes which cause the temperature gradients in the upper layers of the ocean to change. They can conveniently be grouped into four general processes, and these will be discussed first. Their effects in the form of daily, seasonal, and geographic changes of the temperature gradients will then be described. Finally, the more detailed analysis of the general processes will be given.

## 4.2 THE GENERAL PROCESSES AND THEIR INTERACTION

### 4.2.1 General Survey

The surface layers of the ocean are subjected to heating, cooling, and mixing; moreover, they may flow at a speed different from that of the underlying water. These are the four general processes just mentioned. All four processes are closely interrelated but each has its own characteristic effect on the temperature gradients that are revealed by bathythermograms. Each of them is caused by a variety of factors; all four, however, are affected by the condition of the atmosphere at the ocean surface. The immediate effect of each is to alter the dynamic state of the surface layers.

TABLE 1. Outline of processes influencing temperature changes.

| General process | Cause | Dynamic effect |
|---|---|---|
| 1. Heating | Sunshine, Warm moist air | Stability of surface layer |
| 2. Cooling | Evaporation, Radiation, Cold dry wind | Instability of surface layer |
| 3. Mixing | Wind and waves, Instability, Turbulence | Neutral stability of surface layer |
| 4. Flowing | Wind and waves, Internal waves, Currents | Variable; turbulence if strong |

Table 1 presents an outline of the general processes, their causes and dynamic effects. A characteristic complication is illustrated by processes 2 and 3: cooling has the effect of making the surface layer unstable, and instability in turn is a cause of mixing. In the same way, strong currents may cause turbulence, which again results in mixing. There are other chains of cause and effect linking all the processes.

## 122 Stability

### Stratification of the Ocean—an Equilibrium Condition

Bathythermograms show that the ocean is more or less stratified. Two points separated by several hundred yards but at the same depth beneath the surface will have practically the same temperature. If the ocean were in equilibrium, this stratification would be complete: the warm, lighter water being at the surface, the lower strata consisting of cooler, heavier water, and the boundaries between strata being horizontal surfaces. The equilibrium is disturbed by three of the four general processes. The observed stratification is thus the result of other processes tending to bring the ocean to equilibrium.

### Density a Function of Temperature and Salinity

It is a general hydrodynamic principle that when a mass of fluid is in stable equilibrium under the force of gravity its density must everywhere increase in the downward direction and be constant in every horizontal plane. A commonplace illustration of this principle is furnished by a bottle containing oil and water.

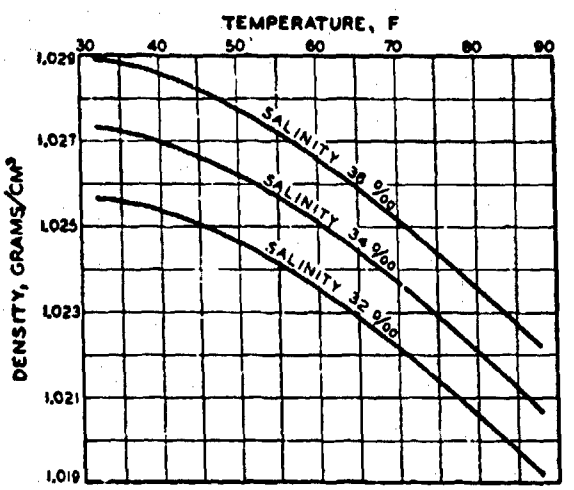


Figure 1. Variation of the density of sea water with temperature and salinity.

The density of sea water is primarily determined by its temperature and salinity, as shown in Figure 1. The changes due to temperature are the largest, just as in the case of the velocity of sound (see Figure 1 of Chapter 2). However, salinity has a proportionately greater effect on the density of sea water than on the velocity of sound.

In the open ocean, where the salinity is practically constant, the lighter water will thus always be the warmer water, and it is to be expected that the temperature will either remain constant or decrease with increasing depth. With very rare exceptions, this is found to be the case. Near the shore, salinity differences may sometimes dominate the density distribution so that a layer of cold dilute water may overlie warmer water of high salinity.

### Thermal Structure and Stability

The concept of stability is a convenient one to apply. Stability depends on the rate at which density increases with depth. If the temperature in a layer decreases rapidly with depth, as in the thermocline, the layer has a high stability, for in this case the density increases rapidly. On the other hand, a layer in which the density decreases with depth is unstable and will exist only transiently. Mixing processes are retarded by high stability; thus wind of a given strength may easily mix a surface layer in which the temperature gradient is small and the stability, therefore, low. The same wind may have little mixing effect if the temperature gradients near the surface are large. The development of a sharp thermocline tends to retard mixing to greater depths.

A completely mixed isothermal layer has indifferent stability. Cooling at the surface increases the density of the surface layer. So also does evaporation, because of the cooling and the increase in salinity that accompany it. Hence these processes tend to make the density of the surface water greater than that of the water immediately below it and to produce a condition of instability. This unstable density distribution near the surface results in convective mixing.

The stability can be estimated from a bathythermogram if it is assumed that salinity gradients are negligible. Density decreases with increasing temperature (see Figure 1) and for most practical purposes the isotherms on the bathythermogram grid can be interpreted as lines of equal density. The slope of the temperature trace is therefore a measure of the

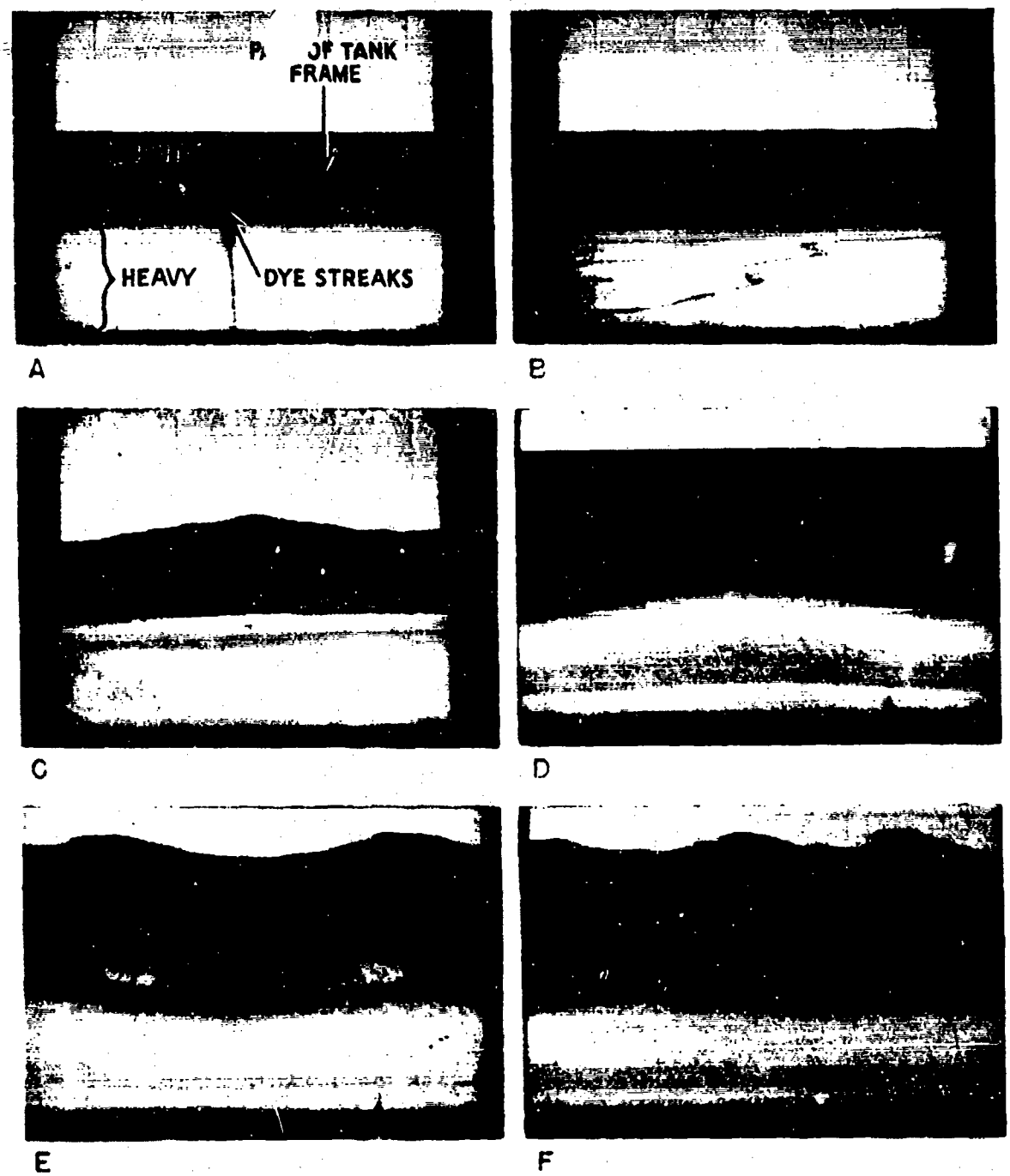


FIGURE 2. Experiments with density layers. (A) Both layers at rest. (B) Dye streaks showing particles transported by currents. (C) Surface waves do not disturb the boundary of the lower layer. (D) Internal waves do not disturb the surface. (E) and (F) Mixing in the upper layers due to long-continued surface waves.

rate of change of density with depth; that is, of stability. With this in mind, the bathythermograph traces can be interpreted in terms of the four major processes.

## 4.2.3 Laboratory Experiments on Stratification

The high stability of negative thermal gradients is due to the fact that there is little exchange of heat between neighboring layers unless they are mixed by some stirring action. This is readily shown by laboratory experiments. If a tank is partly filled with warm water, and water of room temperature is then run in through a hose lying on the bottom, the warm water will float on the colder. Thermometers placed in the two layers will show that the cooler water is not heated by the overlying warm water. The latter will cool, as described below.

Photographs of experiments with density layers are shown in Figure 2. The layers were produced in a tank having transparent walls, and the upper, lighter layer was colored to facilitate observations. Figure 2A shows both layers at rest. The dark vertical streaks were obtained by dropping bits of dyestuff into the water. Figure 2B shows how these particles are transported by currents set up in the top layer. The boundary of the lower layer persists undisturbed by surface waves, as seen in Figure 2C; conversely, Figure 2D shows an internal wave causing changes in the level of the boundary of the two layers without showing on the surface. The internal waves were created mechanically and are not caused by the surface disturbance. Figures 2E and 2F show the effect of long-continued surface waves on mixing in the upper layer.

This stability of layers when the temperature gradients are negative is in marked contrast to the instability of positive temperature gradients. Returning to the experiment of warm and cold layers of water in a tank, the surface of the warm layer may be cooled by blowing a gentle stream of cold air over it. The cooling of the layer at the immediate surface causes it to become heavier than the water beneath it. Consequently it sinks and in so doing mixes with and cools the underlying water. Two thermometers at different depths in the warm layer will show that cooling proceeds nearly simultaneously at all depths, without the development of large positive temperature gradients. The mixing which accompanies cooling is called *convective overturn*.

## 4.2.4 Effects of the General Processes on Temperature Structure

### Heating

The progressive or intermittent effects of the four processes—heating, cooling, mixing, and flowing—lead to the complicated and variable conditions illustrated in Figure 4. The manner in which any one of these processes will operate individually to change the bathythermogram is shown in Figure 3. The change in temperature distribution produced by solar heating is illustrated by curves 1, 2, and 3 in Figure 3A. Initial conditions, indicated by curve 1, are assumed to be isothermal. The absorption of heat together with some mixing results in curve 2 and finally curve 3. Negative gradients extending from the surface downward are characteristic of recent heating. The negative gradients, and consequently the stability, will be greater the smaller the amount of mixing that occurs during the heating. Under these conditions, wind is the principal cause of mixing.

### Cooling

The cooling that takes place during the night and during the winter is essentially a reversal of the process of heating. Starting with curve 1 in Figure 3B, assumed to be the same as curve 3 in the preceding diagram, surface cooling with its accompanying convective overturn produces curve 2 and ultimately curve 3 and if continued for a long enough period would finally produce completely isothermal water. Although the cooling takes place at the surface, measurable positive gradients do not develop because of the mixing involved in the convective overturn. Winds hasten this mixing process, but convective overturn takes place even in very calm weather. Theoretically, the upward transfer of heat must be associated with slight positive gradients, but these are so small that they usually escape detection.

### Mixing

The result of vigorous mixing by the wind, when there is no gain or loss of heat by the surface layer, is illustrated in Figure 3C. It will be noted that in

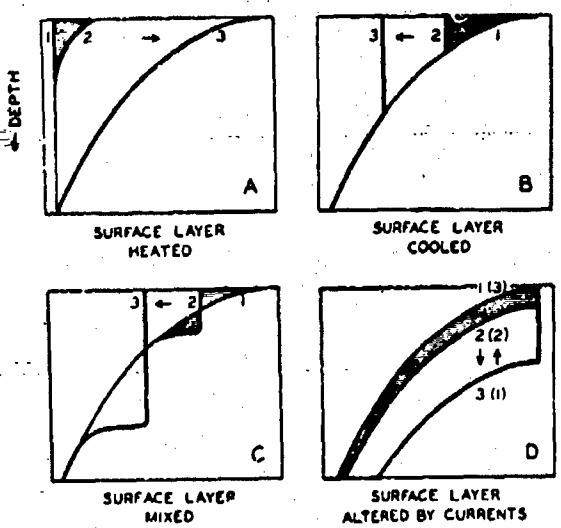


FIGURE 3. Manner in which the general processes working individually change the bathythermogram. (A) Development of negative gradient by heating of surface layer. (B) Development of isothermal surface layer by cooling. (C) Development of isothermal surface layer by mixing. (D) Effect of currents: 1, 2, 3, show development of an isothermal layer; (1), (2), (3), of a negative gradient.

this example surface isothermal layers develop just as they did in Figure 3B, and the surface temperature decreases, but the temperature distribution immediately below the mixed layer is of a different character. The wind mixes warm water with cooler water beneath it, increasing the temperature at intermediate depths, and thus produces a very sharp thermocline instead of retaining the initial gradients (as was the case when cooling was the primary cause of the mixing). Curve 1 in Figure 3C is the same as curve 1 in Figure 3B, but the result of wind mixing without cooling produces distributions quite different from those resulting from cooling alone. Obviously, conditions intermediate between those of Figures 3B and 3C will often develop, since cooling and wind mixing can occur simultaneously.

### Flowing

The effect of addition or removal of water by currents is illustrated in Figure 3D. The transfer of water can be produced by various causes, among them winds. If warm surface water is carried over the top of cooler water, a progressive change in temperature distribution may occur, as illustrated by curves 1, 2, and 3. If warm surface waters are removed, the reverse sequence may develop, that is, the one indicated by numbers (1), (2), and (3). It will be noted that the gradients remain unchanged and are merely lowered or raised. Internal waves, similar to those illustrated by Figure 12, which periodically raise and lower the thermocline, can cause similar effects in a very short time. These waves may be single or have a well-defined periodic character and are accompanied by single or periodic surges of current.

### Temperature Distribution

The processes described above all involve passage of time, that is, *continued* heating, cooling, wind mixing, or flowing produce *progressive* changes in the temperature distribution. In the sea the temperature distribution in a given locality is the result of interplay of all four processes. For a limited time, say, during one afternoon, one of them may dominate, so that it is possible to say that the temperature conditions near the surface are the result of heating, or of cooling, or of wind mixing, or of currents. The *complicated* distributions illustrated in Figure 4 are usually the result of *intermittent* action of the four general processes.

### Thermal Structure at Great Depths

It should be noted that all these processes except the flowing originate at the sea surface and that their effects are propagated to greater depths by convective overturn or mixing or both. These effects are rarely noticeable at depths greater than 600 to 700 ft. Below this level, stable stratification exists at all times, and the only changes are due to slow seasonal currents. This deep region is therefore characterized by the so-called *permanent thermocline* or negative temperature gradient, discussed in Section 2.2.[2]

The density of sea water increases with decreasing temperature down to the freezing point (about 28.5°F), which sets a lower limit for the temperature in the sea. Below 6,000 ft the temperatures everywhere are less than about 37.5°F and decrease with depth; they also decrease towards the south, where the coldest water is formed.[48] The circulation of the deep, cold water is exceedingly slow, probably of the order of 1 ft/minute. For all practical purposes the conditions in the deep sea do not change with time; they do, however, vary slightly from one region to another. In any one locality below about 3,000 ft the temperature decreases slowly and the salinity is either constant or increases slightly with depth. The effects on the velocity of sound of the oceanographic

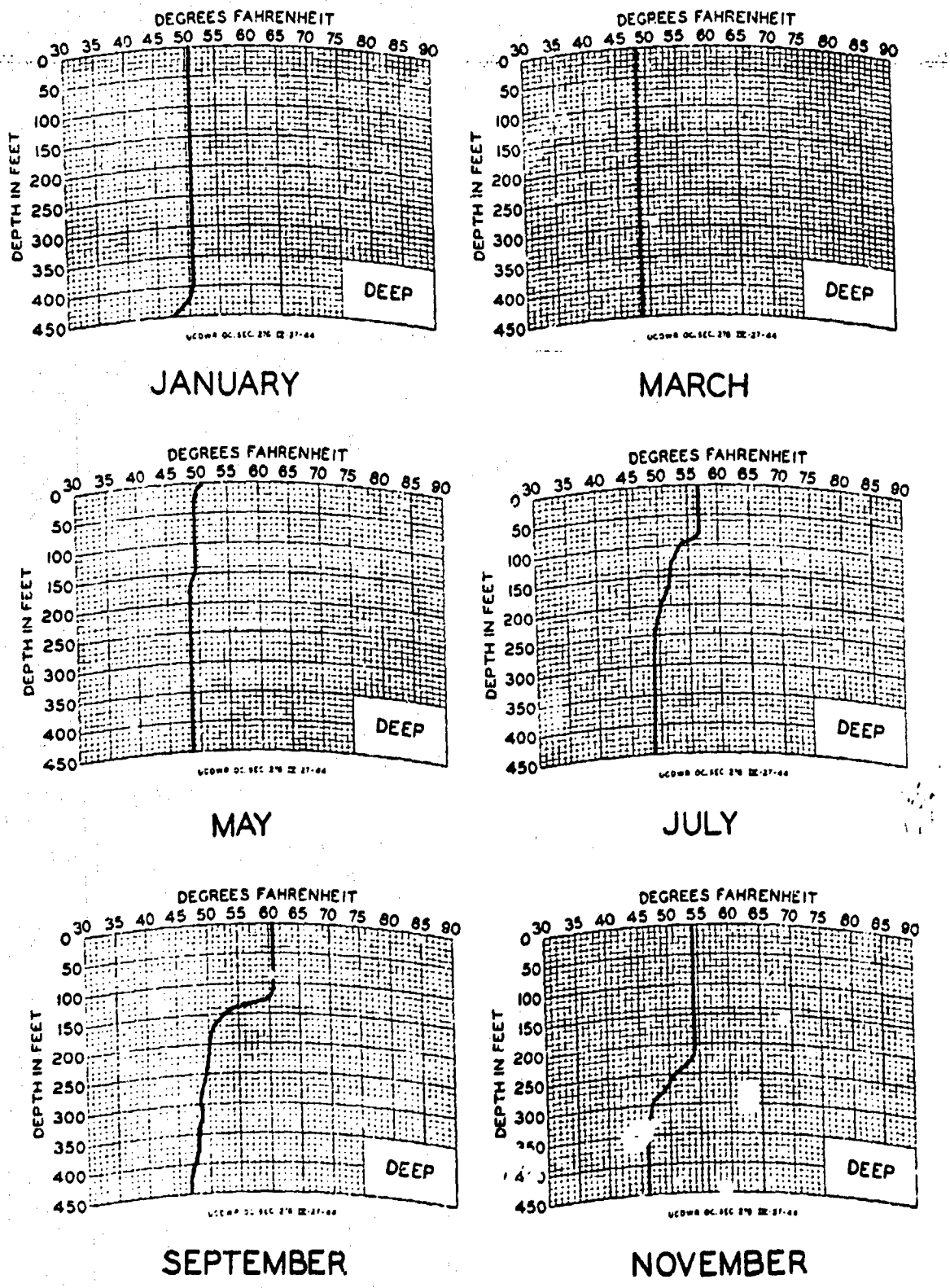


FIGURE 4. Annual cycle of ocean temperature gradients (40° N 170° W).

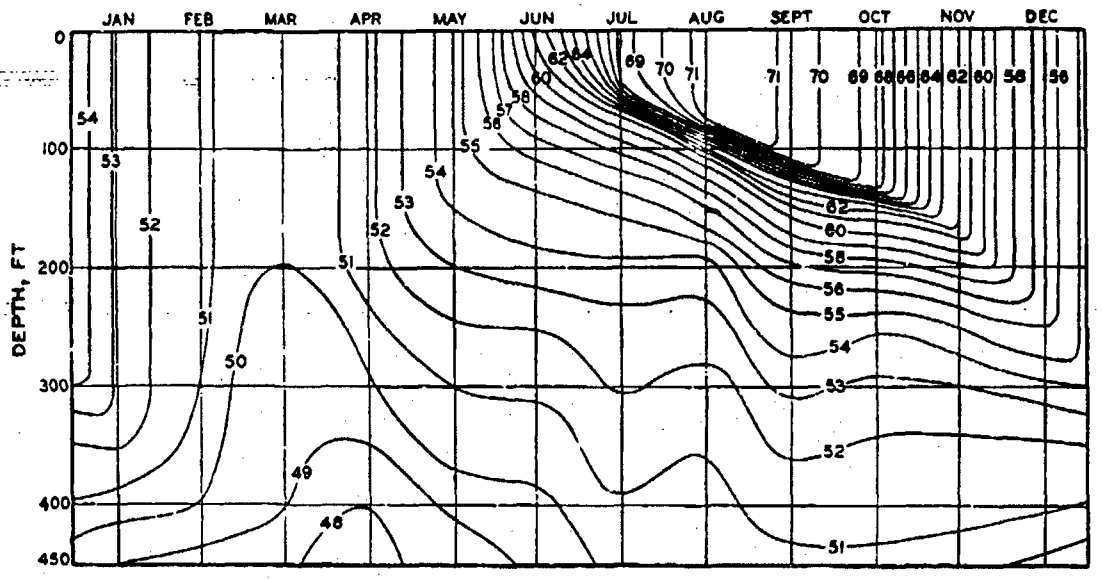


FIGURE 5. Annual cycle of temperature in the ocean. The curves show the depth at which the indicated temperature occurs at various times of the year.

conditions at great depths have been mentioned (see Sections 2.2 and 2.3.3). Transmission of sound at great depths was discussed in Chapter 3.

### 4.2.5 The Annual Cycle

In middle and higher latitudes, there is a marked annual cycle in temperature conditions. The cycle can be observed in Figure 4, which is based on bathythermograms taken in the open ocean, in latitude 40° N in the North Pacific. It is convenient first to consider conditions in March: the isothermal layer is more than 450 ft thick, and was produced by cooling and by mixing induced by winter's storms. In May some heating of the surface layers has occurred, and mixing by winds has produced an upper isothermal layer of a slightly higher temperature than the original; thus, there is a small thermocline at a depth of about 150 ft. The negative gradient at the surface probably represents heating during the day and will either be obliterated by wind mixing or disappear during the night because of cooling and convective overturn. Progressive heating continues through the summer months so that the temperature near the surface increases, as shown by the July and September bathythermograms; but wind maintains a mixed layer with a rather sharp thermocline which increases in depth as the season progresses. In the fall, cooling once more exceeds heating; the surface isothermal layer becomes cooler and, with the added effect of strong winds, the thermocline goes deeper, until in January it is below 400 ft. Cooling and mixing continue until about March.

Figure 5 is another way of summarizing the annual cycle. The curves are isotherms that show the depth at which a given temperature occurs, as a function of time throughout the year. The gradual variation of thickness of the isothermal surface layer is very apparent. The close spacing of the curves noticeable from June to November indicate steep gradients. The discussion of Figure 4 applies to this figure with minor changes, e.g., the negative gradient caused by surface heating does not become marked until early June. These differences are probably within the normal variability of the seasons.

In general, the systematic seasonal changes are subject to modification by local weather co[illegible]. The mixing of the surface layer by wind [illegible] important in this connection. In Figure [illegible] temperature decrease in the top 30 ft is [illegible] each season as a function of wind force. It [illegible] that high winds can practically obliterate the seasonal trend.

### 4.2.6 The Diurnal Cycle

The diurnal cycle in temperature conditions is in many ways a miniature replica of the annual cycle, but it must be remembered that during the spring and summer progressive heating will occur

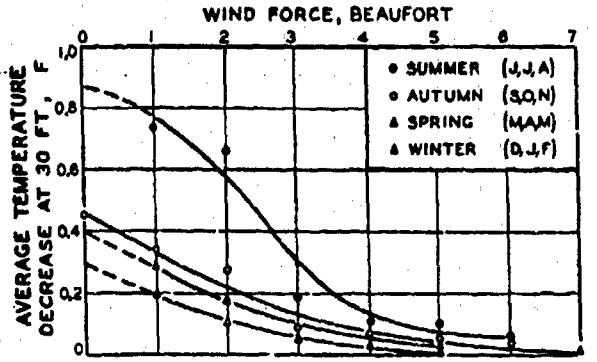


FIGURE 6. Effect of wind on average temperature gradient in surface layer during various seasons.

and that during the fall and winter there will be progressive cooling and mixing. Consequently, the daily cycle will sometimes be practically obliterated by the progress of the seasonal changes.

Four selected examples of diurnal changes are given in Figure 7. The data are from the open ocean and are based on bathythermograms taken over periods of from 23 to 48 hr during the summer months. Each set has been adjusted so that the temperature at a depth of 50 ft is used as the reference. The heating is indicated by shading.

Series A was taken during a day when winds averaged Force 3 at all times. Although heat was added to the water, the stirring action of the wind caused a mixed layer to persist near the surface throughout the day. The layer is so shallow, however, that poor sonar conditions would prevail during the afternoon. During the night, cooling and mixing resulted in isothermal conditions to a depth of 50 ft.

Series B is an example of heating on a day with light winds when negative gradients extended to the surface during the late morning and afternoon. Beginning at 1800, a mixed layer was present and cooling continued during the night. It is of interest that an observation at 0600 next morning showed a small positive gradient which had disappeared at 0800.

Series C covers a period of approximately 48 hours with variable winds. No progressive heating is noticeable and there is a return to isothermal condition each night.

Series D is an example of heating when a negative gradient existed early in the morning. The shallow isothermal surface layer had practically disappeared at noon; the gradient became progressively more pronounced during the day, and persisted during the following night.

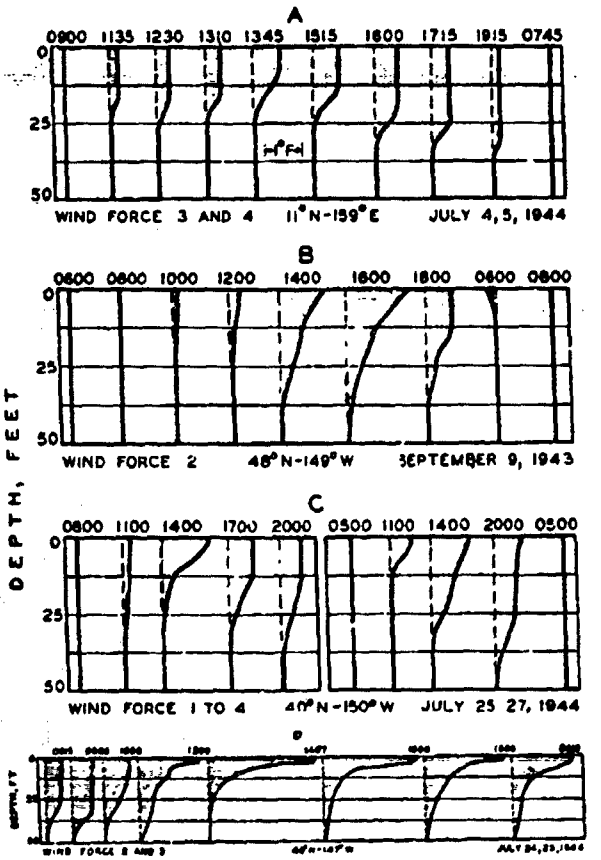


FIGURE 7. Diurnal cycle of ocean temperature gradients. (A) Persistent mixed surface layer. (B) Typical diurnal cycle with light winds. Note slight positive gradient at 0600. (C) Variable winds with changeable pattern. No progressive heating. (D) Persistent negative gradients.

As in the case of the annual cycle, high winds can obliterate the daily cycle in the upper 30 ft. This is shown by Figure 8.

## THE AFTERNOON EFFECT

In general, strong, negative surface gradients are most common in the afternoon. Because of its importance, this has been called the *afternoon effect*. The gradients reach a maximum at about 1600, and have a minimum in the morning, about 0600. They are more common during the summer months than during the winter. This is easily explained, since the solar radiation is greatest in the summer.

This simple explanation is essentially correct, but fails utterly to provide an explanation of the geographical distribution of afternoon effect. Instead of being most frequent at the equator, where solar

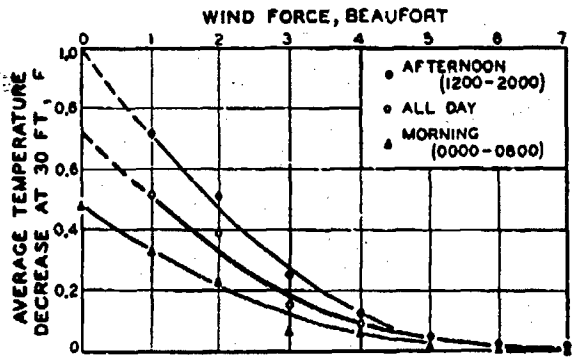


FIGURE 8. Effect of wind on average temperature gradient in surface layer at various times of day.

radiation is greatest, the afternoon effect is actually less frequent there than in high latitudes. Solar radiation is undoubtedly the primary cause of the negative surface gradients, but the magnitude of its effect is modified by the other three factors, especially wind mixing and evaporation. (See below.)

While afternoon effect in the open ocean is most frequent in high latitudes, this is not necessarily true inshore. The waters off Southern California, for example, are notorious for the prevalence of afternoon effect.

## 4.3 DETAILED ANALYSIS OF THE FOUR PROCESSES

The preceding sections have indicated the general types of temperature distribution encountered in the sea and the four major processes which affect the temperature conditions. Their causes will now be discussed.

### 4.3.1 Heating and Cooling

The temperature structure of the ocean is determined primarily by its heat content, which is a constantly varying quantity. There is a continuous exchange of heat at the surface of the ocean. The ocean *receives* heat by *absorption* of the sun's radiation and by the *condensation* of water vapor in the air, when the water is colder than the air. The ocean *loses* heat by *radiation* to the sky, by *evaporation* of water vapor when the water is warmer than the air, and possibly by conduction. Of the received heat, by far the largest quantity is due to incoming solar radiation. Over the ocean as a whole it is balanced by the cooling resulting from reradiation and evaporation. The effects of other processes are comparatively negligible.

#### INCOMING RADIATION

The incoming radiation includes the invisible infrared and ultraviolet as well as the visible light. Since it is received from the sun and sky it obviously varies with latitude, time of year, time of day, and the atmospheric conditions, particularly the cloud cover. The total energy received during the year decreases with increasing latitude, and in the lower latitudes of the tropical regions the seasonal variation is small, but with increasing latitude the difference between the amounts received during summer and winter becomes very great. The effect of clouds is very pronounced: a heavy cover of cloud may reduce the incoming radiation to less than 25 per cent of that received on a clear day.

Direct heating of the water by the sun is limited to relatively shallow depths (Figure 9). Only about 3 per cent of the radiation penetrates below 300 ft and over 50 per cent (all of the infrared) is absorbed in the first few inches. If there were no compensating heat losses and no mixing, fantastically high-surface temperatures and extremely sharp negative gradients just below the surface would occur. The penetration of light varies somewhat from place to place depending upon the amount of suspended debris and organic pigments in the water. The foregoing discussion applies to the open ocean; near shore and in areas of vigorous plant growth the water is practically opaque to all wavelengths.

In addition to the direct solar radiation, the sea surface also receives some infrared from the air. While this is an appreciable source of heat, it is customary to subtract it from the corresponding infrared radiation emitted by the sea surface.

#### EFFECTIVE BACK RADIATION

*Effective back radiation* is the term used for the excess of infrared emitted by the sea surface over that received from the air.[38] This balances somewhat less than one-half of the incoming solar radiation, on the average. It decreases with increasing water temperature and with increasing humidity and cloud cover. With heavy, low-lying clouds present, the effective back radiation drops to less than 25 per cent

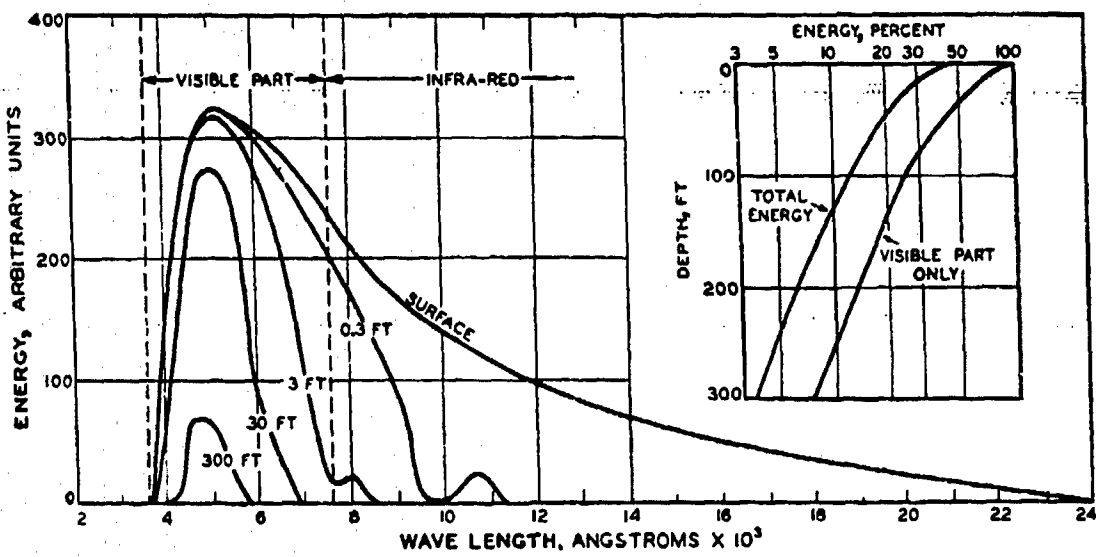


FIGURE 9. Spectrum of radiant energy at various depths in the ocean. Inset: percentage of incident radiation reaching various depths. (From: *The Oceans*, Sverdrup, Johnson, Fleming, Prentice Hall, 1942.)

of that on a clear day, largely because the clouds are themselves sources of infrared and radiate heat into the ocean on their own account. It was mentioned above that clouds prevented direct solar radiation from reaching the sea surface. Heat losses from back radiation occur in the uppermost fraction of an inch of the water and are transmitted to greater depths by convective overturn and wind mixing.

### EVAPORATION

*Evaporation* depends primarily upon the temperatures of the water and the air, the humidity and the wind strength. Evaporation can best be understood by considering the process as one of transfer of water vapor away from the surface. The greater the water-vapor gradient the more rapid the evaporation and hence the greater the heat loss. Cold, dry air overlying warm water therefore favors rapid evaporation. High winds increase evaporation by removing the water vapor.

The relative importance of the heat losses through evaporation and back radiation can be seen from the average heat budget between 70° S and 70° N.

Heat Budget of the Ocean[1]

Total heat received = 0.221 cal/cm²/min

| | |
|---|---|
| Evaporation losses | = 0.118 cal/cm²/min |
| Effective back radiation | = 0.090 cal/cm²/min |
| Conduction to atmosphere | = 0.013 cal/cm²/min |
| Total heat lost | = 0.221 cal/cm²/min |

## 4.3 2 Mixing Processes

### CONVECTIVE OVERTURN

Thus far only the cooling effect of evaporation has been considered. When surface water cools, its density increases and causes convective overturn. Equally important is the *increase in salinity* resulting from evaporation; the increased density arising from this cause contributes greatly to overturn and the development of isothermal surface layers. Thus, cooling by evaporation is even less likely to be accompanied by positive temperature gradients than is cooling by back radiation.

Conditions that tend to lessen the salinity of the surface layer would, of course, have the opposite effect, and would tend to favor the development of positive gradients. Such a condition might result from precipitation. For the ocean as a whole, however, evaporation exceeds precipitation; this is shown in Figure 10. It will be noted that regions of excess evaporation in low and mid-latitudes correspond to regions of relatively high surface salinity and deep thermoclines. Just north of the equator and in latitudes above 40°, where precipitation exceeds evaporation, the surface salinity is low.

The deficit in the water content of the ocean that is caused by the general excess of evaporation over precipitation is made up by runoff from land. Near land, and especially near the mouths of rivers, surface salinities are lower than in the open ocean,

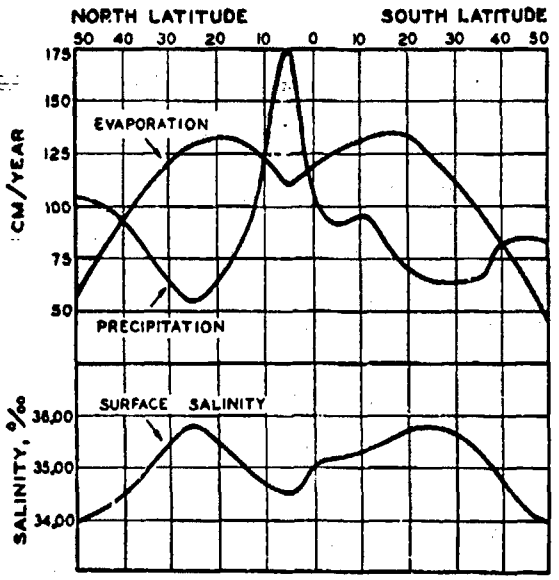


FIGURE 10. Variation of average evaporation, precipitation, and salinity with latitude. Shaded areas show regions where precipitation exceeds evaporation.

or at depth. This favors the development of positive temperature gradients, since it increases their stability.

### MECHANICAL MIXING

Mechanical mixing is caused by wind and does not necessarily involve any gain or loss of heat; nevertheless it may modify the temperature distribution, as has already been seen. The effect of winds depends not only upon their strength, but also on their duration and on the distance over which they have blown. It is quite obvious that the first effect of the wind will be confined to the immediate surface, but that the turbulence will extend to greater depths after the wind has been blowing for some time. The original density distribution of the surface layer will affect the rate at which the turbulence penetrates the layer. A very stable layer will be less easily mixed.

### EFFECT OF ROTATION OF THE EARTH

It is a remarkable fact that the daily rotation of the earth about its axis also affects the depth to which the wind mixing penetrates. A discussion of current theories [3b,4] of this effect would lead beyond the scope of this book, but all agree that a wind of given force will ultimately produce a deeper mixed layer in low latitudes than in high.

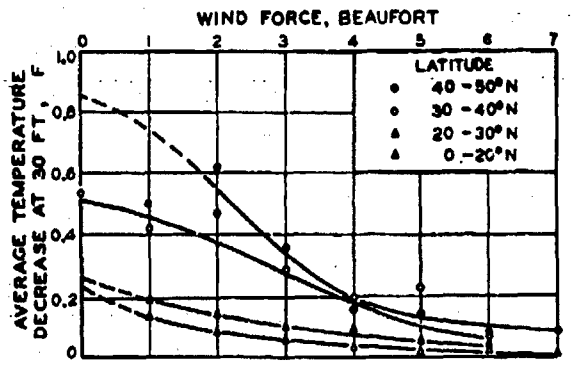


FIGURE 11. Effect of wind on temperature gradient in the surface layer at various latitudes.

This is probably part of the explanation of the data shown in Figure 11, which indicate that strong negative gradients are most apt to be formed in high latitudes. If negative surface gradients are interpreted naively as being the result of solar heating alone, this is most unexpected, since heating is greatest at the equator. The necessity of considering all four of the major processes, together with the detailed mechanisms causing them, is emphasized by this figure.

## 4.3.3 Transport by Currents

### DRIFT CURRENTS

The frictional drag of the wind sets up *drift currents* which flow at less than 3 per cent of the wind velocity. These drift currents do not flow with the wind, but are deflected 45 degrees to the right in the northern hemisphere and 45 degrees to the left in the southern hemisphere. This is caused by the earth's rotation and is closely related to its influence on the depth of mixing which was just discussed. The same sources may be consulted for details.

### PERMANENT CURRENTS

The redistribution of density resulting from the wind-drift currents in turn maintains the *permanent currents*. Under the influence of the steady wind systems, such as the trade winds in the lower latitudes and the westerlies in higher latitudes, these permanent currents form the large-scale current system of the oceans. They are thus partly the indirect result of geographic differences in the heating and cooling of the water and partly the result of wind action. The character of the currents is also influenced by the configuration of the oceans, but in general there are

clockwise gyrals in the northern hemispheres and counterclockwise gyrals in the southern hemisphere. Smaller currents related to land topography and local climate exists near the continents. A countercurrent flows eastward between the two westward-flowing equatorial currents.

The permanent currents have several effects on the temperature conditions. Currents with poleward flow tend to carry warm water into cooler regions; conversely, equatorward flow carries cool water into warm regions. Within the currents themselves the distribution of density produces a temperature gradient such that, in the *northern* hemisphere, the water on the left side of the current has a lower average temperature than water on the right side. This may be reflected by a thinner mixed layer or even by lower surface temperatures. In the *southern* hemisphere the structure is reversed.

#### Divergence and Convergence of Surface Currents

Divergence of the surface currents may occur under the influence of the wind. Examples of this effect are found along the western coasts of the continents and in the vicinity of the equator in the eastern parts of the Atlantic and Pacific. In these areas *upwelling* brings water towards the surface from moderate depths and the thermocline may be shallow or, in extreme cases, absent. The opposite effect, namely *convergence*, occurs in the center of the subtropical gyrals in the northern and southern hemispheres. In these regions the surface water accumulates and consequently the thermocline may be very deep.

#### Tidal Currents

*Tidal currents* in partially isolated, shallow areas have a marked effect on the temperature conditions because they also cause turbulent mixing. In areas of strong tidal currents, for example in the English Channel, the water may remain virtually mixed throughout the year, although there is, of course, heating and cooling of the water column as a whole.

#### Internal Waves

*Internal waves* also affect the temperature distribution. The effect of these waves is reflected in a periodic rise and fall of the thermocline. Periods as long as 12 and 24 hours are known to exist, and recent studies have shown that waves of only a few minutes period may occur. Whether there is a continuous spectrum of frequencies is not known. An example of the effects of internal waves on temperature structure is shown in Figure 12.

## 4.4 GEOGRAPHICAL VARIATIONS

### 4.4.1 Dependence of the Annual Cycle on Geographical Location

The annual cycle in temperature conditions represents the net effect of the annual sequence in the various factors described, particularly in the amount of radiation received, the heat losses associated with evaporation, and the character of the prevailing winds. In low latitudes where these factors do not vary appreciably there is little change in conditions throughout the year, except that near the continental boundaries changing monsoon winds may introduce variable conditions.

It is in the latitudes of 40° to 50° that the annual cycle is most conspicuous. This is to be expected, since in these regions the surface experiences the greatest range of temperature. The effects of this great variation in temperature are magnified by the fact that in winter the cooling due to low temperatures is increased by the greater evaporation that occurs at this season; the resultant increase in the density of the surface water facilitates mixing and thus contributes to the seasonal variation. The typical cases shown in Figures 4 and 5 illustrate this point; they are based on observations in the open ocean in an area of relatively strong winds, far from land and where salinity changes are relatively small. The annual cycle is even more pronounced in regions near land, or in areas where heavy precipitation occurs and light winds are prevalent during the spring and summer. These conditions tend to induce even more extreme negative gradients than those shown in Figure 4. This can also be observed generally in areas of flow towards the equator, in which cool water is being heated; an example of this is the region off the California coast.

### 4.4.2 Dependence of the Diurnal Cycle on Geographical Location

The diurnal change in temperature gradients is essentially similar in principle to the annual cycle,

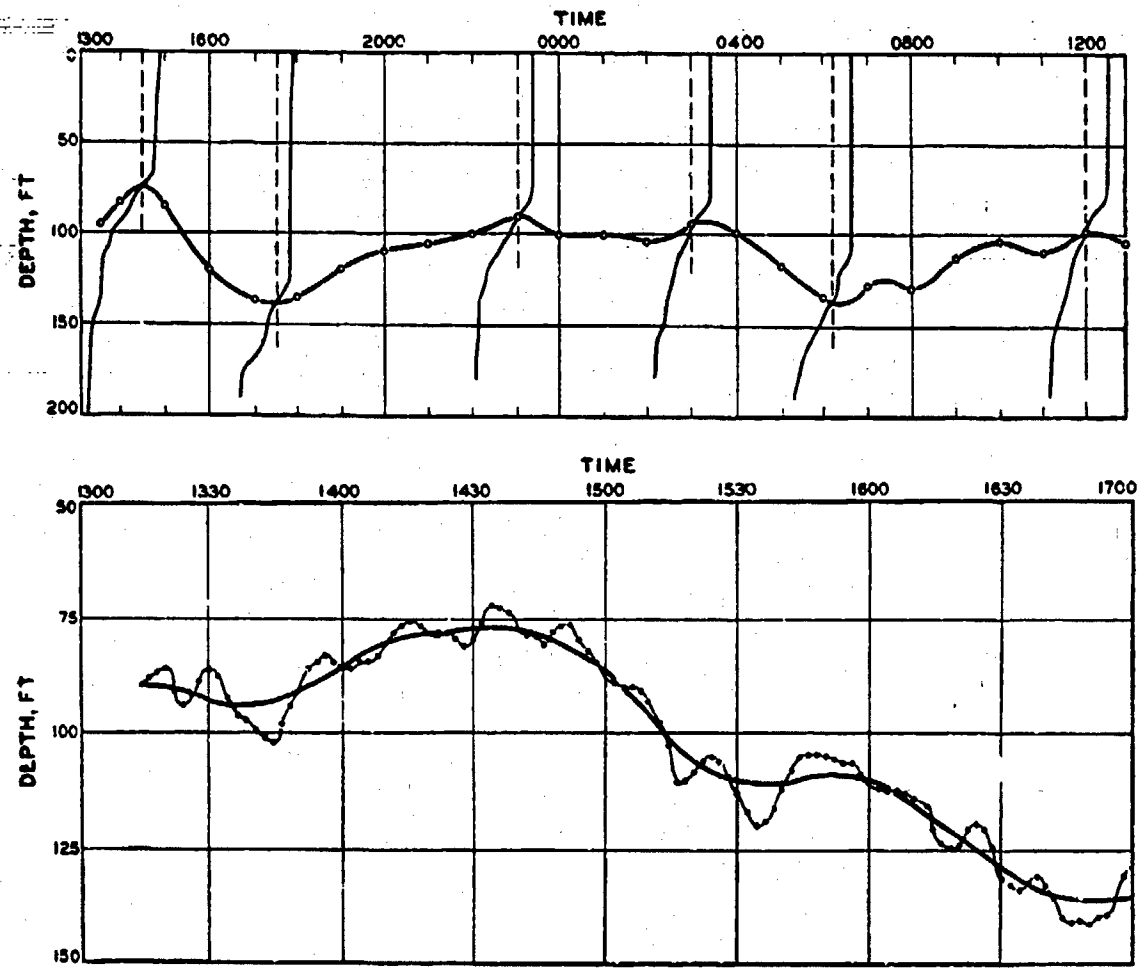


FIGURE 12. Effects of internal waves on temperature structure. (A) Internal waves shown by the progressive variation of depth at which a given temperature exists. The experimental points are plotted at the depths at which the middle of the thermocline occurred, as indicated by the vertical dotted lines adjacent to the bathythermograms. (B) Internal waves from bathythermograph readings at 2-minute intervals, and the smoothed curve.

but the temperature changes are smaller and do not extend to such great depths. The incoming solar radiation depends upon latitude, time of year, time of day, and the cloudiness. The diurnal cycle of incoming radiation changes during the year, the variation being least near the equator and increasing towards the poles. Above the polar circles, of course, there are days of complete darkness during the winter and continuous daylight during the summer. It should be recognized that the diurnal change is not necessarily cyclic, as is the annual change, and that progressive heating or cooling of the water will be characteristic in middle and high latitudes. Within the tropics where the annual variation is small, the diurnal changes are more nearly cyclic.

Even if the total heat absorption be the same, the character of the changes in temperature gradients may be quite different, since these depend upon the previously existing gradients and on the wind conditions. A negative gradient near the surface will be increased by incoming heat unless a strong wind (force 4 or greater) springs up. On the other hand, the changes in an initially mixed (isothermal) layer will depend critically upon the wind strength. Development of surface gradients is common when the wind force is 3 or less but is rare with winds above force 4 (see Figures 6, 8, and 11). In the tradewind belts, therefore, development of surface gradients during the day is a rather rare condition; this is probably another factor to be considered in explaining Figure 11.

443 ## Summary

The regional differences in temperature structure can be explained in terms of the factors described.

The discussion can be summed up as follows:

An *isothermal layer near the surface* is the result of mixing. The factors inducing mixing are (1) wind, (2) radiative cooling, (3) evaporation, with its consequent cooling and salinity increase.

Strong *negative gradients* are the effect of heating a stable surface layer, without much wind mixing. Strong winds may more or less prevent the formation of negative gradients.

*Positive gradients* are produced only in areas where cool, dilute water flows, or is formed, on top of warm, more saline water. Measurable positive temperature gradients are most common during the fall and winter months in the northwestern Atlantic and Pacific oceans, where cold, dilute coastal waters are driven offshore by the wind and flow over the warm but saline ocean water of higher density.

Chapter 5

# ECHOES, SCATTERING, AND REVERBERATION

## 5.1 THE GENERAL NATURE OF REVERBERATION IN THE SEA

When a short tone pulse is sounded in a large, empty room, the sound echoes and re-echoes from the walls, ceiling, and floor for a considerable time. This phenomenon is called reverberation. It has been studied extensively by acoustic engineers, because it interferes with the understanding of speech and the enjoyment of music. Suitable wall covering deadens the room and eliminates reverberation.

When an echo-ranging pulse of sound is emitted into the ocean, a very similar phenomenon is observed, and the name "reverberation" was early applied to it. However, while the ocean has a floor and a ceiling, it lacks the four walls of a room, and both the laws and the causes of underwater reverberation are somewhat different.

Theoretically, if the sea surface and bottom were mirror-flat and if there were no suspended matter (including fish) in the water, there would be no reverberation. Every departure from these ideal conditions results in an echo, usually a very weak echo. However, there are very many irregularities on the ocean bottom, and each wavelet on the surface probably contributes its individual echo. The combined result is a scattering of sound in all directions. Some of this scattered sound comes back to the transducer, and is heard in the sonar loudspeaker. It is the reverberation.

Reverberation is therefore to be considered as the resultant of a large number of very weak echoes. Some of the targets producing these echoes are not very obvious nor is very much known concerning them. They may be air bubbles, suspended solid matter, organic matter such as plankton and the fish feeding on plankton, or minute inhomogeneities in the thermal structure. On the other hand, minor irregularities of the ocean bed are very effective scatterers, and when the sound beam strikes the bottom reverberation is very high. The surface waves undoubtedly contribute appreciably to it.

Reverberation is easily distinguished from extraneous noise because it is a tone of fairly definite pitch, whereas noise has a wide band of frequencies. The individual echoes mentioned above as forming the reverberation are not perceptible as such; they overlap each other in time, causing marked fluctuations in the intensity. If the signal is of constant frequency, transmitted horizontally, it is succeeded by a quavering, ringing tone of rapidly decreasing loudness, interspersed with very occasional bursts of sound that might be mistaken for echoes by an inexperienced observer. In shallow water a crescendo effect may be perceived after a certain interval due to sound scattered backward by the bottom.

If relatively long pings (of about 200-msec duration) of constant frequency are used, reverberation has a musical sound. With shorter pings, the musical character disappears; although pitch can still be distinguished, the tone becomes rough and grating.

When a frequency-modulated signal is used, the reverberation is quite accurately described by comparing it to the clatter made by coal sliding down a metal chute. Some frequency modulation may occur because of improper functioning of the sonar oscillator. If the reverberation from long pings of supposedly constant frequency is not musical, the oscillator should be examined by a competent maintenance man.

The pitch of the reverberation from a constant-frequency ping depends on the speed of the echo-ranging vessel and the relative bearing of the projector.

While this description of reverberation has been linked to the operation of echo ranging, the phenomenon occurs whenever sound is transmitted through the sea. The reverberation "tails" visible on Figure 52 of Chapter 3 have already been mentioned and will be more fully discussed below.

The mechanism of scattering or reverberation, and the mechanism of echo formation are very similar. It is convenient to discuss them at the same time.

In the sections that follow we shall consider first the formation of echoes and then apply the principles to echoes from small solid and liquid particles and from bubbles, and we shall also devote some attention to the scattering of sound from nonspherical objects (Section 5.2). This will be followed by an empirical discussion of reverberation in the ocean (Sections 5.3 and 5.4).

## 5.2 THEORY OF SCATTERING BY SINGLE PARTICLES

### 5.2.1 Elementary Theory of Echo Formation

When a sound wave passes over an obstacle suspended in the medium, the latter is set into vibration and becomes a secondary source of sound. The amplitude of the vibration is proportional to the amplitude of the primary sound, and consequently the intensity of the secondary sound is also proportional to the primary intensity.

The simplest case to consider is that of an object like a submarine or a large fish, with dimensions which are large compared to the wavelength of the sound. This intercepts a certain amount of sound and casts an acoustic shadow. The intercepted power is reradiated as the secondary sound or, as it is more usually called in this case, the echo.

#### Target Area

The amount of power intercepted is determined by the *target area* of the obstacle. For the present, the target area may be defined in a picturesque manner by imagining a shadow cast by the obstacle to fall on a plane perpendicular to the sound rays. The shaded area is the target area $\sigma$. In the case of a sphere of diameter $d$, for example, it follows that the target area would be a circle of area

$$\sigma = \tfrac{1}{4}\pi d^2. \tag{1}$$

In the case of irregular objects, the target area will depend on the direction from which the sound is incident.

Let $F$ be the energy flow (in w unit area) at the obstacle and $W$ the total power intercepted. Then

$$W = F\sigma. \tag{2}$$

If the target is perfectly reflecting, all this energy is reradiated as sound. If the target is not perfectly reflecting, only a fraction, $\varkappa$, of this energy will be reradiated. Thus the secondary sound power will be

$$W_s = F\varkappa\sigma. \tag{3}$$

The effect of absorption is thus the same as if the target area were reduced in the proportion $\varkappa$. This secondary sound is radiated in all directions, though not necessarily equally in all directions.

A large rigid plane would reflect the secondary sound into a single direction, like a mirror; such mirror-like targets almost never occur in the sea. The sea surface is perhaps the closest approach to such a target, but even the sea surface has properties different from those commonly associated with a mirror. It may be sufficient to recall the way in which the sun and moon are reflected by the sea surface; it reflects supersonic sound in an analogous manner.

A sphere reradiates the sound equally in all directions and is thus the simplest case to treat. It may seem that the existence of a shadow is in contradiction to this statement; however, at great distances from the sphere, diffraction causes the shadow to disappear. Consequently, the statement is strictly correct only at a considerable distance from the spherical target. This is discussed in detail in the appendix to this chapter.

At a great distance $r$ the power $W_s$ that is reradiated from the target, flows through the whole area $4\pi r^2$ of an imaginary spherical surface centered at the target. Hence the energy flow of the secondary sound is

$$F_s = \frac{F\varkappa\sigma}{4\pi r^2}, \tag{4}$$

or, in the case of a sphere

$$F_s = \frac{F\varkappa d}{16r^2}, \tag{5}$$

If the target is not spherical, it will radiate more sound in some directions and less in others than is predicted by equation (4). But this equation will still be valid, on the average. The target area $\sigma$ already depends on the direction of the incident sound; by a slight generalization, we may consider it also to depend on the direction in which the sound is scattered and on the reflecting properties of the target as well and thus take into account these variations of $F_s$ with sound direction and target reflectivity. Target area is then defined by the equation

$$F_s = \frac{F\sigma}{4\pi r^2}, \tag{6}$$

and the picturesque definition given above no longer applies. This abstract definition of $\sigma$ is the more useful of the two.

#### Intensity of the Scattered Sound

Since the energy flow $F$ is in this case proportional to the intensity $I$ ($= p^2$) (see Section 1.2), equation (6) may also be written

$$I_s = \frac{I\sigma}{4\pi r^2}. \tag{7}$$

It should be noted that, in this equation, $r$ is the distance from the target to the point at which the scattered intensity is being calculated. The primary intensity itself, $I$, will depend on $r'$, the distance from source to target, and in the general case $r'$ will not equal $r$. Neglecting refraction (this has been implicit in all of the above), equation (11) of Section 1.2 is applicable:

$$I = \frac{I_1}{r'^2}.$$

Therefore

$$I_s = \frac{I_1 \sigma}{4\pi r^2 r'^2}. \tag{8}$$

If the echo is received at the source of the sound, as in practical echo ranging, $r = r'$, and hence

$$I_s = \frac{I_1 \sigma}{4\pi r^4}. \tag{9}$$

### Echo Level and Target Strength

The echo intensity is generally measured at the source, in decibels; this is called the *echo level* $E$ and is defined by

$$E = 10 \log I_s. \tag{9a}$$

Taking logarithms of both sides of equation (9),

$$E = L_1 + T - 40 \log r, \tag{9b}$$

where

$$L_1 = 10 \log I_1,$$

and

$$T = 10 \log \left(\frac{\sigma}{4\pi}\right). \tag{9c}$$

The quantity $T$, defined in this way, is called the *target strength* of the scatterer. It gives a quantitative idea of the reflecting characteristics of the target and is a very useful concept.

## 5.2.2 Echoes from Small Particles

The phenomenon of scattering or reverberation differs from echo formation only in that it results from the action of many relatively small targets rather than from one large target. The action of a single scatterer can still be described by equation (9).

The picturesque definition of target area fails completely when the scatterer has dimensions which are less than the wavelength of the sound. The target area, or the *effective cross section*, of small solid or liquid particles is much less than their actual cross section, in a ratio which is roughly $(\pi d/\lambda)^4$, $d$ being the diameter of the particle and $\lambda$ the wavelength of the sound. This result was first obtained by Rayleigh but has since been studied by many others. The effective cross section also depends on the density and elasticity of the particle and the medium.

Figure 1 illustrates the variation of target area with wavelength for the two extreme cases of a heavy, rigid sphere and an air bubble. The ratio of the target area $\sigma$ to the actual cross-sectional area $4\pi d^2$ is plotted as a function of $\pi d/\lambda$, which is the ratio of the circumference of the scatterer to the wavelength of the sound. When the latter is greater than 2, both curves coincide and show oscillations about the mean value of unity for the ratio $\sigma/\frac{1}{4}\pi d^2$.

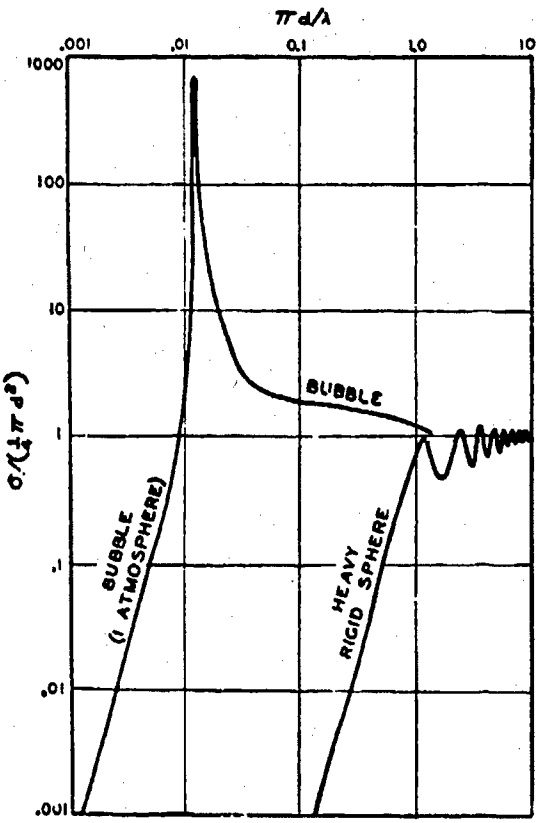


FIGURE 1. Variation of target area with wavelength, in the case of small bubbles and heavy, rigid spheres. The ratio of the target area $\sigma$ to the actual cross-sectional area $\frac{1}{4}\pi d^2$ is plotted as a function of the ratio of the circumference of the scatterer $\pi d$ to the wavelength $\lambda$ of the sound.

Where $\pi d/\lambda$ is greater than 10, both curves indicate that the target area is practically equal to the actual area. For values of $\pi d/\lambda$ less than unity, the two curves differ markedly.

In the case of a heavy, rigid sphere, the graph slopes off sharply when $\pi d/\lambda$ is less than unity. The graph for a gas bubble first rises to a very large value, reaching a maximum at a value of $\pi d/\lambda = 0.012$, and then drops rapidly for smaller values. This difference in the behavior of bubbles and other scatterers will be discussed in detail in the next two sections.

## 5.2.3 Target Area of Small Solid or Liquid Scatterers

The equation of the lower part of the curve for a heavy, rigid sphere was worked out by Rayleigh.[4] It is

$$\frac{\sigma}{\frac{1}{4}\pi d^2} = \frac{4}{9}\left(\frac{\pi d}{\lambda}\right)^4 (C_0^2 + \tfrac{3}{4}C_1^2), \qquad (10)$$

where

$d$ = diameter of sphere,
$\lambda$ = wavelength of sound,
$C_0$, $C_1$ = constants depending on the density and elasticity of the particle. (See Table 1.)

TABLE 1. Values of the parameters $C_0$ and $C_1$, equation (10), for various substances when suspended in sea water.

| Substance | $C_0$ | $C_1$ |
|---|---|---|
| Iron | 0.99 | 0.81 |
| Clay | 0.93 | 0.50 |
| Granite | 0.98 | 0.57 |
| Marble | 0.94 | 0.53 |
| Wood (balsa) | −3.5 | −0.50 |
| Wood (ironwood) | −0.87 | −0.25 |
| Turpentine* | −0.43 | −0.07 |

* Included as an example of an organic liquid, without implying that it might occur in the ocean.

For simplicity, only the average value of $\sigma$ is given, and the dependence on angle is ignored. The value of the factor

$$\tfrac{4}{9}(C_0^2 + \tfrac{3}{4}C_1^2)$$

is not much different from unity for most substances. Table 1 lists the values of $C_0$ and $C_1$ for several substances, and it is seen that only balsa wood and turpentine provide exceptions to this statement. In the case of the former, the factor is somewhat greater than unity, in the case of the latter, somewhat less. Thus, for a given diameter and wavelength, the equation shows that a balsa-wood sphere scatters about ten times as much sound power as a clay sphere, while a globule of turpentine scatters only about one-sixth as much as the clay.

The scattering power of a small object is much more profoundly affected by its size and the wavelength of the sound. For 24-kc sound, $\lambda = 3$ in., approximately. Hence a sphere greater than 30 in. in circumference will have a value of $\pi d/\lambda$ that is greater than 10. The graph shows that such a sphere will have a target area equal to its actual cross section. Rayleigh's equation will apply only to spheres with a circumference less than 3 in. A simple calculation shows that the target area of a sphere 0.3 in. in circumference will be only one-millionth that of a sphere 3 in. in circumference. This is also the ratio of the sound power scattered by the two.

A small sphere will scatter less sound of long wavelength than of short. For example, the wavelength of 2.4-kc sound is ten times that of 24-kc sound; the equation shows that a small, solid sphere will therefore scatter 10,000 times more sound of 24-kc frequency than of 2.4-kc frequency. This marked dependence on frequency is very characteristic of scattering by small objects.

## 5.2.4 Target Area of Bubbles

It is difficult to understand how bubbles can exist permanently in the sea, since sea water is not saturated with air except very near the surface. There are several obvious sources of intermittent bubble formation: whitecaps; the breaking of the bow wave, which causes bubbles to be washed under a ship and into its wake; the rotation of the propellers of ships or submarines, even when the latter are submerged. There are thus occasions when air or vapor bubbles might be expected to exert an appreciable influence on the transmission of sound. This was first investigated by H. F. Willis, of H. M. A/SEE. The discussion and the equations which follow are based on work of the staff of CUDWR.[5,6]

A gas bubble is much more compressible than the surrounding water. Under the influence of a sound wave, it will therefore pulsate with a relatively large amplitude. In order to follow the pulsation, the water immediately surrounding the bubble must oscillate with an amplitude considerably greater than that of

the water at a distance. The mass of this surrounding water coupled with the compressibility of the air results in resonance at a frequency $f_0$ which depends on the diameter of the bubble $d$ and on the average pressure $P$ of the gas in the bubble. The dependence on $P$ arises because the compressibility of a gas depends on its pressure. An approximate formula for the resonant frequency is

$$f_0 = \left(\frac{3P}{\rho\pi^2 d^2}\right)^{\frac{1}{2}}, \tag{11}$$

$\rho$ being the specific gravity of the medium. When $f_0$ is in kilocycles, $d$ in inches, and $P$ in feet of water this becomes

$$fd = 0.02P^{\frac{1}{2}}. \tag{12}$$

For example, at a depth of 66 ft, $P = 100$, since the atmospheric pressure at the surface of the sea is about 34 ft of water. Hence, at this depth, $f_0 d = 0.2$. A 1-in. bubble thus resonates at 0.2 kc and a 0.01-in. bubble at 20 kc. For a bubble at the surface, $P = 34$ ft, so that $f_0 d = 0.12$. Since frequency is inversely proportional to wavelength, this is equivalent to the equation

$$\frac{\pi d}{\lambda_0} = 0.012,$$

where $\lambda_0$ is the wavelength corresponding to the resonant frequency $f_0$.

The graph for bubbles in Figure 1 shows a sharp maximum just at this value; it is caused by the high amplitude with which the bubble vibrates when sound of the resonance frequency is incident on it.

The sharpness of the resonance peak of the bubble is determined by a parameter $Q$, analogous to that familiar in the theory of electrical circuits. The value of this parameter cannot readily be calculated, but is certainly less than $\lambda_0/d$. Experiments by Carstensen and Foldy indicate that the empirical formula

$$Q = \frac{17.5}{1 + f/10} \tag{13}$$

is valid in the range $f = 5$ to 35 kc.[7]

For sound frequencies near resonance, the effective cross section of a bubble becomes very large ($\sigma = \pi d^2 Q^2$, approximately) and may approach $\lambda_0^2$. Thus at a depth of 65 ft a bubble 0.01 in. in diameter has a target area of several square inches for 20 kc sound. This surprising result comes about because of the high amplitude of oscillation of the bubble, which causes it to reradiate a large amount of secondary sound. It is difficult to calculate the exact value of the effective cross section for the resonance frequency, and experimental evidence is not exact.

For frequencies more than an octave above resonance, the target area is about equal to the actual cross section of the bubble.

For frequencies more than an octave below resonance, the target area is considerably less than the actual cross section, and can be approximately calculated from equation (8) with

$$C_0 = -450P, \qquad C_1 = -2.0. \tag{14}$$

Comparing these values with those of Table 1, it is seen that gas bubbles scatter low-frequency sound considerably more effectively than do solid particles of the same size. This is also shown by Figure 1.

## 5.2.5 Target Area of Nonspherical Objects

The mathematical investigations just discussed have been confined to the case of spheres. Their extension to nonspherical objects is not simple, but has been carried out for some cases.[7] It is clear that the same general laws will govern the more general shapes. For example, a fish that is not too flat or elongated will cast a shadow roughly equal in area to that of a sphere of the same volume. This estimate may be in error by a factor of 2 or 3, but it is unlikely to be in error by a factor of 10. Another uncertainty in the calculation is caused by our ignorance of the reflection coefficient. This will depend largely on the compressibility of the fish. If the fish has a swim bladder (air cavity) this will probably be the most effective portion in reflecting sound. Similar remarks apply to kelp and other forms of marine life. As is well known, these plants have gas-filled floats, and are therefore very good reflectors of sound.

The bottom is especially important in the production of reverberations. Boulders, pebbles, shells, coral, etc. are all potential scatterers of sound. A smooth sand or mud bottom will theoretically behave more or less like a mirror, and scatter little sound back to the source. The experimental facts in this connection will be discussed below.

The waves on the sea surface will also act more or less like separate targets. The large surfaces will reflect supersonic waves more or less like curved mir-

rors. The effect of the smaller ripples is not clearly understood, but they will probably scatter the sound more or less equally in all directions.

## 5.3 THEORY OF REVERBERATION

### 5.3.1 General Ideas of the Theory

None of the small scatterers just discussed would return an appreciable echo by itself. As has been indicated, it is the simultaneous reception of the echoes from a large number of them that constitutes what we call reverberation.

#### Train Length

To understand the manner in which the scatterers cooperate in producing reverberation, one must consider the manner in which a pulse of sound (a "ping") is propagated. If the duration of the pulse is $t_0$ seconds, it will consist of a train of waves whose total length is $ct_0$, $c$ being the velocity of sound. This distance will be called the *train length* of the pulse. Since $c = 1{,}600$ yd/sec, approximately, a pulse of duration 0.1 sec ( = 100 msec) will result in a wave train 160 yd long. If the frequency is 24 kc, there will be $24{,}000 \times 0.1 = 2{,}400$ complete waves in the train.

#### Ping Length

One-half the train length is called the *ping length*; a pulse lasting 0.1 sec thus has a ping length of 80 yd. The ping length is a more useful concept than the train length, for two reasons. In echo ranging, the time required for the pulse to travel from projector to target and back to the receiver is measured. The clock is the range dial and is calibrated in terms of the range of the target that returned the echo, not in terms of seconds. If a target is at range $r$, the travel time is $2r/c$. Therefore, if the echo is a pulse of duration $t_0$, the range indication will increase by the amount $r_0 = ct_0/2$ during the reception of the echo. This is just the ping length as defined above.

In the second place, if there are many targets or scatterers, the echoes that are heard simultaneously come from those scatterers for which distances from the sonar differ by less than $r_0$. At a given instant, therefore, echoes will be received from all scatterers that lie in a spherical shell, with a thickness $r_0$, as shown in Figure 2. At this instant, the actual train of waves will no longer be passing over this particular lot of scatterers; it will have moved onward during the time the echoes were returning to the sonar. The instantaneous relation between the volume $A$, from

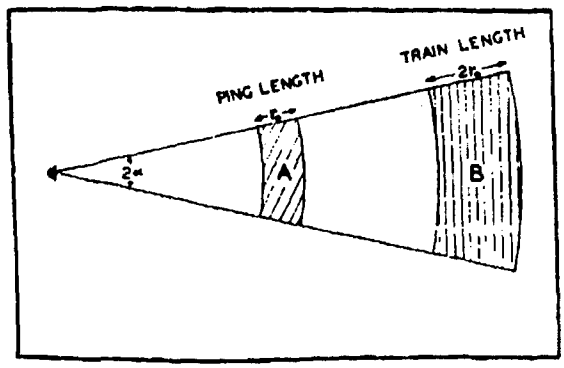


FIGURE 2. Diagram showing the instantaneous relation between the regions from which echoes are being heard ($A$) and the volume occupied by the wave train ($B$), in the case of a beam whose angular half width is $\alpha$ radians.

which the echoes are being heard, and the volume $B$ that is occupied by the wave train, is shown in Figure 2.

This figure also shows graphically how the ping length and train length are related. Very little further reference will be made to the train length, as almost no interest centers on the region $B$. On the contrary, frequent reference to region $A$ will be needed, and these will bring with them references to the ping length.

### 5.3.2 Intensity of Volume Reverberation

The effect of scatterers suspended in the volume of the sea can now be calculated. Consider the simplest possible case:

1. There are $N$ scatterers per unit volume.
2. Each scatterer has the target area $\sigma$.
3. The sonar has a sharply defined beam of half-width $\alpha$, its directivity pattern being as shown in Figure 3.
4. The sonar is in such a place that all effects of surface and bottom can be ignored.

The intensity of the echo from a single scatterer will be given by equation (9), provided it is in the beam, and will be zero otherwise. There will be many scatterers in the active shell (region $A$, Figure 2) at any instant. If $V$ is the volume of this region, the

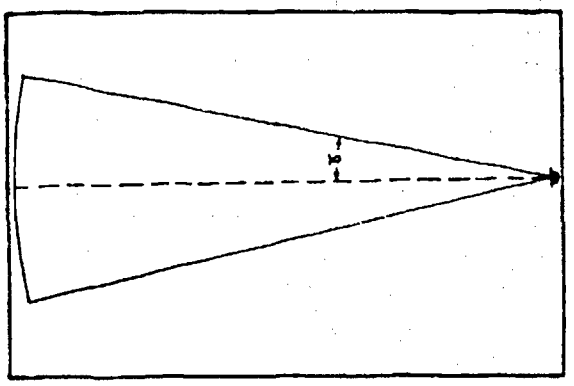

FIGURE 3. Diagram illustrating an ideal beam pattern of half width $\alpha$. The dotted line represents the axis of the beam.

number of scatterers whose echoes are being received will be $NV$. Combining this with equation (9), the intensity of the reverberation will be

$$I_R = \frac{I_1 NV\sigma}{4\pi r^4}. \tag{15}$$

Now the volume $V$ is easily calculated. It is given approximately by

$$V = 2\pi r^2 r_0 (1 - \cos \alpha), \tag{16}$$

where $r$ is the range to the center of region $A$. Hence finally

$$I_R = I_1 \frac{(N\sigma r_0)(1 - \cos \alpha)}{2r^2}. \tag{17}$$

A number of conclusions can be drawn from this equation, as will be seen in the following chapters. A brief list of the simpler conclusions follows.

1. The reverberation intensity $I_R$ is proportional to the source intensity $I_1$: increased sound output increases the reverberation.

2. The reverberation is proportional to the ping length $r_0$: a long ping causes more reverberation than a short one (see Figure 4).

3. Since $(1 - \cos \alpha)$ increases as $\alpha$ increases, it is seen that a broad beam causes more reverberation than a narrow one. In general, doubling the width of the beam will cause $I_R$ to increase about fourfold.

4. The (volume) reverberation intensity varies inversely as the square of the range $r$; this should be compared with equation (9), which shows that the echo from a single target varies inversely as the fourth power of $r$. The reason for the difference is the increase in the active volume $V$ (region $A$) as $r$ increases.

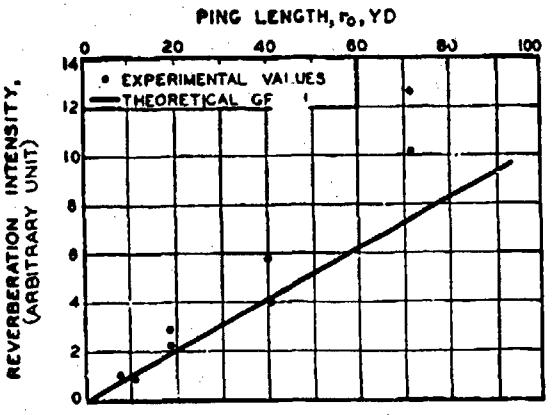


FIGURE 4. Data showing relation between ping length and reverberation intensity. If the latter were strictly proportional to the ping length, the dots would lie on the solid curve.

## 5.3.3 Intensity of Surface and Bottom Reverberation

The theory of volume reverberation, as presented in the previous section, requires only slight modifications when the scatterers are located on either the surface or the bottom. These two cases are, in many ways, identical. Instead of an active volume $V$, one

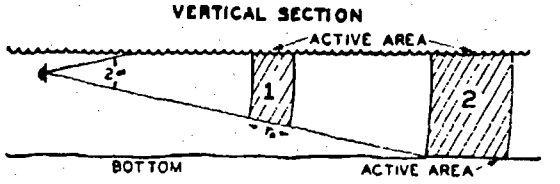


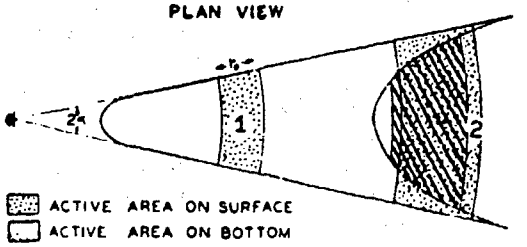


FIGURE 5. Similar to Figure 2, showing active areas on surface and bottom for two different positions of the wave train.

must deal with an active area $A$, namely, the area of the intersection of the surface (or bottom) with the region $A$ of Figure 2, already discussed. In Figure 5,

two successive locations of the active volume are shown. Until the beam intersects the bottom, there is no active area on the bottom; at position 1, there is an active area on the surface, but none on the bottom. After some time, position 2 is reached and there is an active area on the bottom as well as on the surface. The figure is drawn for the case of a sonar mounted on a surface vessel; if the sonar were on a submarine near the bottom, the situation would be reversed. Note that at very short range there is no active area on either bottom or surface; this is shown in greater detail by Figure 6.

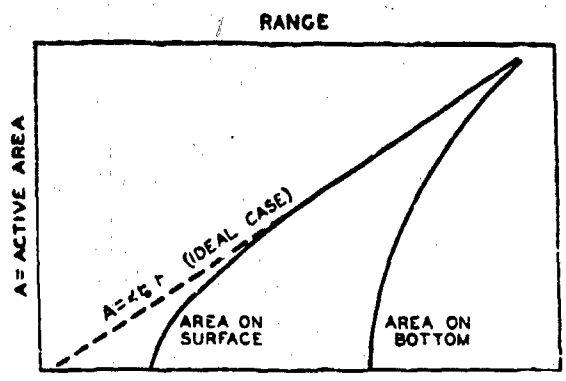


FIGURE 6. Graph showing variation of active areas on surface and bottom as a function of range, for the case where the projector is very close to the surface.

The mathematical expressions for the active areas are rather complicated, except in the special case that the projector is very close to the surface. Then

$$A = 2\alpha r_0 r, \tag{18}$$

where $\alpha$ is to be expressed in radians. The graph of this equation is shown as a dotted line on Figure 6. The departures at short ranges are obvious.

It will be assumed, for simplicity, that there are $N'$ scatterers per unit of active area and that each scatterer has the target area $\sigma$. Then the intensity of reverberation is [compare equation (15)]

$$I_R = \frac{I_1 N' A \sigma}{4\pi r^4}. \tag{19}$$

If the range $r$ is great enough so that equation (18) can be used for $A$,

$$I_R = \frac{I_1 N' \sigma r_0 \alpha}{2\pi r^3}. \tag{20}$$

Conclusions (1) and (2) given above apply to this equation also. The third conclusion requires only slight modification, because $(1 - \cos \alpha)$ is replaced by $\alpha$. Consequently, doubling the width of the beam increases surface reverberation only by a factor of two rather than four. Finally, surface reverberation varies inversely as the third power of the range, while volume reverberation varies as the inverse second power.

If the range is not great enough so that equation (18) can be used, somewhat more elaborate calculations are needed. The first three conclusions concern-

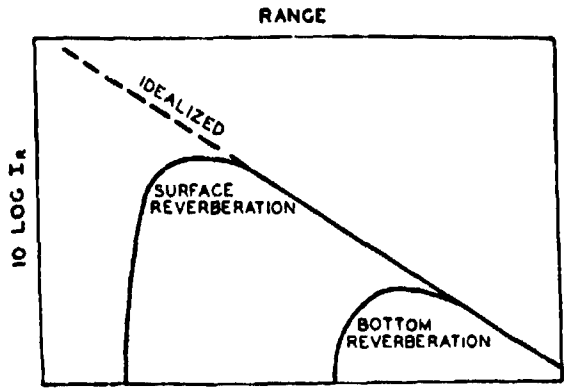


FIGURE 7. Dependence of surface and bottom reverberation on range. It is assumed that the scattering coefficient is the same for both surface and bottom. Actually this number is much greater for the bottom than for the surface. This results in shifting the graph of bottom reverberation upward relative to the surface graph.

ing volume reverberation apply without appreciable change, however, and only the dependence on range is changed. The graphs of Figure 7 show this dependence on range for surface and bottom reverberation. In this Figure it has been assumed that $N'$, the number of scatterers per unit area has the same value for both surface and bottom. Actually $N'$ has a much greater value for the bottom than for the surface. This results in shifting the graph of bottom reverberation upward relative to the surface graph.

Figure 8 shows comparative levels of an echo from a single target, of volume reverberation, and of surface (or bottom) reverberation, as calculated from equations (9), (17), and (20), respectively. In order to give a standard of comparison, it is assumed that all three have the same level at 1,000 yd, which will not necessarily be the case in practice. It will be noted that, at shorter ranges than 1,000 yd, the levels *increase* in the order *volume reverberation*, *surface* (or bottom) *reverberation*, *echo*. At longer ranges, they *decrease* in this same order. The graphs diverge 10 db from their neighbors for each tenfold increase or decrease in range.

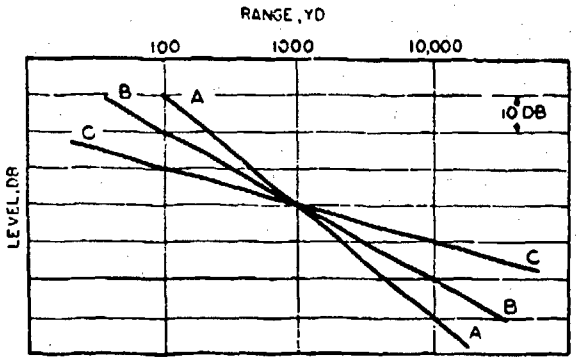


FIGURE 8. Comparative levels of (A) echo from a single target, (B) surface (or bottom) reverberation, (C) volume reverberation. In order to give a standard of comparison, it is assumed that all three have the same level at 1,000 yd, which will not necessarily be the case in practice.

It should also be remembered that Figure 8 is quite schematic as far as surface and bottom reverberation are concerned and should be modified in accordance with Figure 7.

## 5.3.4 Extension of the Theory to Nonideal Conditions

All of the preceding calculations have been based on a number of simplifying assumptions that cannot be expected to be correct under actual conditions, but are useful in presenting the basic ideas. The complications introduced by departures from the ideal cases just examined will now be considered.

### Scattering Coefficients

The first simplification was that the scatterers all had the same target area $\sigma$ and that there were $N$ of them in each unit volume (or $N'$ on each unit area). Obviously, the scatterers will not all be the same, but since only the combination $N\sigma$ enters the final equation, this does not cause any particular trouble. It is seen that $m = N\sigma$ is the total target area of all the scatterers in a unit volume. This quantity is called the *volume-scattering coefficient*. Since $N$ is measured in $\text{yd}^{-3}$ and $\sigma$ in $\text{yd}^2$, $m$ is measured in $\text{yd}^{-1}$; that is $1/m$ is a length. It is essentially the distance a wave train can travel before much of its energy is scattered.

In the same way, $n = N'\sigma$ is the total target area of all the scatterers located on a unit area; it is called *the surface- or bottom-scattering coefficient*. Since $N'$ is measured in $\text{yd}^{-2}$ and $\sigma$ in $\text{yd}^2$, $n$ will be dimensionless, i.e., it will have the same numerical value whether yards or feet are used as units.

Replacing $N\sigma$ by $m$ and $N'\sigma$ by $n$ will remove this oversimplification from equations (17) and (20).

### Beam-Pattern Correction

The second simplification is the assumption that the projector emits the sound in a sharply defined beam, with no sidelobes. When actual projectors are involved, the factor $(1 - \cos \alpha)$ in equation (16) and the factor $\alpha$ in equation (18) must be replaced by others, the exact values of which depend on the beam patterns of the projector. Call these factors $K_v$ and $K_s$, respectively; equations (17) and (20) then become

$$I_R = \frac{I_1 K_v m r_0}{r^2} \quad \text{(volume reverberation)}, \tag{21}$$

$$I_R = \frac{I_1 K_s n r_0}{2r^3} \quad \text{(surface reverberation)}. \tag{22}$$

The two factors $K_v$ and $K_s$, like the ones they replace, bear a simple relation to the half-width of the main lobe of the transducer.[5] Let $\alpha$ be redefined as the angle (in degrees) at which the beam pattern has a value 6 db below the maximum (or axial) level. Then the values of $K_s$ and $K_v$ are given approximately by the equations:

$$K_s = 4.2 \times 10^{-3} \alpha, \tag{23}$$

$$K_v = 4\pi K_s^2 = 5.5 \times 10^{-5} \alpha^2. \tag{24}$$

It should be noted that the scattering coefficients are independent of the projector, whereas $K_s$ and $K_v$ are independent of the ocean.

### Reverberation Levels

Finally, it has implicitly been assumed that the sound rays are straight lines, and that the inverse square law determines the whole transmission loss. In actual cases, the departures from these ideal laws introduce marked effects, which can be ascribed to departures from the inverse square law of transmission loss.

In order to deal with these complications in as simple a manner as possible, it is convenient to define the *reverberation level* $RL$ by

$$RL = 10 \log \frac{I_R}{I_1} \text{ db}. \tag{25}$$

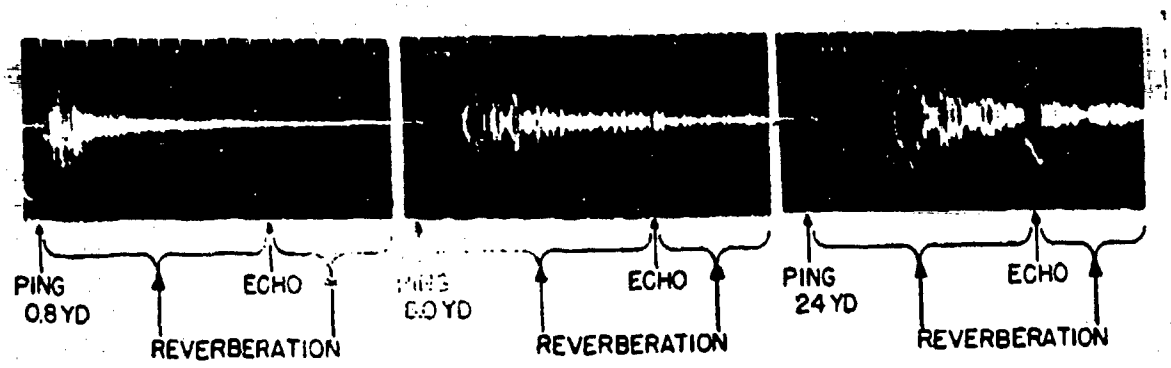


FIGURE 9. Oscillograms of reverberation and echo. Range marks are spaced 40 yd apart at the upper edge.

It will be noted that $RL$ is independent of the sound output of the sonar.

The *volume* and *surface-reverberation indices* $J_v$ and $J_s$ are defined by

$$J_v = 10 \log K_v, \tag{26}$$

$$J_s = 10 \log K_s. \tag{27}$$

and with these substitutions, equations (21) and (22) become

$$RL_v = J_v + 10 \log (nr_0) - 20 \log r \text{ (volume)}, \tag{28}$$

$$RL_s = J_s + 10 \log \left(\frac{nr_0}{2}\right) - 30 \log r \text{ (surface)}. \tag{29}$$

These equations are correct only if the transmission of sound is accurately given by the inverse square law. It can be shown that the departures from the inverse square law are in most cases properly taken into account in the following equations:

$$RL_v = J_v + 10 \log (nr_0) - 2H_v + 20 \log r, \tag{30}$$

$$RL_s = J_s + 10 \log \left(\frac{nr_0}{2}\right) - 2H_s + 10 \log r, \tag{31}$$

where $H_v$ and $H_s$ are the actual transmission losses from the sonar to the active regions responsible for the reverberation. It is easily seen that if $H_v = H_s = 20 \log r$, equations (30) and (31) reduce to equations (28) and (29).

### 5.3.3 Fluctuation of Reverberation Amplitude

The form of equations (28) and (29) suggests that the reverberation decreases steadily with time from an initial high level. This is not true. The "ringing" sound mentioned earlier in the discussion indicates that rapid changes in the intensity occur which are not predicted by these equations. The oscillograms of recorded reverberation show these changes very clearly, as can be seen by an examination of Figure 9.

These are specimens typical of the experimental data in this field and will be discussed in some detail. The three oscillograms were taken in rapid succession with different ping lengths of 0.8 yd, 8 yd, and 24 yd. The electric input to the transducer was coupled to the oscillograph and is recorded at the extreme left. This is followed by a blank interval of about 0.025 sec, during which the connections were changed from "send" to "receive." The portions of the trace to the right of this are reverberation, except for the echo, which is clearly visible in each. The early reverberation is so intense that it is off scale in the two right-hand cases. The ordinates of the three oscillograms are comparable, except that the electric circuit for recording the outgoing ping did not respond fully to the very short 0.8-yd ping. The receiving circuits, however, responded fully to its echo. It will be noted that this echo is rather weak, but that the other two echoes have the same amplitude. This point will be discussed later.

The theory presented above asserts that the intensity of the reverberation should be proportional to the ping length $r_0$. Consequently, the reverberation amplitudes should be proportional to $r_0^{\frac{1}{2}}$ so that the three oscillograms should show amplitude ratios of 1 : 3.2 : 5.5 approximately. It is obviously difficult to verify this by a *single* measurement, because of the rapid and irregular fluctuations in the amplitude of the reverberation. On the average, these ratios are quite close.

A more detailed study of the problem shows that the theory developed above refers only to such average values, and that there is a good explanation of the

rapid changes in amplitude. Two possible causes immediately suggest themselves:

1. The number of scatterers in the active region varies as the latter moves outward.

2. The echoes from the different scatterers interfere.

The first of these is easily seen to cause some fluctuation, but it is often relatively unimportant as compared to the second. If there are many small scatterers, only the second cause need be considered. As the number of scatterers in the active region decreases, the relative importance of the first cause increases.

One consequence of this is that the second cause would dominate in the case of long pings (large active regions), and the first, in the case of exceedingly short pings (small active regions). An inspection suggests, however, that even for the 0.8-yd oscillogram, the second kind of fluctuation is important, although some of the long "spines" may be caused by single scatterers. It would be interesting to study even shorter pings, so that an exact estimate of the number of scatterers per unit volume could be made. The difficulty of constructing transducers with sufficiently short response times has hitherto prevented such work. For longer ping lengths, there is no doubt that only the second cause is important.

The theory of fluctuation due to the second cause has been developed by Lord Rayleigh and others.[18] Let $A$ be the rms amplitude of the reverberation; at any given instant, the actual amplitude $a$ may be greater or less than $A$. The probability that $a$ is greater than some given value $x$, is

$$P = \exp\left(\frac{-x^2}{A^2}\right). \qquad (32)$$

Some values of this probability are given in Table 2.

TABLE 2. Probability that the actual amplitude $a$ is greater than $x$.

| $P$ | $x/A$ | $10 \log x^2/A^2$ |
|---|---|---|
| 0.90 | 0.32 | −10.0 db |
| 0.50 | 0.84 | − 1.6 |
| 0.368 | 1.00 | 0.0 |
| 0.10 | 1.52 | + 3.6 |
| 0.001 | 2.53 | + 8.4 |
| 0.00005 | 3.16 | +10.0 |

A number of conclusions can be drawn from this table.

1. The reverberation amplitude is greater than its rms value about 37 per cent of the time, and less than its rms value 63 per cent of the time. There is thus a marked tendency for the reverberation to be below the rms value at any given time. The median value is 84 per cent of the rms value.

2. The reverberation is more than 10 db *below* rms 10 per cent of the time.

3. The reverberation is more than 10 db *above* rms only 0.005 per cent of the time, or practically never.

4. During 80 per cent of the time, the level is between − 10 and + 3.6 db, relative to the rms amplitude.

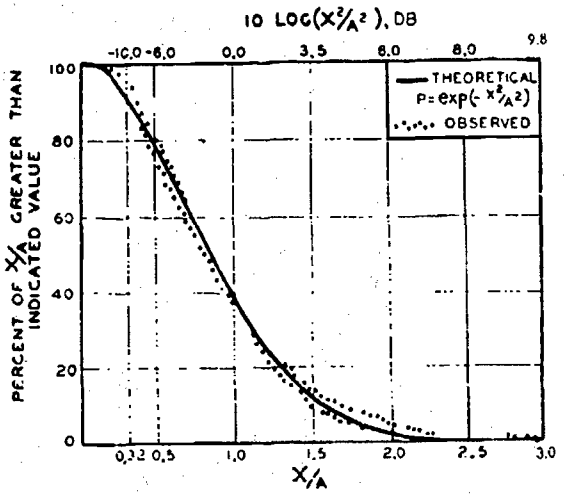


FIGURE 10. Comparison of observed reverberation with the Rayleigh formula.

The Rayleigh formula was checked against experimental results [9,10] shown in Figure 10, which is based on several hundred measurements of the reverberation amplitude at various ranges. Some of these are shown in the figure as circles; the two sets of

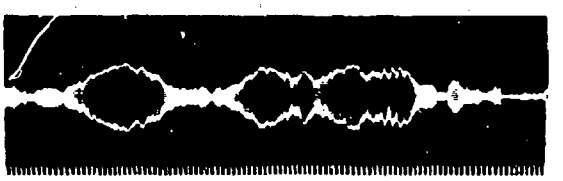

FIGURE 11. High-speed oscillogram showing coherence of reverberation. Similar to the oscillograms of Figure 9 except for the scale; the range marks in Figure 11 are spaced 2.5 yd apart.

circles represent two separate sets of measurements. The solid curve is the graph of equation (32). The experimental points are seen to fall very near the theoretical curve. Such close agreement is usually, but not always obtained. The reasons for the exceptional cases are not known.

The large fluctuations in the reverberation ampli-

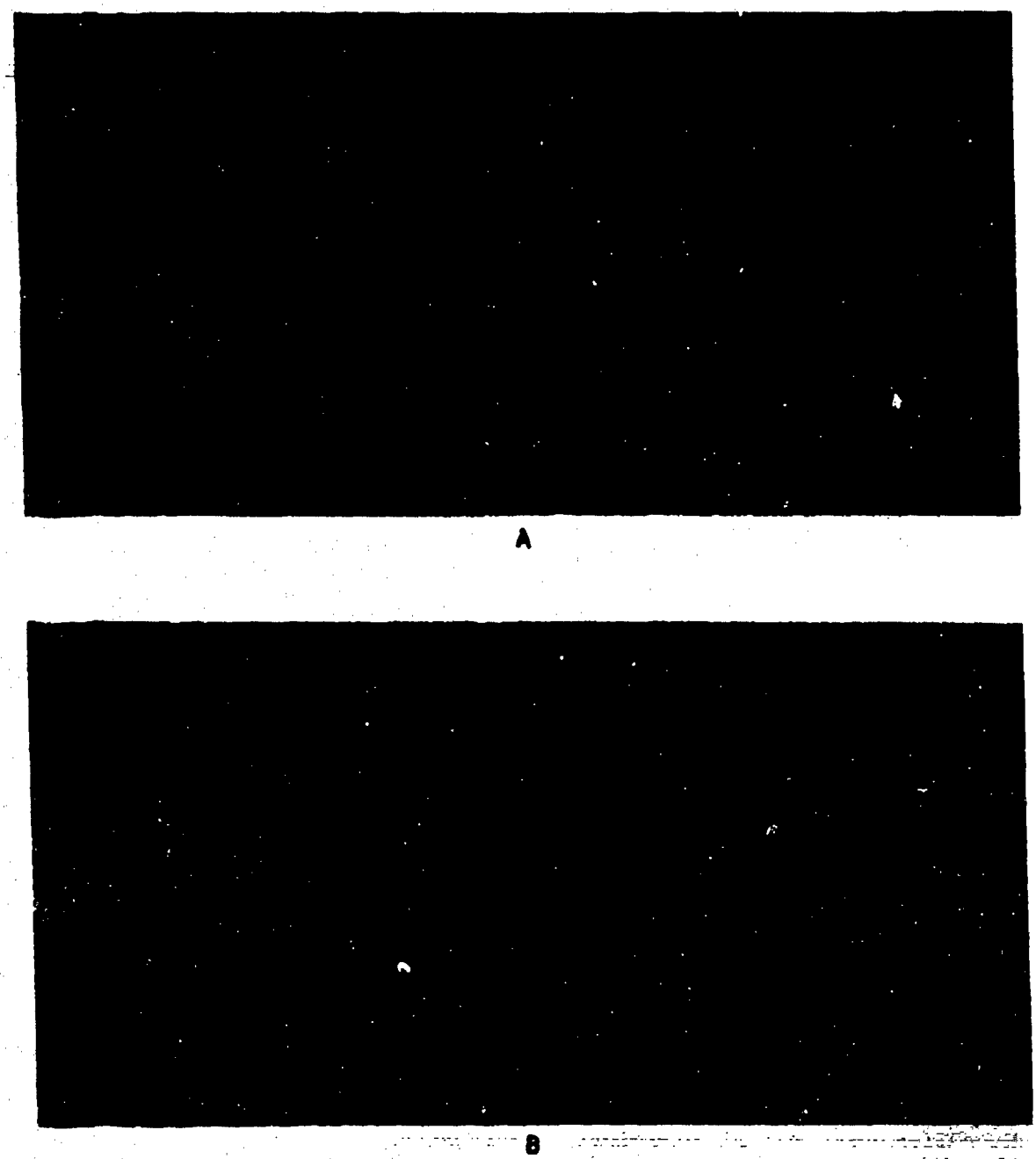


FIGURE 12. (A) Oscillogram of unheterodyned 24-kc reverberation. (B) Oscillogram of the reverberation shown in A heterodyned to 800 c.

tude make it essential to average the results of experimental measurement. That is, the theoretical values of $RL$, derived above, are all values of 20 log $A$ and not 20 log $a$. Consequently, the procedure is to measure a large number of values of $a$ and to compute their mean. This mean differs from $A$, the rms value, by a negligible amount.[39]

### 5.3.6 Coherence of Reverberation

While the amplitude of reverberation fluctuates widely, its envelope changes more or less gradually, as shown in the high-speed oscillogram of Figure 11. This is similar to those of Figure 9 except for the scale; the range marks of Figure 11 are spaced 2.5 yd apart.

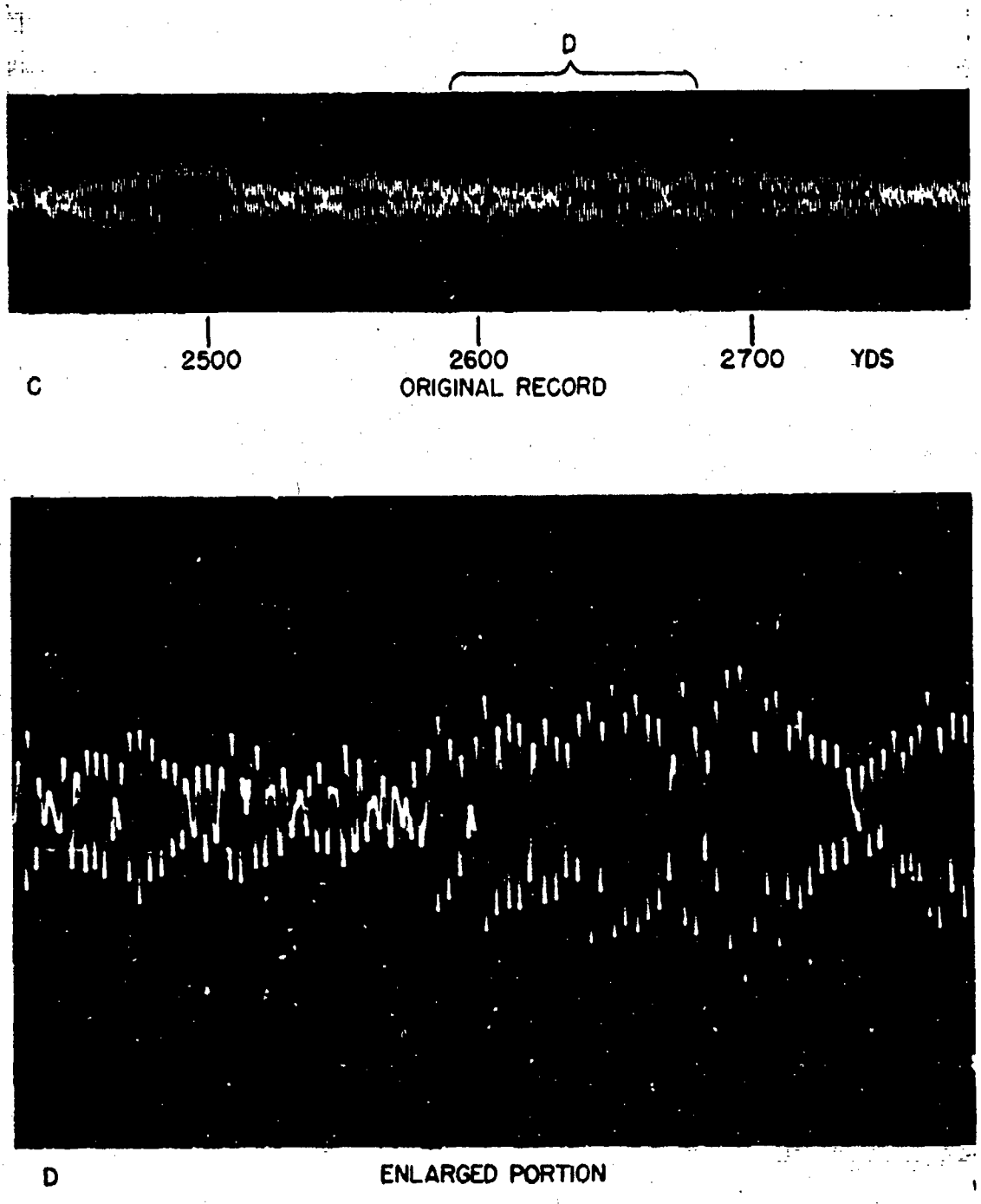


FIGURE 12. (C) Oscillogram of heterodyned 800-c reverberation. (D) Enlarged portion of heterodyned reverberation indicated in C.

It is seen that, while the amplitude is constantly undergoing small changes, the large changes occur rather gradually.

A somewhat greater enlargement of an oscillogram of reverberation is shown in Figure 12. Figure 12A is the record of the unheterodyned 24-kc current, Figure 12B, on which the successive cycles are clearly resolved, of the heterodyned 800-c current. Figures 12C and D show this even more clearly. It is seen that the changes occur even during a single cycle of

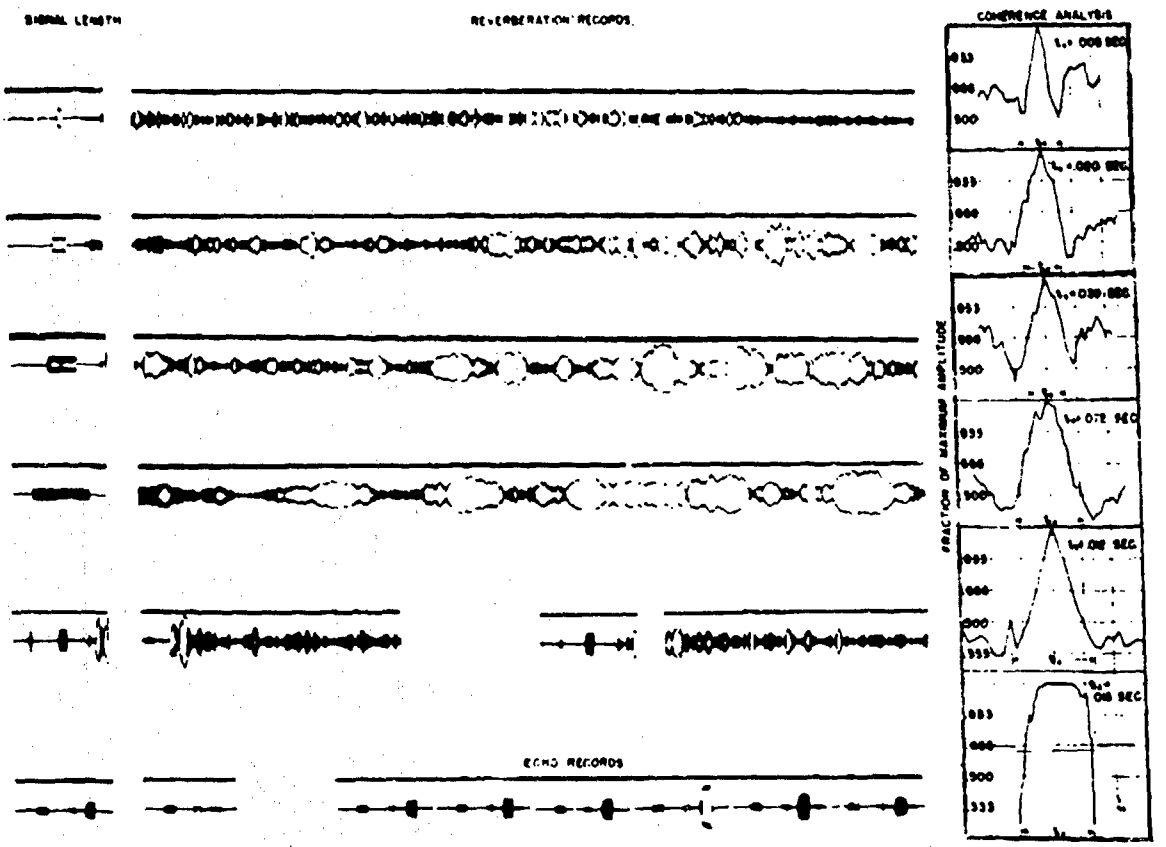


FIGURE 13. The coherence of reverberation. The graphs on the right are drawn from calculations based on the oscillograms. The ping lengths are indicated on the left. The lowest strip (and the corresponding curve on the right) show the coherence of echoes instead of reverberation.

the heterodyne frequency, and distort the wave form, particularly when the amplitude is small.

In general, the major changes require a number of cycles, and take place gradually. This is sometimes expressed by saying that the reverberation "coheres" in "blobs," the latter term being descriptive of the oscillogram rather than of the sound. The "rolling" character of the sound, however, is indicated by the blobbly character of the oscillogram.

The duration of the blobs tends to be about the same as that of the ping or echo. This is shown in a qualitative way by the three oscillograms in Figure 9, each of which was made with a different ping length. The quantitative aspects are more clearly shown by Figure 13. These graphs were made by selecting a number of blobs of reverberation from oscillograms made with a given ping length. Each blob was measured at a number of points, spaced at equal distances from its maximum. The measurements at a given distance to left or right of the maximum were averaged and plotted in Figure 13. For comparison, the ping length is indicated on each.

The graphs furnish good evidence that the duration of the blob increases with ping length and is about equal to the ping length. The very longest ping shows some departure from this last rule; this may be caused by fluctuations in the transmission loss (see Chapter 3).

The coherence of echoes is more pronounced than that of reverberation, as can be seen in the lowest strip of Figure 12.

### 5.3.7 Wave Form of Reverberation

Reference has already been made to the distorted wave form of the reverberation. These distortions are most obvious when the amplitude is small, but they occur at all times. This is indicated, for example, by the difference in amplitude of successive cycles in Figures 12 and 12A.

A convenient measure of the distortion is the time interval between alternate zeros of the voltage. In the case of an undistorted wave, all these intervals would be the same, and equal to the reciprocal of the frequency.

It has been possible to construct an instrument, called a periodmeter, to record the interval between zeros.[9] It traces a dotted line, for which the height above a reference line is a linear function of the intervals. Examples are shown in Figure 14. The upper trace was made with an 800-c sine wave from a standard oscillator. The lower trace was made by recording the same tone on a phonograph disk and playing it back. The irregular line of dots shows that the speed of the turntable varied sufficiently to cause variations of more than 20 c in the frequency of the reproduced sound.

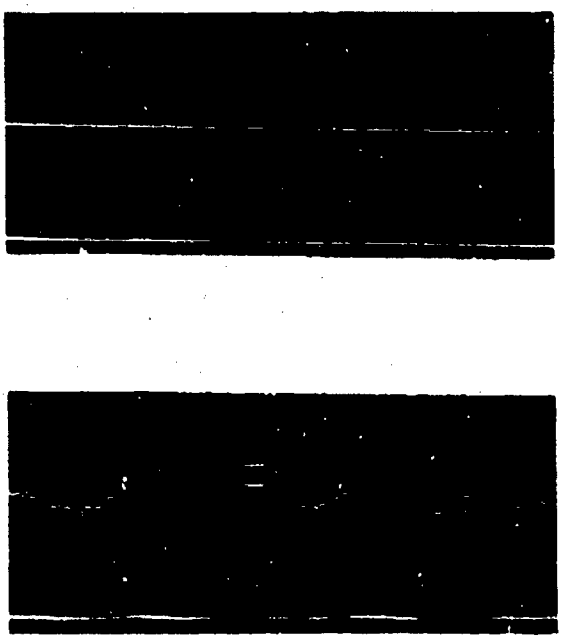

FIGURE 14. Periodmeter record, showing distortion of wave form. Upper trace was made with an 800-c sine wave from a standard oscillator. Lower trace was made by recording the same tone on a phonograph disk and playing it back. The irregular line of dots shows that the speed of the turntable varied sufficiently to cause variations of more than 20 c in the frequency of the reproduced sound.

and oscillator. The lower trace was made by recording the same tone on a phonograph disk and playing it back. The irregular line of dots shows that the speed of the turn table varied sufficiently to cause variations of more than 20 c in the frequency of the reproduced sound.

The instrument has been found useful in locating troubles in the wave form and frequency of the power supply of sonars, which in turn affects the wave form and frequency of the reverberation and echo. Figure 15 illustrates this. Figure 15A shows a fairly good wave form, but a moderate change in frequency (less than 5 c) from beginning to end of the ping. Figure 15B shows a large frequency drift, together with a periodic frequency modulation. This modulation apparently resulted from an overtone of the 60-cycle ship's power. A more complicated type of frequency modulation, the cause of which was never completely determined, is shown in the lowest trace, Figure 15C.

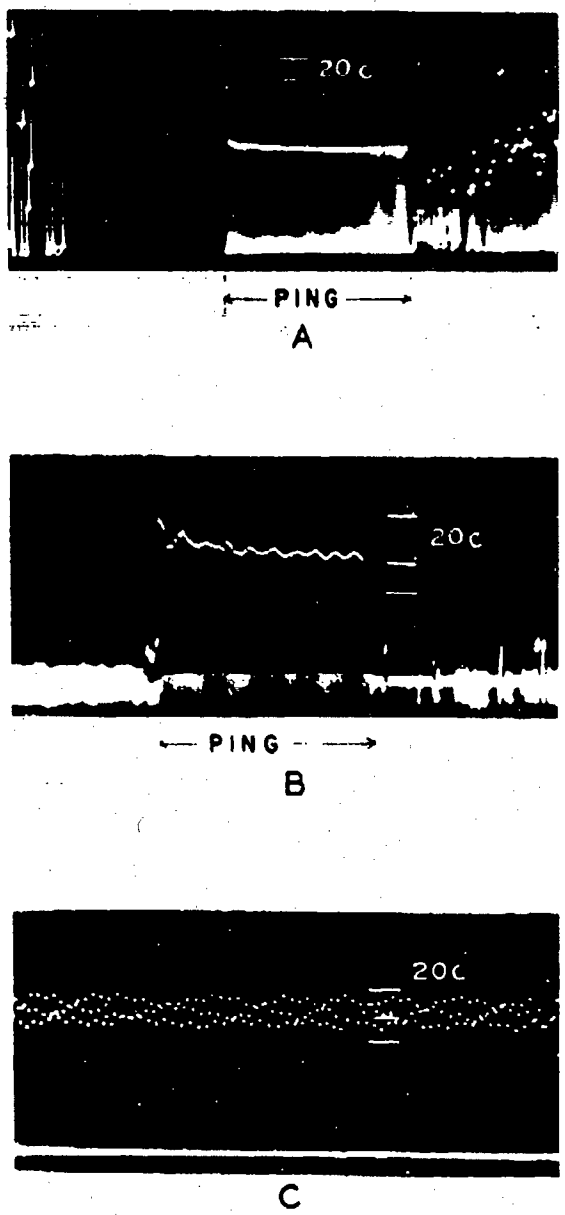


FIGURE 15. Periodmeter record, showing distortion of the wave form recorded in (A) apparently by an overtone of the 60-c ship's power. (B) Shows large frequency drift and periodic frequency modulation. In (C) a more complicated frequency modulation is seen. The cause was not completely determined.

Under good conditions (very strong echoes) the echo practically reproduces the frequency modulation of the current supplied to the sonar projector, as shown in Figure 16.

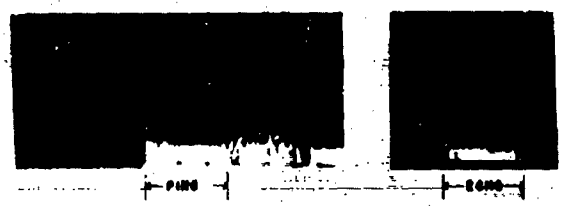


FIGURE 16. Periodmeter record of an echo. The echo is seen to reproduce the frequency modulation of the current supplied to the projector.

Reverberation shows much wider changes in the values of successive periods, as shown in Figure 17. Some caution must be exercised in interpreting these traces in terms of frequency. They are indicative of the distorted wave form and are caused by the irregular amplitude, as well as by the frequency modulation (see Figure 12A).

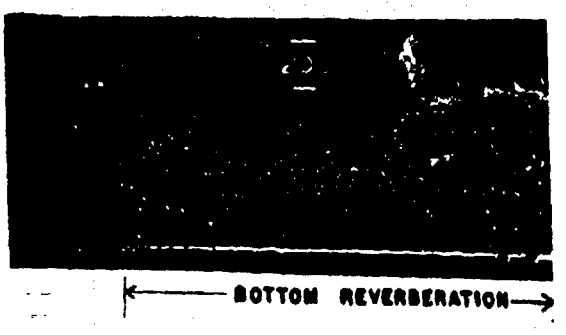


FIGURE 17. Periodmeter records of reverberation, showing changes in the values of successive periods. (A) shows volume reverberation; (B), bottom reverberation. They are indicative of the distorted wave form, and are caused by the irregular amplitude as well as by the frequency modulation. (See Figure 12A.)

When the echo is comparable to the reverberation in intensity, the periodmeter yields traces like those in Figure 18. The trace *A* shows an echo with no doppler, as well as reverberation. The greater stability of the wave form of the echo is apparent. Trace

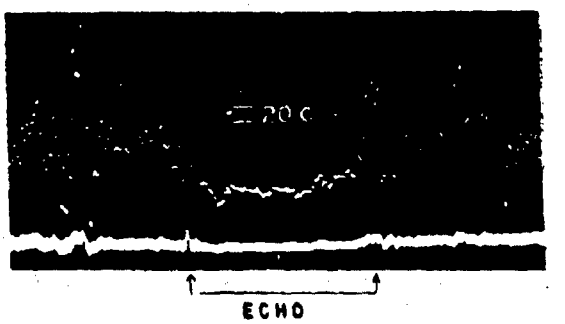


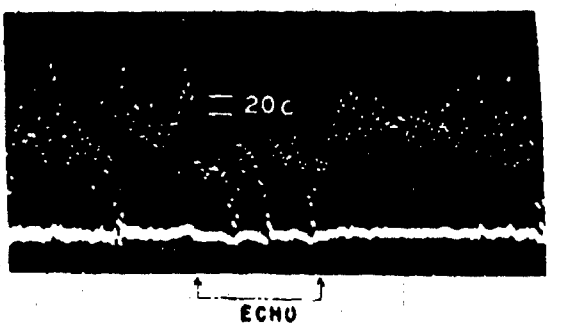


FIGURE 18. Periodmeter traces of echoes comparable in intensity with the reverberation. (A) shows an echo with no doppler, as well as reverberation. (B) shows an echo whose frequency has been shifted by doppler effect. The large but fairly regular changes in the row of dots are caused by beats.

*B* shows an echo whose frequency has been shifted by doppler effect. The large but fairly regular changes in the row of dots are caused by the well-known phenomenon of beats.

There is a widespread opinion that the pitch of reverberation rises as the range increases. To test this, the periodmeter records were interpreted as an indication of frequency (thus ignoring the caution mentioned above) and plotted as shown in Figure 19. Some of the very rapid and irregular changes were eliminated by averaging the records over 100-msec (80-yd) intervals. There is some indication of a rise in frequency with range, but the systematic rise is often obscured by the larger irregular changes. Of 16 reverberations treated in this way, 10 showed sufficient systematic increase in pitch to be noted; if

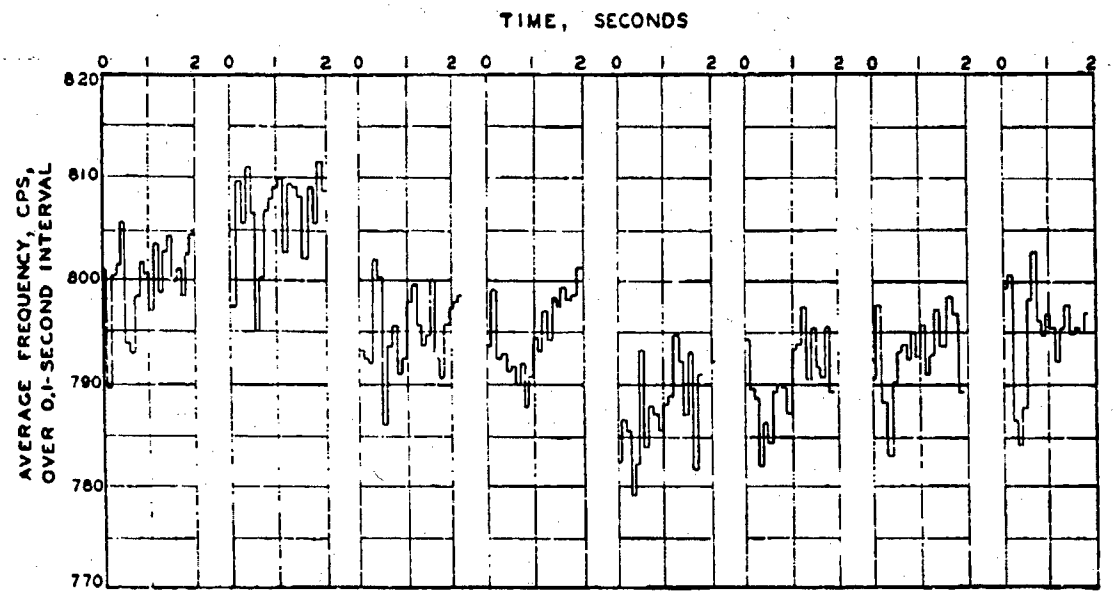


FIGURE 19. Graphs of reverberation frequency as a function of range. Average frequencies over 0.1-sec intervals computed from periodmeter records.

there was such an increase in the other six, it was obscured by the irregular changes. In no case did the increase exceed 10 cycles in 2 sec (1,600 yd).

While the periodmeter records are very useful for obtaining qualitative information about the modulation and distortion of reverberation and echoes, their quantitative evaluation is both laborious and uncertain. Slight modifications [illegible] equipment would simplify the work. This would seem to be a fruitful field for further experimental and theoretical research.

## 3.3.8 Reverberation from Chirps

It has been suggested, for various reasons, that it might be advantageous to use modulated signals in echo ranging, rather than the constant frequency pings. If the frequency of the sound is increased during the transmission of the signal, it will sound like "chirp" rather than "ping". The chirp is the form of modulation most often used. If the frequency increases from $f$ c at the beginning of the transmission to $f+s$ at the end, the quantity $s$ is called the sweep of the chirp. While a constant frequency ping is characterized only by its duration $t_0$ (or ping length $r_0$), a chirp is characterized both by its sweep and its duration.

If the product $st_0$ is less than unity, the chirp will differ only slightly from the ping in most respects. Only if the product $st_0$ is much greater than unity will there be much difference. Thus a 1-msec ping and a 1-msec chirp with a sweep of 1,000 c will not differ greatly, but a 50-msec ping and a 50-msec chirp with a 1,000-c sweep will differ markedly.

Theoretical analysis has established three general conclusions that are valid when $st_0 > 1$.

1. The average intensity of the reverberation from a chirp is the same as that from a ping of the same duration.

2. The fluctuation or blob length of the reverberation from a chirp is the same as that for a ping of duration $1/s$.

3. The duration of the echo from a concentrated target is approximately the duration of the chirp.

These theoretical conclusions have not been very carefully checked by experiment, but they seem to be correct, as is illustrated by Figure 20. The oscillogram $A$ shows reverberation from a 40-yd ping, and $C$ that from a 0.8-yd ping. The oscillogram $B$ shows reverberation from a 40-yd chirp whose sweep was 1,000 c. It is seen that the intensity of the chirp reverberation is comparable to that of the 40-yd ping, while the duration of the blobs of the chirp reverberation is comparable to that of the 0.8-yd ping. The echo shown on all three oscillograms is from the same target and is in accord with the third conclusion.

Several applications of these principles have been suggested, but further research is needed.

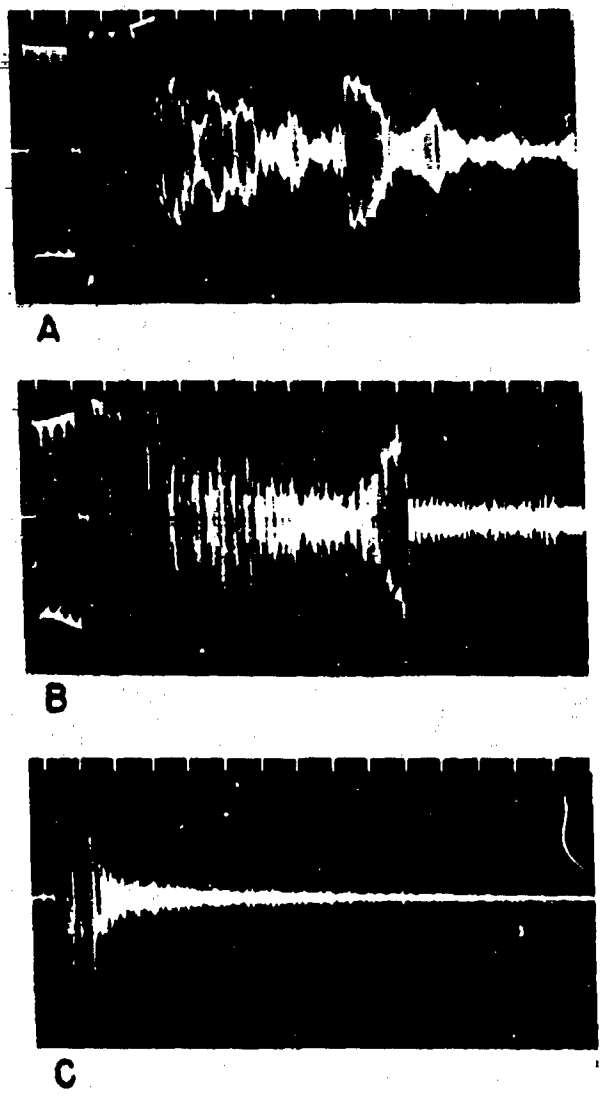


FIG. 20. Oscillograms showing effect of pulse length and modulation upon reverberation. (A) Forty-yard ping; (B) 40-yd chirp having 1-kc sweep; (C) 0.8-yd ping.

## 5.4 REVERBERATION IN DEEP WATER

### 5.4.1 General Remarks

The experimental study of reverberation as a function of range is greatly facilitated by the proper choice of two parameters: water depth and beam tilt. Thus, by observing reverberation from horizontal beams in deep water, it is usually possible to eliminate the effect of bottom reflections so that the ocean may be treated as a semi-infinite medium bounded by the surface. This allows comparison of the experimental results with the theory developed in Section 5.3.

In the study of volume reverberation a further simplification is gained by tilting the sound beam downward at a large angle, thus eliminating surface reflection and surface reverberation. The results of such tilted beam experiments are described in Section 5.4.2.

With the beam directed horizontally the observed reverberation is a combination of both surface and volume reverberation. Moreover, both beam pattern and refraction effects are important. All these factors make the interpretation of these data more difficult. The results of such experiments are discussed in Section 5.4.3.

Finally, in Section 5.4.5, a brief discussion will be given of forward scattering from the same volume scatterers which are responsible for volume reverberation, or backward scattering.

With the exception of the discussion of the dependence of volume reverberation on frequency, all the data described in this section were taken at 24 kc. It is also important to note that the data and the conclusions drawn therefrom are representative of the oceanographic conditions within a few hundred miles of the coast of California and Lower California. Since no deep-water reverberation data are available from other geographical regions, it is impossible to estimate the validity of these conclusions for oceanic waters in general.

### 5.4.2 Volume Reverberation with a Tilted Beam

The primary objective in using a tilted beam is the elimination of surface reverberation. To achieve this, it is necessary to employ a highly directional beam tilted at a dip angle of 30 degrees or more below the horizontal. This procedure also eliminates two other complicating factors: surface reflection and refraction, and the transmission anomaly is thus determined entirely by losses due to absorption and scattering. Neglecting the attenuation loss due to absorption and scattering, the transmission is therefore inverse-square.

#### Dependence of Volume Reverberation on Range

It will be recalled (Section 5.3) that if the volume scatterers are uniformly distributed and the trans-

mission is inverse square, the intensity of volume reverberation decreases as the square of the range (or, with a vertical beam, the depth). Thus the theoretical reverberation level (equation 28) decreases 20 db per tenfold increase in range. Figure 21 shows an example of this dependence.[10] The data were taken

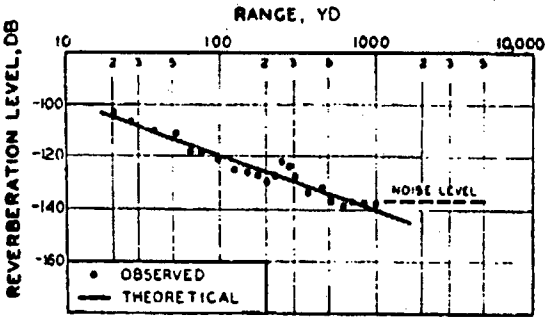


FIGURE 21. Dependence of volume reverberation on range. The straight line represents an inverse square variation. Experimental data taken in 600-fathom water with the transducer tilted downward 60 degrees. The close fit is exceptional.

in 600-fathom water with the transducer tilted downward 60 degrees. The observed points are seen to fit the theoretical solid line quite closely.

Such good agreement between observed levels and equation (28) is not often experienced. Usually the reverberation graphs, while exhibiting an overall decrease with range more or less in conformity with the equation (28), have maxima and minima much more pronounced than those in Figure 21. This is illustrated in Figure 22, which is the graph of reverberation measured in the same location as that of

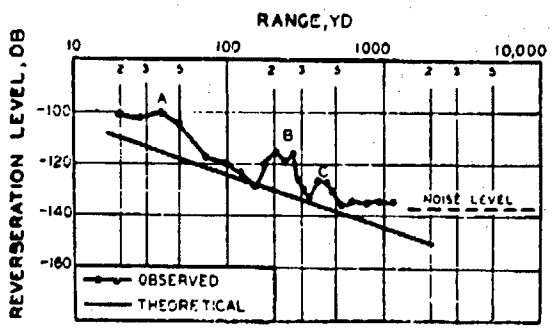


FIGURE 22. Volume reverberation measured under the same conditions as in Figure 21, five days later. The data shown here are more typical than those of Figure 21.

Figure 21, five days later. It is seen that the spread between maximum and minimum values is as much as 10 db greater than in Figure 21.

## DEEP SCATTERING LAYERS

These departures from the theoretical variation of reverberation with range are ascribed to the fact that the scatterers in the ocean are not distributed uniformly throughout the medium, as was assumed in deriving the equations; rather, the shape of the curves implies that they occur in horizontal layers at various depths and in varying concentrations.

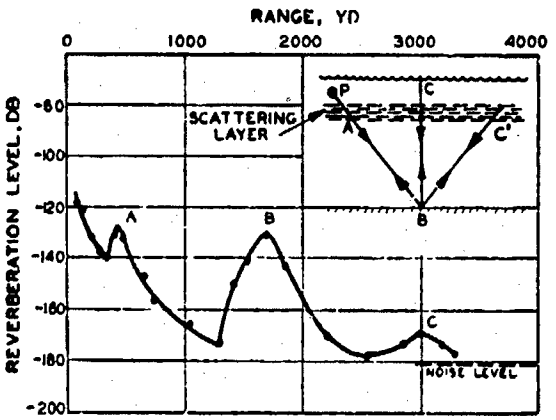


FIGURE 23. Reverberation from the deep scattering layer. The insert shows the geometry. The peak at *A* at a range of 400 yd is ascribed to scattering from this layer (marked *A* in the insert), the average depth of which was 300 yd. The peak at *B* is ascribed to bottom reverberation; the one at *C* may be due to sound traveling via *PABC'BAP* or *PABC"BAP*.

There is ample experimental evidence for the existence of such scattering layers at considerable

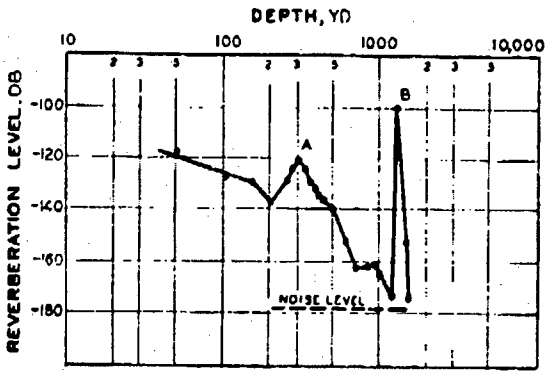


FIGURE 24. Reverberation from the deep scattering layer, with the beam directed vertically downward. The peak at *A* is ascribed to this scattering; the one at *B* is sound reflected from the bottom.

depths. Figures 23 and 24 are typical specimens of reverberation graphs from data taken in deep water with tilted beams. The data of Figure 23 were taken in water 1,300 yd deep; the transducer was tilted

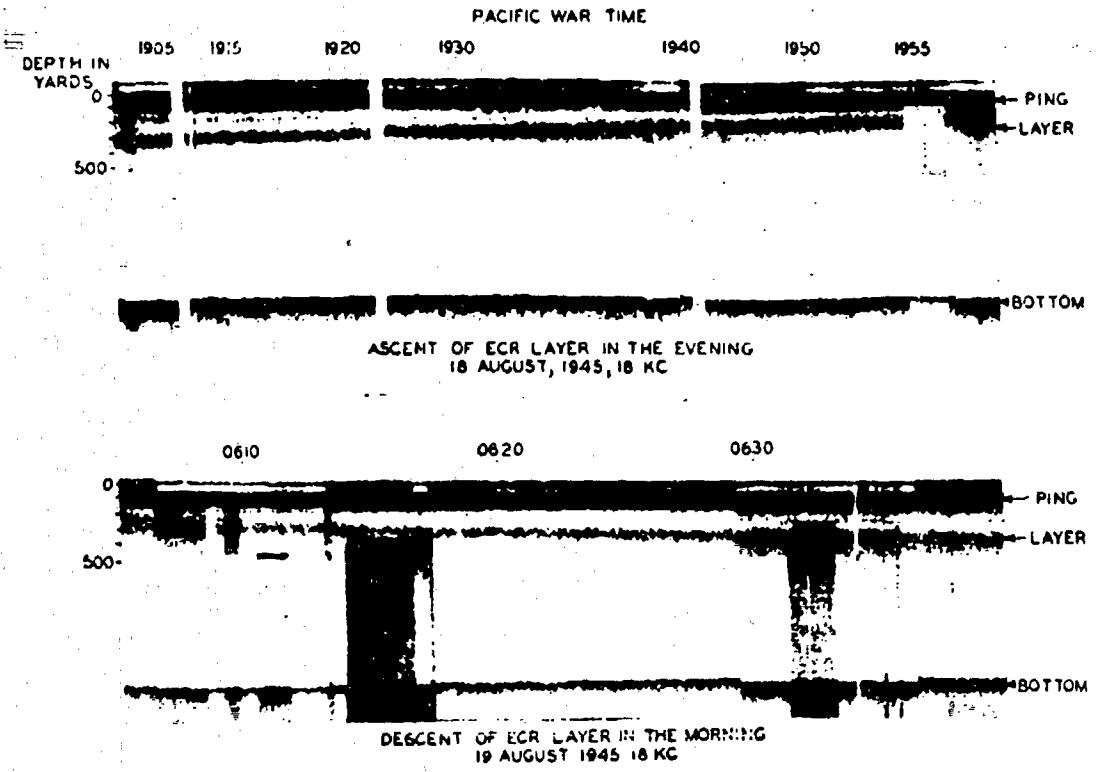


FIGURE 25A. Diurnal variation of the deep scattering (ECR) layer.

downward 49 degrees. The sharp peak (*A*) at a range of about 400 yd is ascribed to scattering from a layer at a depth of about 300 yd, in which the scatterers are more numerous than in the neighboring water; from the width of the peak the layer appears to be about 100 yd thick. The insert shows the geometry. The large peak (*B*) at 1,800-yd range is reverberation from the bottom; the third peak (*C*) at 3,000 yd is probably due to sound scattered from the bottom a second time, after the first bottom-scattered sound was reflected to the surface and thence scattered back to the bottom—sound that traveled the path *PABCBAP*, or to the scattering layer and back, via *PABC'BAP*.

The data of Figure 24 were taken at the same time, the beam in this case being directed vertically downward. The presence of the deep scattering layer at 300 yd is again evident (*A*). The sharp peak (*B*) is due to sound reflected from the bottom at normal incidence.

The presence of the deep layer off the southern California coast was first discovered in the summer of 1942 in the course of experiments of the type described above. It was found that in a given area the same deep scattering layer tended to persist for periods of a month or more, although it occasionally became diffuse, with the result that the sharp peak in the reverberation curve disappeared. Subsequent studies using a vertically directed beam, were made off Lower California during cruises of the USS *Jasper* to Guadalupe Island in 1943 and to La Paz in 1945, as well as in the San Diego area and as far north as San Francisco. These experiments indicate that throughout the year such layers are common from as far north as San Francisco to as far south as Cape San Lucas, and extend 400 miles out to sea from the California coast. In many cases two or more distinct layers were detected at various depths.

These investigations have shown that the deep scattering layer undergoes a diurnal cycle (see Figure 25A). This is shown schematically in Figure 25B and may be described as follows:

1. During the day the layer is more or less concentrated at one depth, 300 yd being typical.

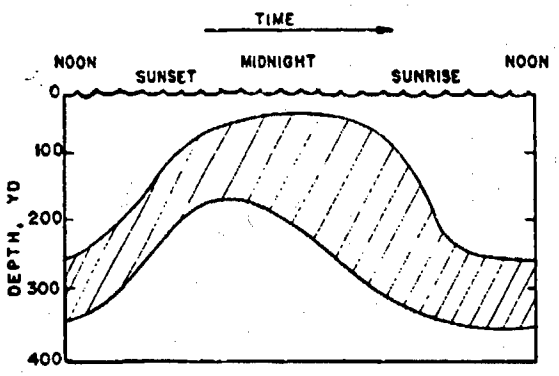


FIGURE 25B. Diurnal variation of the deep scattering (ECR) layer.

2. In the late afternoon and early evening the layer moves toward the surface.

3. From midnight to sunrise some of the scatterers move downward and the layer becomes diffuse, with the scatterers distributed between the surface and a depth of 200 or 300 yd.

4. Finally, from sunrise to midmorning the remaining scatterers near the surface move downward and the layer again becomes concentrated.

These facts suggest the occurrence of scatterers that migrate with a daily schedule. Their nature has not been definitely established. However, biological studies have shown that plankton (the passively floating or weakly swimming organic life found in bodies of water) executes a diurnal migration cycle, going to depths of at least 200 yd. It appears reasonable to conclude that these scattering layers may be colonies of plankton, or fish feeding on it, or possibly bubbles generated by it.*

## THE DETERMINATION OF THE VOLUME-SCATTERING COEFFICIENT

It is possible to calculate the volume-scattering coefficient $m$ by comparing observed and theoretical reverberation levels. The most suitable data for this purpose are those taken with a vertically directed beam and a short ping length, such as those shown in Figure 24. There are two reasons for this. First, the geometry is such that at each range the scatterers are essentially uniformly distributed within the active volume, as assumed in the theory developed in Section 3. Second, the transmission loss is the same for all scatterers and is given by

$$H_t = 20 \log r + ar. \qquad (33)$$

The first term, 20 log $r$, is the inverse square loss, $r$ in this case being the depth; the second, $ar$, takes account of losses by absorption amounting to $a$ db/yd. Using this value of $H$ in equation (30) the volume reverberation level becomes

$$RL_v = J_t + 10 \log mr_0 - 20 \log r - 2ar. \qquad (34)$$

This equation contains seven variables: of these, $J_t$, $r_0$, $r$, and $RL_v$ can be determined quite accurately by measurement. The value of $a$ appropriate to vertical transmission is not accurately known (see Chapter 3). The error inherent in this estimate is serious only for large values of $r$ (great depths) and for high frequencies.

The scattering coefficient $m$ can then be calculated from equation (34). An example using the reverberation levels plotted in Figure 24 is shown in Figure 26. In this example $r_0 = 8$ yd, $J_t = -25$ db, and $a$ is estimated to be equal to 0.0045 db/yd. It is seen that the

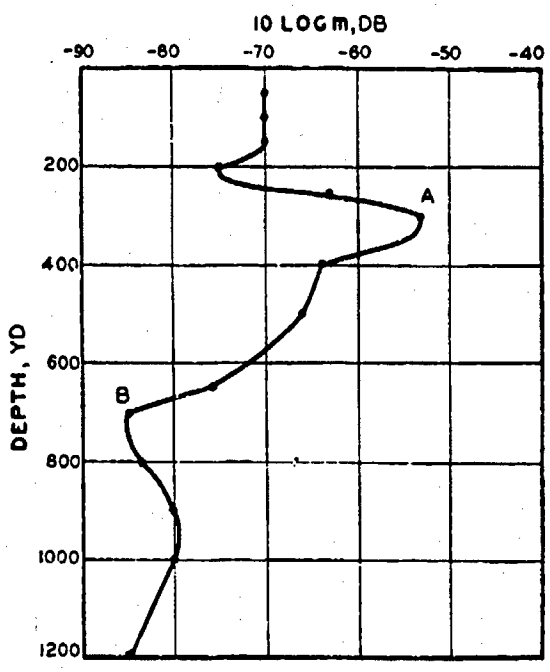


FIGURE 26. Volume-scattering coefficient, 24-kc.

value of 10 log $m$ ranges from a maximum of $-53$ db in the ECR layer to a minimum value of $-85$ db at a depth of 700 yd. The values of $m$ corresponding to these are respectively

$$m = 5 \times 10^{-6} \text{ yd}^{-1},$$

and

$$m = 3 \times 10^{-9} \text{ yd}^{-1}.$$

* It has been suggested that this layer be called the "ECR layer." "ECR" was the designation of the research group that discovered and studied it as well as the initials of the three leaders of the group, C. F. Eyring, R. J. Christensen, and R. W. Raitt.

They are typical of the maximum and minimum values commonly observed. Values as low as $10^{-10}$ have been observed. The minimum values that can be measured are determined by the level of the background noise in the receiver. It is probable that with lower noise levels even smaller values would be obtained on occasions.

While it is difficult, because of the wide spread in the observed values, to give a single average value, the values summarized in Table 3 may be considered fairly representative.

TABLE 3. Values of the surface scattering coefficient $n$ at 100-yd ranges.

| Wind speed | 10 log $n$ | $n$ |
|---|---|---|
| 8 mph | −54 db | $4 \times 10^{-6}$ |
| 10 | −45 | $3 \times 10^{-5}$ |
| 15 | −33 | $5 \times 10^{-4}$ |
| 20–40 | −24 | $4 \times 10^{-3}$ |

### SCATTERING DOES NOT CAUSE APPRECIABLE ATTENUATION

It has been remarked that scattering is theoretically responsible for some attenuation. These numerical results can be used to estimate the importance of this cause of attenuation. If scattering were the only cause, the attenuation of 20-kc sound in the ECR layer would be only about one-tenth that due to viscosity and much less than 1 per cent of that actually observed. In regions of smaller scattering coefficient, and for higher frequencies, these ratios are even smaller. It may therefore be concluded that scattering is not a cause of the anomalously high-attenuation coefficients (see Chapter 3).

### DEPENDENCE OF VOLUME REVERBERATION ON FREQUENCY

The discussion of volume reverberation has thus far been limited to data taken at 24 kc. During January and February 1943, an extensive series of measurements was made with vertical beams at four other frequencies: 10, 20, 40, and 80 kc. The observations were made at nine stations between San Diego and Guadalupe Island, about 250 miles south. The ocean depth varied from 600 to 2,000 fathoms.

The ECR layer was observed at all positions and at all four frequencies. Figure 27 shows the average scattering coefficient at each frequency as a function of depth. The curves were obtained from the measured reverberation levels, using equation (34). The values of the attenuation coefficient $a$, based on available data on attenuation of sound in the sea,[12] are as follows:

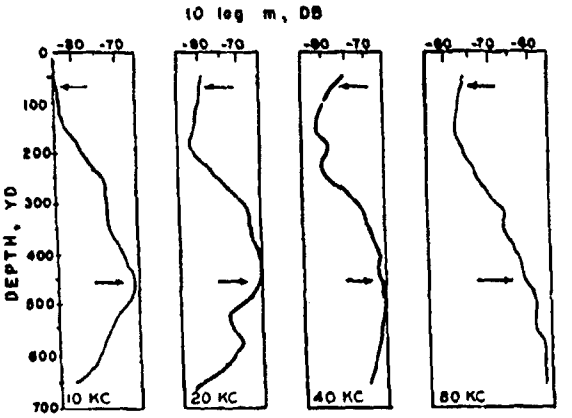


FIGURE 27. Volume-scattering coefficient at various frequencies.

| Frequency (kc) | $a$ (db per yard) |
|---|---|
| 10 | 0.00135 |
| 20 | 0.0036 |
| 40 | 0.0097 |
| 80 | 0.024 |

The four curves are seen to be very similar, with comparable values of $m$ both near the surface and at the depth of maximum scattering (about 450 yd). Below this depth the 10-kc and 20-kc curves are similar but the 40- and 80-kc curves do not show a decrease in the value of $m$; this is probably only apparent, and may be the result of experimental errors caused by higher noise levels at these frequencies. It is probable that had the noise levels been lower at the two higher frequencies, the observed values of 10 log $m$ would have decreased again below the 450-yd depth.

A comparison of $m$ at the four frequencies is made in Figure 28. Curve 1 represents average values in the upper 250 ft of the ocean (indicated by arrows in Figure 27). These values are essentially independent of the values assumed for the attenuation, since even at 80 kc the term $2ar$ in equation (34) is less than 5 db. The values of 10 log $m$ show an increase with frequency which is only slightly greater than the experimental error and is considerably less than the irregular variations at a single frequency. Thus $m$ may vary as the first power of the frequency or, at most, as the second power. It is decidedly less than that of curve 3, which shows the Rayleigh fourth-

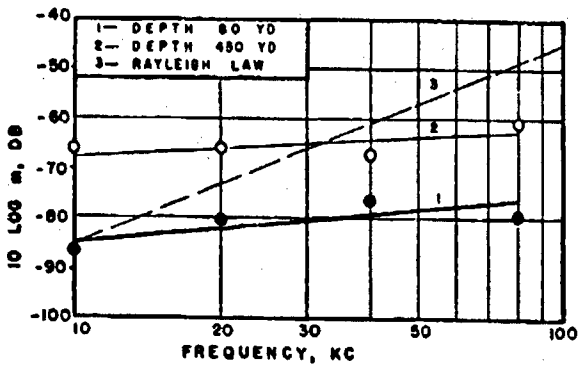


FIGURE 28. Comparison of volume-scattering coefficients at different depths with the theoretical Rayleigh scattering. The data are those of Figure 27.

power variation (Section 5.2.2) predicted for small solid or liquid particles having dimensions less than the wavelength of the sound.

### A Paradox Concerning Reverberation

These results are very difficult to reconcile with other facts concerning reverberation. This may be illustrated by a simple calculation. The lack of dependence on frequency may be explained if the scatterers have diameters greater than one wavelength of 10-kc sound, i.e., $d \geq 0.16$ yd. For these, Figure 1 shows that their target areas will be constant (to within 5 db) for all higher frequencies. The target areas of each scatterer will then be $\sigma = \frac{1}{4}\pi d^2$, or $\sigma \geq 0.02$ yd$^2$. Since the scattering coefficient is approximately $m = N\sigma$, where $N$ is the number of scatterers per cubic yard, we can estimate $N$. If $m = 10^{-6}$ yd$^{-1}$, it follows that $N \leq 5 \times 10^{-5}$ yd$^{-3}$, if $m = 10^{-8}$, then $N \leq 5 \times 10^{-7}$ yd. That is, there will be about one scatterer per million cubic yards of water.

This may be compared to the active volume of a ping at 250 yd from the projector. The width of the beam is involved in this calculation; supposing it to be 6 degrees, the active volume is 2,000 $r_0$ yd$^3$, $r_0$ being the ping length. Taking $r_0 = 50$ yd, it follows that the active volume is $10^5$ yd$^3$. In general, therefore, there should be no scatterer in the active volume. Only once in every two or three transmissions would there be any reverberation at the given range of 250 yd; on this one occasion, the intensity would be several times that which is actually observed.

To put the matter in another way, two causes for the fluctuation were suggested in Section 5.3.5. The experimental evidence cited there is conclusive that the second cause is the dominant one. These calculations indicate that the first cause should be dominant and that the fluctuations of reverberation intensity should be much greater than is actually observed.

These calculations have been based on the assumption that the scatterers are solid particles or liquid droplets. If they should be gaseous bubbles, Figure 1 shows that their *actual* diameters might be much less than the value deduced above. However, the *effective* target areas of the resonant bubbles are so much greater than the actual cross section that the argument is not greatly changed, and the paradox remains for all except the longest pings.

It is worth noting that the paradox is a contradiction between two theoretical conclusions, drawn from different experimental data. Its resolution will therefore require theoretical as well as experimental research.

## 5.4.3 Volume and Surface Reverberation with a Horizontally Directed Beam

When the transducer is directed horizontally in deep water, both surface and volume reverberation are generally observed. The intensity of the resulting reverberation at each range will therefore depend on which of these two types of reverberation is dominant. Thus, as will be shown below, volume reverberation is always dominant at long ranges, while at short ranges surface reverberation usually dominates.

It is convenient to begin the discussion with average reverberation-range curves obtained under practical echo-ranging conditions. Surface and volume reverberation will then be considered separately in more detail; finally, average values of the scattering coefficients will be given.

### Average Reverberation Curves

Two reverberation curves are shown in Figure 29A; they are averages of an extensive set of observed reverberations at high and low wind speeds. About 110 reverberation curves were obtained, each being an average of five successive pings. The spread of the individual points about each of the two average curves was very small, the quartile deviation being only about $\pm 5$ db. The measurements were made at 24 kc, using echo-ranging equipment with the trans-

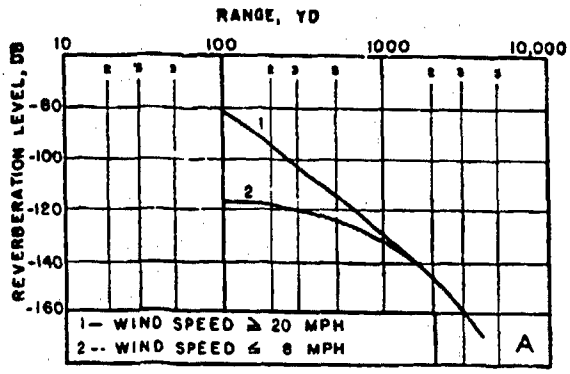


FIGURE 29A. Effect of wind speed on average reverberation level.

ducer mounted at a depth of 16 ft. Ping lengths of 16 to 80 yd were employed but the reverberation levels were all corrected to a standard ping length of 80 yd.

The two curves exhibit the following features:

1. At short ranges (less than 500 yd) the average reverberation level depends strongly on the roughness of the sea surface as measured by wind speed.

2. At long ranges (beyond 1,000 yd) the average reverberation is independent of wind speed.

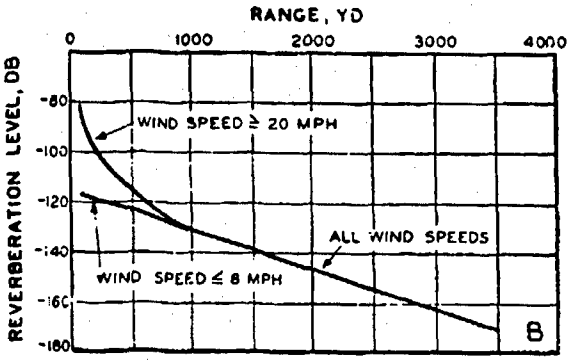


FIGURE 29B. Same data plotted on linear range scale.

3. With high wind speed the reverberation level drops rapidly, the slope of the average curve (curve 1) indicating a dependence on range as about $r^{-3}$.

4. With low wind speeds the reverberation drops more slowly, the average slope (curve 2) between 100 and 1,000 yd being roughly inverse square.

The curves are also shown in Figure 29B on a linear range scale.

The dependence of the short-range reverberation on wind speed clearly indicates that at ranges shorter than 500 yd and at high wind speeds, surface reverberation completely dominates volume reverberation. This conclusion is supported by observations made at nearly the same time with horizontal and vertical beams. At high wind speeds it is found that at short ranges the reverberation levels obtained with a horizontal beam are much higher than those obtained with a tilted beam. Figure 30 shows data of this type taken at a wind speed of 17 mph. Comparison of the two curves shows that in the first 100 yd the horizontal reverberation is about 20 db above the vertical reverberation. Two scattering layers (*A* and *B*) are also shown in Figure 30 at depths of 80 and 400 yd.

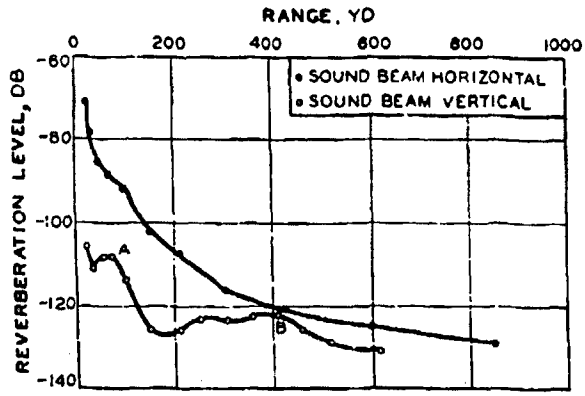


FIGURE 30. Comparison of reverberation at wind speed of 17 mph with horizontal and vertical beam. Points *A* and *B* represent deep scattering layers.

At low wind speeds (curve 2 of Figure 29A) the short-range reverberation is *volume* reverberation. The evidence for this statement is afforded by experiments of the type described in the previous paragraph. When such measurements are made at very low wind speeds, with the sea dead calm, it is found that the horizontal reverberation is much lower than in Figure 30 and agrees well with the vertical reverberation. From this it is concluded that at very low wind speeds volume reverberation is dominant and surface reverberation is negligible.

Finally, at long ranges, Figure 29A shows the reverberation to be independent of wind speed. This is taken as evidence that at these ranges volume reverberation always dominates surface reverberation.

Thus three main conclusions may be drawn regarding deep-water reverberation with a horizontal beam.

1. At short ranges and high wind speeds, surface reverberation is high and dominates volume reverberation (curve 1, Figure 29).

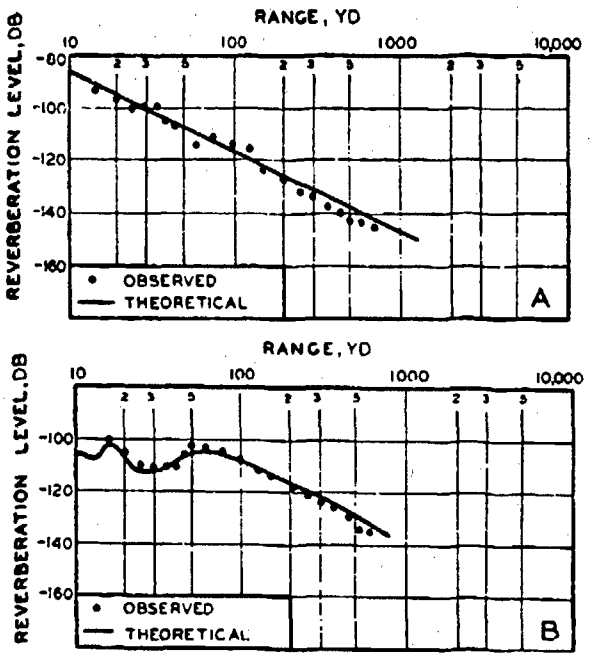


FIGURE 31. Comparison of observed and calculated surface reverberation. (A) Measurements made with transducer that was almost nondirectional in the vertical plane. Horizontal beam. (B) Data taken the same day under similar conditions, but with transducer turned so its directionality in the vertical plane was high. The theoretical curve takes account of the beam pattern.

2. At short ranges and low wind speeds surface reverberation is negligible and volume reverberation is dominant (curve 2, Figure 29).

3. At long ranges (beyond 1,000 yd) volume reverberation dominates at all wind speeds and is independent of wind speed.

Surface and volume reverberation will now be considered in more detail.

### SURFACE REVERBERATION

The discussion of surface reverberation given in Section 5.3 predicts an inverse third-power dependence on range. An example of this is shown in Figure 31A. The data were taken with a transducer almost nondirectional in the vertical plane and mounted at a depth of 20 ft. Short pings, 6.4 yd long, were used. Wind speed was about 15 mph, so that the resulting reverberation can be identified as surface reverberation. It is seen that the observed points agree well with the theoretical inverse cube law.

Figure 31B is a reverberation curve taken the same day under similar conditions. In this case, however, the transducer had a pattern in the vertical plane which was highly directional (the axis of the beam was horizontal in both cases). At very short ranges the active surface area is insonified by the outer portions of the beam, beyond the angle $\alpha$; these portions emit sound of a lower intensity than the main beam, and the receiver has a lower response at large angles than on the axis; thus there occurs a noticeable drop in the reverberation level. This can be calculated from the beam pattern as is shown by the solid curve. At ranges greater than 80 yd the active area is insonified by the main beam only, and the measured reverberation levels are seen to fit the inverse third-power line closely.

The curves in Figure 31 must not be regarded as universal. Examples of reverberation curves that show an inverse fifth-power variation of the reverberation with range are frequent. (Curve 1 of Figure 29 is an example.) The reason for this rapid decay is not understood.[10]

One case in which the surface reverberation is frequently observed to drop off more rapidly than

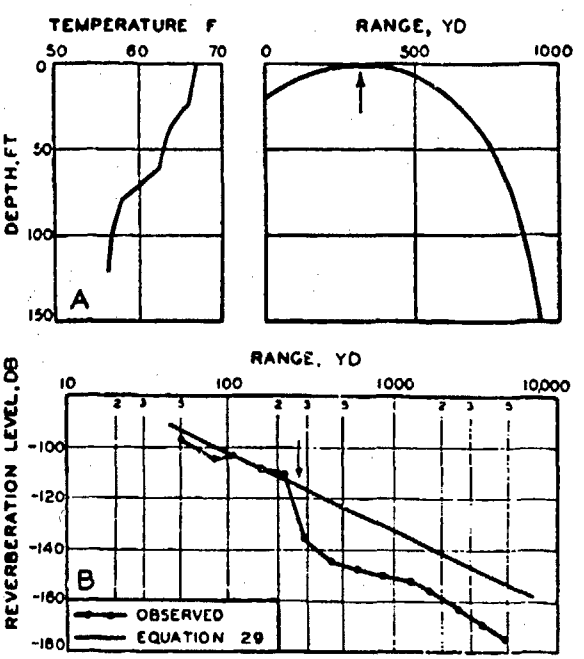


FIGURE 32. Effect of downward refraction on reverberation. (A) Bathythermogram and corresponding ray diagram. (B) Comparison of observed results with those calculated from simple theory. A sharp drop in the reverberation level at the arrow corresponds to the range at which the sound beam leaves the surface.

the inverse cube can be explained. Under conditions of strong downward refraction the reverberation would be expected to decrease at that range where the sound beam is bent away from the layer of sur-

face scatterers. Figure 32B shows an example of this drop, indicated by the arrow. It occurs at about 300 yd; at greater ranges the reverberation level is some 20 db below the value as given by equation (29). The data were taken with short (9-yd) pings. The transducer depth was 20 ft and the wind speed 12 mph. From the ray diagram based on the bathythermogram shown in Figure 32A, it is seen that the limiting ray leaves the surface at about 300-yd range (indicated by an arrow), thus affording support for the explanation suggested above.

The dependence of surface reverberation on wind speed is very marked at short ranges, as can be seen in Figure 29: at 100 yd the reverberation level at high wind speeds is some 35 db above that for low speeds, but at 500 yd the difference is only 10 db. The rapid increase of reverberation at 100 yd is seen more clearly in Figure 33 in which the average reverberation level is plotted against wind speed. The quartile deviation of the individual points about the smooth curve of Figure 33 is about $\pm 5$ db.

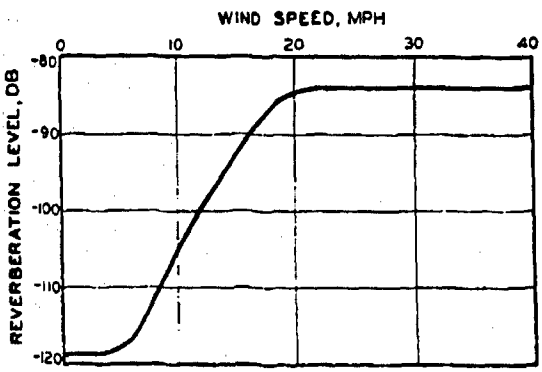


FIGURE 33. Dependence of reverberation level at short range (100 yd) on wind speed.

It is seen that the reverberation level is constant for wind speeds up to 8 mph. This confirms the conclusion that volume reverberation is dominant at these low wind speeds. For wind speeds of 8 to 20 mph the reverberation increases 35 db; the curve then levels off and above 20 mph there is little further dependence on wind speed. This dependence on wind speed is closely correlated with the roughness of the sea. At 8 mph the wind is strong enough to roughen the surface appreciably; occasionally wavelets may slough over, but no well-developed whitecaps are observed. At about 10 mph small whitecaps begin to appear, and when the wind has reached 20 mph the sea is liberally covered with them. When this stage is reached, further increase in whitecaps has no effect on the reverberation.

Correlation of reverberation with other measures of surface roughness (sea state, wind force, and swell) show similar results. In all cases, the reverberation level shows a marked dependence at short ranges and negligible dependence at long ranges.

### Surface Scattering Coefficient

It has been pointed out that surface reverberation in the ocean rarely exhibits the inverse third-power dependence on range which is predicted by the simple theory. This lack of agreement is found even at short ranges (100 to 500 yd), as shown by the steep slope of curve A in Figure 29. Thus it is clear that even the average surface reverberation cannot be fitted by equation (29) at all ranges. It is possible, however, to apply the equation to the observed reverberation level at *one* range to obtain the scattering coefficient as a function of wind speed. Table 3 shows values of $n$ obtained in this way from the observed levels at 100 yd (Figure 33).

Values of $J_s = -15$ db and $r_0 = 80$ yd were used, corresponding to standard gear using 80-yd pings at 24 kc. Since the projector was at a depth of 16 ft, these values correspond to an incident grazing angle at the surface of about 3 degrees.

### Volume Reverberation

The simple theory of volume reverberation developed in Section 5.3 assuming inverse square transmission and uniform distribution of volume scatterers predicts an inverse square dependence on the range. The first assumption is approximately valid at short ranges but breaks down at long ranges because of refraction and attenuation effects. The second assumption is sometimes valid over a limited region; in general, however, the horizontal stratification of the scatterers (Section 5.4.2) invalidates the assumption that they are uniformly distributed. Thus it is clear that the two basic assumptions made in the simple theory are usually not satisfied.

In order to take account of refraction and the uneven distribution of scatterers, it would be necessary to carry out a volume integration over the active scattering volume at each range. There is insufficient data to warrant such a complex theory. The correction for attenuation, however, is easily made [equation (34)] and has already been discussed

in Section 5.4.2, in connection with the calculation of the volume scattering coefficients. Finally, it can be shown that surface reflection will, on the average, raise the reverberation given by equation (34) by an additional 3 db. Thus, for a horizontal beam, the theoretical volume reverberation, corrected for surface reflection and attenuation, is given by

$$RL_v = J_v + 10 \log mr_0 - 20 \log r - 2ar + 3. \quad (35)$$

The observed volume reverberation beyond 1,000 yd agrees very closely with the theoretical reverberation given by equation (35) for typical values of $a$ and $m$. This is shown in Figure 34. Curves 1 and 2 are the observed averages at high and low wind speeds shown in Figure 21 and are repeated here for convenience. Curves 3 and 4 were calculated from equation (35) using attenuation coefficients of $a = 0$

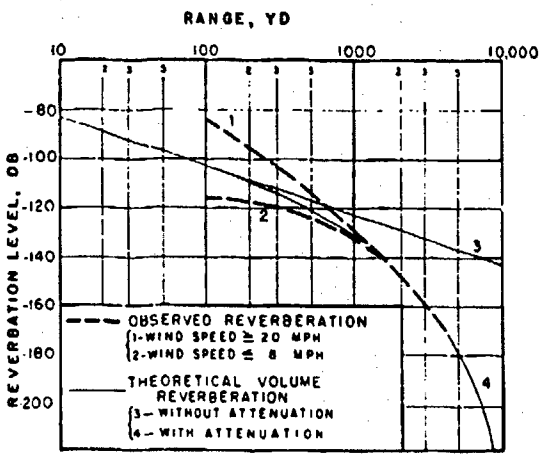


FIGURE 34. Comparison of calculated and observed volume reverberation, showing the close agreement.

and $a = 0.0045$ db/yd, the latter typical of good transmission at 24 kc. For the remaining parameters the following values were used:

$$J_v = -25 \text{ db},$$
$$r_0 = 80 \text{ yd},$$
$$m = 10^{-6} \text{ yd}^{-1}.$$

The value of $m$ is the average value given in Table 3 for the deep scattering layer.

The importance of attenuation at long ranges is strikingly shown by the large differences between curves 3 and 4. Thus, at 5,000 yd the attenuation reduces the reverberation level by some 45 db below the inverse square value of curve 3. It should also be noted that the *shape* of the theoretical curve 4 beyond 1,000 yd is determined largely by the particular value of the attenuation coefficient $a$.

To return to the fit between equation (35) and the average curve at long ranges: not only does curve 4 fit the average volume reverberation, but it also gives a fair fit to most individual reverberation curves. This is shown by the small spread of the individual points around the average curve, half of the points lying within ± 5 db of the average. These results indicate that the long-range volume reverberation is due largely to the ECR layer. Further evidence for this conclusion is afforded by the fact that at short ranges, where the sound beam has not yet reached the ECR layer, the observed volume reverberation (curve 2) falls below the theoretical curve.

It has been remarked that beyond 1,000 yd most individual reverberation curves fit curve 4 quite closely. This is true over a wide range of oceanographic conditions, with one exception: no significant dependence has been found on wind speed, sea state, location, season, or thermal structure of the ocean.

The exception occurs under conditions of extremely sharp downward refraction and provides an interesting check on the importance of the ECR layer.

The effect of sharp downward refraction is to concentrate the sound beam into a relatively narrow cone. This produces a maximum in the reverberation curve at the range where the sound beam reaches the layer. An example of this effect is shown in Figure 35, where refraction and reverberation are compared for two days. The data were taken late in the afternoon off La Paz, using standard gear and 80-yd pings.

On the first day there was a deep mixed layer extending from the surface to a depth of 40 yd. Figure 35A shows the ray diagram and the deep scattering layer. The angle shown on each ray is the angle of the ray at the projector, measured downward from the horizontal; the 6-degree ray is the effective lower edge of the sound beam. Two days later, on March 17, the same deep layer was still present, but thermal conditions had changed radically, producing the strong downward refraction shown in Figure 35B. (The dotted rays 1 and 2 will be discussed later in connection with forward scattering.)

Typical reverberation curves for each day are shown in Figure 35C together with the theoretical reverberation (curve 4) of Figure 34. It is seen that the reverberation observed when there was a mixed layer (curve 1) agrees well with the theoretical

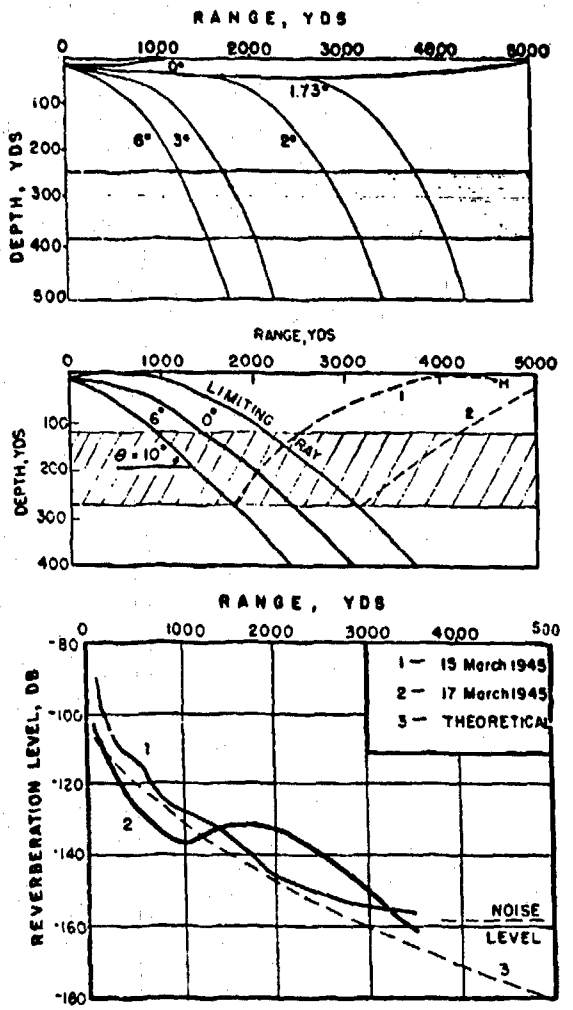


FIGURE 35. Comparison of reverberation and refraction for two days. (*Top*) Ray diagram for March 15, 1945. The shaded portion indicates the ECR layer. (*Center*) Ray diagram for March 17, 1945. (*Bottom*) Observed reverberation for these two days compared with calculated values.

curve 3 between 1,000 yd and 2,500 yd; beyond 2,500 yd it reaches the noise level and flattens out. Curve 2, on the other hand, observed when there was sharp downward refraction, shows a large maximum at about 2,000 yd, corresponding to the range at which the central portion of the sound beam reached the depth of maximum scattering (Figure 35B).

At short ranges, curve 1 rises steeply with decreasing range. This rise is due to surface reverberation and is to be expected, since the data were taken at a wind speed of 20 mph. The data of curve 2 were taken at a wind speed of 12 mph; it shows a corresponding rise in the reverberation level at very short ranges (100 yd), but there is a minimum when the sound beam has left the surface and has not yet reached the scattering layer. When the lower edge of the beam reaches the deep layer (about 1,000 yd) the reverberation begins to increase with increasing range, culminating in the main maximum.

## 5.4.4 Bottom Reverberation

Since in echo ranging the transducer is generally near the surface, the sound scattered back from the sea bottom will provide an important contribution to the reverberation only in shallow water; here, however, it may well be the dominant factor in limiting the range from which detectible echoes can be obtained.

### Types of Sea Bottom

In the case of surface reverberation, it is the state of the sea that determines the intensity of the scattered sound; bottom reverberation levels, it may be expected, will depend on the character of the sea bed. In practical work four types of bottom are recognized—*Rock*, *Sand*, *Mud and Sand*, and *Mud*. The criterion of classification is the size of the particles constituting the sea bed, as determined by examining samples obtained by sounding with special devices. Recently, also, techniques of underwater photography have been perfected and have proved useful in studying the bottom. The difference in reverberation intensities among these various bottom types will be discussed below in connection with the discussion of bottom scattering coefficients.

### Transmission Loss—Surface Reflection

It is obvious, from the discussion of Figure 5 in Section 5.3.3, that any bottom reverberation that occurs will be combined with volume reverberation, and, when a horizontally directed beam is used, with surface reverberation. Thus we can not expect that the measured levels of what is, from the geometry of the experiment, predominantly bottom reverberation, will necessarily have the levels predicted by the simple theory expressed by equation (31). (It will be recalled that equation (31) applies to bottom reverberation as well as to surface reverberation.) However, in shallow water over a bottom that scatters strongly, such as rock, the bottom reverbera-

tion may be so much greater than either the surface or volume reverberation that a rough check of the theory is possible. In attempting this, however, the simple inverse square loss will not provide a very reliable guide to the transmission loss. One must consider also the loss due to attenuation.

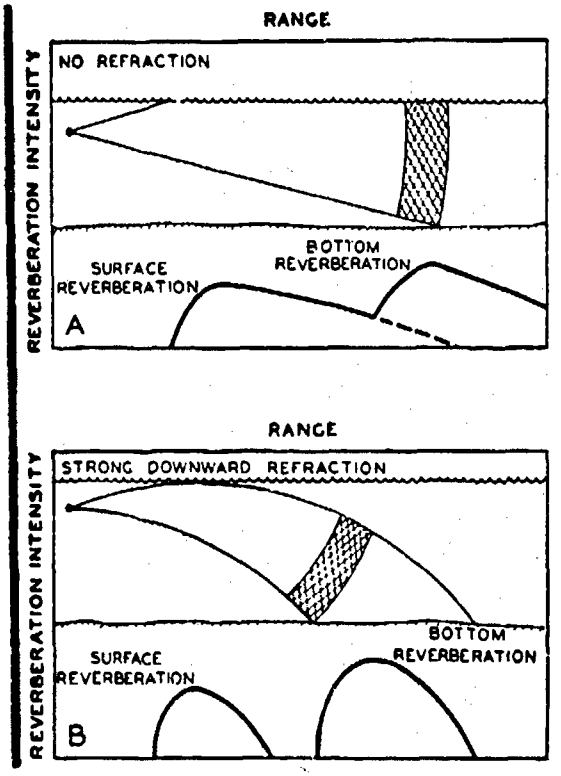


FIGURE 36. Schematic diagrams illustrating surface and bottom reverberation and comparing the cases of no refraction (A) and strong downward refraction (B).

In addition, the effect of the surface in reflecting the sound incident on it toward the bottom, from which it may be scattered back to the transducer either directly or by way of the surface a second time, must be taken into account. Considering the surface to act as a perfect reflector, it is evident that, if refraction is neglected, the intensity of the direct sound at the bottom will be doubled, thus doubling the intensity of the scattered sound. Moreover, the reflection of this scattered sound from the surface causes the intensity at the transducer to be doubled. Hence, the surface increases the intensity of the reverberation fourfold, or, expressed in decibels, raises the reverberation level 6 db.

These deviations from the inverse square loss can, in discussions, be conveniently combined with the latter in the term $H$, of equation (31).

### EFFECTS OF REFRACTION

The effects of the refraction of the sound are more difficult to evaluate. The bending and distortion of the sound beam affects the intensity of the bottom reverberation in several ways. If the beam is bent sharply downward, the sound strikes the bottom at

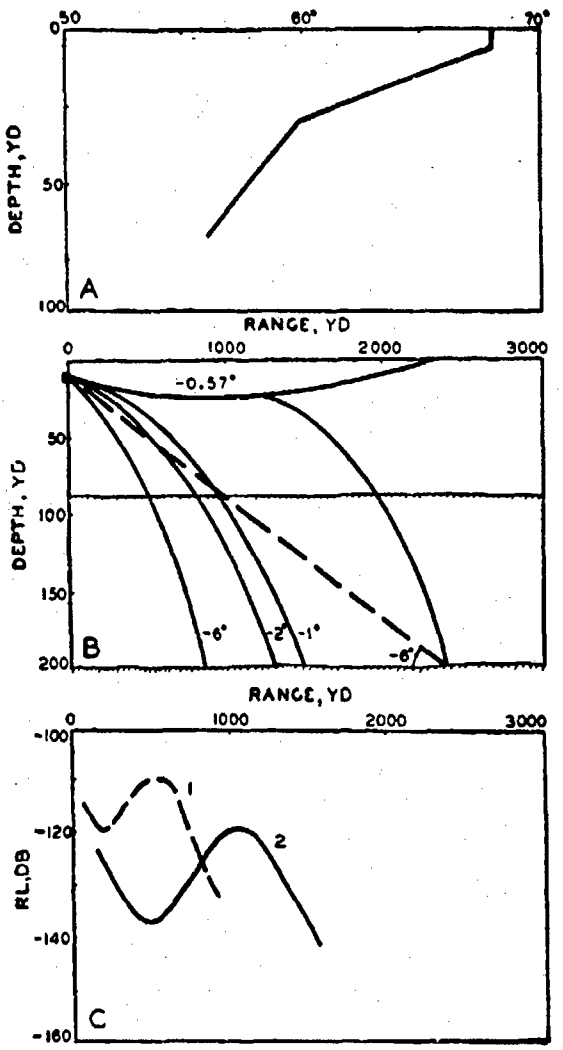


FIGURE 37. Data of an experiment illustrating the conditions shown in Figure 36. (A) Bathythermogram; (B) ray diagram; (C) observed reverberation, curve 1, water depth 87 yd, curve 2, water depth 210 yd.

a shorter range and may be more concentrated; the surface reverberation will decay very rapidly, and the bottom reverberation may be more intense. This is illustrated schematically in Figure 36A and B. It is clear from A that, if the beam is not refracted downward, surface reverberation will be received continuously after the beam first strikes the surface.

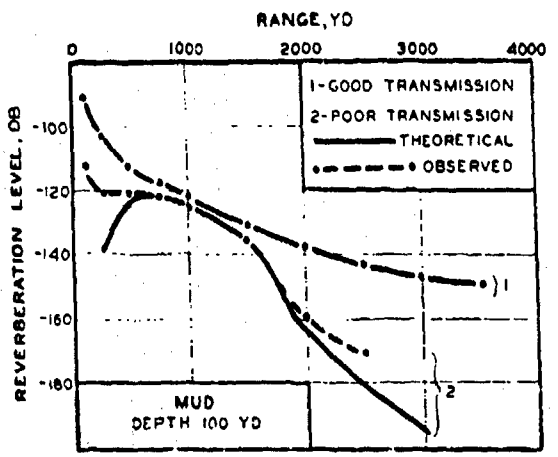


FIGURE 38. Comparison of calculated and observed reverberation in shallow water over mud bottom.

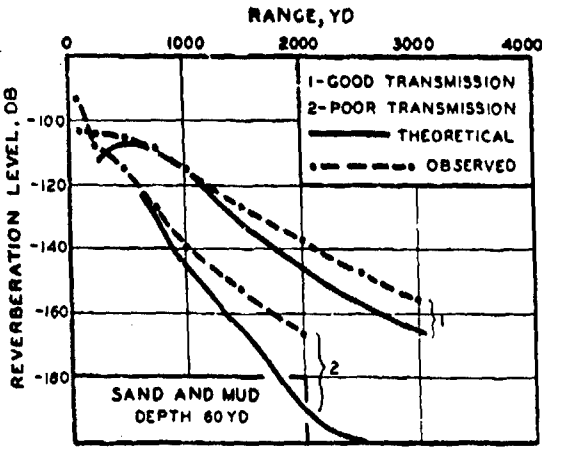


FIGURE 39. Like Figure 38, sand and mud bottom.

On the other hand, as seen from B, a sharply refracted beam strikes the surface in a limited area only; thus the surface reverberation consists of a burst of sound that dies away very rapidly, to be followed by a second burst of sound as the bottom reverberation comes in.

These effects are shown clearly in Figure 37. The bathythermogram shows the thermal pattern of the sea when the reverberation shown by curves 1 and 2 in Figure 37B was measured. The two curves represent reverberation in two different depths of water (87 and 210 yd, respectively). The bending and distortion of the beam is seen in the ray diagram; a dotted line showing the path of the −6-degree ray in the absence of refraction is drawn in. The refracted −6-degree ray strikes the bottom at ranges shorter by 500 and 1,200 yd at the two depths. Moreover, the beam is concentrated between the −1-degree and −6-degree rays, but diverges strongly between the −1-degree ray and the upper limiting ray. One would therefore expect the reverberation to decrease rapidly as soon as the upper half of the beam strikes the bottom, and both curves 1 and 2 show this. The expected rapid decrease of the surface reverberation is also clearly shown. The difference in levels between the two curves is due to the difference in ranges to the bottom in the two cases.

### Comparison of Observed and Calculated Reverberation Levels

A large number of bottom reverberation records have been plotted and compared with the graph of $RL_r$ as a function of $r$, as given by equation (31):

$$RL_r = J_s + 10 \log \left( \frac{H r_0}{2} \right) - 2H_s + 10 \log r. \quad (31)$$

Of the terms in this equation, $J_s$ and $r_0$ are known; the value of $H_s$ must either be predicted or else obtained by making transmission measurements as nearly simultaneously with the reverberation runs as is practicable. The magnitude of the scattering coefficient $n$ is, of course, not known, hence that value of $n$ which will give the best fit with the experimental points is considered to be the appropriate scattering coefficient. In determining the best fit, the region of the graph between 500 and 1,000 yd is given the greatest weight.

The agreement between the calculated and observed reverberation is illustrated by Figures 38 to 41. Each of these exhibits results of measurements taken over a particular bottom type. Two theoretical curves are drawn for each bottom type except mud, in which case transmission data were available only for the case of poor transmission. The curves labeled 1 represent good transmission conditions, those labeled 2, poor transmission. The values of $H_s$ were measured in conjunction with the reverberation measurements.

The experimental points represent averages of from 5 to 30 reverberation runs. The quartile deviation is about ± 5 db on the average. All measurements were made using 80-yd pings.

It should be stressed that these experimental data are not to be considered as representing bottom reverberation generally in shallow water. The measurements which yielded them were taken over particular small patches of particular bottom types.

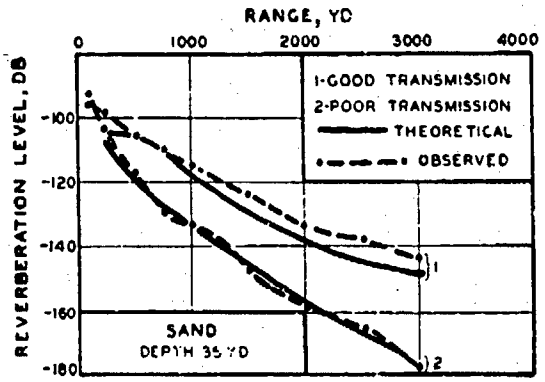


FIGURE 40. Like Figure 38, sand bottom.

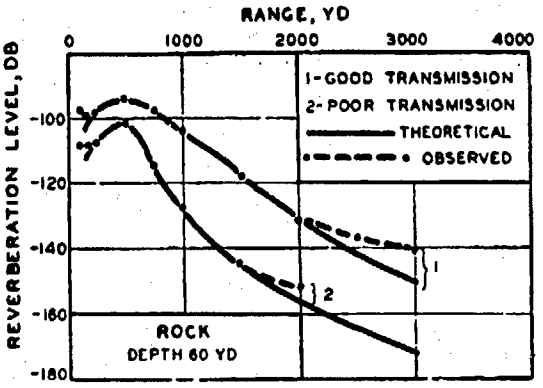


FIGURE 41. Like Figure 38, rock bottom.

The curves will serve, however, to convey a fairly realistic picture of the main features of reverberation in shallow water.

The four figures have certain features in common. The fit in all cases is quite good for ranges less than 1,500 yd. Beyond this range the measured reverberation is consistently higher than the calculated; over *mud* bottom, the difference at 2,500 yd is 10 db; over *sand and mud*, it is 20 db at 2,000 yd. The reason for this divergence at longer ranges is not known.

BOTTOM SCATTERING COEFFICIENTS

| Bottom type | 10 log $n$ |
|---|---|
| Rock | −22 |
| Mud and Mud-Sand | −30 |
| Sand | −31 |

The errors, systematic and random, may be as much as 5 db.

## 5.4.5 Forward Scattering from the ECR Layer

Simple refraction theory predicts a "black" shadow zone under conditions of strong downward refraction. This is not confirmed by 24-kc transmission runs made in deep water off the southern California coast (see Chapter 3). Instead, sound of very low intensity is observed out to ranges of 5,000 yd (some 4,000 yd beyond the limit of the strong direct sound field), which can be explained neither as direct nor as bottom reflected sound. Instead, there appears good reason to believe that it is sound scattered in the forward direction from the ECR layer.

Figure 42 illustrates this phenomenon diagrammatically. Two transmission curves are shown. The dotted curve indicates the level of the direct sound and is seen to drop rapidly with range. This drop occurs at roughly the range of the shadow boundary predicted by the ray diagram. The solid curve represents the level of the sound observed in the predicted shadow zone. It is seen that the transmission anomaly is of the order of 50 db and changes slowly with range.

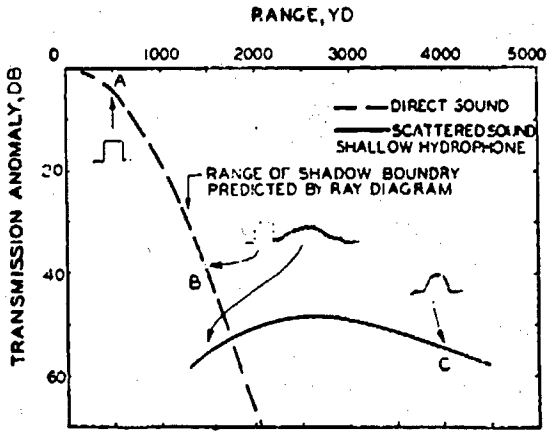


FIGURE 42. Diagram illustrating forward scattering. Transmission with strong downward refraction showing the signal form received at various ranges.

The form of the signal as it is received at various ranges is illustrated schematically. At short ranges (*A*), well inside the direct sound field, only the strong direct signal is observed. In the region of the shadow boundary (*B*) the direct signal is much weaker and is followed by a "tail" which resembles reverberation in appearance. The intensity of sound in the tail is shown by the solid curve. Finally, at ranges far beyond the shadow boundary (*C*), the direct signal has disappeared entirely and the reverbera-

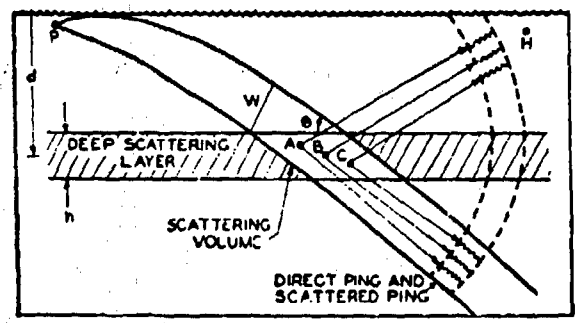


FIGURE 43. Diagram showing forward scattering from the deep scattering layer. Sound scattered from each of the three scatterers *A*, *B*, *C* has a ping length (~~~~) equal to the ping length of the direct sound. Since the travel distances *PAH*, *PBH*, and *PCH* are nearly equal, the three pings of scattered sound are received in the forward direction almost simultaneously at hydrophone *H*, thus constituting a pulse of scattered sound having a ping length equal to that of the direct sound.

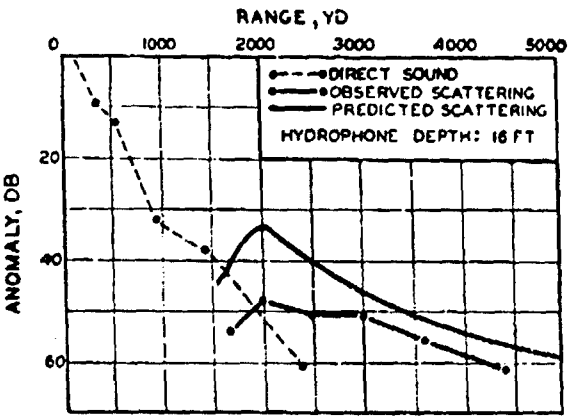


FIGURE 44. Comparison of observed and calculated scattering. In this experiment a 24-yd ping at 24 kc was projected into water 1,500 fathoms deep.

tion tail has contracted to a ragged pulse whose signal length is approximately that of the direct signal. If long signals are used, the intensity of the sound in the shadow zone is unchanged but the duration of the signal is correspondingly longer.

Figure 43 shows schematically how forward scattering can explain the short pulse observed at long ranges. The explanation depends on the fact that the path differences, via the various scatterers, are small, so that all the scattered sound reaches the hydrophone at nearly the same time. With the hydrophone at shorter ranges the path differences are larger and the scattered sound is received over a longer period. This "smears" out the pulse and explains the presence of the tail.

The level of the scattered sound which this mechanism predicts depends on the projector output and beam pattern, the scattering coefficient and thickness of the deep layer, and the angle between the incident sound and the horizontal (Figure 43).

A check of the theory is possible in a few cases where vertical-beam reverberation measurements were made in conjunction with transmission runs. From the vertical reverberation data the scattering coefficient and layer thickness can be found. These can then be used to predict the level of the forward scattering. One such experiment was performed on March 17, 1945, the second of the two days compared in the previous section, with the refraction conditions and deep layer as shown in Figure 35B. Figure 44 shows the observed and predicted scattering for this case. Beyond 3,000 yd the scattered sound is no longer a short pulse but is spread out, and the predicted level is too high. When the hydrophone range is greater than 4,000 or 5,000 yd the observed level should drop rapidly because the scattered sound will be refracted downward (along rays 1 and 2 in Figure 35B) before it reaches the hydrophone. No observations are available at such long ranges to check this, however.

The general good agreement between the theory and the observations, in the few cases which can be checked, indicates two main conclusions:

1. Sound observed in the shadow zone under conditions of sharp downward refraction is forward scattering from the deep scattering layer.

2. The scatterers in the deep scattering layer are approximately isotropic, i.e., scatter sound nearly equally in all directions.

## Appendix

*The reflection of sound by a large, perfectly reflecting sphere.* Let the sound be incident in the direction *QP*, as shown in Figure 45. Consider the cap *APB* on the sphere which is cut out by a plane perpendicular to the incident sound rays. It intercepts sound at the rate

$$W = \tfrac{1}{4}\pi d^2 F \sin^2 \theta \text{ watts}, \qquad (36)$$

where $F$ is the energy flow in watts per unit area at the target of the incident sound energy. All this energy is reflected, and since the angles of incidence and reflection are equal, all of it will be reflected in directions that make angles not greater than $2\theta$ with the incident beam.

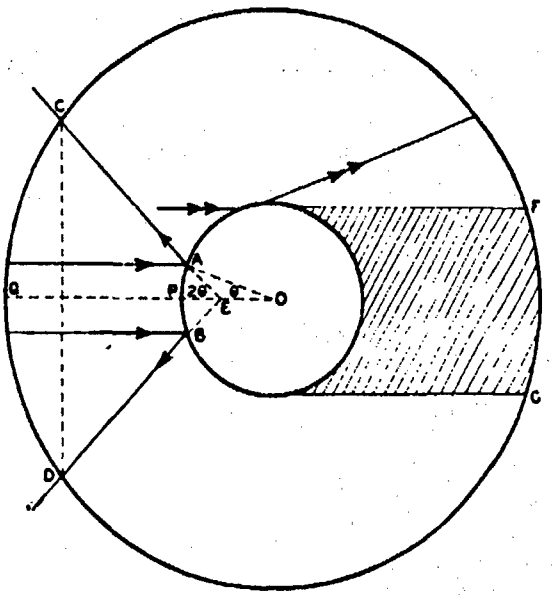


FIGURE 45. Diagram illustrating the calculation of the target strength of a sphere.

Now consider a large sphere of radius $r$, concentric with the target. The reflected energy will pass through the cap $CQD$ of the surface of this sphere. When $r$ is much greater than $d$, and the angle $\theta$ is not too large, the error involved in assuming that the points $E$ and $O$ are the same will be comparatively small. With this assumption the area of the cap is

$$a = 2\pi r^2 (1 - \cos 2\theta) = 4\pi r^2 \sin^2 \theta \qquad (37)$$

to a close approximation. It will be seen that, when $\theta$ is large, this estimate of the area involves neglecting the shadow $FG$ of the sphere. On the other hand, when $r$ is much greater than $d$, this shaded area $FG$ is only a small fraction of the whole area of the sphere. Thus, the proportional error involved will be negligible.

The average rate at which energy passes through the area $CQD$ is given by

$$\frac{W}{a} = \frac{Fd^2}{16r^2}, \text{ watts/yd}^2 \qquad (38)$$

and since it is independent of the angle $\theta$, it follows that it is also the rate at any point of the cap.

Therefore, the energy is reflected (reradiated) equally in all directions, as stated in the text.

# Chapter 6

# WAKES

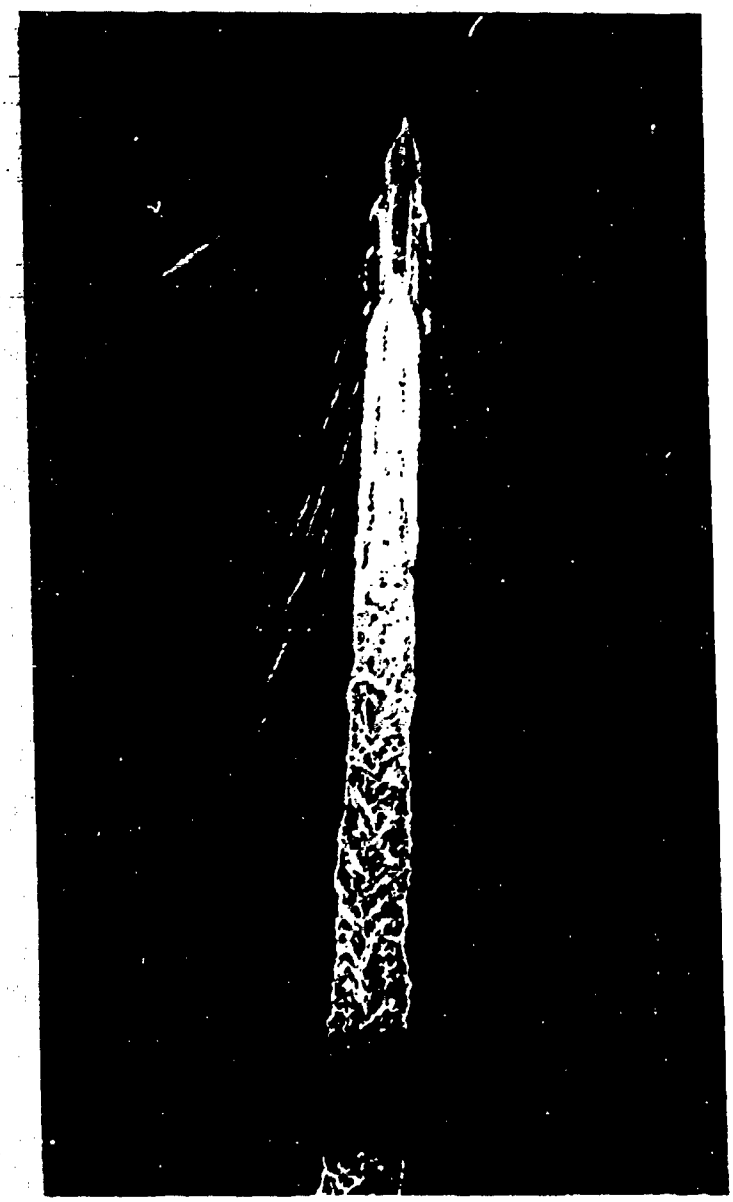

FIGURE 1. Wake of USS *Moale* (DD) at 20 ks from 2,500 ft.

## 6.1 GENERAL DESCRIPTION

### 6.1.1 Visual Appearance

THE GENERAL NATURE of the wake of a ship is most readily seen from the air (Figures 1 to 4). The surface waves that spread out in a V behind the vessel and form a navigational hazard for near-by small craft are relatively inconspicuous from the air. Even the white bow wave, which breaks and sends foam back along the sides of vessel, is seen to be minor compared to the wake of turbulent, foamy water that fans out from the screws.

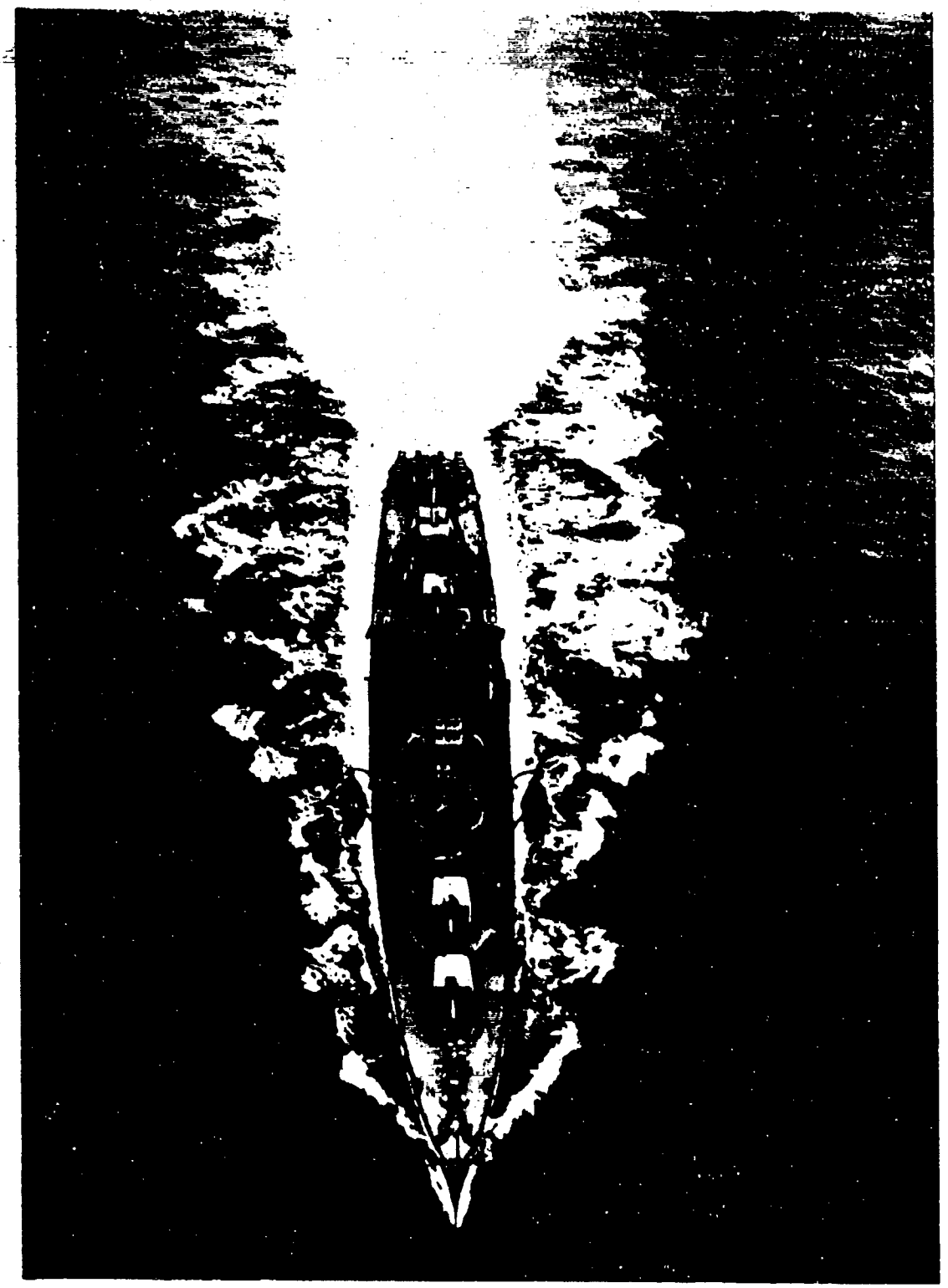

FIGURE 2. USS *Ringold* (DD) from 300 ft.

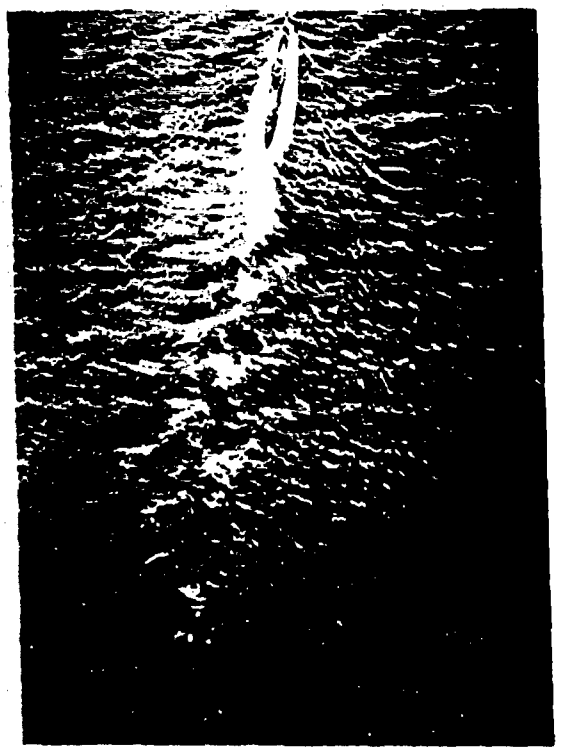

FIGURE 3. Wake of surfaced submarine at 15 kts.

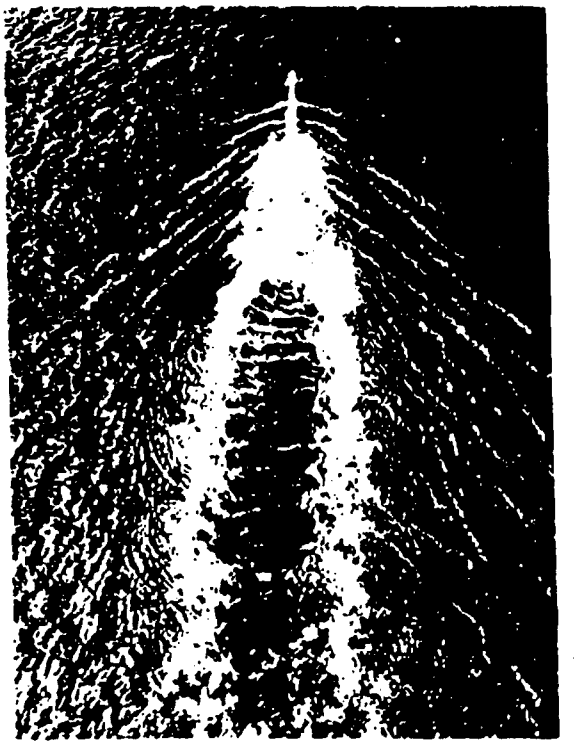

FIGURE 4. Swirl behind submarine after crash dive.

This turbulent wake spreads rapidly for a fraction of the ship's length, and thereafter widens only slightly. The divergence has been measured for various wakes and found to vary from 0.5 to 5 degrees. The foam, which makes it visible from a distance, gradually disappears, but not until long after the ship has passed. The visual wake of a high-speed vessel extends twenty or even fifty ships-lengths astern.

## 6.12 Other Properties of the Wakes of Surface Vessels

It is fairly obvious that the violent disturbance which creates the turbulent wake will give it physical properties that differ to a greater or lesser extent from those of the undisturbed ocean surrounding it.

### Temperature Effects

For example, if there is a temperature gradient in the upper part of the ocean, the mixing of the surface water with that of lower layers will give the water in the wake a different temperature from that of the nearby water at the same depth. This effect has been observed by the use of sensitive recording thermometers. The mixing of water from different depths may also result in anomalous density gradients. While these have not been investigated experimentally, they may be important in causing the ultimate disappearance of the wake.

### Acoustic Properties of Wakes

Of most interest from the present standpoint are the acoustic properties of the wake. They are probably all associated with the presence of entrained air bubbles. The aerial photographs show that large numbers of bubbles remain in the wake for several minutes, and it is likely that some will remain suspended in the water even after the visible foam has disappeared.

These acoustic properties of the wake are easily demonstrated with sonar gear. Figure 5 shows a record of echoes obtained from the wake of the *E. W. Scripps*. This vessel ran between the echo-ranging vessel and a small sphere, the echoes from the latter being recorded simultaneously with those from the wake.

Two general conclusions can be drawn from Figure 5. The wake echo gradually lengthens as it becomes

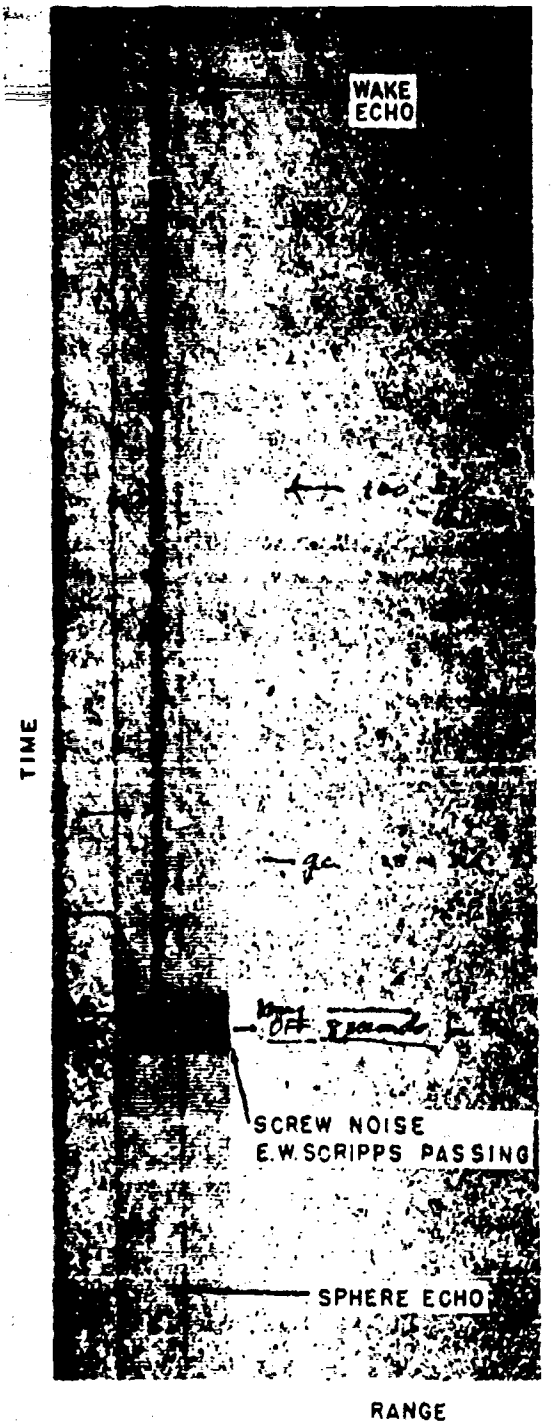


FIGURE 5. Range recorder trace of wake echoes from *E.W. Scripps*.

fainter, presumably because of the spreading of the turbulent wake and the gradual disappearance of the bubbles. Secondly, the sphere echo is weakened slightly, but noticeably, by the presence of the wake between the sonar and the sphere.

In another experiment, a 40-ft motor launch, having a draft of only $2\frac{1}{2}$ ft but with a wake extending to a depth of about 15 ft, passed between a standard 24-kc sonar and a moored buoy. The echo from the buoy was reduced by 13 db after the passage of the launch and did not return to its original level for some 2 minutes.

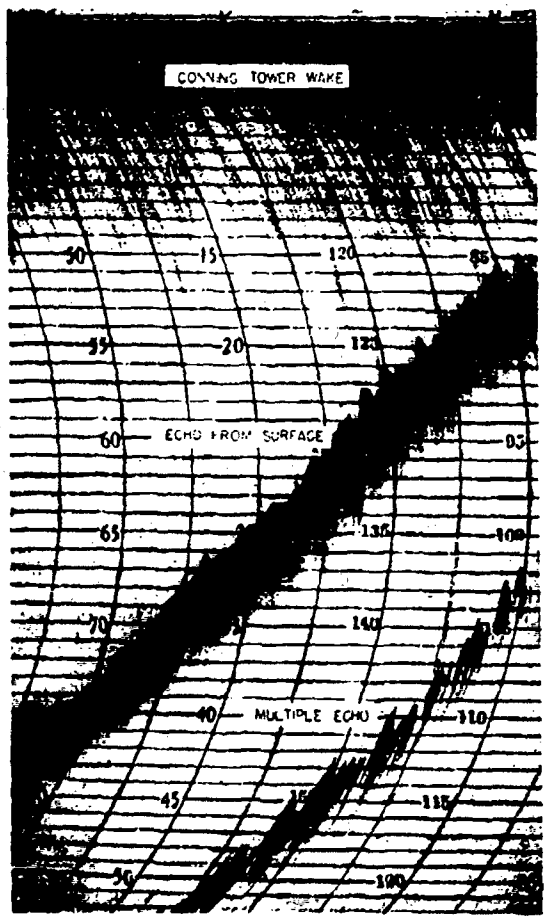


FIGURE 6. Echo-sounding record from surface. Taken on submarine during a dive (photograph from USNEL, San Diego).

These conclusions are substantiated by a series of experiments performed by USNRSL (San Diego). An echo sounder was mounted in an inverted position on the deck of a submarine. When submerged, it was thus possible to echo range on the surface and record the depth of the submarine. This is illustrated by Figure 6, which is the record of a dive. The increasing depth during a dive is clearly indicated, as are the waves on the surface.

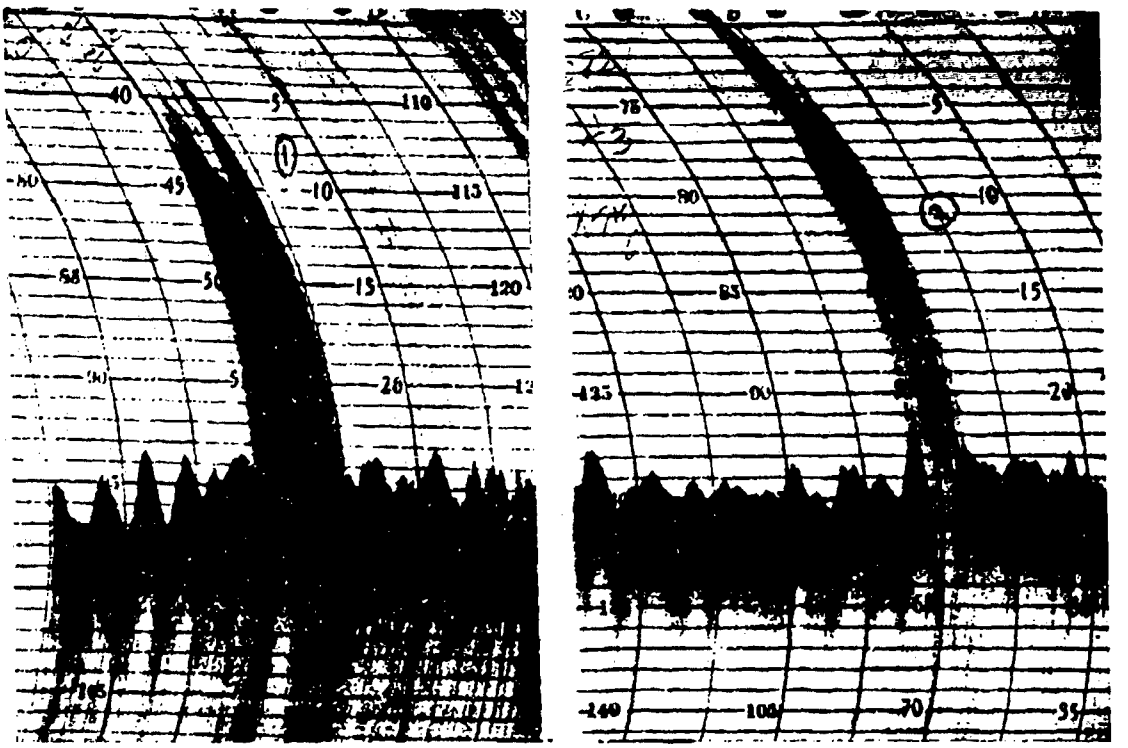

FIGURE 7. Similar to Figure 6. Record made while submarine was passing under the wake of a surface vessel. (Photograph from USNEL, San Diego.)

Figure 7 shows similar records made while the submarine passed under the wake of a surface vessel. In each of the two examples, it can be seen that the wake returned sound to the receiver, and also that it reduced the amount of sound returned from the surface.

It may thus be concluded that the wakes of surface vessels have two major acoustic properties: they return echoes that are readily detectable by ordinary sonar gear, and they act as acoustic screens, reducing the intensity of the echoes from targets on their far side.

## 6.3 THEORY OF THE ACOUSTIC PROPERTIES OF WAKES

### 6.3.1 Air Bubbles As the Cause of Wake Echoes

The two most obvious differences between a surface wake and the undisturbed ocean are its turbulence and its content of bubbles. It is therefore reasonable to assume that one or both of these are the cause of its acoustic properties.

The possibility that turbulence is the cause of wake echoes is ruled out by theoretical considerations. It is true that when a sound wave passes through turbulent water it is scattered. But two facts exclude the assumption that this scattering is the cause of echoes. First, the scattering from turbulence is very weak unless there are great differences in velocity between pairs of points separated by one wavelength of the sound. Second, the intensity of the scattered sound depends strongly on the direction of scattering, and the intensity in the backward direction is zero. Thus, although turbulent water scatters sound, it does not return an echo.

Turbulence might be an indirect cause of the echoes by mixing the warmer surface water with that from below. In this way, irregular differences of temperature are produced by the irregular differences in the turbulent velocity. Again, however, the magnitude of the expected effect is too small; in order to produce the observed echoes, temperature differences of nearly 1°F would have to occur between points only one wavelength apart. Such large temperature differences are very improbable. Moreover, if they were formed in some way, they would persist for a very long time, longer than wakes are observed to persist.

Thus, it may be concluded that the air bubbles in the wake are the major cause of the acoustic properties of a wake. Several objections have been urged against this conclusion. One objection is based on the supposed short life of bubbles in water. Bubbles rise to the surface and break, so that they disappear from the wake in a short time; their disappearance is also hastened by solution of the air by the sea water. On the other hand, echoes have been obtained from wakes more than 10 minutes after the vessel passed, and there have been reports of echoes from wakes several hours old. The latter reports may be discounted, since it is very difficult to be certain of the position of a wake so long after the ship has passed, and it is quite possible that a school of fish, etc., might be mistaken for a wake under such circumstances. It is therefore only necessary to show that some bubbles will remain suspended for periods of 10 to 30 minutes.

Experimental evidence on this point was obtained by stirring the water of the pool at USNRSL with an outboard motor. The acoustic properties of the water were studied with an echo sounder. It was found that sound was returned from the body of the water after stopping the motor. This return continued even after all of the more obvious bubbles and turbulence had disappeared. Closer examination showed, however, that a relatively small number of small bubbles remained suspended. They were very difficult to see except when they drifted into a region of favorable illumination, so that neither their number nor their size could be accurately determined. It was concluded that sufficient bubbles were present to explain the observed effects. This was based on the consideration that very small bubbles are quite effective in scattering sound but rise very slowly (see Figure 1 of Chapter 5 and Figure 8 of this section) and are especially difficult to observe.

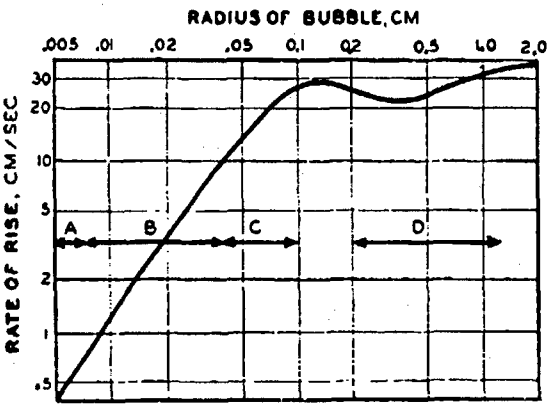


FIGURE 8. Rate of rise of air bubbles in still water: *A*. Rectilinear motion, spherical shape. *B*. Helical and twisting motion, flattened shape. *C*. Irregular. *D*. Rectilinear motion, distorted mushroom shape.

Theoretical and experimental studies on the rate of rise of bubbles in still water are summarized in Figure 8. The rate of rise of the bubbles which are most effective in scattering is seen to be about 1 yd/minute. These results for still water do not apply directly to wakes or turbulent water. The long-lived bubbles observed in the USNRSL pool did not show any marked tendency to rise, but were carried in irregular paths by the motion of the water. This is analogous to the effect of air currents in keeping dust from settling. It is reasonable to suppose that the moderate turbulence in an old wake will have this same effect and prevent the disappearance of the bubbles.

## 6.2.2 Propeller Cavitation as a Source of Bubbles

The second objection is based on the fact that echoes are obtained from the wakes of submerged submarines and the idea that most of the bubbles in a wake come from the breaking bow wave. The aerial photographs strongly suggest that this idea is not correct, since most of the foam appears to come directly from the screws. This is borne out by the observation that the wake laid by a vessel under sail is less acoustically active than the wake of the same vessel under power.

Hence it is probable that most of the bubbles are caused by cavitation at the propellers. Photographs of this phenomenon are shown in Figures 9 and 10. The bubbles are seen to be formed far from the air-water interface and are not sucked under from the atmosphere. The mechanism of cavitation is apparently very similar to that of boiling. Because of the motion of the screws, the hydrostatic pressure is reduced; the boiling point of water is lowered by this reduced pressure, so that it is below the actual temperature of the water, and boiling occurs. For example, pure water will boil at 60°F if the pressure is reduced much below one-sixtieth of an atmosphere.

FIGURE 9. Cavitating propeller. The water in the jet is moving away from the observer. The back of each blade is left covered with cavitation bubbles and a cavitation void which extends for some distance behind the blade, whereas the face of each blade is clean. (Photograph by David Taylor Model Basin.)

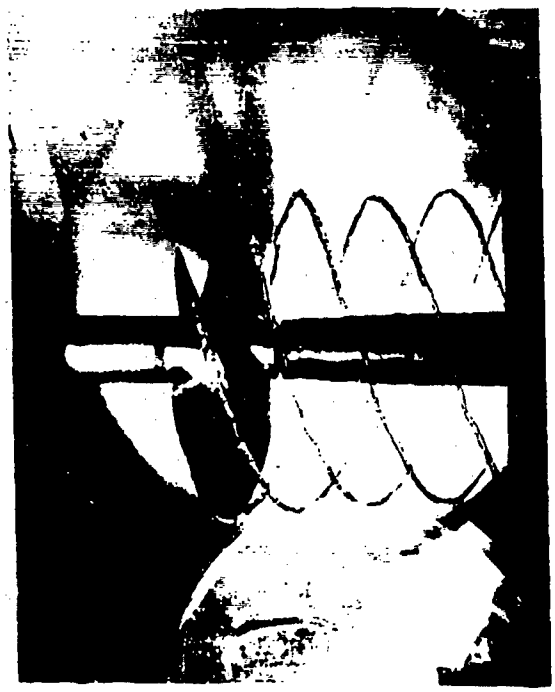

FIGURE 10. Tip vortices emanating from a propeller. The combination of the rotation of the propeller and the flow of the water in the jet from left to right gives a spiral pattern to the vortices. (Photograph by David Taylor Model Basin.)

However, sea water is not pure. In the present connection, dissolved air is the most important impurity. This is present in such quantities that sea water will boil at 60°F whenever the pressure is reduced much below one atmosphere. The bubbles produced by this boiling are filled principally with air, rather than water vapor. Once formed, these bubbles are apparently quite stable, i.e., the rate at which the air is redissolved is very slow.

Laboratory experiments[5] show that the diameter of the bubble decreases at a constant rate at any given depth. Figure 11 shows that at a depth of 50 m the diameter of a bubble decreases 1 mm every 10 minutes. Thus, a bubble initially 1 mm in diameter would require 9 minutes to reach a diameter of 0.1 mm and a further 1 minute to reach a very small diameter or disappear.

It appears likely that, even in the wakes of surface vessels, much of the foam is the result of cavitation, and that only a part of it is caused by air dragged under from the atmosphere. In the wakes of submerged submarines, the only sources of air other than cavitation might conceivably be a leaky high-pressure air line.

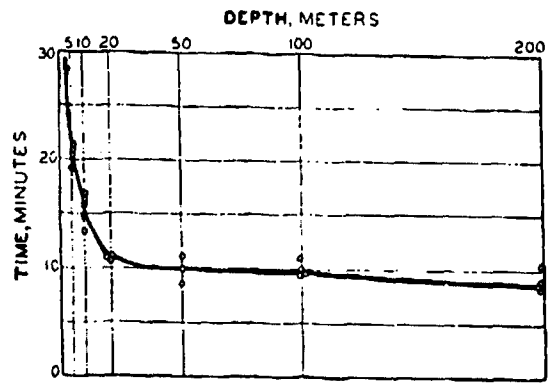


FIGURE 11. Rate at which the size of bubbles varies at various depths. The curve shows the time required for the diameter of a bubble to decrease 1 mm.

## 6.2.5 Dependence of Cavitation on Depth and Speed

It is found that cavitation depends critically on propeller rpm. A given propeller at a given depth of submergence will produce no bubbles unless its speed exceeds a certain critical value. Let $N_0$ rpm be this critical value; when the speed exceeds $N_0$,

the number of bubbles formed increases very rapidly, but not according to any known law.

The critical speed itself, however, depends in a simple manner on $h$, the depth of the propeller beneath the sea surface. This dependence is given by

$$\frac{N_0^2}{h} = \text{constant.} \qquad (1)$$

Thus, if a given propeller begins to cavitate at 50 rpm when at a depth of 15 ft, it will begin to cavitate at 100 rpm when at a depth of 60 ft, and not until 200 rpm when at a depth of 240 ft.

The constant in equation (1) depends on the design of the propeller, and on any accidental changes in its shape that may occur in service. A scratch or nick caused by some accident will usually reduce the value of the critical speed very appreciably. One remarkable property of cavitation is that the bubbles themselves scratch and scar the metal surface on which they are formed.[2]

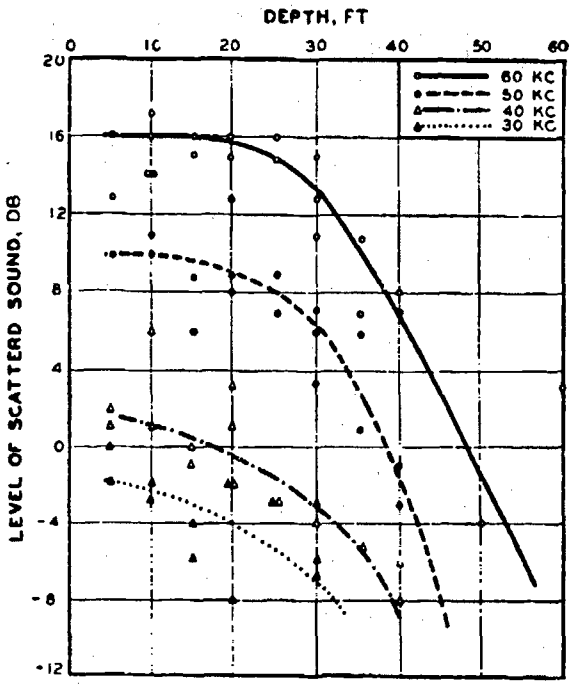


FIGURE 12. Dependence of level of scattered sound on depth. The sound was scattered from the wake of a 10-in. propeller run at 1,600 rpm. The direct signal was constant for each frequency.

This theory of the connection between cavitation and the acoustic properties of wakes has certain consequences that can be qualitatively checked. Thus the wake of a submerged submarine should return echoes, but they should be considerably weaker than when the ship is moving on the surface. They should also become progressively weaker as the depth of submergence increases. Finally, they should increase rapidly with propeller speed. All these conclusions are in general agreement with experience.

Experiments designed to test the theory were performed by Woods Hole Oceanographic Institution. A small propeller (10 to 20 in. in diam) was operated when suspended from a wharf at various depths up to 60 ft. The possibility of atmospheric air being entrained in its wake was thus definitely excluded. No echoes were obtained when the propeller speed was below the critical speed for cavitation; echoes were obtained at higher speeds. The wake was also observed to attenuate sound passing through it. Figure 12 summarizes the measured scattering of sound by the 10-in. propeller, as a function of depth and frequency.

The propellers are probably not the only source of cavitation bubbles. Since the ship as a whole is moving through the water, cavitation can occur at other places. In general, the smaller the object, the lower is the critical speed at which cavitation occurs. Thus small fittings or hand rails on the deck of a submarine may become sources of cavitation bubbles when submerged. This effect is probably the explanation of the blackening in the upper part of Figure 6. Such "conning tower wakes" probably contribute only slightly to the reflection of sound from the submarine, although the only experimental evidence on this point is that of Figure 6.

### 6.2.4 The Propagation of Sound in Water Containing Bubbles

The theoretical discussion of the acoustic properties of water containing air bubbles is complicated, and the studies are not complete.[3] In order to present the general ideas of the theory without confusion, it is convenient to introduce certain terms for the description of water containing bubbles.

In *foamy water*, the average distance between neighboring bubbles is less than the average diameter of the bubbles. In the extreme case, the walls separating the bubbles may be very thin, as in the case of soap suds. The acoustic theory of foamy water has not been studied at all, but this is no serious lack, since wakes probably contain foamy water only at

the air-water surface, where the bubbles tend to accumulate.

In *bubbly water*, the average distance between neighboring bubbles is considerably greater than the average diameter of the bubbles, but much less than the wavelength of the sound involved. For practical purposes, the water may be considered to be bubbly if it contains less than one part per 1,000 (by volume) of air, and foamy if it contains much more than this. The bubbles are *dispersed* if the average distance between neighbors is greater both than one wavelength of the sound and than the average diameter. Thus a portion of a wake may be dispersed for supersonic frequencies and bubbly for sonic frequencies.

It would be very useful to have information concerning the foamy, bubbly, and dispersed regions of typical wakes. Unfortunately, there is relatively little information of this sort other than that which can be obtained from the inspection of aerial photographs or deduced indirectly from acoustic measurements. It is probable that the wake reaches the dispersed state some 5 to 10 ship-lengths astern of the screws, and is foamy only in the immediate neighborhood of the screws, or of the air-water surface.

## 6.2.5 Scattering and Absorption of Sound in Wakes

The theory of dispersed wakes is very similar to the theory of reverberation, with the exception that somewhat greater attention must be given to detail.

Consider a single bubble of diameter $d$, in a region where the flow of acoustic energy is $F$ w./yd$^2$. This bubble will remove power from the beam at the rate

$$P = F\sigma_0 \text{ watts removed,} \qquad (2)$$

where $\sigma_0$ will be called the *total effective cross section* of the bubble. Of this power, a fraction $\varkappa$ will be reradiated as sound, so that

$$\varkappa P = F\varkappa\sigma_0 = F\sigma \text{ watts scattered.} \qquad (3)$$

The quantity $\sigma = \varkappa\sigma_0$ will be called the *scattering cross section* of the bubble. It is the quantity which was discussed in Section 5.4 and may be very much greater than $\pi d^2$ (see Figure 1 of Chapter 5). The remainder of the power will be converted into heat, i.e., absorbed by the air of the bubble and, to a lesser extent, by the water surrounding it; thus

$$(1-\varkappa)P = F(1-\varkappa)\sigma_0 = F\sigma_a \text{ watts absorbed.} \qquad (4)$$

The quantity $\sigma_a$ is called the absorption cross section of the bubble. Note that

$$\sigma_0 = \sigma + \sigma_a. \qquad (5)$$

There are theoretical reasons for believing that $\sigma_0/\sigma$ is about 10.

Figure 13 shows the variation of the scattering and absorption cross sections with the diameter of the bubble, the sound frequency being 24 kc. The abscissa shows the ratio of the actual diameter of the bubble to the resonance diameter calculated from equation (11) of Chapter 5. Note that the absorption of sound by the bubble causes a slight shift of the resonance peak to smaller diameters than given by that equation. The ordinate is the ratio of the scattering or absorption cross section to the geometric cross section of the bubble.

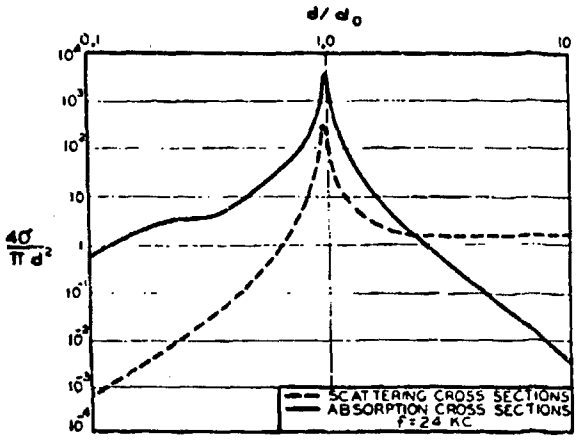


FIGURE 13. Variation of scattering cross section and absorption cross section of a bubble with its diameter for 24-kc sound. The abscissa is the ratio of the actual diameter of the bubble to the resonance diameter calculated from equation (11) of Chapter 5. The ordinate is the ratio of the scattering cross section or absorption cross section, respectively, to the geometric cross section of the bubble.

In the theory about to be developed, it will be shown that it is the total effective cross section $\sigma_0$, which determines the screening caused by a wake, while the strength of the wake echo is determined by the scattering cross section $\sigma$.

Even though the wake is dispersed, so that the distance between neighboring bubbles is large, the whole wake will still contain many bubbles. Some of these will not be in the sound beam, and thus can be neglected. This is indicated diagrammatically in Figure 14. In plan, the wake is shown as a parallel strip, the sound beam as a divergent one. In section,

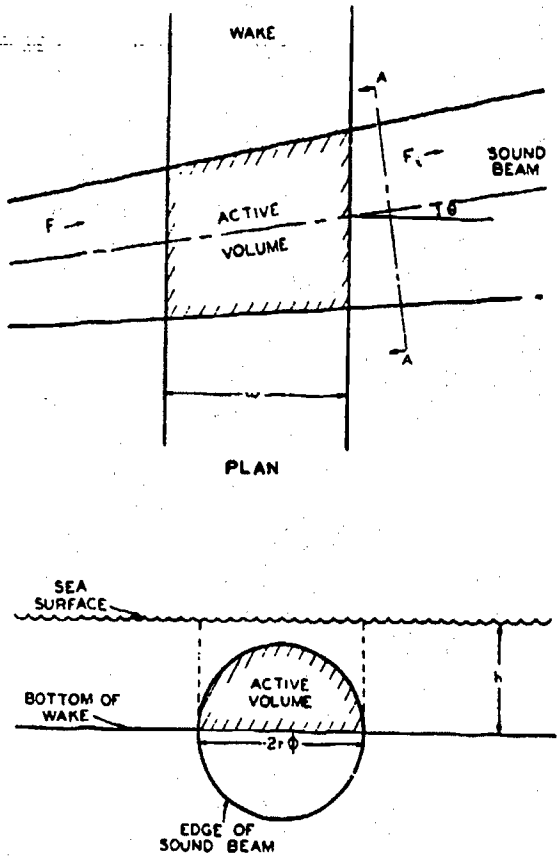


FIGURE 14. Diagram showing intersection of sound beam and wake in plan (upper figure); the lower figure shows section A-A. $F$ = energy flow in incident beam; $F_t$ = energy flow after traversing the wake; $\theta$ = angle between axis of sound beam and axis of wake; $\phi$ = angular half width of sound beam; $r$ = distance from sonar to wake; $h$ = vertical dimension of wake; $w$ = width of wake.

the sound beam is shown as a sharply bounded circle, and the wake as a sharply bounded layer. These sharp boundaries are probably not realized in practice, but are convenient idealizations. Only those bubbles in the intersection of the two, i.e., in the region marked "active volume," contribute to the acoustic effects. The total number of bubbles that are effective thus depends on $w$, the width of the wake; on $\theta$, the angle between the wake and the axis of the sound beam; and on $A$, the area of the sound beam that is intercepted by the wake.

The theory of wide wakes is rather different from the theory of narrow wakes, so that the distinction between the two kinds will be considered in some detail. Figure 15 is an enlarged schematic of the Section AA of Figure 14. The position of each bubble is indicated by a dot; the circles surrounding the dots are supposed to have the area $\sigma_0$ appropriate to each bubble. (Scale relations are obviously exaggerated.) The total number of bubbles in the active volume is small in the case illustrated, so small that their projected areas overlap in only a very few cases. When this condition is fulfilled, the wake will be called *narrow*. When, on the other hand, there

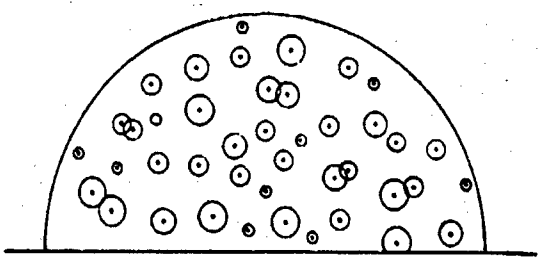

FIGURE 15. Enlarged schematic of section A-A of Figure 14. The dots represent bubbles; the circles surrounding the dots are supposed to have the area $\sigma_0$ appropriate to each bubble. (Scale relations are obviously exaggerated.)

are so many bubbles that their projected areas usually overlap, the wake will be called *wide*. It should be noted that this definition depends on the total number of bubbles in the active volume, not merely on the number of bubbles in unit volume.

## 6.2 6 Theory of Narrow Wakes

### The Screening Action of Wakes

The approximate calculation of the screening effect and target strength of a narrow wake can be made as follows.

Let $N$ = average number of bubbles in unit volume of the wake (1/yd³),
$\sigma_0, \sigma$ = average total and scattering cross section of one bubble (yd²),
$w$ = geometric width of wake (yd) (see Figure 13),
$\theta$ = angle between axis of sound beam and axis of wake,
$A$ = area of sound beam intercepted by the wake (yd²) (see Figure 12).

Then the active volume will be approximately given by

$$\frac{Aw}{\cos\theta}\ (\text{yd}^3). \qquad (6)$$

The total number of active scatterers will be $N$ times this volume, and their effective area will be

$$\frac{N\sigma_0 A w}{\cos\theta} \text{ (yd}^2\text{)}. \tag{7}$$

In this calculation, all effects caused by the overlapping of the projected areas in Figure 15 have been neglected, since the wake is narrow. The total power removed from the sound beam will be

$$\frac{FN\sigma_0 A w}{\cos\theta} \text{ (watts removed)}. \tag{8}$$

The power in the incident beam is $FA$, and after it has traversed the wake, the power in the beam is $F_t A$; consequently,

$$F_t A = FA\,\frac{1 - N\sigma_0 w}{\cos\theta}. \tag{9}$$

The ratio of the transmitted energy flow to the energy flow incident on the wake measures the transmission loss in traversing the wake. It obviously applies only to that part of the sound beam that has passed through the wake, and not to the part that has passed under it.

The transmission loss $H$ in decibels is given by

$$H = 10 \log \frac{F_t}{F} = 10 \log \frac{1 - N\sigma_0 w}{\cos\theta}. \tag{10}$$

### The Scattering Action of Wakes

The total power removed from the beam by scattering will be obtained from equation (8) on replacing the total cross section $\sigma_0$ by the scattering cross section $\sigma$,

$$\frac{FN\sigma A w}{\cos\theta} \text{ (watts scattered)}. \tag{11}$$

At a great distance $r$ from the active volume of the wake, this scattered power will be spread over a sphere of area $4\pi r^2$. Hence, the average energy flow at this distance will be

$$\frac{FN\sigma A w}{4\pi r^2 \cos\theta} \text{ (w/yd}^2\text{)}. \tag{12}$$

Comparing this with equations (6) and (9c) of Chapter 5, which are

$$F_s = \frac{F\sigma}{4\pi r^2},$$

and

$$T = 10 \log \left(\frac{\sigma}{4\pi}\right),$$

it is seen that the target strength of the wake is

$$T = 10 \log \left(\frac{N\sigma A w}{4\pi \cos\theta}\right). \tag{13}$$

This expression is noteworthy in that it contains $A$, the cross section of that part of the sound beam intercepted by the wake. This was not true in the case of the screening ratio $F_t/F$. Since the sound beam diverges, $A$ will increase with the range of the wake from the sonar projector, so that the target strength of a distant wake will be greater than that of a nearer one, all other things being equal.

### The Strength of the Wake

The accurate calculation of $A$ is complicated, and the values of many of the quantities entering it are uncertain. Consequently, a very rough calculation will suffice for the present. Let the angular half-width of the sound beam be $\phi$ radians. Then the diameter of the beam at a range of $r$ yd from the sonar will be $2r\phi$ yd. If the wake has a vertical dimension of $h$ yd (see Figure 14), an approximate expression of $A$ is

$$A = 2r\phi h. \tag{14}$$

Substituting this in equation (13), one obtains

$$T = 10 \log \left(\frac{N\sigma w h}{4\pi}\right) + 10 \log \left(\frac{2r\phi}{\cos\theta}\right). \tag{15}$$

This expression has been separated into two terms, the first of which contains only quantities characteristic of the wake, the second only quantities describing the position of the sonar, and the bearing and width of the sonar beam. The first term of equation (15),

$$W = 10 \log \left(\frac{N\sigma w h}{4\pi}\right) \text{ db}, \tag{16}$$

is called the *strength of the wake*. Since $2r\phi$ is essentially the length of the wake that lies in the sound beam, $W$ may be interpreted as the *target strength of 1 yd of the wake*.

One objective of the research on wakes has been to determine $W$ for the wakes laid by various types of vessels under various conditions.

## 6.2.7 Theory of Wide Wakes

In the case of wide wakes, the total number of bubbles in the active volume is so great that there is much overlapping of the projected areas in Figure

15. If equation (8) were used to calculate the power removed from the sound beam, this quantity would be greater than $FA$; the wake would, according to this formula, remove more power than was incident on it. This is obviously absurd, and results from the neglect of the overlapping projected areas.

One might be tempted to allow for the overlapping by assuming that the bubbles nearest the source of sound cast shadows on those farther away, thus rendering them ineffective in removing power from the beam, or in returning echoes. Without going into the details of the calculation, this would replace equation (10) by the equation

$$\frac{I_t}{F} = \exp\left(-\frac{N\sigma_a w}{\cos\theta}\right) \tag{17}$$

and replace equation (13) by

$$T = 10 \log \frac{.1\sigma}{8\pi\sigma_a}\left[1 - \exp\left(\frac{2N\sigma_a w}{\cos\theta}\right)\right] \tag{18}$$

These equations are free from the obvious absurdity of equations (10) and (13) when applied to wide wakes and are probably reasonably accurate. Several theoretical objections to them will be discussed, since the discussion brings out important characteristics of wakes. In the first place, obstacles smaller than one wavelength in diameter do not cast sharp shadows, even though a cloud of them does weaken the train of waves passing through it. In the second place, sound scattered by one bubble may reach a second bubble and be scattered a second time. Neither of these facts are considered in the derivation of equations (17) and (18).

Theoretically, the possibility of multiple scattering is the more important reason for doubting the validity of these equations. They are based on the assumption that most of the sound energy is traveling in the direction of the incident wave, and that sound traveling in other directions has been scattered only once. If the scattering cross section $\sigma$ were much greater than the absorption cross section $\sigma_a$ (or, in other words, if $\sigma_a$ were about equal to $\sigma$), this would not be true. In the interior of a wide wake, most of the sound would have been scattered many times; and waves traveling in all directions would be present. The most common example of this phenomenon is presented by the sun's light on a foggy day: from the interior of the fog, it is impossible to determine the direction of the sun. A further consequence of the diffuse illumination is that even large objects cast no shadows. To pursue the analogy, the interior of a narrow wake would be similar to a hazy day, in which the sun can be seen distinctly but is dimmed by the haze.

It is probable that this condition is not present in wakes. As has been remarked, the ratio of $\sigma$ to $\sigma_0$ is of the order of magnitude 0.1. Consequently most of the energy intercepted by a bubble will be absorbed and only a small part will be scattered. By the time this process has been repeated, the multiply-scattered radiation will be so weak as to be negligible. The analogy to daylight in a fog breaks down under these conditions, and the situation is rather more like looking at the sun through a dark glass. The direct, unscattered radiation is weak, but the scattered radiation is even weaker.

## 6.28 Theory of Bubbly Wakes

### Change in Velocity of Sound Due to Bubbles

The mathematical theory of bubbly water is similar to the theory of the index of refraction of light in a gas composed of separated molecules. In both cases, the velocity of the waves is determined by the number and nature of the particles in their path.

Small amounts of air bubbles can produce very appreciable changes in the velocity of sound. There is little experimental evidence on this point, and the theory is complicated by the fact that the bubbles are not all the same diameter. Figure 16 shows the theoretical change in the velocity of sound caused

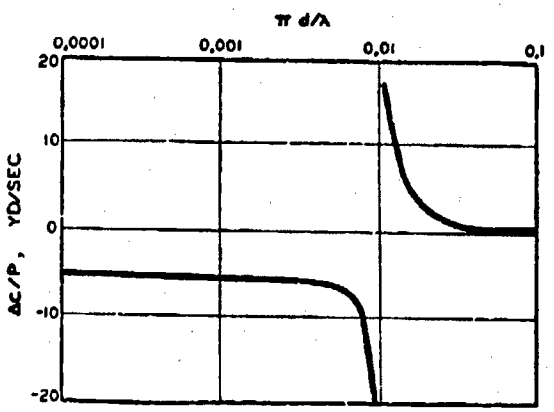


Figure 16. Change in velocity of sound as a function of ratio of circumference of bubble to wavelength of sound. $\Delta C$ = change in velocity of sound. $P$ = parts per million of air bubbles, by volume. $d$ = diameter of bubble. $\lambda$ = wavelength of sound.

by 1 part/million (by volume) of air bubbles, as a function of $(\pi d/\lambda)$, where $d$ is the diameter of the bubbles and $\lambda$ the wavelength of the sound. The wavelength is to be measured in bubble-free water, and it is assumed that the air in the bubbles is at a pressure of one atmosphere.

For other concentrations, the change in the velocity of sound is proportional to that shown in the figure, provided that the change is not more than a few hundred yards per second. Concentrations producing larger changes than this require special computations that have not yet been carried out.

The significance of this changed velocity of sound for the theory of wakes is not clear. If the wake had very sharp boundaries, the abrupt change in velocity would result in reflection of the sound. However, the boundary of an actual wake is probably never sharp, and hence this reflection will not occur. However, sound rays passing through the wake will be refracted. The angular deflection of the rays is difficult to determine, either experimentally or theoretically.

### Scattering and Absorption

Apart from this change in the velocity of sound, scattering and absorption also occur. Qualitatively, these effects are entirely similar to those in dispersed wakes. The quantitative differences have not been studied theoretically, but some guesses concerning the results of such a study can be made. The individual bubbles in a dispersed wake have been assumed to act, each as though the others were not present. In bubbly water, this will no longer be the case. One effect of this "cooperation" among the bubbles is the change in the velocity of sound.

### Other Cooperative Effects

It is possible that other cooperative effects become important in bubbly water. For example, consider two bubbles, widely separated, having scattering cross sections $\sigma'$ and $\sigma''$. If these same bubbles are brought close together, so that the distance between their centers is not more than 2 or 3 diameters, the numbers $\sigma'$ and $\sigma''$ will cease to have any significance. It will not be possible to distinguish between the energy scattered by one and that scattered by the other. Moreover, the total amount of energy scattered will not be determined by the sum $\sigma' + \sigma''$, but will depend also on the distance between their centers. Thus, it is certain that the theory of foamy water will be primarily concerned with cooperative effects. Bubbly water is a transition stage; it may be that cooperation in scattering begins when the average distance between bubbles becomes comparable to one wavelength, for it is certain that cooperation is well developed when the distance becomes comparable to one diameter.

## 6.2.9 The Importance and Interpretation of Scattering Experiments

Historically, the study of scattering and absorption has played an important part in the development of various branches of physics. This is especially true of those branches dealing with radiations that are not perceptible by the unaided human senses, such as X rays, $\alpha$ rays, $\beta$ rays, $\gamma$ rays, cosmic rays, and more recently, neutron rays. The scattering of visible light explains the color of the clear sky and other meteorological phenomena. The scattering of sound waves had not been studied in any systematic manner prior to World War II. During the war, such studies were begun but are still far from complete.

Modern knowledge of the structure of matter, atoms, and nuclei is largely based on scattering experiments. It is unlikely that experiments on the scattering of sound and radio waves will contribute much to this fundamental body of knowledge concerning the imperceptible structure of matter. It is almost certain, however, that they will contribute much to the knowledge of the inaccessible parts of the ocean and the atmosphere. It is for this reason that studies of reverberation and of the scattering of sound by wakes are considered to be very important, even apart from immediate practical objectives.

The literature on the scattering of other forms of radiation is voluminous, and there is no one source book. The interpretation of the experiments has been the subject of much careful thought, and has resulted in many major advances in knowledge. However, examples of misinterpretations on the part of conscientious and able experimenters are also numerous. For this reason, some words of caution are appropriate at this point.

The most common error is the measurement of extraneous radiation along with that which it was intended to measure. Thus, in measuring the intensity of sound transmitted through a wake, it is most important to shield the hydrophone from all sound

that passes beneath the wake (see Figure 14). This may be a difficult thing to accomplish.

The interpretation of many laboratory experiments has been simplified by the use of opaque screens to shield the detector from extraneous radiation. Sometimes these screens have not been completely opaque, and often their edges have been the source of scattered radiation. In performing scattering experiments at sea, it is not possible to use such screens, so that the possibility of extraneous sound is particularly great.

Another error is the application of theoretical equations to circumstances that do not conform to the assumptions made in deriving them. Thus, equations (17) and (18) are derived on the assumption that the source and receiver of sound are both well outside the wake and are highly directional. If one or both are in the wake, or even if the receiver is near the wake, these equations may be considerably in error. If the receiver is nondirectional and is in or near the wake, it must not be assumed that all of the sound measured comes from the direction of the source. The scattered sound may obviously come from any direction. Moreover, when a transducer is in a wake, its diaphragm may be covered with adhering bubbles, and these will have a marked influence on its sensitivity or power output.

## 6.3 EXPERIMENTAL RESULTS

### 6.3.1 Transmission of Sound through Wakes of Surface Vessels

A series of experiments on the wakes of destroyers and destroyer escorts was performed by the University of California Division of War Research [UCDWR].[4] The procedure was as follows. One vessel carried a hydrophone and was dead in the water, while the destroyer ran past it on a straight course at a fixed speed. As soon as the destroyer had passed, a small launch got underway and carried the sound source from one side of the wake to the other. In this way it was possible to measure the intensity of the sound both when the wake intervened between source and receiver, and when the source was on the same side of the wake as the receiver. After making allowance for the difference in range when the source was on one side or the other of the wake, the apparent transmission loss caused by the wake was calculated.

However, it is not certain that the result is free from error. In the first place, when the sound source is on the far side of the wake, it is possible that some sound may pass under the wake and reach the hydrophone. This error was minimized by suspending both source and hydrophone at about one half the depth of the wake. In spite of this precaution, it must be emphasized that the values of transmission loss so obtained are possibly too low.

This source of error can be eliminated by making the measurement while the source is in the wake, but then the measurement may be too large because of the effect of bubbles in reducing the output of the source. To some extent, this will be balanced out because only part of the wake will be between source and receiver. The true value will probably lie between the two measured values.

The results of an extensive program have been summarized by the following equations:

$$H = 1.5(Vf)^{\frac{1}{2}} - 3.0T \qquad (19)$$

when the source is on the far side of the wake, and

$$H = 2.4(Vf)^{\frac{1}{2}} - 4.8T \qquad (20)$$

when the source is in the wake. The symbols have the following meanings:

$H$ = transmission loss (db),
$V$ = speed of destroyer (knots),
$f$ = frequency of sound (kc),
$T$ = age of wake (minutes).

These equations have no theoretical foundation, and the experimental data which they summarize are rather scattered. The results of a typical experiment are compared with equation (19) in Figure 17. Eight experiments of this kind were performed at speeds of 10, 15, 20, and 25 knots. Three frequencies (3, 8, 20 kc) were used in all, and a fourth (40 kc) in a few of the runs. Equations (19) and (20) agree with the results of all these experiments in much the same manner as with the one shown in detail on Figure 17.

### 6.3.2 Wake Strengths—Surface Vessels

#### Dependence on Age of Wake

Early experiments were performed with a single vessel (the USS *Jasper*) which ran on a straight course, then circled and echo ranged on its own wake.[5] These experiments showed that the level of the echo decreased fairly rapidly with the age of

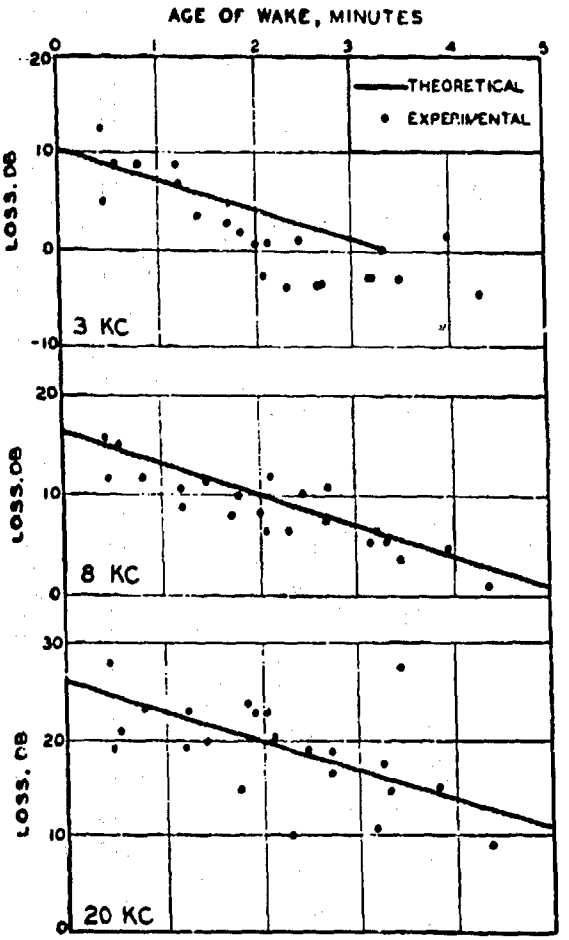


FIGURE 17. Comparison of observed values of transmission loss in wakes with values calculated from $H = 1.5\,(Vf)^{\frac{1}{2}} - 3.0\,T$.

the wake; the results of various experiments ranged from 1.5 db/min to 8 db/min, with an average of about 4 db/min. The levels of the echoes were compared with those of reverberation on the same day at the same range from the sonar. On one day, this range was about 235 ft and the echoes were about 40 db higher than either volume or surface reverberation. These two kinds of reverberation were about equal at this range. On another occasion, the range was 140 ft and the echo was 17 db higher than surface reverberation. A sea state 2 and wind force 3 prevailed on this occasion. In view of the variability of reverberation from day to day, these observations have little absolute significance, but serve to give some idea of the strength of echoes from the wake of a small slow-speed vessel. The values obtained for the rate of decrease of the wake echo have greater claim to validity, and are in good agreement with all other observations.

The difficulties inherent in performing experiments on wakes at sea led to an extended series of experiments in San Diego Harbor, a 40-ft motor launch being used to lay the wakes which extended from the surface to a depth of about 5 yd.[6] There was some evidence that sound reflected from the bottom increased the strength of the echo; in order to minimize this effect, only echoes obtained at ranges less than 100 yd are included in the following averages.

Echoes were obtained using 15-, 24-, and 30-kc sound. It was found that these did not reach their maximum value until some time after the passage of the launch through the sound beam. Average values of the time of the maximum echo are shown in the second column of Table 1. Thereafter, the echo intensity diminished at an average rate of about 7 db/min for all three frequencies. The wake strength (see Section 6.2) at the time of the maximum echo level was computed for each experiment, and average values are shown in the third column of Table 1.

TABLE 1. Dependence of wake strength on age of wake.

| Frequency (kc) | Time of max. echo (sec) | Wake strength at time of max. echo (db) |
|---|---|---|
| 15 | 30 | −2.9 |
| 24 | 50 | +3.1 |
| 30 | 70 | +8.4 |

Figure 18 serves to give further information concerning the behavior of wake echoes. The early period, during which the echo from the wake increases in level, is clearly evident, as is the later period

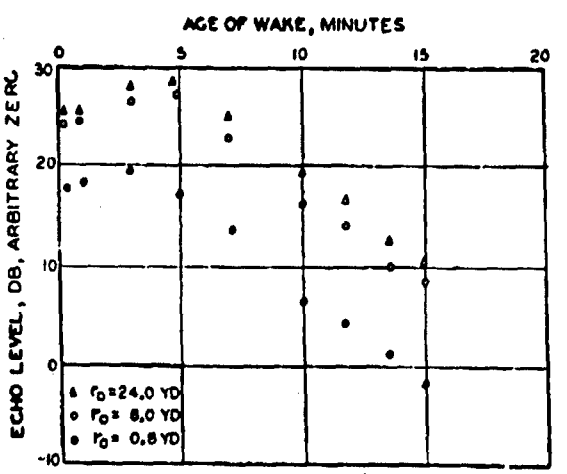


FIGURE 18. Variation of the wake echo level with age of the wake, for various ping lengths at 24 kc.

during which the echo level decreases at a rate of about 1.8 db/minute.

During the work in San Diego Harbor, echoes were obtained from the wakes of passing vessels. Values of the wake strengths of these are shown in Table 2. While there are marked differences from vessel to vessel, there appears to be a tendency for the wake strength to increase with frequency.

TABLE 2. Wake strengths of various types of vessels.

| Vessel | Wake strength 15 kc | 24 kc | 30 kc |
|---|---|---|---|
| Tanker | 8.1 | 7.7 | 9.0 |
| Fishing boat | 0.7 | 10.7 | 9.0 |
| Fishing boat | 0.0 | −0.6 | ... |
| Fishing boat | .... | −0.4 | .... |
| Kelp barge | 7.3 | 5.5 | 12.2 |
| Kelp barge | 4.5 | 9.1 | 14.3 |
| Launch 150-ft | 2.7 | 7.9 | 12.9 |
| Transport | 18.9 | 17.5 | 22.9 |
| Tank boat | 10.9 | 10.3 | 14.7 |

All later work was conducted at sea, in order to avoid the disturbing effect of bottom reflections. Figure 19 shows echoes from the wake of a destroyer (DD, 5th Group, 1917) traveling at 15 knots. The sound frequency was 24 kc, and the three oscillograms marked 41, 42, 43 were obtained with an 80-yd ping length, about 20 sec after the destroyer's screws had passed through the sound beam. Oscillograms 51, 52, 53 were obtained with a 9-yd ping length, about 15 sec later. The duration of the echo from the long ping is almost entirely determined by the ping length; that of the echo from the short ping shows definite elongation caused by the extent of the wake. Oscillograms 173, 174, 175, obtained with the short ping 870 sec after passage of the destroyer, show the increased echo elongation and the decreased amplitude of the echo caused by this spreading and dispersion.

Table 3 summarizes measurements of similar oscillograms obtained from the wakes of a number of vessels, using ping lengths of 8 to 24 yd. The speeds of the vessels were all within the normal range of operation.

### Dependence on Ping Length

Figure 18 also brings out a dependence of echo level on ping length. The theoretical discussion has emphasized the analogy between wake echoes and reverberation. Essentially, the wake is a part of the ocean from which the reverberation is especially high. If the ping length is shorter than the width of the wake, the distinction between reverberation and wake echoes disappears. The number of scatterers returning echoes at any moment is determined, not by the extent of the wake, but by the ping length. Under these conditions, illustrated by oscillograms 173, 174, 175 of Figure 19, the echo level should be proportional to ping length. If, on the other hand, the ping length is long compared to the width of the wake (see 41, 42, 43 of Figure 19), the echo level should be independent of ping length. These effects are also evident on Figure 18.

## 6.3.3 Wake Strengths—Submarines

Experiments on the wakes of submerged submarines encounter many difficulties. The problems of navigation and seamanship involved in the maneuvers are not always solved successfully, even by the ablest submariners. The low levels of the wake echoes, together with these practical difficulties, account for the conflicting reports that have been made on the subject.

On one occasion, echoes from the wake of an S-type submarine were recorded with standard echo-ranging

TABLE 3. Dependence of wake strength on wake-laying vessel.

| Type of wake vessel | 24 kc | | | 60 kc | | |
|---|---|---|---|---|---|---|
| | Average $W$ (db) | Standard deviation of $W$ (db) | Number of wakes | Average $W$ (db) | Standard deviation of $W$ (db) | Number of wakes |
| CVE's and AP's | − 7.7 | 4.1 | 5 | ..... | ... | .. |
| DD's and DE's | − 9.0 | 6.3 | 5 | +7.0 | 1.1 | 2 |
| Laboratory yachts (*Scripps & Jasper*) | − 13.6 | 2.6 | 5 | +1.6 | 3.0 | 8 |
| Small boats | − 18.2 | 2.0 | 2 | − 3.7 | 2.1 | 2 |

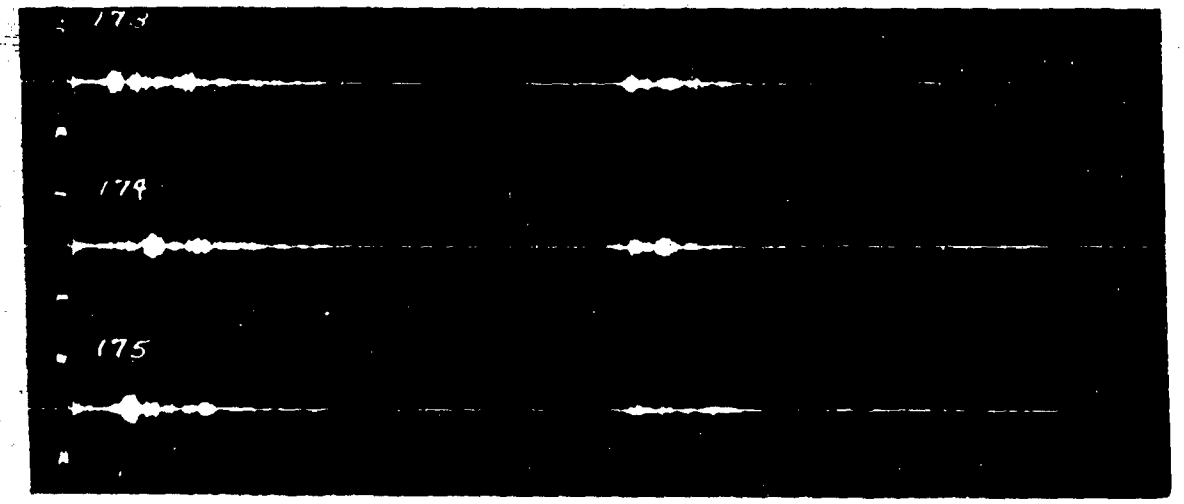


FIGURE 19. Echoes from the wake of a destroyer (DD, 5th group, 1917) traveling at 15 knots. Frequency ≈24-kc. Oscillograms marked 41, 42, 43 were obtained with an 80-yd ping length, about 20 sec after the destroyer's screws had passed through the sound beam. Those marked 51, 52, 53 were obtained with a 9-yd ping length, about 15 sec later. Oscillograms 173, 174, 175 were obtained with the short ping 870 sec after the passage of the destroyer. They show the increased echo elongation and the decreased amplitude of the echo caused by this spreading and dispersion.

gear operated at 24 kc. When running at a depth of 45 ft, contact was maintained with the wake at a distance of 3,000 ft astern of the screws. At depths of 90 and 125 ft, the lengths of the contacts were 700 and 300 ft, respectively.

On a second occasion, it was attempted to use a recording echo sounder for the study. As noted above (Figures 6 and 7), this instrument had been successfully used in the study of the wakes of surface vessels. Consequently, it was mounted on a launch, and the submarine (fleet-type) ran on a straight course designed to carry it directly under the launch. This maneuver proved difficult to execute, but echoes from the hull of the submarine were obtained on several occasions. The depth of the submarine varied from 65 to 200 ft. On no occasion were echoes from the wake obtained at distances more than 50 to 100 ft astern of the screws.

It had been hoped that this experiment would show whether the wake had a tendency to rise to the surface, as might be expected if bubbles are the primary cause of its acoustic activity. The results were inconclusive. It has been reported that, on several occasions, the wake of a submarine running at a depth of 45 to 60 ft could be seen from the deck of a nearby surface vessel. This visibility was apparently due more to turbulence, which disturbed the surface, than to bubbles.

On a third occasion, some fifteen experiments were performed to measure the wake strength of a fleet-type submarine running at various depths from 45 to 400 ft. None of these yielded echoes that were positively identified as caused by the wake, although echoes from the hull of the vessel were obtained. Some few echoes may have come from a short distance astern of the screws. Frequencies of 20 kc and 45 kc were used; 45-kc echoes from the wake would have been recorded unless they were more than 14 db below those from the submarine itself. At 20 kc, the difference must have been more than 28 db.

The operational problems were reduced to manageable proportions by the following procedure. The submarine started on the surface, running a course parallel to that of the echo-ranging vessel. The latter ran at a slow speed, so that the submarine overtook it and passed through the sound beam while still on the surface and at a range of 100 to 300 yd. About 90 sec after passage, the submarine dived rapidly to 90 ft and slowed down. Simultaneously the surface vessel increased speed, so as to overtake the submerged submarine about 10 minutes later. It was found that these operations could be carried out satisfactorily except that it was difficult to adhere to the prearranged time schedule, and that the submarine's submerged course often diverged appreciably from that of the surface vessel. The timing of events was critical because of the limited supply of film in the magazine of the recording oscillograph.

Data recorded during such an experiment are summarized in Figure 20. It is seen that the wake

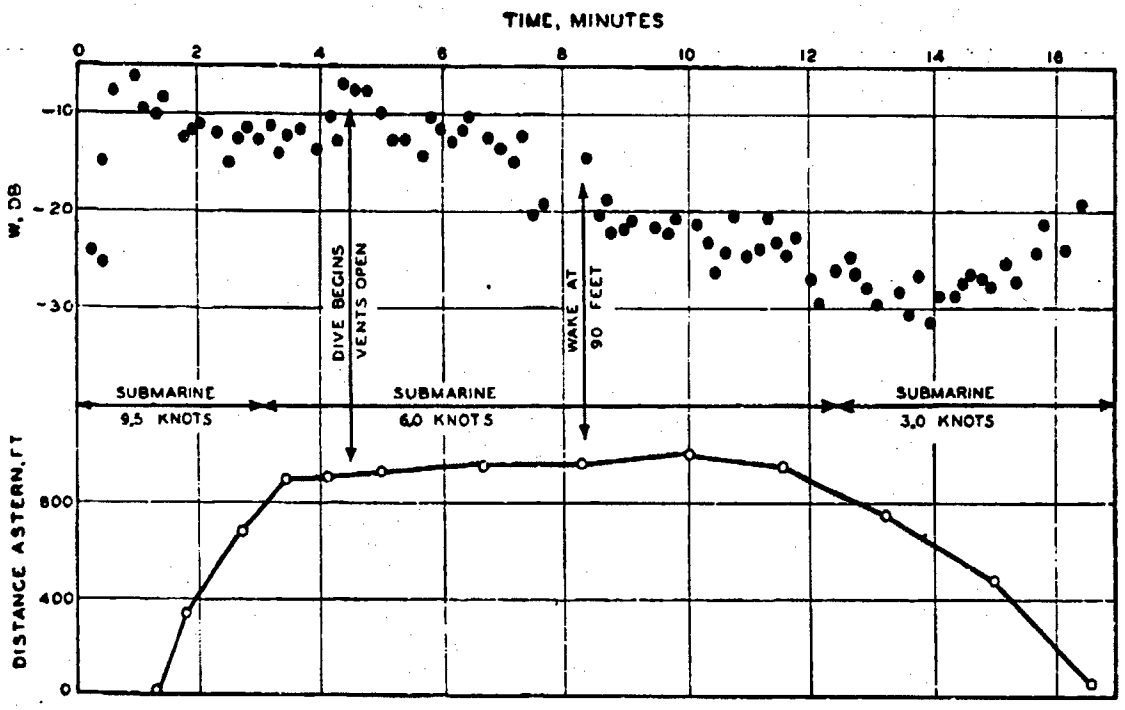


FIGURE 20. Wake strength of submarine. The lower half of the figure shows the distance astern in feet.

strength while running on the surface was −10 to −15 db. This was momentarily increased as the echo-ranging vessel passed the site of the dive, where the venting of air from the ballast tanks presumably increased the bubble content of the wake. After the submarine reached the depth of 90 ft, the wake strength varied between −20 and −30, even while the distance astern remained practically constant at about 900 ft. As the echo-ranging vessel overtook the submarine, the wake strength again increased to −20 db.

The results of other experiments with submarines are listed in Table 4. Ping lengths of 8 to 24 yd were used in all of the work summarized. It is seen that the strengths of submarine wakes are very small, even when the vessel is running on the surface. This is probably to be explained by the low speeds at which the vessel moves.

TABLE 4. Wake strengths of submarines

| Submarine type | Freq. (kc) | Wake strength surfaced 9 knots (db) | Wake strength submerged 6 knots (db) | Depth (ft) |
|---|---|---|---|---|
| S | 60 | −18 | −26 | 90 |
| S | 45 | −13 | −24 | 90 |
| Fleet | 45 | −13 | −20 | 90 |
| S | 45 | ..... | −33 | 45 |
| S | 20 | ..... | −20 | 45 |

# PART II

# ECHO RANGING

In echo ranging, a sound signal is projected into the water, in the expectation that it will strike a target and be reflected back to the transmitter. The time interval between the emission of the signal and the detection of the echo gives the range of the target; if $c$ is the velocity of sound in the sea and $t$ the elapsed time between signal and echo, the range $r$ is given by

$$r = \frac{ct}{2}. \qquad (1)$$

Provided the emitted sound energy is concentrated in a narrow beam, the bearing of the target can be determined from the orientation of the transmitter. If the transmitter can be rotated about a horizontal axis, the depth of the target can also be determined. Various characteristics of the echo can provide information concerning the size, speed, and aspect of the target.

Discussion of the manifold problems of echo ranging centers around the four basic ones that are involved. (1) The target must be insonified:* energy must be transmitted into the water and out to the target. (2) Some of this energy must be reflected by the target. (3) The reflected energy must be transmitted back to the echo-ranging vessel. (4) The echo must be received, amplified electrically, and then perceived by the operator.

The problem can be approached from several points of view. The projection of the signal and the detection of the echo suggest the immediate importance of the equipment. Thus the design of gear that will function over long ranges is one aspect of the problem. Equally important is the training of the operator to utilize the equipment to the fullest extent of its possibilities. Thirdly, the transmission of sound in the sea must be understood because it affects both design and operation of equipment. Finally, a foreknowledge of the maximum echo ranges for given targets under existing oceanographic conditions is of importance for tactical reasons, over and above the mere operation of the gear; the prediction of probable maximum ranges thus becomes a fourth important aspect of the problem.

Selecting any one of these points of view would lead one to go into detail about some matters and to minimize the discussion of others. It is the purpose, in this book, to consider the problem as a whole, in sufficient detail to enable the reader to arrive at critical conclusions concerning our knowledge of it, but not in such detail as to lose perspective.

Referring to the four steps in the echo-ranging process listed above, we can introduce the major items that must be examined in a general survey of this sort.

The insonification of the target includes the production of the signal and its transmission to the target. The production of the signal involves consideration of the frequency to be used, the power output of the transmitting system, and its directivity. These three items will form the subject matter of the next chapter. The transmission of the sound energy to the target was discussed in Part I, and thus need enter only incidentally.

A quantitative discussion of the reflection of the sound by the target will involve the concept of target strength, introduced in Chapter 5. The numerical values of this quantity and the implications for design and operation will be discussed in Chapter 8.

The third process is very similar to the first, dealing with the transmission of the reflected sound back to the transmitter.

The fourth process, the perception of the echo, is complicated by the fact that the echo must be detected against a background consisting of airborne sounds, noise produced by the echo-ranging vessel itself, noise inherent in the sea, and the multitude of unwanted echoes called reverberation. This necessitates the study of methods of portrayal (aural and visual) and the design and operation of the receiver; moreover, the perception of the echo involves psychophysical factors which must be investigated. Discussion of these factors will occupy the remainder of Part II.

To sum up, the problems of echo ranging will be discussed under the following titles:

1. "The Acoustic Output of Sonars," Chapter 7.
2. "Target Strength and Echo Level," Chapter 8.
3. "Maximum Echo Ranges when Background Noise is Limiting," Chapter 9.
4. "Maximum Echo Ranges when Reverberation is Limiting," Chapter 10.
5. "Miscellaneous Echo Ranging Applications," Chapter 11.

* Just as a searchlight illuminates a target, a sound source is said to insonify the target.

Chapter 7

# THE ACOUSTIC OUTPUT OF SONARS

## 7.1 IMPEDANCE OF PROJECTORS

### 7.1.1 Mechanical Impedance

PROJECTORS DESIGNED for the generation of supersonic waves in water have a construction that is markedly different from that of the familiar loudspeakers for the generation of sound in air. It is not possible to do justice here to all the factors entering into these designs, but some of the basic principles are easily summarized.

The objective, in both cases, is to set the medium into periodic motion. To accomplish this, a force must be applied to the medium, and this is most readily accomplished by means of a plate, or diaphragm, to which the force is applied more or less directly. This plate is often a circular disk. Suppose it is desired to give a point on its surface the velocity

$$v = v_0 \cos \omega t \text{ cm/sec}, \tag{2}$$

where $v_0$ is the maximum value of the velocity, $\omega = 2\pi f$, and $f$ is the frequency of the sound to be produced. If this can be accomplished, the water or air in immediate contact with the plate will probably move with this same velocity. (At least, this will be the case if $v_0$ is not too great. In Section 7.5, the possibility will be considered that the medium does not follow the motion of the plate, but for the present such lost motion will be ignored.)

The first problem is the calculation of the force required to produce the motion. This force will be proportional to $v_0$, and to a quantity $Z$. This is analogous to the relation between voltage and current in an electric circuit, and $Z$ is, by analogy, called the *mechanical impedance* of the plate. The resistance and the inductive and capacitive reactances which make up the electric impedance have their mechanical analogies. The value of $Z$ depends on the mass, size, and shape of the plate and on its mechanical properties, such as stiffness; also on the density of the medium, the velocity of sound in the medium, and on $\omega$.

The required force will usually not be in phase with the velocity. In general, it may be written

$$F = v_0 (X_0 \cos \omega t - Y_0 \sin \omega t) \text{ dynes}. \tag{3}$$

The quantities $X_0$ and $Y_0$ are called the mechanical resistance and reactance, respectively, of the plate.

The power required to maintain the motion will be

$$P_0 = \tfrac{1}{2} X_0 v_0^2 \text{ ergs/sec} = \tfrac{1}{2} \times 10^{-7} X_0 v_0^2 \text{ watts}. \tag{4}$$

In the simplest possible case, that of a perfectly rigid plate suspended by light threads in a vacuum, the resistance $X_0$ would be zero, so that no power is required to maintain the motion. The reactance $Y_0$ would be given by

$$Y_0 = M\omega, \tag{5}$$

$M$ being the mass of the plate.

### 7.1.2 Radiation Impedance

In practical cases, when the plate is placed in an actual medium and supported in a more complicated manner, the expression for the impedance becomes more complicated. In general, we may write

$$X_0 = X + X_p, \quad Y_0 = Y + Y_p, \tag{6}$$

where $X_p$ and $Y_p$ are the impedances that would apply when the projector is *in vacuo*, and $X$ and $Y$ are additional impedances which result from the motion imparted to the medium. These added impedances, $X$ and $Y$, are called *radiation impedances*.

The two forces $X \cos \omega t$ and $Y \sin \omega t$ result from different processes. The former results from the compression and rarefaction of the medium, which constitutes the sound radiated to a distance. The power radiated as sound will be given by

$$P = \tfrac{1}{2} \cdot 10^7 \times v_0^2 \text{ watts}. \tag{7}$$

The component $Y \sin \omega t$ results from a purely local motion of the water in the neighborhood of the plate. The energy involved in this motion is not radiated to distant points.

Strictly speaking, while the term radiation resistance accurately describes the quantity $X$, the quantity $Y$ should not be called the radiation reactance. The ratio $Y/\omega$ is the mass of water that moves back and forth with the vibrating projector. If the medium were incompressible (infinite velocity of sound), $X$ would be zero. The quantity $Y/\omega$, however, would be finite.

The radiation impedances are more or less independent of the mechanical properties of the plate but depend on its size and shape, and on the acoustic properties of the medium. They may be written

$$X = \rho c S U, \quad Y = \rho c S V, \tag{8}$$

where $\rho$ = density of the medium (gm/cm³),
$c$ = velocity of sound in the medium (cm/sec),
$S$ = area of the plate,
$U, V$ = quantities to be discussed below.

It is immediately clear that the radiation impedance of a given plate will be vastly different in air than in water, for the numerical value of the product $\rho c$ is about 150,000 for water and only 42 for air. This comes about largely because water is 800 times more dense than air; the velocity of sound is also nearly five times greater. To cause a given velocity of the plate in water will thus require a force which is nearly 3,600 times greater than that which would cause the same motion in air. Consequently, to cause the plate to radiate a given power into water will require 60 times the force that would be needed in air. Conversely, to radiate a given power into water requires only one-sixtieth of the velocity that would be needed to accomplish the same thing in air.

The fact that $S$, the area of the plate, enters into equation (8) will be obvious; it therefore remains to discuss the factors $U$ and $V$. These depend largely on the ratio of the size of the plate to the wavelength of the sound in the medium, and to a lesser extent on the shape and mechanical properties of the plate. Figure 1 is a graph of their values for a rigid circular plate, as a function of the ratio $\alpha = \pi d/\lambda$, $d$ being the diameter of the plate and $\lambda$ the wavelength of the sound.

It is seen that when $\alpha$ is greater than 6 or 7, the approximation $U = 1$, $V = 0$ is fairly good. On the other hand, when $\alpha$ is less than 1, both $U$ and $V$ become small. This might be considered a desirable circumstance, were it not that $U$ decreases more rapidly than $V$. Thus the power radiated decreases more rapidly than the force required: the out-of-phase component of the force becomes large compared to the in-phase component. This is entirely analogous to the concept of the power factor in alternating current theory. A large plate has a high power factor, a small plate a very low power factor. In the case of supersonic waves, it is fortunately possible to make the projector large enough to take advantage of this fact, but for low frequencies the dimensions required would become prohibitive. Thus, for 1000-c

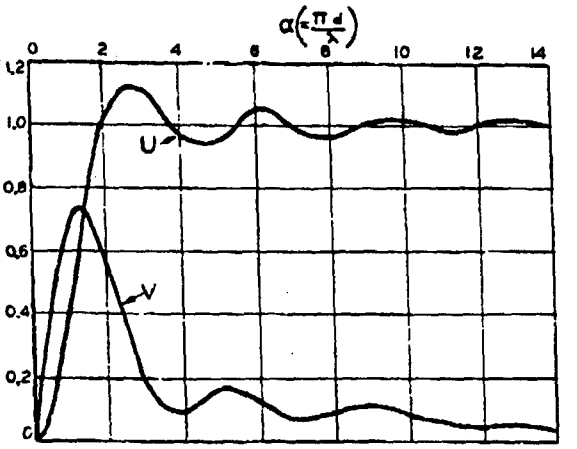


FIGURE 1. Variation of the quantities $U$ and $V$, equation (8), with $\alpha(=\pi d/\lambda)$.

sound, $\lambda = 5$ ft (approximately), so that even $\alpha = 4$ would require $d = 6.5$ ft.

## 7.1.3 The Motor

The force required to drive the diaphragm or plate at the velocity $v_0$ is supplied by an electromechanical device which is called the motor. It is similar to the ordinary motor in that it converts electrical power into mechanical motion, but, since the motion is oscillatory rather than rotatory, the analogy is not very close.

A closer analogy is obtained by considering the motor as a transformer. Then the velocity $v_0$ is analogous to the output current, and the force $F$ to the output voltage of the transformer. The radiation impedance is directly analogous to the impedance of the output circuit of the transformer. This analogy can be used to describe the effect of taking a projector out of water and into air. Suppose the projector has been designed to work under water. Then the lower radiation impedance of air will effectively short-circuit it. The projector will heat up, just as an ordinary transformer when it is short-circuited. Very little power will be usefully transformed.

Conversely, a projector designed to work efficiently in air is analogous to a transformer with a low-voltage, high-current secondary. It will not be efficient under water, where the requirements correspond to a high-voltage, low-current secondary.

The physical differences between a loudspeaker designed to work into air and a projector designed to work into water can be understood by means of this analogy. The former always has a thin diaphragm

of small mass—one that is easily movable. The motor usually applies the necessary small force by magnetic means. In principle, a small bit of magnetized steel attached to the diaphragm might be attracted and repelled by a stationary electromagnet through which an alternating current is passed. Even if such a device could be immersed in water without physical damage, the force obtainable in this way would not be sufficient to move the mass of water in contact with the diaphragm, and it would "stall."

Underwater projectors usually (though not always) have more massive diaphragms, which are appropriately described as plates. The moving part of the motor is in rigid physical contact with the plate. The large force necessary to move the plate and adjacent water is produced by any of several methods. It is possible to design electromagnets to furnish this force, but most motors in use at the present time depend on the magnetostrictive or the piezoelectric effect for this purpose. These effects are capable of producing large forces without the complications that would result from the use of large electromagnets.

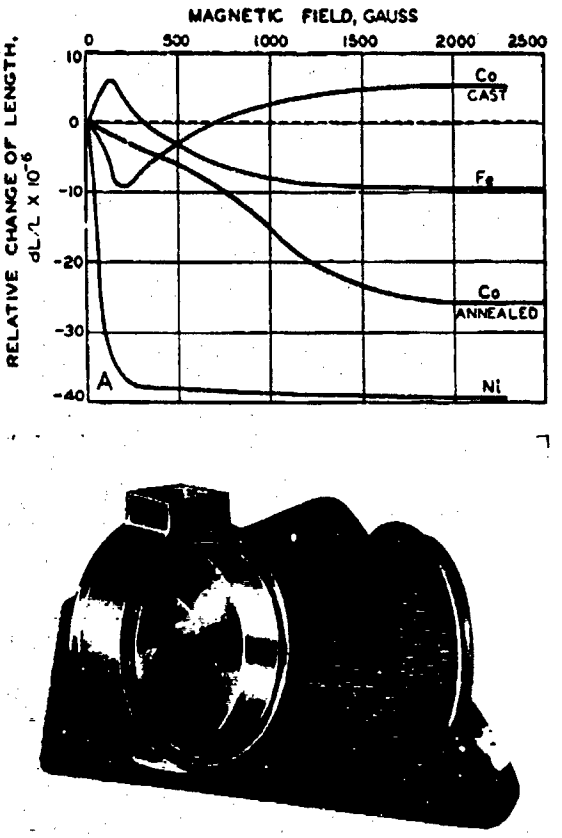


FIGURE 2. (*Top*) Magnetostriction in iron, nickel, and cobalt. The curves show the relative change in length of a rod as a function of the magnetic field strength. (*Bottom*) Construction of a magnetostriction projector head.

## 7.2 MAGNETOSTRICTION PROJECTORS

### 7.2.1 The Magnetostrictive Effect

If a rod of a ferromagnetic material is brought into a magnetic field parallel to its long axis, the length is changed slightly. The change in length is independent of the sign of the field, and may be either a decrease or an increase. Its magnitude depends on the material, its heat treatment and present temperature, and on the degree to which it was previously magnetized. The effect was discovered by Joule in 1847 and is called *magnetostriction*.[1]

The phenomenon is not related in any simple manner to other magnetic properties. Figure 2 shows the relative change in length $dL/L$, as a function of the field strength in gauss, for several elements. It is seen that nickel possesses the property of magnetostriction to a much greater degree than any other, even iron. It decreases in length in a fairly regular manner for an increasing field strength up to about 200 gauss; if the field is increased beyond this value, the additional change becomes extremely small. The extreme relative change in length is about 40 parts in a million. However, since the Young's modulus of nickel is great, a large force is exerted against anything which resists this small change in length.

Besides nickel itself, certain of its alloys exhibit marked magnetostrictive properties, among others, Invar, Monel, and Permendur may be mentioned.

Magnetostriction is reversible. If a previously magnetized rod of nickel is stretched, the magnetization of the rod is decreased; if it is compressed (in the direction of its length), the magnetization is increased.[2]

### 7.2.2 The Magnetostriction Oscillator

Magnetostriction is applied to the production of sound waves as follows: a nickel rod is subjected to an alternating magnetic field by winding a coil of wire around it and sending an alternating current through the coil. The rod is shortened periodically

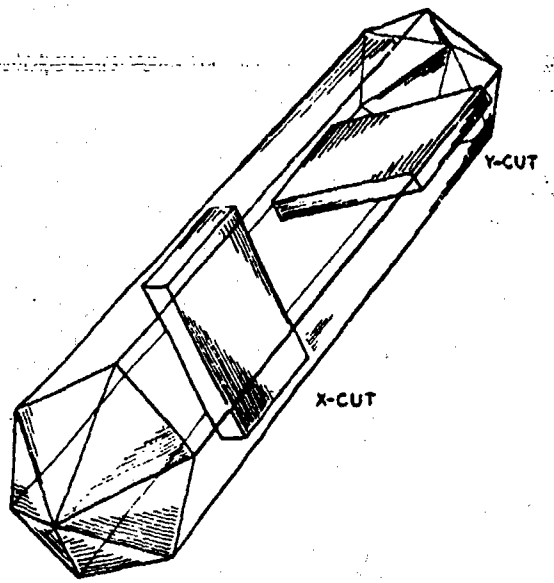


FIGURE 3. Quartz crystal, showing X-cut and Y-cut plates.

in response to the changing field. Since the change in length is independent of the direction of the field, the rod would elongate twice during each cycle of the alternating current. This can be prevented by suitably premagnetizing the rod, or by sending a continuous direct current (a "polarizing current") through the coil.

The natural fundamental frequency of vibration $N$ of a rod of length $L$ is given by

$$N = \frac{1}{2L}\left(\frac{E}{\rho}\right)^{\frac{1}{2}}, \qquad (9)$$

where $E$ is the modulus of elasticity and $\rho$ the density of the material. If a current of this frequency is sent through the coil, the amplitude of the oscillations will be a maximum; relative changes in length may be of the order of one in ten thousand. From equation (9) it can be calculated that a rod of nickel 5 in. long has a fundamental frequency of vibration of about 20 kc; and one 1.6 in. long will resonate at 60 kc. By using harmonics of a higher order, greater frequencies are obtainable, though with a loss in amplitude.

### 7.2.3 Production of Sound Waves

If a nickel rod is set in vibration in the manner just described, sound waves will be emitted from the end of the rod, with a frequency determined by the frequency of the magnetizing current. To obtain the maximum possible intensity, a practical projector is constructed by embedding the ends of hundreds of small nickel-alloy rods or tubes in a steel diaphragm of dimensions which ensure that its resonant frequency is the same as that of the rods. Each rod is excited by its own coil.

The activating current is generated by a vacuum-tube oscillator, and amplified.[3] The polarizing current, as mentioned above, serves to prevent a doubling of the frequency of vibration of the rods, but it has a second function in addition to this. Starting with zero magnetization, the magnetostrictive effect is at first very small, but at a certain critical value of the magnetic field strength the effect becomes decidedly more pronounced (see Figure 2). By using a suitable value of the polarizing current, it is possible to work on the steep part of the curve.

Because of the reversibility of the magnetostriction effect, it is evident that the projector will also act as a receiver. Sound waves impinging on the diaphragm will compress or extend the rods; corresponding changes in the magnetization of the rods will induce alternating currents in the coils, which after amplification can activate some portrayal device.

## 7.3 THE PIEZOELECTRIC PROJECTOR

### 7.3.1 The Piezoelectric Effect

Some crystals develop electric charges on their surfaces when they are subjected to pressure or tension. This phenomenon, called the *piezoelectric* effect, was discovered by the brothers Curie in 1880.[5] The electric charges developed are proportional to the force applied to the crystal. They are of opposite sign for compressions and tensions.

The effect is reversible, so that if a piezoelectric crystal is placed between two electrodes and a charge is applied to the latter, mechanical strains result. These set the crystal to vibrating. Since the elastic properties of such crystals differ in different directions, the vibrations will occur in different ways, depending on the orientation of the crystal relative to the electrodes. In any case, the natural frequency of vibration will be given by an equation similar to equation (9), where the value of the elasticity modulus will differ for different orientations of the crystal.

Three piezoelectric materials are currently used: quartz, Rochelle salt, and ammonium dihydrogen phosphate (ADP). Crystals of these substances are

shown in Figures 3, 4, and 5, respectively. Quartz has the advantage that it is strong and insoluble in water, whereas Rochelle salt and ADP are quite fragile and soluble. The solubility is a disadvantage in all seagoing applications, although it can be overcome by observing suitable precautions in the design and construction of projectors. On the other hand, it is an advantage in that it makes possible the production of good artificial crystals in the laboratory; whereas quartz crystals must be mined, and only a small fraction of those found are large enough and perfect enough for acoustic purposes. Quartz has an additional disadvantage in that it is very hard and more difficult to cut and polish even than glass; while both Rochelle salt and ADP crystals are soft enough so that they can be cut with band saws and shaped with ordinary metal-working power tools, if care is exercised to prevent chipping.

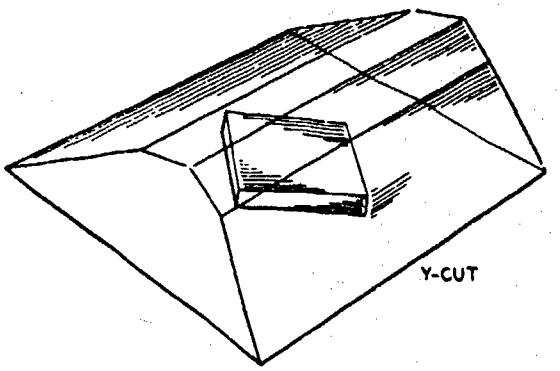


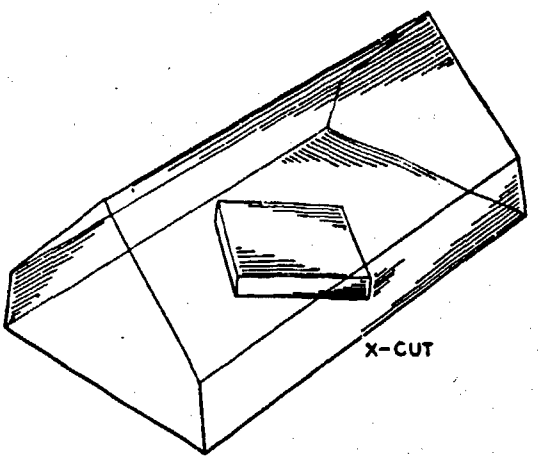


FIGURE 4. Rochelle salt crystals, showing Y-cut and X-cut plates.

For piezoelectric applications, plates are cut from the whole crystal. A few of the possible ways in which plates can be cut are shown in Figures 3, 4, and 5. The designations commonly applied to the plates are indicated.

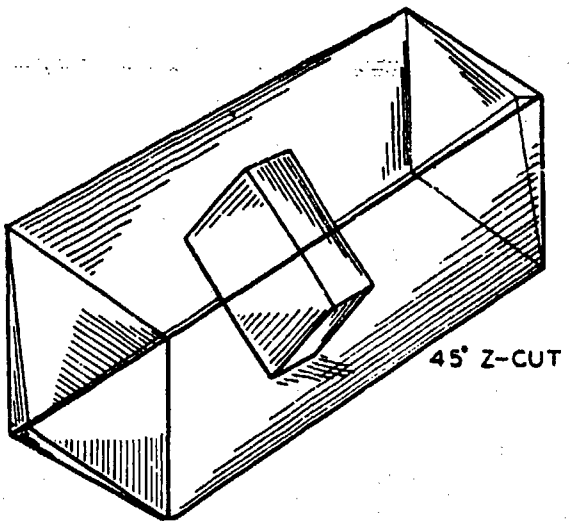


FIGURE 5. Ammonium dihydrogen phosphate (ADP) crystals, showing 45-degree Z-cut plate.

### 7.3.2 Quartz Projectors

The British Asdic utilizes X-cut quartz crystals. These are laid flat on a steel plate, as shown in Figure 6A, arranged in a mosaic so that the plate is adequately covered. An identical plate (not shown in the figure) is then laid on top of the crystals, forming a sandwich. The sandwich is made mechanically rigid by means of clamps at the edges of the plates. Insulating washers make it possible to connect the plates to the terminals of the a-c source.

The deformation of the crystal when the voltage is applied is shown in Figure 6A by the arrows. When the potential of the upper face of the crystal is positive, the thickness increases. Simultaneously, the other two dimensions shrink. The changes which occur in the length, width, and thickness are such that the volume of the plate remains the same. When the potential is reversed, the deformations are in the opposite sense. (The two faces of the plate clearly are not equivalent, hence care must be taken to arrange all the plates in a mosaic so that they expand and contract "in step.") Since the plate will be compressed during one half of the cycle of an a-c field, and extended the same amount during the other half, it will vibrate with the same period as that of the field. If this is the natural period of the crystal, the amplitude of the vibrations will be a maximum. The natural

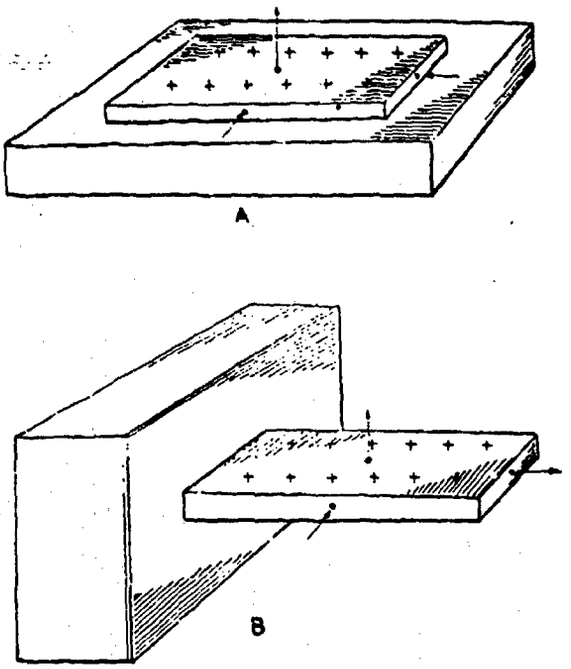


FIGURE 6. (A) Construction of Asdic projector. A mosaic of X-cut quartz crystals is laid on a steel plate as shown; a second identical steel plate (not shown in the figure) is laid on the crystal to form a "sandwich" to which the voltage is applied. The Asdic uses the "thickness" vibrations of the crystal. The arrows indicate the deformation. (B) Mounting of Rochelle salt and ADP crystals. The large faces of the crystal are covered with metal foil, to which the voltage is applied. The crystal is cemented to the heavy backing plate. The arrows indicate the deformation of the crystal. The longitudinal vibration is the one desired.

frequency of the thickness vibrations (the ones utilized in the Asdic projector) calculated from equation (9) is

$$f_0 = \frac{285.5}{t} \text{ kc}, \qquad (10)$$

there $t$ is the thickness of the plate in centimeters. However, experiments[5] showed that this relation is only approximately true,* because the plates will generally execute vibrations in other modes than the ones mentioned; moreover, in addition to compressional vibrations, vibrations due to shear may also be present. Such additional vibrations coupled to the primary ones will tend to change the primary frequency of vibration.

* A. Hund obtained the following experimental relation:

$$f_0 = \frac{287 \pm 5}{t} \text{ kc}.$$

### 7.3.3 Rochelle Salt and ADP Projectors

The plates of Rochelle salt and ADP crystals are mounted so as to utilize the length vibrations instead of the thickness vibrations, as shown in Figure 6B. The two large faces are coated with a metal foil, and

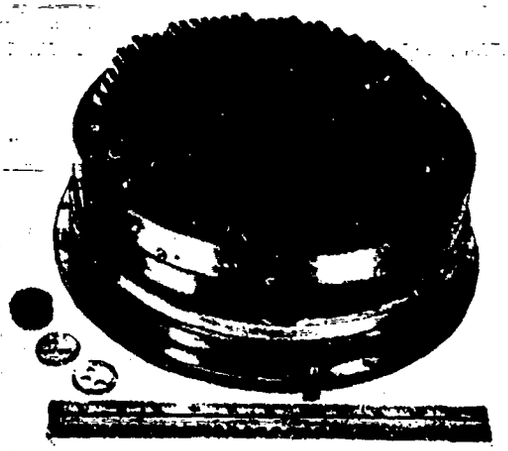

FIGURE 7A. Crystal stack for transducer.

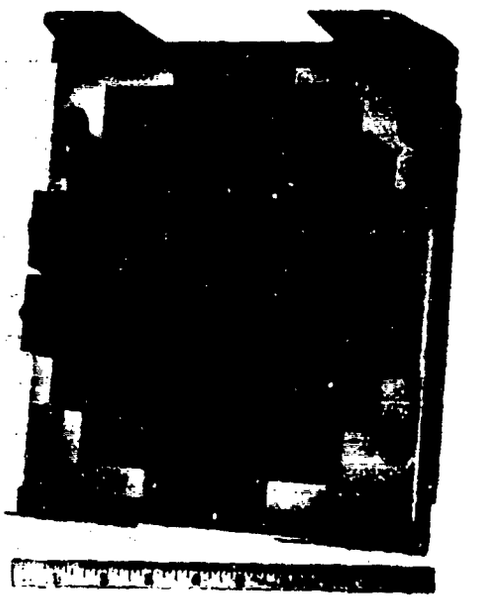

FIGURE 7B. Crystal stack for transducer.

the a-c voltage is applied to the foil. The arrows indicate the deformation resulting from the indicated charge. The crystals are cemented to a

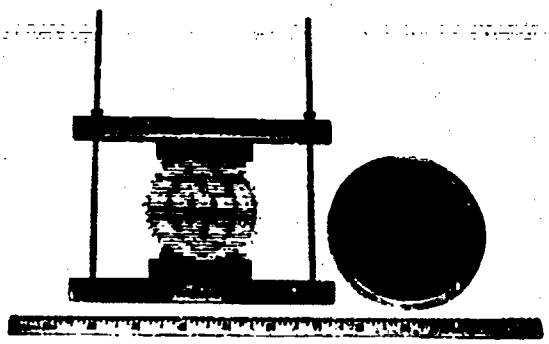

FIGURE 7C. Crystal transducer being built.

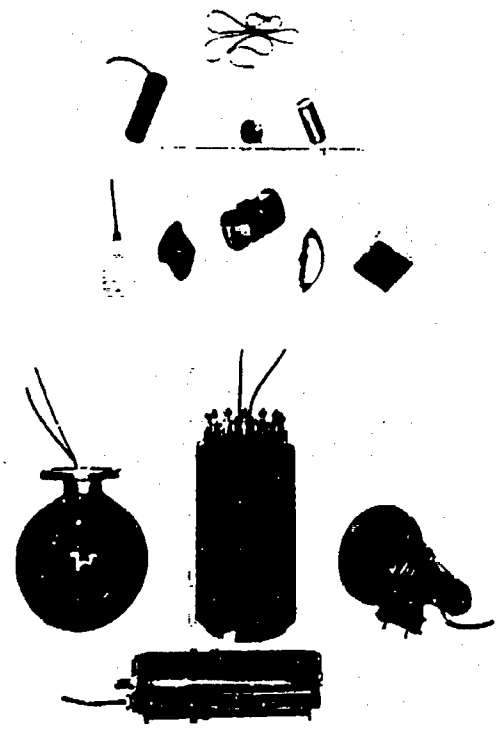

FIGURE 7D. Exterior of crystal transducers.

single heavy backing plate; in order to prevent short-circuiting, the surface of the backing plate must be enameled.

Many crystals are mounted on a single plate, as shown in Figure 7, and the sound is radiated from the free ends of the crystals. They are protected from the action of sea water by a heavy rubber sheet which lies over the free ends. The space between backing plate and rubber that is not occupied by crystals is filled with carefully purified castor oil. Traces of moisture would etch the crystals and short-circuit the electric connections; even small air bubbles would seriously reduce the efficiency of the projector.

ADP crystals possess certain physical characteristics that make them superior to Rochelle salt crystals as elements in underwater sound projectors, and are replacing the latter in standard echo-ranging gear. The resonant frequency of the length vibrations of the 45-degree cut plates shown in Figure 6 is a function both of the length $L$ and width $w$ of the plate; it is generally multiplied by the length to form a term called the "frequency constant," which is given by

$$fL = 64.7 - (13.6)\left(\frac{w}{L}\right)^2 \text{ kc.} \qquad (11)$$

The piezoelectric effect being reversible, a crystal projector acts also as a receiver of sound waves incident on the diaphragm. The compression of the crystals generates corresponding electric currents which, after amplification, can activate a portrayal device.

## 7.4 DIRECTIVITY PATTERNS AND DIRECTIVITY INDICES

### 7.4.1 Directivity of a Projector

In order to locate a target effectively by means of reflected sound energy, it is obvious that the sound must be projected in the form of a narrow beam. This is achieved by using a large source as described in Section 1.2.

A large source is one whose linear dimensions are several times as great as the wavelength of the sound emitted by the source. The significance of the wavelength in determining the directivity of a source can be seen by considering a simple case.

A "point" source can be pictured as an extremely small sphere contracting and expanding sinusoidally; such a source would send out energy equally in all directions. Consider two point sources, vibrating in phase, each of which produces a pressure $p$ at a distant point $A$. (See Figure 8.) If this point $A$ is on the perpendicular bisector of the line joining the two sources, the travel time for the respective waves from the two sources to the point $A$ is the same; thus they will arrive at this point in phase, and the pressure at $A$ will always be $2p$. Consider, however, a point $B$ on the line joining the two sources, at which

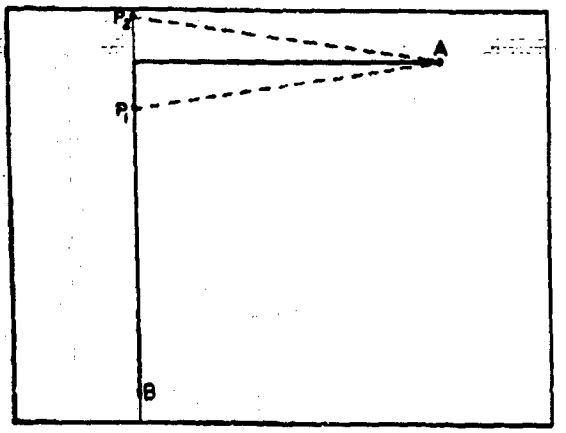


FIGURE 8. Diagram illustrating directional effect of a two-point source.

each source again exerts a pressure $p$. If the two sources are a wavelength, $\lambda$, apart, the waves will arrive at this point in phase, and the pressure will be $2p$. This will also be the case if the two sources are any whole number of wavelengths apart. But if the two sources are an odd number of half wavelengths apart, a wave from the more distant source will be 180 degrees (half a period) behind the wave that left the nearer source at the same instant, and the sound pressure there will be zero. In this case the two sources constitute a directional projector, with a maximum output along the normal to the line joining them and zero output along this line.

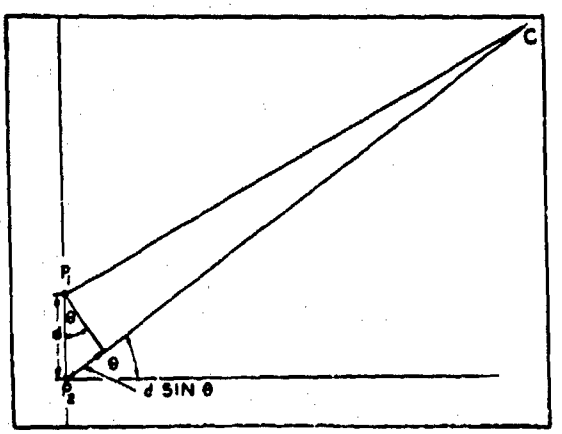


Figure 9. Diagrams illustrating directional effects of a two-point source.

If the two sources are separated by some other fraction of a wavelength, the difference in the pressures at points $A$ and $B$ will depend on the amount of this separation. For example, it can be calculated that if the separation is $\lambda/10$, the difference in pressure at $A$ and $B$ is about 5 per cent; and the smaller the separation of the sources, i.e., the smaller the dimensions of the whole source relative to the wavelength, the smaller will be the difference in pressure between points on the two lines under discussion.

If the point under observation lies in a direction making the angle $\theta$ with the normal to the line joining the two sources, as shown in Figure 9, the wave from one source will lag behind the one from the other by a distance $d \sin \theta$, where $d$ is the distance between the two sources. The phase lag will then be $(2\pi d/\lambda) \sin \theta$. It can be shown that the ratio of the resultant pressure $p$ at the point $C$ to the pressure $p_0$ at the corresponding point $A$ on the normal ($\theta = 0$), is given by

$$\frac{p}{p_0} = \cos\left(\frac{\pi d}{\lambda} \sin \theta\right). \tag{12}$$

A graph of this function shows a series of maxima and minima as $\theta$ is made to vary through 360 degrees (see Figure 10).

Practical sources of sound can be considered to be composed of a number of point sources. By reasoning similar to that just used, the pressure at any point in the field surrounding the source can be calculated. The calculation becomes extremely complicated for all but the simplest possible arrangements; however, they have been made for several simple geometrical configurations and are found in standard works on sound.[9,10] For purposes of illustration, a few formulas are cited:

1. For a set of $n$ equally spaced point sources vibrating in phase with the same amplitude on a straight line, the ratio $p/p_0$ defined above is given by

$$\frac{p}{p_0} = \frac{\sin\left(\frac{n\pi d}{\lambda} \sin \theta\right)}{n \sin\left(\frac{\pi d}{\lambda} \sin \theta\right)}. \tag{13}$$

2. If the elementary sources are arranged in surfaces, such as the square or rhombus, circle, and rectangle, the expressions for $p/p_0$ are different for each shape; but if certain minor approximations are made, none of them differs materially from an equation similar to equation (13), namely,

$$\frac{p}{p_0} = \frac{\sin(ka \sin \theta)}{ka \sin \theta}, \tag{14}$$

where $k = 2\pi/\lambda$, and $a$ is the horizontal half-length of the projector surface. The square of the ratio $p/p_0$ is the function $b(\theta)$ defined in Section 1.2.

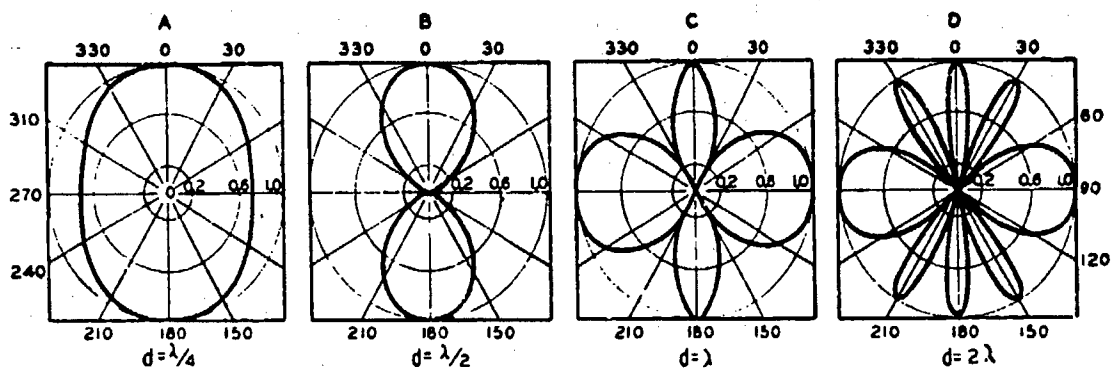


FIGURE 10. Graphs of equation (12) for various values of $d$.

By substituting values of $\theta$ in equation (14), the pressure in all directions relative to the pressure on the normal to the surface can be plotted for arbitrary values of $d$ and $\lambda$. If the plotting is done on polar graph paper, a directivity pattern results. Such a pattern, calculated for a rectangular plate with $a = 2\lambda$, is shown in Figure 5 of Chapter 1. It is found that patterns obtained by measurements from actual transducers are generally similar to those calculated theoretically.

In order to achieve considerable directivity, the linear dimensions of the projector must be several times as great as the wavelength of the sound. Sound of 10 kc has a wavelength of about 6 in. It is obvious that to get directivity at that frequency, or at a lower one, would require a larger projector than for the higher supersonic frequencies.

## 7.4 2 Directivity Patterns

It is customary to plot the directivity function $B(\theta) = -10 \log b(\theta)$ rather than $b(\theta)$ itself; by this means the importance of the side lobes is stressed, as was mentioned in Section 1.2 and as can be seen from Figures 6 and 7 of Chapter 1. In echo ranging, the side lobes are important because an echo may be received along one of them and considered to be due to sound from the main lobe; this would result in a large bearing error. Thus the suppression of side lobes plays an important part in the design of transducers. As an example, it has been found that if a circular disk is constructed of two concentric rings and the inner ring is made to vibrate with greater amplitude than the outer one, the first side lobe may be as much as 10 to 12 db lower than it would be if the diaphragm were a simple circular plate with all points on it vibrating with the same amplitude.

The width of the beam is designated by the angle subtended by the main lobe where it is 6 db below maximum response.

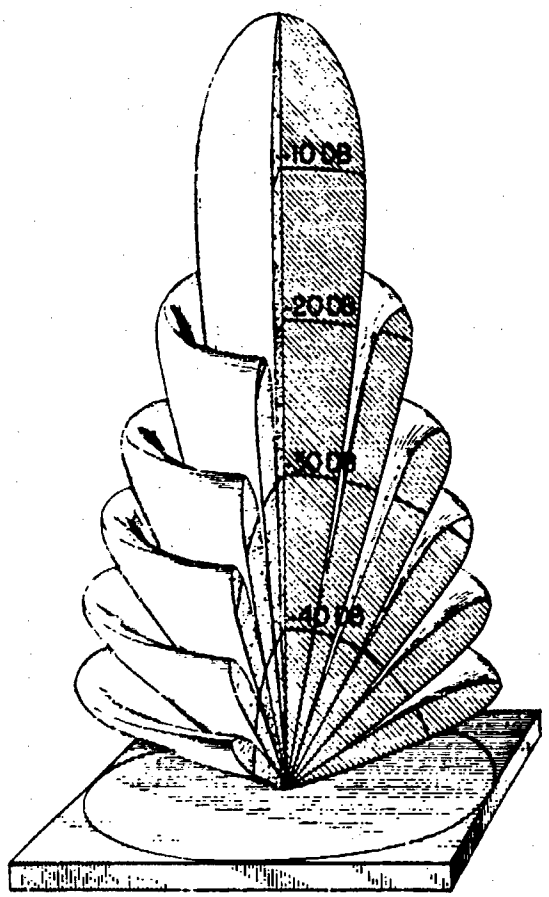


FIGURE 11. Three-dimensional directivity pattern for a circular plate. Frequency = 25 kc; diameter of plate = 15 in.

Since the beam itself is three-dimensional, the plane in which a directivity pattern is measured must be specified. If the projector is a circular piston, the

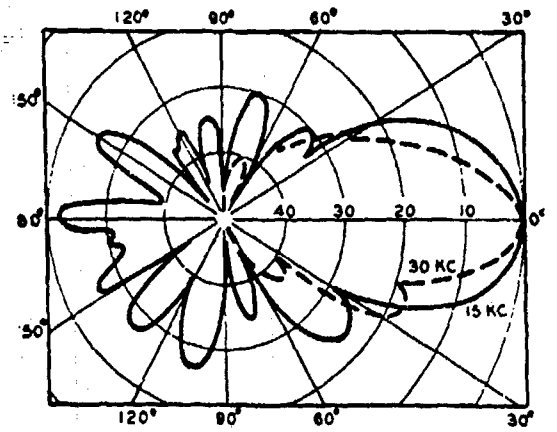


FIGURE 12. Directivity patterns of QGA echo-ranging transducer. The solid curve is the pattern for the 15-kc, the dotted curve, that of the 30-kc projector. The numbers on the axis indicate decibels below the maximum. Directivity index: at 15 kc, −18.1 db; at 30 kc, −23.2 db.

beam may have symmetry about the normal to the projector face, as illustrated in Figure 11; but if the instrument is nonsymmetrical, there exists a directivity pattern for each possible axis of rotation, and in general these various patterns will be different.

Theoretically, any desired directivity pattern can be obtained by using the appropriate combination of the shape and dimensions of the diaphragm, spacing of the sound-generating units, and frequency. Practically, any desired pattern can be approximated more or less closely by designing a projector according to calculations based on the theory.

Detecting submarines under diverse circumstances sets requirements for echo ranging that can be met only by using several projectors. For general long-range search purposes, it is desirable to have a relatively wide beam with circular symmetry and small attenuation; for this purpose a circular piston driven at, say, 15 kc is suitable. For close ranges, a narrower beam could be achieved by using sound of 30 kc; the loss in range due to increased attenuation at the higher frequency is compensated for by the greater concentration of the beam and the greater accuracy in obtaining bearings on the target. The QGA magnetostriction transducer is designed along these lines. The two projectors are mounted in a single dome. The directivity patterns for the two frequencies of the QGA are shown in Figure 12.

Directivity patterns of projectors in current use are shown in Figures 13 to 17. The type of sound generator is designated by a code letter. The QC type uses magnetostriction and the QB type the piezoelectric effect. Figure 13 shows the pattern of the standard QC projector, which consists of 608 hollow nickel tubes arranged on a circular diaphragm. In this gear the tubes are premagnetized by a polarizing current. Another form of QC gear, the QCU, has the directivity pattern shown in Figure 14.

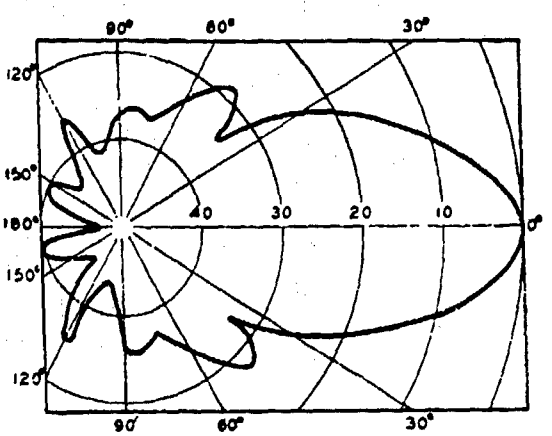


FIGURE 13. Directivity pattern of magnetostriction (QC) 24-kc echo-ranging transducer. Numbers on the axis indicate decibels below maximum. In this gear the tubes are arranged in circular form, and are premagnetized by a polarizing current. Directivity index = −21.4 db.

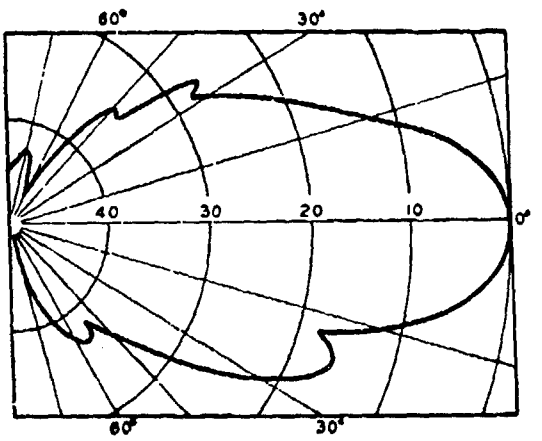


FIGURE 14. Directivity of magnetostriction 25-kc echo-ranging transducer (QCU). Rods are spaced in equilateral triangle; premagnetized by permanent magnets. Numbers on axis indicate decibels below maximum. Directivity index = −22.5 db.

This unit consists of 182 nickel tubes spaced in an equilateral triangle; the tubes are premagnetized by permanent magnets.

Directivity patterns of two types of QB transducers are shown in Figures 15 and 16. Figure 15 is the pattern of the QBF, an echo-ranging projector

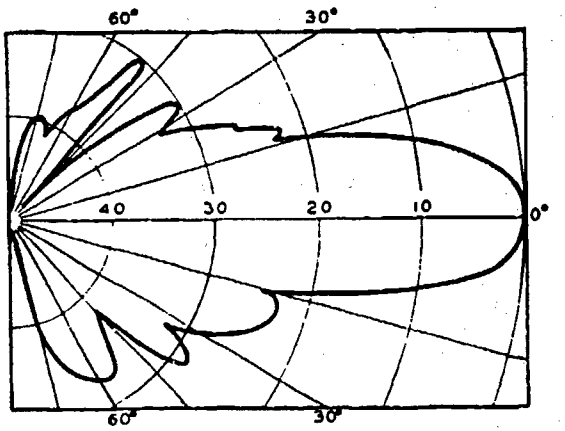


FIGURE 15. Directivity pattern of Rochelle salt (Y-cut) crystal echo-ranging transducer (QBF) at 30 kc. Numbers on axis indicate decibels below maximum. Directivity index = −25.2 db.

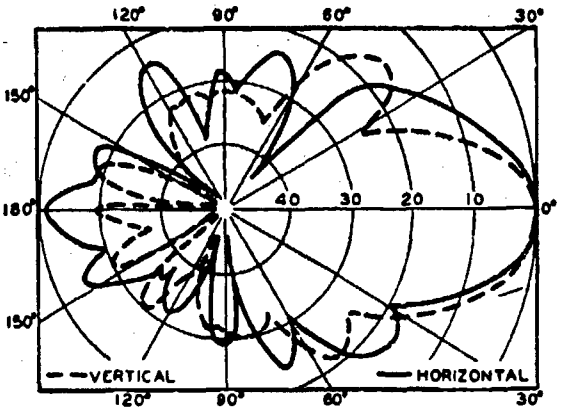


FIGURE 16. Directivity patterns of Rochelle salt crystal (45° Z-cut) echo-ranging transducer (QBG) taken in both the vertical and horizontal planes. Directivity index for horizontal pattern at 22.5 kc = −17.3 db. Numbers on axis indicate decibels below maximum.

consisting of 450 Y-cut Rochelle salt crystals mounted on a steel plate. The active area is about 10.5 in. square. Figure 16 shows the patterns of the QBG projector taken in the horizontal and vertical planes at 22 kc. The QBG is a small Rochelle salt gear intended for small ships.

Very often a third projector is mounted with the QGA system, the function of which is to determine the depth of the submarine. One such projector has a beam pattern that is fan-shaped, i.e., it is very broad in the horizontal plane, whereas in the vertical plane the angular width of the beam is only about 3 degrees. It is a quartz projector driven at 50 kc. This transducer is mounted in such a way that it can be tilted in the vertical plane as well as rotated in the horizontal one. The directivity pattern of this transducer is shown in Figure 17.

When the transducer is used as a hydrophone, the directivity pattern is generally found to be nearly identical with its pattern when used as a projector, provided the electric connections to the acoustic elements, i.e., the crystals or the magnetostriction tubes, are not altered when the gear is changed from send to receive. Hence the directivity function $B$ gives information concerning the response of the transducer to sounds coming from a specified direction. More complicated cases arise, however, in which the sources of sound are more or less uniformly distributed in all directions. The directivity function also gives some information about the response of the transducer to such multidirectional sound fields, for it is obvious that its response will be largely caused by those sources in the direction of the principal lobe, and that sources in other directions will not contribute appreciably.

Such sounds are very often unwanted ones that interfere with the reception of echoes. It will be shown (see Chapter 9) that the interference caused by these unwanted sounds is of considerable importance in echo ranging; thus the response of a sonar projector to them, and their previous measurement under various sea conditions and at various locations, all become important.

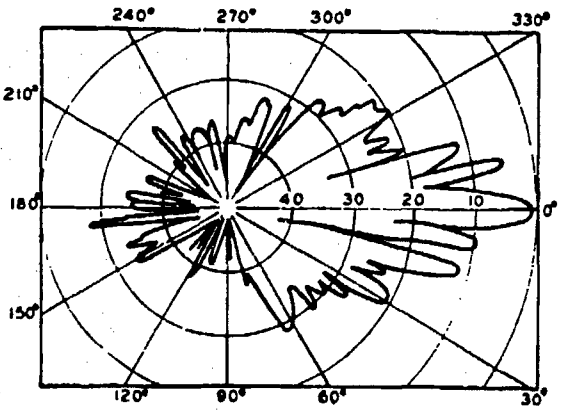


FIGURE 17. Directivity pattern, in vertical plane, of a quartz projector at 50-kc, used for depth determination. Numbers on this denote decibels below maximum. The horizontal pattern of this transducer is quite broad.

The magnitude of a multidirectional sound field is most readily specified in terms of its rms sound pressure $p$. This can be directly measured by means of a nondirectional hydrophone, that is, one for which $b = 1$ in every direction.

The electric connections to the acoustic elements of a transducer may be altered when its function is changed from projector to receiver for the purpose of providing a means for accurate bearing determination. One method that is used is to split the transducer elements into two halves, and connect these in such a way that through one amplifier the transducer is most sensitive to sounds coming from slightly to the right of the transducer bearing; simultaneously through another amplifier, it is most sensitive to sounds coming from slightly to the left. The transducer, as a hydrophone, will thus have two (possibly different) directivity patterns, and these will not be the same as the pattern when the electric connections are not altered. This is discussed in detail in Section 11.2.3.

## 7.4.3 The Directivity Index

### Definition

The directional characteristic of a transducer could be described by stating the fraction of the sound energy that is sent out in the desired direction. This is done essentially by computing the *directivity index*.

Suppose the sound intensity at a fixed distance from the projector is measured in a given plane (for example, the horizontal plane containing the normal to the projector face) in equal angular steps around the circle. If the average of all these intensities is divided by the maximum intensity, this ratio, called the *directivity factor* $K$, evidently provides quantitative information on the directivity. For, if this ratio is unity, the projector is entirely nondirectional, whereas if it is a small fraction, it is evident that a large proportion of the energy is concentrated near the direction of maximum emission, the "acoustic axis."

If the average intensity is $\bar{I}$, and the maximum or *axial intensity* is $I_a$, the directivity index $D$ is defined by

$$D = 10 \log K = 10 \log \frac{\bar{I}}{I_a}. \qquad (15)$$

For a nondirectional transducer, $D$ is zero; for a directional one, $D$ is a negative number. The directivity indices of the various highly directional transducers mentioned in the preceding section range from $-20$ to $-26$ db.

The concept of the directivity index given above can be generalized by applying it to three dimensions. To do this, it is necessary to find the average value of the intensity over a sphere surrounding the projector, from the three-dimensional directivity pattern. This average value depends somewhat on the size of the sphere; since in practice one is concerned with effects at a great distance, the result should apply for this condition, and this will generally be the case if the radius of the sphere is considerably greater than the longest linear dimension of the radiating surface.

### The Calculation of the Directivity Index

The directivity index for an ideal projector of given size and shape can be calculated theoretically from the constants of the apparatus, without involving excessively unwieldy mathematical treatment if certain simplifying assumptions are made. For example, a circular plate whose diameter $d$ is greater than two wavelengths can be shown to have an index that is given approximately by

$$D = 20 \log \left(\frac{c}{\pi f d}\right), \qquad (16)$$

where $f$ is the frequency and $c$ the velocity of the sound.

Generally, $D$ is calculated from the beam pattern, or directivity function, $b$, which was defined by equation (14) of Chapter 1:

$$b = \frac{I}{I_a},$$

where $I$ is the intensity at a given point and $I_a$ the intensity at a point equally distant from the source, but located on the axis. If $b$ is averaged over all directions, this average evidently gives $K$ and hence $D$.

### Directivity Index of a Receiver

When used as a hydrophone, the directivity index of a transducer is defined as follows.

Sound incident on the hydrophone from a standard source located at a point in any direction at a distance $r$ from the source will generate electrical power $R$. The same source placed on the acoustic axis at the same distance will generate electric power $R_a$. The ratio $R/R_a$ can be called $b'$, the directivity function of the receiver. The values of $b$ and $b'$ are equal for a given transducer; unless, as was de-

scribed above, the transducer is split for accurate bearing determination.

As in the case of the projector, $b'$ can be averaged over the directivity pattern, and the value of $D$ calculated as before.

The directivity index of a hydrophone also determines its response to a multidirectional sound source. Consider two sound fields, one caused by a single source located on the axis of the hydrophone, and another by sources distributed equally in all directions from the hydrophone. Let both sets of sources result in the same sound pressure at the hydrophone, and let $E_a$ be the electromotive force generated in the hydrophone by the single source, $E_i$ the emf generated by the isotropically distributed sources. Thus

$$20 \log E_i = 20 \log E_a + D.$$

Since $D$ is a negative number, $E_i$ will be less than $E_a$. This relation is of considerable practical importance.

## 7.5 THE SOUND OUTPUT

### 7.5.1 Electrical Power Input and Acoustic Power Output

A projector is essentially a device for converting electric power applied to the system into acoustic power in the water. In rating a projector, we are interested in knowing how much of the applied electric power is available as acoustic power, and how much of the available acoustic power is concentrated in a narrow beam.

The electrical power input can be measured either from the open-circuit voltage of the generator and the impedance of the circuit, or from the current and impedance.

The acoustical power output can be computed from measured pressure levels. The total power is given by the energy flow per second over a sphere surrounding the projector. The average intensity $\bar{I}$, over a sphere of radius $r$ multiplied by the surface area of the sphere $4\pi r^2$, therefore is a measure of the acoustic output of the projector. Since $\bar{I} = KI_a$, where $K$ is the directivity factor and $I_a$ is the axial intensity, the acoustic power is given by $4\pi r^2 K I_a$.

The axial intensity is commonly measured by mounting a hydrophone at a convenient distance on the acoustic axis of the projector, and transmitting continuous sound, using a constant current.

### 7.5.2 The Efficiency and Response of a Projector

Only that portion of the electric power that is converted into acoustic power is available for echo ranging. The efficiency of a projector is defined in decibels by 10 log $(P_0/P_i)$, where $P_0$ is the acoustic power output and $P_i$ the electric power input. If a system is, say, 50 per cent efficient, the efficiency is given by 10 log $(\frac{1}{2}) = -3$ db; an efficiency of 10 per cent would be $-10$ db, etc. The efficiency of a standard echo-ranging projector ranges from $-2$ db to $-15$ db.

In rating a projector, a convenient method is to state the axial sound level reduced to 1 yd[b] (the axial source level) per volt or ampere of the impressed voltage or current. This is called the *response* of the projector.

The acoustic power output $P$, the axial source level $S_a$, and the directivity index $D$, are related by the equation

$$S_a = 71.6 + 10 \log P - D. \qquad (17)$$

The performance of a given projector is completely described by the response, the directivity index, and the efficiency. The characteristics of some standard echo-ranging transducers are listed in Table 1.

TABLE 1. Characteristics of some standard projectors.

| Code | Type | Resonant freq. (kc) | $D$ | Source level, $S_a$ | Eff. (db) |
|---|---|---|---|---|---|
| QGA-942 | MS* | 30 | −23.2 db | 85 db | −6 |
| QGA-941 | MS | 15 | −18.1 | 77 | −7.5 |
| QBF | RS** Y-cut | 24 | −21.1 (20 kc)<br>−23.5 (26 kc)<br>−25.2 (30 kc) | 88.5 | −3.6 |
| QBG | RS X-cut | 22 | −17.3 (22 kc) | 33 (22 kc)<br>39 (45 kc) | ? |
| QCU | MS | 25 | −22.5 | 84 | −3.8 |
| QC-L | MS | 20 | −21.4 | 43* | −9.5 |
| QC-J | MS | 24 | −22.1 | 46.5* | −9.5 |
| Asdic | Quartz | 15 | −22.0 | 56 | −3.1 |

* MS = Magnetostriction.

** RS = Rochelle salts.

[b] The standard unit distance for calibration adopted by the Navy is 1 m. One yd and 1 m are not sensibly different in this connection.

### 7.5.3 Limitation of Power Output by Electrical Characteristics

It would appear from equation (26) that very long echo ranges might be achieved by increasing the power input into the projector system, and that the only limit on the available power would be set by the permissible size and weight of the gear. This is not the case. There are two limiting factors in determining the power output, aside from structural requirements.

The first of these factors results from electrical characteristics. The voltage across the face of a crystal cannot be increased indefinitely, for at a certain critical voltage a spark will pass. This is referred to as "voltage breakdown." Some idea of the magnitude of the maximum voltage that can be applied can be gained from the fact that the specifications for ADP crystals for echo-ranging transducers require that the crystal must withstand a resonant-frequency voltage of 20,000 v. in. for at least 30 sec.

In the case of magnetostriction transducers, a limitation to the power input is set by the fact that the magnetostriction effect becomes negligible when a certain critical value of the magnetic field strength is reached. Nickel, for example, exhibits practically no magnetostriction for field strengths greater than 200 to 250 gausses (see Figure 2).

### 7.5.4 The Limitation of Power Output by Cavitation

The second factor that limits the power output of transducers is cavitation.

An acoustic projector consists essentially of a vibrating face or piston. The motion of the face is imparted to the water, in which the disturbance is propagated as a wave. This process can proceed efficiently only as long as the water follows the motion of the projector face. When this motion becomes too violent, the face tears away from the water, with a marked loss of efficiency in the process of sound production.

This limitation on the output of a projector is thus closely related to the phenomenon of cavitation discussed in Section 6.2.2. Let $p$ be the rms acoustic pressure at a point where the normal hydrostatic pressure is $p_0$. Then once each cycle of the sound wave, the total pressure will change from $p_0 - 2^{\frac{1}{2}}p$ to $p_0 + 2^{\frac{1}{2}}p$ and back again. Cavitation may occur whenever the total pressure tends to become negative. Accordingly, the maximum acoustic pressure that can be transmitted through a region where the hydrostatic pressure is $p_0$ will be given by $p = p_0/2^{\frac{1}{2}}$ or, in terms of sound level, by

$$\text{Critical level} = 20 \log p_0 - 3.$$

For $p_0$ = 1 atmosphere = 35 ft of water = $10^6$ dynes/cm$^2$, $L$ = 117 db. When the sound level exceeds this critical value, cavitation bubbles may be formed, and cause high transmission losses (see Section 6.2). These bubbles have been observed in laboratory experiments.

Since the acoustic pressure is highest at the face of the projector, cavitation will occur there before it occurs elsewhere. This constitutes the process discussed in the first paragraph. As a result of the process, the power output of the projector, for a given motion of the face, will be reduced.

Aside from the reduction of power output of a projector for a given motion of its face because the water does not follow the moving face, the power output may also be reduced for other reasons. Thus, it has been observed in experimental tanks at Naval Research Laboratory, that small air bubbles may form on the projector when it is warmer than the water. This may also happen under other conditions. Accompanying the formation of these almost invisible bubbles, the sound output of the projector, for a given electric input, was much reduced. Under similar circumstances, its sensitivity as a hydrophone also diminished.

## 7.6 THE SIGNAL USED IN ECHO RANGING

### 7.6.1 The Signal Frequency

Practical considerations set rather definite upper and lower limits to the frequencies that can be used in echo ranging. The use of sonic frequencies (less than 10 kc) has not been considered practicable because of directivity requirements, as discussed above. A second reason for the use of supersonic sound is provided by considerations of the detectability of echoes. The echo must always be detected against a background of interfering noises; while these noises include sound of supersonic frequencies, the greater part of their energy is in the sonic region. Hence, supersonic echoes are masked less than sonic ones.

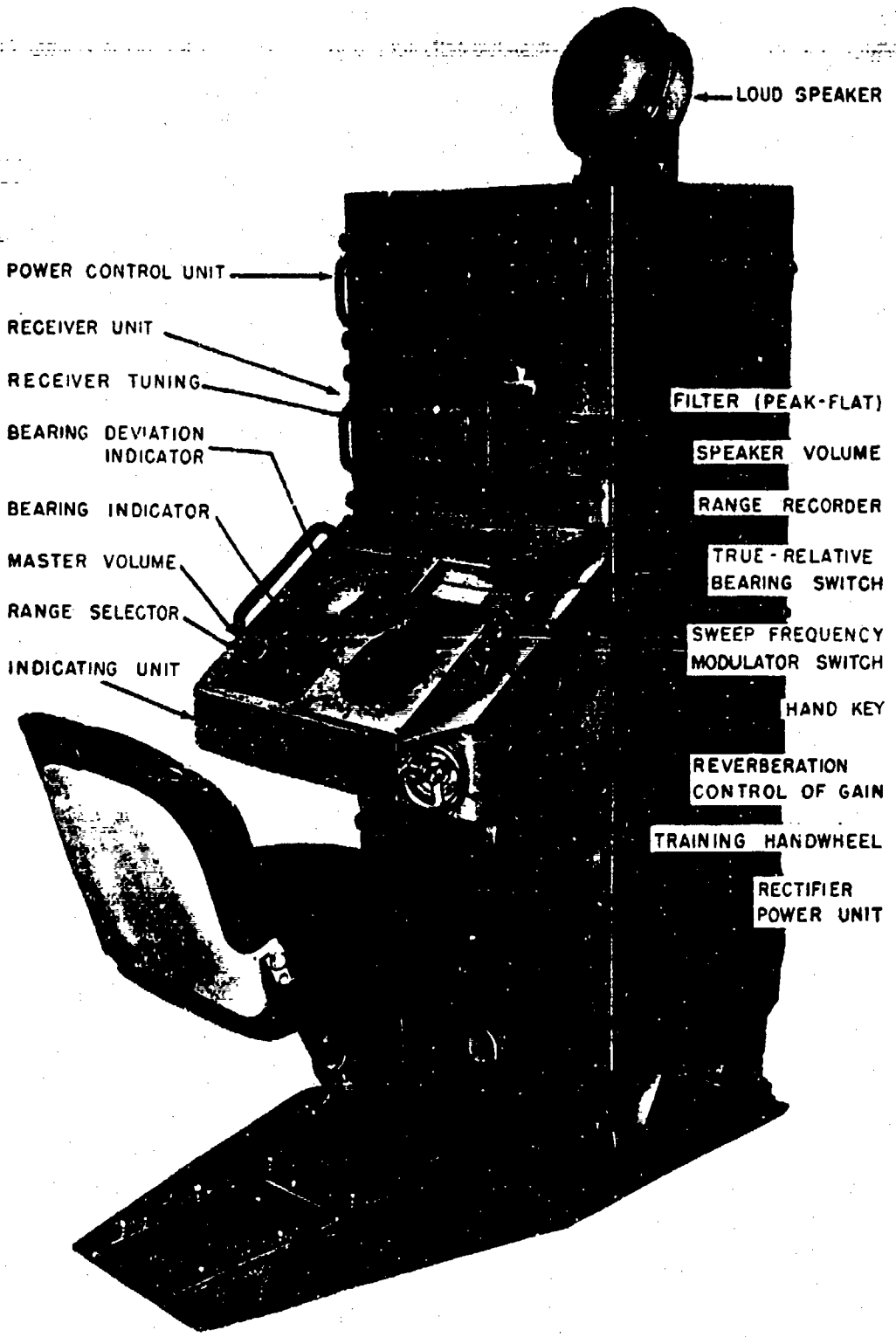


FIGURE 18. Model QGB sonar stack. The QGB equipment employs a magnetostriction projector for echo ranging, listening, and underwater communication on a supersonic frequency that is between the limits of 17 and 26 kc. The principal units in the stack are designated on the photograph above.

An upper limit to the practicable frequency is set by the attenuation of the sound in the sea. The attenuation coefficient increases very markedly with frequency (see Chapter 3, Table 3). Hence, for search purposes, where long ranges are required, a frequency higher than about 25 to 30 kc is not suitable. When the range is being closed, and great accuracy of bearing is needed rather than a long range, the greater directivity associated with higher frequencies is the determining factor, and thus frequencies of 50 to 100 kc may be found useful. This is especially true for depth determination, where an extremely narrow beam is required; and since accurate depth determination is practicable only at comparatively short ranges, the high attenuation consequent upon using high frequencies is not significant.

The U. S. Navy at first adopted a compromise value of 24 kc. This frequency allowed fair directivity to be achieved while the size of the transducer could be kept within practical limits. The attenuation was moderate. It is now being replaced by more elaborate gear that can emit several frequencies, as mentioned above.

A further reason, of minor importance, for using supersonic frequencies is that a high-frequency ping is not so readily detected by the enemy unless his gear is tuned to the particular frequency used.

Further investigation may show that the foregoing considerations are not conclusive and that other frequency ranges merit practical trial.

### 7.6.2 Keying Length and Keying Interval

The best signal duration is a moot question. The amount of energy returned to a transducer obviously is proportional to the amount of energy sent out; hence it would appear that a long signal would provide a better chance for a recognizable echo being obtained than a shorter one. This is discussed in Chapters 8 and 10. Moreover, the signal and echo both fluctuate markedly during transmission; hence, a longer signal would provide a greater chance for a peak value of the echo strength to be received (see Section 3.5). In general practice, signals of a duration of about 50 to 200 msec are used.

A reason for the use of shorter signal duration is provided by the fact that the intensity of the reverberation is proportional to the length of the signal (Chapter 5), whereas under ordinary circumstances the intensity of the echo is not. Consequently, the ratio of echo-to-reverberation intensity is greater for short signals. This advantage may be canceled because aural recognition of the echo is more difficult, but shortening of the ping does not affect the recognition when a chemical recorder is used. However, the echo intensity is independent of signal length only if the linear dimension of the target does not exceed a certain value. In the case of large targets, the echo intensity increases with the signal duration. (This will be discussed in more detail in Chapters 8 and 10.)

In sonar gear, the duration of the signal and the time interval between signals are controlled at the range indicator, a device which enables the operator to give the range to the target by noting the position on a dial of a flash of light caused by the returning echo energy (see Figure 18). One type of indicator contains a revolving disk with a slot through which the light flashes when the echo energy is received. A system of electric motors and gear ratios causes a circular disk to complete one revolution either in 1.25 sec, the approximate time required for sound to travel to and from a target 1,000 yd distant, or in 6.25 sec for a target 5,000 yd distant. The signal may be transmitted automatically at the beginning of each revolution, or at the beginning of each second or third revolution. The time between transmissions is called the *keying interval*. The keying interval is usually given in equivalent yards, e.g., if a signal is transmitted once for each revolution of the dial, the keying interval is expressed as 1,000 or 5,000 yd. A nonautomatic, manual keying device is also provided.

The duration of the signal may be read from the scale on the dial; since this is calibrated in yards, it is customary to express the *ping length* in yards instead of seconds, as has been discussed in Chapter 5. If $t_0$ is the duration of the signal in seconds, the ping length $P$ in yards is given by $P = 800\,t_0$, 800 yd being roughly the two-way distance traversed by sound in 1 sec.

## 7.7 THE EFFECT OF DOMES

### 7.7.1 General

The projector unit, consisting of the projector and the shaft that supports it, is usually installed near the bow of the ship. Since the housings in which projectors are encased are usually spherical, they

would cause excessive turbulence, and possibly cavitation, at even moderate speeds. This would cause excessive background noise, as discussed in Chapter 9. For this reason, transducers are generally enclosed in streamlined metal shells called domes. Several

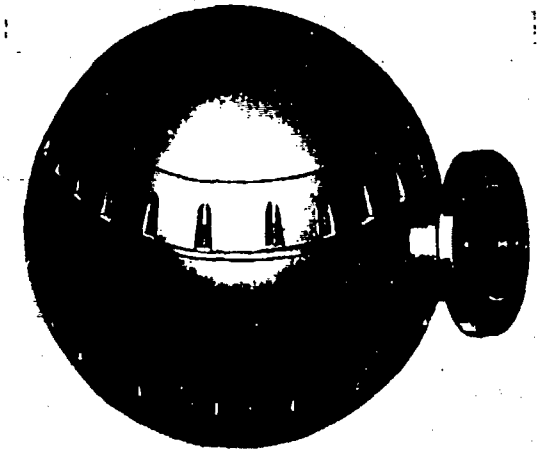

FIGURE 19A. Standard dome.

types of domes are in current use by the Navy. They are all made of corrosion-resistant steel; the front is very thin so as to form a "window" to transmit the sound; the back is made heavy to damp un-

FIGURE 19B. Standard dome.

wanted noise from the propellers. One type is equipped with a bulkhead just aft of the projector, which supports a sound-absorbing baffle on the forward side and a sound-reflecting pad on the after side; both these devices reduce sound reception

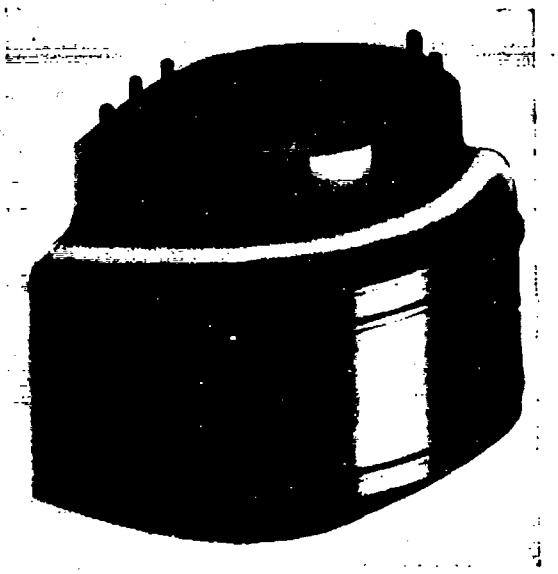

FIGURE 19C. Standard dome.

through the stern section of the dome, and the baffle also aids in reducing multiple reflection within the dome. Some domes are retractable and when not in use are withdrawn into a sea chest built into the hull.

Some standard domes are illustrated in Figure 19.

## 7.7.2 Acoustic Effects of Domes

The acoustic effects of the use of domes are twofold. In the first place, it is observed that the axial source level of a dome-enclosed projector is less than that of the same projector without a dome. In the second place, the directivity pattern of the dome-enclosed projector differs from that of the same projector without a dome.

The two effects are closely related. It is not possible to construct domes of materials that are entirely transparent acoustically. Thus, a certain amount of multiple reflection occurs inside the dome, as a result of which some of the sound energy that is emitted by the projector into the main lobe of the sound beam is diverted from it. This reduces the axial source level.

Any energy diverted from the main lobe, however, must be redistributed in some manner. It is quite possible, therefore, that new side lobes may be added to the directivity pattern, for the regular shape of the dome would preclude a mere random redistribution of the diverted energy. Moreover, it is obvious

that multiple reflections inside the dome may affect the original side lobes of the bare projector pattern.

It can be shown that the decrease in the axial source level due to the distortion of the directivity pattern is equal to the change in the directivity index that ensues when the projector is placed in a dome.

In echo ranging, a loss in the transmission reduces the effective range; and the distortion of the directivity, especially if accompanied by the formation of prominent side lobes, tends to confuse the determination of bearings. Hence, the various factors that have been adduced must be taken into account when designing a dome.

# Chapter 8

# TARGET STRENGTH AND ECHO LEVEL

## 8.1 THE CONCEPT OF TARGET STRENGTH

### 8.1.1 General Principles

THE STUDY of the echoes received from targets obviously constitutes one of the most important problems in echo ranging. The theory of echo formation has been introduced earlier (see Section 5.2); at this time the application of that theory to the conditions encountered in practical echo ranging will be considered.

The sound that is scattered by a target is radiated by it according to the same laws that describe the radiation of sound from primary sources, and which were discussed in Chapter 1. As in the case of primary sources, we shall find it convenient, when discussing echoes, to speak of the source intensity of the insonified target. This concept, and that of the reradiation itself, can be illustrated very clearly by the so-called echo repeater, an artificial target developed for the purpose of training personnel. It consists of a hydrophone and a projector, mounted close together. The hydrophone receives the pings from the distant sonar, and its electrical output is amplified. This amplified signal is then fed into the projector which reradiates it as the "echo."

The source intensity of this target is defined as the intensity of the reradiated sound at 1 yd from the projector on the axis of the latter. Let it be $I_1$. If the intensity of the sound incident on the hydrophone is $I$, the ratio $I_1/I$ would serve to describe quantitatively the reflectivity of the target; it might be called the overall gain of the repeater. It is more usual to convert this ratio to decibels and to call

$$T = 10 \log \frac{I_1}{I} \qquad (1)$$

the *target strength*.

It is found that in order to simulate the echo from a submarine, the ratio $I_1/I$ must be of the order of magnitude 50 to 100. This gives a general idea of the strength of the secondary sources involved in the formation of the echoes from a large target, such as a ship or submarine. The fact that the ratio $I_1/I$ is greater than unity may seem paradoxical, as implying that the intensity of the secondary, reradiated sound is greater than that of the incident sound; for these targets have convex surfaces that cannot focus the reflected energy. It must be remembered, however, that these targets are large objects: the intensity of the scattered sound at all actual points in front of the target is, of course, less than that of the incident sound at the surface of the target; nevertheless, when viewed from a distance, the target radiates like a point source concentrated at its center, and the strength of this hypothetical point source, given by the intensity at a distance of 1 yd, is greater than at the surface of the target, several yards distant, where the actual intensities of incident and reflected sound are equal. This phenomenon is precisely analogous to the radiation of sound from large primary sources, as discussed in Section 1.2 and illustrated in Figure 5 of Chapter 1.

The concept of target strength applies not only to the echo repeater, but to any target. In Section 5.2, it was shown that the intensity of the scattered sound $I_s$ at a distance $r$ from a target, is given by equation (7),

$$I_s = \frac{I\sigma}{4\pi r^2},$$

where $\sigma$ is its target area. If we set $r = 1$ in this equation, we get

$$I_1 = \frac{I\sigma}{4\pi},$$

whence the definition of target strength given in equation (1) yields

$$T = 10 \log \frac{I_1}{I} = 10 \log \left(\frac{\sigma}{4\pi}\right). \qquad (2)$$

### 8.1.2 The Target Strength of Spheres

The concept of target strength, as presented in the foregoing, has been experimentally tested. The simplest case of reflection is provided by a sphere. In this case it is clear that the target area $\sigma$, and therefore the target strength $T$, does not depend on the direction of the incident sound; and it was shown, moreover, that it is also independent of the direction

of the reflected sound (see Appendix, Chapter 5). The target area of a large sphere (Section 5.2) is $\pi d^2/4$, where $d$ is the diameter of the sphere; hence its target strength is given by

$$T = 10 \log \left(\frac{\sigma}{4\pi}\right) = 10 \log \frac{d^2}{16},$$

$$= 20 \log \left(\frac{d}{4}\right) \text{ db.} \qquad (3)$$

The target strength of spheres as a function of the diameter is shown in Figure 1.

Optical experiments carried out at MIT show that equation (3) does represent the target strength of spheres for visible light.[1,2,3] The intensity of the

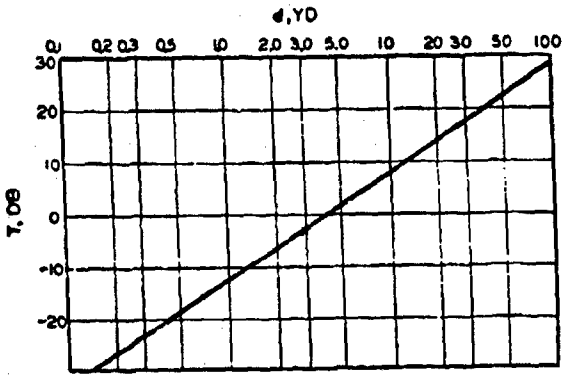


FIGURE 1. Graph of equation (3) for the target strength of a sphere whose circumference is greater than ten wavelengths of the sound. For smaller spheres, consult Section 5.1.

light reflected by spheres of various sizes from 2 to 25 in. in diam. was measured at a point near the source. All the experimental conditions with regard to the projection, transmission, and reception of the light were the same for all the spheres; moreover, the surfaces of the different spheres were alike. Hence, the variation in intensity could be a function only of the size of the sphere. It was found that the level $L'$ of the reflected light, in decibels above the intensity of the reflected light from a sphere of arbitrary diameter, was given by

$$L' = 20 \log d + \text{constant}.$$

The numerical value of the constant could not be determined.

While there is an analogy between the reflection of light and that of sound, it is desirable to check the theoretical formula by acoustic experiments. Unfortunately, these are difficult to make with the necessary accuracy. Perhaps the most instructive series of experiments was carried out at a calibration station.[4] The separation between the sonar and the target was only 11.5 ft. The targets consisted of metal spheres 3 ft in diameter. Several different spheres were used; one was constructed of gores welded together, the others had a smoother construction, but all showed appreciable departures from geometric perfection. Various frequencies of sound were used, to test the theoretical conclusion that target strength should not depend on frequency, provided only that the radius of the target is great compared to the wavelength of the sound. The results are shown in Table 1; the theoretical target strength is $T = -12$ db in each case.

TABLE 1. Target strengths of spheres.

| Frequency (kc) | 3-ft mine case, water-filled ($T$ db) | 3-ft mine case, loaded ($T$ db) | 33-in. sphere, gored construction, water-filled ($T$ db) | 3-ft sphere, badly dented, water-filled ($T$ db) |
|---|---|---|---|---|
| 30 | ..... | −10.8 | ..... | ..... |
| 40 | − 6.9 | − 7.9 | −5.2 | −8.5 |
| 50 | − 6.7 | − 6.0 | ..... | ..... |
| 60 | − 8.2 | − 7.2 | −3.2 | −9.7 |
| 70 | − 8.4 | − 7.7 | ..... | ..... |
| 80 | −10.3 | −10.3 | −5.1 | ..... |
| 90 | −11.9 | − 8.9 | −3.5 | ..... |

The observed values are in general considerably higher than − 12 db, and the differences are not the same for all frequencies. However, there is no systematic dependence, and some of the variability is doubtless due to experimental error.

In order to investigate the sources of error, the echo intensity was recorded continuously while the sphere was rotated. The results are shown in Figures 2 and 3 for the dented sphere and the water-filled mine case. It is seen that a very considerable variation results from the departures of the target from the ideal geometrical shape. This is emphasized by Figure 4, obtained with the gored sphere.

The general conclusion is that the theoretical formula may be used to estimate the target strength of a sphere, but that appreciable departures from theory may be expected in practice.

### 8.1.3 Echo Level

In most of the previous discussion of echo formation it has been tacitly assumed that the transmission loss is described by the inverse square law. This

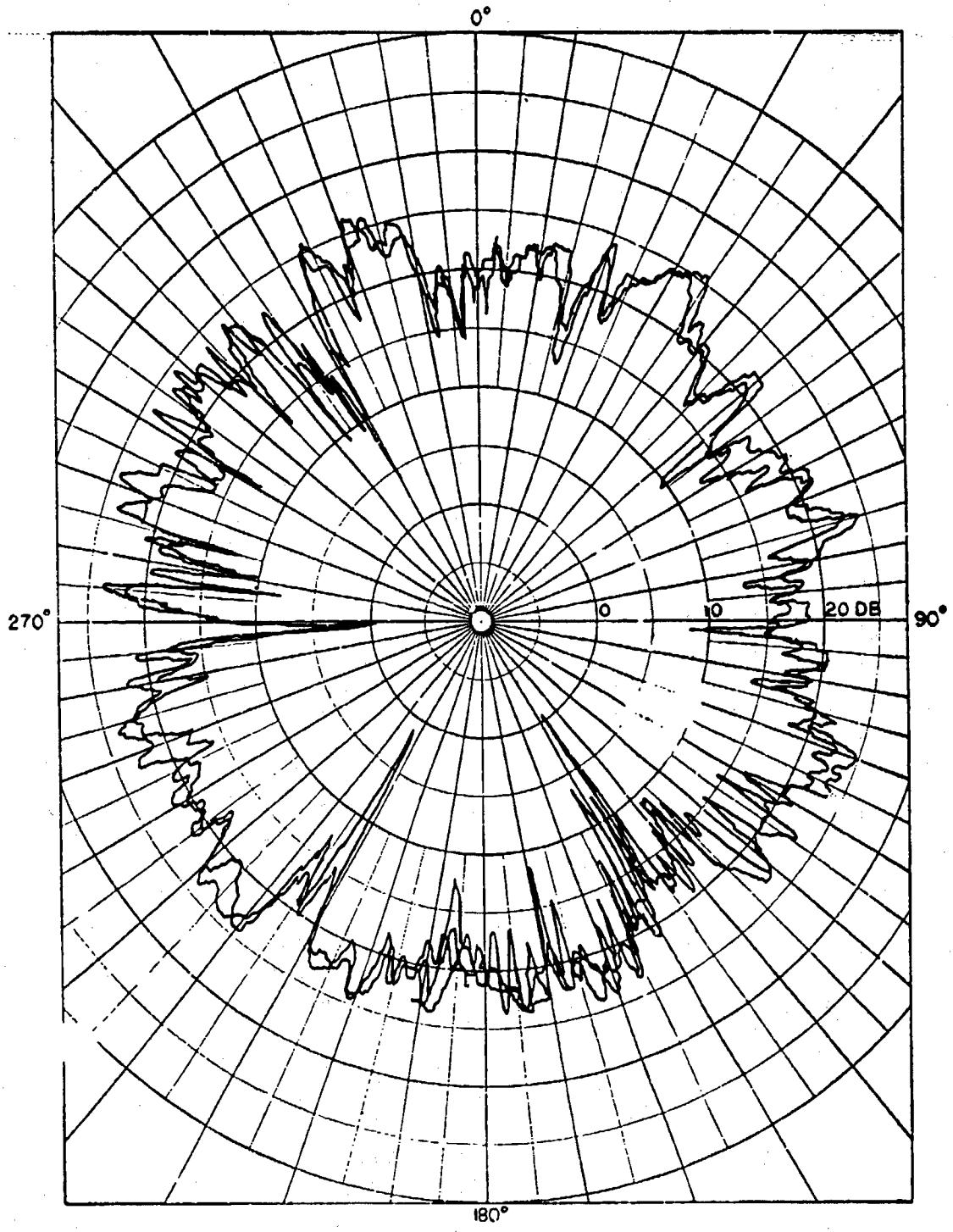


FIGURE 2. Echo from a sphere with large dents, diam. 3 ft. The echo level was recorded continuously while the sphere was rotated through two complete revolutions at a depth of 13 ft. Distance from projector to center of sphere = 11.5 ft. Pressure level of incident sound at front of sphere = 45.7 db. Frequency, 40 kc.[4]

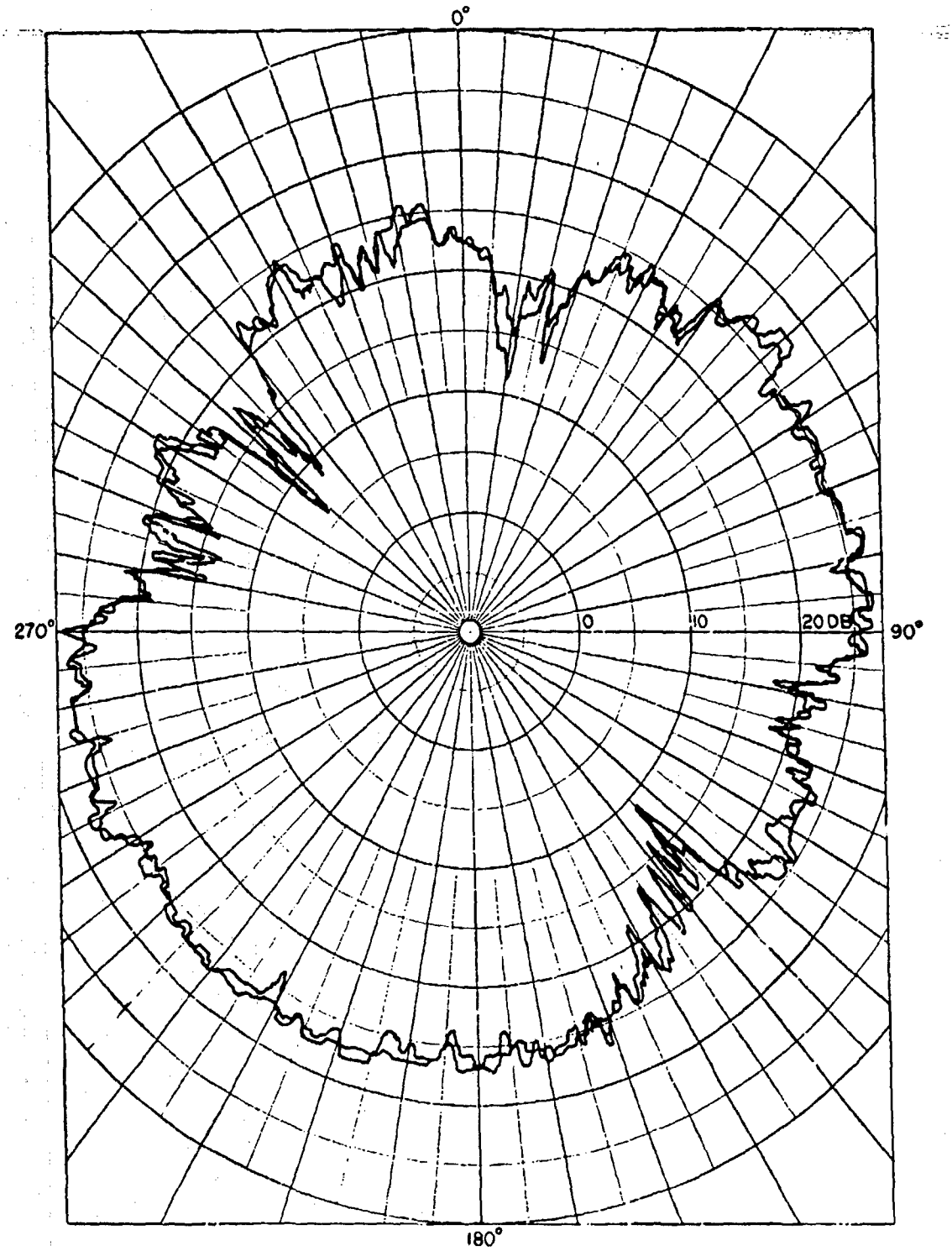


FIGURE 3. Echo from a mine case (water-filled), diam. 3 ft. Experimental procedure and conditions were the same as for Figure 2.[4]

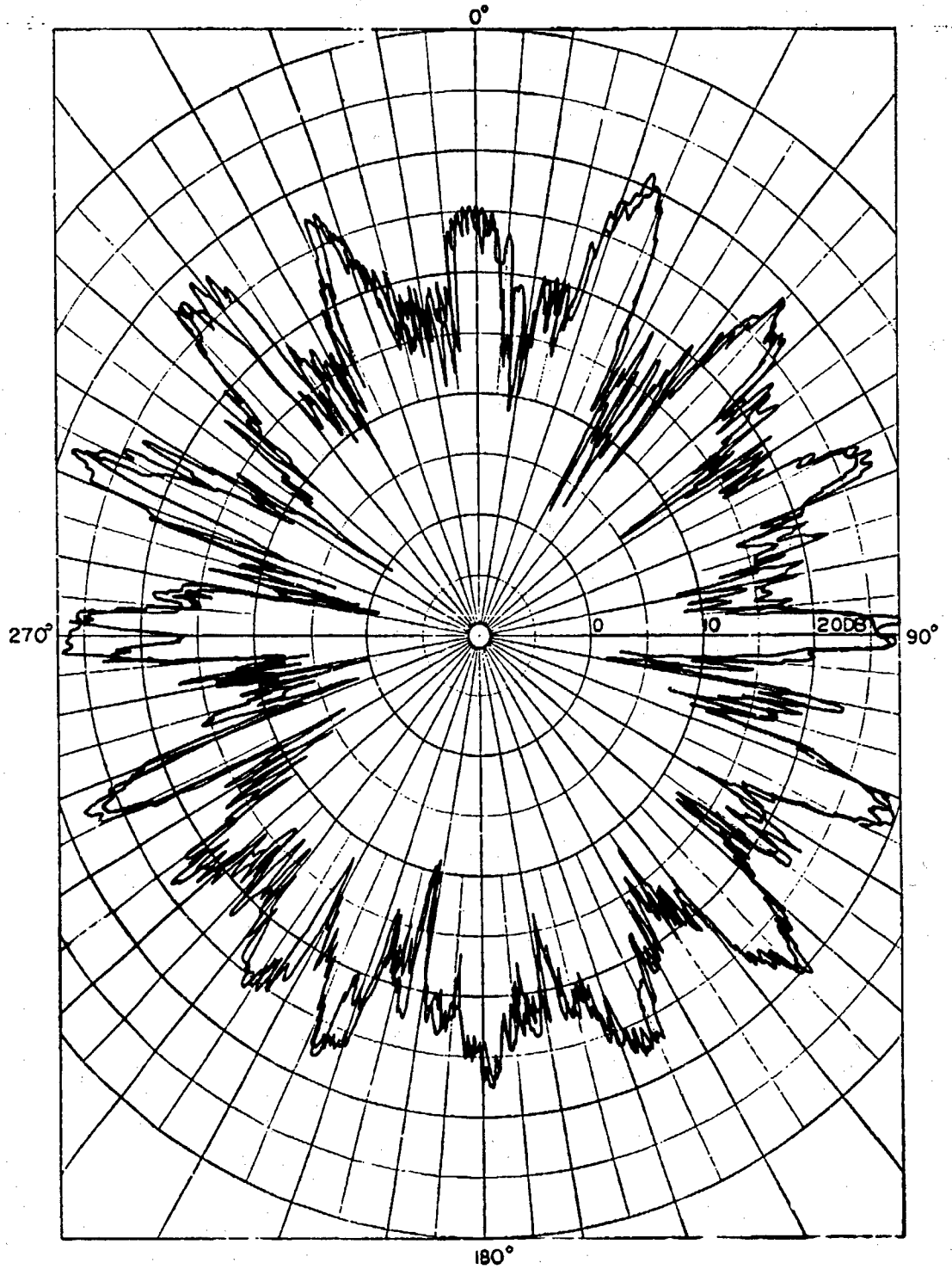


FIGURE 4. Echo from a gored sphere, diam. 3 ft. Experimental conditions and procedure were the same as for Figure 2.[4]

is almost never true at sea, thus it is necessary to derive formulas that describe the general case.

Consider the case of a signal projected by a sonar that has a source level $S$ db. In going to the target, the sound level of the signal will be reduced $H$ db; the value of the transmission loss $H$ depends on the range to the target. At the target, the level of the *incident* sound will thus be

$$L = S - H \text{ db}. \tag{4}$$

If the intensity of the sound at the target is $I$, then

$$L = 10 \log I. \tag{5}$$

Under the influence of this sound, the target becomes a secondary source of sound; the intensity, $I_1$, of the reradiated sound at the standard distance of 1 yd is, according to equation (7) of Chapter 5,

$$I_1 = \frac{I\sigma}{4\pi},$$

where $\sigma$ is the target area. Taking logarithms of this expression, we obtain as the secondary source level

$$\begin{aligned} S_1 &= 10 \log I_1 = 10 \log I + 10 \log \frac{\sigma}{4\pi}, \\ &= L + T, \end{aligned} \tag{6}$$

where $T$ is the target strength.

Since, from equation (4), $L = S - H$,

$$S_1 = S - H + T. \tag{7}$$

As this reradiated sound (the echo) travels back to the sonar, its sound level is again reduced $H$ db, hence the level of the *echo* at the sonar, denoted by $E$, will be given by

$$E = S_1 - H, \tag{8}$$

and, using equation (7),

$$E = S + T - 2H.$$

In this equation $E$ = the echo level,
$S$ = the source level of the sonar,
$T$ = the target strength,
$H$ = the transmission loss from sonar to target.

These four quantities are in decibel units.

Equation (9) is fundamental to all considerations of echo ranging. It may be given another form, since

$$H = A + 20 \log r,$$

(see Chapter 1) where $A$ is the transmission anomaly, equation (9) may be written

$$E = S + T - 2A - 40 \log r, \tag{10}$$

where $r$ now is the range to the target.

It is to be noted that if the target strength depends on the aspect of the target, that value of $T$ appropriate to the situation is to be used in this equation.

## 8.1.4 The Measurement of Target Strength

The discussion up to this point has implied that the target strength of a given reflector is a characteristic of the reflector, determined entirely by the physical properties of the latter—its size, shape, the nature of its surface, and its orientation relative to the direction of the incident sound. It is necessary to investigate the effects of these properties, as well as those of the signal, such as its frequency and ping length. Three major methods have been adopted in this work.

1. Formulas for the target strength of practical targets—for example, submarines—can be derived by mathematical methods similar to that illustrated in the derivation of equation (3). The calculations are complicated and subject to the same uncertainty that has already been noted in the case of the spherical target.

2. A convenient laboratory method for measuring target strengths of practical targets is provided by constructing accurate small-scale models, and comparing the intensity of the echo with the intensity of echoes from spheres. The target strength can then be expressed in terms of a standard sphere. Visible light and high-frequency sound have both been used in such model studies. They will be described in Section 8.2.

3. The most direct and straightforward method of obtaining target strengths obviously is to echo range on the actual targets in the ocean and to study the recorded echoes. The complications introduced by working in a medium as variable and unpredictable as the ocean make it difficult to interpret the results of such measurements. A program of considerable magnitude has been inaugurated and partially completed in order to obtain and analyze a sufficiently large mass of data to warrant definite conclusions concerning the design and operation of gear and the

construction of submarines. The results of these studies up to the time of writing will be summarized in Section 8.4.

## 8.2 MEASUREMENT OF TARGET STRENGTH USING SCALE MODELS

The specific objectives of the experiments with models are:

1. To determine the target strength as a function of the orientation of the target with respect to the echo-ranging beam. The orientation is conveniently described in terms of aspect and altitude angles, defined in Figure 5. In this figure the center of a submarine is shown as the origin of a system of rectangular

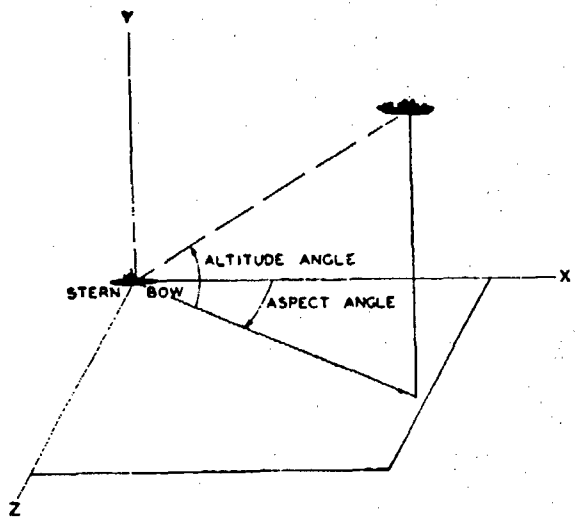


FIGURE 5. Diagram illustrating target aspect and altitude angles.

coordinates. The *aspect* is given by the angle between the $x$ axis and the projection of the beam on the $x$-$z$ plane, measured clockwise in degrees from the bow of the submarine. Thus, bow aspect is 0 degrees, stern aspect 180 degrees, starboard beam aspect 90 degrees and port beam aspect 270 degrees. The altitude of the target is defined as the angle in degrees between the echo-ranging beam and the $x$-$z$ plane. This angle is positive if the projector is above the target and negative if it is below. Thus, if target and projector are the same level, the altitude is 0 degrees; if the projector is directly above the target, the altitude is 90 degrees.

2. To determine which portions of a vessel are mainly responsible for the production of echoes.

### 8.2.1 Optical Experiments

#### METHOD OF DETERMINING THE TARGET STRENGTH

A series of experiments was carried out at MIT in which the target strengths of several classes of submarines were determined by optical methods.[1,2,3] In general terms, the experimental technique was to project light onto the models at different aspects and altitudes and to receive the reflected light by a photoelectric cell located near the source. The resulting electric current was amplified and measured. The models were then replaced by spheres of various sizes (see Section 8.1.2) and the intensity of the light reflected by them measured in the same manner.

The target strength of the submarine represented by a given model was calculated as follows:

From equation (9), the target strength of the model $T'$ is

$$T' = E' - S + 2H,$$

where $E'$ is the intensity level of the reflected light in decibels above some arbitrary reference, dictated by considerations of convenience in using the apparatus. The source level $S$ will, of course, also be in decibels above the same reference level as $E'$. The target strength $T_0$ of a comparison sphere substituted for the model, is

$$T_0 = E_0 - S + 2H,$$

where $E_0$ and $S$ are referred to the same zero level as before. If proper precautions are observed, $S$ and $H$ will be equal in both measurements; hence

$$T' - T_0 = E' - E_0 \text{ db}.$$

If the comparison sphere duplicates the echo level of the model, $E' = E_0$ and $T' = T_0$, and the target strength of the model then is given by equation (3),

$$T' = 20 \log d_0 - 12 \text{ db},$$

where $d_0$ is the diameter of the equivalent sphere. To obtain the target strength of the actual submarine, $d_0$ is multiplied by the scale factor, $k$, of the model; whence finally

$$T = 20 \log (kd_0) - 12 \text{ db}.$$

#### EXPERIMENTAL RESULTS

Some typical results of the measurements described above are exhibited in Figures 6 to 8. Figure 6 shows the reflection from a model of a submarine of the S class. It is evident that echoes from aspects

other than off the beam are negligible compared with the latter; for at aspects more than 30 degrees removed from beam aspect the target strength is nearly 20 db less than the maximum.

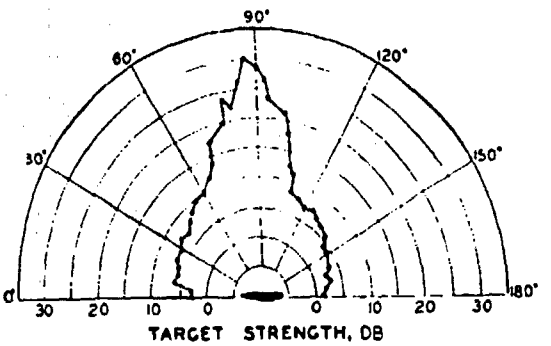


FIGURE 6. Target strength of a submarine (S class) model measured by optical method, showing variation with aspect. Points show averages of both sides of the model. Zero altitude.

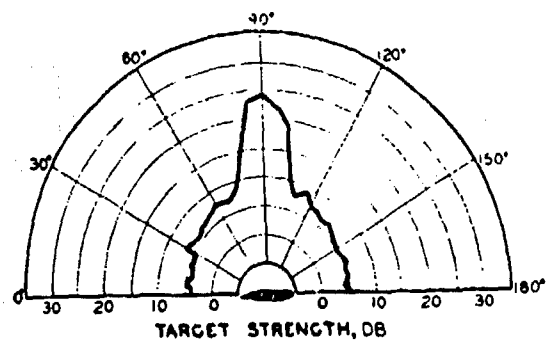


FIGURE 7. Target strength of model submarine of Figure 6 by optical method.[3] Altitude = −45 degrees.

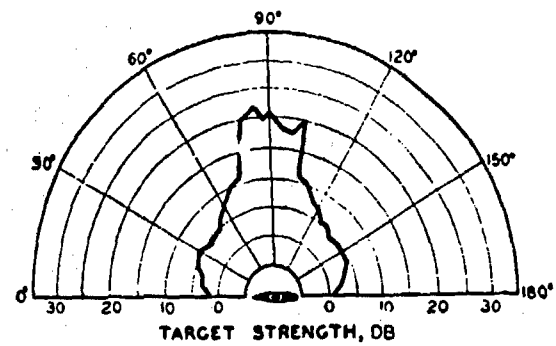


FIGURE 8. Target strength of submarine model of Figure 6 by optical method.[3] Altitude = +10 degrees.

The effect of altitude is shown in Figure 7 and Figure 8, which show the reflectivity from the same model at an altitude of − 45 degrees and + 10 degrees, respectively. The target strength is seen to be considerably less than for 0 degrees altitude, but the general pattern of the curves is similar at all altitudes.

## CRITICISM

The chief criticism of optical experiments on models is based on the fact that the wavelength of the light used is not properly scaled. For example, if a scale factor of 60:1 is used in constructing the model, the wavelength of the light corresponding to the wavelength of 24-kc sound would be 1 mm. This is in the far infrared or ultrashort microwave region, and is not practicable for these experiments. As a consequence of the wrong wavelength, the results may be in error because of the effects connected with the diffraction and nonspecular reflection of the sound. The chief consequence of these errors is that the effect of the conning tower may be overemphasized and that of the bow and stern reduced too much.

An additional handicap in experiments with light is provided by the fact that the effects of inaccuracies in the construction of models are exaggerated. Moreover, it is not possible to reproduce all the ship's fittings in the model, and these may possibly be important. In this connection also the diffuse reflection caused by minor irregularities must be considered; in the experiments these effects were minimized by using glossy surfaces. For all these reasons it is possible that target strengths of submarines estimated from models may sometimes be in error by as much as 10 db.

One objection has been raised, based on the assumption that if a submarine is in motion, its hull is surrounded by a blanket of turbulent water, and perhaps of air bubbles, the effect of which may be to alter the reflectivity considerably. However, there is little experimental evidence to support this assumption of an appreciable acoustic effect of the turbulent blanket surrounding the submarine. It is known, however, that the wakes of both surface vessels and submarines can be detected by echo ranging (see Chapter 6).

## PHOTOGRAPHIC STUDIES

In connection with the experiments just described, the reflected light could also be admitted to a camera, in the expectation that the resulting photographs would give clues as to the most likely areas of submarines that produce strong echoes. Such photo-

graphic studies were also carried out at San Diego.[5] At the latter laboratory, a model HMS *Graph*, finished with glossy white enamel, was photographed from various aspects (see Figure 9). The model was then covered in part by vertical and horizontal cor-

FIGURE 9. Photograph of Model of HMS *Graph*, beam aspect. The model was finished with glossy white enamel.

FIGURE 10. Similar to Figure 9, except that vertical and horizontal corrugations were attached.

FIGURE 11. Similar to Figure 9, with parts of the model covered by emery cloth.

rugations (Figure 10) and by emery cloth (Figure 11), with the objective of reducing prominent reflections.

### 8.2.2 Acoustic Experiments

The inaccuracies associated with the wrong scale factor of the light used in the optical experiments just described were avoided in another study of target strengths by using ultrasonic sound.[6] A model of HMS *Graph*, built to a scale of 1:60, was suspended in water, and continuous sound of 1,565 kc was projected against it. This frequency corresponds to echo ranging on the actual submarine at 26 kc. The echo level was measured for all aspects of the model at distances ranging from 1 to 17 ft, corresponding to actual target ranges between 20 and 340 yd. The target strength of the model $T_M$ was calculated by using equation (9),

$$T_M = E - S + 2H.$$

The transmission loss was assumed to be

$$H = 20 \log r.$$

The value of $T_M$ was increased by 20 log 60 (the scale factor of the model) to obtain the target strength of the actual submarine.

The target strength, for all aspects, measured in this manner is shown in Figure 12; the curve is the average of the two sides of the model. The target

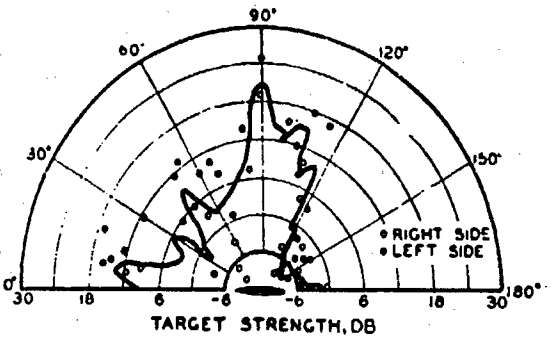


FIGURE 12. Target strength of submarine model of Figures 9 to 11, measured in water with 1,565-kc sound. Echo level measured at distances of 1 ft to 17 ft. The curve is the average of the two sets of experimental points.

strength decreases nearly 20 db from its value at beam aspect for aspects more than 20 degrees from the beam. Bow and stern aspects show greater target strength than the corresponding optical measurements indicate.

Experiments with models are valuable in that they give the order of magnitude, at least, of the target strengths of practical targets; but the great scatter of the observed points indicates the difficulty of obtaining precise results.

## 8.3 MEASUREMENT OF THE TARGET STRENGTHS OF SHIPS AND SUBMARINES

### 8.3.1 General Considerations

All measurements in echo ranging are based on the fundamental equation (9),

$$E = S + T - 2H,$$

whence the target strength is given by

$$T = E - S + 2H. \qquad (11)$$

This equation involves four quantities. If the echo level $E$, the source level $S$, and the transmission $H$

could all be measured while echo ranging on an actual ship or submarine, the target strength of $T$ of the latter could be calculated.

The primary difficulty is that these three independent measurements must all be made at sea. It has been seen that such measurements are rendered difficult by the extreme variability of the ocean. Consequently, each of the three measurements will be subject to errors of considerable magnitude, and the computed value of the target strength will be less accurate than the least accurate of the three measurements involved.

In addition, secondary difficulties are encountered in the work because of the problems of seamanship and navigation that arise when a surface vessel and submarine are required to execute precise maneuvers together.

The accuracy might possibly be improved by using the method of comparison spheres, as described above in the discussion of the optical experiments; this would reduce the required measurements to determinations of echo levels alone, since $S$ and $H$ would cancel out. However, the problem of handling large spheres at sea is so difficult that this method has not been used to any extent.

In the following, some attention will be devoted to the measurement of the three quantities, and to proposed means for surmounting or avoiding the difficulties.

### 8.3.2 The Measurement of $E-S$

In principle, $S$ could be determined by measuring the electric input during transmission, the sonar being calibrated to give the equivalent source level. If $V_S$ is the electric input of the signal, and $K_P$ the calibration constant of the sonar as a projector,

$$S = V_S + K_P. \tag{12}$$

All these quantities are in decibel units. Similarly, the echo level $E$ would be determined from

$$E = V_E + K_H, \tag{13}$$

where $V_E$ is the electric output during the reception of the signal, and $K_H$ the calibration constant of the sonar as a hydrophone. Then

$$E - S = V_E - V_S + K_E - K_S. \tag{14}$$

Of these four quantities, $V_E$ and $V_S$ can be determined quite accurately; at any rate, errors in their measurement are negligible compared with those in the determination of $K_E$ and $K_S$. These constants cannot be determined more accurately than within $\pm 2$ db even under the best conditions. Moreover, their values change from day to day in an unpredictable manner; changes in temperature and humidity, the growth of fouling organisms on the transducer, all contribute to these changes. It is optimistic to suppose that they are both known within $\pm 4$ db, and consequently, errors in the value of $E - S$ will be of the order of $\pm 6$ db. This simple method of determining $E - S$ is, therefore, far from precise. It has been used in most of the experimental work, but more elaborate methods have been devised in order to eliminate the errors in the calibration constants.

The objective of these more complicated methods is, in each case, to obtain an expression for $E - S$ that does not involve the calibration constant of any of the apparatus used. They all require additional equipment and make the operations at sea still more difficult. As a consequence, none of them has as yet been used extensively.

An example will be presented to show how it is possible to attain this objective. It is the simplest of the various methods proposed, but is not the best in practice.

Suppose that, instead of using the same transducer both for transmitting the signal and receiving the echo, two separate transducers are used for the two purposes. They are mounted on separate shafts and have separate electric circuits. The values of $S$ and $E$ will still be given by equations (12) and (13) when these are applied to the appropriate transducer. An auxiliary experiment is also performed as nearly simultaneously with the echo ranging operation as possible. This experiment can be more easily described with reference to Figure 13A. The two sonars are trained so that they face each other; Sonar I serves as the projector, and Sonar II as the receiver of the signal. Sonar I is excited with the input $V_S$, and a signal of source level $S$ is transmitted. This signal will travel directly to the hydrophone of Sonar II, where its level will be given by

$$L = S - H_0,$$

$H_0$ being the transmission loss over the path separating the two transducers. If the electric output of the signal at the hydrophone of Sonar II is $V'_S$, and the calibration constant is $K_H$, we have, since

$$L = V'_S + K_H,$$

$$V'_S = L - K_H = S - H_0 - K_H,$$

or

$$S = V'_S + H_0 + K_H. \tag{15}$$

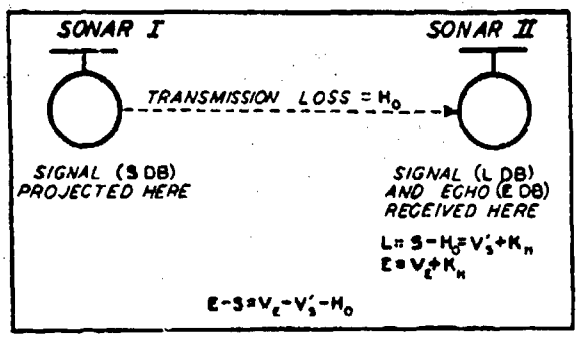


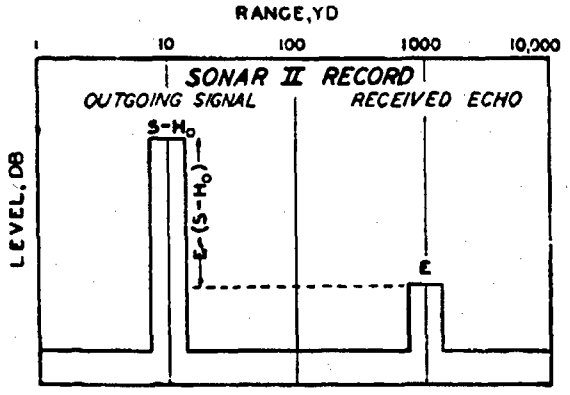


FIGURE 13. Arrangement for eliminating the calibration constants of the sonar in determining $E - S$. (*Top*) Experimental setup. Sonar I and Sonar II are both mounted on the echo-ranging ship but on separate shafts, facing each other. They have separate electrical circuits. (*Bottom*) Schematic of oscillograph record showing how $E - S$ may be read from the record if $H_0$ is known. $S$ = source level of transmitted signal. $E$ = echo level. $L$ = sound level of signal at Sonar II. $V'_S$ = electrical output of the signal at Sonar II. $V_E$ = electrical output of Sonar II during reception of the signal. $K_H$ = calibration constant of Sonar II as hydrophone.

An echo received by Sonar II will have an electric output $V_E$ at its hydrophone, and combining equations (13) and (15), we have finally,

$$E - S = V_E - V'_S - H_0, \qquad (16)$$

an expression that is independent of both $K_H$ and $K_P$, but does depend on $H_0$. Figure 13B shows schematically how the value of $E - S$ may be read from a record if $H_0$ is known.

The advantage of this method results from the fact that the transmission loss $H_0$ is not subject to the same erratic changes that bedevil the calibration constants. Any error in its determination is thus common to all measurements with the same apparatus. Differences in $E - S$ from one set of experimental conditions to another, or from one target to another, should thus be more accurately determinable than by the simple method of measuring $E$ and $S$ independently on the same sonar.

The method has the practical disadvantage of requiring two nearly complete sonar installations on the same ship, and this has contributed to preventing its use. Analogous methods, more complicated on paper but simpler in practical application, have been used in a few instances.

## 8 3.3 The Measurement of $H$

In much of the work on target strengths, the transmission loss $H$ experienced by the signal in traveling to the target could only be estimated, the calculation taking into account the known thermal conditions of the sea, and the other oceanographic factors that enter into the problem. This method results in large errors, and in equation (11) these are multiplied by 2; when these are combined with the already large error in $E - S$, the resulting error in the value of $T$ is rendered very large indeed.

The alternative is to measure the transmission loss directly. This can be done by making transmission runs immediately before or after an echo-ranging run. This has been done in some experiments. However, it has been observed that the transmission loss may change very appreciably even in a half hour, so that the method is not too successful. Moreover, it has usually been necessary to use a vessel other than the target for the transmission run, thus necessitating maneuvers by three vessels.

The obvious way of avoiding both disadvantages is to equip the target with a receiver system supplied with a recorder. Thus it is possible to measure the transmission loss simultaneously with the measurement of $E - S$. This has been done in a few cases. The chief cause of error in this method is found in the difficulties of ensuring that only the direct signal, and no reflections from the target itself are picked up by the receiver. This technique is being perfected at present.

## 8 3.4 Errors Caused by Fluctuation

Even if all the sources of error discussed above could be eliminated, one other source would still remain. The echo level depends on the transmission loss [equation (9)], and since this quantity fluctuates from ping to ping (see Chapter 3), it is to be expected

that the same will be true of the echo. Figure 14 shows how widely two successive echoes may differ in level.

It might be supposed that by making a simultaneous transmission measurement the error due to the echo fluctuation could be eliminated. For, since there

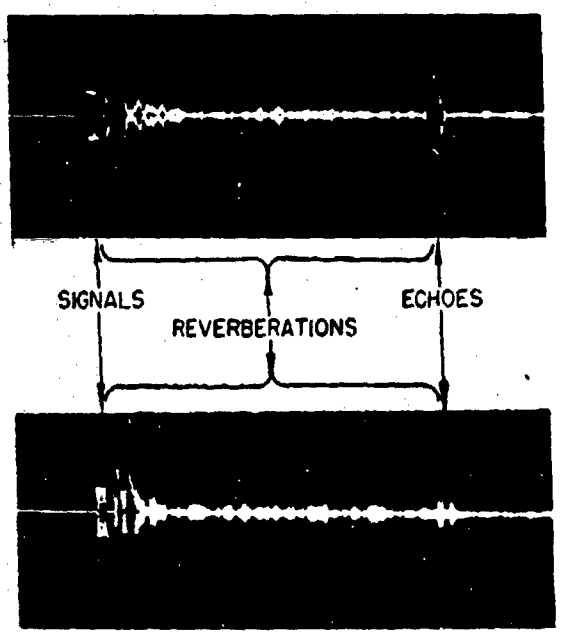


FIGURE 14. Oscillograms of two successive echoes, showing how the echo level may fluctuate from one echo to the next.

is only a short time interval between the transmission of the ping and the reception of the echo, one might assume that the echo level and transmission loss would fluctuate together, or, in other words, that the difference $E - 2H$ would not fluctuate. Unfortunately, the time interval is generally not short enough to justify this assumption. Even at a range of only 400 yd, it is 0.5 sec. Reference to Figure 52 of Chapter 3 shows that quite large changes in transmission loss occur in an interval of this magnitude. Hence the transmission measurement cannot predict reliably how the sound level will fluctuate on the return trip from target to sonar, and it is quite probable that the echo level $E$ will fluctuate as much or even more than the transmission loss.

In practice, some attempt is made to eliminate the fluctuation by averaging sets of five successive echo level measurements. Even with this precaution, the values of $T$, calculated from the average of such sets of five echoes, still fluctuate. An idea of the magnitude of this fluctuation is afforded by Figure 15, which shows that the values are still subject to a

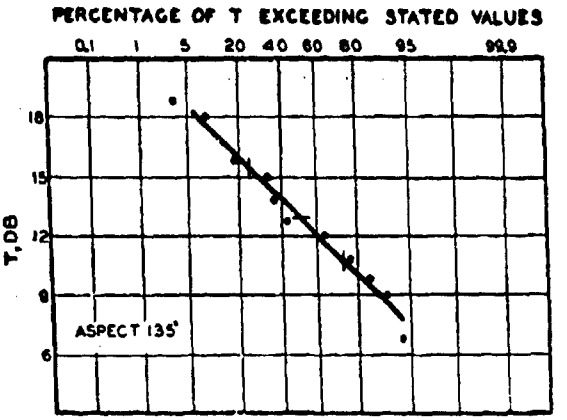


FIGURE 15. Cumulative distribution of target strength $T$ of a submarine at constant range. The median value is indicated by a short horizontal line, the quartiles by short vertical lines, crossing the graph.

random error of some $\pm 3$ db, while errors of $\pm 6$ db occur with noticeable frequency.

The knowledge of the target strength of submarine and surface vessels is fundamental to all sonar design and development problems. It is therefore most unfortunate that the accurate measurement of this parameter should be so difficult. The discussion of the sources of error that has been presented here is by no means exhaustive, but may serve as an introduction to an important series of unsolved problems in sonar research.

## 8.4 RESULTS OF EXPERIMENTS AT SEA

### 8.4.1 Target Strength as Function of Aspect

The dependence of target strength on aspect is shown in Figure 16, which exhibits the results of an experiment on a fleet-type submarine, and is typical of the experiments of this kind carried out at San Diego. The target vessel ran at about 2½ knots submerged at periscope depth; the echo-ranging vessel circled the submarine twice, maintaining a distance of about 500 yd. The transmission loss $H$ was calculated from the relation

$$H = 20 \log r + Ar,$$

and the anomaly $A$ was assumed to be 0.005 db/yd of sound travel. The value of $T$ was computed using equation (13). Each point on the curve is the average of all echo observations with the 15-degree sector centered at the point and represents the average of about 40 echoes.

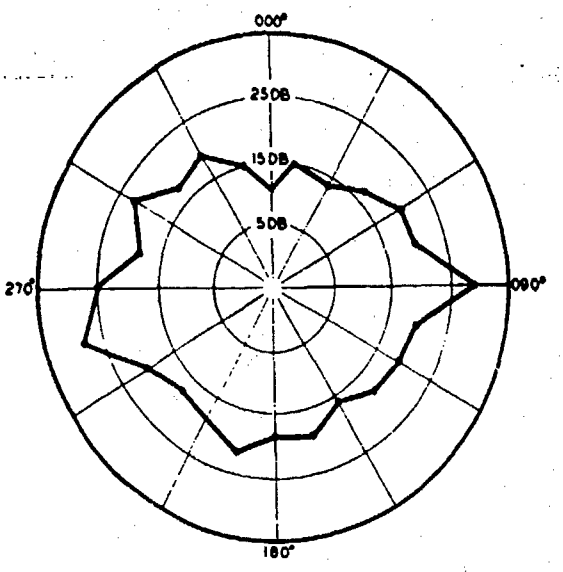


FIGURE 16. Dependence of target strength $T$ of a fleet-type submarine on aspect angle.

It is seen from the figure that the variation with aspect of the target strength measured in this way corresponds roughly to the results obtained by using models. One would not expect a very close correspondence, as there is great variation not only between different classes of submarines, but also between individual submarines of a given class. This can be seen from Table 2, which exhibits the results

TABLE 2. Target strength of submarines for various aspects (15-degree sectors, 24-kc sound).

| Type of submarine | Bow (db) | Stern (db) | Abeam (db) |
|---|---|---|---|
| Fleet | 10 | 18 | 27 |
| S class | | | |
| A | ... | ... | 18 |
| B | 15 | 10 | 21 |
| C | 5 | 10 | 8 |
| D | 1 | 2 | 5 |
| C (repeated 3 months later) | 2 | ... | 14 |
| E | ... | ... | 22 |
| B (repeated 8 months later) | ... | 12 (135° aspect) | ... |
| Average for all S boats | 6 | 7 | 15 |

of many experiments carried out at San Diego. All these measurements were made with 30-msec signals of 24-kc sound.

A systematic dependence of target strength on the class of the ship has not been definitely established, although the above table suggests that the larger fleet-class submarine has a higher target strength, as was to be expected.

Other measurements made at various places and times indicate higher values for S-type submarines. No explanation for this has been offered. The target strengths as measured by model experiments are a few db higher for beam aspects, and slightly lower for bow and stern aspects, than the corresponding values from direct measurements.

### ALTITUDE ANGLE

In operational practice the variation of target strength with altitude is not significant, since the altitude angle is generally quite small. There is practically no experimental evidence of an altitude effect in echo ranging.

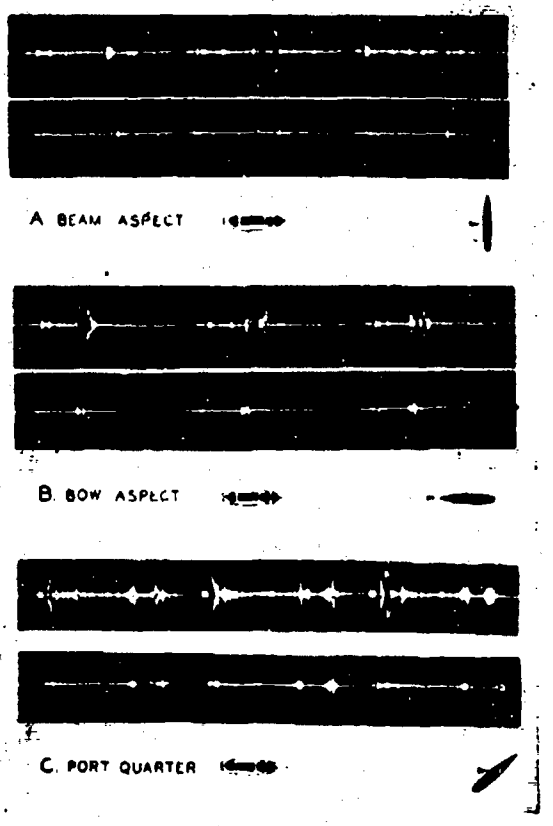


FIGURE 17. Echoes from submarines at various aspects, using long and short pings. The upper oscillogram of each pair is the record of a ping of 26.5-yd length, the lower one of a 4.0-yd ping. As the ping length is decreased, the separate echoes tend to become discrete.

## 8.4.2 The Form of the Echo as a Function of Target Aspect and Ping Length

A submarine must be considered as an aggregate of various targets, rather than as a single one: the secondary sources that cause the echo are not all at

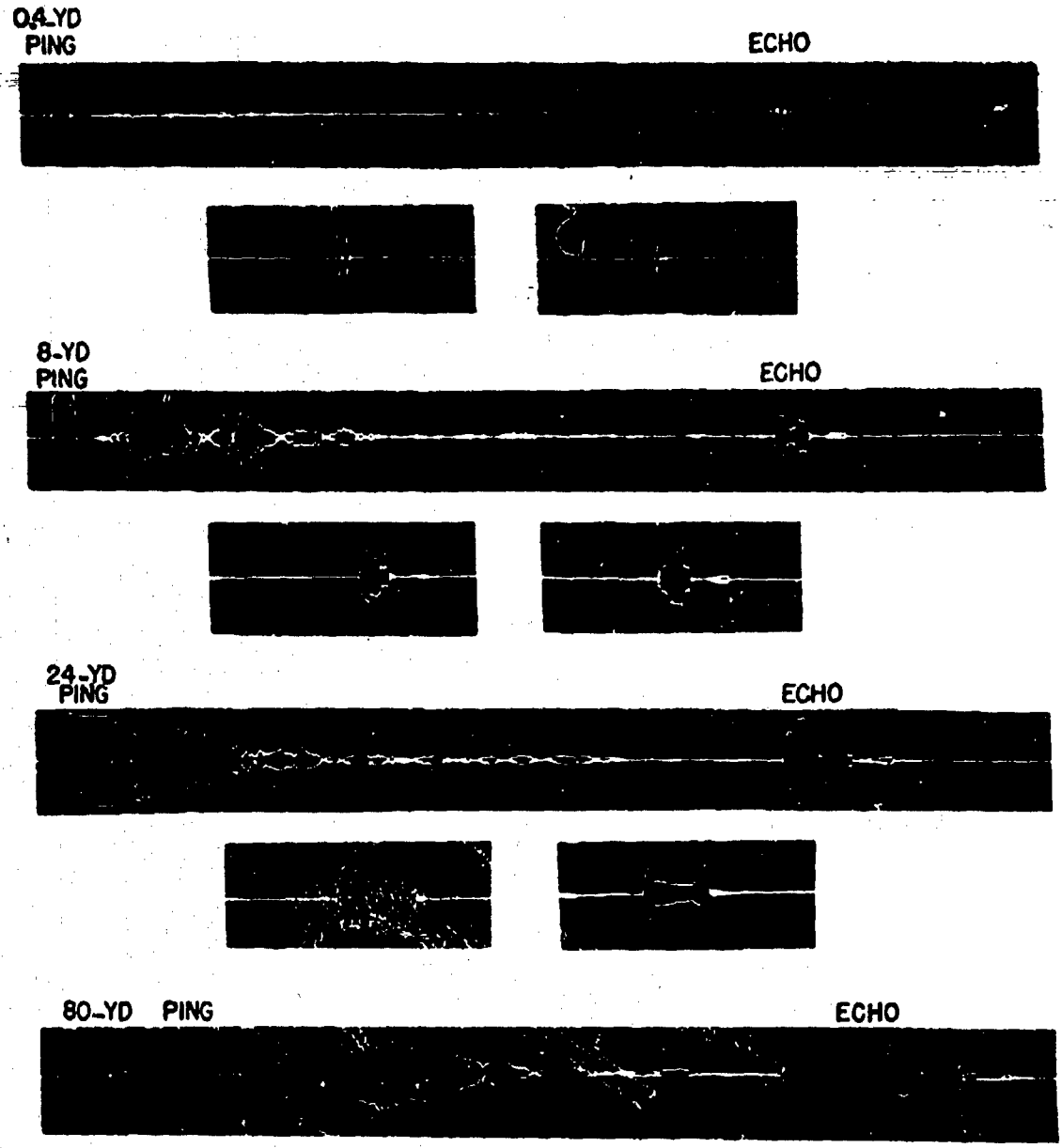


FIGURE 18. Oscillograms of echoes of pings of various ping lengths from a submarine presenting beam aspect. The records are more extended than those of Figure 17. Each of the first three sets shows three echoes received within a period of ten seconds. The echoes are seen to show the effects of interference between the component parts of the echo. (Compare with Figure 52, Chapter 3. The original oscillograms were retouched slightly to bring out the outlines of the echoes; it is not believed that the form has been changed.

the same place. This is clearly illustrated by the photographs of the model submarines shown in Figures 9 to 11; in practice the number of component sources is probably increased by various fittings on the deck and hull. Each of these returns its own echo; thus it is not strictly correct to speak of *an* echo from a submarine. If the range to the various sources is different, each echo will be received at a different time.

With long pings, these separate echoes overlap in time and result in a single burst of sound, the envelope of which is very irregular. If the ping length is very short, the individual echoes can be distinguished on the oscillogram. This is illustrated by Figure 17: the upper oscillogram of each pair is the record of a ping of 26.5-yd length, the lower one of a 4.0-yd ping. As the ping length is decreased, the separate echoes tend to become discrete. This is

more strik evident in Figure 18, in which are shown oscillograms of echoes recorded with the camera speeded up, so that the record is more extended than in Figure 17. The echoes shown are of pings of various lengths from 0.4 yd to 80 yd, and all are for beam aspect. Each oscillogram shows three echoes received within a period of 10 sec, and it will be noted that these echoes have a structure similar to that discussed in Chapter 3 and illustrated in Figure 52 in connection with signals, which shows the effect of interference between the components of the resultant echo. Both "spool"- and "transformer"-type envelopes can be distinguished. There is some reason for concluding that the two main "blobs" noticeable in the shorter ping lengths are due to echoes from the hull and conning tower, respectively. The "tail" that is observable in each case is attributed to sound reflected from the submarine to the surface, back to the boat, and thence to the sonar.

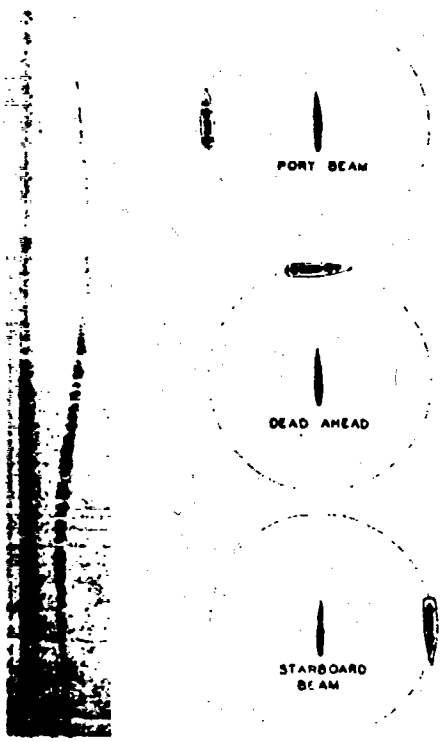


FIGURE 19. Chemical recorder trace made while echo-ranging vessel circled a submarine, showing the variation in echo length at different aspects. It is seen that at beam aspects the echo is of a length comparable with that of the signal.

It is not possible to separate the component echoes by ear, or on the range recorder. On the latter, however, it is possible to see the elongation that results from the extension of the target in the line of sight. This effect is discernible in the oscillograms of Figure 17, but much more clearly evident in the range recorder trace illustrated in Figure 19. This trace was made while the echo ranging vessel circled a submarine. When the latter presents a beam aspect, the echo is short, being about equal in length to that of the outgoing signal; the latter is visible at the left edge of the trace. As the aspect changes, the difference in range to the various secondary sources increases, with an accompanying increase in the length of the echo.

This increase is theoretically equal to the length of the target in the line of sight. This dimension is proportional to the cosine of the aspect angle; in Figure 20 it is plotted against the aspect angle, shown by the solid curve. The indentations shown at bow and stern aspects are due to the shadows cast by the hull. The experimental values are shown by the dotted curve, which is seen to parallel the theoretical curve quite well. The observed echo lengths are consistently longer than those calculated on the basis of the length of the submarine; since the wake of a moving vessel returns an echo, the length of the wake should be included in the calculation, but this is a rather indefinite quantity.

### 8.4.3 Echo Intensity as a Function of Aspect and Ping Length

The separation of the individual secondary sources on a complex target has an effect also on the intensity of the echo. Let the target areas of the several parts of the target be represented by $s_1, s_2, s_3, \ldots s_n$. The $n$th one will then return an echo of intensity proportional to $s_n$. If the sources are close enough together so that their echoes overlap, the intensities of all of them will add, so that the resultant intensity will be proportional to $s_1 + s_2 + s_3 + \ldots + s_n$.

If the individual sources are spaced more widely than the ping length, the echoes will not overlap, and the result will be an echo intensity that is successively proportional to $s_1$, then to $s_2$, then to $s_3$, and so on. It follows that, under these circumstances, the echo intensity will vary rapidly, but will be lower, on the average, than when there is overlapping.

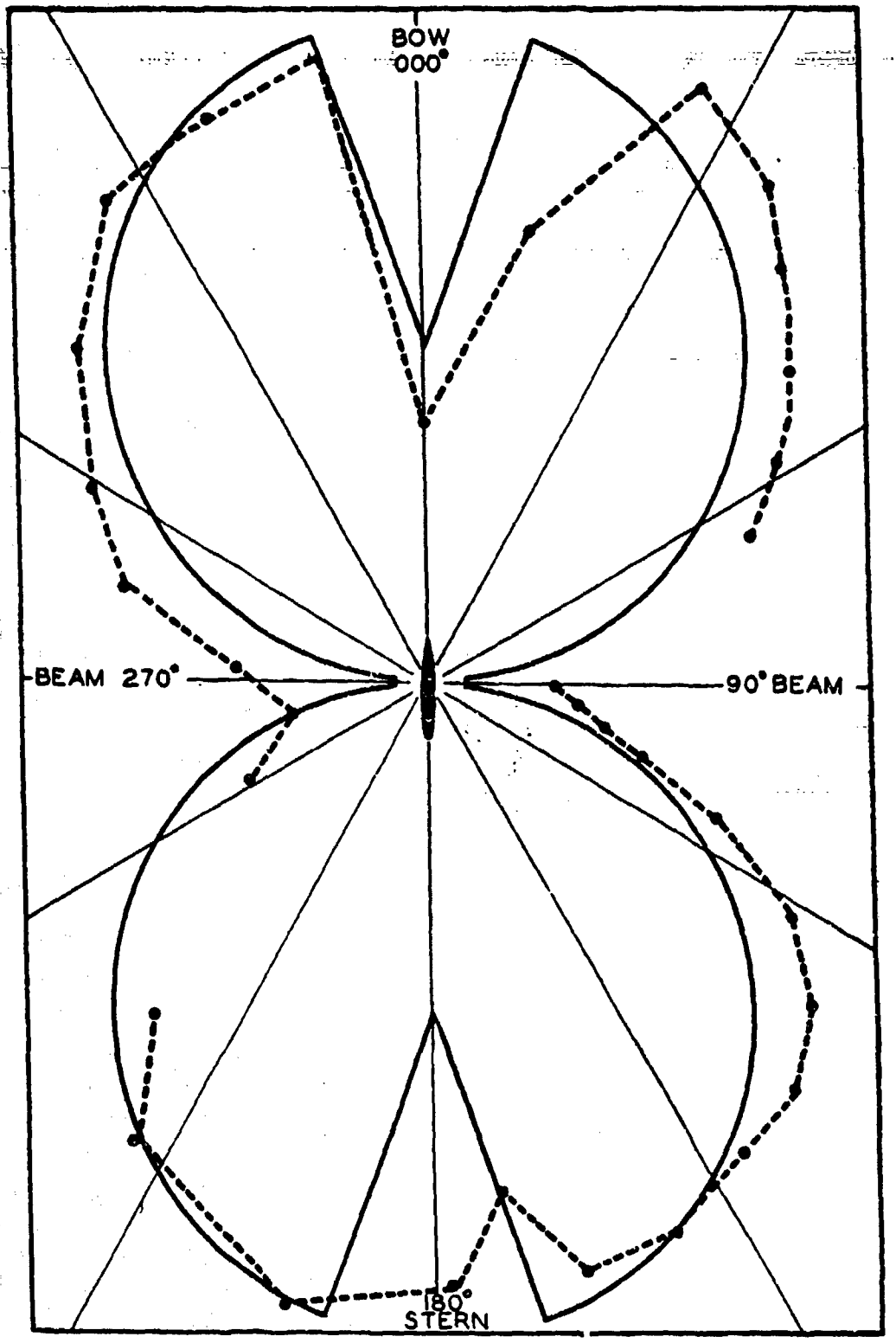


FIGURE 20. Elongation of the echo from a submarine for various aspects. The solid curve is the theoretical length of the echo for a very short ping. The dotted curve connects observed values of the echo length after correction for the actual ping length. They are seen to parallel the theoretical curve fairly well. The indentations at bow and stern aspects are due to the shadow cast by the hull of the target.

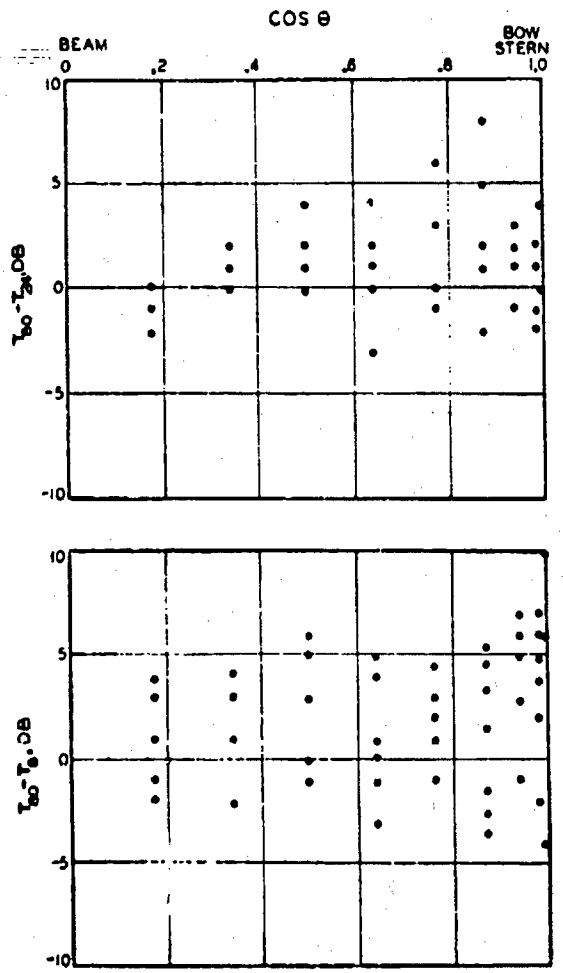


FIGURE 21. Target strength as a function of ping length and aspect. The difference in target strengths between 80-yd and 24-yd signals ($T_{80}-T_{24}$) and between 80-yd and 8-yd signals ($T_{80}-T_8$) are plotted against the cosine of the aspect angle, θ. (From NY STR.)

This effect is shown very clearly by Figure 17. It is seen that at bow and quarter aspect the amplitude of the echoes from the 26.5-yd pings are noticeably larger than those from the 4.0-yd pings. However, the simple theory presented here has not been completely verified by experiment. Early measurements made at San Diego at 24 kc indicated that echoes of 4.0-yd signals averaged about 4 db lower than those from 26.5-yd signals; and that echoes at beam aspect showed less dependence on signal length than echoes from bow and quarter aspects. Later measurements, however, reported no very significant dependence of target strength on signal length, for signals of 8, 24, and 80 yd. These measurements are portrayed graphically in Figure 21, in which the differences in target strengths between 80-yd and 24-yd signals ($T_{80}-T_{24}$) and between 80-yd and 8-yd signals ($T_{80}-T_8$) are plotted against the cosine of the aspect angle $\theta$. The differences are very small, and in view of the large scatter, not much significance can be attached to them.

### 8.4.4 Dependence of Target Strength on Frequency

Theoretical considerations suggest that the target strength of a scatterer will depend on the frequency of the incident sound only when the principal part of the echo is due to scattering by irregularities, the dimensions of which are of the order of magnitude of the wavelength of the incident sound.

The evidence of direct measurements is inconclusive. On one occasion it was found that the values of the target strength for sound of 60 kc were as much as 14 db higher than those obtained when 24-kc sound was used; on another occasion the target strengths of the two frequencies were nearly equal. In these experiments the transmission loss was estimated from earlier measurements. In view of the small amount of data on transmission at 60 kc and the known variability at all frequencies, the estimated values of $H$ are of doubtful accuracy.

Experiments performed at sea with spherical targets at frequencies ranging from 10 to 40 kc also provide no decisive evidence of systematic variation of target strength with frequency; any variations that were observed were less than the uncertainty of the calibration of the sonar gear. This agrees with the results obtained at very short range, already discussed in 8.1.

### 8.4.5 Dependence of Target Strength on Range and Speed of Target

The target strength of a submarine might be expected to depend on the speed provided the motion resulted in a layer of turbulent water or of bubbles surrounding the submarine. There is no experimental evidence of such an effect, but most measurements have been made on creeping submarines, where the effect, if it exists, might be expected to be small.

Concerning the effect on target strength of range, it is evident that if the target is at a range sufficiently large to act as a point source, its target strength is independent of the range, for under such circumstances it will always be completely and uniformly

insonified by the beam at all ranges. At close ranges, this might not be the case, and then the target strength would vary with range, depending on just how much and which part of the target was insonified. This can be seen from Figure 22.

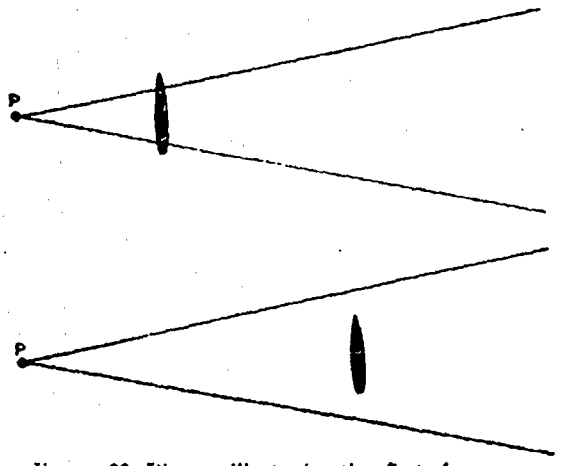


FIGURE 22. Diagram illustrating the effect of range on target strength at close range, the target will present a greater or smaller surface to the sound beam as the distance between it and the projector ($P$) increases or decreases; at long ranges it is completely immersed in the sound beam, and a change of range does not affect the surface area exposed to the ping.

## 8.5 ECHOES FROM WAKES AND ARTIFICIAL TARGETS

### 8.5.1 Echoes from Wakes

The discussion of the acoustic properties of wakes in Section 6.1 makes it clear that wakes are factors to be reckoned with in echo ranging, for two reasons.

1. The wake may act as an acoustic screen, and as a result the echoes from real targets that are beyond the wake may be weakened. In Section 6.1.2 it was mentioned that the echo from a buoy was reduced by 13 db after the passage of a 40-ft motor launch between the buoy and the sonar, and that the echo did not return to its original level for some 2 minutes.

2. The wake itself may produce echoes that are so similar, in both intensity and character, to the echo produced by real targets, as to be easily confused with them (see Figure 5 of Chapter 6).

The latter effect has been used by submarines in evasive tactics; the presumption being that if the submarine made a sharp turn the resultant curved wake ("knuckle") would leave the enemy sound operator an extended false target to echo range on and increase the submarine's chances for favorable action. However, the value of this maneuver has not been established. On the other hand, the wake left by a target vessel might conceivably provide means by which the vessel could be tracked acoustically, especially since the acoustic properties of a wake are known to persist over periods of half an hour or more, long after the visible traces of the ship's passage have disappeared.

The concept of target strength as applied to wakes is fully discussed in Sections 6.2.5 and 6.2.6.

### 8.5.2 Artificial Targets

Mention was made in Section 8.1 of the echo repeater, an artificial target designed for training personnel. An artificial target that has proved to have a variety of uses is the triplane.

#### THE TRIPLANE

The most obvious substitute for a submarine as an echo-ranging practice target is a large sphere, but the difficulty encountered in handling it at sea precludes its use. Theoretical investigation shows that

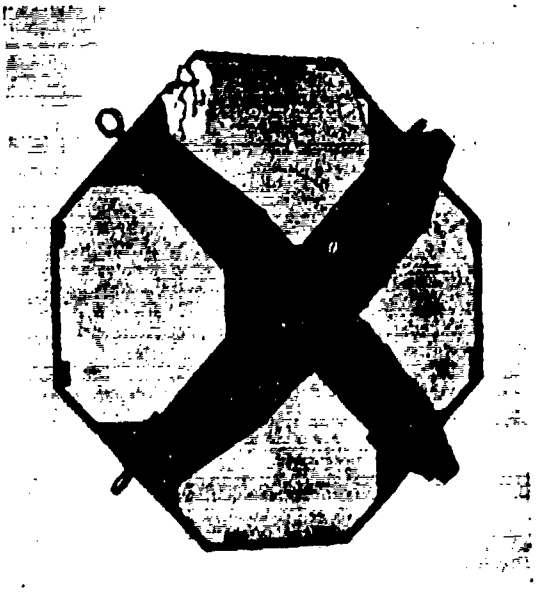

FIGURE 23. Triplanes viewed from different aspects.

a system of three mutually perpendicular square planes of length $L$ has a target strength equivalent to that of a sphere of diameter $d$ given by

$$d = \frac{4.34\,L^2}{\lambda}, \qquad (17)$$

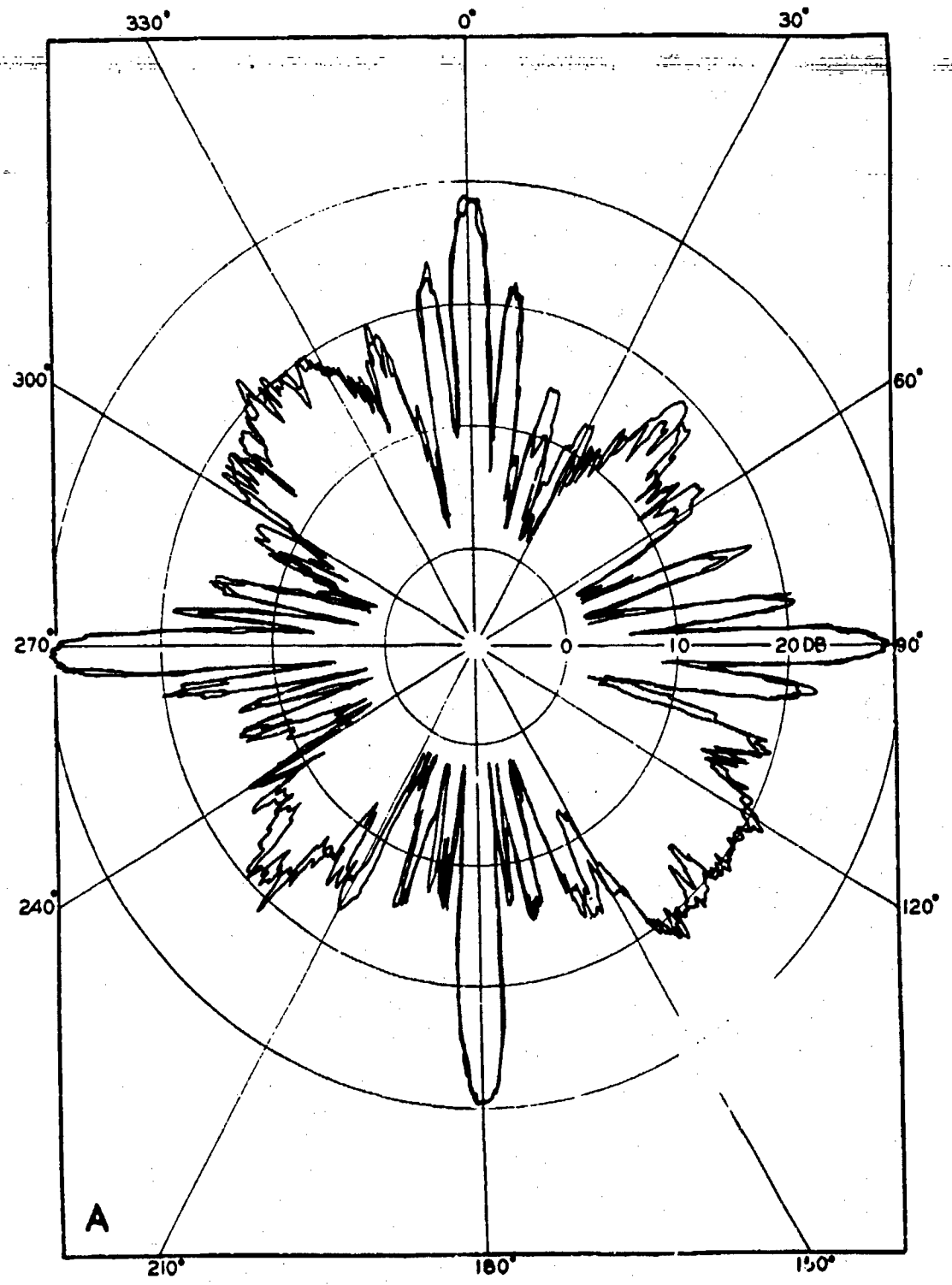


FIGURE 24A. Echo levels from 8-in. triplane at close range. Frequency = 40 kc; distance to triplane = 11.5 ft; sound level at triplane = 43.5 db. Three orientations are shown in Figures 24 A, B, and C. (A)—(0, 0, 1) Plane, $Z = 0$.

where $\lambda$ is the wavelength of the sound. The target strength is expected to vary with the orientation and this value is for the favorable aspect. Thus a triplane with planes 1 yd square has a theoretical target

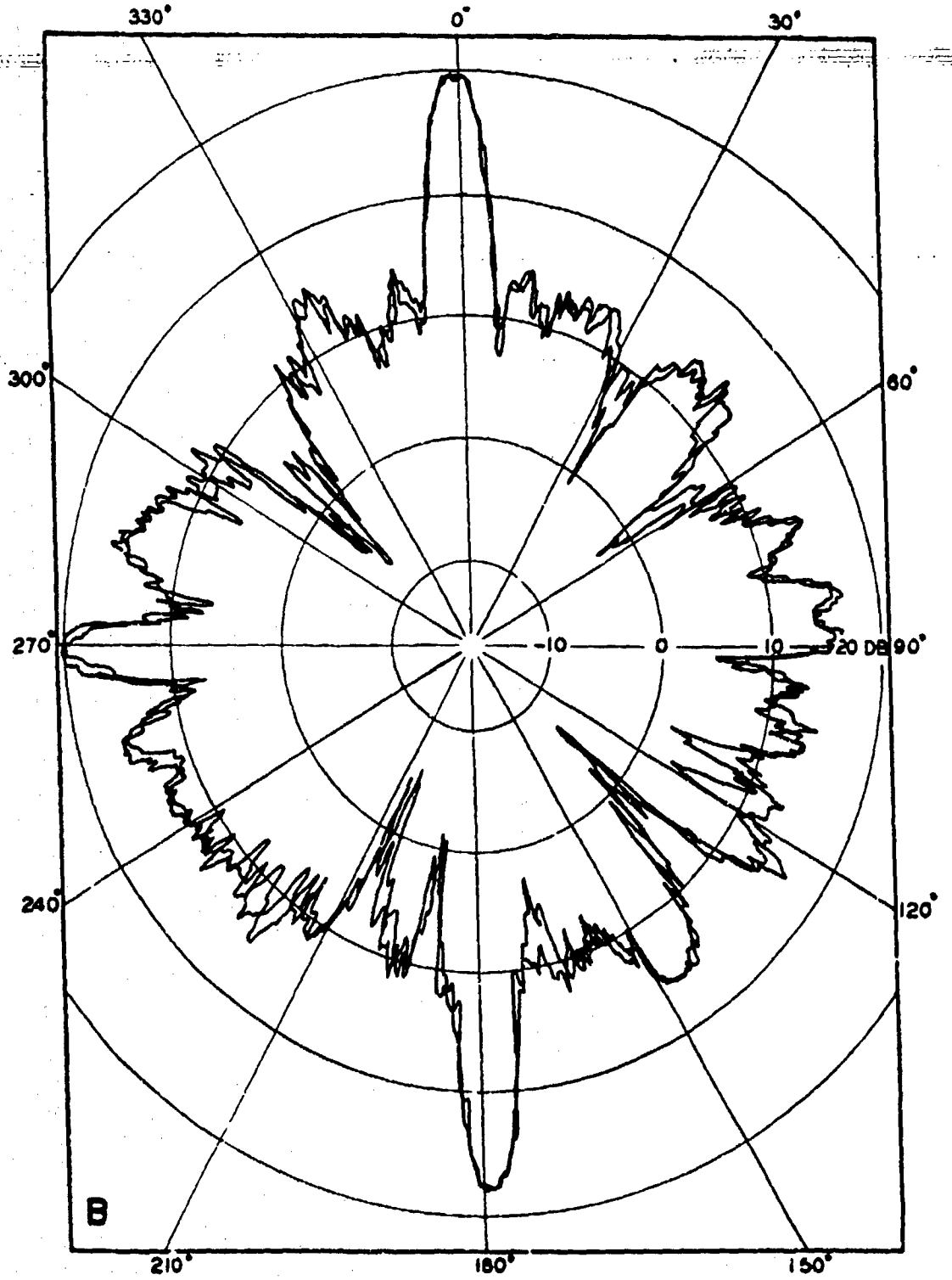


FIGURE 24B. Orientation: (0, 1, 1) Plane, $Y+Z=0$.

strength with 24-kc sound equivalent to that of a 60-yd sphere, or about 23 db, which is roughly the target strength at beam aspect of a submarine. A triplane of the given size is easy to handle. Triplanes 2 yd square have been extensively used to provide strong echoes for training purposes. Such a triplane is illustrated in Figure 23.

Triplane targets must be very accurately con-

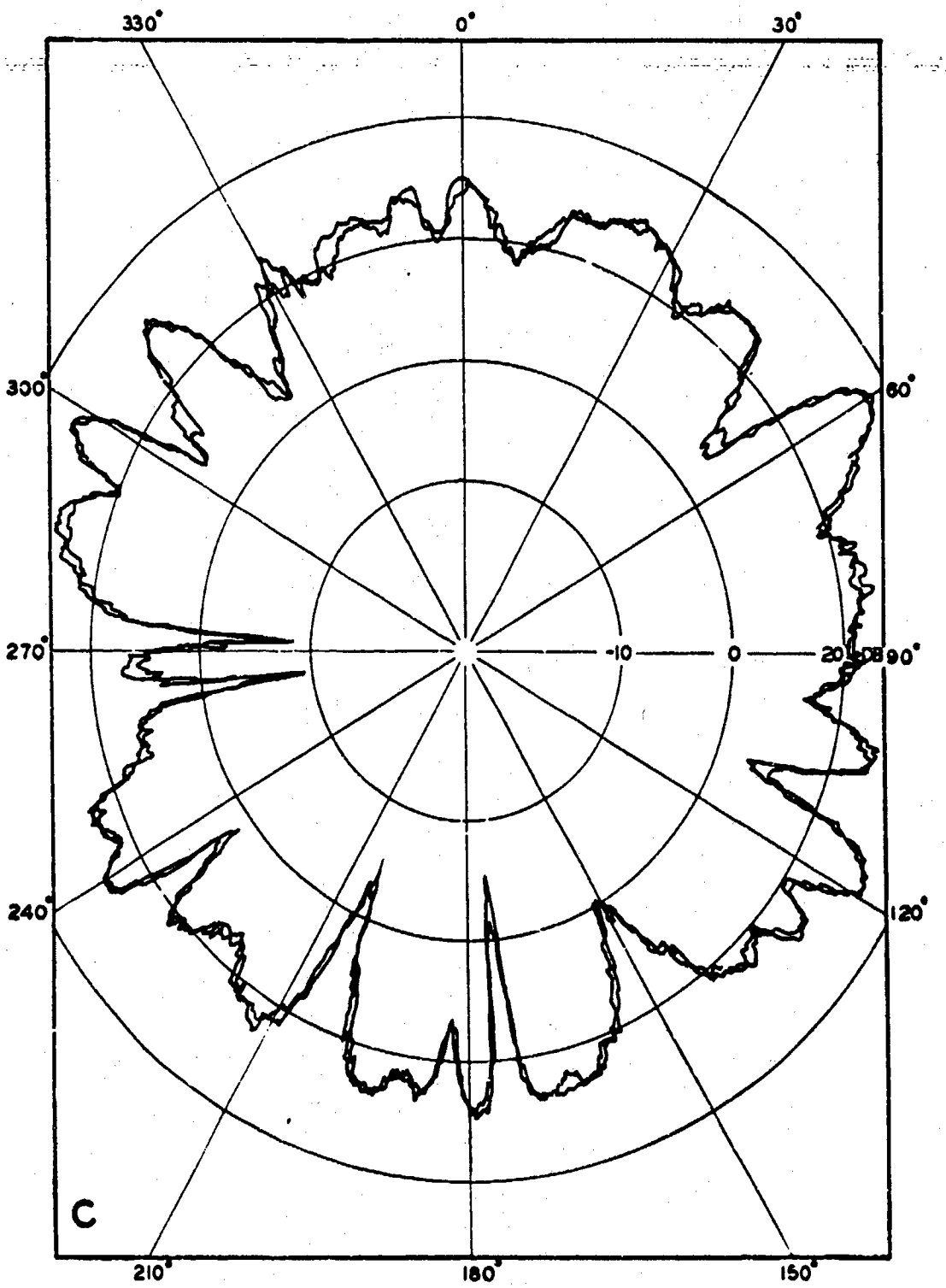


FIGURE 24C. Orientation: (1, 1, 1) Plane, $X+Y+Z=0$.

structed; unless the faces are perfectly perpendicular, the echo will be distorted and probably weakened.

The target strength of a triplane depends on its orientation with respect to the sound beam. Among the measurements of target strengths that were mentioned above[4] were a large number of data on triplanes. These triplanes were small, the planes measuring 8 or 10 in. It was observed that the target

strengths of these specimens varied as much as 10 db at a given frequency for different orientations; for example, the actual target strengths for 30-kc sound varied from −6 db to −16 db (see Table 3). The theoretical target strength, according to equations (17) and (3), is zero db. Thus, while the measured values of the target strengths of spheres is consistently higher than the theoretical values (see Table 1), that of triplanes appears to be consistently lower.

TABLE 3. Target strengths of 8-in. metal triplanes.[4]

| Plane of orientation (frequency, kc) | 0, 0, 1, $z=0$ ($T$, db) | 1, 1, 0, $x+y=0$ ($T$, db) | 1, 1, 1, $x+y+z=0$ ($T$, db) |
|---|---|---|---|
| 20 | −12.7 | −14.2 | −20.2 |
| 30 | − 5.7 | − 5.0 | −16.4 |
| 40 | − 4.1 | − 4.0 | −15.1 |
| 50 | − 1.5 | + 0.9 | −10.1 |
| 60 | + 0.3 | + 1.8 | − 8.2 |
| 70 | + 1.2 | + 2.2 | − 7.3 |
| 80 | + 1.6 | + 3.1 | − 7.9 |
| 90 | + 2.1 | + 4.7 | − 4.9 |

The departure of actual triplanes from geometric perfection undoubtedly contributes to this. The variation in echo level of an 8-in. triplane is illustrated in Figure 24A, B, C, for three different orientations of the triplane, which was slowly rotated while being insonified. Measured values of target strengths for various orientations and frequencies are shown in Table 3.

## Bubble Targets

The fact that wakes of submarines are sources of perceptible echoes suggested that artificial wakes might form a deceptive target that would confuse an echo-ranging vessel in the attack phase. Investigation of the problem disclosed that by means of chemicals, bubble screens could be laid that were imitations of real submarine echoes, except for the doppler effect. Moreover, it was found that bubble targets could effectively mask or quench an echo from a submarine. The German variety of device for generating bubble targets became quite generally known under the name Pillenwerfer. The effectiveness of this device was not great, since an experienced sonarman had no difficulty in distinguishing the echo from the submarine and ignoring that from the bubbles.

## Chapter 9

# MAXIMUM ECHO RANGES WHEN BACKGROUND NOISE IS LIMITING

## 9.1 RECEIVER SENSITIVITY AND BACKGROUND NOISE

### 9.11 Reception in General

WHEN THE SIGNAL has been emitted, the transducer connections are changed so that it can act as a receiver of sound waves, or hydrophone. The oscillations of the hydrophone plate reproduce the sound incident on it, but the frequency of this sound is too great to be perceptible to the human ear. This makes some kind of portrayal device necessary. The mechanical pressure of the sound waves is converted into alternating currents by the magnetostrictive or piezoelectric effect, as described in Chapter 7; these currents are fed into an amplifier, and the amplified currents are utilized to render the incident sounds perceptible in various ways. The customary methods of portrayal are:

1. The amplified currents may be heterodyned to sonic frequencies, converted to airborne sound waves and made audible, by means of a loudspeaker or headphones.

2. The amplified voltage may be rectified and applied to a cathode-ray oscilloscope. The spot of this indicator is usually made to move along a vertical $y$ axis to indicate range. The rectified voltage may be applied so as to cause the spot to deviate from straight line motion (deflection in the direction of the $x$ axis). The echo is then recognized by a greater $x$-axis deflection than that produced by reverberation.

3. In a second method of portrayal involving the use of a cathode-ray oscilloscope, the spot always moves in a straight line to indicate range. Its brightness is controlled by the rectified voltage from the receiver, so that the echo appears as a bright spot on the relatively dim, or invisible, line traced by the spot in the absence of an echo. This is called $z$-axis portrayal. It is possible to combine $z$- and $x$-axis portrayal.

4. By using a chemical effect of the current, the sounds can be recorded on specially treated paper, the blackness of the trace being determined again by the magnitude of the current. This is thus similar to a $z$-axis portrayal. An advantage of this method, not possessed by the other two, is that it provides a comparatively permanent record of the incident sounds. The current is fed to the paper by a moving stylus, so that the range of an echo is also recorded.

Although the three methods of portrayal are quite different, the general principles that govern them are similar. The echo is only one of many sounds picked up by the sonar. Each sound, whether wanted or unwanted, actuates the portrayal device. The echo must be heard in spite of the unwanted sounds that are being heard at the same time, or must be seen among the records of these other sounds.

An ideal sonar would respond only to the echo and not to any other sound. This ideal is unattainable, but some steps can be taken to approach it. For example, in listening to the radio we wish to hear the broadcast of only one station at a time, so we tune our set, with the result that it will respond only to the electric waves of the relatively narrow range of frequencies emitted by the particular station, and not to those of any other. In the same way, since the echo has a definite frequency, it will obviously be desirable to tune the receiver to this frequency, thus excluding much of the unwanted sound. This is more important with visual than with aural methods of portrayal, for the ear has the ability to ignore unwanted sounds and to hear a note of definite pitch even in the presence of noise (see below and also Chapter 14).

The tuning of the sonar receiver can be accomplished at various stages. The first is the so-called *radio-frequency* (r-f) stage: the receiver can be tuned to the frequency of the incoming echo. In the second stage, the receiver is tuned to the *intermediate frequency* (i-f), which is the first heterodyne stage. Finally it is possible also to tune the receiver in the *audio-frequency* (a-f) stage, when the once-heterodyned signal is heterodyned a second time to an audible frequency. The tuning is under the control of the operator, and can be accomplished at any one stage, or in several of them at once.

Another line of approach is found in the fact that the echo is sound coming from a particular direction,

while background noises may come from all possible directions. The unwanted noise can be reduced by using directional hydrophones, as discussed in Section 7.4.3. The obvious disadvantage of such a receiver is that it cannot then be alert in all directions simultaneously (although means have been found for circumventing this difficulty, as described in Chapter 11); but this drawback is offset by the consideration that, if an echo is received on a directional sonar, the bearing of its source is at once known.

## 9.1.2 Response Curves of Hydrophones and Amplifiers

### The Response of Hydrophones

The electromotive force generated by the hydrophone is a function of the sound pressure on its diaphragm. This response of the hydrophone partially determines the response of any system into which it may be connected. Hydrophone *sensitivity* at the frequency $f$ is defined as the electromotive force developed in the hydrophone when it is in a sound field of frequency $f$ and rms pressure of 1 dyne/cm². If $e$ is the emf generated by the hydrophone when in a sound field of $p$ dynes/cm², the ratio

$$k = \frac{e}{p}, \tag{1}$$

defines the sensitivity of the hydrophone. It is measured in volts/dyne/cm². The quantity

$$K = 10 \log k^2 = 10 \log \frac{e^2}{p^2} = 20 \log k, \tag{2}$$

is called the *response* of the hydrophone. The response is the decibel ratio of the power generated by the hydrophone per ohm resistance of the external circuit to the intensity of the sound field at the hydrophone. For if

$P$ = the power per ohm resistance,
$I$ = the intensity of the sound,

then, since $P = e^2$, and according to equation (4) of Chapter 1, $I = p^2$,

$$K = 10 \log \frac{e^2}{p^2} = 10 \log \frac{P}{I}. \tag{3}$$

### Response Curves

The graph showing the response at each frequency is called the *response curve* of the system. The response curves of two QC magnetostriction transducers are shown in Figure 1. They respond well only to sounds in the neighborhood of the resonance frequency $f_0$. In the case of the *QCJ*, Figure 1A, $f_0$ is

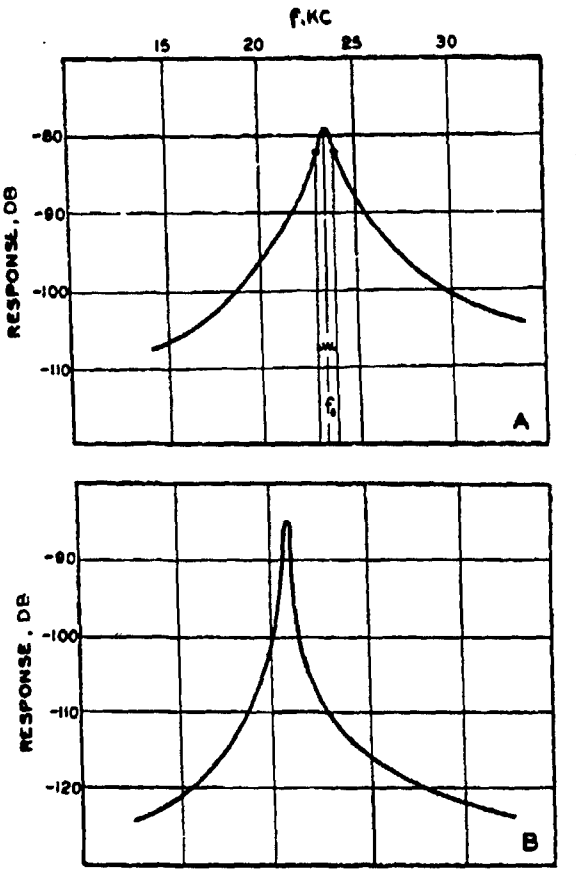


Figure 1. (A) Response curve of QCJ transducer; (B) response curve of QCL transducer.

24 kc; the transducer is said to *resonate* at 24 kc. The width $w$ of the resonance peak, shown in the figure, is usually defined as the frequency separation of the two points on the curve which are 6 db below the maximum. In the given curve, $w$ is seen to be about 1 kc.

Another commonly specified quantity is the resonance parameter $Q = f_0/w$. If $Q$ is greater than 10 or 20, the system is said to be highly resonant; if $Q$ is less than 4 or 5, the system is nonresonant. The *QCJ* transducer has a $Q$ of about 24. The *QCL* shown in Figure 1B is seen to be more sharply resonant than the *QCJ*; its $w$ is about 200 or 300 c, and, since it

resonates at 21 kc, its $Q$ is 60 or 100. Because of the resonant character of these transducers, they themselves are tuned, i.e., the echo frequency must be near the resonant frequency, otherwise they will not respond effectively.

### Response of Amplifiers

The amplification ratio of an amplifier is similar to the hydrophone sensitivity. It is the ratio of the output- to the input-voltage. The response is defined in terms of amplification ratio in exactly the same manner that the response of a hydrophone is defined in terms of its sensitivity. Response curves can be plotted for amplifiers as well as hydrophones, and the same terminology is applied to them.

## 9.1 3 Spectrum Level and Response Time

### Power Spectrum Level of Noise

The response curve shows the emf generated by a hydrophone in responding to a sound of a definite frequency. Most of the unwanted sounds encountered in echo ranging do not have a definite frequency, and it is necessary to consider the emf generated by the hydrophone in response to such a sound.

Consider an ideal hydrophone whose response curve is rectangular, as illustrated in Figure 2. Sup-

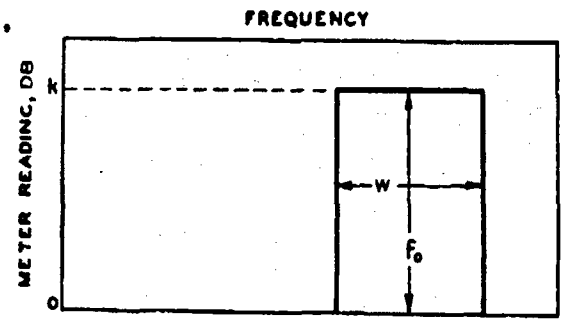


Figure 2. Schematic response curve of ideal hydrophone.

pose that it is possible in some way to vary both $f_0$ and $w$, while the hydrophone is exposed to a constant noise. The emf generated will then depend on both $f_0$ and $w$. If $w$ is made successively smaller and smaller, it will be found that the power $P$ of the generated emf finally becomes proportional to $w$:

$$P = k^2 I(f_0) w. \qquad (4)$$

The two other factors in this equation are $k$, the sensitivity of the hydrophone to a sound of the frequency $f_0$, as defined by equation (1), and a function $I(f_0)$ which is found to be characteristic of a particular noise. This function has not been given a simple name, but is sometimes called the intensity of the noise in a 1-c band. The function

$$N(f_0) = 10 \log I(f_0) \qquad (5)$$

is called the *spectrum* of the noise, or its *spectrum level* at $f_0$. In order to distinguish the spectrum of a continuous noise from that of a pulse, it is often necessary to call the former a *power spectrum* and the latter an *energy spectrum*. Equation (4) then becomes

$$10 \log P = K + N + 10 \log w. \qquad (6)$$

In Part III, it will be necessary to consider the generalization of equation (4) for hydrophones whose response curves are not rectangular and narrow. For all wide-band noises encountered in echo ranging, however, it will be sufficiently accurate to use equation (4) even for resonant hydrophones like the $QC$, whose response curves are far from ideal. The definitions of $K$ and $w$ given in Section 9.1.2 are to be used. Equation (4) indicates that the power generated by a wide-band noise is proportional to the width of the resonance peak of the transducer.

### Energy Spectrum Level of a Pulse

Although the intensity of an uninterrupted, constant sound is most conveniently measured in terms of power (energy/sec), the intensity of a pulse is better measured in terms of energy, i.e., power times duration. The energy spectrum of a pulse can be defined in much the same manner as the power spectrum of an uninterrupted sound was defined above.

If the pulse consists of a train of sinusoidal waves, it will have a more or less definite pitch, say $f$ c, provided the train contains many complete waves. The definite pitch of such a pulse indicates that its energy spectrum will have a sharp maximum at the frequency $f$. If the number of waves in the train is diminished, the height of this peak decreases, and its width $w$ increases. The complete mathematical discussion of this effect can be given an elaborate form, but the essential result is simple.

Let the duration of the wave train be $\tau$ sec. Each wave requires $1/f$ sec to pass a given point; therefore,

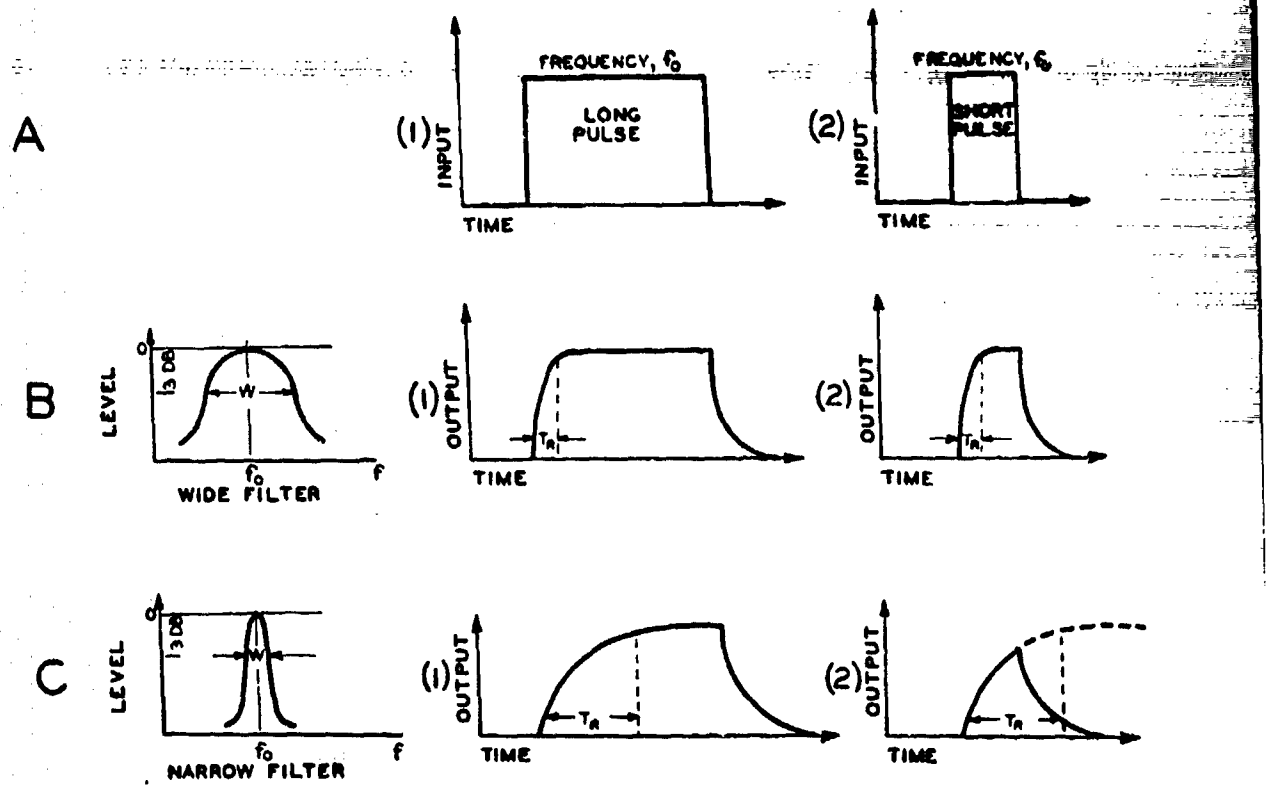


FIGURE 3. Response time of a filter in relation to its bandwidth. (A) Curves (1) and (2) represent diagrammatically the input of a long and short pulse respectively; (B) Graph at left is a schematic response curve of a wide filter. Curves (1) and (2) show diagrammatically the output of such a filter for the long and short pulse shown in A. The time response for the filter is indicated as $t_r$; (C) similar to B for a narrow filter.

if the wave train contains many complete waves, $\tau \gg 1/f$. The duration of the pulse $\tau$ and the width of the resonance peak of the pulse $w$ are connected by the approximate equation

$$w\tau = 1. \tag{7}$$

The greater width of the resonance peak associated with a shorter pulse duration makes it appear that a short pulse can be analyzed into a much wider group of frequencies than a long one. The human ear behaves in a manner consistent with this mathematical fact. If a listener hears pulses consisting of trains of sinusoidal waves, his sensations will depend on the number of waves in the train. If the pulse contains many complete waves, the sensation will be that of a short tone of well-defined pitch. As the number of complete waves diminishes, and the pulse becomes shorter, the listener finds it more and more difficult to be sure of the pitch. Finally, very short pulses consisting only of two or three waves lose all tonal characteristics and are best described as "clicks" or "pops."

## RESPONSE OF BAND FILTERS TO SHORT PINGS

Since the width of the spectrum peak of a pulse is inversely proportional to the pulse duration, it might be expected that in designing filters intended to pass only a restricted group of frequencies centered at $f$c, the duration of the pulse would have to be taken into account. For since a very short pulse has a wider peak, it seems obvious that if a filter is to pass it with a minimum diminution of intensity, the width of the filter will have to be greater than is necessary for a longer pulse with its proportionately narrower peak.

This can be stated in another way. There is a relation between the width of the filter and the speed with which it will respond to sudden changes of input. This is illustrated in Figure 3. The two upper graphs, A(1) and A(2), represent the input of a long and a short pulse, respectively. The graph at the left in row B shows the frequency response curve of a wide filter; the one at the left in row C, that of a narrow filter. The remaining curves, B(1) and B(2), C(1) and C(2), represent the outputs of the filters

when excited by the corresponding pulse shown in A.

The input, in each case, begins and ends abruptly, as shown in A(1) and A(2). The output, however, in each case begins and ends gradually. It requires a certain time interval $t_R$ to come anywhere near its maximum value.* This time interval is indicated in each of the diagrams, and it is seen that it is much shorter in the case of the wide filter B than of the narrow one C. The relation between the response time $t_R$ sec and the width $w$ c of the filter is given by the inequality

$$t_R \gtrsim \frac{1}{w}. \qquad (8)$$

In a well-designed filter, the equality may be assumed to hold; but a poorly designed filter may have a response time considerably greater than $1/w$.

The diagrams show that if the pulse is long enough, as illustrated by the curves marked (1), the response time is short enough so that the pulse can come near its maximum value even in the case of the narrow filter C(1). If the pulse is short, however, as illustrated by the curves marked (2), it is seen that while the response time of the wide filter is short enough to permit the pulse to come up to maximum value B(2), this is not true for the narrow filter C(2): before the response time has elapsed, the input ceases. Thus the output never attains its steady-state value, but is less than this.

It follows that if a receiver is to respond fully to pings of a length $r_0$ yd, whose duration is thus $2r_0/c = r_0/800$ sec, the pass band of the receiver must be at least so wide that $w = 800/r_0$ cycles per second.

## 11.4 Limitations on the Use of Sharply Tuned Receivers

There are a number of factors that prevent full exploitation of tuning as a method of eliminating the unwanted sounds besides the limitation on filter width set by the ping length. Several of these factors will be discussed briefly.

### Doppler Effect

Even if the frequency of the emitted signal remains constant, the frequency of the echo will not always be the same, but will depend on the rate at which the range of the target is changing. (See the discussion of the doppler effect in Section 10.2.) The tuning cannot be made indefinitely sharp, therefore, without endangering the reception of echoes from targets whose range rate is high.

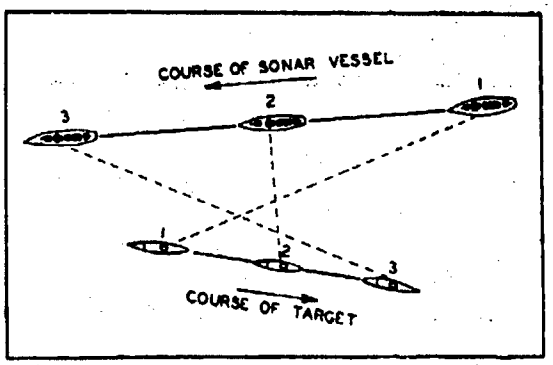


Figure 4. Diagram showing how the range rate depends on the relative bearing of the target.

The change in frequency due to the doppler effect can be very considerable. In Chapter 10 it is shown that if the emitted frequency in kilocycles is $f$ and the range rate of the target in knots is $v$, the frequency of the echo is changed by $\Delta f$ c, where

$$\Delta f = 0.7vf \text{ c}. \qquad (9)$$

The change $\Delta f$ is an increase if the range is closing and a decrease if it is opening. If the sonar vessel has a speed of 20 knots and the possible targets have speeds up to 4 knots, the possible echoes may have any frequency within a range of nearly 900 c. The pass band of the receiver must therefore be at least as wide as that.

It is appropriate to note here that the range rate depends not only on the speeds of sonar vessel and target, but also on the relative bearing of the target. This is illustrated in Figure 4, which shows three successive positions of two vessels passing on constant courses at constant speeds. At time 1, the target is off the bow of the sonar vessel, and the range is closing rapidly. At time 2, the target is abeam, and the range rate is zero. At time 3, the target is on the quarter, and the range is opening rapidly. The change from closing to opening range occurs continuously as the bearing changes.

### Reverberation

Reverberation occupies a peculiar position, as it is in some ways an unwanted sound and in others a

*Theoretically, it requires an infinite time to reach its maximum value, hence the rather vague wording of this sentence.

wanted sound. It can mask the echo and is therefore an unwanted sound. From this point of view, it is unfortunate that its frequency is very close to that of the echo, so that extremely sharp tuning is needed if the receiver is to respond to the echo and not to the reverberation.

Reverberation consists essentially of a large number of echoes, hence its frequency will also be affected by doppler. Since the scatterers responsible for the echoes are presumably at rest in the water, the range rate, and therefore the magnitude of the doppler effect, will be determined solely by the speed of the sonar vessel and the relative bearing of the sound beam. For this reason the doppler effect of reverberation is called *own doppler*. If an echo is received from a moving target, there will be a difference between its frequency and that of the reverberation; this difference is called *target doppler*. The magnitude of the target doppler is a measure of the speed and approximate bearing of the target, hence an important item. As it enables the determination of target doppler, reverberation is a wanted sound.

It will be shown in Chapter 10 that, when the difference in frequency between echo and reverberation is large and the echo is detected by ear, the masking power of the latter is reduced. It then functions primarily as a wanted sound. On the other hand, when the speed of the target through the water is small or at right angles to the transducer heading, the unwanted masking effect of reverberation is dominant. This unwanted effect is always the dominant one with visual methods of portrayal, since the range recorder cannot distinguish between sounds of various frequencies.

### Own-Doppler Nullifier

It was seen above that the major limitation on the use of narrow band receivers is the necessity of allowing echoes of many different frequencies to pass through the receiver. The limitation would not be so severe if the sonar vessel were at rest, or if its motion did not affect the frequency of the echo: for the speed of the most common targets is relatively small, and it would be possible to reduce the width of the receiver band if this were the only cause of doppler shifts.

It would be possible to operate with a narrow band receiver if the operator could constantly change the frequency of the transmitted signal by an amount just sufficient to compensate for the own doppler. The reverberation frequency would then remain constant, and the only frequency shift to be accommodated would be that of target doppler. Because of the necessity of sweeping the sound beam over a wide range of bearings, the own doppler changes rapidly, and it is not feasible for the operator to make this adjustment and still perform his other duties.

A device has therefore been developed that automatically accomplishes this result to a high degree of approximation. This is known as the *own-doppler nullifier*.[4] If this device is set for some one frequency $f$, the heterodyne frequency is automatically adjusted to this value during the first fraction of a second after transmission; thereafter the adjustment remains constant. In this way, the frequency of the reverberation is kept quite constant, and considerably narrower filters can be used in the receiver. This device may be less useful if submarines capable of high underwater speeds become more common.

## 9.15 Discrimination of the Hydrophone against Noise

Thus far it has been tacitly assumed that the hydrophone is nondirectional, or else that the noise source is located on the acoustic axis of the hydrophone. In general, the sources of background noise are located at random, and it may be assumed that the noise is isotropic. This means that the sound energy incident on the hydrophone from any one direction is the same as that from any other direction.

If the hydrophone is directional, it will then be relatively insensitive to sounds from most directions, and the emf generated will be only a fraction of that given by equation (4). This fraction, when converted into db, is the directivity index $D$ of the hydrophone (see Section 7.4). It is a negative number, since the fraction is less than unity. Equation (6) becomes

$$10 \log e = K + N + D + 10 \log w \qquad (10)$$

for a directional hydrophone and nondirectional noise.

## 9.16 The Inherent Threshold of a Hydrophone

Any system capable of acting as a hydrophone, i.e., of generating an emf when a mechanical pressure is applied to it, will spontaneously generate an elec-

tromotive force [emf] even when no sound is incident on it. This is a consequence of the kinetic theory of heat. According to this theory, all the molecules of matter are constantly in motion. The energy of this motion is measured by the temperature. The higher the temperature, the greater the spontaneous internal motion.

The effect of the spontaneous motion is in many ways similar to that of the forced motion caused by a sound pressure. In particular, it causes an emf. When the hydrophone is connected through an amplifier to a loudspeaker, this emf is heard as a hiss or crackle. It is in all respects similar to the sound of a wide-band noise received with the same hydrophone.

Heat motion is not the only cause of spontaneous emf: joints on which soldering acid has been used are another source; loose connections of all kinds contribute.

Let $e_0$ be the magnitude of the spontaneously generated emf of a hydrophone, whatever its cause. Since the sound produced by it when connected to a loudspeaker is similar to that of a wide-band noise, it is natural to calculate the spectrum level of the isotropic noise equivalent to the spontaneous emf. Referring to equations (6) and (10), this is

$$N_0 = 10 \log \frac{e_0}{w} - K - D. \qquad (11)$$

The quantity $N_0$ is called the *inherent threshold of the hydrophone*. A noise whose spectrum level is much less than $N_0$ will not be audible above the spontaneously generated noise. The inherent threshold of the hydrophone thus sets a lower limit to the level of the sounds that can be detected by it.

### 9.1.7 Two General Specifications for the Echo-Ranging Receiver

Everything that has been said concerning hydrophones can be extended almost verbatim to the complex system composed of a hydrophone connected to a heterodyne amplifier. The emf generated in the output stages of the amplifier when a sound is incident on the hydrophone can be plotted as a response curve for the system as a whole. Adjustment of the amplifier gain will shift the response curve parallel to itself; adjustment of the tuning in any stage of the receiver will alter the value of the resonance frequency or the width of the resonance curve, or possibly both.

The following discussion will be couched in terms of the loudspeaker presentation but can be applied with slight modification to any of the other methods of portrayal. If the transducer is trained on the bearing of a target and $E$ is the sound level of the echo in the water, the sound emitted by the loudspeaker will have the level $E_{air}$ where

$$E_{air} = E + A \qquad (12)$$

and $A$ is the gain of the receiver system. If there is an isotropic noise of spectrum level $N$ incident on the transducer, the spectrum level of the sound emitted by the loudspeaker will be $N_{air}$, where

$$N_{air} = N + D + A. \qquad (13)$$

The entire receiver will also have an inherent threshold, the spontaneous emf being generated partly in the hydrophone, partly in the other portions of the circuits. Some additional increase of the inherent threshold may result if these circuits are not adequately shielded from other electrical equipment aboard ship.

The inherent noise of the whole receiver can be specified in two ways. Perhaps the most natural is to specify the spectrum level of the noise which issues from the loudspeaker when no underwater sound is incident on the transducer; this will be called $N_{0,air}$. If this has been measured, one can calculate the underwater noise that is equivalent to it, $N_0$, by inverting equation (13)

$$N_0 = N_{0,air} - D - A. \qquad (14)$$

The operator will have to hear the echo in spite of the fact that he also hears the noise $N_{air}$ that has been picked up by the receiver from the water, and the noise $N_{0,air}$ that has been generated by the receiver. In addition to this, he will also be disturbed by other extraneous sound resulting from activities aboard ship—suppose that their spectrum level is $N_{ship}$.

In order to obtain some idea of the proper design for the sonar receiver, three cases will be considered in turn. Suppose first that the shipboard sounds are more disturbing than the other two noises: $N_{ship} > N_{0,air}$ and $N_{ship} > N_{air}$. The operator may try to remedy this by increasing the gain $A$. According to equation (12), this will increase $E_{air}$ and thus increase the loudness of the echo.

If the shipboard sounds are not too loud, this will be an effective remedy, but there is a limit to the useful increase in gain. According to equation (13), the level of the noise picked up from the water will be increased by the same amount as the echo. The

inherent noise will probably also be increased. The optimum gain setting will be such that one or both of these last two noises, $N_{air}$ and $N_{0,air}$, are comfortably audible above the shipboard noises. When this is the case, the shipboard noises do not affect the audibility of the echo.

This results in a first general specification for the design and location of sonar receivers.

*Specification 1.* The gain of the receiver amplifier and loudspeaker system and their location aboard ship should be such that water noise or inherent noise, or both, can always be heard despite the sound of nearby activities.

Neither the inherent noise at a given gain setting nor the water noise are under the control of the sonar operator. However, the former can be reduced by proper design, installation, and maintenance of the electronic components of the receiver. The reduction of water noise is more difficult than the reduction of inherent noise. Good practice will therefore require that $N_{0,air} < N_{air}$ or, which is the same thing, that $N_0 < N$. This results in a second general specification.

*Specification 2.* The inherent noise of the receiver should be so low that it is possible to hear the water noise.

If these two specifications are complied with, the audibility of the echo will be determined solely by the reverberation level and the spectrum level of the water noise. The effect of reverberation will be discussed in the next section of this chapter. No discussion of the ways and means of complying with these two general specifications will be given in this book.

While it is essential to use enough gain so that water noise is comfortably audible, additional gain will have an adverse effect. Not only will the excessive level of the speaker output be a source of discomfort to the operator, but there is danger that a signal may raise the level to the point of overloading the amplifier, causing it to operate inefficiently and reduce the audibility of the signal.

## 9.2 BACKGROUND NOISE IN ECHO RANGING

### 9.2.1 General Classification

The background sounds have many causes, a partial list of them being given in Table 1. From the foregoing discussion it appears that it is convenient

TABLE 1. CLASSIFICATION OF AMPLIFIED SOUNDS IN ECHO RANGING.

I BACKGROUND NOISE. Extraneous sounds of various kinds.
- A. *Self noise* produced at or on own ship.
  1. Caused by motion of ship and/or gear relative to water, or by the slapping of waves against the ship when stationary.
  2. Caused by mechanical vibration incident to operations aboard own ship and picked up by hydrophone.
  3. Circuit noise, caused by thermal agitation of the electrons, by instability of electric circuits in the receiver, by operation of ship's power system, etc.
- B. *Ambient noise* produced at a distance from own ship.
  1. (a) Sea noise, principal cause unknown—heard even in deep water.
     (b) Rain, surf, whitecaps are occasional causes.
  2. Biological noise: certain fish, shrimp, etc., produce sounds that are audible in sonic and supersonic gear.
  3. Traffic noise, caused by ship traffic and, in or near harbors, by industrial operations.
- C. *Target noise* produced at the target. This is the wanted sound in listening but an unwanted background in echo ranging, and may prevent accurate determination of the range of the target.

II REVERBERATION. A sound which is an intrinsic accompaniment to all echo-ranging operations, caused by scattering of the emitted sound by
1. Irregularities of sea bottom.
2. Irregularities of sea surface.
3. Unknown scattering mechanisms widely distributed throughout the volume of the sea.

to distinguish between airborne noise that does not issue from the loudspeaker, and the noise from the loudspeaker, which may be called "amplified" noise.

The amplified noise is of two general kinds. One kind is extraneous to the operation of the echo-ranging gear, and is heard even when no pings are emitted. This is the background noise. A sound that is inherent in echo ranging is reverberation, which has very nearly the same frequency as the ping or echo. In discussing the limitation of range in echo ranging, it is convenient to differentiate between the case where the range is limited by background noise and the case where reverberation is the limiting factor. The latter case is treated in Chapter 12, the former in the present chapter.

The general classification of noise is given in Table 1. A detailed description of the background noise will be found in Chapter 13. Table 2 supplements

TABLE 2. Typical spectrum levels of amplified noise at 24 kc.

| | Decibels |
|---|---|
| Self-noise | |
| Circuit noise | −104 to −94 |
| Submarine self-noise | −72 to −46 |
| Surface vessel self-noise | |
| DD or DE, 10 to 20 kc | −65 to −35 |
| Ambient noise | |
| Sea noise | −74 to −54 |
| Biological noise | |
| Snapping shrimp | −39 |
| Croakers | −20 |
| Traffic noise (includes sea noise) | −55 to −50 |
| Target noise (source level) | |
| Submarine, 6 kt periscope depth, 12 kt surf. | 8 |
| Battleship | 27 |
| Cruiser | 20 |
| Destroyer | 15 |
| Passenger | 13 |
| Corvette | 8 |
| Freighter | 3 |

the brief outline of Table 1 by giving some levels of the noise. These are the power spectrum levels defined in Section 9.1.3.

## 9.2.2 Ambient Noise

A comprehensive discussion of ambient noise will be found in Section 13.4. In echo ranging, ambient noise is important if the echo-ranging vessel is comparatively quiet; in this event echoes may, under favorable circumstances, be received from long ranges, limited only by the masking effect of the inherent noise of the sea.

While the mechanism of sea noise is not known in detail, it is known that it increases with wind force and sea state, and that its spectrum level decreases about 5 db each time the frequency is doubled. (See Figure 7 of Chapter 13.)

Biological noise is not very important in echo ranging. Most of it is intermittent, or localized in small areas. The only incessant source of this type of noise is the snapping shrimp; but these animals live only in shallow water (less than 30 fathoms). In such areas the echo will nearly always be masked by reverberation from the bottom; for it is precisely the rocky, uneven type of bottom affected by snapping shrimp that is the source of the strongest bottom reverberation. However, shrimp noise may be annoying, especially in harbor echo-ranging installations in latitudes less than 40°.

An important contribution to ambient noise is made by other ships moving in the neighborhood of the echo-ranging vessel, for example, in convoys. In and near harbors the noise of industrial and commercial operations (dredging, riveting on the hulls of ships in docks, etc.) is added to that of passing ships. This background noise is often dominant in harbor installations.

The noise produced by the target vessel itself can perhaps be considered as traffic noise. In listening, these sounds are the wanted ones; and even while engaged in echo ranging, the operator will, between pings, listen for what the British call "hydrophone effect," and attempt to gain some information about the target from its sounds. But the target noise may prevent an accurate determination of range and must therefore be considered as part of the masking background.

## 9.2.3 Self-Noise

In echo ranging from fast-moving vessels it is the noise produced at the vessel itself that is likely to limit the range. The chief causes of self-noise are cavitation at the screws or near the transducer and the impact of air bubbles, caused by the passage of the hull through the water, against the transducer. The lower limit of self-noise is the inherent noise of the receiving system which is usually included in this category, although its cause is quite different.

The level of self-noise increases with the speed of the echo-ranging vessel, as much as 3 db per knot increase in speed above 15 knots in the case of destroyers. Below 15 knots self-noise is not likely to be

the limiting background, provided adequate maintenance has kept the inherent noise of the system from becoming too great.

Self-noise decreases rapidly with frequency; at 24 kc it drops, on the average, about 8 db per octave increase in frequency. This is an argument in favor of the use of the highest practicable frequency in echo ranging.

Self-noise is not likely to be important in echo ranging from submarines. When the submarine echo-ranges, it depends generally on a single ping for the echo; since the self-noise of submarines proceeding at high speed is appreciable, it will be reduced if the motors are shut down when echo ranging. It has been observed that this may reduce the self-noise by as much as 20 db.[1]

That part of the self-noise caused by the motion of the sonar projectors through the water can be reduced by enclosing them in streamlined structures. A first step in this direction was the construction of projectors having a spherical shape, even though their diaphragms were plane. This was probably dictated as much by a desire to reduce the force required to move the projector through the water, as by consideration of the self-noise.

However, this construction did not eliminate that part of the noise caused by the motion of bubbly water past the projector, and it became the practice to enclose the spherical projector in a larger streamlined dome. In one case, it was found that the presence of the dome decreased the noise level by 23 db when the ship was moving at 25 knots.[1] The problems connected with the design and use of such domes were discussed briefly in Chapter 7.

## 9.3 THE RECOGNITION OF THE ECHO

### 9.3.1 Definition of Recognition and Maximum Range

A signal of any kind will be clearly identified as such against a background of noise if it produces a sufficiently great change in the sound. The change may be in loudness, or pitch, or quality, or any combination of these three characteristics. As this change becomes smaller, a point will be reached at which repeated signals may be heard sometimes and not heard other times. By convention, *recognition* occurs when 50 per cent of the signals are correctly identified.

When applying this definition to echoes, it can be stated in another way. When the target is at very long range an occasional echo may be received that can definitely be identified as such. As the range is closed, more and more of the transmitted pings will return identifiable echoes; when half of them do so, we say that recognition occurs. The range at which this occurs is called the *maximum range*, a term that has no other significance than this. It does not mean, on the one hand, that echoes will not be received from ranges longer than the maximum; nor, on the other hand, that at shorter ranges every ping will necessarily return a detectable echo.

The 50 per cent criterion is arbitrary. The range recorder may exhibit a pattern which definitely indicates that echoes are being received even if the fraction of perceptible ones is considerably less than 50 per cent; conversely, it is possible to be well within the maximum range and still fail to get a detectable echo if only a few pings are sent out.

This definition of recognition is therefore inadequate if the echo-ranging vessel is restricted to 1 or 2 pings, as is the practice on submarines. In this case it is necessary to have practical certainty of recognition, that is, 80 or 90 per cent probability of recognition instead of 50 per cent. When any probability other than 50 per cent is required, the per cent recognition is specified.

### 9.3.2 The Recognition Differential

The intensity required for a given signal (a pure tone, say, or a certain frequency) to be recognized depends on the intensity and character of the background noise. The ratio, in db, of the power of the signal at recognition to the power of the noise in the pass band of the receiver is called the "recognition differential" for the particular set of conditions existing during the measurement of the signal-to noise ratio. If the recognition differential is denoted by $M$, then

$$M = E - L \text{ db}, \tag{15}$$

where $E$ = sound level of the echo at 50 per cent recognition,

$$L = N + 10 \log w = \text{sound level of the background noise}, \tag{16}$$

$N$ = spectrum level of the noise,

$w$ = bandwidth of the receiver, c.

The factors that determine the recognition differential can be classified into three general categories.

1. Physical properties of the signal, its frequency and duration, as well as the physical character of the background noise.

2. The characteristics of the gear and of the portrayal apparatus. The chief of these is the width of the frequency band to which the receiver will respond; this also affects the physical characteristics of the signal and noise. Its effect is only partially included in the equation $L = N + 10 \log w$.

3. Psychoacoustic factors, such as the subjective acuity of the observer, his skill and training, etc. These are related to the bandwidth and to the method of portrayal.

We shall discuss the recognition differential at present with the main emphasis on the effect of bandwidth and ping length, leaving the more detailed discussion of the psychoacoustic factors to Chapter 14. A few remarks concerning the method of portrayal are pertinent here.

### 9.3.3 Method of Portrayal

Listening to the echo enables the operator to exploit the difference in quality between the echo and the background. Provided the signal is not of excessively short duration, the echo will be a musical tone of definite pitch contrasting markedly with the more or less steady hissing or crackling background. If the background is reverberation, the echo from a moving target will differ from the background in pitch, because of the doppler effect. These advantages are lost in visual portrayal methods; in these the distinguishing characteristic of the echo is primarily its greater intensity (see Figure 19 of Chapter 8).

The range recorder has one advantage, resulting from the permanence of its record, which enables the operator to compare any number of echoes with each other. This "memory" is very valuable in the identification of echoes that are so weak that they can be heard, or seen on the record, only a small fraction of the time.

### 9.3.4 Recognition

The problem of recognition has many aspects. By way of introduction, an oversimplified case will be discussed, to serve as a basis for the later account of the complications. It will first be assumed that the recognition differential is independent of both the bandwidth of the receiver and of the spectrum level of the noise. The three graphs of Figure 5 illustrate this oversimplified case of a constant recognition differential. An increase of either the spectrum level $N$ or bandwidth $w$ causes a corresponding increase in the noise level $L$, according to equation (16),

$$L = N + 10 \log w.$$

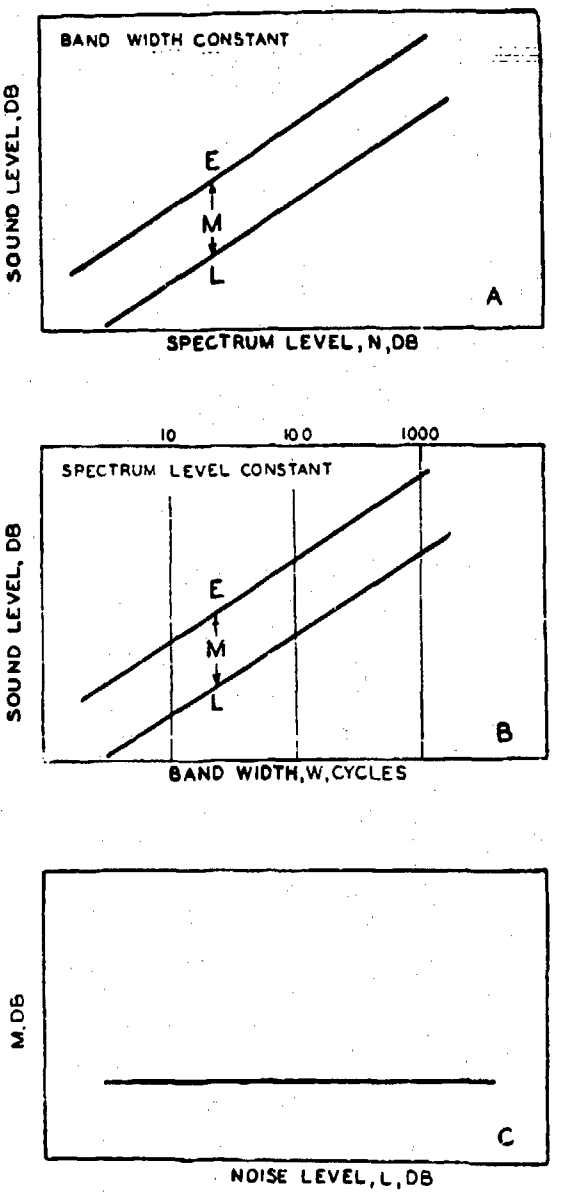


FIGURE 5. Diagram illustrating the case of a constant recognition differential. (A) Graph of $L = N + 10 \log w$, ($w$ = const.), and $E = L + M$; (B) graph of $L = N + 10 \log w$, ($N$ = const.) and $E = L + M$; (C) graph of $M = E - L$ ($M$ = const.).

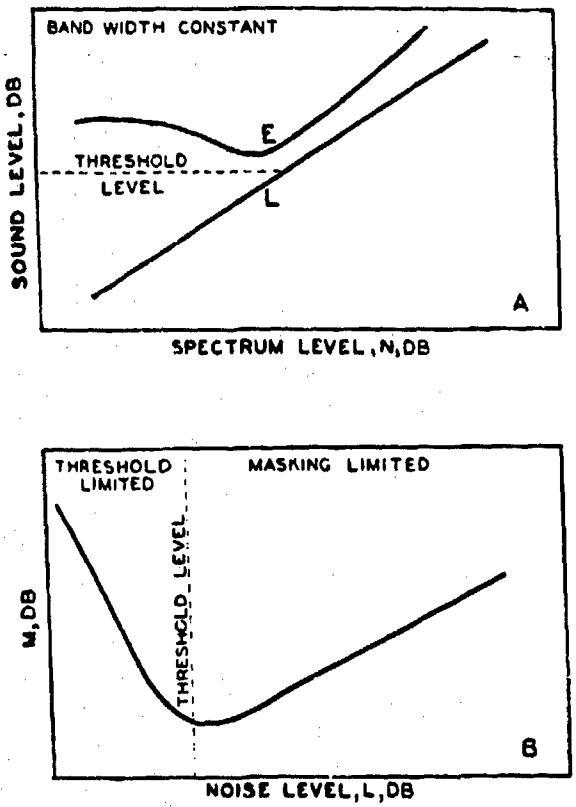


FIGURE 6. Diagram illustrating recognition with visual methods of portrayal. (A) Graphs of $N = L + 10 \log w$ ($w$ = const.) and $E = L + M$; (B) value of recognition differential corresponding to the sound levels in A.

The actual echo level is, of course, independent of both $N$ and $w$, as is determined by quite other factors. However, the level $E$ which is necessary for 50 per cent recognition will be

$$E = L + M \text{ (for 50 per cent recognition).} \quad (16a)$$

For convenience, this will be called the *recognition level* of the echo. If the actual level is less than the recognition level, the echo will usually be lost. If it is greater, the echo will usually be detected.

This simple case of a constant recognition differential is not realized in practice by any of the methods of portrayal. A pair of graphs for the visual methods of portrayal are shown in Figure 6. The upper graph shows that, as the spectrum level increases, the noise level also increases. (Both the noise and echo levels are here to be interpreted in terms of the voltage applied to the range recorder or oscillograph.) However, the echo level necessary for recognition remains more or less constant until a certain critical value of the noise level is reached, whereupon it increases more rapidly than the noise level. The lower graph shows the values of the recognition differential that correspond to the sound levels of the upper graph.

The diagram is divided into two regions, marked *threshold limited* and *masking limited*. The noise level separating the two is called the *threshold level* of the recorder or oscilloscope. When the noise level is less than the threshold, no trace of the noise is visible on the recorder paper or oscillograph. When the noise level exceeds the threshold, the noise produces a record.

In the threshold-limited region, the recognition level of the echo remains more or less constant and is very nearly equal to the threshold level of the noise. That is, the condition for detection is that the echo voltage be great enough to make a mark on the paper, or to deflect the oscillograph appreciably. The slight drop as the noise level approaches the threshold level is caused by "sensitization." The echo voltage is actually assisted in making a record by the presence of the noise. This is a well-known effect in photography: films that have been exposed to a very weak light are more sensitive than those which have been kept completely dark until use. To pursue the analogy, if the films have been exposed to stronger light before use, they are fogged. The masking-limited region, where the noise obscures the echo, is analogous to photographs on fogged film.

Obviously, it will be good practice to operate at the region of minimum recognition level, if that is possible. Adjustment of the gain will accomplish this objective, provided the equipment is well designed.

Recognition of heterodyned echoes by ear obeys much the same laws as visual recognition. The concepts of threshold and masking limitation are applicable almost without change. It is not known whether the ear also exhibits the sensitization phenomenon. These matters will be discussed in Chapter 14. The principal difference between visual and aural detection lies in the effect of receiver bandwidth $w$. The *recognition differential* for visual detection is (presumably) independent of $w$, but when the ear is used under masking-limited conditions, the bandwidth is important in determining its value. However, since the overall level of the masking noise is also dependent on bandwidth, the situation in regard to *recognition level* is almost the exact reverse. This is strongly dependent on $w$ for visual detection, and almost independent of $w$ for aural detection.

It will be assumed, in what follows, that the echo is a tone of constant frequency and rather long

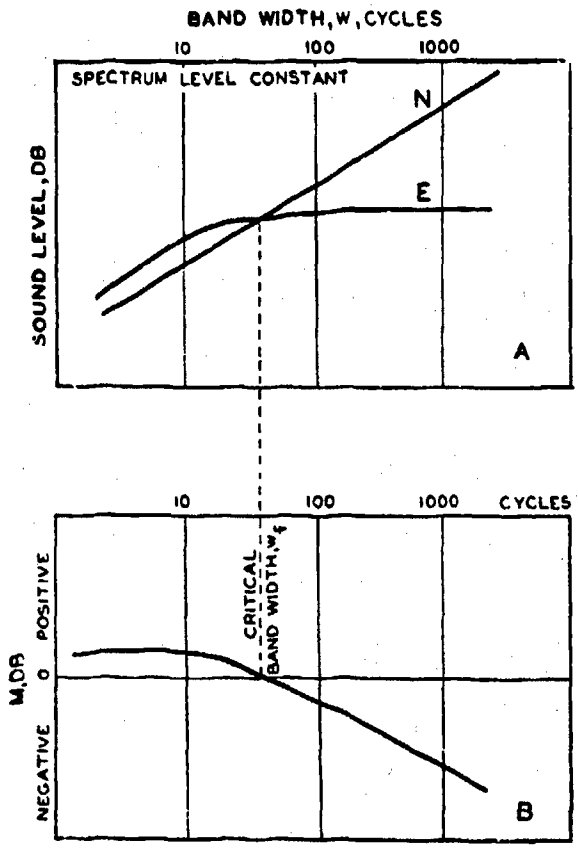


FIGURE 7. (A) Diagram illustrating recognition of an echo of constant frequency and rather long duration, when the noise level is great enough to cause masking limited conditions for all bandwidths; (B) changes in recognition differential corresponding to (A).

duration, and that the spectrum level is high enough to cause masking-limited conditions to prevail for all bandwidths. Then the facts are as illustrated in Figure 7. The upper graph shows that, for small bandwidths, the recognition level of the echo increases parallel with the increase of noise level. At a certain critical bandwidth, $w_f$, the two curves cross, and the necessary echo level becomes almost independent of bandwidth. The lower graph shows the corresponding changes in the recognition differential $M$. It has a small positive value for bandwidths less than $w_f$, becomes zero at $w_f$, and for larger widths, becomes negative. The large negative values are one of the major advantages of the audio presentation.

The sensations of the operator when listening to echoes parallel these graphs rather closely. When the bandwidth is less than $w_f$, echo and noise are heard as a single blended sound, and recognition is caused almost entirely by a noticeable increase in loudness when the echo comes in. When the bandwidth is greater than $w_f$, echo and noise are heard as two distinct, though simultaneous sounds, and the operator feels that he is able to ignore the noise and concentrate on the echo. To a very considerable extent, this feeling is not an illusion.

The theory of the critical bandwidth will be discussed in Chapter 14. For the present purpose, it is sufficient to remark that its numerical value depends on the frequency, and increases below 300 c and above 1,000 c. This is one reason for the choice of 800 c as the standard audio frequency in echo-ranging devices.

## 9.3.3 The Effect of Ping Length on Recognition

In the case of audio presentation, the duration of the echo becomes important because the ear needs a finite time—about 0.2 sec—to respond completely to a sound, and hence a signal of shorter duration than this will not sound so loud as an equally intense one of longer duration. Moreover, it is probable that recognition occurs when the peak values of a fluctuating echo intensity coincide with minimum values of the noise intensity, and this will be more likely to occur if the signal is long.

Some experimental data on the effect of ping length on recognition are exhibited in Figures 8 and 9. Figure 8 shows the variation of the recognition differential for pulses of 800-c sound when masked by noise. The pass band used in taking the measurements was 1,000 c wide. The recognition differential, however, is calculated in terms of the spectrum level of the noise. It is seen to decrease with the pulse duration up to about 0.2 or 0.3 sec. Further increase in the duration causes less change in the recognition differential. Figure 9 shows the results of experiments in which actual (recorded) echoes from a submarine were masked by wide-band thermal noise; echoes from other aspects might have given different results. A similar reduction in the recognition differential is seen, but the spread for the short ping length is more than 10 db. Two different pass bands centered at 800 c were used, and the values of $M$, as before, converted to the standard bandwidth of 1 c. The right-hand ordinate scale shows the values of $M$ when the noise level is measured in a 40-c band—the critical bandwidth at 800 c.

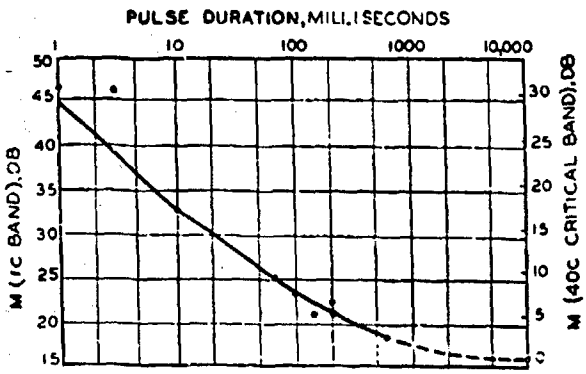


FIGURE 8. Effect of pulse on recognition of 800-c pulses masked by noise.

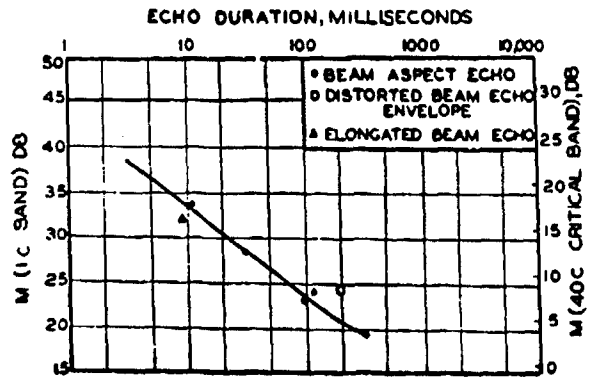


FIGURE 9. Effect of echo duration on recognition of echoes masked by noise.

### MULTIPLE PULSES

A difficulty encountered in the use of extremely short pings is that their echoes are easily overlooked because they so closely resemble the occasional "pops" of noise. It was thought that the use of two or more pings in close succession might eliminate the difficulty. An experimental study indicated that recognition was improved somewhat by the use of double pings.[2]

## 9.3.6 Values of the Recognition Differential

It is not feasible to measure the recognition differential experimentally while actually echo ranging at sea. The experimenter, therefore, endeavors to simulate, as closely as is possible in the laboratory, the condition encountered in practice. The ambient noise in the sea is replaced by artificially generated thermal noise; its bandwidth and level are at his control. With regard to the signal, two kinds are used. Actual echoes from submarines can be recorded, and then played back at various known, controlled levels, or pure tones of various frequencies, generated by oscillators, can be used. In the following, the term "signal" will be restricted to the latter kind. They differ from echoes in that they have a rectangular envelope, i.e., the level remains constant throughout the duration of the signal; echoes, on the contrary, have irregular envelopes, because their level fluctuates more or less widely throughout their duration. For this reason, if one listens to two echoes of the same average level against the same background noise, the recognition differential may be different. For this and other reasons, the recognition differential for echoes is usually stated within a range of several decibels (see Table 3). For convenience, the recognition differentials for 800-c signals and echoes are tabulated in Table 3.

TABLE 3. Recognition differential (RD) for 800-c signal and echo in noise background (1-kc band).

| Ping length (msec) | RD of signal (db) | RD of echo (db) |
|---|---|---|
| 1 | 16 | .... |
| 9 | .... | $5 \pm 5$ |
| 10 | 2 | .... |
| 36 | .... | $-6 \pm 1$ |
| 70 | −5 | .... |
| 80 | .... | $-3 \pm 1$ |
| 100 | −7 | .... |
| 140 | −9 | .... |
| 200 | −9 | .... |
| 300 | .... | $-10 \pm 1$ |
| 600 | −12 | .... |

Values of the recognition differential of echoes in a background of reverberation will be given in Chapter 10.

## 9.3.7 Recognition Probability

From the above discussion, it is clear that the recognition differential determines only the echo level necessary for a 50—50 probability of recognition. The importance of other recognition probabilities has already been stressed and will now be considered in greater detail.

Figure 10 presents data obtained in the laboratory by playing recorded echoes at a definite level $L'$ and allowing listeners to hear them when masked by noise. The 50—50 level is $L$, and the abscissa of the

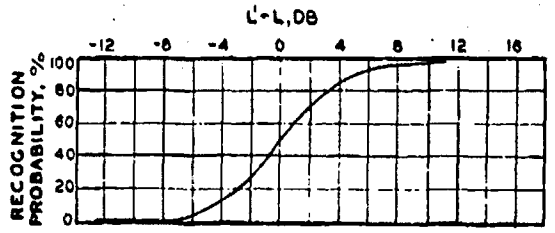


FIGURE 10. Recognition probability. The 50 per cent recognition level is $L$. Listeners heard recorded echoes at a level $L'$. The abscissa of the graph shows the amount by which $L'$ exceeded $L''$, the ordinate is the recognition probability.

graph shows the amount by which $L'$ exceeded $L$; the ordinate is the recognition probability. A recognition probability of 90 per cent means that 9 out of 10 echoes are identified as such, the tenth one being inaudible. It is seen that 90 per cent recognition requires a level 4 or 5 db higher than does 50 per cent recognition. Conversely, if the level is 4 or 5 db lower than the 50 per cent level, only 10 per cent of the echoes are heard.

This laboratory experiment does not reproduce conditions at sea in one very important respect. It has been remarked that the echoes are played back at a fixed and definite level. At sea, successive echoes have quite different levels. This is shown by Figure 11; if the average level of the echoes is $E$, this graph shows that only about 35 per cent of the echoes have

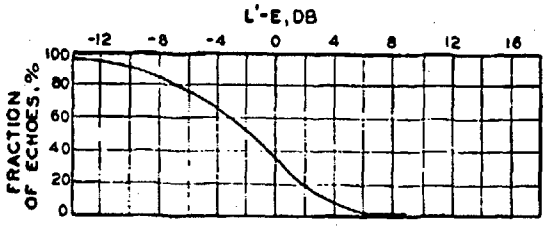


FIGURE 11. Graph showing the fraction of echoes that have levels $L'$ greater than the average level $E$.

levels $L'$ that are greater than $E$. About 10 per cent have levels $L'$ more than 4 db greater than $E$, and 10 per cent have levels more than 10 db less than $E$.

This raises the question: what is the recognition probability when $E$, the *average* echo level *at sea*, exceeds the 50 per cent *laboratory* value $L$ by a certain amount? The data of Figures 10 and 11 can be combined to give Figure 12, which answers this question. It shows that when $E = L$, the large number of echoes that are below average reduce the recognition probability from 50 to 35 per cent. The 50 per cent value is not reached until $E$ is about 2 db

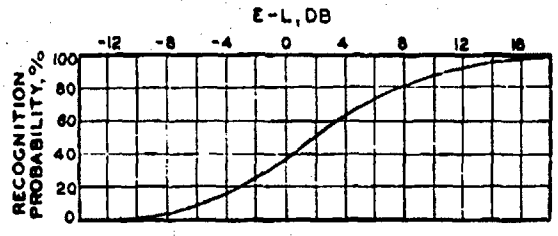


FIGURE 12. Graph showing recognition probability when $E$, the average echo level at sea, exceeds the 50 per cent laboratory value $L$ by the amounts shown by the abscissas.

greater than $L$, and the 90 per cent value requires $E$ to be nearly 12 db greater than $L$.

In view of the importance of the 90 per cent recognition probability for submarine operations, it would be desirable to be able to predict, in advance of transmission, whether the echo will be above or below average. The outlook for such a development is not favorable.

## 9.4 MAXIMUM ECHO RANGES WHEN BACKGROUND NOISE IS LIMITING

### 9.4.1 General Principles of Range Calculation

From the discussion of the preceding sections it appears that an echo will be recognized 50 per cent of the time if its level $E$ satisfies the relation

$$E = N + D + M + 10 \log w. \qquad (17)$$

where $N$ is the equivalent water-noise spectrum level, $D$ the directivity index of the transducer, and $M$ the recognition differential. The quantity $N + D + M + 10 \log w$ is the *recognition level* defined above.

From equation (9) of Chapter 8 the echo level $E$ is given by

$$E = S + T - 2H(r), \qquad (18)$$

where $S$ is the source level of the projector, $T$ the strength of the target, and $H(r)$ the transmission loss to the target, presumed to be equal for both outgoing and reflected sound. Comparison of equations (17) and (18) indicates that one may expect to detect more than 50 per cent of the echoes from the target if

$$2H(r) < S + T - (N + 10 \log w + D + M). \qquad (19)$$

The right-hand member of equation (19) can, for convenience, be defined as the *available signal output*. The actual level of the echo must be greater than

the recognition level; the total transmission loss must be less than the available signal output. As the range to the target increases, the value of $H(r)$ will increase. At some range $r_{max}$ it will become equal to the available signal output; for longer ranges, the echo will be heard less than half the time and will rapidly become inaudible all of the time.

The *maximum range* $r_{max}$ is defined as the greatest range at which the available signal output is at least equal to the two-way transmission loss. Equation (2) shows that the maximum range will depend on a large number of terms. Each of these has already been discussed in detail, but it will be useful to summarize the salient facts about each term that enters into equation (19).

The *source level* $S$ is characteristic of the sonar projector and its power supply. It is also conditioned by the dome in which the projector is mounted. A typical value for standard Navy installations is 110 db.

The *target strength* $T$ is characteristic of the submarine or target. An average value for a submarine is 15 db, but if the target is small or presents an unfavorable aspect, the value may be as low as 5 db. For an especially favorable aspect, a large submarine may have $T = 25$ db.

The *noise level* $N + 10 \log w$ depends both on the noise sources near and on the ship, and on the bandwidth of the receiver. A typical value of the latter is 1 kc ($10 \log w = +30$ db). The spectrum level $N$ varies from $-60$ db in a favorable case to $-30$ db for a destroyer at 20 knots. A typical value is $-45$ db.

The *directivity index* $D$ characterizes the directionality of the receiver. Its value is adversely affected by the use of sound domes unless the latter are very carefully designed and installed (Section 7.7). Neglecting this cause of variation, its values for standard Navy sonars range only over a few db, the average being $-23$ db.

The *recognition differential* $M$ depends on the method of portrayal, the bandwidth of the receiver, and the acuity and training of the operator. The average value for a bandwidth of 1,000 c may be taken to be 0 db, but values of $+10$ and $-10$ db are not uncommon. The value of $+10$ is perhaps very high for a trained operator, and should be considered to apply only to untrained personnel with little aptitude.

The *transmission loss* $H(r)$ depends on oceanographic conditions, the most important being the thermal conditions in the ocean, although wind, sea, and (in shallow water) the bottom character all influence its value.

The *gain of the receiver* is conspicuous by its absence from equation (19), although common sense might lead one to expect it to exert an influence on the maximum range. The reason for its absence is to be found in the two general specifications for sonar gear that were formulated in Section 9.1. If the operator makes full use of the gain provided under these specifications, a further increase in the gain will not affect the maximum range until the amplifier overloads. At that stage, the maximum range will be reduced by an increase in gain.

When operated at proper gain, the available signal output is almost independent of the receiver bandwidth for aural presentation. This is because $(N + 10 \log w) + M(w)$ is independent of $w$. For visual presentation, the term $M$ is independent of $w$, and the term $10 \log w$ is not canceled out (compare Figures 5 and 7).

## 9.4.2 Values of the Available Signal

The numerical values given above are summarized in Table 4. It should be noted that even the favorable and unfavorable cases do not represent extremes, and that the variation in the available signal may be even greater than is shown by the table. However, it is thought that the most common values of the available signal will be within $\pm 10$ db of the value 160 db.

TABLE 4. Available echo levels.

| | Unfavorable case | Average case | Favorable case |
|---|---|---|---|
| | (db) | (db) | (db) |
| $S$ | 110 | 110 | 110 |
| $T$ | 5 | 15 | 25 |
| $N + 10 \log w$ | 0 | $-15$ | $-30$ |
| $D$ | $-23$ | $-23$ | $-23$ |
| $M$ (1-kc band) | 10 | 0 | $-10$ |
| Available signal | 128 | 163 | 198 |

## 9.4.3 Calculation of the Maximum Range

The maximum range is to be calculated, according to equation (19), by equating the two-way transmission loss to the available signal. If the transmission

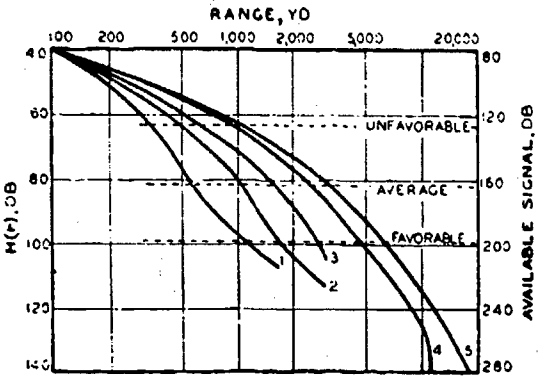


FIGURE 13. Graphical calculation of maximum echo ranges under various thermal conditions. The curves 1 to 5 correspond to the anomaly curves of Figure 14, Chapter 3.

loss were given by the inverse square law, the calculation could be made with a table of logarithms, from the equation

$$40 \log r = \text{Available signal.} \qquad (20)$$

Using the available signals of Table 4, this equation results in the following values of the maximum range:

| Unfavorable case | Average case | Favorable case |
|---|---|---|
| 1,600 yd | 10,000 yd | 90,000 yd |

Except for the unfavorable case, these values are far in excess of the ranges actually observed. The reason is obvious; this calculation assumes that the transmission anomaly is zero, whereas it actually has very appreciable values.

In order to obtain more reasonable values for probable ranges, the empirical values of the transmission loss must be used. The anomaly graphs of Figure 14, Chapter 3, have been used to calculate the transmission loss curves of Figure 13. If the curves are to be used simply to obtain values of the one-way transmission loss, the left-hand scale is to be used. The right-hand scale shows the two-way loss, which is to be equated to the available signal. The dotted lines show the unfavorable, average, and favorable values of the available signal, as tabulated above. The intersection of these lines with the graph appropriate to the different thermal conditions are shown on the graphs. The resulting estimates of the maximum range are shown in Table 5.

TABLE 5. Estimates of maximum range.

| Thermal condition | Unfavorable | Average | Favorable |
|---|---|---|---|
| 1 | 350 | 600 | 1,200 |
| 2 | 500 | 1,050 | 2,000 |
| 3 | 650 | 1,800 | 2,800 |
| 4 | 100 | 2,200 | 5,500 |
| 5 | 1,200 | 3,100 | 6,500 |

## Chapter 10

# MAXIMUM ECHO RANGES WHEN REVERBERATION IS LIMITING

## 10.1 REVERBERATION IN ECHO RANGING

### 10.1.1 General Remarks

IN ECHO RANGING, background noise, in general, limits only the longer ranges. At short, and possibly medium ranges, the echo must be detected against a background of reverberation. As a masking background, reverberation differs from a noise in several ways. Reverberation is a background concentrated around a definite frequency, whereas the spectrum of noise comprises a very wide range of frequencies. The level of reverberation depends on the power output of the projector and decreases very rapidly, with range being very high at short ranges and very low at long ranges. Noise, on the contrary, is independent of the projector output and is the same at all ranges. Echoes are usually tones of a definite pitch and thus are not likely to be confused with such noise, except when very short ping lengths are used. The occasional strong bursts of reverberation, however, may easily be mistaken for echoes.

### 10.1.2 Spectrum of Reverberation

The dependence of reverberation on power output and ping length were discussed in Chapter 5, where it was shown that the intensity of reverberation was proportional to these two factors. The spectrum of reverberation is of particular importance in discussing the masking effect of reverberation.

Figure 1 shows a typical spectrum of heterodyned reverberation from an 80-yd ping. The reverberation is seen to be concentrated around 840 c, the peak being only 24 c wide at the −3-db points and 50 c wide at the −10-db points.

Theoretically, the power spectrum of reverberation should be the same as the energy spectrum of the ping which causes it. This conclusion depends on several assumptions, and it is not surprising that it is confirmed only in a general way. With long pings, the spectrum of reverberation has a well-defined peak, but its width is probably greater than that of the energy spectrum of the ping. As was noted above, this latter is $1/\tau$, where $\tau$ is the duration of the ping in seconds. There are many possible reasons for this, but the effect has not been adequately studied. For sufficiently short pings, it may be that the spectrum of reverberation and ping become more nearly identical. In any case, it is safe to assume that the width of the spectrum peak for reverberation is not less than $1/\tau$. For pings of 0.1-sec duration such as are used in much echo-ranging work, Figure 1 shows that the width is about 24 c, rather than 10 c.

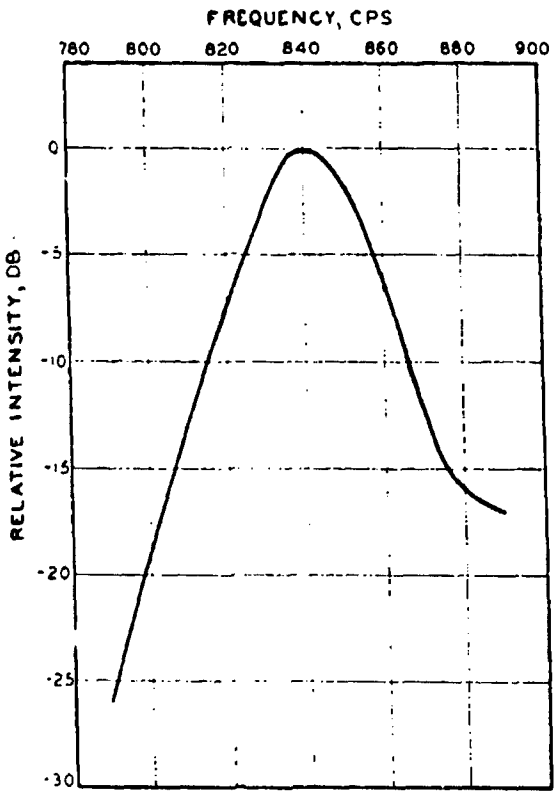


FIGURE 1. Spectrum of heterodyned reverberation.

The concentration of the reverberation about one frequency leads to a further important difference between reverberation and noise. This difference concerns the effect of the receiver bandwidth. If the

bandwidth is wide enough to admit frequencies about 50 c to each side of the reverberation frequency, further increase in bandwidth will have no effect on the intensity of the reverberation emitted by the loudspeaker. Unlike noise, therefore, the airborne level of reverberation does not increase with bandwidth. Thus for a receiver having a response curve of the type shown in Figure 1 of Chapter 9 with a bandwidth of about 1,000 c or even less, the airborne reverberation level is simply

$$R_{air} = R + A, \tag{1}$$

just as for the echo equation (12) of Chapter 9.

## 10.2 DOPPLER EFFECT

### 10.2.1 Explanation of Doppler Effect

When an observer is in motion toward a source of sound, he hears a note the pitch of which is higher than when he is at rest. If the observer is in motion away from the source, he hears a lower note than when he is at rest. Thus the apparent frequency of the sound is increased when an observer moves toward a source and decreased when he moves away from it. Similarly, if the source is moving toward the observer, the frequency is higher; if the source moves away from the observer, it is lower. This change in pitch is known as the doppler effect.

The apparent frequency of the sound is found as follows. When the observer is at rest, the number of waves he receives each second is $F_0$, the true frequency of the sound. When the observer is in motion toward the source, he receives more sound waves in each second than when he is at rest. If his mean range rate is $v$, the additional number of waves received per second are those which occupy this distance, $v$, by which the range is changed in 1 sec. Since the distance between successive waves is the wavelength $\lambda$, this number is $v/\lambda$. Using the relation for the velocity $c$ of the sound,

$$c = F_0\lambda,$$

the number of additional waves received is $F_0v/c$. The *apparent frequency* $F$ is the total number of waves received each second, and is therefore given by

$$F = F_0\left(1 + \frac{v}{c}\right). \tag{2}$$

For the case in which the observer is in motion away from the source, the plus is replaced by a minus:

$$F = F_0\left(1 - \frac{v}{c}\right). \tag{3}$$

If the source is receiving echoes from a target, the doppler effect will occur twice, so that the frequency of the echo $F_E$ received at the source is

$$F_E = F_0\left(1 \pm \frac{2v}{c}\right). \tag{4}$$

Equation (4) gives the apparent frequency of the echo when the range rate is $v$, the positive sign being used if they are moving toward each other, the negative if they are moving away.

The equations apply to the supersonic frequency of the sound in the water. In order to make this sound audible, the received waves are heterodyned in the receiver. This heterodyne receiver reduces the frequency by a constant amount. It is important to note that this reduction is subtractive and not proportional, i.e., the receiver subtracts a constant amount $F_H$ from the received frequency $F$, so that the audio frequency of the output is

$$f = F - F_H. \tag{5}$$

Applying this to equation (4), it is seen that the audio frequency of the echo is

$$f_E = F_0 - F_H \pm \frac{2F_0v}{c} \tag{6}$$

$$= f_0 \pm \frac{2F_0v}{c}. \tag{7}$$

Here $f_0 = F_0 - F_H$ is the audio frequency of the echo for a zero range rate. The difference $f_E - f_0$, i.e., the quantity $\pm 2F_0v/c$, is called the *absolute doppler shift*. It is seen to be proportional to $F_0$, and independent of $F_H$ or $f_0$. Since the transmitted frequency $F_0$ is much greater than the heterodyned audio frequency $f_0$, this is a very important point. Using $c = 2{,}800$ knots, and expressing $v$ in knots, $F_0$ in kc, the doppler shift is

$$f_E - f_0 = 0.7F_0v \text{ c, approximately.} \tag{8}$$

If $F_0 = 24$ kc,

$$f_E - f_0 = 17v \text{ c, approximately.} \tag{9}$$

This shift can be very appreciable. If the sonar ship and target are on opposite courses, the one moving at 24 knots, the other at 5, the shift is $30 \times 17 = 510$ c. Since $f_0$ is commonly 800 c, this is a very large

effect. Its importance in determining the width of the pass band of sonar receivers has already been discussed in Chapter 9. Other consequences will now be considered.

## 10.2.2 Application to Echo Ranging

In echo ranging the operator does not hear the outgoing ping, since the equipment is on "send" and the receiver is blocked. It is therefore impossible for him to compare the frequency of the returning echo with that of the outgoing ping. He can, however, compare the frequency of the echo with that of the reverberation heard immediately after the ping is emitted, and this has an important effect. The difference between the reverberation and echo frequency depends only on the submarine's absolute motion through the water, and its direction relative to the sound beam. It is independent of the motion of the ship.

The reason for this may be explained as follows. Suppose the ship is moving with velocity $V$, its sound beam being directed dead ahead; then, just as in the case of an echo, the relative motion between the source and the scatterers will cause the reverberation frequency to increase, its value after heterodyning being given by equation (7):

$$f_R = f_0 + \frac{2F_0V}{c}. \tag{10}$$

If a submarine is approaching the echo-ranging ship with a speed $V'$, the relative speed $v$ is

$$v = V + V', \tag{11}$$

and the audio frequency of the echo is, from equation (7),

$$f_E = f_0 + \frac{2F_0V}{c} + \frac{2F_0V'}{c}. \tag{12}$$

Comparing equations (10) and (12), it is seen that *the audio frequency of the echo exceeds that of the reverberation by*

$$\Delta f = \frac{2F_0V'}{c}, \tag{13}$$

an expression that does not contain $V$, the speed of the sonar vessel.

If $F_0 = 24$ kc,

$$\Delta f = 17V' \text{ c, approximately;} \tag{14}$$

thus, for an approaching 5-knot submarine, the frequency of the echo is 85 c above the reverberation frequency. As has already been mentioned, the quantity $\Delta f$ is known as the target doppler; because operationally it is much more important than the absolute doppler shift, it is frequently called simply doppler. It is "up-doppler" if the submarine is moving toward the echo-ranging ship and "down-doppler" if it is moving away.

In the above example, it has been assumed that the course of the target is directly toward (or away from) the echo-ranging gear. It may be shown that, in general, $V'$ is not the actual speed of the target, but its range rate relative to a stationary point $P$. This point $P$ momentarily coincides with the sonar projector, but must be considered stationary even though the sonar is moving.

## 10.2.3 Importance of Target Doppler

The importance of target doppler in echo ranging is immediately evident. It is a common experience that a difference in pitch between two tones is a great aid in hearing them, and even a very weak tone can often be distinguished from others if its pitch differs markedly. Thus target doppler is a great aid in detecting echoes against a reverberation background. (It does not enter, of course, when the echo must be recognized against noise.) This application of target doppler to echo ranging will be discussed in the next section.

A second important exploitation of target doppler derives from the fact that it is proportional to the speed of the target. Hence it can give information concerning the motion of the latter. If the echo is of higher frequency than the reverberation (up-doppler), the range must be closing; if the echo frequency is lower than that of the reverberation, the range is opening. A trained operator can also estimate the probable aspect of the target with considerable accuracy from the change in target doppler.

The ability of the operator to estimate the difference in frequency between reverberation and echo depends on the ping length. This has been mentioned in Section 9.1. It is shown quantitatively by Figure 3 of Chapter 14.

Many "false" echoes are received from floating debris, kelp, and from unknown causes. These do not show the effect of target doppler, so that a final important application of the latter is this identification problem.

## 10.3 RECOGNITION OF THE ECHO AGAINST REVERBERATION

The definition of recognition and maximum range are the same for reverberation as for noise (Section 9.3.1). Thus recognition occurs when 50 per cent of the echoes are correctly identified against the reverberation; the range at which this would occur is the *maximum reverberation limited range*. This may be the actual maximum range, or not, as will be explained in Section 10.4.2.

### 10.3.1 The Recognition Differential

The recognition differential for reverberation is defined by

$$M_R = 10 \log \frac{I_s}{I_R}, \tag{15}$$

where $I_s$ = echo intensity at 50 per cent recognition,
$I_R$ = reverberation intensity

Using equation (9a) of Chapter 5

$$E = 10 \log I_s,$$

and defining the absolute reverberation level $R$ by

$$R = 10 \log I_R, \tag{16}$$

equation (15) can be written

$$E = R + M_R \tag{17}$$

and is exactly analogous to equation (16a) of Chapter 9:

$$E = L + M_N.$$

The subscripts $N$ and $R$ will be used with $M$ to distinguish between the two recognition differentials. In either case $M$ is seen to be the number of decibels by which the echo must exceed the background (noise $L$ or reverberation $R$), in order to be detected 50 per cent of the time. The quantities $R - M_R$ and $L - M_N$ will be called the *recognition level for reverberation* and *recognition level for noise*, respectively.

In general, the factors that determine the recognition differential for reverberation are the same as those discussed in Section 9.3.2 in connection with noise. Very little work, however, has been done to investigate any but aural recognition. This is primarily due to the almost universal use of the ear for detection, even when other methods are used in addition. The discussion in the remaining sections of this chapter will therefore be restricted to aural detection. The method of calculating maximum ranges, however, is applicable to all methods of presentation, provided, of course, the values of $M_R$ which are used are appropriate to the particular presentation employed.

### 10.3.2 Aural Recognition

In Section 9.3.4 it was pointed out that in the case of the ear, the masking effect of background noise is restricted to a certain critical band of frequencies. In listening to an echo, the only part of the background which is effective in masking is that part which is contained in the critical band centered at the echo frequency. For a heterodyned output of 800 c, the critical band of the ear is about 40 c.

For this reason it is clear from Figure 1 that if the echo has no doppler, i.e., its frequency is the same as that of the reverberation, virtually all of the reverberation power will be included in the critical band, and the ear has no advantage over other methods of presentation. On the other hand, when doppler shifts the echo 40 c or more away from the reverberation frequency, the level of reverberation in the critical band will be relatively low. Its masking effect will be correspondingly lower, with the result that weaker echoes can be detected.

The effect of doppler shift on recognition can also be described in terms of the sensations of the operator. When the echo and reverberation have the same f[illegible]ency, he will hear the echo only as a louder [illegible] of sound. As the frequency difference increase[illegible] will become increasingly aware of a difference in pitch, until finally this will be the primary sensation. The difference in loudness will not be noticed unless it is extreme.

### 10.3.3 Values of the Aural Recognition Differential

The value of $M_R$ for aural presentation depends on the duration of the echo and upon its doppler shift. Figure 2 shows the dependence of $M_R$ on ping duration for a beam echo having no doppler. For long signals (more than 200 msec) the recognition differential is nearly zero, indicating that the echo can be heard half the time if its level is equal to that of the reverberation. For signals shorter than 30 msec the echo level must exceed the reverberation by about 12 db in order for 50 per cent recognition to

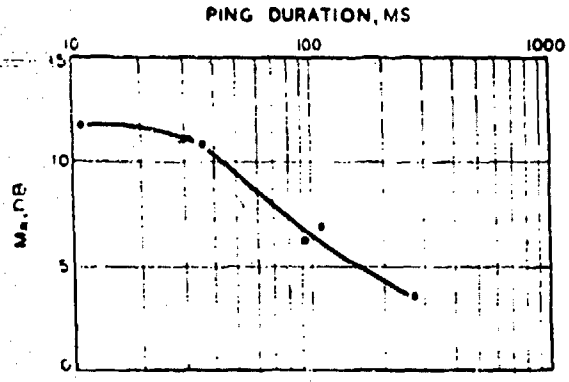


FIGURE 2. Dependence of the recognition differential on ping duration for a beam echo without doppler, when masked by reverberation.

occur. Between 30 and 200 msec $M_R$ decreases approximately inversely as the ping duration.

Now suppose the echo has doppler; as the magnitude of the doppler shift increases, the recognition differential decreases. This is shown in Figure 3 for

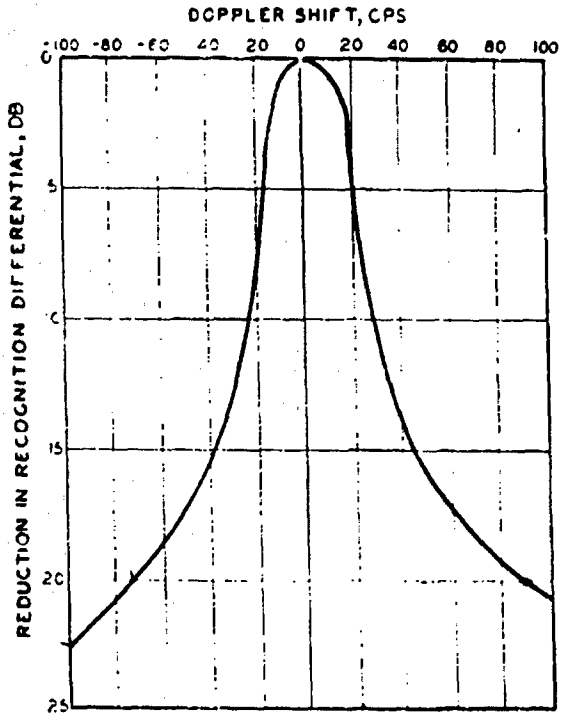


FIGURE 3. Graph showing the reduction in recognition differential for dopplered echoes. Echo duration = 114 msec. Note the asymmetry of the curve.

114-msec echoes. The data were obtained by UCDWR using relatively well-trained subjects, representative of the best sonar operators. It is seen that the recognition differential is reduced 10 db by a target doppler of about $-25$ c or $+30$ c; and 20 db by a target doppler of $-70$ c or $+90$ c. The asymmetry of the curve is interesting, as appearing to indicate that recognition is somewhat easier when the range is closing than when it is opening. Data obtained by other experimenters show this same asymmetry, but differ in some respects from Figure 3.

This curve shows the great importance of target doppler in the recognition of echoes. From Figure 2 it is seen that the recognition differential for a 114-msec echo is 6 db without doppler; if the range rate is 1.5 knots, the recognition differential is $-4$ db, and for a range rate of 5 knots, the recognition differential is about $-14$ db.

For ping lengths shorter than 114 msec the pitch discrimination of the ear is less, and the decrease in $M_R$ will not be so great. For longer pings the discrimination improves and the decrease in $M_R$ will be somewhat greater. Relatively little quantitative information is available.

## 10.4 MAXIMUM ECHO RANGES WHEN REVERBERATION IS LIMITING

### 10.4.1 General Principles of Range Calculations

The calculation of reverberation-limited ranges differs from the calculation of noise-limited ranges only in one important feature: reverberation is a function of range, whereas noise is essentially constant. When reverberation is limiting, therefore, both the echo level and the background depend on range, and a slightly different method must be used to calculate the limiting range.

By definition, the maximum range is the range for which equation (17) is satisfied,

$$E = R + M_R. \tag{17}$$

To find the maximum range we may first plot a curve of $E$ as a function of range, and next, a curve of $R + M_R$; the point at which the two curves intersect gives the maximum reverberation-limited range.

Curves of $E$ and $R + M_R$ for a shallow target are shown in Figure 4 and will be discussed quantitatively in the next section. The recognition level for noise $L + M_N$ is also shown. The five echo-level curves correspond to the five thermal conditions used in Figure 11 of Chapter 9 in the discussion of noise-limited

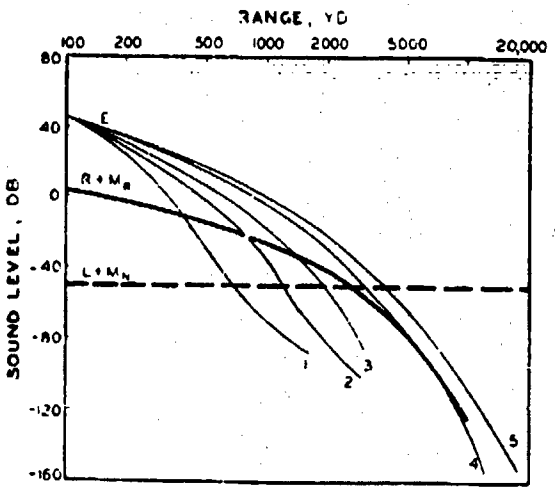


FIGURE 4. Graphical estimation of maximum echo ranges limited by either reverberation or noise, for the 5 thermal conditions shown in Figure 14 of Chapter 3 and used to construct Figure 11 of Chapter 9. Curves 1 to 5 show the echo level calculated for these thermal conditions. The curve marked $R + M_R$ shows the recognition level with a reverberation background, and the broken curve marked $L + M_N$ gives the recognition level when the masking background is noise.

ranges. At very short ranges the echo level is seen to be far above both reverberation and noise, so that an echo at these ranges would rarely be masked. At longer ranges the echo level drops into either noise or reverberation. Thus the echo-level curves 1, 2, and 3 drop into reverberation before they reach the noise background. For these curves, therefore, reverberation is the masking background. Curve 4, on the other hand, drops into noise before it reaches the reverberation, and noise is the masking background. Curve 5 is also masked by noise; it does not intersect the reverberation curve at any range.

The manner in which the various parameters enter into the range calculation may be shown as follows:

1. The echo level is given by equation (9) of Chapter 8,

$$E(r) = S + T - 2H(r).$$

2. Using equation (16) and equation (25) of Chapter 5, the absolute reverberation level is $S + RL$, so that the *recognition level for reverberation* is given by equation (17),

$$R + M_R = S + RL + M_R. \qquad (18)$$

3. The *recognition level for noise* is given by equation (17) of Chapter 9,

$$L + M_N = N + D + 10 \log w + M_N. \qquad (19)$$

These three equations show explicitly all the main factors affecting the range.

The qualitative effect of these factors on the range is easily shown by reference to Figure 4. For example:

*Source Level S.* A change in $S$ will shift the curves of $E$ and $R + M_R$ by equal amounts, and *will therefore not affect the reverberation-limited range.* An increase in $S$ will raise the $E$ curves and thus *increase the noise-limited range;* a decrease will shorten it.

*Target Strength T.* A change in $T$ will affect $E$ but leave $R + M_R$ and $L + M_N$ unchanged. Thus *increase in T will increase both noise- and reverberation-limited ranges.*

*Transmission Loss H.* As $H$ increases, the echo-level curve drops, as shown by the change in going from curve 5 to curve 1, which corresponds to going from good transmission conditions to poorer. Thus *increase in H will decrease both noise- and reverberation-limited ranges.*

*Reverberation Level RL.* An overall increase in the reverberation level, caused, for example, by using a longer ping length, will tend to shorten reverberation-limited ranges. It is worth emphasizing that, to a first approximation, the reverberation level is independent of thermal conditions.

*Recognition Differential M.* For both noise and reverberation an increase in the recognition differential effectively increases the background and therefore shortens the range.

The above parameters are not independent. One example, concerning source strength, has already been discussed. Two others are of particular interest.

1. Effect of *ping length* $r_0$. An increase in $r_0$ *increases RL* proportionately; according to Figure 2, however, it *decreases* $M_R$, at least in a region of considerable practical interest (30 to 200 msec). These two effects offset each other in equation (18) and leave $R + M_R$ almost unchanged. *Changing ping length, between 30 and 200 msec, therefore does not greatly affect reverberation-limited ranges.* It should be pointed out, however, that since this involves $M_R$, the recognition differential for aural detection, this statement will require modification for other modes of portrayal. There is good evidence that with certain methods of visual presentation, a decrease of ping length increases the reverberation-limited range. The effect of ping length on target strength has been discussed in Chapter 8, and will also have an influence on the maximum range.

2. Effect of *target speed and aspect.* The target strength $T$ is high for beam aspect and low for bow

or stern aspect. If the target is not moving, therefore, the echo will be weaker, and both noise- and reverberation-limited ranges will be shorter for stern or bow aspects than for beam aspect.

If the target is moving, however, doppler effect will be present for the stern and bow echoes and will decrease $M_R$, thereby lowering $R + M_R$ and increasing the reverberation-limited range. At beam aspect, of course, there will be no doppler effect and the range will be unchanged.* The noise-limited ranges will, of course, be independent of the target speed, since $M_N$ is unchanged by doppler effect.

The net result is that, with increasing target speed and any aspect except beam aspect, the reverberation-limited range will be increased. Reverberation-limited ranges at beam aspect or noise-limited ranges at any aspect will be theoretically unaffected by target speed.

## 10.12 Calculation of the Maximum Range

To illustrate the method of calculating maximum ranges, three cases will be considered, corresponding to those in Chapter 9. It will be assumed that standard 24-kc echo-ranging gear is being used in deep water, that the ping length is 100 msec, that the receiver has a wide-band ($w = 2{,}000$ c) response, and that aural detection is employed. The values of the parameters $S$, $T$, $M_R$ are given in Table 1. The same values of $S$ and $T$ are used as in Chapter 9, the values of 5 db, 15 db, 25 db for $T$ representing stern or bow, quarter, and beam aspect, respectively. For $M_R$ the value of 6 db in the unfavorable case corresponds to no doppler; taken with the value of $T = 5$ db, the combination represents a submarine dead in the water at stern aspect, a decidedly unfavorable situation. For the average case $M_R = -4$ db corresponds to slight doppler and, with $T = 15$ db, the combination represents a creeping submarine under way at about 6 knots at quarter aspect. The favorable case $T = 25$ db and $M_R = -4$ db corresponds to a fast-moving submarine seen about 10 degrees off the beam. A more favorable case would have been $T = 15$ db and $M_R = -20$ db, corresponding to high speed and quarter aspect; the case shown in Table 1 was taken in order to retain the large value of $T = 25$ used in Chapter 9.

Table 1. Values of various parameters used in calculating reverberation-limited ranges.

| | Unfavorable case (db) | Average case (db) | Favorable case (db) |
|---|---|---|---|
| $S$ | 110 | 110 | 110 |
| $T$ | 5 | 15 | 25 |
| $M_R$ | 6 | −4 | −4 |

Using the values of $S$ and $T$ in Table 1 for the average case, together with the same values of $H(r)$ as were used in Figure 11 of Chapter 9, the $E$ curves of Figure 4 were constructed. The $R + M_R$ curve was obtained from the average for deep water given in Chapter 5 (curve 4, Figure 34).

The recognition level for noise $L + M_N$ corresponds to the average case used in Chapter 9; the values of the parameters assumed for all three cases are shown in Table 2.

Table 2. Values of parameters used in calculating noise-limited ranges (from Chapter 9).

| | Unfavorable case (db) | Average case (db) | Favorable case (db) |
|---|---|---|---|
| $N$ | −30 | −45 | −60 |
| $D$ | −23 | −23 | −23 |
| $M_N$ | − 3 | −13 | −23 |
| 10 log $w$ | 30 | 30 | 30 |
| Recognition level for noise | −26 | −51 | −76 |

The reverberation- and noise-limited ranges for the average case were read from Figure 4 and are shown in Tables 3 and 4, together with the corresponding values for the other two cases, determined

Table 3. Estimates of maximum range (reverberation-limited).

| Thermal condition | Unfavorable case (yd) | Average case (yd) | Favorable case (yd) |
|---|---|---|---|
| 1 | 300 | 400 | 500 |
| 2 | 550 | 800 | 1,000 |
| 3 | 900 | 1,400 | 2,000 |
| 4 | 2,500 | 5,000 | .... |
| 5 | .... | .... | .... |

*This sentence is based on a very simple theory. Experimental evidence on the effect of target motion on the intensity of echoes from the beam aspect is puzzling and conflicting. The observed effects have been large on some occasions but not always in the same direction. Further experimental work on this problem is urgently needed.

TABLE 4. Estimates of maximum range (noise-limited).

| Thermal condition | Unfavorable case (yd) | Average case (yd) | Favorable case (yd) |
|---|---|---|---|
| 1 | 400 | 700 | 1,500 |
| 2 | 700 | 1,100 | 2,100 |
| 3 | 900 | 2,000 | 3,000 |
| 4 | 1,400 | 3,200 | 5,600 |
| 5 | 1,700 | 4,200 | 7,400 |

TABLE 5. Estimates of maximum range (noise- and reverberation-limited).

| Thermal condition | Unfavorable case (yd) | Average case (yd) | Favorable case (yd) | Masking background |
|---|---|---|---|---|
| 1 | 300 | 400 | 500 | Reverberation |
| 2 | 550 | 800 | 1,000 | |
| 3 | 900 | 1,400 | 2,000 | |
| 4 | 1,400 | 3,200 | 5,600 | Noise |
| 5 | 1,700 | 4,200 | 7,400 | |

in a similar manner. In general, these numerical data should be considered as illustrative of the calculations and should not be used for operational decisions.

## COMPARISON OF LIMITING RANGES FOR NOISE AND REVERBERATION

In order to determine the maximum echo range in a given situation, the limiting ranges must be calculated for both noise and reverberation and the shorter of the two chosen. This has been done for the cases above; the results are shown in Table 5. It is also useful to consider the range at which $R + M_R$ crosses $L + M_N$: this is the range at which the masking background changes from reverberation to noise. For the average case shown in Figure 4 this occurs at 2,700 yd. Inside this range the limiting ranges must therefore be determined from the reverberation (Table 3); beyond this range they are determined by noise (Table 4).

# Chapter 11

# MISCELLANEOUS ECHO-RANGING APPLICATIONS

## 11.1 OPERATIONAL PLANNING

THE DISCUSSIONS in the preceding chapters of Part II have dealt primarily with the production of the echo-ranging signal and the detection of the echo, without devoting particular attention to specific situations and the problems associated with them. The present chapter is devoted to discussing the attempts that are being made to cope with some of the special operational difficulties encountered in trying to obtain information by echo ranging and to apply such information to tactical problems.

### 11.1.1 Search Operations

Echo ranging is used by the Navy for a number of different purposes, not all of them necessarily connected with naval warfare; its use as an aid in antisubmarine warfare is only one application, although perhaps one of the most important and dramatic. To whatever use it may be put, success is conditioned by the systematic execution of a carefully considered operational plan. Such a plan is based on consideration of the several functions that underwater echo ranging can successfully perform.

1. To establish contact with the target by using sound.
2. To maintain contact with the target and identify it.
3. To obtain accurate determinations of the *range* and *bearing* of the target.
4. To determine the rate at which the range and the bearing are changing—the *range rate* and *bearing rate*.

Each of the last three of these functions successively depends on the preceding ones.

The discussion will fulfill its purpose if we restrict it to the application of echo ranging to *search* operations in antisubmarine warfare prosecuted by a surface vessel.

Employing the terminology of antisubmarine warfare, in a search operation three different missions can be assigned to the surface vessel or squadron.

*Hunt:* to find as many enemy submarines as possible, having little or no information as to their position at any earlier time.

*Location:* to find a specific enemy submarine whose position at an earlier time is known with reasonable accuracy.

*Screen:* to establish a zone (the screen) around a friendly area (a shipping lane or a moving convoy) such that all enemy submarines must pass through the screen in order to attack, and then to detect all enemy submarines while they are in the screen.

There are a number of differences between these three assignments. "Hunt" and "location" missions are offensive, and the submarine may be expected to use evasive maneuvers. The "screen" operation is defensive, and its objective, the prevention of a successful attack, will be partially achieved if the submarine is forced to use evasive tactics.

The success of these missions obviously depends in the first place on the probability of establishing sonar contact, that is, on the probability that when a ping is transmitted a recognizable echo will be returned. Intelligent operational plans can be worked out, therefore, only if all the factors affecting this probability are known and their effects evaluated. Some of these are intuitively apparent, e.g., in the hunt operation, success may be equally probable if one searches a wide area superficially or a smaller area intensively. In the location operation, success is assured if the echo-ranging vessel has sufficient speed to make an exhaustive search of a sufficiently large but limited area; provided, of course, that the self-noise at the high speed does not render the sonar inoperative.

The effects of the other factors are not easy to evaluate. It will help to indicate the scope of the problem if we list the most important of these at this time.

1. The range of the target.
2. Its bearing deviation, i.e., the difference between its actual bearing and the projector heading (see Section 11.2.1).
3. Its relative bearing.
4. Its depth.
5. Its target strength.
6. The prevailing sound conditions.
7. The speed of the echo-ranging vessel.

Some of these factors have been discussed fully in the previous chapters. The problem of bringing the

sonar into such a position as to insure a high probability of obtaining echoes resolves itself into an analysis of the cumulative effect of all the factors. A large number of rules have been formulated, based on experience and a small amount of theoretical analysis.[1] However, no complete analysis of the problem has been made. Further work, experimental as well as theoretical, is needed.

In this section, a few general and qualitative remarks will be submitted, suggesting the type of theoretical analysis referred to. It will be assumed that adequate data is available on the last four factors listed, and the dependence of the probability of establishing sonar contact on the range and bearing of the target only will be examined.

## 11.1.2 The Probability of Detection—Single Ping

Assume that a target is in the neighborhood of a sonar and that a single ping is transmitted. The dependence of the detection probability can conveniently be exhibited on a contour map, like the one shown in Figure 1. It should be clearly understood that this figure is entirely schematic and is presented merely to illustrate the discussion of general principles. It does not represent the facts of any actual situation.

The position of the echo-ranging sonar is indicated at the bottom of the figure. If the target is situated on a given contour, the number shown on the contour designates the probability of detection. For example, if a target is on the 60 per cent contour, a single ping will return a recognizable echo 60 per cent of the time. If the target is inside the 60 per cent contour, this probability will be greater. These numbers are called the *detection probability*.

For all search operations, it is important that the area of each contour be as large as possible. It is also desirable that the maximum value of the detection probability be large. In order to obtain a single number that will describe the contour diagram, the areas between two adjacent contours may be multiplied by the average value of the detection probability, and the various products thus obtained added. The result is called the *effective search area* of a single ping. For example, the area between the 30 and 40 per cent contour is measured and this quantity multiplied by 35 per cent, the average probability in the area; then the process is repeated for all

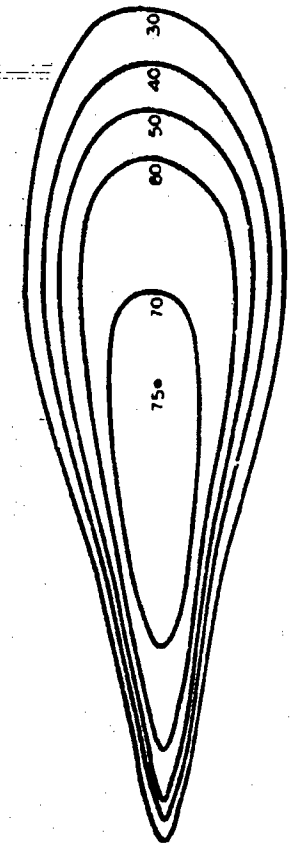


FIGURE 1. Contour map showing detection probability of a stationary target using a stationary sonar. This figure is entirely schematic and is presented merely to illustrate the discussion of general principles.

the zones, and the sum of the individual products computed.

In order to obtain a larger area, the beam width could be increased. However, that might make the bearing determination less accurate, and thus the gain of one advantage would cause the loss of another. In the design of an all-purpose pinging sonar the various requirements must be carefully balanced against each other.

## 11.1.3 The Probability of Detection—Successive Pings

In practice, surface vessels do not rely on a single ping for detection, although the tactical situation

may force a submarine to do so. The analysis of the advantage of repeated pings in operational practice is complex; only a few major principles can be discussed here.

The simplest case is that both sonar and target are at rest, and that two pings are sent out. Then it is possible that an echo will be recognized (1) on both of the pings, (2) on either of the pings, and (3) on neither of the pings.

Let $w_1$ be the probability that a single ping would return a recognizable echo for the given position of the target. Then the probability that the echo would *not* be detected is evidently

$$1 - w_1. \tag{1}$$

Let us assume that the detection probability for the second ping is the same as if the first had not been transmitted. This is not likely, for the operator may have been doubtful of the echo from the first ping and may have ignored it, but a doubtful echo from the second ping will, under these conditions, be very apt to be considered certain. This is especially true if a range recorder is used and becomes an increasingly important effect as the number of pings increases. However, for simplicity, such memory and comparison effects will be ignored.

The probability that the second echo will not be detected is thus also

$$1 - w_1.$$

The probability that neither of the two echoes will be detected is the product of the two probabilities, namely,

$$(1 - w_1)^2. \tag{2}$$

Hence the probability that at least one of the two echoes will be detected is

$$w_2 = 1 - (1 - w_1)^2. \tag{3}$$

In view of the foregoing remarks, this value is apt to be too small.

If $n$ pings are transmitted, the detection probability is

$$w_n = 1 - (1 - w_1)^n. \tag{4}$$

Graphs of this equation for several values of $n$ are shown in Figure 2. Even though these values, as has been said, are likely to be too low, the figure shows an increase of detection probability with each successive ping. This increase is most rapid for intermediate values of $w_1$. *If* $w_1 > 0.5$, five pings will make detection practically certain.

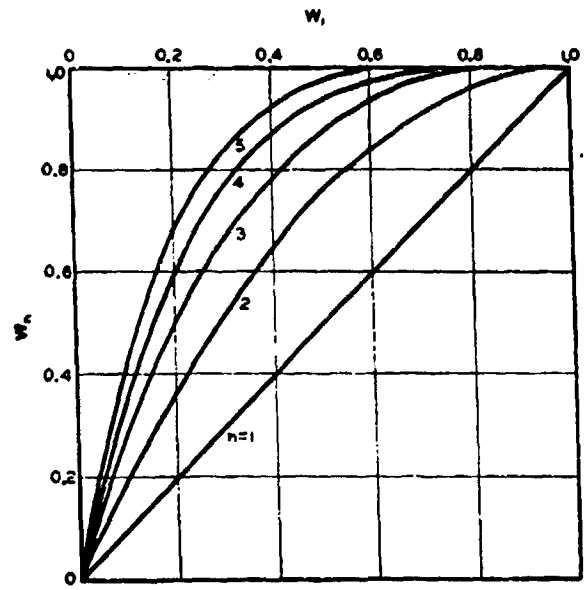


FIGURE 2. Graphs of detection probability $W_n$ for $n$ pings in terms of the detection probability $W$ of a single ping.

## 11.1.4 Effect of Motion of Sonar and Target

If the echo-ranging vessel is in motion, the calculation of the probability of making sonar contact with a target by using successive pings becomes more complicated. If the target is moving, still others arise.

Let the target be on the contour $w'$ of the first ping, and suppose that the motion of the sonar has resulted in placing it on the contour $w''$ of the second ping. Then, by reasoning similar to that in the previous section, and again ignoring memory and comparison effects, the probability of detection by either of the two pings or by both is given by

$$w = 1 - (1 - w')(1 - w''). \tag{5}$$

Values of this function are tabulated in Table 1. Arbitrary values of $w'$ are arranged in the top row, those of $w''$ in the left-hand column, and the corresponding values of $w$ are found in the body of the table. For example, suppose that when the first ping is transmitted the target is on the 60 per cent contour, and that the motion of the sonar has resulted in placing it on the 50 per cent contour for the second ping. Then $w' = 0.6$, $w'' = 0.5$, and from the table, $w = 0.8$.

Table 1 can be used to construct a contour map similar to Figure 1. Such a map is shown in Figure 3.

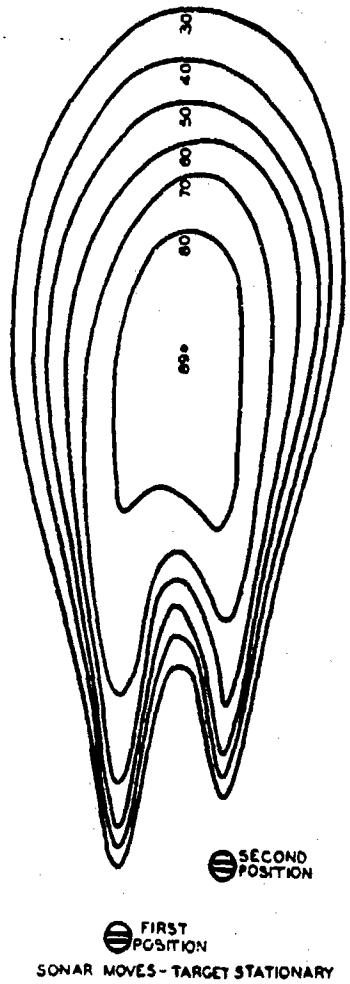


FIGURE 3. Contour map of detection probability, similar to Figure 1, but considering the sonar to be in motion while the target is stationary. This figure should be compared with Figure 1.

TABLE 1. Detection probability for two pings—moving sonar, stationary target.

| $p''$ \ $p'$ | 0.1 | 0.2 | 0.3 | 0.4 | 0.5 | 0.6 | 0.7 | 0.8 | 0.9 |
|---|---|---|---|---|---|---|---|---|---|
| 0.1 | 0.19 | 0.28 | 0.37 | 0.46 | 0.55 | 0.64 | 0.73 | 0.82 | 0.91 |
| 0.2 | | 0.36 | 0.44 | 0.52 | 0.60 | 0.68 | 0.76 | 0.84 | 0.92 |
| 0.3 | | | 0.51 | 0.58 | 0.65 | 0.72 | 0.79 | 0.86 | 0.93 |
| 0.4 | | | | 0.64 | 0.70 | 0.76 | 0.82 | 0.88 | 0.94 |
| 0.5 | | | | | 0.75 | 0.80 | 0.85 | 0.90 | 0.95 |
| 0.6 | | | | | | 0.84 | 0.88 | 0.92 | 0.96 |
| 0.7 | | | | | | | 0.91 | 0.94 | 0.97 |
| 0.8 | | | | | | | | 0.96 | 0.98 |
| 0.9 | | | | | | | | | 0.99 |

The two successive positions of the sonar are shown at the bottom. It is assumed that the detection probability of each ping is identical with that diagrammed in Figure 1, and that the pings were transmitted with the same projector heading. The motion of the projector between pings has been greatly exaggerated for purposes of illustration.

Comparison with Figure 1 shows that each contour, e.g., the 50 per cent contour, has greatly expanded, and encloses more than twice the area of the same contour for a single ping. Moreover, the maximum value of the detection probability has increased from 75 per cent for the single ping to nearly 90 per cent for the two pings. Consequently, the effective search area of the two pings is more than doubled.

The amount by which the effective search area of the overlapping pair exceeds twice the area of a single ping has been exaggerated by the exaggerated motion of the sonar. In practice it will be somewhat less than is shown, but the effect will still be appreciable. In practice, also, more than two overlapping pings will be used, and the effect is increased by this.

The possible motion of the target will have a rather different effect than that of the sonar. To see this, suppose that the target was actually detected at a certain point $P$ at time $t_0$, and that at a later time $t$ it is necessary to estimate its position. In order to illustrate the principles involved, suppose that between $t_0$ and $t$ no further pings were sent out, and that the direction and speed of the target's motion is unknown. Then it is possible to estimate only its speed, not its direction. It will be possible to draw probability contours, giving the probability that the target is at any given point at time $t$. These will be circles with centers at the point $P$. The radii of the various contours will depend on the probability that the target moves with the given speed. As the time interval $t - t_0$ increases, these radii will increase, since the unknown motion of the target has more time to have its effect.

These same considerations can be applied to the time interval between pings. If the ping was sent out at time $t_0$, Figure 1 will show the probability that, if the target is at a given place, it was detected. At a later time $t$, but before the next ping, the target may have moved. Consequently, Figure 1 does not show the probability that, if the target is at a given place at this later time, it would have been detected at the earlier time $t_0$. But it is possible in principle to work out the contours for this "prior-detection" probability. The effect of the unknown motion of the target will be to cause the contours of high probability to shrink as $t$ increases. This is shown

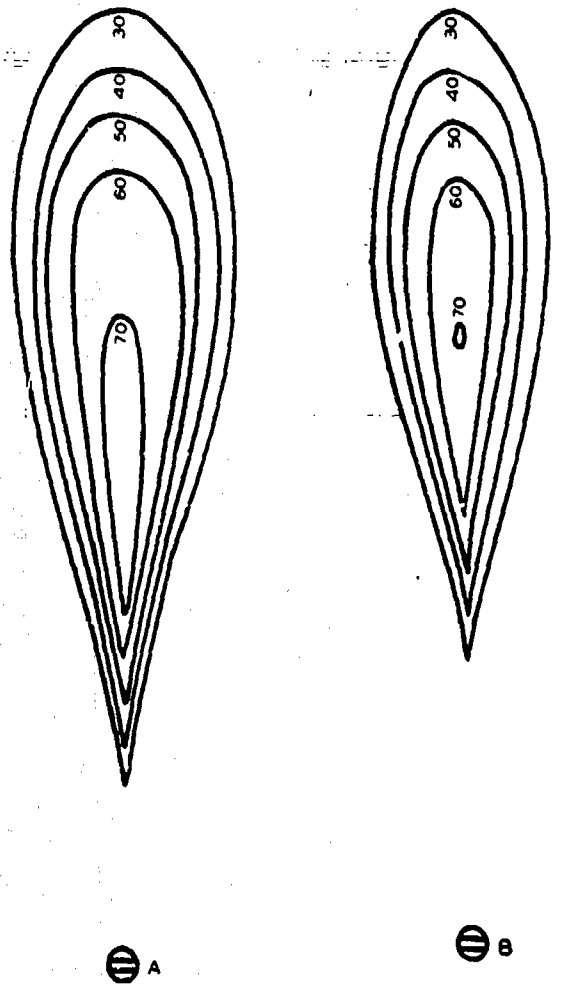


SONAR STATIONARY - TARGET IN MOTION

FIGURE 4. Contour maps of detection probability, similar to Figures 1 and 3, but considering the target to be in motion while the sonar is assumed to be stationary; (A) this figure shows the change that has been brought about in Figure 1 after a certain interval of time; (B) this figure shows the change in Figure 1 after twice the interval.

schematically by Figure 4 for two successive values of $t$.

If several pings are sent out, it is these shrunken prior-detection contours that must be combined as explained in connection with Figure 3. The result of such a succession of pings is shown schematically in Figure 5. This represents the state of affairs at the time the echoes from the third ping are being received, and the contours show the probability that, if the target is then at a given point, it would have been detected either then or earlier.

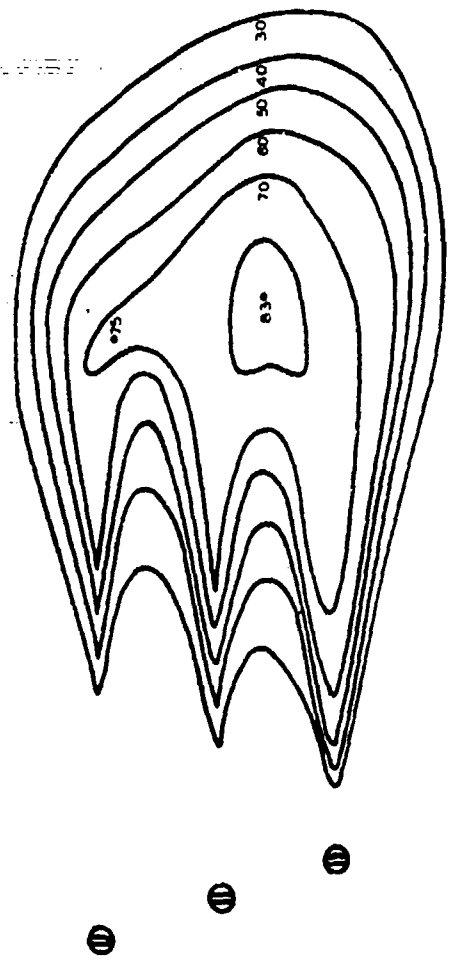


SONAR AND TARGET IN MOTION

FIGURE 5. Probability contours for three successive pings, allowing for the motion of both target and echo-ranging vessel.

The motion of the sonar and target have been exaggerated to emphasize the important points. It will be noted that, because of the unknown motion of the target, the 80 per cent contour of Figure 5 has a much smaller area than the 80 per cent contour of Figure 3—and this despite the fact that the latter is based on three pings, the former on only two.

## 11.2 TARGET BEARING

The foregoing considerations of the probability of establishing sonar contact have been restricted to simple conditions. In general, the possibility of taking action against a target in a given area depends not only on how completely the area can be searched in a short time, but also on the ability of the operator

to maintain sonar contact with the target once he has contacted it. The first of these requirements makes it desirable to design the sonar so that the search area of the ping is large. The second requirement will be seen to be in some conflict with the first. Various special devices have been designed to avoid this conflict. These will be discussed after a preliminary examination of the operational problem in terms of the simplest sonar.

## 11.2.1 Maintaining Contact

After the signal has been transmitted, the sonar operator is on the alert for a sound contact with the target, i.e., a break in the background reverberation or noise, either as he listens to the sound from the loudspeaker or watches the chemical range recorder. (A specimen of a record from the latter is reproduced in Figure 19 of Chapter 8.) Having made a contact, his chief concern is to maintain it.

This is difficult with ordinary sonar gear. The target may move out of the sound beam, either to the right or to the left. Because of the relatively long interval between echoes, the uncertainty as to the direction in which the beam should be rotated is serious.

### Bearing Deviation

The *target bearing* is the direction of the line joining the projector to the center of the target and is not necessarily given by the *projector heading*, which is the direction of the axis of the sound beam. Because of the width of the sound beam, an echo may be received even when the axis does not bear on the center of the target (say, the conning tower, in the case of a submarine). Thus the target bearing and projector heading may not coincide. The difference between them is called the *bearing deviation*. When the bearing deviation becomes greater than a certain amount, the echoes become too weak to be heard.

The projector is under the sonar operator's control, and thus the projector heading is known. The conning officer, however, wishes to know the target bearing. If the bearing deviation were small, it could be ignored. Unfortunately, every attempt to reduce it will increase the probability that the target may move out of the sound beam, and increase the seriousness of the uncertainty mentioned above. Thus every solution must be a compromise between conflicting requirements.

It is not only the beam pattern of the projector and the target width that affect the possible magnitude of the bearing deviation; the echo level and the level of background noise and reverberation are also instrumental. If reverberation is limiting, the possible deviation also depends on the doppler shift of the echo. For present purposes, it is not necessary to consider these matters in detail, but the principles explained in the previous chapters would suffice for their discussion.

### Crossing the Target

The earliest solution of these problems was the operation known as *crossing the target*. In this operation, the projector heading is systematically changed more rapidly than the target bearing changes. When the sound beam leaves the target, the projector motion is reversed, and continued until the sound beam leaves the target on the other side. This eliminates the uncertainty mentioned above. Whenever no echo is obtained, the operator knows on which side of the beam he will find the target. The two limiting projector headings thus obtained are called *cut-ons*. The average of two successive cut-ons is taken as the best approximation to the target bearing.

While the procedure is practicable, it has many disadvantages. The original echo may have come in on either half of the main beam. If the sonar operator begins to cross the target in the wrong direction, he risks losing contact. Moreover, it is time consuming, for it requires at least four, and often more, pings to obtain one value of the target bearing; hence before this value is known to the sonar operator, the target may have moved, rendering the information more or less obsolete.

## 11.2.2 Multiple Hydrophones and Split Transducers

Modern solutions of these problems all involve the use of two hydrophones, and in principle, more than two could be used. The two hydrophones are often constructed in semicircular shape and of such dimensions that they can be mounted in the same space as the older circular transducers. Moreover, by changing electric connections before transmission,

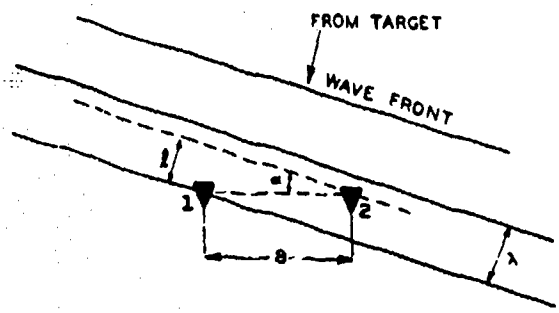


FIGURE 6. Diagram showing three successive stages in the passage of a plane wave front from the target to a transducer having two hydrophones (marked 1 and 2) spaced a unit apart.

the projected sound beam can be made identical with that of the older circular transducer. Such pairs are called split transducers.

The physical principles involved can most easily be explained by considering a pair of identical

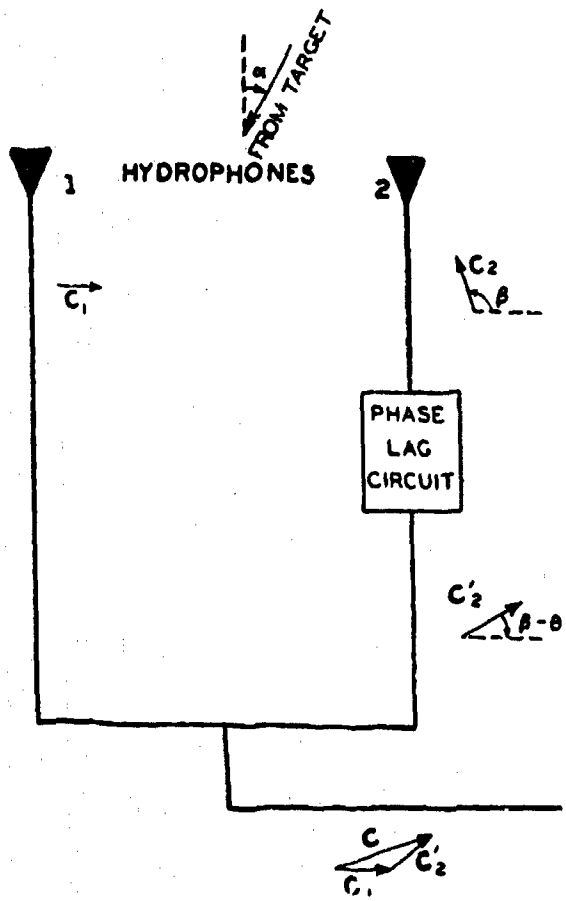


FIGURE 7. Schematic diagram of circuit containing phase lag circuit, showing how a desired phase difference between the currents from the two hydrophones is obtained.

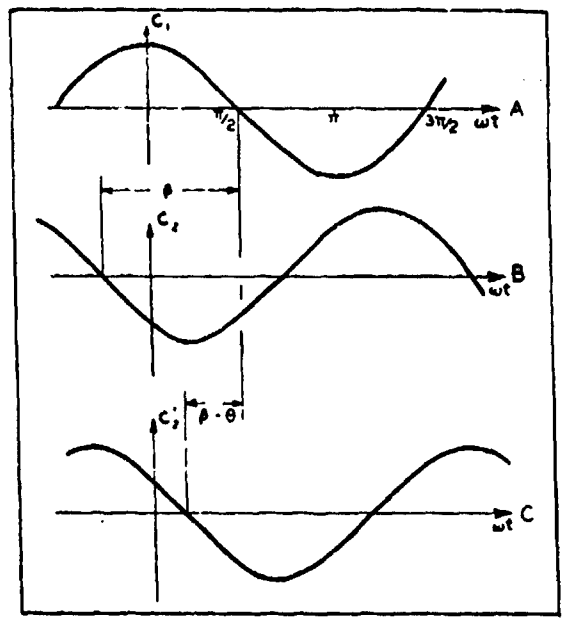


FIGURE 8. Graph of the three currents $C_1$, $C_2$, and $C_2'$, of Figure 7, plotted against the phase angle $\omega t$, and showing the phase differences $\beta$ and $\beta-\theta$ of Figure 7.

hydrophones, mounted a distance $a$ apart, with their acoustic axes parallel to each other and perpendicular to the line joining the two hydrophones. The general arrangement is shown schematically in Figures 6 and 7. It is assumed that the pattern of the two hydrophones consists of a single broad lobe, as shown by the dotted line of Figure 9.

Let an echo or other single-frequency sound be incident on the hydrophones from a direction that makes the angle $\alpha$ with the acoustic axes. Each wave will then reach the hydrophone closest to the target before it reaches the other, and the alternating currents generated by them will not be in phase. Under the circumstances shown in Figure 6, the current for No. 2 will be in advance of that from No. 1. This is shown in Figure 8, curves $A$ and $B$. The phase angle $\beta$ can be calculated as follows: after reaching hydrophone No. 2, the wave must travel a distance $l$ before reaching No. 1. This distance is

$$l = a \sin \alpha. \tag{6}$$

This is $l/\lambda$ wavelengths, and since one wavelength is equivalent to a phase change of 360 degrees, the angle $\beta$ will be given by

$$\beta = 360\left(\frac{a}{\lambda}\right) \sin \alpha. \tag{7}$$

If the current generated by No. 1 is given by

$$C_1 = C(\alpha) \cos \omega t, \tag{8}$$

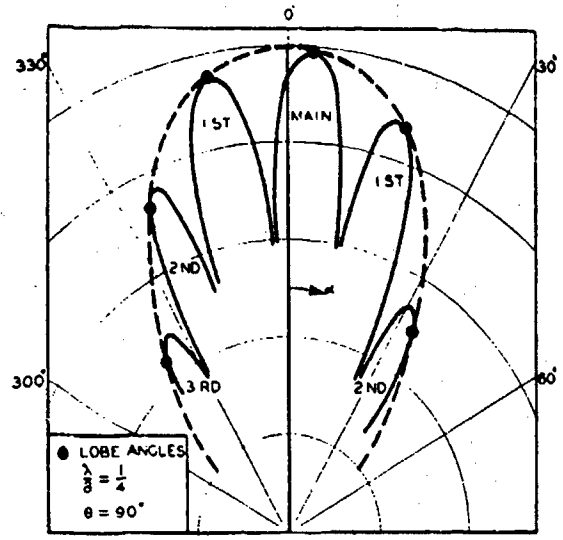


FIGURE 9. Graph of equation (13) for $a/\lambda = 4$, $\theta = 90$ degrees. Note that as a result of the phase shift the single broad lobe of each hydrophone, indicated by the dotted curve, has been broken up into a number of narrower lobes (solid curves); also, that the axis of the main lobe has been displaced. The "lobe angles" are the angles at which the new beam patterns are tangent to the original ones.

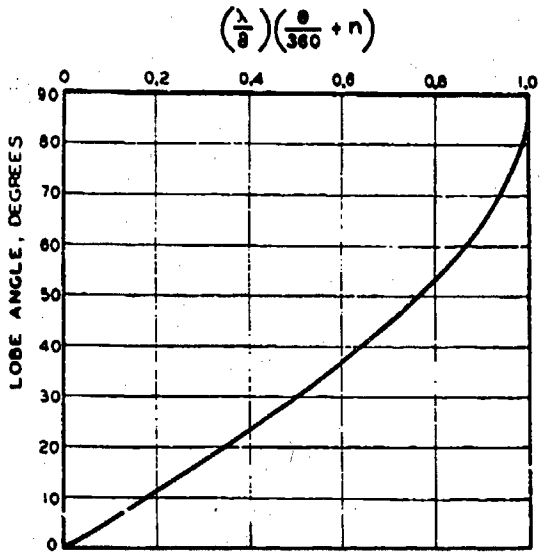


FIGURE 10. Values of the lobe angles, shown in Figure 9, as a function of $\lambda/a$ and $n$, the order of the lobe.

then that from No. 2 will be

$$C_2 = C(\alpha) \cos(\omega t + \beta). \tag{9}$$

The function $C(\alpha)$ is determined by the directivity pattern of the separate hydrophones (dotted curve, Figure 9). The graphs of the two currents $C_1$ and $C_2$ are shown in Figures 8A and B.

If the current from hydrophone No. 1 is passed through a phase shifting network, the phase shift $\beta$ can be altered by any desired amount, say $\theta$. This results in the current

$$C'_2 = C(\alpha) \cos(\omega t + \beta - \theta), \tag{10}$$

shown graphically in Figure 8C. The circuit is shown schematically in Figure 7, and the vector diagrams indicate the relation between the three currents. If $C_1$ and $C'_2$ are combined, the resulting current will be*

$$C = C_1 + C'_2 = C(\alpha)[\cos(\omega t) + \cos(\omega t + \beta - \theta)] \tag{11}$$

$$C_1 + C'_2 = 2C(\alpha) \cos \tfrac{1}{2}(\beta - \theta) \cos[\omega t + \tfrac{1}{2}(\beta - \theta)]. \tag{12}$$

The level of the electrical output is thus

$$L = 20 \log [2C(\alpha)] + 20 \log \cos [\tfrac{1}{2}(\beta - \theta)].$$

* In deriving the equation for $C$, use has been made of the trigonometric formula

$$\cos A + \cos B = 2 \cos \tfrac{1}{2}(A + B) \cos \tfrac{1}{2}(A - B).$$

The first term of this expression is essentially the directivity pattern of the individual hydrophones. The second term also depends on the direction $\alpha$ from which the sound comes, since $\beta$ depends on $\alpha$.

The graphs of the resultant level $L$, for the case $(a/\lambda) = 4$, $\theta = 90$ degrees, is shown by the solid line of Figure 4. It is seen that, as a result of connecting the two hydrophones together, the single broad lobe of each has been changed into a number of narrower lobes.

The axis of the new main lobe does not coincide with that of the original lobe, nor are the side lobes symmetrically located. This is a result of the phase shifting network. Figure 10 can be used to calculate the positions of the lobes for any value of the quantities $\theta$, $\lambda/a$, and $n$, the order of the lobe.

In this graph, the lobe angle is the point at which the new and the original beam patterns are tangent (see Figure 4) and the integer $n$ is zero for the main lobe, $\pm 1$ for the two lobes on either side, $\pm 2$ for the pair of second lobes, etc. The phase lag $\theta$ is to be measured in degrees.

### 11.2.3 Bearing Deviation Indication

Various devices employing the split transducer principles have been designed. They are known by various names: bearing deviation indicators, vector bearing indicators, and phase-actuated locators are several designations. They all use a split projector and differ only in detail.[1]

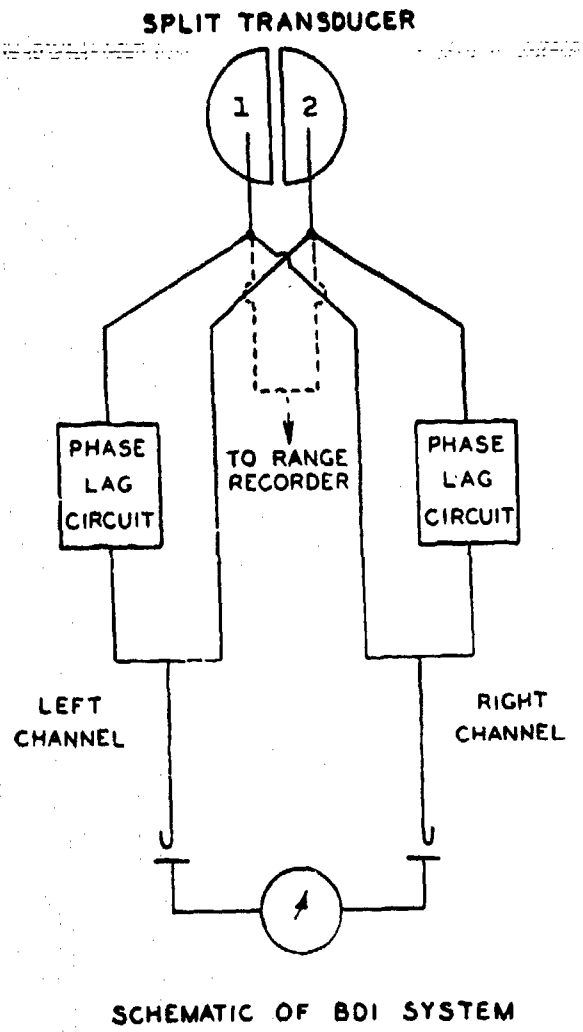


FIGURE 11. Schematic of BDI system.

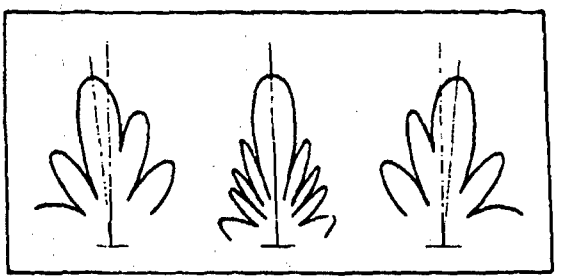

Figure 12. Shift of main lobe of beam pattern in BDI. The center pattern shows the normal beam of a circular diaphragm. For transmission the two halves of the transducer plate are connected together and this pattern is projected. The two side figures show the beam patterns for the two halves of the circuit shown in Figure 11.

For transmission, the two semicircular parts are connected so as to produce the normal beam of a circular diaphragm illustrated by the center curve of Figure 12. For reception, the two halves are connected as shown in Figure 11. It will be noted that there are two symmetric output channels. The connections of the right channel are the same as for the pair of hydrophones in Figure 7. The connections of the left channel differ only in that the phase lag is introduced into the output of No. 1 rather than No. 2. The beam pattern for the right channel thus has its main lobe deflected to the right, as shown by the right-hand curve of Figure 12; the main lobe of the left channel, on the other hand, is to the left. This is perhaps shown more clearly in the rectangular coordinate system used in Figure 13. The ordinates are the currents out of the two channels. In practice, these currents are rectified, as indicated in Figure 13; the diodes are shown in Figure 11.

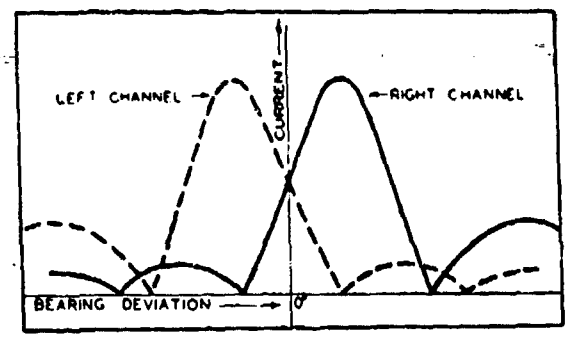


FIGURE 13. Graph of currents from the two channels as a function of bearing deviation.

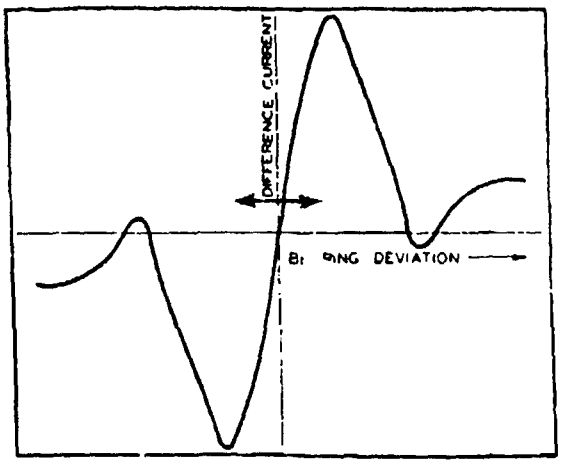


FIGURE 14. Graph of the difference between the currents from the two channels as a function of bearing deviation.

The rectified output currents may be used for various purposes. They are commonly connected to

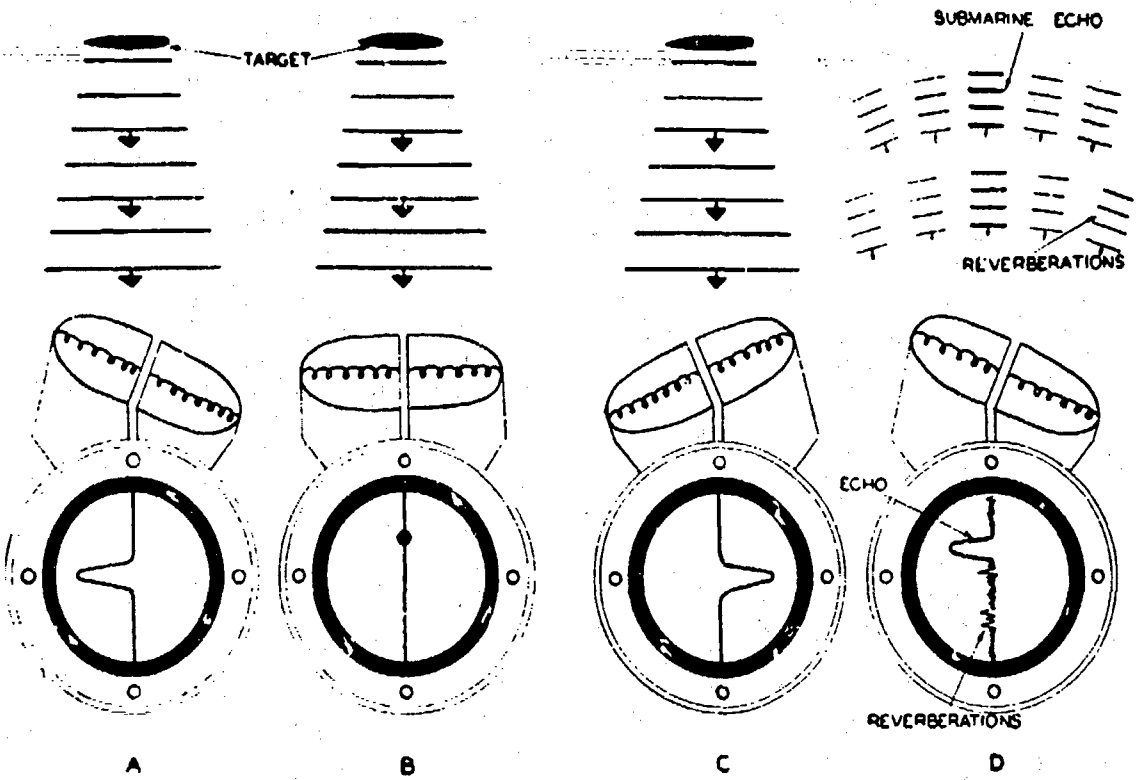


FIGURE 15. Diagrams illustrating BDI. (A) Target to the left of the projector heading causes the dot on the oscilloscope to be deflected to the left; (B) target on dead center causes a brightening of the spot; (C) target to right of projector heading causes the dot to be deflected to the right; (D) echoes must be distinguished from reverberation. For this purpose the visual perception is supplemented by listening to a loudspeaker.

an indicator (*cathode-ray oscillograph* [CRO]) in such a way that its deflection is proportional to the difference between the currents in the two channels. This difference is plotted as a function of bearing deviation in Figure 14. It is seen that, if the latter is not too great, the difference current is proportional to the bearing deviations. It is positive when the deviation is to the right, negative when to the left. Thus the indicator can (in principle at least) be calibrated in terms of bearing deviation. Confusion can occur if the deviation is greater than the limits set by the double arrow of Figure 14.

### 11.24 The Standard BDI

A device designed by the Harvard Underwater Sound Laboratory [HUSL] according to the principles just discussed has become standard equipment in the Navy. It is known as the *bearing deviation indicator* [BDI]. The QGB stack shown in Figure 19 of Chapter 7 has the BDI on its sloping panel.

The BDI provides a visual indication of the sound incident on the transducer. When the transducer is trained on the exact center of the source (Figure 15B), the incident sound strikes both halves of the diaphragm simultaneously; this is indicated by a brightening of the luminous trace on the screen of the CRO. When the transducer is trained slightly off the center of the target (Figures 15A and C), the incident sound waves strike one of the transducer halves before the other. This causes the brightened trace on the screen to be deflected in the direction of the half on which the sound first impinges; a deflection to the left thus would show that the source was to the left of the transducer bearing, and that the operator must train left to get a dead-on bearing. Similarly, a deflection of the brightened spot to the right would indicate that the operator should train right. An accurate bearing can be obtained by getting both a right and a left deflection.

Since the BDI reacts to all sound energy incident on the transducer, it must be used in conjunction with the loudspeaker in order to distinguish between echoes and reverberation, and also between echoes themselves, particularly between the echo from a

submarine and that from its wake (see Figure 15D).

The motion of the spot across the screen is controlled by the range indicator and is synchronized with it. It appears on the bottom of the screen at the beginning of the ping, and travels up the screen in the time required for the range indicator to make one revolution. Hence the spot can move at a rate corresponding to a range of 5,000 yd or to one of 1,000 yd. In addition, a range selector switch is provided by which the operator can control the speed of the spot. It is evident that the position of the bright spot on the screen makes possible a quick estimate of the range of the target.

The rather narrow deflection limits of the indicator make it desirable to employ a *time-varied gain* [TVG] control on the signal transmitted to the indicator. By this means it is possible to have low gain for the strong echoes from nearby targets and reverberations that correspond to short time intervals after the emission of the ping, and progressively higher gains for the weaker echoes from distant targets.

## 11.3 SCANNING SONAR—PULSED TRANSMISSION

The problem of rapidly searching a wide area led to the development of so-called scanning sonars. Two main kinds have been designed: one kind transmits short pulses of sound, the other kind a continuous signal of varying frequency.

### 11.3.1 Objective of Pulsed Scanning Sonar

The original methods of echo ranging all involve a short transmission of sound, followed by a longer period during which the sonar operator is alert for echoes. This period must be long enough so that no further echoes of any one ping can arrive after the next has been transmitted; otherwise the interpretation of the echoes would be uncertain. For example, if a target is located a mile away, over 2 sec are required for the echo of a given ping to be returned to the sonar. Thus, the number of echoes that can be obtained from a given target in a given time is strictly limited, and decreases as the range of the target increases. The corresponding problem in radar is much less serious because of the much greater velocity of radio waves.

A second limitation is that because of its directivity, the sonar is, at a given moment, alert only to echoes from targets in a relatively narrow sector. This is particularly serious when many targets must be anticipated, as for instance, when sonar is used for navigation in a mine field. Under these conditions, the time consumed in training from one bearing to another might well be fatal. Even under less strenuous conditions, it makes it difficult for the operator to be certain of the momentary situation on all bearings.

The objective of the developments discussed in the present chapter is to utilize the necessary interval between pings to search the widest possible sector. In this way, the area searched per ping and the amount of information received per unit time will both be increased.

### 11.3.2 General Principles

This objective can be achieved by flooding the search area by pulses from a transmitter that is nondirectional in a horizontal plane, thus transmitting energy to all bearings with each pulse. The projector need not transmit energy along rays that are much inclined to the horizontal, however. The echoes are received on a rapidly rotating, sharply directional hydrophone. At any instant the outgoing train of waves will thus occupy a ring-shaped region, as shown in Figure 16, marked "wave train." The radius of this ring increases with the velocity of sound. Echoes, on the other hand, can be returned to the hydrophone, at a given instant, only from a small region—the "active volume" defined in Chapter 5, and shown in the figure crosshatched—determined by the ping length $r_0$ and the angular width of the beam. This region is located at half the range of the wave train, and has half the extent of the latter in range; its width, or extent in bearing, is limited by the directionality of the hydrophone. Since the latter is rotating, the active region will describe a spiral path. The radius of the spiral increases with half the velocity of sound; the speed of the active volume in the spiral path will, of course, be much greater than this.

In order that every possible target should at some time be encountered by the active region, the hydrophone must not be rotated too slowly. Otherwise the condition illustrated in Figure 17 results: there is a dead area between the rings of the spiral traced out by the active volume. This dead area is shown unshaded and echoes from targets in it will not be

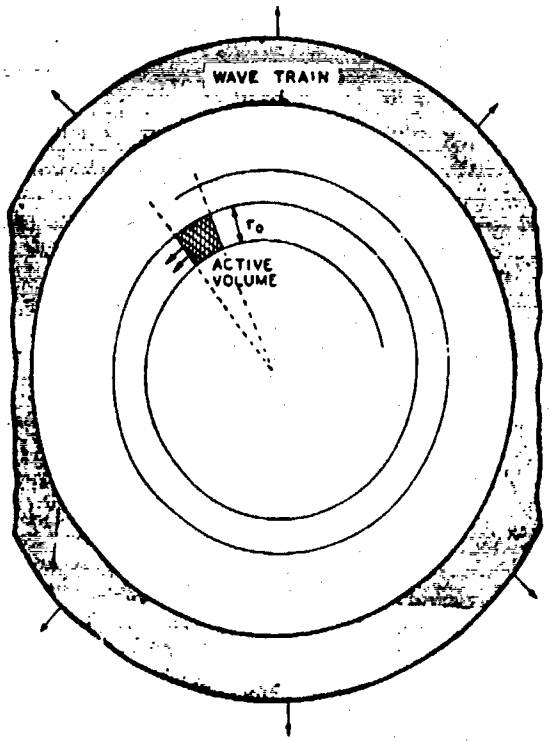


FIGURE 16. Diagram of wave train and active region, for the case of a rotating hydrophone. The sound at a given instant occupies the ring-shaped shaded region, marked "wave train." The radius of this ring increases with the velocity of sound. Echoes can be received to the hydrophone, at a given instant, only from the "active volume," *shown cross-hatched, determined by the ping length, $r_0$, and the angular width of the beam.* The active region describes a spiral path.

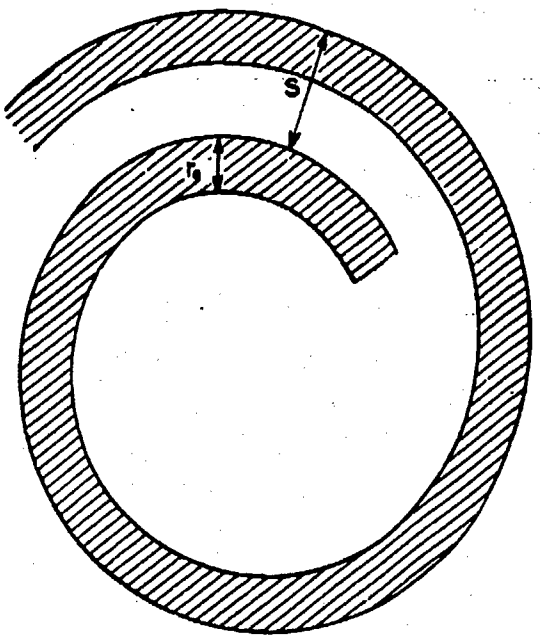


FIGURE 17. Diagram showing the result of rotating the hydrophone too slowly. There is a dead area between the rings of the spiral traced out by the active volume—this area is shown unshaded.

received. The pitch $s$ of the spiral, in this case, is greater than the ping length $r_0$. If the hydrophone makes one revolution during the ping duration $t_0$ of the signal, $s$ will equal $r_0$, and there will be no dead areas. If $t_0$ is expressed in milliseconds and $r_0$ in yards, $r_0 = 0.8t_0$, since $t_0 = 2r_0/c$ sec.

Conversely, if the rotation of the hydrophone is fixed, the ping must have a duration of at least one revolution. Thus, if the hydrophone is rotated at 1,800 rpm, one revolution takes place in 33.3 msec, and consequently, the ping length must be greater than $0.8 \times 33.3 = 26.7$ yd. A value of $r_0 = 30.0$ yd would be safe if the ping is truly rectangular.

A consequence of the rotation of the hydrophone is that the echo will not have the same duration as the transmitted pulse. The echo will be received only while the hydrophone beam is passing over the target. If the effective width of the hydrophone beam is $\theta$ degrees, the echo from a point target, i.e., a target smaller than the active area, will be received during $\theta/360$ of a revolution. Taking $\theta = 11$ degrees and 1,800 rpm as an example, the duration of the echo will be approximately 1 msec. Expressed in yards, the echo length $r_1$ is 0.8 yd. The echo length $r_1$ must thus be distinguished from the ping length $r_0$. In every case, $r_1$ will be smaller than $r_0$, and will be independent of the ping length, provided the latter is of the required order of magnitude, as explained above.

This shortness of the echo duration is a consequence of the increased velocity with which the active volume moves. In fact, it may be said that this increased velocity of the active region is the primary characteristic of pulsed scanning sonar.

The short duration of the echo, in its turn, has a number of consequences:

1. Doppler discrimination will be much impaired (see Section 10.2).

2. Since the spectrum of the short echo extends over many critical bandwidths of the ear, the advantage of the ear over other methods of perception is lost (see Section 9.3.4).

3. The pass band of the receiver must be at least wide enough to pass the short echo. This will involve increased noise levels (see Section 9.1).

4. The level of the reverberation, being determined by the volume of the active region, will be compar-

able to that of standard sonars transmitting pings of length $r_0$ (see Section 5.3.2) and thus greater than for pings of duration $r_1$.

5. The coherence of the reverberation will be comparable to that of sonars transmitting pings of length $r_1$ (see Section 5.3.6).

All these effects will tend to reduce the maximum range obtainable on a given target unless compensated by a suitable device for detecting the echo or by the sixth effect:

6. The target strength of an extended object is determined by the size of the active volume, and will therefore be that which is characteristic of standard sonars transmitting pings of length $r_0$.

### 11.3.3 Plan Position Indicators

The high rate of rotation of the hydrophone makes it impossible for an operator to follow the changes in its heading with his unaided senses. This, together with effects 1 and 2 listed above, makes it necessary to use special devices to portray the echo and render the bearing and range of the target perceptible. These devices are called *plan position indicators*.

The only device of this kind which is feasible for the high rates of rotation contemplated above is a persistent-screen cathode-ray oscilloscope. The spot of this scope is made to describe a spiral path in synchronism with the active area. The path of the spot on the screen is thus a map of the path of the active volume. The brightness of the spot is controlled by the intensity of the received sound, so that an echo will be seen as a brighter spot than the background of reverberation and noise. Because of the synchronization of the spot with the active volume, the echo will appear at the proper range and relative bearing on the screen.

If there are several targets in the field, these will be portrayed in their proper relative positions. If echoes are obtained from reefs or sand banks, these will appear on the screen as brightened areas. Thus scanning sonar with a plan position indicator presents the operator with a complete map of the underwater situation.

### 11.3.4 CR and ER Sonars

In principle, the receiver of a scanning sonar could be a directional transducer rotated about a vertical axis. However, the high speeds required make this impracticable.

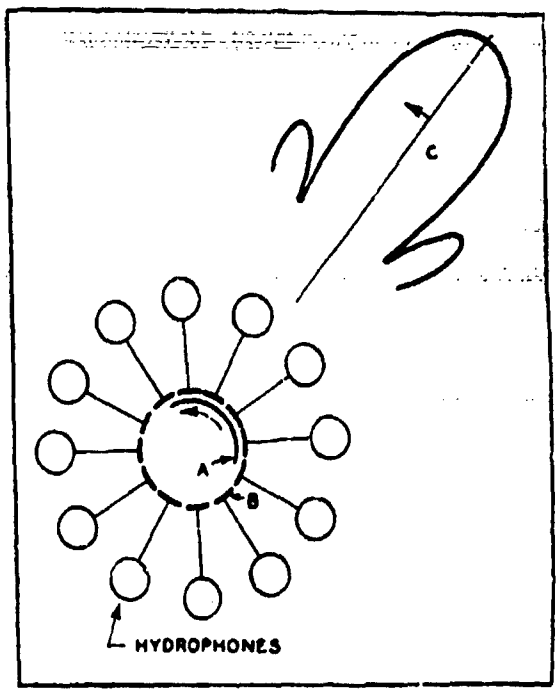


FIGURE 18. Schematic diagram illustrating CR scanning sonar. The twelve hydrophones are connected each to a segment ($B$) of a stationary commutator. These are contacted by a rotating brush ($A$) which connects five or six hydrophones to the receiver at any one time. In practice, the power is transmitted from commutator to brush by capacitive coupling rather than by actual contact. The receiving pattern of the array is markedly directional and rotates with the brush $A$. This is indicated at $C$.

The same result can be accomplished by using a ring of stationary hydrophones and connecting the receiver to them in succession by means of a commutator. This is shown in Figure 18, twelve hydrophones being shown. Each of these is connected to one segment $B$ of a stationary commutator. These segments are contacted by a rotating brush $A$, which connects five or six hydrophones to the receiver at any one time. As the brush rotates, these are disconnected in succession and replaced by others farther along the ring. The result is that the receiving pattern of the array is markedly directional, and rotates with the brush $A$.

Since sliding contacts would generate too much electrical noise, a small gap is provided between the moving brush $A$ and the commutator segments, forming an electric condenser. The electrical power is thus transmitted by capacitative coupling, rather than by conduction. This does not entirely eliminate

commutator noise, however. Scanning sonars operated on this principle are often designated by the initials CR (for capacitative rotation of the beam).

A second proposal for avoiding electric noise involves the elimination of all moving parts, and the use of electronic switches to perform the commutation. The initials ER (electronic rotation) are applied to this system.

### 11.3.5 Sector Scan Sonar

The echo length resulting from the necessarily rapid motion of the active volume can be somewhat increased by scanning only a sector rather than the complete horizon. In this case the path of the active volume must be somewhat as shown in Figure 19, and its speed can be reduced.

The oscillation of the receiver beam can be accomplished by a modification of the principles already discussed in connection with the BDI. Several stationary hydrophones are continuously connected to the receiver amplifier, each hydrophone having a phase shifting circuit interposed between it and the amplifier. The phase lags are so chosen that a sharp hydrophone pattern results, and they are varied, by electronic means, so that the axis of the beam oscillates with the required frequency. The basic principles that permit this to be accomplished have already been discussed in Section 11.1.

A plan position indicator is also required for sector scanning, the CRO spot again tracing a synchronous map of the motion of the active region.

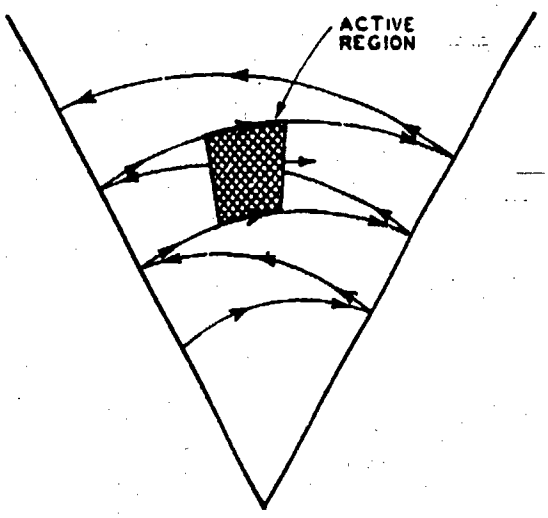


FIGURE 19. Schematic diagram illustrating the principle of scanning a sector rather than the complete horizon.

### 11.3.6 Rotating Projectors

One disadvantage of the pulsed scanning sonar is the relatively large power output that is required to obtain an adequate echo level. To insure this, the sound energy must be radiated in all directions at a level that must be at least as great as that which conventional sonars radiate in a narrow cone. Another disadvantage is that the reverberation level is high out of all proportion to the echo length $r_1$.

It might be supposed that this could be overcome by using a rotating directional projector and a nondirectional hydrophone; but a moment's reflection makes it apparent that this would make it impossible to determine the bearing of the target. The result achieved would not differ essentially from that obtained by having both hydrophone and projector nondirectional and stationary.

The possibility of rotating both projector and hydrophone presents itself. Detailed consideration of this proposal shows that the necessary output and the reverberation-echo ratio could both be reduced, but probably not by more than 10 db. It is doubtful whether this advantage would compensate for the additional complication of the gear.

In general, the rotating projector contributes little to accomplishing the basic function of the pulsed scanning sonar, which is to increase the speed of the active region beyond its normal value of half the velocity of sound. Consequently, rotating projectors can be considered only in connection with refinements of the gear and not in connection with its basic design.

It may be possible to abandon the basic principle of pulsed scanning sonar and to design useful systems operating on other principles and using rotating projectors. For example, if a directional projector makes one complete revolution and transmits sound of constantly increasing frequency during that time, the bearing of a stationary target can be identified by the frequency of its echo. The pitch of the echo from a moving target, however, will be determined both by its bearing and speed. Thus the problem of correctly estimating both bearing and motion of a target becomes complex. Moreover, the own-doppler caused by the motion of the sonar through the water, will introduce complications. The theory of this type

of sonar has not been carefully examined, but is somewhat similar to that of FM sonar, which will be discussed in the next section.

## 11.4 SCANNING SONAR—CONTINUOUS TRANSMISSION

### 11.4.1 Principle of FM Scanning Sonar

It was pointed out earlier in this chapter that the long delay between the transmission of the signal and the reception of the echo, caused by the low velocity of sound, is a handicap in search operations. Pulsed scanning sonar, as has been seen, utilizes this delay to scan all bearings, thus effectively increasing the speed of the active area.

The possibility of using the delay period to make other transmissions presents itself. Obviously, if this were done, it would be necessary to be able to associate a given echo with the particular signal that caused it. The idea can be illustrated very simply.

Assuming that the maximum practical range is about 3,000 yd, the maximum time delay is about 4 sec. Suppose that during these 4 sec eight pulses were transmitted at ½-sec intervals, the frequency of each pulse differing from its predecessor by a stated amount. They might form the tones of the major diatonic scale. Then a musically inclined listener would be able, on hearing an echo, to state its pitch and thus identify the ping responsible for it, provided, of course, both source and target were stationary, as otherwise the doppler effect would alter the pitch of the echo. Some means would have to be provided for recording the time and projector heading for each ping, to enable the determination of range and bearing of the target.

While this illustration is greatly oversimplified, it can serve as a point of departure for the discussion of a sonar that uses the principle.

In practice it is simpler to change the frequency more or less continuously than by abrupt steps. The frequency is allowed to decrease at a constant rate for some seconds; when it approaches the lower limit of the pass band of the receiver, it is suddenly increased to its original value, and the constant rate of decrease begins again. The principle is explained by the time graph of the transmitted frequency shown as the solid curve in Figure 20A. This kind of

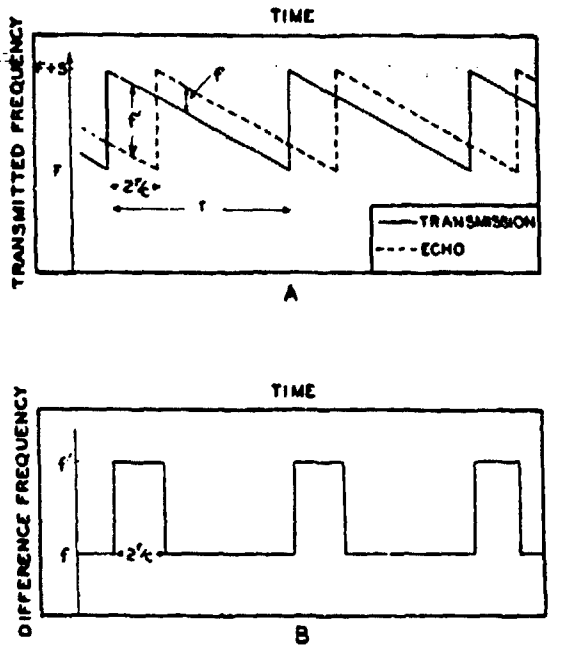


FIGURE 20. (A) Diagram illustrating the principle of FM sonar. The solid curve is the frequency-time graph of the "sawtooth" signal, the dotted curve that of the echo. The echo lags behind the signal by $2r/c$ sec; this causes a difference in the frequency $f$ or $f'$. *The time interval $T$ is the sawtooth interval;* (B) graph of the frequency difference as a function of time.

transmitted signal is known as a "sawtooth." The intensity of the transmitted sound is kept constant during the transmission.

A target located in the sound beam will return a continuous echo and, if both the sonar and target are stationary, this echo will reproduce the constant frequency change of the transmitted signal. However, because of the time delay between transmission and echo, the sawtooth graph of the echo will lag behind that of the signal, as shown by the dotted line in Figure 20A. During a portion of the sawtooth interval (indicated in the figure by $T$), the echo frequency will be less than the transmission frequency by a difference $f'$. During the remainder of the time $T$ it will be greater by a difference $f$. This is further illustrated by Figure 20B, in which the difference in frequencies between signal and echo is plotted as a function of the time. The frequency difference $f$ is seen to remain constant for relatively long periods, and then to jump suddenly to the value $f'$.

It is possible to perform the subtraction of the frequencies, i.e., to determine $f$ or $f'$, electrically, by applying the heterodyne principle: a voltage tapped from the transmitter is combined with the hydro-

phone output in a heterodyne stage of the receiving amplifier.

From either of these frequency differences $f$ or $f'$ the range can be determined; the calculation is given below.

Up to this point we have supposed that there is only one target in the sound beam. If there are more than one returning echoes, each echo will have its time graph of frequency, the displacement of which, relative to the graph of the signal, will depend on the range of the target. The output of the receiver will thus contain components of several frequencies, one pair of frequencies for each target in the sound field. This complex output must be analyzed into its components in order to determine the range of the several targets.

The active region from which echoes are being received occupies the whole of the sound field. Moreover, it is stationary if the projector and receiver headings are not changing. Thus the basic objective of continuous transmission sonar is to increase the size of the active region rather than its speed. The method just outlined for accomplishing this has been called FM sonar.

When used with stationary projector and hydrophone, FM sonar is not a bearing scanning device. However, it can also be used with a nondirectional projector and rotating directional receiver, and then becomes a scanning sonar but of a different type from that described in Section 11.3.

It is possible that other methods of increasing the size of the active area could be devised, but FM sonar is the only sonar of this class that has yet been built.

## 11.42 The Parameters of FM Sonar

### The Relation Between Target Range and Echo Frequency

How the frequency difference between the echo and the transmitted signal determines the range will be apparent from the following discussion and reference to Figure 20.

The duration of one sawtooth is $T$ sec. During this interval the frequency varies at a constant rate from $F+s$ to $F$; $s$ is called the *sweep* of the frequency. In one model, the QLA, $F = 36$ kc, and $s = 12$ kc. $T$ is usually from 1 to 12 sec.

The following relations exist between the several parameters:

1. The constant rate of frequency decrease is $s/T$ kc.

2. The delay time for an echo from range $r$ is $2r/c$ sec.

3. In $2r/c$ sec the frequency will therefore decrease by $(2r/c)(s/T)$ kc, and the frequency difference $f$, shown in Figure 20A, will be

$$f = \frac{2r}{c}\frac{s}{T} \text{ kc.} \tag{14}$$

4. From equation (14), the range $r$ is given by

$$r = cT\frac{f}{2s}. \tag{15}$$

5. The frequency difference $f$ will be maintained for $T - 2r/c$ sec. At the end of this interval, the transmitted signal has reached the bottom of the frequency sweep and returns to the top of the sweep. During a succeeding time interval equal to $2r/c$ sec, the echo frequency will be *less* than the transmitted signal frequency by $f'$ kc (see the figure), where

$$f' = s - f. \tag{16}$$

If the sawtooth interval $T$ is several times greater than the delay time of echoes from the maximum range, the frequency $f$ will be less than $s/2$, and the frequency $f'$ greater than $s/2$.

6. The duration of the frequency $f'$ will be considerably less than the duration of the frequency $f$. Consequently, it is economical to ignore the frequency $f'$ and concentrate on the determination of the frequency $f$.

### The Determination of $f$ and $r$.

From equation (15) it is evident that $f$ must be known to determine $r$. This is done as follows:

Suppose the heterodyned output (the hydrophone output mixed with a sample of the signal) is passed through a band-pass filter centered at $f$ kc, and of a width $w$ kc. This filter will then pass an echo only if its frequency lies within this band, namely, between $f - w/2$ and $f + w/2$. This is equivalent to saying that the sound energy admitted by this filter comes from a certain active area (see Figure 21) which will be a sector of a circular ring. By using a battery of such filters, a series of channels is established, each of which is constantly alert to echoes coming from a certain active area. The dimensions of the area corresponding to a given filter are easily calculated. The greatest ranges from which the particular filter under

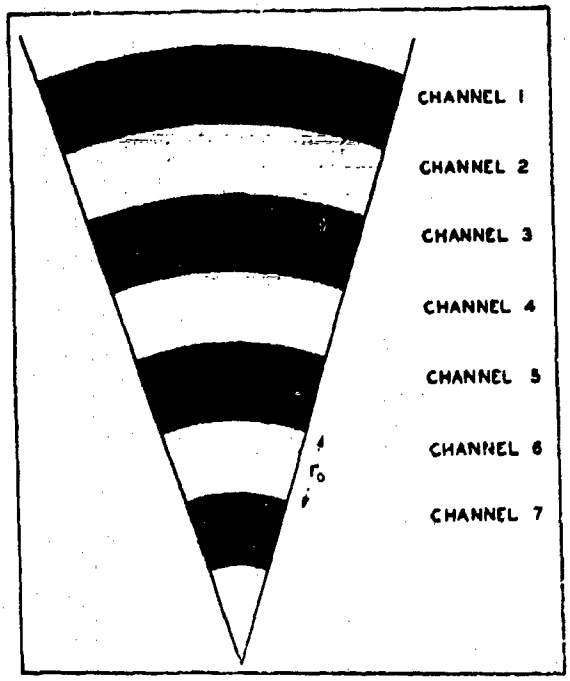


FIGURE 21. Active areas associated with the individual channels in FM sonar.

consideration will accept an echo is, from equation (15),

$$cT\frac{f+\frac{1}{2}w}{2s}$$

and the smallest range,

$$cT\frac{f-\frac{1}{2}w}{2s}.$$

The radial extent $r_0$ of the area is the difference between the two ranges, and thus

$$r_0 = cT\frac{w}{2s}. \qquad (17)$$

The other dimension of the active area is determined by the range and the width of the hydrophone beam; and from elementary geometry its mean value is the product of the mean range times the angular width of the beam expressed in radians.

The dimensions of the active area are proportional to the sawtooth interval $T$ and, insofar as they are determined by $T$, are under the operator's control. For example, if $T = 12$ sec, $s = 12$ kc, and $w = 35$ c, then $r_0 = 30$ yd. Reducing the value of $T$ to 1 sec would make $r_0 = 2.5$ yd.

As has been remarked, each of the channels will be almost constantly alert to targets in the particular

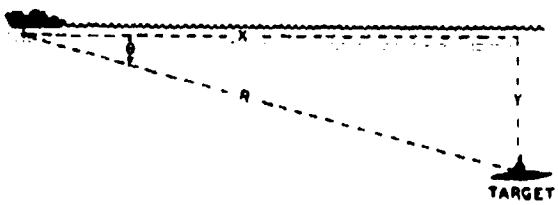


FIGURE 22. The geometry of depth determination. The range indicator shows the slant range $R$, the depth of the target below the projector is $Y$, and its horizontal range is $X$. Knowing the angle of tilt $\theta$, the value of $X$ and $Y$ can be calculated from $X = R\cos\theta$, $Y = R\sin\theta$.

area associated with it. These areas are indicated in Figure 21. The active area of each channel is stationary, and by making the areas of adjacent channels overlap slightly, the whole sound field can be covered, as shown in the figure.

Because of the exclusion of the frequencies $f'$, each channel would normally be inert for a part of each sawtooth cycle. However, this fraction can be made as small as desired or can even be completely eliminated by a recent ingenious development.

Since the active areas are stationary, it might seem that the range could not be determined so precisely as is possible with pinging sonars. Actually, however, the precision is the same as for a ping length equal to $r_0$. The quantity $r_0$ defined by equation (17) can be called the *effective ping length* of FM sonar.

## RANGE AND BEARING INDICATION

The range is read on an oscilloscope with a persistent screen. The filters corresponding to the various mean ranges of the several channels are arranged so that their output lights up the oscilloscope trace at a point whose distance from the center is proportional to the frequency $f$ and thus to the range.

An additional device makes the bearing of the echo spot on the oscilloscope correspond to the hydrophone heading. Figure 2? is a diagram of the FM sonar screen.

For complete details the reader is referred to the discussions presented in several previously published reports.[2,3,5,6]

## ECHO DURATION

The duration of the echo will depend, in the first place, on whether or not the hydrophone is stationary or is being rotated. If the projector is nondirectional,

then the echo in a stationary hydrophone will have a duration nearly equal to the sawtooth period $T$. If the hydrophone is rotated, the echo duration may be reduced, becoming equal to the time required for the hydrophone beam to sweep across the target. The rate of rotation can be made as small as is required to obtain an echo of any desired duration less than $T$. In this respect FM sonar differs from the pulsed scanning sonars described previously.

The rotation rate cannot be increased beyond a certain critical value, however. This limitation is a consequence of the use of filters, which require a finite time interval to respond fully to the echo. The minimum time interval depends on the width $w$ of the filter, and must be greater than $1/w$ sec, if $w$ is in cycles per second.

Suppose the hydrophone is rotated at a rate of $N$ rpm and that its beam width is $\theta$ degrees. A complete revolution requires $1/N$ minutes $= 60/N$ sec. The beam occupies $\theta/360$ of a revolution; thus the time required for it to sweep across a given point is $\theta/360$ times $60/N = \theta/6N$ sec. Hence, it is necessary that

$$\frac{\theta}{6N} > \frac{1}{w},$$

from which it follows that $N$ must be less than $\frac{1}{6}\theta w$.

As an example, let $\theta = 11$ degrees and $w = 35$ c; then $N$ must be less than 65 rpm. The echo duration for 65 rpm is 29 msec; the echo length corresponding to this is 23 yd. If the rotation is slower, the echo length will be increased.

### 11.43 The Doppler Range Error

It is clear that, since FM sonar uses the frequency of the echo to determine the range of the target, the doppler shift resulting from a possible relative motion of sonar and target will introduce an error into the indicated range. The magnitude of this error must be evaluated.

FM sonar is calibrated so as to indicate the range $r_I$ ($I$ for "indicated") according to equation (15),

$$r_I = \frac{cTf}{2s}.$$

This is the correct range if the range of the target is not changing, but it is necessary to calculate the error in $r_I$ caused by the doppler change of frequency when the range is opening or closing.

In all echo-ranging operations, three instants of time must be considered. These are (1) $t_1$, the time at which the primary sound was transmitted from the projector; (2) $t_T$, the time at which the echo was reflected from the target; and (3) $t_E$, the time at which the echo was received.

If there is any relative motion of sonar and target, the range will be different at these three times. Call the corresponding ranges $r_1$, $r_T$, and $r_E$. In the case of pulsed sonar, the range indicated is always $r_T$, regardless of the possible motion of sonar and target. The differences between $r_1$, $r_T$, and $r_E$ are negligible. This can be quickly verified when it is remembered that a speed of 1 knot is equivalent to 0.56 yd per sec, so that a speed of 25 knots would involve an error of less than 50 yd in a range of about 3,000 yd.

None of the three ranges just defined is the range indicated by FM sonar. This range $r_I$ is defined by equation (15). In order to calculate $r_I$, one must distinguish between three supersonic frequencies.

1. $F_1$, the frequency that was being transmitted at the time $t_1$.

2. $F_E$, the frequency that was being transmitted at the time $t_E$.

3. $F'_E$, the frequency of the echo that was being received at the time $t_E$.

The quantity $f$ of equation (15) is obviously $F'_E - F_E$, hence

$$r_I = \frac{cT}{2s}(F'_E - F_E). \tag{18}$$

Let us examine the frequencies $F_E$ and $F'_E$ more closely. To simplify the calculation, it may be assumed that the sonar is stationary. No error is introduced by this assumption provided $v$ of equation (20) is interpreted as the range rate. When the target reflects the sound, its range is $r_T$, and the transmitted frequency at the time $t_E$ will have been reduced by $(2r_T/c)(s/T)$. The possible motion of the target will not affect this quantity. Thus the frequency being emitted at the instant when the echo is received is given by

$$F_E = F_1 - \frac{2s}{cT} r_T. \tag{19}$$

The frequency of the echo, on the other hand, is affected by the motion of the target. From the theory of the doppler effect, the value of $F'_E$ will approximately be

$$F'_E = F_1 \pm \frac{2v}{c} F_1, \tag{20}$$

where $\dot{r}$ is the range rate of the target. Subtracting equation (19) from equation (20) we have

$$F'_E - F_E = \frac{2s}{cT} r_T \pm \frac{2v}{c} F_1, \qquad (21)$$

and substituting equation (21) into equation (18) gives

$$r_I = r_T \pm \frac{vT}{s} F_1. \qquad (22)$$

The error in the indicated range is therefore proportional to the velocity of the target, and is zero only for stationary targets.

As an example, let $T = 12$ sec, $s = 12$ kc, and $F_1 = 36$ to 48 kc, then

$$\frac{TF_1}{s} = 36 \text{ to } 48 \text{ sec.}$$

The range error is thus the distance moved by the target in 36 to 48 sec, the larger error occurring when the sawtooth frequency $F_1$ is high, the smaller when it is low. The distance traversed in 48 sec by a submarine at 10 knots is slightly over 200 yd.

It should be noted that the error is also proportional to the sawtooth period. Thus if in the example, $T$ had been 1 sec rather than 12, the range error would be the distance moved by the target in 3 to 4 sec, about 20 yd at a speed of 10 knots.

It may also be remarked that this range *error* is very similar to the range *correction* which must be made in determining the time to fire on a moving target. It has been proposed to utilize this similarity so that the indicated range of FM sonar can be used without this correction in fire-control problems. For this application, it is essential that the frequency increase, rather than decrease, during each sawtooth period.

Recent development of the gear gives promise of utilizing the doppler effect for the determination of the range rate, and of eliminating the range error.

### 11.4.4 Comparison of FM and CR Sonars

Since FM and CR sonars have very similar functions and both result in plan position indication, it is desirable to make a detailed comparison of the two. For this purpose the points listed in Section 11.3.2 will be considered, and in the same order as was done there.

1. The use of doppler to determine the velocity of the target is difficult with both systems but may be more feasible in the case of FM sonar. The range error of FM sonar must be minimized by proper choice of its parameters, unless it can be utilized as suggested.

2. In practice, it is found advantageous to listen to the echo with FM sonar as well as to watch its position on the plan position indicator. It is possible that this is also the case with CR sonar.

3. CR sonar must use a high rate of rotation and a wide-band receiver. FM sonar must use a low rate of rotation and a narrow-band receiver. Thus FM sonar will be less affected by background noise than is CR sonar. On the other hand, the slow rate of rotation may be a disadvantage for FM sonar in certain applications.

4. The level of reverberation will in both cases be determined by the quantity $r_0$. This is the radial extent of the active area in each case, and can be made the same by suitable choice of parameters.

5. The duration of the echo and the coherence of the reverberation will in both cases be determined by the rate of rotation. Since FM sonar can be rotated slowly, its echo duration can be made longer than that of CR sonar. This is an advantage of FM sonar since the ear can detect and interpret long echoes more efficiently than short ones.

Both systems differ from the standard sonars in that the intensity of reverberation is determined by other parameters than those that determine the echo duration. It does not appear possible to use this advantageously in the case of CR sonar. The corresponding problem in the case of FM sonar deserves attention.

6. The target strength is, in both cases, determined by $r_0$. Both systems have been unexpectedly successful in detecting weak echoes from small targets. It may be that this is related to the use of a plan position indicator.

The bearing accuracy achievable by either system is determined by the hydrophone directivity. In both cases, an increased directivity results in a shorter echo. This is less serious with the long echoes of FM sonar than with the short echoes of CR sonar.

In principle, both systems can be adapted to sector scanning as well as to the complete 360-degree rotation. A number of technical problems are different in the two cases, but have not yet been fully explored.

The maximum ranges achievable by the two systems can be estimated from the foregoing principles. It appears that noise is apt to be the limiting factor with CR sonar, while reverberation is apt to limit the maximum range of FM sonar. There have not yet been sufficient experimental measurements, nor enough development work, to determine whether either system has an ultimate advantage over the other.

## 11.5 THE DETECTION OF SMALL OBJECTS

### 11.5.1 General Principles

The echo-ranging gear in use at the beginning of World War II was designed for the detection of relatively large submarines. As the war progressed it became imperative to design equipment for the detection of mines and other small objects. The standard test object in this development work was a sphere 3 ft in diameter. Its target strength is some 20 db lower than that of a large submarine. Because of the small target strength, the ranges in small-object detection will generally be comparatively short, and thus limited by reverberation rather than background noise.

In order than an echo be detected against a background of reverberation, it is necessary that the total target strength of all the scatterers in the active region of a ping should be less than the target strength of the sphere; otherwise the reverberation intensity will be greater than that of the echo, and masking will prevent detection.

The target strength of the reverberation can be decreased by reducing the size of the active region. There are two ways in which this can be accomplished: (1) the ping length can be decreased, and (2) the beam can be made narrower. The latter method is not suitable for shipboard installations since it involves a decrease in the effective search area and thus would cause great difficulties in maintaining contact with the target. That leaves only the ping length as an available parameter for this purpose.

The use of short pings is thus a characteristic of many sonars designed for small-object detection. The reasons for the success, in this phase of echo ranging, of CR and FM scanning sonars, which do not use short pings, are not clearly understood; as was suggested above, their success probably depends on the plan position presentation of the echo. The present discussion will be concerned largely with the use of short pings.

### 11.5.2 Echo: Reverberation Ratio as Function of Ping Length

The theories developed in the previous chapters indicate that the reverberation intensity should be proportional to the ping length $r_0$; the echo level, on the contrary, should be independent of ping length. The latter statement is subject to modification when the ping length becomes less than the extent of the target in range. If the target is a complicated one, its target strength will be less for short pings, as has been explained (Chapter 8). This is because the echoes from some parts of the target will no longer overlap those from other parts. However, if the target has a smooth surface, with no irregularities of dimensions comparable to one wavelength of the sound, this reduction in target strength will probably not occur. The theory of echo formation has not been worked out with sufficient completeness to cover this point.

The results of some experiments are summarized in Table 2.[9] Although they were not suitable for the calculation of the target strength of a smooth 3-ft sphere, they show that the echo-reverberation ratio increases with decreasing ping length even when the latter is as small as one-eighth the diameter of the sphere. They also show that this ratio decreases with

TABLE 2. Echo ranging on a 3-ft sphere.

| $r_0$ = ping length (yd) | Range (yd) | Echo: reverberation (db) | Reverberation (db, arbitrary reference level) | $10 \log \frac{r_0}{0.13}$ |
|---|---|---|---|---|
| 0.13 | 82 | 23 | 26 | 0 |
| | 200 | 19 | 9 | ... |
| | 360 | 11 | 15 | ... |
| 0.8 | 315 | 15 | 21 | 8 |
| | 370 | 7 | 25 | ... |
| 2.4 | 85 | 15 | 35 | 13 |
| | 300 | 5 | 27 | ... |
| | 380 | 4 | 30 | ... |
| 8.0 | 85 | 14 | 46 | 18 |
| | 300 | 5 | 27 | ... |

increasing range out to 400 yd, thus supporting the idea that reverberation, rather than background noise, is the limiting factor in this work. This is rather surprising, since a wide-band receiver is necessary for the use of these very short pings. The qualitative distinction between reverberation and noise largely disappears at these ping lengths, for the two sound alike to a listener and have a similar appearance on an oscillogram. Consequently, these experiments are the best evidence that reverberation and not noise is the masking agent. This high level of reverberation is due to a combination of factors, principally the shallowness of the water and the shortness of the range. Both are typical of the conditions under which the gear must operate.

In the right-hand column the ratios of the ping lengths to the shortest ping length is given. Comparison with the adjacent column shows that the reverberation intensity actually is roughly proportional to the ping length, as predicted by the theory.

## 11.6 VARIATION OF GAIN

In Chapter 9, it has been shown that the optimal gain setting is one which makes the masking background just audible. If the gain is less than this, weak signals will not be heard, even though they are stronger than the background. If the gain is much greater than this, there is danger that a signal will overload the amplifier, resulting in distortion and a reduction of the signal-background ratio in the airborne output.

This situation is complicated when reverberation is the masking background, because the reverberation level varies greatly during the period following transmission. Many of the oscillograms reproduced in this volume show overloading during the early period, indicating that the gain setting was too high for this period (see Figures 9 and 20 of Chapter 5). During a later period, the reverberation is not readable, indicating that the gain setting was too low. Other figures show abrupt changes in gain at various times, these changes being made automatically to avoid these difficulties.

The obvious solution for this problem is to devise a sonar receiver in which the gain continuously increases during the period following transmission of the ping. The receiving circuits for accomplishing this *time variation of gain* [TVG] are controlled by the discharge of a condenser that was charged during the transmission. By altering the resistance of the discharge circuit, the rate at which the gain increases can be controlled. By altering the voltage to which the condenser is charged, the total increase in gain can be adjusted.[10]

While TVG improves the operation of echo-ranging gear, it fails to meet all requirements. One disadvantage is that the gain is increased in a regular manner; this would be satisfactory if reverberation decreased in an equally regular manner, but, as has been seen, this is not always the case, especially in shallow water. Consequently, the possibility of using the background to control the instantaneous gain was explored.

Circuits, called *automatic volume controls* [AVC], that could accomplish this had been used in radio receivers. The inclusion of these devices in sonar receivers proved to be very disadvantageous. The AVC circuits can be adjusted so that they respond rapidly or slowly to changes in the input. It was found that, if they respond to the rapid fluctuation of reverberation, they also respond to the change in intensity due to the echo. This is unavoidable, since the duration of the reverberation blobs is about the same as that of the echo from a point target. With this adjustment, AVC reduces the gain during the time the echo is being received, an obviously undesirable situation. If, on the other hand, the AVC is adjusted so that it does not reduce the gain during the echo, it becomes so sluggish that it fails to respond to the slower changes in mean reverberation level, e.g., to the peak of bottom reverberation.[11,12]

A compromise solution, called *reverberation controlled gain* [RCG], has been developed. This is similar to TVG in that the gain constantly increases during the period following transmission. It is similar to AVC in that the momentary level of the receiver input controls its operation. However, it is the *rate of increase* of gain that is controlled and not the *gain* itself. It is obvious that such a device cannot reduce the gain when the echo arrives; it will merely reduce the amount by which the gain increases during the echo. It will thus not have the disadvantage of AVC. It will respond somewhat to the special characteristics of reverberation at a specific time and place, and thus not suffer the disadvantage of a TVG circuit that is improperly adjusted for the momentary conditions.

## 11.7 DEPTH DETERMINATION

### 11.7.1 Tilting Beam Mountings for Transducers

In Chapter 1 it has been noted that a horizontal directional beam may pass over a deeply submerged target at close range. As a result, the intensity of the sound incident on the target, and consequently that of the echo also, are reduced. This renders it difficult or impossible to maintain contact at close ranges, and the difficulty is increased because of the high level of reverberation at short ranges, requiring an increased echo level for recognition.

This can be overcome by mounting the transducer after the fashion of a searchlight, so that it can not only be rotated about a vertical axis but also tilted about a horizontal axis. By depressing the axis of the beam toward the deep target, and hence away from the surface, the echo level can be increased, and the surface reverberation decreased. While such a mounting is complicated, both from the standpoint of construction and operation, its advantages are great.

### 11.7.2 Depth Determination with Tilting Beams

In addition to making it possible to maintain contact at short ranges and great depth, the tilting beam makes it possible to determine both depth and horizontal range. The geometry of the situation is shown in Figure 22. The range indicator of the sonar shows the *slant range* $R$; the *depth* of the target below the projector is $Y$, and its *horizontal range* is $X$. Knowing the angle of tilt $\theta$, the values of $X$ and $Y$ can be calculated from the equations

$$X = R \cos \theta, \qquad Y = R \sin \theta. \tag{23}$$

Various automatic or semiautomatic methods of performing this calculation have been devised.

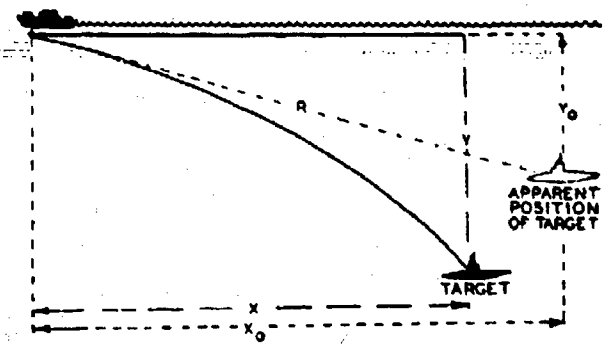


FIGURE 23. Effect of downward refraction on the situation shown in Figure 22. The values of the depth and horizontal range calculated as above would yield $Y_0$ and $X_0$ instead of the actual values $Y$ and $X$.

### 11.7.3 Refraction Error in Depth Determination

Equation (23) assumes that sound rays are straight lines. If the rays are refracted, the values computed from this equation (call them $X_0$ and $Y_0$) will not be the true values, as is shown in Figure 23. The errors $Y - Y_0$ and $X - X_0$ can be quite large, especially when there is marked downward refraction.

The errors arise from two causes: the sound does not travel in a constant direction, and it does not travel at a constant speed. The determination of the corrections to be applied is similar to a problem in exterior ballistics. The problem can be solved by the same methods, but when there is a marked thermocline, the magnitude of the correction required, and consequently the required accuracy of the approximate calculation, is increased.

It has been possible to reduce these calculations to a semiautomatic form. Several characteristics of the bathythermogram are noted, and are used to enter a table. This table indicates a single number, which designates the proper scale to be used on the sonar indicator. These scales are too numerous to be engraved on a single plate, so that interchangeable plates must be provided. Once the proper plate is in position, the correction is applied automatically.

# *PART III*

# *LISTENING*

## Chapter 12

# THE ACOUSTIC OUTPUT OF SHIPS AND SUBMARINES

## 12.1 INTRODUCTION

### 12.1.1 Listening to Underwater Sounds in Warfare

THE OFFENSIVE function of all applications of underwater acoustics in warfare is the detection and location of enemy craft; the defensive avoidance of detection on the part of the patrolling vessel is an important corollary. The role of echo ranging in subsurface warfare has been described in Part II of this book; Part III is devoted to the problems presented by listening. A brief comparison of the two operations can serve to introduce the subject.

Echo ranging and listening differ essentially in several ways. In echo ranging, the searching vessel projects a sound signal into the water intentionally in the expectation that the sound will strike a target and that enough of the energy will be returned by the target to the transducer to activate the receiver so that the operator can recognize the echo. The primary source of the sound is in the searching vessel; the target is only a secondary source. The transmission of the sound is a two-way process. In listening, the signal is sound emitted involuntarily by the target itself, which therefore is the primary source. The transmission is a one-way process. This first consideration suggests that losses by transmission will be smaller in the case of listening, and that detection should be possible at longer ranges by listening than by echo ranging, provided only that the sound output of the targets is comparable to that of the standard echo-ranging projector. This last is not often the case.* The noisiest type of ship, a large battleship moving at high speed, has an overall output of sound of about the same level as a standard projector; but whereas the sound from a projector is a pure tone, and the echo has frequencies that are restricted to about 100 c in the neighborhood of the transmitted frequencies, the sound from a battleship has components of a wide range of frequencies, and hence is more easily masked by background noise. Nevertheless, conditions are frequently such that ships are detected by listening at ranges of 10,000 yd and more, whereas echo ranging is rarely effective above 3,000 yd. Echo ranging, however, enables the range and bearing of the target to be determined accurately; listening gives the bearing quite accurately, but in its most elementary form it provides little or no information on the range.

Listening is used chiefly by submarines. A surface vessel produces considerable noise, and this noise interferes with the detection of the sounds of other ships. This is especially true of the low sounds of submarines. On the other hand, this difference in the noise output enables a submarine to detect the presence of a surface vessel rather easily. An antisubmarine surface vessel, moreover, will generally not use evasive tactics. Therefore it will not hesitate to emit a powerful signal into the water, and thus gain the advantages of echo ranging; whereas a submarine will hesitate to reveal its presence by echo ranging except in the last stages of an attack.

Listening plays an important part in the detection of submarines by harbor protection stations. It is true that a submarine executing a sneak attack is nearly noiseless; still it is not possible to suppress all noise, and so a listening watch may provide several minutes of warning. The expendable radio sono buoy, dropped from aircraft, carries a hydrophone and radios the received sound back to the aircraft. Anchored radio sono buoys are used in harbor defense installations, as are cable-connected hydrophones mounted on the ocean bottom.

In order that listening be a tactical aid, the sound operator must be able:

1. To distinguish the sound emitted by the target from the usual background noise. This requires familiarity with both.

2. To distinguish between the various kinds of ship sounds with a view to possible identification of the type of vessel emitting them and to obtain information on its operating conditions.

3. Having detected and perhaps partially identified a target, to obtain information concerning its approximate location and motion while it is still at comparatively long range.

These considerations suggest the value and purpose of the investigation of ship and submarine

* An obvious and important exception occurs when the target is pinging. The enemy can hear the pings at much longer ranges than those at which echoes can be detected.

sounds. Other applications of such information immediately present themselves, besides those just discussed. One application is to the problem of the control or possible elimination of revealing noises. The basic principle in this problem is the same as that underlying visual camouflage: to render the target inconspicuous by making it resemble its background. This means that the sounds that are unintentionally and unavoidably emitted should, in the ideal case, have spectra that are very similar to that of the background noise. This study, however, is still in its beginning stages.

Another application is found in the design and operation of acoustic mines and in the prediction of their actuating ranges. This, as well as the defense against mines of this type, evidently requires a knowledge of the sounds emitted by the vessels against which they are to be used.

### 12.1.2 Basic Factors in Listening

The physical factors involved in listening are the same as those in echo ranging. The target acts as a source of sound that must be transmitted to the receiver through the water and detected against a background of masking noise. The ability of the ear or automatic mechanism to recognize the signal depends on certain basic factors.

1. The nature of the signal radiated by the source. This will form the subject matter of this chapter.
2. The transmission loss of sound in water. This has been discussed in Part I and will enter only incidentally into the discussion here.
3. The nature of the masking sounds. This forms the material of Chapter 13.
4. The response and directivity of the listening gear. This is discussed in Section 12.3.
5. The recognition differential. This is taken up in Chapter 14, which deals with psychoacoustic effects.

The remaining part of this section will discuss the nature and method of measuring underwater sounds in general; following this, the listening gear in current use is described in Section 12.3, and the characteristics of the various target sounds are discussed in detail in the succeeding sections of this chapter.

### 12.1.3 Underwater Sound in General

Underwater sounds are of many diverse kinds. The simplest way to distinguish among them is to classify them functionally as *wanted* and *unwanted* sounds. Wanted sounds come from a localized source. They can be conveniently designated by their source, as ship sounds, submarine sounds, torpedo sounds, and the like, or generically by the term "signal." Unwanted sounds come from many possible sources and tend to make the detection of the wanted sounds more difficult. They are the background noises that were decribed in Chapter 9 and include self-noise and ambient noise. A more detailed description of the spectra of these sounds will be presented in Chapter 13.

Underwater sounds are usually complex; that is, they comprise components that have frequencies which may range from a few cycles to many kilocycles per second. The *overall intensity* of the composite sound from a given source, as well as the manner in which the sound energy is distributed among the different frequencies, may fluctuate greatly from moment to moment. Hence the complete description of an underwater sound will concern itself with the *spectrum*, which shows how the sound energy is distributed among the several frequencies, and also with the *time pattern*, which describes the audible fluctuation of the sound. Other audible characteristics are usually not given a quantitative description, and are called the *quality* of the sound.

Two general forms of listening gear are used: sonic and supersonic. The former consists essentially of a hydrophone connected to a loudspeaker through a simple amplifier. The latter is similar, but a heterodyne stage is included, to convert the supersonic vibrations into audible sound.

## 12.2 THE MEASUREMENT OF UNDERWATER SOUND

### 12.2.1 Response Curves

Underwater sounds are measured by means of a hydrophone connected through an amplifier to some form of electrical meter. The latter may be of the recording type, or a simple milliammeter. Two kinds of recording instruments are used, oscillographs and power-level meters. Oscillographs respond rapidly, and their record is a more or less faithful graph of the instantaneous pressure of the sound on the hydrophone. Power-level meters respond less rapidly, and are designed to record the logarithm of the average

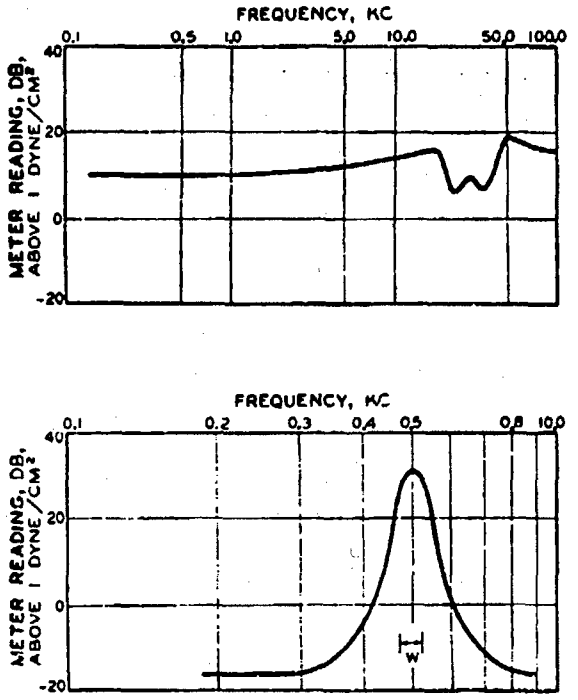


FIGURE 1. Two extreme types of response curves. The upper curve is that of a "flat" system which responds about equally to sound of any frequency between 0.1 and 5.0 kc, whereas the lower curve is that of a "resonant" system which responds only to sounds in the neighborhood of 500 c.

intensity, i.e., the sound level as defined in Section 1.2.

All measuring systems must be calibrated. In principle, this is accomplished by placing the hydrophone in a sound field of known frequency and level and noting the reading. The graph showing the reading corresponding to 1 dyne per sq cm at each frequency is called the response curve of the system, and has already been discussed in connection with echo-ranging gear. For the reader's convenience, the discussion is summarized here.

Response curves of two extreme types are shown in Figure 1. The upper curve is that of a *flat* system which responds about equally to sound of any frequency between 0.1 and 5.0 kc, while the lower curve is that of a *resonant* system which responds only to sounds in the neighborhood of 500 c. Both kinds of system have their uses. A flat system can be converted into a resonant system by the insertion of a filter.

Systems whose response curves have a maximum at a frequency $f$ are said to resonate at that frequency. The width $w$ of the resonance peak (see lower curve, Figure 1) is usually defined as the frequency separation of the two points on the curve which are 3 db below the maximum. Another useful quantity is the resonance parameter $Q = f/w$. If $Q$ is greater than 10 or 20, the system is said to be highly resonant. If $Q$ is less than 4 or 5, the system is nonresonant.

The various components (hydrophone, amplifier, loudspeaker) are all characterized by response curves. Examples of response curves for some hydrophones are given in Section 12.3.

## 12.2.2 Overall Levels

Most sounds encountered in listening are not pure tones of a definite frequency or pitch. When a composite sound is measured with two systems having different response curves, the two meter readings will usually be different. In order to obtain comparable results, some correction must be made.

This correction is simple only in the case of flat systems, where response is practically independent of frequency. In that case, the meter reading minus the numerical value of the response (10 db in the system represented by the upper curve of Figure 1) is a number which is independent of the system. It is called the overall level of the sound.

Ideally, the overall level should be measured with a system in which the response curve is a horizontal line extending from 0 c to infinity. Practically, such systems are impossible to build, and a compromise is necessary. In the present book, the overall level is supposed to be measured with a system that responds equally to all frequencies between 0.1 and 10 kc, but with a response curve which drops rapidly outside this range.

The overall level is a useful characteristic of a sound, but does not completely describe it. There are circumstances in which one sound of given overall level may be audible, while another of the same overall level is inaudible.

## 12.2.3 Spectrum Level

In order to discuss those properties of sounds that are not determined by their overall level, it is convenient to use the concept of spectrum level, which was defined in Chapter 9.

The spectrum level is defined in terms of an ideal system, but can also be determined from the reading of an actual system, provided its response is suf-

ficiently peaked. The effective bandwidth $w$ of an actual system must be determined in a way that need not be discussed here. Often the definition of $w$ as the width of the resonance peak between the 3-db points can be used. Spectrum-level meters are of two kinds, one of which is furnished with a series of filters of known width and mid-frequency. The other kind is arranged so that the mid-frequency of its response is continuously variable, the bandwidth remaining constant.

For any sound, the spectrum level can be plotted as a function of the frequency (see Figure 15). Such a graph is called the spectrum of the sound.

It sometimes happens that more or less pure tones are emitted simultaneously with a sound having a continuous spectrum. This occurs, for example, when a propeller is driven through a gear train that has not been quieted, or when the propeller blade vibrates like a whistle because of the flow of water past its blades. Such single-frequency sounds can be shown on the spectrum as very high, narrow peaks. The accurate measurement of these peaks presents practical problems that need not be considered here.

For convenience, these peaks are called "lines." A spectrum that does not contain lines is a continuous one. A line spectrum may be superposed on a continuous one (see Figures 23 and 24) or may occur without any noteworthy continuous spectrum (as in the case of a musical instrument).

### 12.2.4 Oscillograms

A sound is not determined uniquely even by its spectrum. For many purposes, however, two sounds having the same spectrum may be considered as equivalent, even though they may be recognizably different to the ear. Descriptive terms, such as "hissing," "burbling," "crackling," are often useful in this connection.

If more detailed information about the sound is needed, an oscillogram recorded with a flat system is obtained. This is essentially a graph of the instantaneous pressure in the sound wave as a function of time.

### 12.2.5 Distortion

If a sound is passed through a system whose response is not flat, it will be distorted. That is, if the output stage of the system is a loudspeaker, the sound emitted will not be a faithful reproduction of the incident sound. If the output of the system is a voltage, the changes in this voltage will not be proportional to the changes in the sound pressure.

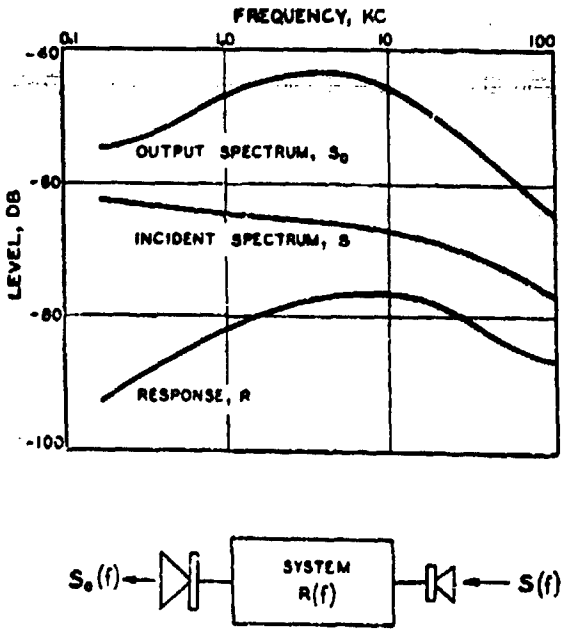


FIGURE 2. Diagram illustrating the effect of the response of a system on the spectrum of an incident sound. If $S(f)$ is the spectrum of the incident sound and $R(f)$ the response of the system, the output will have the spectrum $S_0(f) = S(f) + R(f)$.

If $S(f)$ is the spectrum of the incident sound and $R(f)$ the response of the system, the output will have the spectrum $S_0(f) = S(f) + R(f)$. This is illustrated by Figure 2.

### 12.2.6 Inherent Threshold

Most measuring systems are arranged so that their sensitivity can be varied in steps, resulting in a shift of the response curve parallel to itself by a known number of decibels. For sounds of high level, a low sensitivity is sufficient; for sounds of low level, high sensitivity is needed.

As the sensitivity is increased, a stage will ultimately be reached when the meter shows a reading even though the hydrophone is in a very quiet place. This is caused by electrical and other noise originating in the measuring system itself. The inherent threshold has already been discussed in Chapter 9, and is the sound level which would, in the absence

of the system noise, cause the same meter reading as the system noise.

Sounds which are much below the inherent threshold cannot be measured. Sounds at the threshold level can be detected by a change in the meter reading (theoretically, 3 db) but a correction must be applied to the reading in order to obtain the true sound level. Not until the incident sound is 6 or 10 db above the threshold level can the meter reading be used without correction.

This concept of threshold is an important one, and can also be applied to the components of a system, as well as to the ear itself.

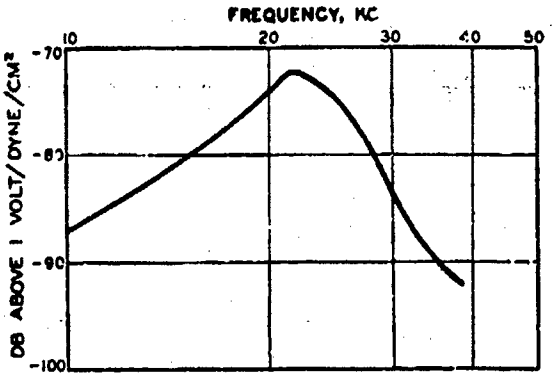


FIGURE 3. Response curve of a standard supersonic hydrophone.[10]

## 12 3 HYDROPHONES

### 12 3.1 The Response of Hydrophones

When a hydrophone is placed in an underwater sound field its diaphragm oscillates in response to the variations in hydrostatic pressure at its face. These oscillations of the diaphragm are transformed into electric energy as discussed in Sections 7.2 and 7.3.

The magnitude of the voltage generated in the receiver is a function of the pressure on the diaphragm of the hydrophone. This response of the hydrophone partially determines the response of any system into which the hydrophone may be connected. Hydrophone response at the frequency $f$ is defined as the electromotive force developed in the hydrophone when it is in a sound field of frequency $f$ and rms pressure of 1 dyne per sq cm.

If $e$ is the emf generated by the hydrophone when in a sound field of $p$ dynes per sq cm, its response is $20 \log (e/p)$ db. It will, in general, be a function of the frequency, as discussed above. Very few hydrophones have flat response curves; exceptions are a few specially designed for scientific measurements. In Table 1, typical values of the response of various hydrophones are given in Column 7. Figures 3 and 4 show detailed curves for standard sonic and supersonic hydrophones.

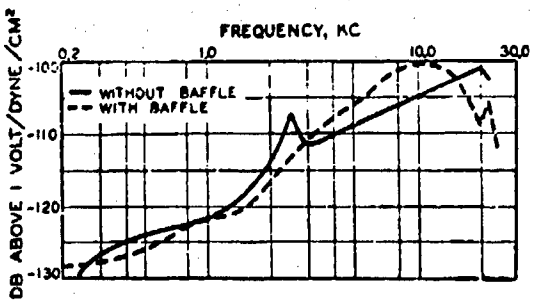


FIGURE 4. Response curves of a standard sonic hydrophone, used with and without a baffle.[10]

TABLE 1. Characteristics of some commonly used hydrophones.[10]

| Code | Type | Approximate diaphragm diam (in.) | Resonant frequency (kc) | Directivity index (db) | Resonance parameter ($Q$) | Hydrophone response (db above 1 v per dyne per sq cm) | Threshold (db above 1 dyne per sq cm) |
|---|---|---|---|---|---|---|---|
| QC | MS* | 15¾ | 24 | −22 | 10 to 110 | −80 to −85 (24 kc) | −92 |
| QBG | RS* | 8¼ | Broad | −17 | 3 to 6 | −80 (24 kc) | −98 |
| JK | RS | 15¾ | Broad | −23 | 3 | −64 (24 kc) | −105 |
| British ASDIC | Quartz | 15 | 15 | −22 | 55 to 80 | −42†(15 kc) | −107 |
| JP | MS | 2×40 (tube) | Broad | 0 (0.1 kc) −8.0 (5.0 kc) −11.0 (10 kc) | | −135 to −105 (0.1 to 10 kc) | −48 to −67 |

* MS Magnetostriction unit; RS Rochelle-salt unit.
† This is not the emf but the measured response in the actual operating gear.

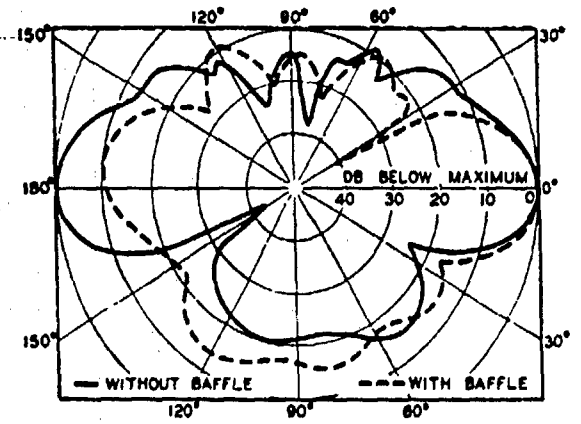


FIGURE 5. Directivity patterns of the sonic hydrophone whose response curves are shown in Figure 4.[10]

## 12.3.2 The Directivity of Hydrophones

The response of large hydrophones depends on the direction from which the sound is incident (see Section 7.4). In interpreting response curves, it may be taken for granted that they refer to the direction of maximum response, unless specifically stated otherwise. The direction of maximum response is usually called the axis of the hydrophone, although other definitions of this term are used occasionally.

In the following comparisons of a directional and a nondirectional hydrophone, it is assumed that the latter has the same response curve for all directions as the former has for its axis.

Directional hydrophones are usually mounted so that they can be rotated about a vertical axis. The bearing of a target can thus be determined by noting the direction in which its sound is a maximum. Since a change of 3 db in sound level is usually quite perceptible, reasonably accurate bearings can be obtained even with hydrophones with patterns similar to those of Figures 5 or 6.

While the possibility of obtaining bearings is the primary reason for installing directional hydrophones, they have several other advantages over nondirectional systems. These all arise from the necessity of distinguishing between the signal and the background of unwanted sound.

If the source of the background noise is localized (e.g., at the propellers of the listening ship) on some bearing other than that of the target, the directional hydrophone will suppress the unwanted sound relative to that of the target. Thus listening may become

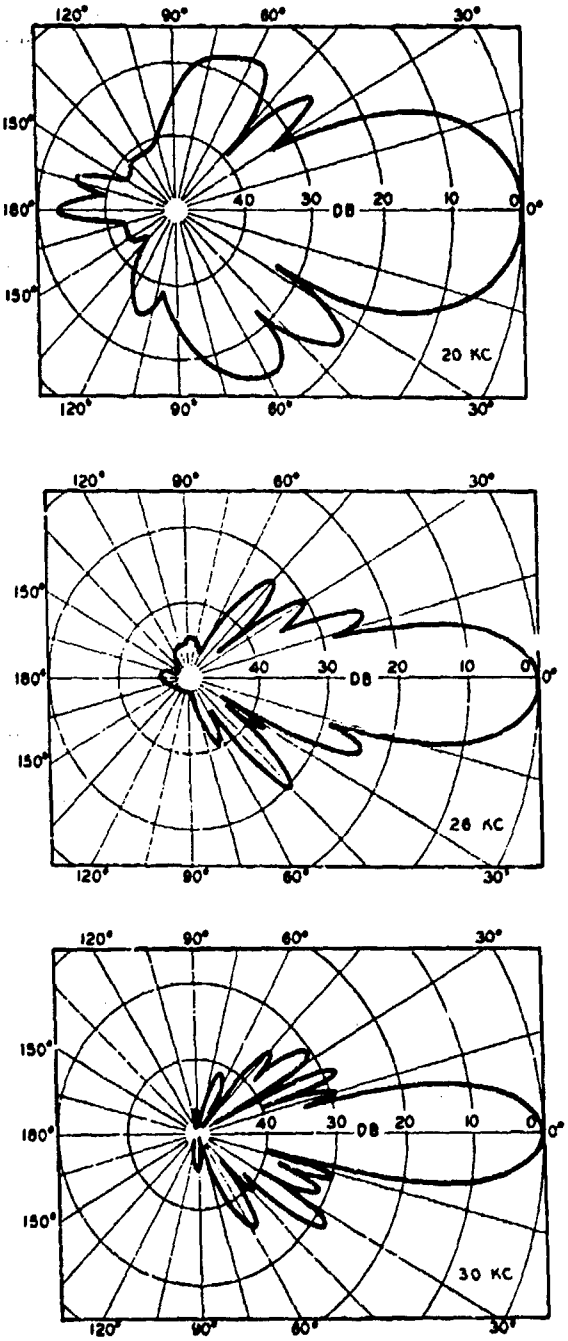


FIGURE 6. Directivity patterns of a standard hydrophone for frequencies of 20, 26, and 30 kc.[10]

possible with a directional system even though the background is too high for the use of a nondirectional system.

This is true even of the background of ambient noise, for which the sources are distributed in all directions. The directional hydrophone will respond mainly to those sources that lie on its axis. Thus its

FIGURE 7. The JP sonic listening hydrophone.

response to ambient noise will be less than that of a nondirectional one. Its response to a target located on its axis will, however, be the same as that of the nondirectional hydrophone. The difference in the background heard by a given nondirectional hydrophone and that heard by the directional unit is called the directivity index of the latter (see Section 7.4). Column 5 of Table 1 gives typical values of the directivity indices.

Finally, the listener can control the level of the signal from a localized target by training a directional hydrophone on and off. Since the background of ambient noise remains constant during such a sweep, this procedure is an aid in verifying a sound contact.

### 12.3.3 Sonic Listening Gear

These general remarks can be illustrated by considering the directivity pattern of a particular hydrophone. The JP hydrophone is a cylindrical nickel tube about 3 ft long and 2 in. in diameter which serves as a magnetostriction unit. It is mounted, with the tube horizontal, on a vertical shaft about which it can be rotated, as indicated in the illustration of Figure 7. The directional properties are determined by the ratio of the tube length to the wavelength of the incident sound. When sound pressure reaches all parts of the tube simultaneously, as it does when the tube is at right angles to the direction of the impinging wave, the generated voltage will be at a maximum. When the tube is turned to intercept the wave obliquely, the pressure on a given area will be greater or less than the pressure on an adjacent area. As a consequence, if the wavelength is small, as it is at the higher frequencies, some parts of the tube will be caused to expand while other parts will be compressed. These opposing effects on different parts of the tube tend to reduce the response of the hydrophone. If the wavelength is long compared to the length of the tube, all parts of the tube will be compressed or expanded in nearly the same phase, hence the orientation of the tube will have little effect on the response; in other words, the hydrophone will be practically nondirectional. Thus, the hydrophone becomes more directional as frequency increases and wavelength decreases.

Figure 5 is a directivity pattern of the JP unit for sound of a frequency of 4.7 kc. The patterns were taken in a plane containing the axis of the cylinder. They show two main response peaks or lobes and numerous side lobes. The JP is usually provided with a sound-absorbing baffle, and it is seen by comparing the two patterns that the baffle causes a drop of 10 db in the rearward direction; this additional directivity aids in discriminating against the self-noise due to the propellers, and also helps to prevent errors of 180 degrees in target bearings. At the frequency of about 5 kc, the main lobes are seen to be about 20 degrees wide (between the −3-db points); at higher frequencies they become narrower and the hydrophone correspondingly more directional. In a plane perpendicular to the axis of the tube, the JP hydrophone without baffle is nondirectional.

The JP amplifier has five filters of the high-pass type. The cutoffs are at 0.2, 0.6, 1.5, 3.0, and 5.5 kc. The operator, using headphones, will begin by listening with the lowest filter frequency switched on, for many of the wanted incidental sounds have very strong components at low frequencies. On identifying a signal, he will successively switch on the higher frequency filters in order to utilize the progressively increasing directivity of the unit. There is a "tuning

eye" permanently connected to the output of the 5.5-kc filter, which facilitates the determination of the bearing. A skilled operator may expect to obtain bearings that are accurate to within 1 degree with the JP gear.[1]

### 12.3.4 Supersonic Listening Gear

Supersonic listening has certain advantages associated with the greater directivity and sharper response at the higher frequencies. The JK hydrophone illustrates this. It is a Rochelle salt crystal unit, with a circular diaphragm, and is mounted in a spherical housing to reduce the water noise. On surface vessels, the sphere may itself be enclosed in a streamlined dome. Directivity patterns shown in Figure 6 illustrate the increase in directivity as the frequency increases. Figure 3 shows the response curve of this unit for sound incident along the axis. It is seen that there is a broad peak at 24 kc. The response drops 3 db below the maximum at 24 kc in the frequency band from 21.5 to 27.5 kc. The value of the resonance parameter $Q$ is thus 24/6 or 4. In contrast to this broad response band with the low value of $Q$ is the very narrow response band of echo-ranging transducers like the QC, which at a resonant frequency of 24 kc have values of $Q$ ranging from 10 to 110. A $Q$ of 25 would restrict the listening to a band of a few kilocycles centered at 24 kc, if a nonresonant amplifier is used.

The narrower pass band associated with a high-resonance parameter is advantageous in echo ranging, but not in listening. If the incident sound has a more or less uniform spectrum level throughout the frequency band in question, the output of the listening gear is proportional to the pass-band width. Most background noise is of this description and its level is reduced by narrowing the pass band. This is an advantage in echo ranging (see Section 9.1). In listening, however, the signal is also reduced in level, and no advantage is gained. The pass band would thus appear to be immaterial. However, listening through a narrow-band system distorts the sound so that everything sounds the same; the operator thus loses the advantage of any qualitative difference between signal and background, unless the former has a characteristic time pattern.

The higher directivity of the supersonic hydrophone makes it possible to avoid receiving much of the noise caused by the motion of the listening vessel. As a result of this and other factors, supersonic listening is possible at ship speeds of 15 to 20 knots, compared with the maximum speed of about 5 knots that limits sonic listening.

### 12.3.5 Enemy Listening Gear

The German and Japanese navies have stressed sonic listening more than have the United States and British. They have tended to use several small hydrophones, mounted some distance apart. The outputs of these are combined in such a way that the installation as a whole is directional. By means of variable elements in the electric circuits, it is possible to alter the direction of maximum sensitivity of such hydrophone arrays. The sound beam can thus be steered without the necessity of moving parts outside the hull.

## 12.4 SOUNDS OF SUBMARINES

### 12.4.1 Objectives

From the antisubmarine standpoint, a knowledge of the sound output of submarines is needed for the prediction of maximum listening ranges. The design of listening gear, in particular the decision between sonic and supersonic devices, depends on the spectrum of the sound to be detected.

From the pro-submarine standpoint, it is important to know the relative sound output of various maneuvers, so that evasive action will not be nullified by excessive detectable sound. The problem of noise control, and the design of propellers, engines and auxiliaries, all demand measurement of sound output.

### 12.4.2 The Sources of Submarine Sounds

Submarine sounds have their origin chiefly in the machinery and in the propellers.

The machinery of the submarine is extremely diversified and complicated. There are more than fifty auxiliaries, all of which are potential sound

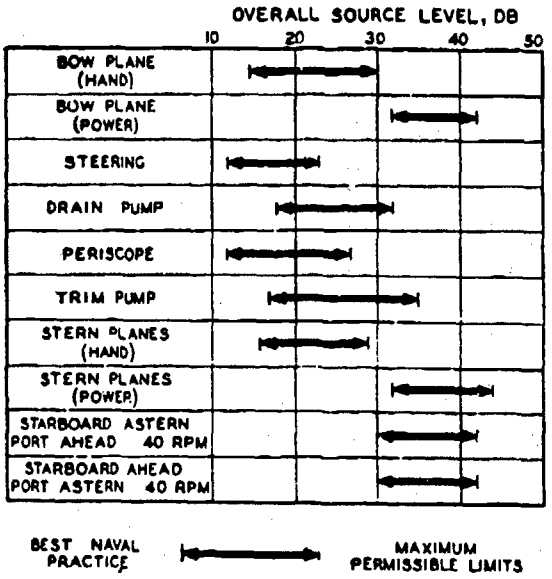


FIGURE 8. Suggested limits of overall sound level of several auxiliaries on submarines, and the levels representing best naval practice.

sources. Figure 8 lists a few of these sources, and shows the source levels that have been proposed as best naval practice and also the maximum permissible limits.

In general, these sounds have a continuous spectrum, with a maximum at low frequencies. Sometimes, however, the machinery will produce a strong line spectrum which is superposed on the continuous spectrum. The importance of such single-frequency components warrants a rather detailed discussion, and this will be found in Chapter 14.

Propeller sounds are of two general kinds, (1) *singing*, due to vibrations of the propeller blades, and (2) *cavitation* sounds. The latter are the most important of all submarine sounds. Vibrations of the propeller blades may be due to faulty design or manufacture and are generally not difficult to eliminate.

Cavitation results when the propellers are turning so rapidly that the water does not close in behind the blades. Thus a stream of bubbles is formed. These may be caused by reduced pressure on the back of the propeller blade (Figure 9) or by vortices at the tip of the propeller blade (Figure 10). Acoustically, tip cavitation appears to be much more important than blade cavitation. This may be because the blade cavitation has a more serious effect on propeller thrust, and is usually prevented by the designer of the ship. These bubbles cause noise in much the same way as those in a boiling kettle.

Besides these two main sources of submarine sounds, there are some minor sources, such as the splashing of water at the bow and in the wake when the submarine is at the surface; when submerged, the fittings of the vessel, such as handrails, may be set into vibration by the turbulent flow of water past them. These sounds are considered to be of small significance compared with those due to cavitation.

The activities of the crew are a source of incidental sound. It is interesting that, according to some British measurements, overall source levels of 45 to 50 db may be produced by dropping a spanner or by the use of the engine-room telegraph, levels comparable to those produced by the submarine itself under conditions of evasive operations. The transitoriness of such sounds makes them comparatively unimportant, except when evading detection by an alert enemy.

## 12.4.3 The Measurement of Submarine Sounds

The measurement of source levels involves (1) the sound levels, (2) the distance between the hydrophone and the source of the sounds.

If the measurements are taken in a sound range, the hydrophones are moored to the bottom at accurately determined positions. The submarine carries out its maneuvers both on the surface and at periscope depth. Its position at all times can be accurately determined from shore and recorded, and thus the range which the signal sound has traversed at any given moment can be calculated from simple geometry. The levels of the sounds received at the hydrophones are also measured ashore, as a function of time. This method is at present restricted to relatively shallow water. It would be desirable to have a sound range at least 400 ft deep, to enable maneuvering at greater depths.

A second method is used when no sound range is available or when measurements in deep water are desired. The sounds are recorded on a surface vessel equipped as a sound laboratory, and dead in the water. The hydrophone is streamed out on buoys to avoid the effects of the noise originating at or on the vessel. The submarine follows a straight course past the hydrophone, approaching it as closely as possible. Unless the submarine is on the surface or at periscope depth, unavoidable inaccuracies enter the range measurement.

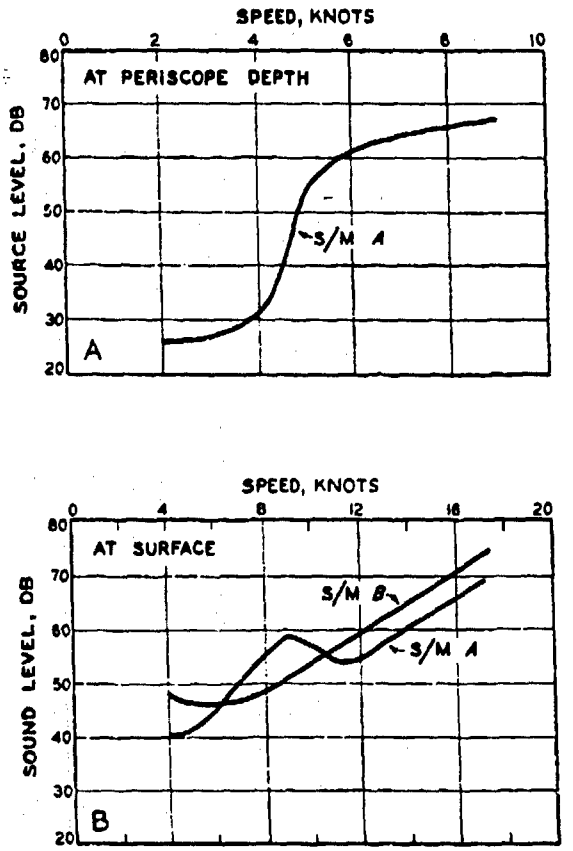


FIGURE 9. Overall source levels of submarine sounds. (A) Submerged variation with speed; (B) two submarines, surface operation, illustrating the variability between ships.

In such experiments, the received sounds have also been sent by frequency-modulated radio to a laboratory on shore, where high-fidelity sound-on-film records are made for later detailed study and measurement.

The sounds produced by individual sources may also be measured at dock by hanging hydrophones overside and operating various auxiliaries successively.

The sound output may also be monitored by the submarine crew while the vessel is on actual operations. This can be done with the standard JK and JP listening units by making a sweep from 0 to 360 degrees and noting the readings on a meter. However, a special noise-level monitor is preferable for such purposes.[2,3] This is an installation of four small magnetostriction hydrophones placed near the noisiest auxiliaries but outside the pressure hull; a fifth hydrophone is installed near the propellers. The signals from each of these hydrophones can be amplified and measured at will. The output of the several hydrophones is recorded when the submarine is quiet, and this is compared with their respective output when the vessel is operating.

## 12.4.4 Overall Source Levels of Submarine Sounds

The sound output of a submarine varies widely with the size and type of vessel. For a given vessel it varies with speed and operating conditions. If the submarine is submerged, its sound output depends strongly on the depth of submergence.

The overall source level may range from about 40 db under evasive conditions to more than 75 db at top speeds.[4] An average based on a large number of measurements[5] gives the following values. (1) Running submerged at 6 knots or at 12 knots on the surface, the overall source level is about 72 db. (2) At top surface speeds, the overall source level is about 77 db.

The dependence of the overall source level on speed is shown for two submarines in Figure 9. In diagram A the overall source level is plotted against the ship speed for a submerged submarine, and in the right-hand diagram, for two submarines operating at the surface.

The variability of source level from ship to ship is indicated by the curve of vessel B included in diagram B. The values of source levels of various submarines may vary by as much as 10 to 15 db under identical operating conditions.

The curve pertaining to operation at periscope depth is typical of ship sounds in general. At very low speeds the source level is quite low. At a certain critical speed, in this case 4 knots, the sound output increases very rapidly with speed, so that an increase of 2 knots is accompanied by an increase in the source level of 30 db. If the speed is increased beyond 6 knots, the curve flattens off.

This abrupt increase in the sound output at the critical speed is due to cavitation, which is related to many factors but chiefly to the shaft rate or speed and to the hydrostatic pressure. Other things being equal, the speed at which cavitation occurs is inversely proportional to the square root of the static pressure. (See Chapter 5.) Hence one would expect the sound output at a given speed to be less when the submarine submerges to greater depths. This is

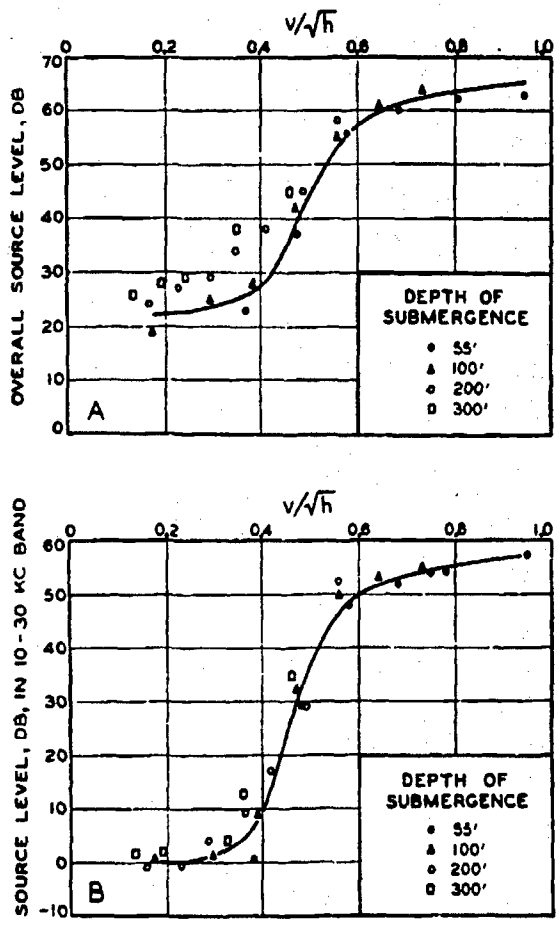


FIGURE 10. Dependence of overall source levels of submarine sounds on depth of submergence $h$(feet) and speed $V$(knots). The steep rise between $V/h^{1/2}=0.4$ and $V/h^{1/2}=0.6$ is due to cavitation. The solid curve is drawn on the assumption that the speed at which cavitation occurs is inversely proportional to the square root of the hydrostatic pressure.[5] Figure 10A plots the levels measured in the 0.1- to 10-kc bandwidth; Figure 10B the levels in the 10- to 30-kc band.

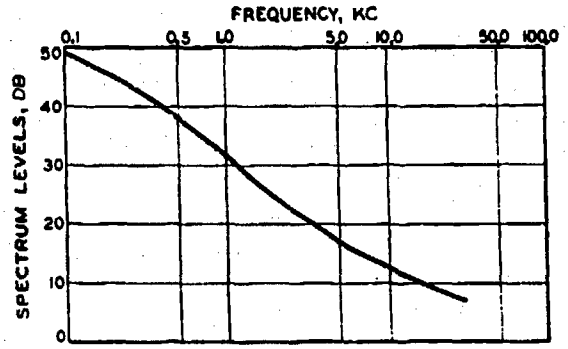


FIGURE 11. Average spectrum of a submarine running at 6 k at periscope depth or 12 k at the surface. It must be stressed that the spectra of individual ships may deviate decidedly from this figure.[5]

shown to be the case in Figure 10,[5] in which overall source levels are plotted against $V/h^{1/2}$, where $V$ is the speed in knots and $h$ is the total hydrostatic pressure head. The value of $h$ is calculated from $h = 33 + d$, where $d$ is the depth in feet and 33 ft is the head of sea water equivalent to 1 atmosphere. The experimental points are seen to fit the empirical curves fairly well. They are based on a small number of data obtained from two submarines of the same size and design.

It has been found that the speed required for cavitation to set in is, in general, higher for submarines of new design. This is the result of a persistent effort to decrease the sound output of American submarines. It has been decreased, on the average, about 20 db; however, individual submarines occasionally are still found which produce prominent and very undesirable single-frequency tones below 1,000 c. There is considerable evidence that these have their origin almost entirely in the reduction gears.

The relation between sound level and speed is quite different for surface operation. Referring to diagram B of Figure 9, it will be noted that the increase in source level of submarine A is gradual and does not show the abrupt rise due to cavitation that is observed with submerged operation. The higher levels associated with surface operation are to be attributed to the diesel engines used for operating on the surface; the electric drive is considerably more quiet. The hump shown in the curve for submarine A is caused by a singing propeller.

### 12.4.5 Sound Spectra of Submarine Sounds

Figure 11 gives the spectrum of a submarine running at 6 knots at periscope depth or at 12 knots on the surface. These values are averages based on a large number of measurements. It must be borne in mind that there is a great spread in individual measurements, and thus the sounds from a given submarine may deviate decidedly from the values in the figure.[5]

It is seen from Figure 11 that the intensity of submarine sounds decreases rapidly with the frequency; the drop in level is about 6 db per octave on the average. In other words, the spectrum level is about 20 db higher at 100 c than at 1,000, and this same proportionate variation continues at least until

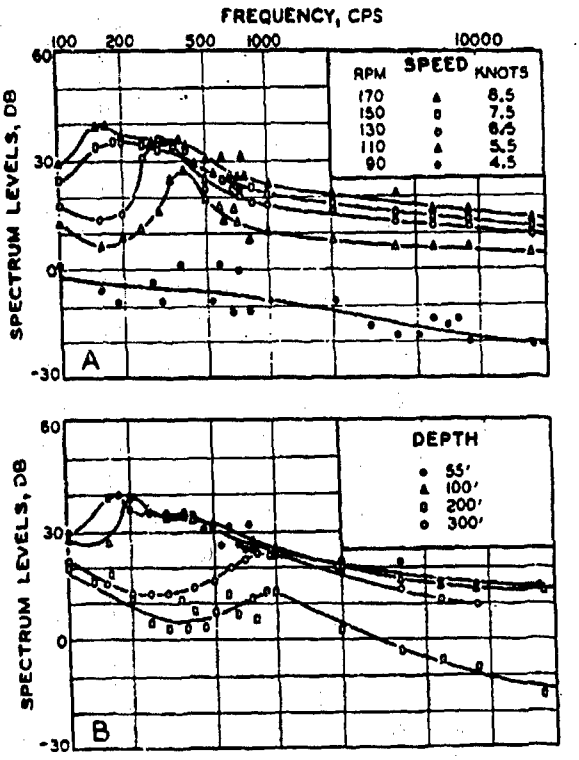


FIGURE 12. Spectra of individual submarines. (A) The variation of spectra with speed of submerged submarine; (B) effect of increasing depth on the spectra. The peak which characterizes the curves at low frequencies is ascribed to cavitation.

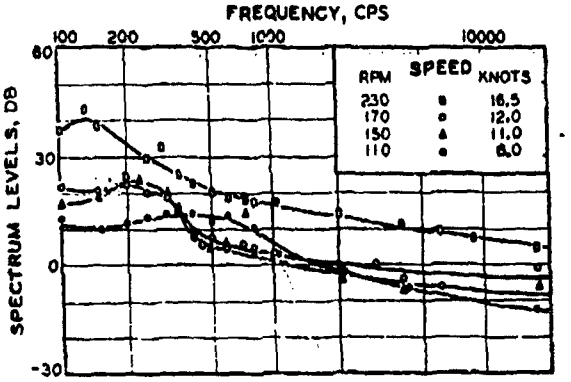


FIGURE 13. Variation of spectra of individual submarines with speed. Surface operation.

30 kc. As a result, the overall level is largely determined by the lower frequencies.

If the threshold of listening gear were independent of frequency, sounds with such a spectrum would be much more readily detected with sonic than with supersonic devices. However, the threshold also decreases with increasing frequency, especially for gear mounted on a moving surface vessel, and until recently this has more or less nullified the advantage of sonic listening. These problems will be discussed again in Chapter 15. On sailing vessels, sonic listening retains its advantage, especially if the auxiliaries can be periodically shut down for listening. An effective antisubmarine watch can thus be maintained from such vessels. The same is true of bottom-mounted hydrophones and sono buoys, both of which use the sonic band.

Sound-level spectra of individual submarines are shown in Figures 12 and 13 for various operating conditions. A characteristic feature of these curves is a peak at low frequencies, and a tendency for this peak to occur at lower frequencies as the speed increases. This behavior is ascribed to cavitation effects. It is thought that higher propeller speeds produce progressively larger bubbles. The resonant frequency of a bubble is inversely related to its diameter (see Chapter 5), and thus an increase in speed results in the production of sound of a lower frequency.

The exact position of these peaks also varies from submarine to submarine. Consequently they do not show on the average curve of Figure 11. It will be noted that even the peaks of these two submarines lie well below the average curve for frequencies less than 1 kc.

Figure 12B shows the effect of increasing depth on the sound-level spectrum. It will be noted that the peaks tend to shift toward higher frequencies with increasing depths. It is thought that the increase in hydrostatic pressure with depth reduces the size of the cavities formed at a given speed, and thus results in a higher resonance frequency.

### 12.4.6 The Directivity of Submarine Sounds

Very little is known concerning the location of the particular point, or points, on the ship which can be considered as the effective source of the radiated sound. There is reason to believe that at periscope depth the engine room is the principal source of sounds at very low speeds, while at speeds above 3 to 4 knots the propeller is chiefly responsible. However, even at high speeds the engine room may contribute materially to the sound at frequencies below 150 c. During surface operations the propeller and wake are probably the principal sources of sound at practically all speeds with electric drive; with diesel drive the engine room is the main source at low speeds, and a material contributor at all speeds.

The sounds from submarines are radiated in such a way as to produce approximately a uniform sound field at a distance of several ship lengths from the source. Some observers[5] report a slight decrease in the sound level in the region within 10 or 20 degrees on either bow; at 200 yd it amounts to from 2 to 4 db. A similar shadow astern of the ship has also been reported; this is ascribed to the wake.

## 12.5 SOUNDS OF SURFACE SHIPS

### 12.5.1 Objectives of the Study of Ship Sounds

The sounds emitted by surface vessels may provide considerable information to an experienced sound operator aboard a submarine. Various forms of underwater mines are detonated by the ship's sound. Ship sounds vary greatly from ship to ship, and from one class of ship to another, in intensity and spectrum, and for a given ship, both vary with speed. From the viewpoint of defense, it is obvious that every ship that is likely to enter water harboring hostile submarines, would benefit by an analysis of its own sounds. Such an analysis would discover any revealing single-frequency components, such as the one shown in Figures 23 and 24. These undesirable components are due to causes which can often be easily remedied. The analysis would also make possible more accurate estimates of the range at which the ship is liable to be detected by an enemy submarine.

### 12.5.2 The Measurement of Ship Sounds

The following procedure[6] is typical of the methods used for measuring the acoustic output of surface vessels. A series of hydrophones was mounted on tripods on the sea bottom in water 40 ft deep. As a ship passed over the hydrophones, the sound output was recorded, together with data on the type and speed of the vessel, its changing position, etc. In tabulating the results, the maximum response from the various hydrophones was used. The recorded pressure levels were reduced to source levels. Both overall pressure levels and spectrum levels were recorded.

### 12.5.3 The Overall Sound Output of Ships

The extreme values of observed overall source levels range from about 50 db for launches and small auxiliary craft at low speeds to 110 db for battleships at 20 knots.[7] The latter value is approximately the source level of a standard sonar projector. It will be recalled that the average overall source levels of submarines ranged from about 30 to 75 db.

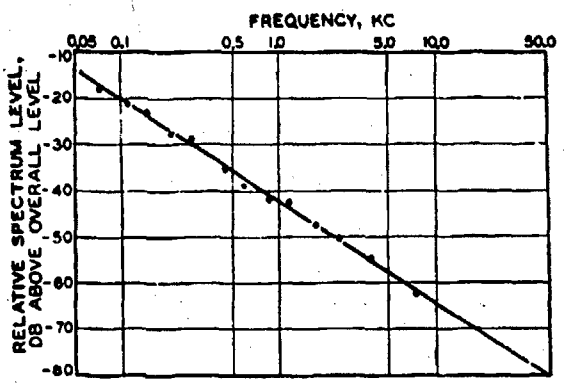


FIGURE 14. Spectrum of surface ships, representing the average of measurements made of 52 vessels of 12 different types of warships and commercial ships.

Besides being affected by the speed of the vessel, the overall source level is a function also of the load or displacement of the ship.[b]

### 12.5.4 Spectra of Ship Sounds

The sources of ship sounds are extremely diversified, and a given source may change its sound output with ship speed. Hence ship sounds are variable and complex, and are distributed through the whole range of frequencies. As in the case of submarines, the chief sources are the screws, where cavitation produces the sound, and the hull, which transmits the vibrations of the machinery and engines.

Single-frequency components due to propeller singing or to vibrations of the propulsion machinery are common. Ordinarily such sounds occur below 1 kc, but sometimes these single-frequency components

[b] An empirical formula is given in *Survey of Underwater Sound*, Report No. 4,[7] which has been found fairly accurate when applied to ships of over 400 tons' displacement. It is

$$S = 60 \log K + 9 \log T - 25,$$

where $S$ = spectrum level at 5 kc at 1 yd from source,

$K$ = the speed of the ship in knots,

$T$ = the displacement in tons. If this is not known, the gross tonnage either can be estimated or is listed for the type of a given vessel. Even a large error in $T$ does not affect the value of $S$ significantly. For instance, if a 3,000-ton ship displacement were estimated as 6,000 tons, the error in $S$ would be less than 3 db.

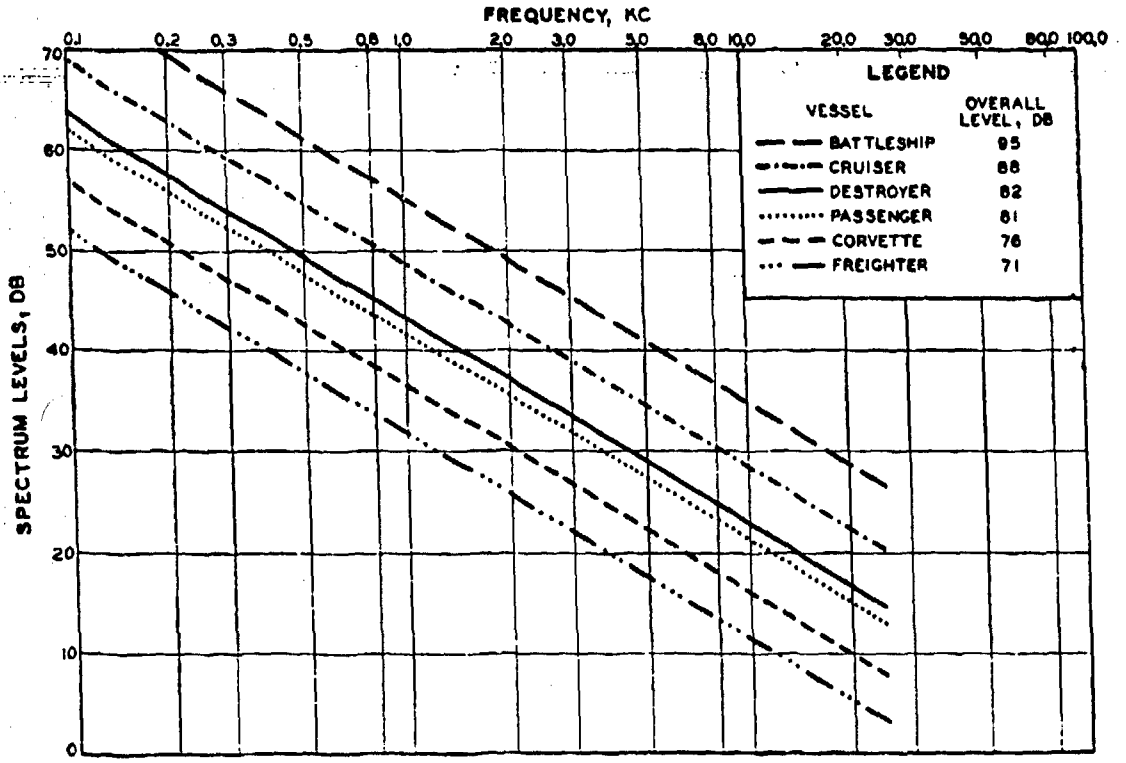


FIGURE 15. Average spectra of six different classes of ships.

are encountered well above this frequency. They are discussed in some detail in Chapter 14.

Figure 14 shows the average spectrum-frequency distribution of sounds from a large number of surface ships.[7] The data on which this figure is based were provided by measurements made according to the method described above on 52 ships comprising 12 different types, including both warships and commercial vessels. The ordinates on the graph are the values of relative spectrum levels, i.e., of the spectrum level, defined above, minus the overall (0.1- to 10-kc) level. These differences are averaged for all types of ships in order to obtain the graphs. The total spread of the measurements on the individual ships was considerable, and due allowance for this must be made when using data from this graph and the following graphs.

The level of the sound is seen to decrease with increasing frequency, at a rate of 7 db per octave. This is very similar to that shown in Figure 11 for submarines. Spectra of the different ships varied in average slope from about 5.5 to 8.6 db per octave. Figure 15 shows average spectrum levels for six different classes of ships at normal cruising speeds. The average overall levels are also indicated.

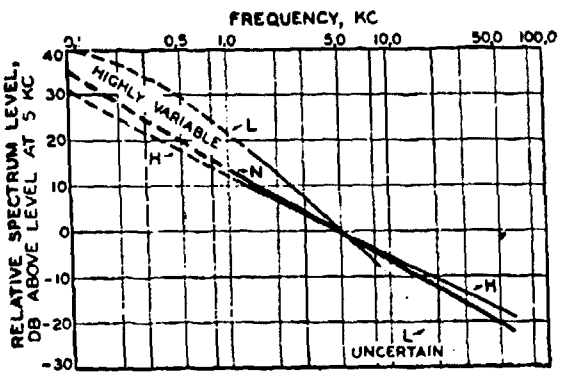


FIGURE 16. Effect of varying speed on ship spectra. The curve marked *L* represents the average spectrum at low speeds, *H* that at high speeds, and *N* that at normal cruising speeds.

Figure 16 illustrates the effect of varying speed on the spectral distribution. At very low speeds the chief source of the sound is found in the machinery, and all the machinery contributes materially. Much of the sound from this source is concentrated at the lower frequencies; therefore in this region the spectrum is highly variable, as was previously noted in the case of submarines (Section 12.4). The curve marked *L* indicates the approximate shape of the

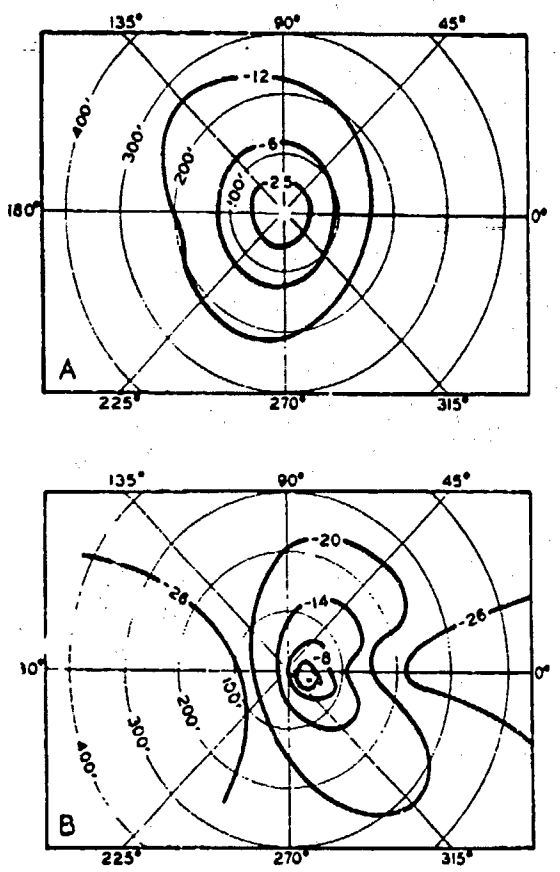


FIGURE 17. Contours showing the average directionality of ship sounds. (A) Average patterns for 15 freighters for low frequencies (200-400 c); (B) contours of sound levels for a typical freighter at 8 k. The outline of the ship is indicated by the shaded area.[7]

spectra for low speeds. It is seen to differ markedly from the spectrum at normal cruising speeds, which is very similar to Figure 14 for frequencies above 1,000 c, but is also quite variable at lower frequencies. The variability of the spectra in the lower frequency region may again be ascribed to cavitation, which is the chief source of ship sounds at all but the lowest speeds. The sound due to cavitation has a continuous spectrum, whereas machinery sound generally is more likely to consist of many discrete components more or less closely spaced. Above 1 or 2 kc, the spectral slope of cavitation sound is very nearly $-6$ db per octave; but in the region of lower frequencies there is usually a peak (see Figure 12). The frequency at which this peak occurs depends on various factors connected with the type and size of ship and its speed, and thus may provide some information tending toward identification of the vessel.

At high speeds, cavitation may introduce components in the supersonic region. This is shown in Figure 16 by the curve marked *H*.

### 12.5.5 The Distribution of the Sound Field around Surface Ships

The sound emitted by ships has very little directivity, particularly in the sonic region of frequencies. Average directionality patterns for 15 freighters for the low frequencies (200 to 400 c) are illustrated in Figure 17A, where sound levels are exhibited as contours, lines joining points of equal intensity. The levels were measured with a bottom-mounted hydrophone.[7]

The contours are somewhat difficult to reconcile with the observation that many ships have two dominant sources of sound, one at the engine room, the other at the screws. In the case of large destroyers, these two sources are of equal level at about 12 knots. At 8 knots, the engine room dominates, while at 16 knots the screws are the dominant source.[8] In Liberty ships, however, the two sources are of approximately equal level at all speeds. The dominance of the propellers as the source of sound for the 15 ships in Figure 17A possibly indicates that the Liberty ships are not typical of all freighters.

If the source of sound from a ship is concentrated at the screws or over a small part of its hull, the audible sound would be quite independent of direction except for the shadow effect of the hull and wake. This effect is illustrated graphically in Figure 17B, which shows the contours of pressure levels for a typical freighter cruising at 8 knots. The outline of the ship is shown by the dotted lines. The shadow and screening effects are highly variable from ship to ship. This, together with the variable distribution of the sound sources, makes it difficult to generalize about the sound distribution. It is probable that for large ships the pressure level 400 to 500 ft ahead or astern of the main source of sound is 5 to 10 db below the level at the same distance abeam.[7]

## 12.6 TIME PATTERNS AND PROPELLER BEATS

### 12.6.1 Rhythms and Other Time Patterns

The necessary prerequisite for the detection of a ship or submarine is that its sound have sufficient

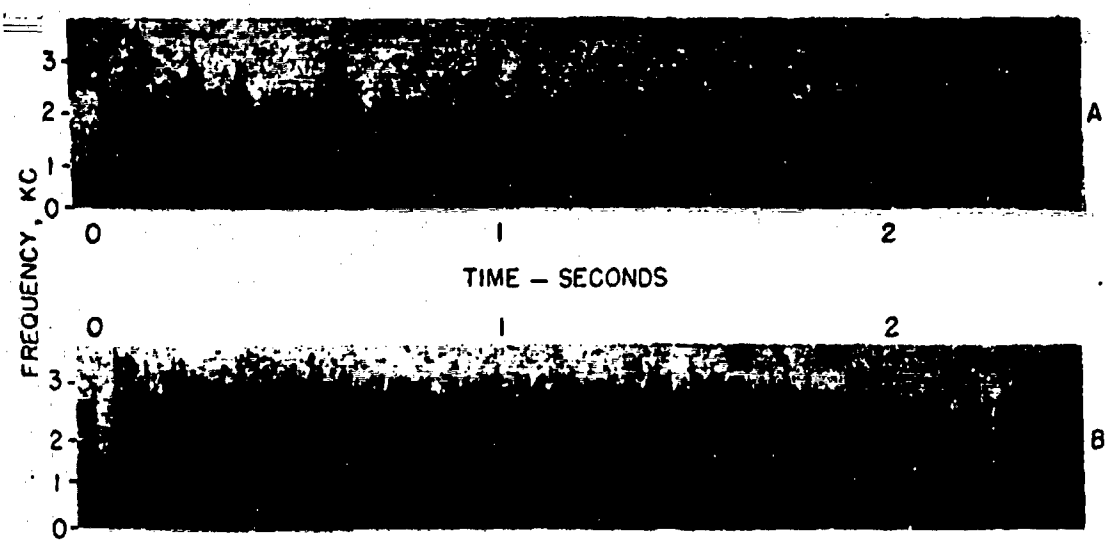


FIG. 12.18. Sound spectrograms of ships sounds. Time is plotted horizontally, frequency in kilocycles vertically, and the spectrum level indicated by the degree of darkening of the print. (A) Spectrogram of supersonic noise from medium-sized A-S vessel, twin screws, 5 k. Heterodyned to 850 c; (B) spectrogram of supersonic self noise of S-type submarine, speed 3 k at 90-ft depth. Heterodyned to 800 c.

intensity at the hydrophone to be heard above the background noise. Since the level of background noise usually varies in an irregular manner, a rhythmic sound having a periodic pattern of beats, may be more readily recognized than a nonrhythmic one.

Moreover, intensity alone conveys no information other than that something in the neighborhood is making a noise. Additional information about the source is obtained from the spectrum (high or low pitch) and from any rhythm that may be inherent in the sound.

The propeller sounds of a large ship, although produced by cavitation, usually pulsate periodically. In some ships, the beat may be unaccented and occur once per propeller revolution (shaft frequency). Other propeller sounds pulsate several times per revolution; a three-blade propeller will give 3, and a four-blade, 4 beats per revolution (blade frequency). If the beat is unaccented, it is difficult to determine which frequency is involved. However, one blade will often be noisier than the others, resulting in an accent repeated at shaft frequency, while unaccented beats occur at blade frequency. In favorable cases, therefore, both the number of blades and the propeller rpm can be determined. These items will partially identify the class of ship, and certainly differentiate its sound from various intermittent background noises.

Somewhat similar in its effect on recognition is the variation in sound level that can be produced by training a directional receiver on and off the target in a systematic manner. This, however, contributes very little to the identification of ship class.

Quite dissimilar is the effect of aperiodic fluctuations in transmission loss. These produce irregular variations in sound intensity, and tend to obscure any rhythm that may be present in the source. It is possible that these fluctuations make ship sounds heard at great distances so similar to background noise that they are not recognized, even when they have an appreciable level.

### 12.6.2 Perception of Time Patterns

The manner in which fluctuations in sound level are heard depends on their rate or frequency. Very slow changes in level are not perceived unless they are relatively large; they are often called "fading." Rhythms are most easily heard and counted when the beats occur two or three times a second. At high rates, counting becomes difficult; with practice, it can be done by counting every third or fourth beat. If accented beats are present, this method is easy.

When the frequency becomes greater than 15 or 20 per second, the individual beats are no longer heard. The rhythm is then heard as a "flutter" or "tremolo."

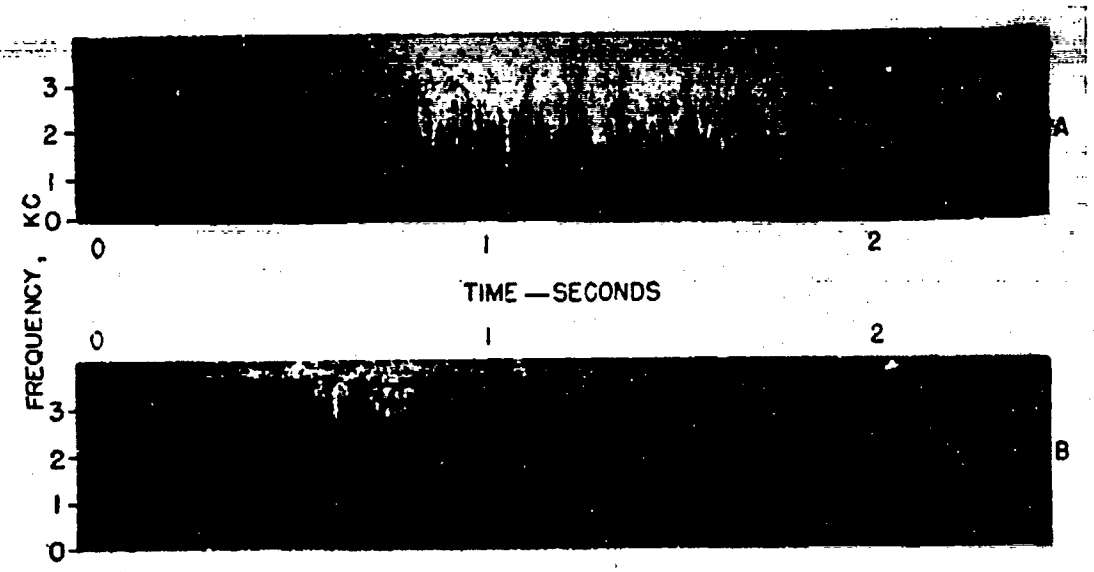


FIGURE 19. (A) Spectrogram of sonic noise from a destroyer, speed 15 k; (B) spectrogram of sonic deep sea ambient noise.

Frequencies much above 100 c are not recognized as periodic, but as a pitch that is inherent in the sound.

### 12.6.3 Changes in Spectrum

The time pattern of a sound may consist either of changes in level or of spectrum or both. The analysis of rapid changes in spectrum requires special equipment. A sound spectrograph designed by the Bell Telephone Laboratories makes it possible to show the intensity of the sound as a function of both time and frequency.[2] Some spectrograms of noise from this analyzer are shown in Figures 18 and 19. Time is plotted horizontally, the frequency in kc vertically, and the spectrum level is indicated by the degree of darkening of the print. Such records are useful in giving a qualitative representation of fluctuating sound levels. The quantitative analysis of spectral fluctuations is still in the incipient stage.

Figure 18A is an analysis of the sound of a twin-screw vessel, as heard with supersonic listening gear. Most of the audible output is below 2,000 c, but beats of higher-frequency sound occur at a rate of about 8 c. Figure 18B shows the self-noise of the same gear at increased gain and without any signal. The striated appearance of the record indicates irregular fluctuations in the sound. Figure 19 is a pair of records obtained with sonic listening gear.

## 12.7 SINGLE-FREQUENCY COMPONENTS

### 12.7.1 The Audibility of Single-Frequency Components

The discussions of previous sections of this chapter have pointed out that ship sounds in general have continuous spectra, that is, the emitted sound energy is distributed over a more or less wide range of frequencies, and on the average the distribution of the energy over the frequency range follows a fairly simple pattern—a decrease in the sound level of about 6 db per octave increase in frequency. Mention has been made at various times, however, of the occurrence in ship sounds of relatively pure tones of audible frequency. On a spectrum plot an absolutely pure tone would be one-dimensional, having sound level but no frequency width; a spectrum composed predominantly of such discrete components would be a line spectrum. Actually the so-called single-frequency components comprise a more or less narrow band of frequencies; but if the width of this band is smaller than the width of the band that can be resolved by ear, it will have a definite pitch. It is in this sense that the terms "single-frequency component" and "pure tone" are used.

The ear very readily detects pure tones against a background of complex noise. This is possible because

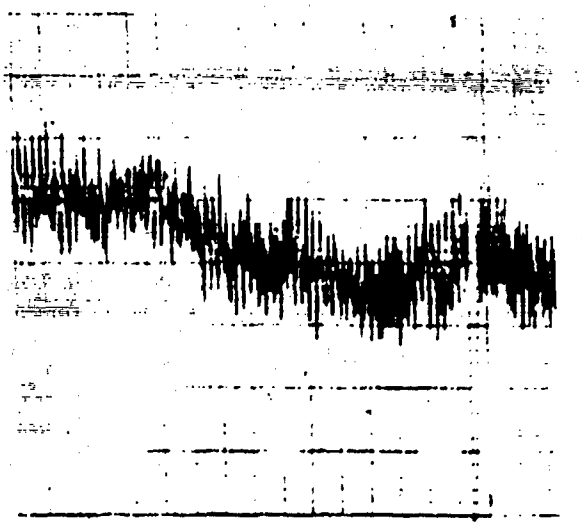

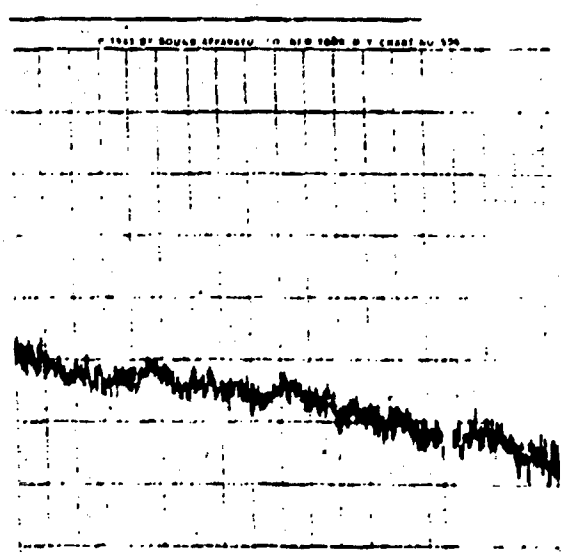

FIGURE 20. Power-level record of a 550-c component in the sounds from a carrier. The periodically recurring variation in average intensity is apparent. An entirely comparable trace from a second carrier of the same class, but fitted with different propellers, is shown in the lower half of the figure. This sound has a random pattern and a lower level than the former.

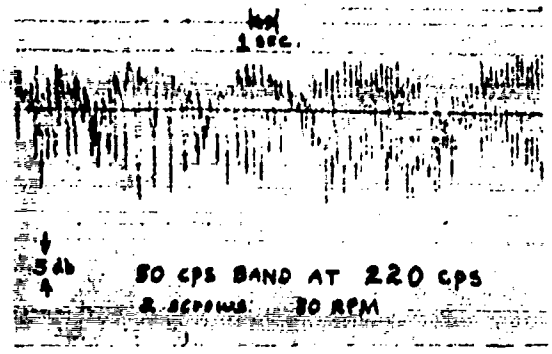


FIGURE 21. Oscillogram of 220-c component in the sound of a submarine running on two screws. The beats may be due to different shaft rates of the two screws.

the ear is a very efficient analyzer of comparatively high selectivity, and because a pure tone has a distinctive quality that contrasts strongly with random noise, which has no definite pitch. These characteristics make it possible for the ear to detect a pure tone in the audible region even when its sound level is considerably lower (sometimes as much as 20 db) than the overall level of the background noise. Tests have shown that a pure tone can be heard when its level is at least equal to the level of the background noise in a band of a certain width at the frequency of the tone. The width of the band depends on the frequency. These *critical bands* are from 30 to 50 c wide for tones between 100 and 1,000 c; this gives an indication of the great effectiveness of the ear in discriminating against random noise. This topic will be dealt with more fully in Chapter 14.

## 12.7.2 Time Patterns of Single-Frequency Components

It sometimes happens that pronounced rhythmic time patterns occur in single-frequency components originating in propeller vibrations. An example of this effect is shown in the upper part of Figure 20, which is a power-level record of a 550-c component in the sounds from a carrier. The periodically recurring variation in average intensity is quite apparent. An entirely comparable trace from a second carrier of the same class, but fitted with different propellers, is shown in the lower half of the figure. It is seen that this sound has a random time pattern with no discernible periodicity, and considerably lower level.

A rhythmic time pattern in the case of single-frequency components may originate in another way. Many single-frequency components have their source in the reduction gears. If a ship has twin screws, the two propellers may have slightly different shaft rates. This would result in the reduction gears' producing two tones that differ only by a few cycles per second. In this case one would perceive fluctuations in resultant level, as the two tones came in and out of phase.

The oscillogram shown in Figure 21 may be an example of this effect. The figure is the trace of a

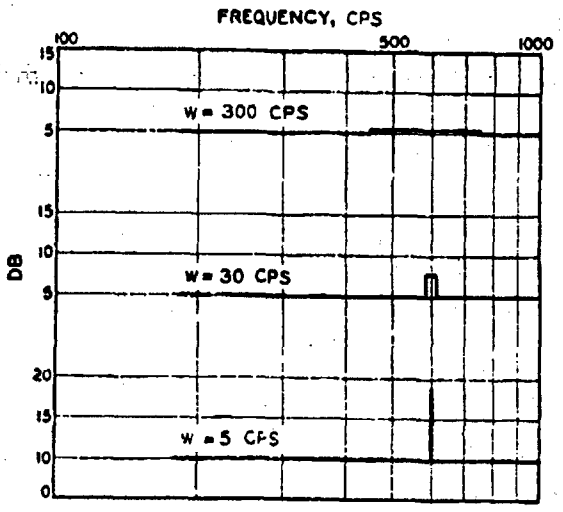


FIGURE 22. Schematic illustrating the measurement of the level of a single-frequency component.

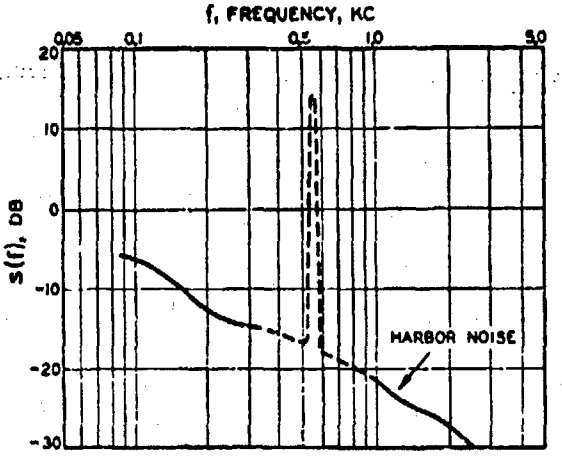


FIGURE 23. Spectrum of the sound whose time pattern is shown in Figure 21. Because of the difficulties in measurement, the single-frequency component is shown as a dotted line.

record of the variation of the sound level with time of a 220-c component in the sound of a submarine running on two screws. The trace shows a well-defined periodic fluctuation, but the frequency of the fluctuation changes; during some time intervals there are 3 or 4 per second; during others they may occur as slowly as 1 per second. It is evident, therefore, that they are not due to simple propeller modulations, which would be regular. The variation in the rate at which the beats occur is probably due to a small variation in the shaft rates.

The extreme audibility of single-frequency components, as compared to sounds of continuous spectrum, introduces complications into the techniques of sound measurement. For example, suppose the overall level of a submarine is being measured at dock, and that, with a motor secured, it has a continuous spectrum of certain overall level. The motor may produce a pure tone which increases the audibility of the submarine's sound very materially, but may scarcely affect the overall level.

In order to obtain reliable measurements of single-frequency components, the spectrum level must be determined with a system using a very narrow filter. Even then corrections for the bandwidth must be applied. To see this, suppose the spectrum level of a sound is $S$ and that a pure tone of level $I$ can be turned on or off at will. Let

$$S = 10 \log I_1,$$

$$L = 10 \log I,$$

and let both be measured with a system having the bandwidth $w$. The power output in the absence of the pure tone will be

$$P = I_1 w,$$

and when the pure tone is added, will be

$$P' = I_1 w + I.$$

If the system is calibrated in spectrum-level units, the meter reading corresponding to $P$ will be $S$ and that corresponding to $P'$ will be $S + s = 10 \log P'$. Hence

$$s = 10 \log \left(1 + \frac{I}{wI_1}\right).$$

As $w$ becomes very great, $s$ will approach zero.

It will be shown in Chapter 14 that the ear behaves like such a system, with a bandwidth $w_c = 30$ to 50 c over most of the audible range. As explained above, $w_c$ is called the critical band of the ear. It is found that the pure tone will just be audible above the background when $I = w_c I_1$. The increase in meter reading caused by the pure tone at this level is thus

$$s_0 = 10 \log \left(1 + \frac{w_c}{w}\right).$$

If $w_c = 30$ c and $w = 300$, the increased reading will be only $s_0 = 0.4$ db. If $w$ is reduced to 30 c, the increased reading due to the pure tone will be 3 db; and if $w = 5$ c, $s_0 = 8.5$ db.

These considerations are illustrated in Figure 22, which shows, in idealized form, the uncorrected spectra obtained with three analyzers using different pass bands. All three are supposed to be applied to the same sound, which has a continuous spectrum

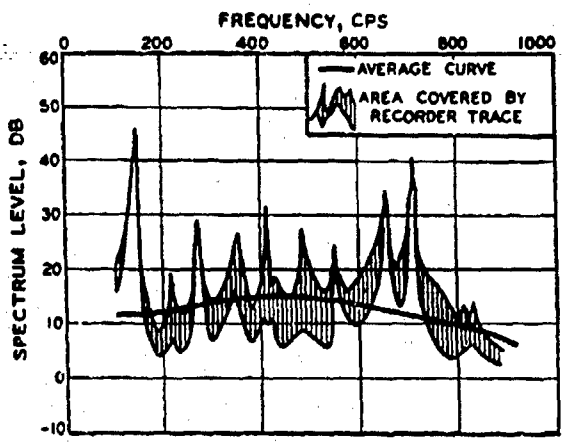


FIGURE 24. Spectrum of a submarine. The heavy line was obtained with an analyzer using a wide band; the analysis with a narrow filter shows many sharp peaks.

plus an audible single-frequency component at 600 c. In actual practice, the graphs will not be so simple for various reasons. The filter edges will not be sharp, and the time patterns of the sound levels cause the graphs to be irregular lines rather than straight.

Figure 23 shows the spectrum of the sound whose time pattern is shown in Figure 21. Because of the difficulties in measurement, the single-frequency component is shown as a dotted line. Its level is probably 35 db above the level of the other ship sounds. It was distinctly audible as a whine. Similar screw sounds have been heard over distances of 30 miles. Yet the contribution of this whine to the overall level of the sound output was very small. The importance of spectral analyses (even if only made by ear by a trained listener) in supplementing overall level measurements cannot be overemphasized.

As a further example, Figure 24 shows the spectrum of a submarine's sound. The heavy line was obtained with an analyzer using a wide band, and shows no values above 20 db. The analysis with a narrow filter shows many sharp peaks, several of which rise above 40 db. These, together with the marked time pattern, indicated by the shaded area, make this submarine far more vulnerable to detection than would be thought from a consideration of the solid line alone.

# Chapter 13

# BACKGROUND NOISE

## 13.1 BACKGROUND NOISE IN GENERAL

### 13.1.1 Airborne Noise

IN LISTENING the operator depends almost entirely on his ears, unaided by any form of recorder, etc. Occasionally, a decibel meter or "magic eye" may be available for supplementary quantitative information. His task reduces to detecting and recognizing a wanted signal against the background of all the other sounds that impinge on his ear. They are many and complex. As a first step in the discrimination process, the operator will distinguish between the sounds that are airborne from his surroundings, and those that issue from the loudspeaker or headphones, and have been picked up or generated by the receiver system. Airborne sounds may, in some cases, be a limiting factor. Listening in an airplane for the signals of a radio sono buoy is sometimes limited by this type of noise, which is often referred to as "local noise" or "room noise."

Against airborne noise, the signal can be made more perceptible by increasing the amplification of the receiver; for in this case the background noise is not amplified, and the signal-to-noise ratio will be increased.

### 13.1.2 Amplified Noise

The wanted signal is only one among many different sounds that are incident on the hydrophone, and that originate in the sea and in the listening vessel itself. These sounds constitute a masking background for the signal. Increasing the gain of the amplifier system obviously does not benefit in this case, for the background noise will be amplified together with the signal, and the signal-to-noise ratio will not be improved.

Finally, as has already been discussed in Chapter 9, the receiver system itself is a source of noise voltages, which are amplified and converted into sound, and these sounds form a part of the masking background noise against which the signal must be detected. Again, in this case, increasing the gain will increase the noise as well as the signal, and will not increase the signal-to-noise ratio.

All of the amplified background noise is distributed over a considerable frequency band, although in bad cases 60-c hum may dominate. The first principle for obtaining a good signal-to-noise ratio is that the frequency band to which the receiver is made to respond be no wider than is necessary to accommodate the signal; for the intensity of the background noise emitted by the loudspeaker is roughly proportional to the bandwidth in which it is received. Unfortunately, the wanted sounds or signals are also wide band. Their spectra do not differ in any systematic way from those of the background. Consequently the application of the principle is not very simple in this case.

### 13.1.3 The Classification of Amplified Background Noise

Because of the diversity and complexity of the sounds that make up the background noise, it is convenient to have a more or less rigorous terminology. A classification of background noise was given in Section 9.2. In Figure 1 essentially the same classification of background noise is submitted in diagrammatic form. It will be convenient to summarize the discussion again before taking up the several kinds of noise in detail.

The amplified noises are classified according to their physical origin into (1) *self-noise*, the sounds originating in the listening vessel and the receiver system; and (2) *ambient noise*, the sounds inherent in the sea itself, which would be detected by even a perfectly noiseless stationary receiver.

The sources of self-noise are threefold:

1. In the absence of all other sound the receiver system itself generates noise. This is called *circuit noise*.

2. The hydrophone may be caused to vibrate by motion through the water, and thus sound will be emitted from it and from its housing and will be directly translated to electrical impulses.

3. The ship sounds from the listening vessel itself tend to mask the sounds from possible targets.

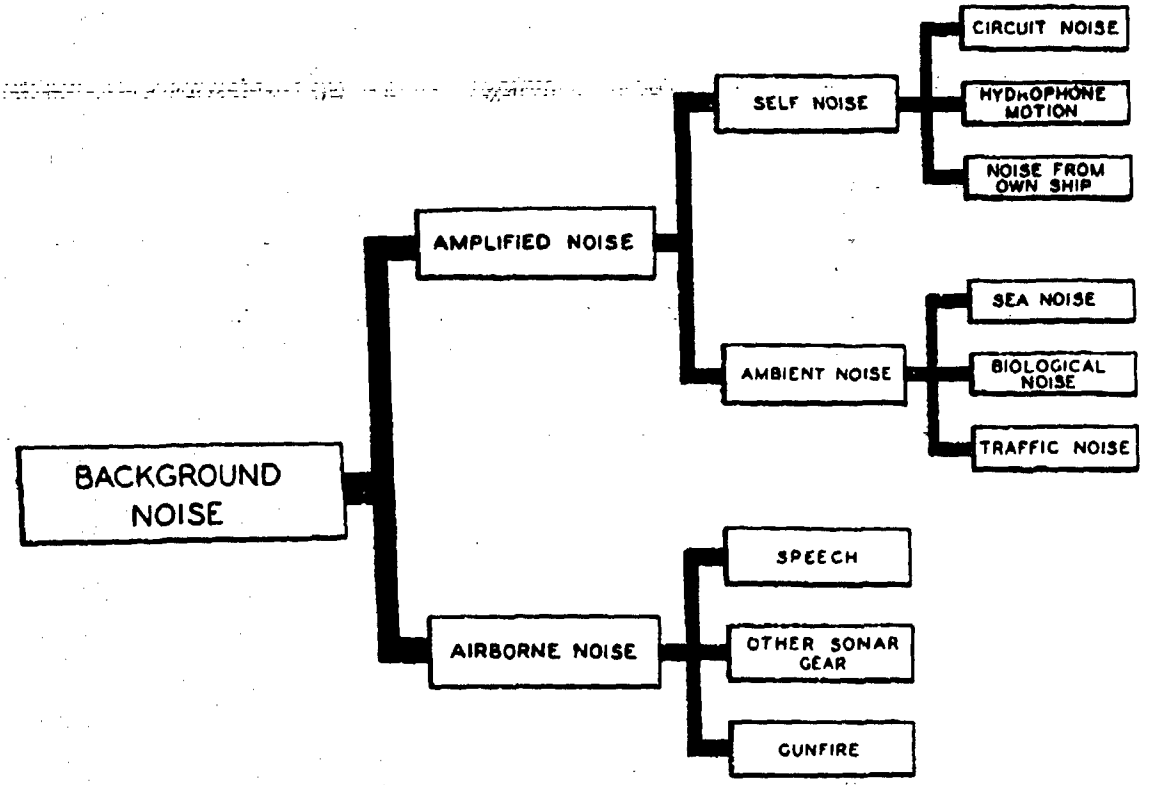


FIGURE 1. Classification of background noise.

The sources of *ambient noise* are also threefold:

1. *Sea noise*, caused by the action of the wind and weather, the patter of rain and hail, etc.

2. *Biological noise*, produced by various species of marine animals.

3. As distinct from the natural sources mentioned in 1 and 2, one encounters unwanted sounds from man-made sources whose character depends strongly on locality. They include passing ships, industrial establishments on shore, the incidental underwater sounds of battle, etc. These are designated *traffic noise*, for want of a better term.

It will be noted that in this classification no provision is made for including reverberation in the background noise. It is evident that since in listening no ping is transmitted, there will be no reverberation. If the target vessel projects pings, and these are received by a listening device, the pings themselves as well as the forward reverberation, if any, resulting from the pinging, will form part of the wanted signal sounds and hence are not part of the background.

In echo ranging, on the other hand, reverberation is likely to be the most important factor in the unwanted background noise. The masking properties of reverberation have been discussed in connection with echo ranging (Chapter 10). For the simplification of an essentially complicated subject like background noise, it seems advisable to omit reverberation from a classification of background noise.

### 13.1.4 Summary of Overall Levels of Amplified Background Noise

Table 1 is a summary of average values of background noise of different kinds. These values are

TABLE 1. Overall levels of amplified noise (0.1 to 10 kc).

| | Decibels |
|---|---|
| Self-noise | |
| Circuit noise | −30 to 0 |
| Submarine self-noise | 0 to 20 |
| Surface vessel self-noise (DD or DE) 10 to 25 knots | 5 to 40 |
| Ambient noise | |
| Sea noise | |
| Deep sea | − 5 to 6 |
| Near surface | −17 to 9 |
| Biological noise | |
| Snapping shrimp | 5 to 7.5 |
| Croakers | 36 (max) |
| Porpoises | 40 (max) |
| Evening noise | 8.5 (max) |
| Traffic noise (includes sea noise) | 0 to 22 |

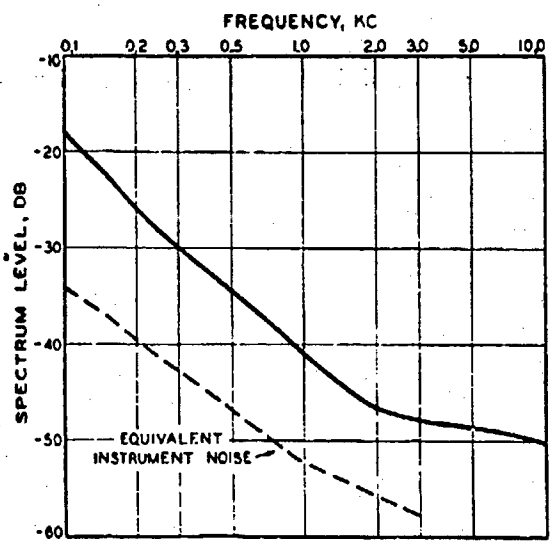


FIGURE 2. Spectrum of circuit noise (dotted curve). The spectrum of sea noise as measured with this system is also drawn in for comparison. The circuit noise level is seen to be from 10 to 12 db below that of sea noise on this occasion, but the two curves are roughly parallel.

approximate. It is apparent that since the sources of specific kinds of noise cannot always be isolated, values assigned to them are based on estimates. As an instance, traffic noise cannot be measured distinct from other ambient noise, and the noise due to hydrophone motion is necessarily included in a measurement of the self-noise produced by the ship on which it is mounted.

## 13.2 CIRCUIT NOISE

### 13.2.1 Sources of Circuit Noise

An acoustic receiver converts sound pressures into electric impulses, amplifies these, and finally portrays them in some manner that makes them perceptible to the operator. Each of these three functions has its own distinctive set of problems. The present discussion is concerned primarily with the perception of sounds; it deals with the other two functions only as they affect the perceptibility of the sound incident on the hydrophone. It is from this viewpoint that circuit noise is discussed here.

Circuit noise has been mentioned as being an important factor in determining the threshold of a receiver system (Section 12.3). It is important in two respects: it contributes to the total of background noise, and it sets a definite limit to the number of stages of amplification that can be used. Any slight change in the currents flowing in the plate or heater circuit of an amplifier tube, especially if it is one of the first tubes, will be amplified and may finally produce a very large change in the plate current of the last tube and a consequent loud click in the loudspeaker. If these changes occur with sufficient frequency, the result may overload the tubes in the last stage of amplification. Even before this state is reached, the noise may completely hide the wanted sound, thus making additional stages of amplification useless.

The spectrum of circuit noise of a certain receiving system is shown in Figure 2.[1] The spectrum of sea noise as measured with this system is also drawn in for comparison. It is seen that the spectrum level of the instrument noise was from 10 to 12 db below that of the sea noise on this occasion, but that the two curves are roughly parallel. The overall level of the circuit noise is about $-10$ db.

The sources of circuit noise are (1) the thermal agitation of electrons in the tuned input circuit, (2) tube noise, (3) hum due to man-made disturbances of various kinds, (4) mechanical vibration of the elements of the tube, resulting in "microphonics."

It will be recalled (Section 12.2) that it is circuit noise which, together with the response of a hydrophone, determines the receiving threshold of a receiver.

### 13.2.2 Thermal Noise

Thermal noise is unavoidable in a receiver circuit. A conductor will show a fluctuation of potential between its terminals even when no external source of voltage is applied to it. This fluctuating potential is due to the thermal agitation of the electrons in the conductor, a phenomenon analogous to the thermal agitation of molecules in matter.

The frequency of fluctuation of this thermally generated voltage ranges from zero to frequencies higher than any used in communication. The sound that results when the voltages are amplified and sent through a loudspeaker therefore has a continuous spectrum.

The magnitude of the thermally generated voltage is determined by the resistance and temperature of the conductor, and for a given conductor the mean-square voltage is proportional to the width of the

frequency band over which the voltage is measured.[2a] These thermal voltages set a lower limit to the smallest voltage, resulting from sound incident on the hydrophone, that can be amplified without being lost in a background of noise. In other words, the ultimate limit of signal-to-noise ratio (restricting the term "noise" in this connection to circuit noise) is obtained when (1) the receiver bandwidth has the minimum possible value and (2) all the noise in the receiver output is caused by thermal agitation in the input circuit to the first tube of the amplification system. It should be added that while this limit is determined by the width of the band that is being amplified, it is not affected by the position in the frequency spectrum at which the band is located.

It need hardly be said that the ultimate limit of signal-to-noise ratio just described is never attained in practice. It is impossible to eliminate all other circuit noise except under very carefully controlled laboratory conditions.

### 13.2.3 Tube Noise

Tube noises have their source in fluctuation in the currents associated with the electrodes of the tube. These fluctuations also are amplified and result in spurious voltages that contribute to the circuit noise. Usually tube noise, rather than thermal noise, sets the lower limit to the voltage that can be amplified without being completely masked.

Tube noise differs from thermal noise in that it can be controlled or reduced to a certain extent by proper design and construction of tubes.

### 13.2.4 Hum

Man-made electrical disturbances are responsible for the third class of circuit noises, generally designated hum. The chief source of hum is found in poorly filtered power supply systems, and in stray magnetic fields resulting from faulty transformers. Currents of the power frequency and its harmonics introduced into the amplifier circuits in the low-level stages may be amplified and thus become troublesome, particularly in high-gain audio-frequency amplification.

Hum can be controlled by intelligent design of circuits, proper electric and magnetic shielding, and careful design and installation of the electric grounds of both sonar and other gear aboard ship.

### 13.2.5 Microphonics

Mechanical vibrations of parts of circuits associated with the amplifier tube will modulate the voltages being amplified. This will result in a circuit noise called "microphonics." The mechanical vibrations may be the result of vibrations of the receiver unit or even of the vessel containing it, or they may result from the direct mechanical action of the sound waves issuing from the loudspeaker. The control and elimination of microphonics evidently is obtained by rigid construction of the affected circuit element, by reducing vibration of the whole unit by shock-mounting, and finally by protecting the unit against the direct action of sound waves.

## 13.3 OTHER SELF-NOISE

### 13.3.1 Sources of Self-Noise

If it were possible to construct a hydrophone that generated no circuit noise and if this hydrophone were placed in water that was absolutely silent, it would record no sound if it were kept stationary. But if it were moved through the water, the motion would cause vibration of the diaphragm, resulting in amplified noise.

If the hydrophone is mounted on a ship, it is probable that it encounters air bubbles in the water under the ship, and their impact on the hydrophone will increase the noise. Moreover, the sounds emitted by the vessel would be added to the sounds incident on the hydrophone; and there would be the intermittent noise due to the slapping of waves against the hull.

### 13.3.2 The Character of Self-Noise

If listening is being done on board a moving ship, the noise of the ship itself is probably the chief source of self-noise. Ship sounds were discussed in detail in Chapter 12. It was stated there that at low speeds the noise originated mainly in the machinery and that, as the speed increases to a certain critical value, cavitation sets in and the level of the ship noise rises abruptly.

Another important source of self-noise in the case of listening from surface vessels is turbulence at the

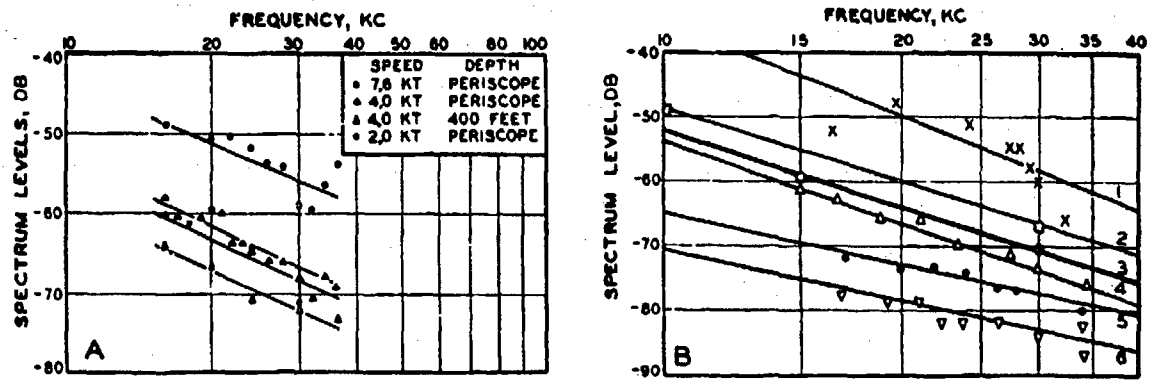


FIGURE 3. (A) Spectra of supersonic self-noise of a submarine at various speeds and depths.[3] (B) Spectra of supersonic self-noise of submarines submerged at periscope depth at 8 knots.[4]

| Curve | Symbol | Ship |
|---|---|---|
| 1 | X | *Cavalla* |
| 2 | □ | *Pipefish* |
| 3 | O | Average of the five |
| 4 | △ | *Sea Lion* |
| 5 | ● | *Shark* |
| 6 | ▽ | *Tarpon* |

hydrophone. Entrained air bubbles were mentioned above. The effects of both can be mitigated by enclosing the projector head in a streamlined dome.

The high level of self-noise on surface vessels makes listening less useful there than on submarines. For this reason most observations of self-noise have been made on the latter, and very little is known quantitatively concerning self-noise of surface vessels.

A listener on a submarine has described his impression of the self-noise as follows.

1. A random noise, apparently not related to the motion of the submarine, together with steady whines.
2. Short bursts of sound which occur at the blade rate.
3. A swishing sound occurring at the rotation rate of the shaft.
4. A steady hiss in addition to the preceding intermittent sounds.

These observations as well as others suggest that it is a composite of three effects.

1. A fixed background noise that is independent of the speed of the vessel, probably circuit noise with added ambient noise. This may decrease somewhat with depth.
2. Self-noise proportional to the speed.
3. Cavitation noise.

As stated in the previous chapter, the speed at which the submarine begins to cavitate depends on the depth of submergence.

The characteristic quantitative features of self-noise are shown in Figures 3[1,6] and 4.[4,6] The data given in these figures are expressed in terms of rms pressure of a plane wave in the water, the direction of which is parallel to the acoustic axis of the hydrophone. This differs from the general convention in regard to noise as adopted elsewhere in this book, according to which the results of measurement are expressed in terms of equivalent isotropic noise. The relation between the noise level in terms of the plane wave convention $N$ and the level $N_i$ in terms of the isotropic convention is given by

$$N = N_i + D,$$

where $D$ is the directivity index of the hydrophone.

Figure 3A shows how the spectrum level of self-noise of supersonic frequencies varies with ship speed in the case of a submerged submarine. The spread in the self-noise levels of different submarines is shown by Figure 3B, which shows the supersonic spectra of the self-noise of five different submarines traveling at 8 knots at periscope depth. It is seen that there may be as much as 30 db difference in the spectrum levels of the self-noise of different submarines. Figure 4A shows the spectra, for sonic frequencies, of the self-noise of a submarine at periscope depth for speeds of 2, 4, and 8 knots. Figures 4B and C compare the self-noise in the sonic band of frequencies (0.1 to 10 kc) with that at 24 kc; in this figure the overall sound level is reduced to an equivalent spectrum

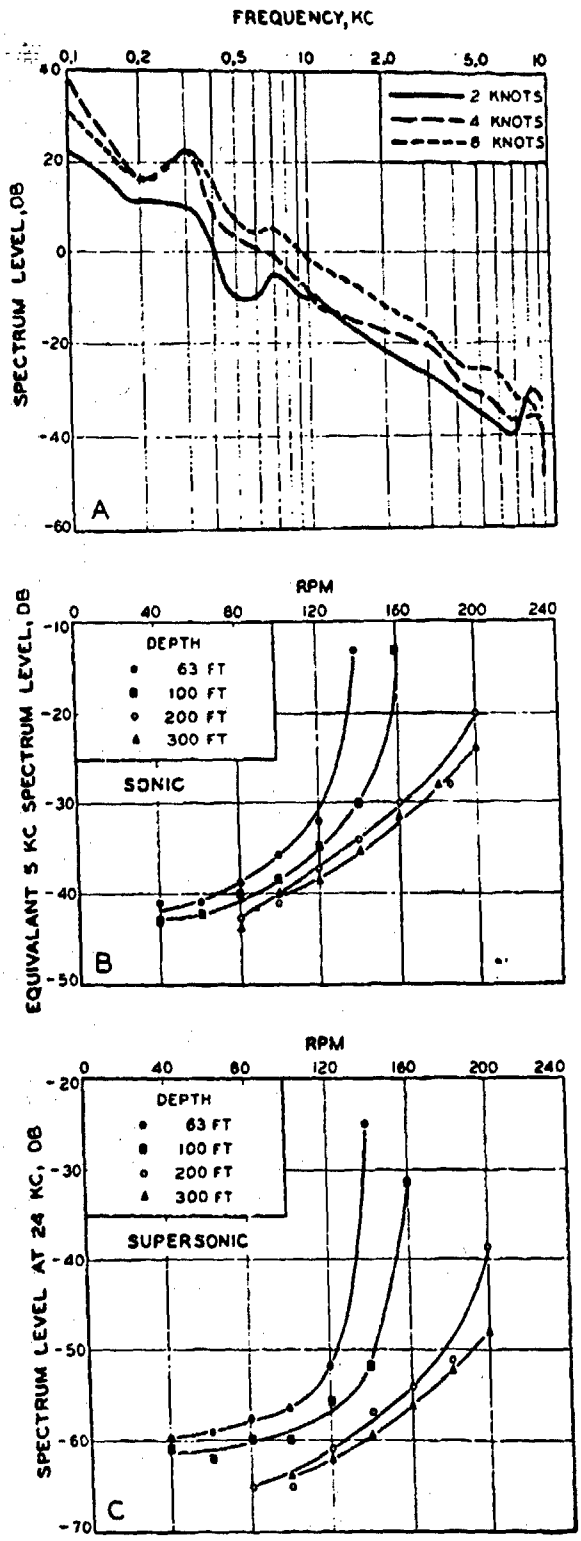


FIGURE 4A. Spectra of sonic self-noise of a submarine at various speeds, submerged at periscope depth.[6] B. Variation with shaft rate of equivalent 5-kc spectrum level of sonic self noise of a submarine. C. Same as Figure 4B for supersonic self-noise.[6]

level (1-c band) centered at 5 kc, and this is plotted against shaft rate for several depths. It is seen that the corresponding supersonic and sonic curves are quite comparable in shape.

The directionality of high-frequency self-noise of a submarine is shown in Figure 5. The level of the self-noise in a 1-c band at 24 kc is plotted for various relative bearings of the directional hydrophone.

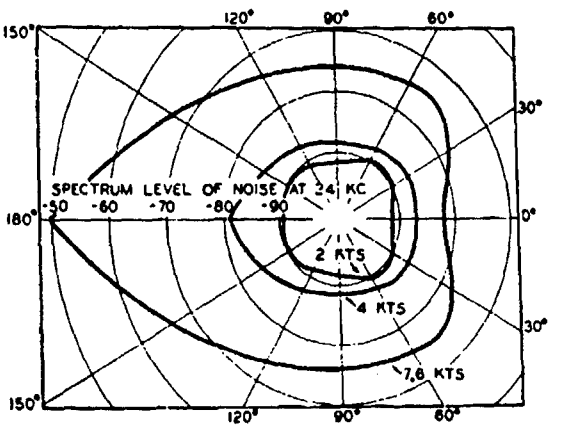


FIGURE 5. Directionality of high-frequency (24 kc) self-noise at various speeds.

It will be seen from Figure 5 that at low speeds the self-noise is practically nondirectional. As the speed increases from 4 to 7.6 knots, the self-noise from dead astern (180 degrees) increases more than 30 db. This increase is due to cavitation, which sets in at a speed of about 6 knots.

## 13.4 AMBIENT NOISE

### 13.4.1 Sources of Ambient Noise

If a hypothetical, perfectly noiseless, stationary receiver were placed in the sea, it would convey to a listener many diverse sounds. The ocean is by no means a region of silence. It is never at rest, and the splashing of the water as it encounters solid objects and the breaking of waves generate noise. Many forms of marine life produce characteristic sounds, and at times such sounds may swell into a chorus. Near cities and harbors industrial noise may be transmitted by the sea, and ship traffic and underwater sounds incident to battle may add their contribution. All the various noises associated with, or resident in,

the sea itself, as distinct from self-noise, are collectively designated by the term "ambient noise." Corresponding to the chief agents just mentioned, ambient noise is classified into three categories: (1) sea noise, due to wind action, rain, and hail; (2) biological noise, due to marine life; (3) traffic noise, due to man-made conditions.

These three classes of ambient noise are taken up in some detail in the succeeding sections. It is worthy of mention that little underwater sound can be produced by sources in the air itself. The air-water surface reflects most of the sound incident on it from either side, and transmits so little that it can be neglected for practical purposes.

## 13.4.2 The General Character of Ambient Noise

The outstanding characteristic of ambient noise is its great variability. At a given locality one or another of the three classes just mentioned may be the dominating one. In the open deep sea it will likely be chiefly sea noise; in or near harbors, traffic noise; near certain coasts various forms of marine life may be the main contributors. Or the ambient noise may be composed at the same time of two or of all three of the classes more or less equally presented.

Besides the variability in the quality of ambient noise from place to place, the listener at a given locality will observe considerable fluctuations in its intensity; for the range and bearing of a localized source will probably change, as for example in the case of passing ships or a school of musically inclined fish. The transmission of sound in the sea is subject to changes, which affect the number of sources that contribute to the ambient noise at a given place. Finally, the sources of ambient noise themselves exhibit definite diurnal and seasonal variation.

For all these reasons ambient noise cannot be specified as a definite, constant quantity, but must be described in statistical terms; that is, an estimate can be made of the most probable or average amount of noise which is to be expected under given circumstances. In addition, it is frequently possible to estimate the degree of variability in terms of a frequency distribution or of the standard deviation of the distribution, when the distribution is known to follow the normal law.

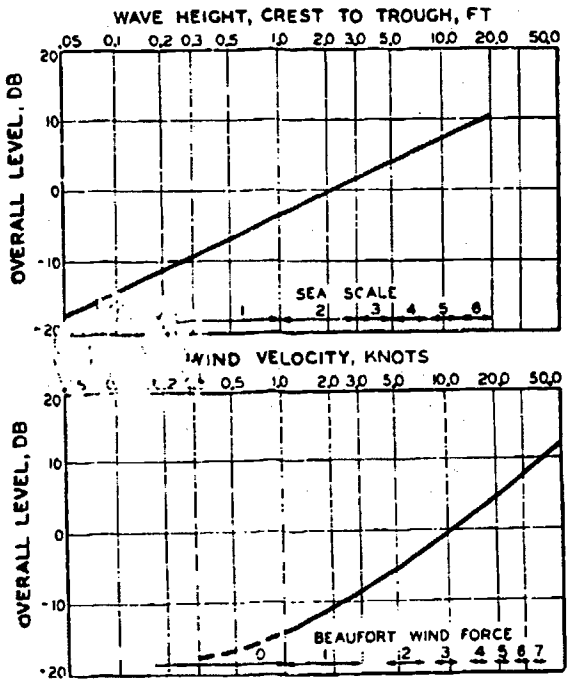


FIGURE 6. *Top:* Sea noise, overall level (0.1 to 10 kc) as a function of wave height. The Weather Bureau sea scale is inserted. *Bottom:* Overall level of sea noise as a function of wind velocity. The Beaufort scale is shown.

## 13.5 SEA NOISE

### 13.5.1 Sea Noise due to Wind Action

Sea noise usually is the prevailing form of ambient noise in open and deep water but may also dominate in shallow water. It is produced mainly by the agitation of the sea surface, and hence is related to wind strength and sea state. Most observers conclude that it is chiefly *breaking wave crests* at the sea surface that produce sea noise, and that very little sound is generated by the unbroken undulations of the surface.

The dependence of sea noise on sea state is illustrated in Figure 6 where the overall sound level, (0.1 to 10 kc), is plotted against sea state and wind velocity. The wave heights are estimated by eye. These graphs represent average values, and considerable deviation from them can be expected.

### 13.5.2 Spectra of Sea Noise

Sea noise has its energy distributed chiefly over the sonic band. Average spectrum levels to be ex-

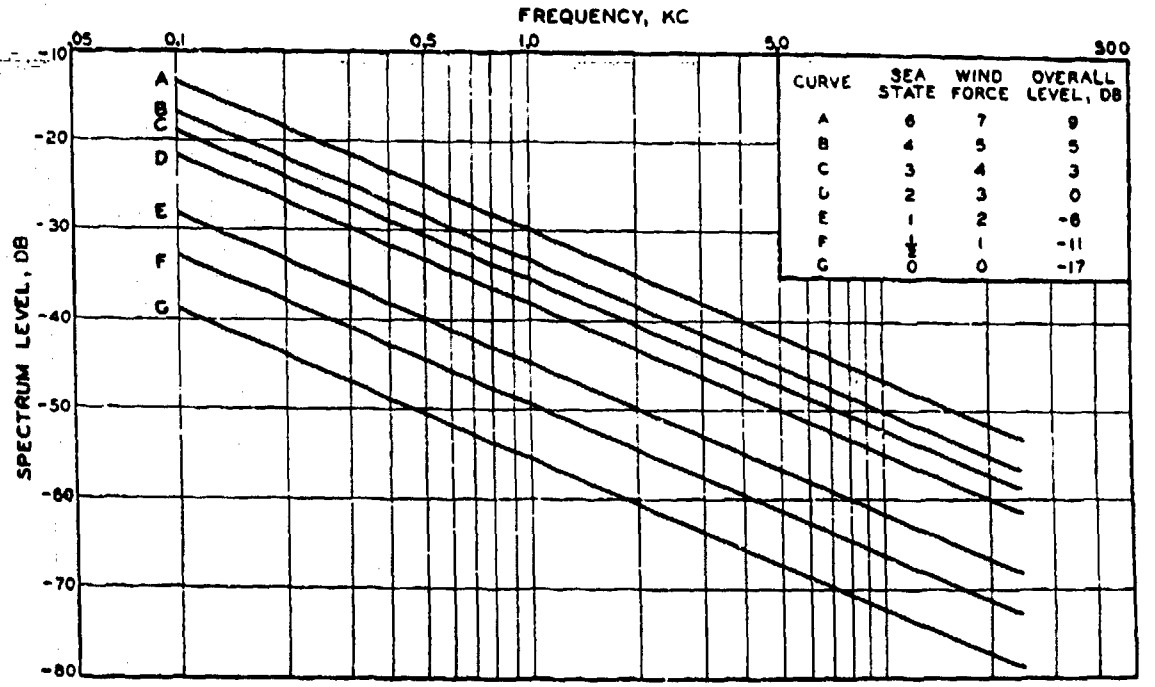


FIGURE 7. Spectra of sea noise for various sea states. The overall (0.1- to 10-kc) level is also given.

pected under various conditions of sea state and wind force are shown in the graph of Figure 7. It is interesting to note that the sea state appears to have no systematic effect on the average spectral distribution of sea noise; consequently all the curves show a uniform decrease of noise level with frequency amounting to about 5 db per octave. On any specific occasion, appreciable random departures from the curves are to be expected.

Deep-sea noise is presumed to be isotropic, i.e., to come equally from all directions, for neither the overall noise level nor the spectrum levels are dependent on depth. However, the character of the noise is different at different depths. Near the surface the noise from individual waves can be discerned, and the fluctuations in the noise level are more pronounced there than they are at greater depths.

### 13.5.3 Other Sources of Sea Noise

The thermal agitation of the water molecules, sometimes called "water noise," produces sound of intensity equal to that caused by the thermal agitation of electrons in the first input stage of the receiver system and is indistinguishable from the latter. The level of sea noise actually observed, even when the sea is very calm, is of a much higher level than this thermal noise.

Rain and hail undoubtedly cause noise, but no quantitative data are available on this subject. It has been informally reported that at New London a rise of 20 db in the overall noise level was observed during a heavy but not torrential rainstorm.

The contribution of surf noise has been measured. It was observed that the overall sound level, measured near the bottom 300 yd offshore, during "rough weather" was 4 db. This corresponds to deep-sea conditions of sea state 4 and wind force 4 to 5, according to Figure 6.

It is possible that the movement of bottom material may contribute to sea noise near shore, although there is little evidence of such movement on a scale large enough to be a significant factor in noise production. No measurements have been attempted.

## 13.6 BIOLOGICAL NOISE

### 13.6.1 Sources of Biological Noise

Surprisingly large numbers of different species of marine life can and do produce sounds of various

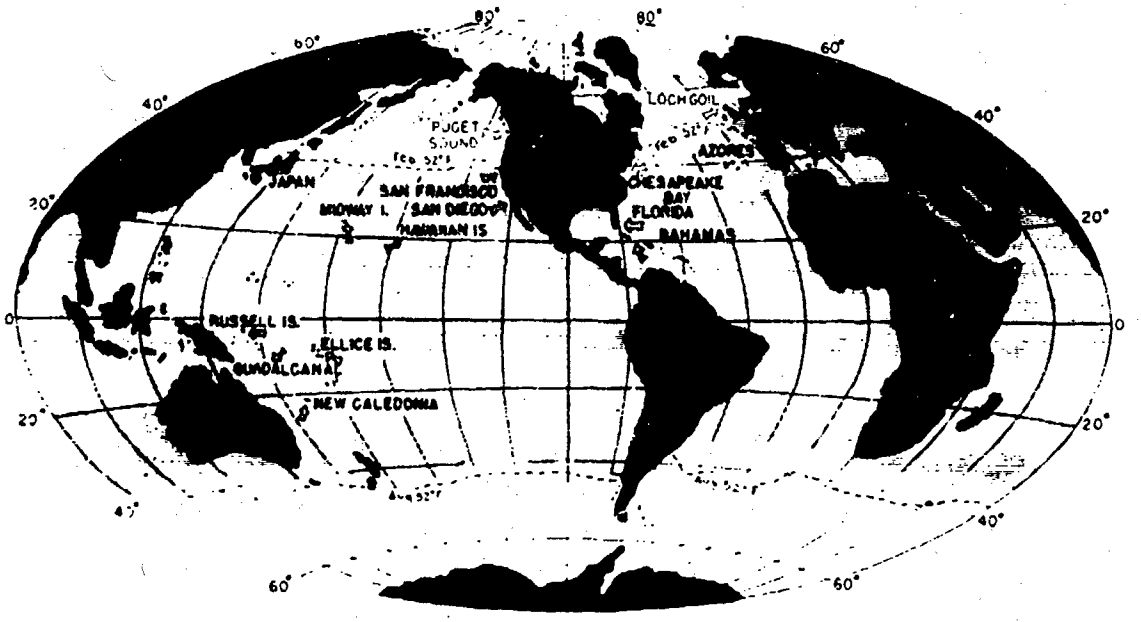


DISTRIBUTION OF SNAPPING SHRIMP

FIG. 8. The distribution of snapping shrimp. Shaded areas show regions where shrimp occur when water depth and bottom characteristics are favorable.

sorts. They are mostly crustaceans and vertebrates. Biological noise is an important factor in limiting listening ranges in shallow water only in tropical and subtropical regions. To discuss the complicated subject conveniently, it is customary to group the various sounds from marine life into three categories, which in the order of their importance from an operational viewpoint are (1) shrimp noise, (2) pergolic fish choruses or croaker noise, (3) miscellaneous biological noise.

## 13.2 Shrimp Noise

Early in World War II, it was observed that as one approached shallow water, the ordinary ambient noise was sometimes replaced by sounds resembling the sizzle of frying fat; on coming close to the shore, the sound approximated the crackle of burning twigs or the crashes of static noise heard in a radio receiver. This noise was encountered only in tropical and subtropical regions, and it was observed to be more common over rocky boulders or cobblestone bottoms. It was sometimes confused with noise due to surf. Investigation disclosed the source of this noise to be colonies of certain species of snapping shrimp not to be confused with the ordinary edible species) that close their pincers with a loud audible click, similar to that which can be caused by snapping a fingernail. The rate at which a single shrimp produces clicks and the reason for this activity is not known. The combined activity of hundreds of thousands of

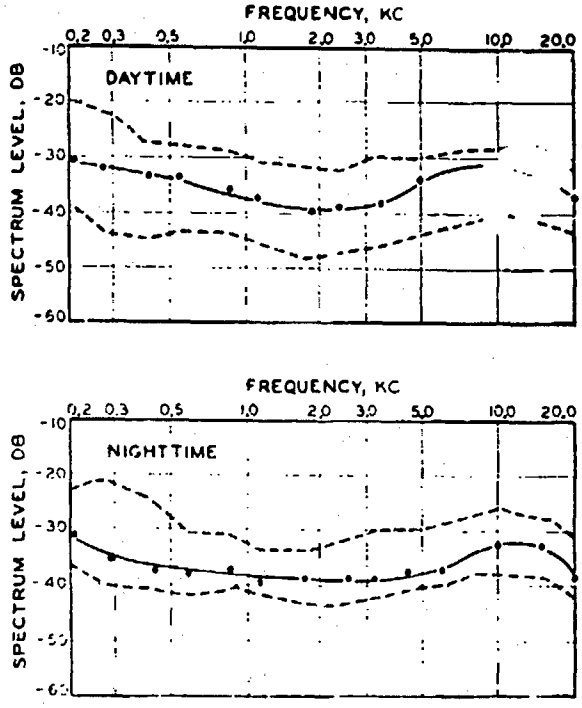


FIG. 9. Spectra of shrimp noise for daytime and nighttime. The dots indicate average values, the dotted curves show the spread of the spectrum levels.

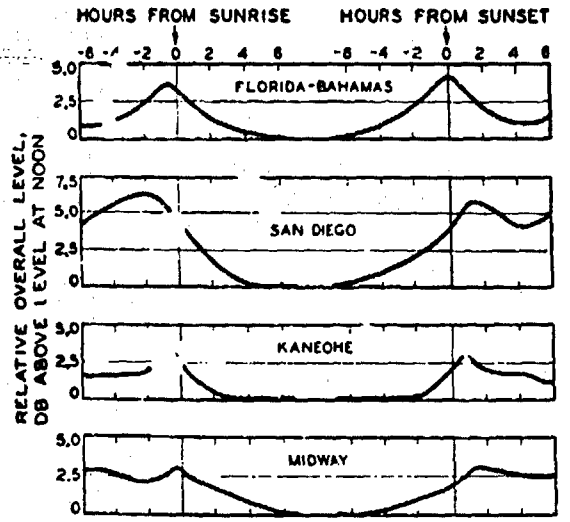


FIGURE 10. Diurnal variation of shrimp noise, overall level at various locations.

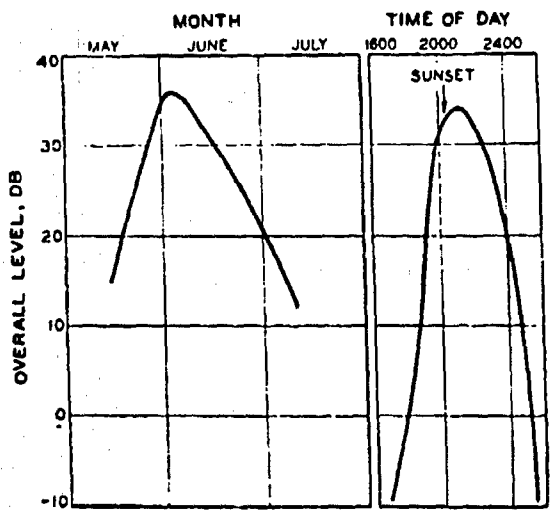


FIGURE 11. Seasonal and diurnal variation of overall levels of croaker noise.

the animals is required to produce the observed sizzle. They are very widespread all over the world in tropical and subtropical regions (see the map shown in Figure 8.) Their habitat is rocky sea bottom in water less than 30 fathoms deep. Few are found on mud or sand bottom, but coral is a very favorable environment.

Shrimp noise is a serious masking noise in listening, both because of its intensity and because of its spectral distribution. While it has a measured frequency range of 1.5 to 45 kc, the main components lie between 1.5 and 20 kc. The spectrum level at 10 kc may be of the order of $-39$ to $-29$ db, as can be seen from Figure 9. It is evident that shrimp noise is a serious complication in both sonic and supersonic listening.

Directly over a shrimp bed the sound output of a directional hydrophone appears to be independent of the hydrophone orientation, both in the horizontal and vertical directions. It is also independent of the depth of the hydrophone. At the edge of or at a distance from the bed the noise level depends very strongly on the hydrophone bearing.

Shrimp noise is remarkably constant throughout the year, no appreciable seasonal variation having been observed. There is a small diurnal variation: the noise is from 2 to 6 db higher at night than in the daytime, small maxima occurring about an hour before sunrise and after sunset (see Figure 10).

## 13.6.3 Periodic Fish Choruses

The chief noise makers among fish are found in certain species of croakers and drumfish, which are common, especially on the Atlantic Coast. An individual croaker emits sounds resembling 4 to 7 rapid blows on a hollow log.

At certain periods of the year, large schools of croakers infest certain localities: in the Chesapeake Bay the croaker season extends from May to July. During this season there is an evening chorus of croaker noise lasting several hours, with a peak just

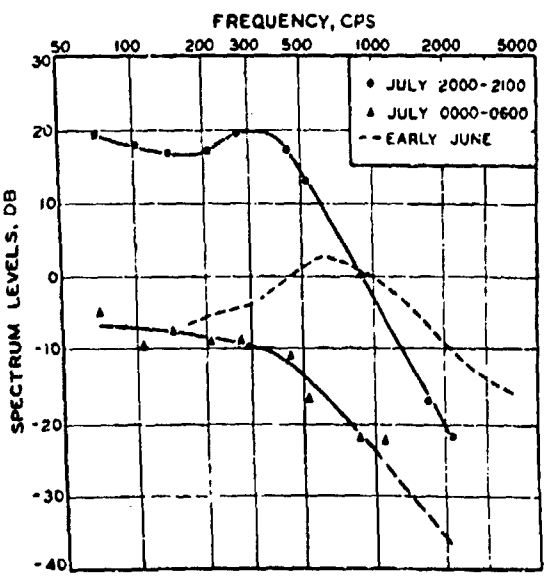


FIGURE 12. Spectra of croaker noise. The solid curves show the difference in average level between early evening and the period after midnight during July. The dotted curve is the average spectrum for early June.

after sundown. Overall levels of croaker noise showing seasonal and diurnal variation are shown in Figure 11.

The spectrum levels of a sample of croaker noise are shown in Figure 12. When it occurs, croaker noise may completely mask wanted signals, for the frequency range lies almost entirely below 1 kc, the region where the most prominent components of ship sounds occur.

### 13.6.4 Miscellaneous Biological Noises

Besides the crackle of shrimp in some regions and the daily chorus of croakers in others, the sonar operator will hear at various times an assortment of clicks, squeaks, honks, groans, barks, gobbles, whistles, beats, or moans, all of which doubtless have their origin in some form of marine life. Drumfish, groupers, crabs, lobsters, pompano, porpoises, sea lions, seals, and sea robins have all been identified as active members of the marine band. As a rule, these sounds are not very important factors in masking wanted sounds.

One of the few of these miscellaneous noises that have been investigated to any extent is a noise encountered at Oahu, T. H., and at Midway Island. It occurs from about sunset to midnight and resembles the discordant sound of a peanut vendor's whistle. It is a serious factor in limiting sonic listening ranges; the frequency range is around 3 kc, and its level is about 15 db above the normal background noise. This noise is referred to as "evening noise" in the literature and should not be confused with the "evening chorus" of the croakers. Overall sound levels of ambient noise measured at Pearl Harbor, showing the occurrence of evening noise, are given in Figure 13.

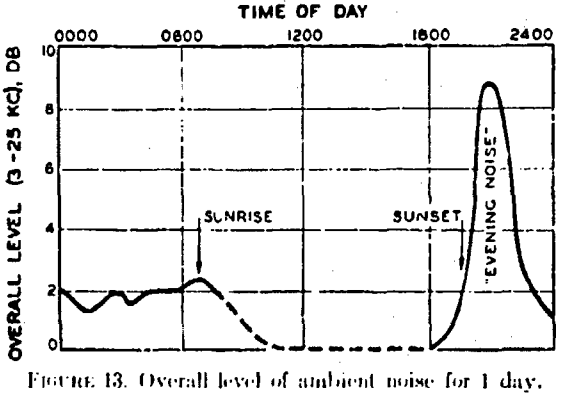


FIGURE 13. Overall level of ambient noise for 1 day, showing "evening noise"

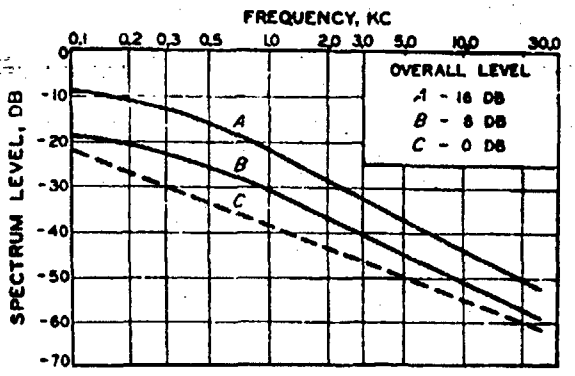


FIGURE 14. Spectra of traffic noise in New York Harbor and its approaches during the daytime. Curve *A* is the spectrum of the noise in the harbor, Curve *B* the average levels measured in upper Long Island Sound near the ship lanes. Curve *C* is the spectrum of sea noise for sea state 2, included for comparison.

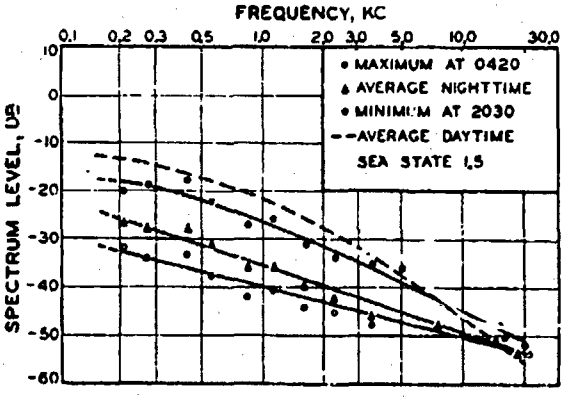


FIGURE 15. Same as Fig. 14, but for nighttime. The average daytime spectrum is shown by the dotted curve.

## 13.7 TRAFFIC NOISE

In and near busy harbors, the ordinary sea noise (and biological noises if present) are overlaid with the sounds associated with the movements of ships, especially small high-speed craft, and by the noise of industrial operations on the beach. Listening in harbors thus becomes extremely difficult; hence installations off the harbor entrance have been devised to ensure protection for harbors against the sneak attacks of enemy submarines.

Traffic noise is essentially variable, but a certain periodicity is to be expected. Measurements made in New York Harbor and its approaches are shown in Figure 14. Curve A shows the spectrum level of the noise in the harbor in the daytime, and curve B the average levels measured in upper Long Island Sound near the ship lanes. The latter is seen to be about 8

to 10 db below the harbor level at all frequencies. For comparison, the curve of sea noise for sea state 2 is included as curve C. In the region of sonic frequencies the harbor noise is seen to be from 10 to 18 db above this level. Overall sound levels (0.1 to 10 kc) for the noise in the harbor itself is about 16 db, compared with 6 db in the harbor approaches, and 0 db for water noise with sea state 2.

Nighttime levels of ambient noise in New York Harbor approaches are shown in Figure 15 with a curve showing average daytime levels added for comparison.

# Chapter 14

# HEARING AND RECOGNITION

## 14.1 THE HUMAN EAR

### 14.1.1 Introduction

CONFUSION SOMETIMES ARISES between the objective physical phenomenon of sound and its subjective perception by a listener. The reader is doubtless familiar with a philosophical problem that agitated the ancients, which was formulated somewhat as follows. A tree crashes in the middle of a forest, and no living being is present to perceive the fact. Was there any sound?

Most of the lengthy arguments that were expended on this question could have been av ·ided had there been adequate theories of sound and hearing. Today *sound* means waves, which travel in the air, water, or other medium. Thus the answer to the question is yes. Sound is to be distinguished from the sensation of hearing, or auditory sensation, which is a phenomenon occurring in a human being or animal. There was no auditory sensation in the above example. In order to clarify the distinction between the sensation produced by a sound, and the sound itself, the latter is often called the stimulus. This is a useful word, for supersonic waves are sound, but they do not stimulate the sensation of hearing in human beings; they are thus not a stimulus of auditory sensation.

The most elaborate listening gear is useless unless there is an operator to hear and interpret the sound waves produced by its loudspeaker. The capabilities and limitations of the operator whose task it is to interpret the sounds issuing from the listening gear are important in determining the success or failure of its mission. For this reason, the present chapter on the physics, physiology, and psychology of hearing is included, even though it is not strictly a part of the theory of underwater sound. Throughout this chapter, the subject matter will be airborne sound. This is not to say that a diver cannot hear when completely submerged in water; but this aspect of underwater sound will be ignored.

### 14.1.2 The Anatomy of the Ear

Figure 1 is a simplified diagram showing the structure of the ear and the terms used in its description. Three general regions are distinguished: the *outer*, *middle*, and *inner* ears.

The outer ear is open to the air, and the *pinna* (*P*) and *external canal* (*E*) form a sort of horn for collecting sound energy.

The middle ear is also filled with air, obtained through the *Eustachian tube* (*T*) that connects it with the throat.

The inner ear is filled with liquid and contains the nerve endings, the stimulation of which by the vibrations of the liquid produces the sensation of hearing.

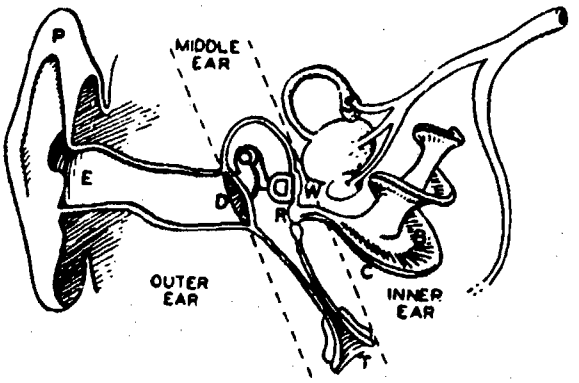


FIGURE 1. Structure of the ear. The parts shown are: in the outer ear, the pinna (*P*) and the external canal (*E*); in the middle ear, the eardrum (*D*), the ossicles (*O*), and the oval window (*W*) and the round window (*R*); in the inner ear, the cochlea (*C*) with the basilar membrane (*B*); the semicircular canals (*S*) are also shown.

The principal physical problem that is solved by the structure of the ear is that of transmitting the airborne sound into the liquid of the inner ear. This cannot be done directly, since an air-liquid surface is a very good reflector of sound. Only a small fraction of the incident airborne energy would be transmitted into the liquid. The function of the middle ear is to provide an efficient transmitting mechanism.

The middle ear is separated from the outer by the *eardrum* (*D*) which is a membrane that vibrates in response to airborne sound. Three small bones are contained in the middle ear. They are called *ossicles*, shown at *O*, and are in contact with each other. One of them is also in contact with the eardrum, and one with a membrane, the *oval window* (*W*) that separates the middle ear from the fluid in the inner ear. The

ossicles form a lever system that efficiently transmits vibrations from the air to the fluid of the inner ear; they are analogous to impedance-matching transformers in electrical systems.

The inner ear itself consists of two major parts: the *cochlea* (*C*) and the *semicircular canals* (*S*). The latter are primarily a stabilizing mechanism, enabling the brain to transmit the necessary nerve impulses to keep the body in equilibrium. These canals have little or nothing to do with hearing.

The cochlea, on the other hand, has a major part in the hearing process. It is a spiral tube, about 30 mm long, divided into two galleries by a longitudinal membrane—the basilar membrane (*B*) which is a sort of carpet of nerve endings. One of the two galleries is terminated by the oval window (*W*) mentioned above, and the other by the *round window* (*R*). As the ossicles press in on the oval window, the fluid presses down on the basilar membrane, which in turn causes the fluid in the other gallery to press out on the round window.

## 14.13 A Theory of Hearing

The nerve endings of the basilar membrane are transverse fibers that vary systematically in length. The short fibers located near the oval window respond to sound waves of higher frequencies; the longer fibers at the other end, to those of low frequencies. That is, the position of the point of maximum stimulation depends on the frequency of the tone.[a]

In response to a complex sound, the basilar membrane vibrates with a certain pattern, perhaps having several maxima, depending on the frequency components in the stimulus. The auditory nerve endings are distributed along the basilar membrane in such a way that they can transmit this pattern to the brain, which interprets it in terms of the pitch, loudness, and quality of the sound. The location of the vibration pattern on the basilar membrane determines the pitch sensation, while loudness is associated with the magnitude of the vibration.

[a] The structure of the basilar membrane suggests that the cochlea might be considered as an instrument containing a series of resonators, which can be excited by vibrations of appropriate frequency; the nerves corresponding to the individual resonators then transmit the reaction to the brain. This theory was proposed by Helmholtz. There are serious defects in the theory: there is a large damping resulting from the fact that adjacent fibers are closely coupled and are embedded in liquid; and the small differences in length and the small number of vibrators seem inadequate to cover the wide range of 10 or 11 octaves.

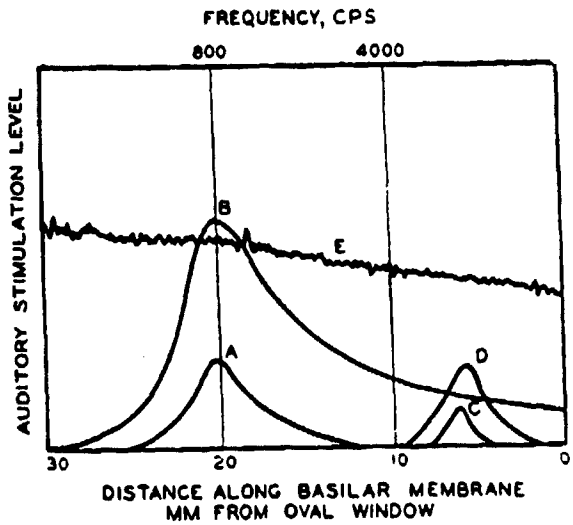


FIGURE 2. Hypothetical stimulus patterns on the basilar membrane for several different stimuli. Curve *A* represents the stimulation by a pure tone of low frequency and low level; curve *B* a tone of the same frequency at high level. The stimulation pattern increases in both amplitude and extent for greater sound intensity. Curve *C* represents a high frequency tone of low intensity, curve *D* one of higher intensity. Curve *E* represents the pattern resulting from a sound having a continuous spectrum. The area under any of the curves is associated with the loudness of the sound.[1]

Some hypothetical stimulus patterns[1] on the basilar membrane representative of several different stimuli are shown in Figure 2. Curve A represents the stimulation produced by a single frequency (pure tone) at a low frequency and low intensity level. Curve B shows a high intensity level at the same frequency. It is apparent that the stimulation pattern increases in both amplitude and extent for greater sound intensity. The broadening of the pattern toward the high frequencies is significant and indicates that the ear is a nonlinear sound receiver. Curve C represents a high-frequency tone of low intensity, Curve D one of higher intensity. Curve E represents the pattern resulting from a sound having a continuous spectrum, such as ambient water noise. The area under any given curve is associated with the loudness of the sound.

The relation between the perceived loudness of a sound and the magnitude of the stimulus on the basilar membrane is explained as follows: the auditory nerve contains about 3,000 nerve fibers which, analogous to a telephone cable, connect the cochlea to the brain. Each nerve fiber responds according to the "all-or-none" law, that is, when it is stimulated sufficiently to respond at all, it responds at full

strength. The response of a nerve fiber is analogous to the discharge of a condenser. The strength of the discharge is independent of the intensity of the sound, but the number of discharges per second does depend on the magnitude of the stimulus in the following manner.

The discharge of a given nerve fiber is followed by a "refractory period" during which the nerve cannot react. This period is about 0.001 sec; thus no single nerve fiber can respond at a rate greater than about 1,000 times per second. The refractory period is followed by a "relative refractory period" of about 0.003 sec during which the nerve gradually recovers its sensitivity. Thus a very weak tone of, say, 1,000 c may cause a given nerve fiber to discharge no more rapidly than about 300 times per second, while in the case of an intense tone of that frequency the nerve may respond up to 900 times per second. The number of responses of a given nerve fiber depends on the strength of the stimulus; moreover, the number of nerve fibers excited increases with the intensity of the stimulus because (1) a greater area of the basilar membrane is activated and thus the stimulus pattern on the membrane takes in nerve endings over a wider area; and (2) the high intensity excites nerve fibers having higher normal thresholds of stimulation. It seems reasonable, therefore, to correlate the sensation of loudness with the total number of nerve impulses arriving at the brain.

That the periodicity of the stimulus is retained in the nerve current reaching the brain is demonstrated by the ability of individuals to localize binaurally the direction of a pure tone because of the phase difference at the two ears. This phenomenon does not require each nerve to discharge on every cycle of the tonal stimulus but may be the result of certain nerve fibers, discharging every other cycle, while others may discharge every third or fourth cycle. It is only necessary to assume that each nerve fiber discharges at the same phase of the vibration of the basilar membrane. This mechanism also may complement the vibration pattern in bringing about pitch perception.

## 14.14 Numerical Data Concerning the Human Ear

This theory suggests how the structure of the ear enables it to respond to frequency and intensity characteristics of a sound. It is a theory which has not been verified in all details and is subject to revision. The following facts are independent of the correctness of the theory outlined above.

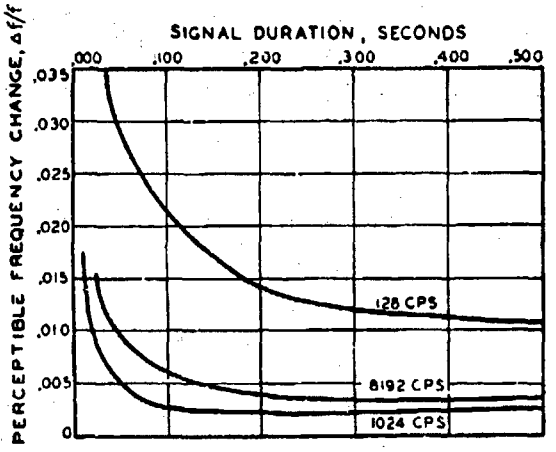


FIGURE 3. Graphs of the threshold of frequency discrimination for several frequencies as a function of signal duration.[2]

Frequencies from 20 to 20,000 c can be heard by a normal, young ear. A change in frequency of less than one-half of 1 per cent results in a perceptible change in the pitch of a pure tone. This is true for long continued tones of frequencies from 500 to 10,000 c and only if the listening level is comfortably loud.[2] If the tone signal has a short duration, the ability to hear pitch changes decreases. This is shown in Figure 3, where the least perceptible frequency change is plotted against the signal duration. It is interesting to note that at 1,024 c, the length of the signal affects pitch discrimination only if the signal length is less than 0.1 sec.[3] This fact is important in doppler discrimination in echo ranging.

The ear is most sensitive at frequencies between 1,000 and 5,000 cycles, where a sound of approximately $10^{-16}$ watt/cm$^2$ intensity can be heard. Sound of approximately $10^{-4}$ watt/cm$^2$ intensity produces a sensation of pain rather than of hearing. Thus the ear has a dynamic range of about 120 db at frequencies around 1,000 cycles.

A rapid change of 1 db, or slightly less, in the level of a pure tone can ordinarily be perceived at all frequencies between 50 and 10,000 c if the listening level is comfortably loud.[4]

The ability to detect changes in level will be less for randomly fluctuating sounds such as noise, than for pure tones. However, a simple rhythmic variation is very easily perceived, particularly if it is cyclic at the rate of about 3 per sec.

The ear requires approximately 0.2 sec for the

sensation of loudness to catch up with a sudden increase[5,6] or decrease of sound level. These dynamic properties seem to be determined by neural rather than mechanical processes. They influence the response of the ear to tones of short duration such as are used in echo ranging.

Sounds producing the same sensations of pitch and loudness still produce different sensations if their spectra are different. The general term "quality" is used to describe the difference in the complex sensations they stimulate. These differences may be sufficient to influence the masking of one sound by another. Since masking is a primary factor in preventing the detection of signals, its general principles will be discussed in greater detail than has been accorded to the other aspects of hearing.

## 14.1.5 The Threshold of Hearing

Imagine the following experiment. A microphone is placed near a sound source which produces a pure tone of controllable intensity. Apart from this sound, the experimental location is to be very quiet. The microphone will convert the mechanical energy of the sound to electric energy which can be used to operate some device, say an oscilloscope.

Beginning with a sound intensity of moderate value, the intensity of the tone is gradually reduced. It will be found that the oscilloscope will fail to operate properly before the sound intensity has reached zero. This minimum intensity to which the oscilloscope will respond depends on two factors. One is the amount of energy dissipated in the various parts of the microphone; the other is the self-noise of the oscilloscope, the microphone, and the circuit. The oscilloscope will not operate properly unless the signal is at least as intense as the self-noise. The minimum sound level that will cause the device to operate properly is its threshold, a concept that has been discussed earlier in this book.

Suppose that the receiver is now replaced by a human ear, and the same procedure followed. A precisely analogous situation results, and for much the same reasons. The ear receives the sound energy incident on it, is stimulated mechanically, and the mechanical energy then is converted to some form of nerve energy which activates the brain. Some of the incident energy is dissipated in this process. Corresponding to the self-noise of the receiver, there are sounds generated by breathing and by the circulation of the blood. Thus there is a minimum level which must be exceeded by a sound before it can be heard. This *threshold of hearing* corresponds to the threshold of the microphone-oscilloscope system.

The value of the threshold of hearing differs from person to person. We say that their *acuity* is different. The average value of the threshold of hearing also depends on the frequency. At 64 c it is 0.12 dyne/cm$^2$; it decreases more or less uniformly with increasing frequency up to about 2,000 c, at which frequency it is 0.00041 dyne/cm$^2$. This corresponds to the lowest limit of sensitivity mentioned in Section 14.1.4. Above 5,000 c it increases with frequency until at 18,000 c it is 4.1 dynes/cm$^2$.

## 14.1.6 Masking

Common experience shows that under all ordinary circumstances, we hear many sounds at once but are usually able to concentrate on the wanted sounds and ignore the unwanted background. This background is always present; as remarked above, even in a very quiet place the self-noise produced by the normal internal processes of the human body becomes audible. Thus there is complete analogy between the ear and an electronic receiver of sound. It will be seen that this analogy is close enough so that it is often possible to use the word "receiver" so as to include reference to the ear as well as to electronic devices.

While one can ignore the unwanted sounds to a considerable extent, their presence does interfere with the ear's ability to detect another sound. This effect is technically called *masking*; it can be described as the increase of threshold level caused by the unwanted sound, and has already been discussed in Chapters 9 and 10.

The laws governing masking are most easily understood if several cases are distinguished, the classification depending on whether the wanted or unwanted sound is a pure tone or a complex one. These will be discussed in detail in Section 14.2, but various generalities remain to be mentioned in preparation for that discussion.

## 14.1.7 Psychological Characteristics of Sound

How does the ear distinguish between a specific sound and all the other sounds that form a back-

ground for it? One's own experience suggests the answer. A bosun shouting orders may rely chiefly on his ability to produce sounds of an intensity great enough to override the clamor of winches, etc. However, a shrill whistle will produce a sound that will be audible, even though the intensity of the background is incomparably greater than that of the whistle. In this case the perception is due partly to the pitch difference between the signal and the background noise, and partly to a decided difference in the quality of the two sounds. Again, a rhythmic drum beat is audible over many noises; before the days of telephone and radio the common method of transmitting orders to masses of troops was to use drum beats of various rhythmic patterns; bugle calls with very decided rhythm utilized the advantages of all the factors mentioned.

To sum up, the sensations produced by sound have at least four distinctive characteristics:[b] (1) loudness, (2) pitch, (3) quality, and (4) time pattern. In recognizing a particular sound, it is probable that all four of these characteristics contribute to differentiate it from others heard simultaneously. In experiments, however, the effect of each characteristic can be isolated.

*Loudness*, *pitch*, and *quality* are psychological, rather than purely physical, terms. That is, they directly characterize the sensation and only indirectly the sound. It is customary to say loosely that loudness is determined by the level of a sound, pitch by its dominant frequency, and quality by the spectrum. This explanation is oversimplified. A more careful examination discovers that in determining any one of the three, all the physical characteristics of the sound play a part. Loudness, it is true, is primarily determined by the level of the sound, but it is influenced also by the frequency and spectrum. It has been demonstrated experimentally that a moderately high frequency is perceived as being louder than a low frequency of the same intensity. This is almost implicit in the discussion of the threshold of hearing given above. If the frequency exceeds 12 or 14 kc, the reverse is true, and supersonic sound of any level is inaudible. Pitch, in its turn, is determined largely by the dominant frequency of the sound waves, but is influenced also by the level and the other characteristics of the spectrum. Quality is principally a matter of spectral distribution, and the time pattern may consist of systematic changes in any of the other three psychological characteristics.

One point is worthy of particular emphasis. Ignoring the fact that intensity is not the only factor that determines loudness, we may inquire as to the mathematical relation between the two. It appears that this is not a simple proportionality: that is, when one sound is said, by most people, to be "twice as loud" as another, the intensity of the one is not twice the intensity of the other. In general, loudness is more nearly proportional to the level of the sound in db above 0.0002 dyne/cm$^2$. A just-perceptible increase of loudness usually accompanies a sudden increase of 1 db in sound level, whether the original level was 5 or 50 db.

### Binaural and Similar Effects

A final characteristic that can be used in differentiating between sounds is their direction of arrival. In simple cases, this coincides with the direction of the source from the listener. The ability of a human being to determine the direction of travel of a sound wave depends on the fact that he has two ears, and the adjective *binaural* is frequently used. The judgment of direction apparently depends largely on the difference in loudness as perceived via the two ears. Difference in the arrival time of the sound waves also contributes to the effect, but appears to be less important; this second mechanism is similar in principle to the split transducer used with *bearing deviation indicators* [BDI].

The current underwater-listening systems make little use of the ability of the listener to determine the direction of a sound. A few experiments have been performed in which the two halves of a split transducer were connected (without phase-lag circuits) separately to the two earphones of a headset, as shown in Figure 4.

The sensation of a listener as the source moves across the axis of the projector is very vivid. The source of sound appears to move rapidly along a line some distance ahead, until it is about to change from left to right, or vice versa. At this moment, when the actual source is presumably on the axis of the projector, the apparent source suddenly seems to be overhead, or even inside the listener's head. There is no doubt that the listener can, in this way, function very effectively as a BDI. An apparent motion of 180 degrees corresponds to about 6 degrees of actual motion. Whether the masking of a signal

[b] Other descriptive terms used by musicians, such as timbre, and clarity, could also be considered, but are of less importance for the present purpose.

by background is reduced correspondingly, is not known.

In these experiments, the underwater sound was supersonic, so that the directivity of the transducer was great, and it was made audible by heterodyning. Similar effects have been obtained with sonic frequencies and arrays of hydrophones spaced on the hull of the ship, at separations comparable to or greater than the sonic wavelengths. During World War I, similar arrays of geophones were used to detect and locate tunneling operations during trench warfare.

## 14.2 THE PRINCIPLES OF AUDITORY MASKING

### 14.2.1 The Masked Threshold

The level at which a particular sound becomes audible differs from the threshold of hearing by an amount depending on the extent to which the background noise masks the signal. As defined above (Chapter 9), this level is the *masked threshold*; it is the level of the signal when it is audible above a particular background noise, 50 per cent of the time. This term therefore applies to the signal-noise pair, not to the signal alone, although it is *measured* by the level of the signal alone. The value of the masked threshold is, however, *determined* by the level of the noise. Raising the level of the noise raises the masked threshold of the signal.

The variable acuity of a listener introduces the need for the phrase "50 per cent of the time"; not only does the threshold of a signal under identical conditions vary from individual to individual, but the same individual will sometimes hear a signal and sometimes not, even though the level of signal and masking noise are the same on the various occasions. Thus, a statement of the probability of recognition of a signal is required to fix a definite value for the threshold level.

This has already been mentioned in earlier chapters, but as greater detail now is needed, it may be further clarified by describing a typical experiment designed to measure the masked threshold. Arrangements are made so that a number of listeners will hear the background noise at a constant and known level. Other arrangements are made for producing the signal at various levels, and various times. Care is taken so that the listeners cannot determine when or at what level the signal is produced except by hearing it; they receive no cues from the person administering the test, nor from each other. The

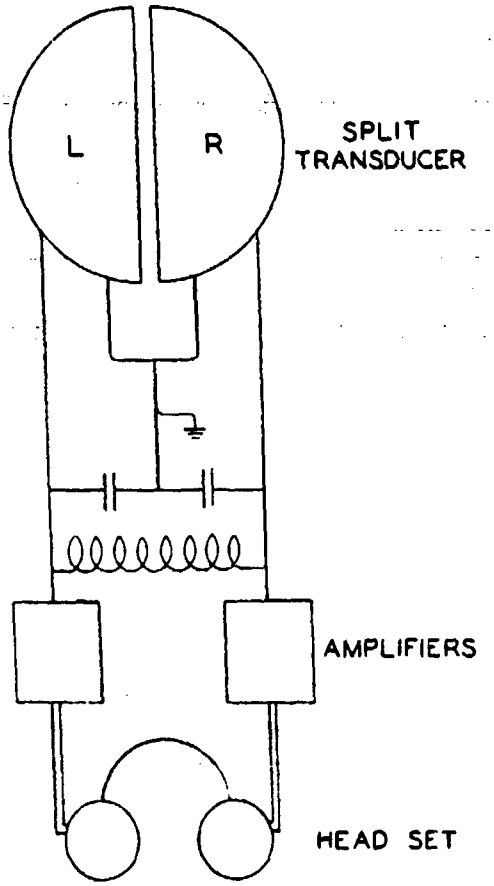


FIGURE 4. Schematic of circuit of split transducer, the two halves of which are connected (without phase lag circuits) separately to the two earphones of a head set. This has been used in some experiments in connection with the binaural effect in listening to underwater sound.

TABLE 1. Probability of the recognition of a signal in presence of a noise background (background level, 12 db).

| Signal level (db) | Vote | | Recognition probability (%) |
|---|---|---|---|
| | Yes | No | |
| 10 | ... | 50 | 0 |
| 11 | ... | 50 | 0 |
| 12 | 2 | 48 | 4 |
| 13 | 9 | 41 | 18 |
| 14 | 16 | 34 | 32 |
| 15 | 32 | 18 | 64 |
| 16 | 43 | 7 | 86 |
| 17 | 49 | 1 | 98 |
| 18 | 50 | ... | 100 |
| 19 | 50 | ... | 100 |
| 20 | 50 | ... | 100 |

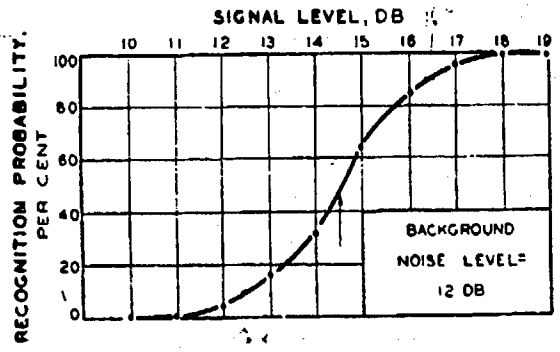


FIGURE 5. Probability of recognition of a pure tone in a background of a noise at a constant level 12 db. Illustrates Table 1.

administrator records the level of the signal, and, after a suitable interval, instructs the listeners each to vote yes or no according as they heard or did not hear the signal.

A typical table of data from such an experiment with ten listeners is given in Table 1. Each level of the signal was presented five times, so that the total number of votes for each level is 50. The recognition probability is the percentage of yes votes for a given level. This is plotted as a function of signal level in Figure 5.

It is seen that there is no abrupt transition from inaudibility to audibility. Instead, the probability of hearing the signal increases gradually from zero to 100 per cent over a 5-db range of levels. This is a complication that was not considered in discussing threshold levels in the preceding pages. Fundamentally, there is no one level at which the signal is "just audible." To avoid confusion, threshold levels are usually defined as the level at which the recognition probability is 50 per cent, but when necessary other percentages may be used provided they are specifically indicated. From Figure 5, it is seen that in the example, the 50 per cent masked threshold is 14.5 db, the 90 per cent threshold is 16.4 db, and the 10 per cent threshold is 12.6 db.

This, also, has already been used in the earlier discussion of echo ranging, as has the recognition differential. This is the difference between the threshold level of the signal and the level of the background. In the example, the recognition differential for 50 per cent recognition is thus $14.5 - 12.0 = 2.5$ db.

Two variants of the above experimental procedure are in common use. In the first, the level of the signal is increased after each presentation, until 100 per cent recognition is definitely attained. Thereafter, the experiment may be started over at a low-signal level, or the level may be successively decreased after each presentation. This is called the *method of minimal changes*. In the second method, the levels are changed in a haphazard manner; this is the *method of random presentation*. Each has its advantage.

## 14.2.2 The Theory of Masking

The theory of hearing presented above can be applied to the masking problem. A given sound activates a particular area of the basilar membrane. This causes a certain fraction of the auditory nerve fibers to be stimulated. The number of discharges per second of these nerve fibers depends on the intensity of the sound. Suppose that while this sound is incident on the ear, a second sound is received and stimulates the same area. Two effects may occur. (1) Additional nerves may be stimulated and their discharges added to the number occurring previously; or (2) the nerves which already have been stimulated may be caused to discharge more rapidly. The effect of the second sound will thus be only to change the stimulation of an already stimulated area. Unless the change is great enough, it will not be perceived.

If the second sound has a markedly different spectrum than the first, it may stimulate a different area of the basilar membrane, and the second sound may be perceived just as though the first were absent.

It appears from these considerations that the masking of one sound by another depends on the areas of the basilar membrane which are stimulated, and hence on the spectral character of the two sounds, as well as on their intensity. In the following pages a résumé will be submitted of the experimental results observed in experiments on masking of (1) one pure tone by another pure tone; (2) a pure tone by background noise having a continuous spectrum; and (3) a complex sound by a second complex sound.

## 14.2.3 The Masking of One Pure Tone by a Second Pure Tone

Experiments on the masking of one pure tone by another pure tone have already been discussed in Chapter 9. The results will be summarized here for completeness.

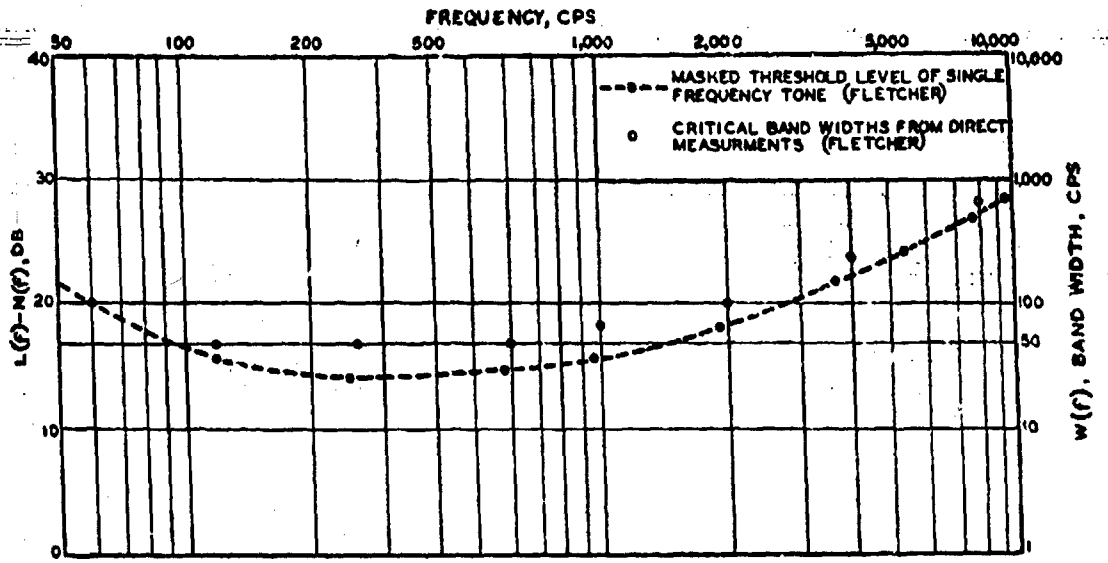


FIGURE 6. Masked threshold level of single-frequency tone and critical bandwidths from direct measurements.[13]

1. Masking is greatest at frequencies in the vicinity of the masking tone; in the presence of a 1,300-c masking tone of 60-db[c] level, the masked threshold of a tone of 1,250 c is raised 46 db above the threshold of hearing, whereas the masked threshold of a tone of 3,000 c is raised only 8 db.[7]

However, when the frequencies of the two tones are very close together, the resulting beats enable the listener to hear the masked tone more easily, and the masking is reduced to some extent. In the example cited above, the masking in the immediate neighborhood of 1,200 c is nearly 10 db lower than that at 1,150 or 1,250 c.

2. Masking is not reciprocal; that is to say, a 60-db masking tone of 1,250 c will not necessarily raise the threshold of a 1,300-c sound 46 db. In general, the masked thresholds are higher on the high-frequency side of a pure tone; for example, a 1,200-c tone of 60-db level will raise the threshold of a 1,400-c tone 36 db, but that of a 1,000-c tone only 30 db. Moreover, it is found that the harmonics of the masking tone have a masking effect.

3. The increase in the masked threshold is roughly the same as the increase in the level of the masking tone. Thus, a 1,200-c masking tone of 80 db will mask a 1,250-c tone about 66 db, compared with the 46-db masking of the 60-db tone mentioned in paragraph 1. For very low and very loud tones, this simple relation is no longer true.

[c] Here and elsewhere in this chapter the levels of airborne sounds are specified in db above 0.0002 dyne/cm² (see Chapter 1, Figure 1).

## 14.2.4 The Masking of a Pure Tone by Complex Sound

Most masking noises encountered in practice are complex, and have their power distributed over a wide band of frequencies. Correspondingly, they stimulate a larger area of the membrane, although the stimulus at any point will be weaker, than in the case of a pure tone of the same level.

Since the masking effect of a pure tone is largely confined to a relatively narrow band of frequencies, we may expect that, conversely, a pure tone will be masked only by those components of a complex sound whose frequencies are adjacent to that of the sound being masked. That is to say, there should be a more or less definite critical bandwidth $w(f)$ such that any components of the noise beyond $w(f)$ do not raise the masked threshold. This critical bandwidth should be the same (or nearly so) as that already discussed in Chapter 9. The masking effect of a complex sound at each frequency will thus be determined by the power level in the critical band involved. Call this $C(f)$; it is related to the spectrum level of the noise $N(f)$ by the relation

$$C(f) = N(f) + 10 \log w(f).$$

The quantity $C(f)$ is called the *critical band* spectrum level.

If this hypothesis is correct, the threshold of a pure tone of frequency $f$, when masked[d] by a complex

[d] This ignores the increased masking when the levels are unduly high.

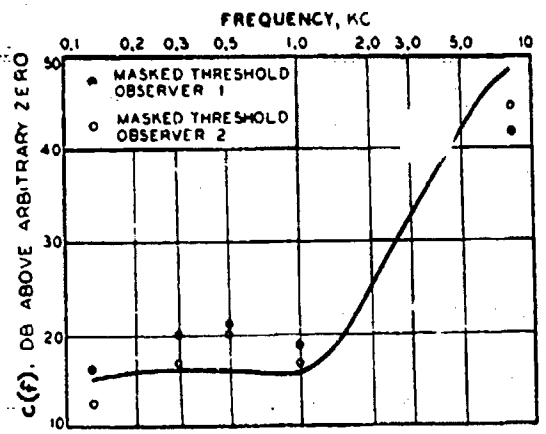


FIGURE 7. Experimental data on critical band levels, using two observers. The solid curve is plotted from the data in Figure 6.

sound, should be just equal to $C(f)$. The verification of this theory by experiment is shown in Figure 6.[1,8] If $L(f)$ is the masked threshold level of a pure tone of frequency $f$, it is expected that $L(f) = C(f)$, or, in other words, that

$$L(f) - N(f) = 10 \log w(f).$$

The masking was by thermal noise, which had a spectrum level $N(f)$ that was the same for all frequencies. The signals were pure tones, for which threshold levels were determined experimentally as described above and plotted as circles. The values of $L(f) - N(f)$ calculated in this way are shown by the open circles and the left-hand scale. The values of $w(f)$ were determined by experiments on the masking of one pure tone by another. The agreement between theory and experiment is very satisfactory.

Figure 7 shows the agreement between theory and experiment in another case. The curve is the graph of $C(f)$, the critical band spectrum of the masking noise, while the points are the masked thresholds $L(f)$ of pure tones, as determined by two listeners. It should be clearly noted that, while $C(f)$ and $L(f)$ are equal, the two numbers are determined by different experimental and computational procedures.

The recognition differential for this case is still defined as the masked threshold level of the pure tone minus the overall level of the noise. However, the overall level of the noise depends on its whole spectrum, while the masking effect is determined only by the spectrum in the immediate critical band of the pure tone signal. Consequently, the laws of masking cannot be easily formulated in terms of recognition differentials. The latter are useful in many cases, but when either or both of the sounds are not pure tones, the critical band spectrum yields more information and should be used whenever possible.

### 14.2.5 The Masking of One Complex Sound by Another Complex Sound

The success of the critical band theory in predicting the masked thresholds of pure tones leads one to anticipate that it will be equally successful in predicting the masking of one complex sound by another.

Let $C_s(f)$ and $C_n(f)$ be the critical band spectra of the signal and masking noise, respectively. It has been found that if $C_s(f)$ is greater than $C_n(f)$ for some frequency $f_1$, then the sudden starting or stopping of the signal can be heard at least 50 per cent of the time. If $C_s(f)$ is less than $C_n(f)$ for all frequencies, the signal will be heard less than 50 per cent of the time.

These relationships are shown schematically in Figure 8. The three parts of the figure show the same signal and noise, the level of the signal being low in A and high in C.

Several other interesting conclusions can be reached from a study of these figures. Thus, Figure 8B shows that, as the signal level is increased, it will first become audible as a sound of pitch $f_T$. This is called the threshold frequency. Figure 8C shows that at higher level many (though not all) frequency components are audible. The audible components of the signal are indicated by shading. The components between $f_1$ and $f_2$ remain inaudible even at this higher level. This theory has been fairly well confirmed by experiment.[9]

As in the case of the masking of a pure tone by a complex sound, the laws are not easily formulated in terms of the recognition differential. The latter is sometimes a useful practical concept, but its use may lead to mistakes unless the critical band spectra are available as supplementary information.

### 14.2.6 Adjacent Masking

In using the critical band spectrum criterion, it is necessary that the masking noise have a continuous spectrum or at least that single-frequency compo-

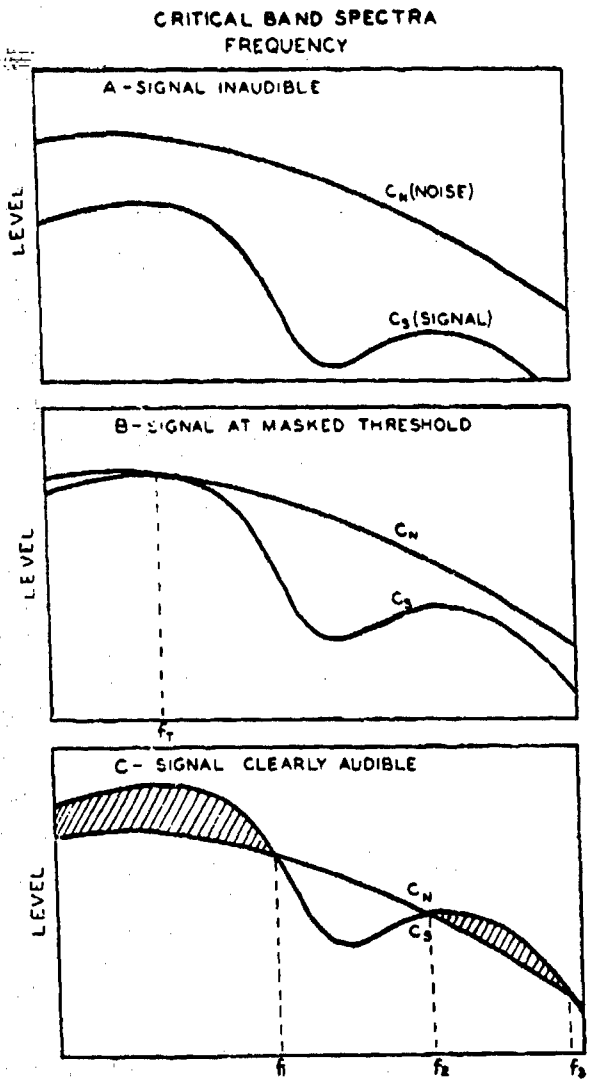


FIGURE 8. Schematic diagrams illustrating recognition of complex signal against a complex noise background. The three parts of the figure show the same signal and noise spectra, the signal spectra being shown at different levels.

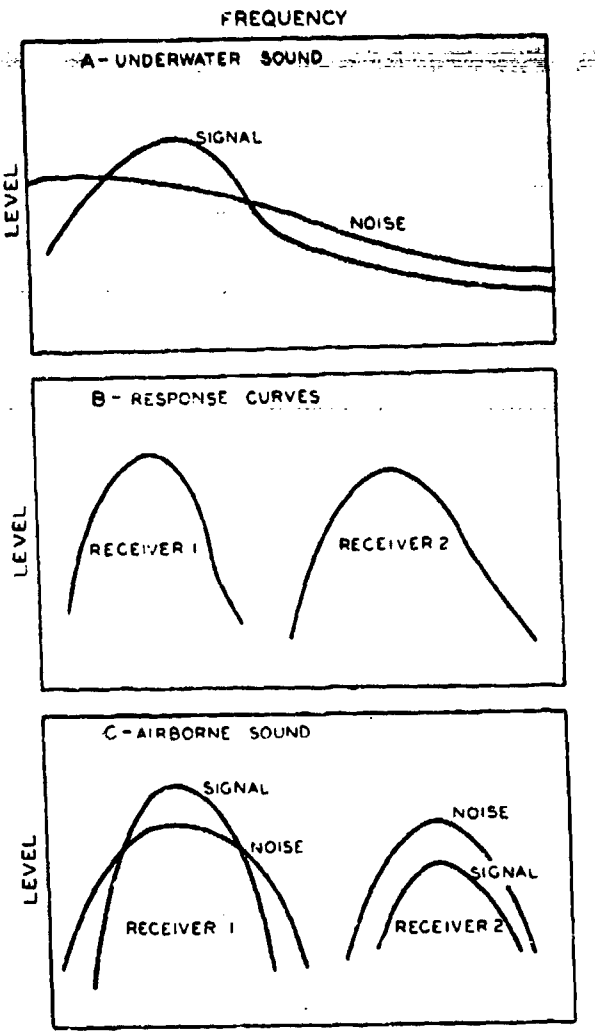


FIGURE 9. Diagram illustrating the effect of the receiver in detecting underwater sound signals. (A) The spectra of the underwater signal and sound. (B) The response curves of two receivers. (C) The signal and noise spectra at the output of the receiver systems.

nents do not have too high a level. Very strong pure tones mask a much wider region on the basilar membrane than their critical band spectra indicate; there occurs a "spilling over" of masking onto frequencies adjacent to the ones at which the energy is located. This effect is called *adjacent masking*. It follows that if components outside the critical band of a particular tone under consideration contribute appreciably to the masking in the band itself, a greater sound level will be required for the tone to reach the masked threshold.

From the shape of the stimulation patterns on the basilar membrane it is apparent that a very loud sound will stimulate several critical bands on either side of its own. It may happen that, in the critical band centered at frequency $f$, the stimulation due to the noise components of this frequency is weaker than the stimulation due to unusually strong components of considerably lower or higher frequency. It is only when this is the case that adjacent masking becomes significant; and it is with this qualification that the term is used to designate the effect.

### 14.2.7 Variable Levels

The preceding discussion of masking applies to sounds that have a constant loudness and quality. Ship sounds are usually not constant, but may have a variable overall level, or a variable spectrum, or both. For example, the main engine and gear train driving the screws may contribute a sound of constant level and spectrum. The screw itself may contribute a sound of different spectrum, the level of which changes as the screw turns. The resultant is a sound for which level and spectrum both change periodically.

In such cases, it is reasonable to suppose that the highest values of $C$, attained during the changes will be the important ones in determining recognition. In addition, the changes, particularly if they are rhythmic, may "call attention" to the presence of the signal.

The quantitative laws governing this increased audibility of rhythmic sounds have not been carefully worked out, but the existence of the effect is certain. It must be considered in any application of the foregoing principles.

### 14.2.8 Influence of the Receiver on the Audibility of Underwater Sound

In this chapter, the discussion has been entirely concerned with airborne sound levels and spectra; that is, with the sound output of listening gear. In most other parts of this book, the discussion has dealt with the underwater sound levels and spectra. Since the receiver amplifies the sound and may modify its spectrum, it may have an effect on the recognition of signals.

To see this two receivers may be compared (Figure 9). The graphs A show the critical band spectra of the underwater signal and noise. Graphs B are the response curves of two receivers, and curves C are the sound outputs of the two receivers, determined by combining graphs A and B as discussed in Section 14.2.5.

For receiver No. 1, the signal will be clearly audible, but for receiver No. 2, the signal will be inaudible. This is perhaps an extreme case, but serves to illustrate the manner in which the response curve of a receiver can influence the audibility of a signal.

# Chapter 15

# SONIC AND SUPERSONIC LISTENING

## 15.1 THE MAXIMUM RANGE EQUATIONS

### 15.1.1 Two Specifications for Listening Receivers

IN SECTION 9.1.7, two general specifications for echo-ranging receiver amplifiers were given. The purpose of these specifications was to prevent the limitation of echo ranges by factors under the control of the electronics designer, and to insure that only those limitations inherent in the sea need be considered in this book. Similar specifications for listening receiver amplifiers can be written, but they are somewhat more complex.

This increased complexity results from the need for wider pass bands in listening than in echo-ranging receivers. This is especially true of sonic listening gear. Even in the discussion of echo-ranging receivers, the concept of spectrum level was used, but it was only necessary to consider a single frequency. This was because the spectrum levels could be considered as approximately constant over the whole range of frequencies within the pass band of the receiver.

In order to simplify a fairly complicated discussion, it is well to begin with the second specification of Section 9.1.7, and to reformulate it as a definition.

The *listening band* of a receiver-hydrophone system is that range of frequencies over which the inherent noise is so low that it is possible to hear water noise, if the loudspeaker is in a quiet place. More precisely, if the inherent noise spectrum is recalculated in terms of the spectrum of an equivalent noise in the water, the listening band is the range of frequencies for which this equivalent spectrum is below the actual water-noise spectrum. In this discussion, the critical band spectrum level is to be used, rather than the 1-c spectrum level, although often the conclusions will not be much affected if the 1-c spectrum level is used. An exception occurs if there are many single-frequency sounds (such as overtones of the 60-c ship's power) in the self-noise. In principle also, such single-frequency tones may introduce gaps in the listening band; for this and other reasons, they are undesirable.

Two general classes of listening systems can be distinguished. The first includes those whose listening band falls in the supersonic region, and whose output is made audible by a heterodyne change of frequency. The other class has its listening band in the audio frequencies, and does not need a heterodyne stage to render its output perceptible.

The choice of a suitable listening band is obviously one of the designer's first problems. It can only be determined by a consideration of all possible factors affecting listening.

With the aid of this definition of the listening band, the first specification for listening amplifiers can be formulated simply:

*Specification 1.* The gain of the listening amplifier and loudspeaker, and their location on board ship, should be such that all frequency components of water noise within the listening band can be heard despite the sound of nearby activities.

When this specification is fulfilled, the airborne noise will never prevent the detection of a signal. The variation in spectrum level over the listening band introduces complications that were not present in the echo-ranging case. As a possible example, consider a listening band extending from 100 to 10,000 c: over this frequency range the spectrum levels of self-noise and water noise may vary by 50 to 70 db, and that of the wanted signal by at least as much. This brings two dangers with it: the intense low-frequency components may overload the amplifier when its gain is sufficient to give the high-frequency components an adequate level; and if this is not the case, the very loud lower frequencies may deafen the listener, so that he cannot hear the weaker high frequencies. This is the "adjacent masking" discussed in the previous chapter.

These dangers can be avoided if the response of the early stages of the amplifier is such that the low frequencies are amplified less than the high frequencies. This brings us to the next specification:

*Specification 2.* The overall response curve of the system should be such that all frequency components of water noise are presented to the listener's ear at about the same loudness.

When these two specifications are complied with, the maximum range obtainable with the receiver will depend only on the pass band and on conditions beyond the control of the electronics designer. A less important consequence is that sound levels can be

expressed in terms of their underwater equivalents, rather than by giving their actual levels at the listener's ear. The gain of the receiver thus disappears from the equations which are given in the following sections.

### 15.1.2 The Determination of Maximum Ranges

As in the case of echo ranges, there is no one range at which the target suddenly becomes undetectable. The maximum listening range must again be defined in terms of a given probability of detection, usually 50 per cent.

The analysis of the factors influencing the maximum range at which a target can be heard over a given listening system has the same objectives as the corresponding problem in echo ranging. The designer will need the information so that the best system for a given purpose can be built. The fleet will need more specific predictions, based on prevailing oceanographic conditions, so that appropriate operational decisions can be reached.

### 15.1.3 General Principles of Range Calculation

The problem of listening differs from the corresponding echo-ranging problem in that the target is not insonified from the listening station, but is itself the source of the signal. Consequently, in calculating listening ranges, there is no term corresponding to the target strength $T$ which occurs in echo-ranging calculations. The steps in the listening process are:

1. The emission of the signal by the target.
2. The transmission of the signal to the receiver.
3. The detection of the signal at the listening station.

If the source level of the signal is $S$, its level $L(r)$, at a point $r$ yards distant from the source, is given by

$$L(r) = S - H(r), \tag{1}$$

where $H(r)$ is the transmission loss in decibels.

The signal will be detectable only if $L(r)$ is at least equal to the level of the background noise, plus the recognition differential $M$. The noise level $N$ will be expressed as equivalent isotropic water noise, so that the effective level will be $N + D$ where $D$ is the directivity index of the hydrophone (see Section 13.3). The directivity index is a negative number, so that $N + D$ is less than $N$. The signal will be heard only if its level exceeds that of the noise by an amount greater than the recognition differential $M$,

$$L \geqslant N + D + M, \tag{2}$$

or, using equation (1),

$$S - H(r) \geqslant N + D + M,$$

whence

$$H(r) \leqslant S - (N + D + M). \tag{3}$$

In order to facilitate discussion of these equations, the quantity $(N + D + M)$ appearing on the right of equation (2) is called the *recognition level*, and $S - (N + D + M)$, the *available signal output*. The actual level $S - H(r)$ must exceed the recognition level, and hence the transmission loss must be less than the available signal output.

"Available signal output" is clearly an omnibus term and summarizes the effect of a large number of factors. The individual terms in equation (3) have been discussed quantitatively in the course of the preceding chapters of this book. At present, it is necessary to keep clearly in mind the relation between them as given by equation (3); for the problem of maximum listening ranges can be discussed intelligently only with regard to the manner in which these quantities vary from one set of conditions to another.

### 15.1.4 The Maximum Range Equations in Echo Ranging and Listening

It is instructive to realize, at this point, that each of the terms in equation (3) differs decidedly from the same term in the corresponding equation in echo ranging. The sources in the two operations have almost no characteristic in common. In echo ranging the signal has a very definite quality and particular frequency, and its source level remains reasonably constant. In listening, the exact opposite is true: the signals are extremely variable and unpredictable; they have a wide frequency range and great variability of spectral distribution; their source levels may vary 100 db or more. The echo-ranging projector is highly directional, while sound is emitted almost equally in all directions by a ship's hull and screws.

The background noise (other than reverberation) which causes the masking of the signal in echo ranging is comprised in a relatively narrow band of supersonic frequencies, and is of a different quality from the signal. In listening, it may be more or less similar to the signal in frequency distribution and is thus likely to be even more serious than in echo ranging. On the other hand, in listening there is no reverberation to mask the signal; for that reason there is also no doppler to assist recognition. In echo ranging, the target noise is part of the masking background; in listening, it is the signal.

The directivity index of echo-ranging gear is always a large negative number of the order of $-20$ or more; in present listening practice, the receiving hydrophone is highly directional only for supersonic sound.

The recognition differential in the two operations is essentially different. In echo ranging two recognition differentials must be considered, one for the case when reverberation masks the echo, which happens at short ranges, another for the case when the echo is masked by noise, as it is at long ranges. In listening, the signal is always masked by noise, but it should be noted that the conditions affecting recognition are different because of the different nature of the signal.

Finally, the transmission of the sound emitted by targets in listening differs from that in echo ranging. First of all, it is a one-way process in listening and a two-way process in echo ranging. This would seem to make the transmission loss less important in listening, and result in longer ranges. However, this is not necessarily the case; the source levels are in general lower than in echo ranging. An important exception occurs when the target is transmitting echo-ranging pings, and the listening system is supersonic. In that case, the signals are obviously identical. Moreover, when echo ranging on a large target, the target strength is a positive quantity and partially cancels the additional magnitude of the transmission-loss term in the echo-ranging equation. Secondly, if the listening system uses sonic frequencies, the attenuation is much less than that of the supersonic sound used in echo ranging. The image effect causes additional losses at moderate range in the sonic band, which is, on the other hand, somewhat less affected by thermal gradients. Since the sources are nondirectional, sound reflected from the bottom is very important in listening. Between them, this second group of factors influencing transmission loss is largely responsible for the longer ranges at which detection by sonic listening is possible.

## 15.1.5 Critical Band Spectrum Levels

As has been discussed in Chapter 14, the various frequency components of a wide-band signal have different audibility, so that as the signal level increases, detection usually occurs first at a single frequency. As the level increases still further, other frequencies become audible. Consequently, equations (2) and (3) should be considered as applying to a single frequency band; or better still, as typical of a large number of equations, one for each frequency band. If the levels entering them are based on the critical bands of the ear, the recognition differential will be zero, and the equations simplify to

$$L(f) \geq N(f) + D(f), \tag{4}$$

$$H(r,f) \leq S(f) - N(f) - D(f), \tag{5}$$

where the notation indicates explicitly that the critical band in question centers at the frequency $f$. Thus $N(f)$ and $S(f)$ are the critical band spectra of noise and source, respectively, and $H(r,f)$ is the transmission loss for this frequency. Those frequency components of the signal for which the mean level is higher than the recognition level will be heard; the rest will be inaudible most of the time. If the mean level of all frequency components is less than their recognition levels, the presence of the target will probably be undetected.*

If the range to the target is opened from a very short range, the value of the transmission loss $H(r,f)$ will, in general, increase for each frequency $f$. At some range it will become equal to the available signal output at that frequency; for longer ranges, that frequency will be heard less than half the time and rapidly become inaudible all of the time.

The *maximum listening range* is defined as the greatest range at which the transmission loss at one or more frequencies is less than the available signal output at those frequencies. At this range, the transmission loss at other frequencies may exceed their available signal output.

* This statement may require slight modification. If the critical band spectra of signal and noise are nearly parallel, the signal may be heard even when the level of all signal components is several db less than the noise components. This effect, however, has not yet been definitely established.

The application of this definition and of equations (4) and (5) encounters practical difficulties in that to date most measurements of sound output $S$ and noise levels $N$ have been made in wide bands, so that the critical band spectra are often not known. S ,e data on the spectrum levels of ship sounds have been published, but the experimental methods used in their determination have not always been the best. The spectrum levels of ambient noise are, perhaps, more accurately known, but data on the self-noise of surface vessels is incomplete. The lack of data should be rectified. In the interim, equations (2) and (3) have been used: the levels $S$ and $N$ entering them are overall levels, whose values are tabulated in Chapters 12 and 13. This does not eliminate the effects of our ignorance; that makes itself felt as ignorance of the proper values of the recognition differential $M$ and of the transmission loss $H$.

This could only be overcome by guessing. For example, the overall transmission loss of a given signal depends on its spectrum in a complicated way. This difficulty was often eliminated by the simplifying assumption that the transmission anomaly is zero, so that $H(r) = 20 \log r$, but this was a bad guess (see Chapter 3). Similarly, the directivity index varies with the spectrum; some guess as to its effective value had to be made. The same was true of the recognition differential.

Since submarines have made more use of listening than have surface vessels, data for the calculations have been accumulated.[8] Even here, however, the data has been restricted largely to that relevant to existing installations.

The difficulties in using equations (4) and (5) are largely those of present ignorance; the difficulties inherent in the wide-band calculation are more fundamental. The basic objections to them are less serious in the case of supersonic listening, however, since in this frequency range all spectra are simple and the listening band is relatively narrow.

## 15.2 GENERAL APPLICATIONS OF THE MAXIMUM RANGE EQUATIONS

### 15.2.1 Reduction of Sound Output for Defense

The use of listening by the enemy as a means of detection can obviously be countered by reducing the sound output of friendly vessels. Such a program has been actively pursued in the case of the submarines of the U.S. Navy. No corresponding program has been followed in the case of surface vessels. The narrow margin by which the Battle of the Atlantic was won, coupled with the probability that future submarines will rely even more on listening as a means of detection and fire control, indicates that serious thought should be given this matter. The increased use of homing torpedoes operating on listening principles is a further reason for such a program. The maintenance of radio silence is a recognized countermeasure against attack from the air. The achievement of underwater silence is more difficult but may be essential.

The ideal objective is to make the signal output unavailable to the enemy gear. Since the available output is $S(f) - [N(f) + D(f) + M(f)]$, it involves factors that cannot be determined without knowledge of the enemy gear. However, it is certain that $N$ cannot be made less than the ambient noise level. Some estimate of the directivity index $D$ in various frequency ranges can be made. The recognition differential $M$ will be zero for detection by an operator; for present homing devices, it is presumably a positive number, but the possibility of devices operating with negative values of $M$ is not excluded.

Thus, some estimate can be made of the largest value of $S(f)$, the sound output of a ship, which is tolerable if the ship is to be completely undetectable at that frequency. This may be unachievable, but even so, it may be useful to reduce $S$ as much as possible. It will be shown that the maximum range sometimes depends very critically on the available signal output. Thus a relatively small reduction in $S$ may make a great difference in the range at which the enemy can detect the vessel.

### 15.2.2 Reduction of the Noise Background

Most of the sound sources aboard ship which radiate to a distant enemy also contribute to the self-noise which interferes with use of its own listening gear. The quieting of these sources will thus contribute in some measure to increasing the signal available for the detection of enemy vessels. This is obviously the case with the sound from the ship's screws.

However, not all sources of self-noise radiate sound to a distance. This is especially true of circuit noise,

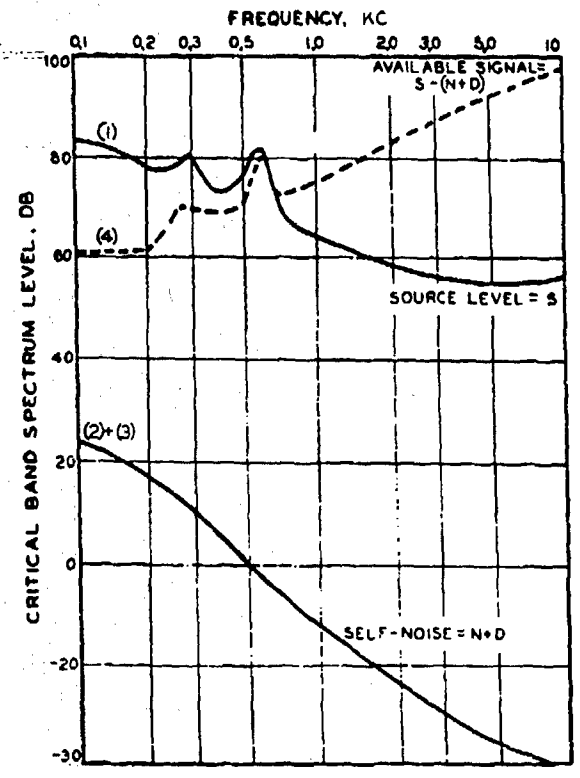


FIGURE 1. The calculation of the available signal level: self-noise background.

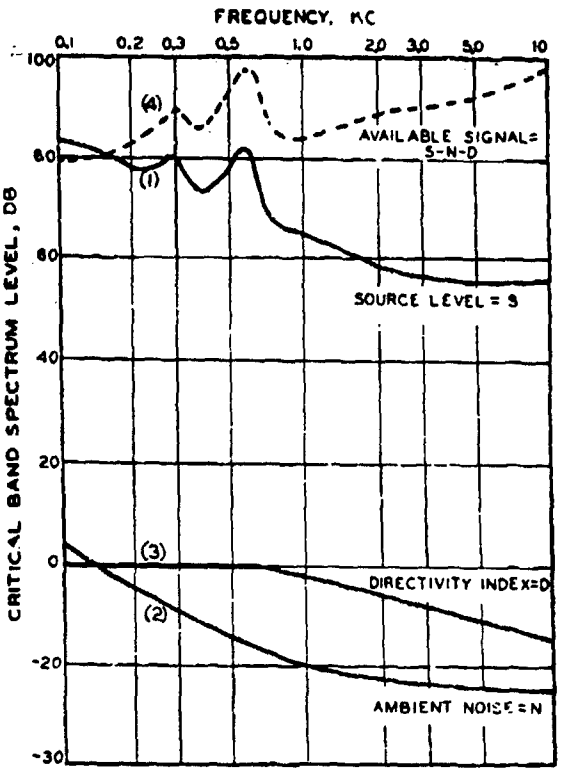


FIGURE 2. The calculation of the available signal level: ambient noise background.

and electrical pickup. The turbulence and bubbles near the hydrophone are probably no great aid to enemy listening and may be the most serious source of self-noise.

The elimination of circuit noise is essentially a problem for the electronics engineer. That component caused by electrical pickup from other equipment aboard ship can be reduced by proper design of all circuits, and by proper maintenance of commutators and other mechanical switches whose operation is semicontinuous. The streamlining of hydrophones and their proper mounting will further reduce the noise background.

A systematic study of the causes of self-noise will undoubtedly result in appreciable improvements over existing installations. However, a lower limit to the value of $N$ is fixed by the ambient noise of the sea itself. The only countermeasure for this is the use of directional hydrophones, which lower the value of $N+D$ when ambient noise is the major component of $N$. In general, directivity will also discriminate against the localized noise sources in the ship's hull, unless the hydrophone happens to be trained toward them.

## 15.2.3 Choice of Listening Band

In Section 15.1.1, the listening band was defined in terms of the characteristics of the receiver and of the noise background. However, these characteristics are to some extent under the control of the designer. This is obvious in the case of the electronic components of the system; but the control of the noise background basically requires the consideration of all designers engaged in the construction of the ship, beginning with the naval architect. Such a focus of attention on the needs of the sound gear has not been possible in the past. The recognition of the critical nature of submarine warfare in World War II may make consideration of control of noise background imperative in the future.

For the present, it may be assumed that the electronic components of the amplifier can be constructed so as to place the listening band in any frequency range desired. It will then be reasonable to use a frequency range in which the available signal is high. This will not necessarily insure the greatest range of detection—that will also depend on the transmission loss at the different frequencies—but for the moment

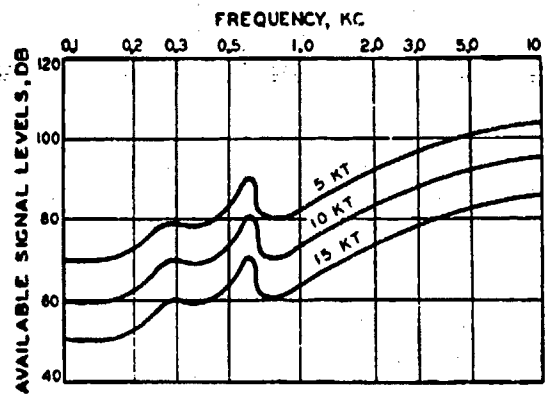


FIGURE 3. Available signal levels at various speeds (schematic).

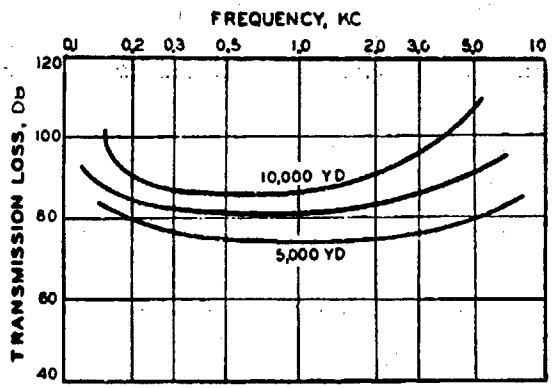


FIGURE 4. Assumed transmission loss $H(r,f)$ of sonic sound at various ranges.

the problem may be simplified by assuming that a high available signal is the major desideratum.

The manner in which the three factors $S$, $N$, and $D$ influence the available signal output is then illustrated schematically in Figures 1 and 2. The spectrum of the actual sound output of the source is schematic but shows machinery peaks in the region of 100 to 600 c, and a general drop until cavitation noise from the screws becomes dominant between 3,000 and 10,000 c. The self-noise curve of Figure 1 is again schematic but shows a steep slope over the whole range. As a result, the whole trend of the available signal output reverses that of the actual source output. The greatest available signal occurs at 10,000 c or higher; and it would seem reasonable to place the listening band in the supersonic region, or at least in the high audible. This figure presumably represents the ideas which prevented Great Britain and America from exploiting the possibilities of the sonic frequencies prior to World War II.

Figure 2 is based on the same actual sound output, but assumes that self-noise has been eliminated, leaving ambient noise as the dominant background. A moderately directional hydrophone is also presupposed. The available signal is then no higher at 10,000 c than is the machinery peak at 600 c. On the basis of available signal output, there is thus little to choose between the sonic band and the supersonic. It has already been seen that the transmission loss of the frequencies below 1,000 c is much less than that of the supersonic frequencies. Hence the case for the sonic frequencies is much more favorable. This figure presumably represents the ideas that caused Germany to develop sonic listening systems.

It should be emphasized that these figures are quite schematic. It would be inappropriate to attempt any final decision between sonic and supersonic listening at this time. The question is a very complex one and its answer is not known. The purpose of the foregoing discussion was to indicate the type of data and the kind of reasoning that will be needed in arriving at the answer.

### 15.2.4 The Range Prediction Problem

In order to provide basic data for operational decisions, it is desirable that the fleet be supplied with summary tables, listing the ranges at which detection of various targets can reasonably be expected under each of a number of conditions (bathythermogram, speed of searching vessel, type of gear, etc.). The purpose of the present section is to indicate the manner in which such tables can be prepared; the graphs presented in the course of the discussion are entirely schematic, especially those of Figure 4.

Again, graphs of available signal level as a function of frequency must first be prepared for each type of target and a given type of listening gear. The speed of the searching vessel will also affect these graphs, so that a typical work sheet may contain several graphs (see Figure 3). Since the sea state and other oceanographic factors, such as snapping shrimp, affect the noise background, these must also be considered. In principle, a large number of such graphs must be prepared, although in practice short cuts can be found to reduce the number needed.

To determine the maximum range, the transmission loss $H(r,f)$ is also plotted, as in Figure 4, using the same scale as for Figure 3. As the transmission loss depends on thermal conditions, etc., several such curves must also be prepared. Since transmission loss

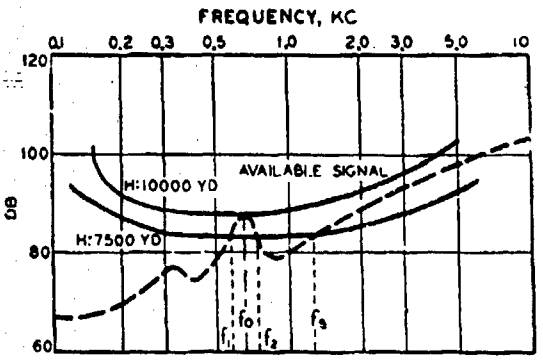


FIGURE 5. Graphical computation of maximum listening ranges (schematic).

and available signal must be compared, it is convenient to plot all curves on transparent paper so that they can be superposed.

The result of the superposition is shown in Figure 5, only one curve of available signal level being shown to avoid confusion. Since the available signal must be greater than the transmission loss, it is seen that at 7,500 yd the components of frequency $f_1$ to $f_2$ or greater than $f_3$ are audible (always provided they are within the listening band of the system). At 10,000 yd, the transmission loss and available signal curves are tangent at $f_0$, hence 10,000 yd is the maximum range.

While this method of calculation may seem complex, the above description is itself only schematic and does not mention all the factors that must be taken into account. These other factors, such as fluctuation, time pattern, etc., can all be considered as influencing either the available signal or the transmission-loss curves. The method having been outlined, the separate factors will next be discussed in greater detail.

## 15.3 SONIC LISTENING

### 15.3.1 The Sound Output

The sources of the signal in listening are surface vessels, submarines, torpedoes, explosions of depth charges, and echo-ranging signals of other vessels. The main source of the high-frequency sound output of ships is the cavitation produced at the screws. Cavitation sounds have a comparatively continuous spectrum, the level of which falls off about 6 db per octave on the average. They are sufficiently uniform in character so that it is possible to determine the cavitation spectrum of a given class of ship at a given speed by taking a single measurement at some frequency, say 1 kc or 5 kc. Enough measurements on cavitation sounds from various sources have been made to enable the prediction of their level for any class of ship at any speed within about 5 db.

This is not true of machinery sounds, which are the dominant source of low-frequency sound (less than 1 kc) at low speeds. These sounds have very complex and irregular line spectra, and differ widely among different individual ships. They are heard as rumbles, squeaks, groans, and whines.

In order to determine the role played by these single-frequency peaks in range prediction, some average value must be chosen. Available data show examples of these peaks with height in a 1-c band ranging from 15 to 40 db above the average spectrum level of the ship sounds. The peaks can be allowed for statistically by replacing the average spectrum by another curve lying above it and indicating the average height of the peaks. At frequencies below 1,000 c, this line of peaks runs above but parallel to the average spectrum, but above this frequency it rapidly approaches the average because machinery sounds are predominantly low frequency.[1]

### 15.3.2 Directivity in Sonic Listening

In sonic listening the problem of hydrophone directivity is usually discussed in connection with the determination of the bearing of the target. However, it enters also in the range problem, and it does this in two ways. In order for a signal to be detected, it is necessary that there be a noticeable change in the sound heard. Since changes are constantly occurring even in the background noise, a gradual change due to a signal of increasing level will not be noticed so soon as would a sudden change due to a signal that is turned on and off. This on-and-off feature may be supplied by the listener, if he trains a directional hydrophone on and off the target bearing. Complete data on the value of this procedure are not available, but it is thought to be appreciably better than would be mere listening on a single bearing.

In the second place, a directional hydrophone discriminates against isotropic ambient noise, the amount of discrimination being given by the directivity index, as already noted.

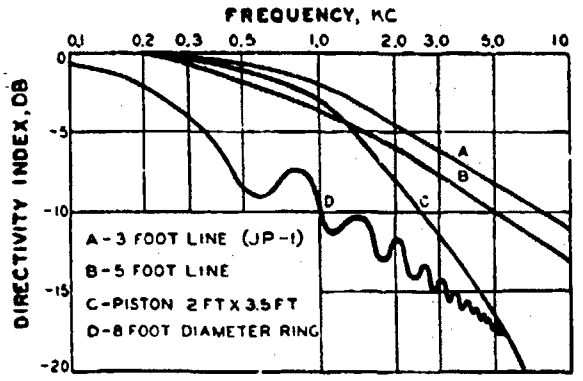


FIGURE 6. Directivity indices of various types of hydrophones for sonic frequencies.

The computed directivity indices of various sonic hydrophones are shown in Figure 6 for frequencies below 10 kc. At the frequency of 1 kc, the directivity index of the 3-ft line and piston hydrophones is only $-2$ to $-3$ db. Compared with these, the directivity index of $-10$ db and of the 8-ft ring hydrophone is outstanding. The structural difficulties of such a large hydrophone can be avoided by the use of arrays of small hydrophones mounted in fixed positions on the hull. The training is accomplished by phase-shifting networks. It is estimated that the increased directivity may increase ranges by as much as 10,000 yd.[2]

### 15.3.3 Directivity and Bearing Determination

The accurate determination of bearings depends very strongly on the directivity of the hydrophone, increasing with directivity up to the point where the narrowness of the beam makes it difficult to maintain contact with the target. Good directivity in the lower frequency range may enable the operator to obtain a more-or-less tentative bearing at long range, and, as the range is closed, the bearing determination can be made with increasing accuracy.

The simplest way to increase the directivity of a given kind of listening gear is to make the hydrophone larger, but the practical limits of size are usually exceeded before the desired directivity for sound of low frequencies is attained. (See Table 1.)

The 3- and 5-ft line hydrophones are typified by the JP and JT hydrophones developed during World War II. The latter consist of nickel tubes, several inches in diameter and of the lengths indicated (see Section 12.3). The general increase in directivity with frequency is indicated in the table for these and the other types of hydrophones. The improved bearing accuracy with increasing size is also apparent.

TABLE 1. Estimated probable bearing error with various hydrophones.

| Hydrophone | Probable bearing error, 1 kc (degrees) | Probable bearing error, 10 kc (degrees) |
|---|---|---|
| 3-ft line | 15.0 | 1.75 |
| 5-ft line | 9.0 | 1.0 |
| Square piston, 1 ft | Nondirectional | 5.25 |
| Rectangular piston, 3.5 ft | 13.5 | 1.5 |
| Circular piston, 10.7 in. | Nondirectional | 7.0 |
| Ring, 2 ft | 19.0 | 2.0 |
| Ring, 8 ft | 4.5 | 0.5 |
| Pressure gradient | 19.0 | 19.0 |

An exception to this rule is the pressure gradient hydrophone. This is a device of small dimensions, the directivity of which is independent of frequency. At low frequencies, it compares very favorably with much larger hydrophones of other types.

The use of split transducer systems for listening was also mentioned in Chapter 14. This enables very good bearing accuracy to be obtained with small hydrophones. The binaural effect was used to obtain bearings during World War I. It has repeatedly been suggested that this might be the basis for a useful sonic listening system. Experimental trials have shown it to be capable of giving accurate bearings. It is doubtful whether the directivity obtained in this way will combat self-noise in the manner obtained with large hydrophones.

### 15.3.4 Ambient Noise Background

The spectra of the various types of ambient noise that are encountered in listening were discussed in Chapter 13. Ambient noise is the limiting factor when the listening hydrophone is stationary, provided the sea state is greater than 1 or 2. For a sea state less than 2, the overall level of ambient noise drops below 0 db, and thus approaches the overall level of circuit noise, which ranges from $-30$ to 0 db; hence in this case the circuit noise will be limiting. Shrimp noise is usually negligible at lower sonic frequencies.

### 15.3.5 Self-Noise Background

The measurements of self-noise discussed in Section 13.3 are typical of the information available on this topic. The measurements have mostly been made

for the specific purpose of evaluating a certain type of listening or echo-ranging system. They have brought to light marked differences between various installations of the same type of gear but have not resulted in a thorough understanding of the problem.

There is great need for a thorough analysis of this problem. The various sources of self-noise should be studied in detail. In so far as the sources are electric, these studies should result in improved specifications for the ship's wiring system, grounds for sonar gear, etc. The maintenance and quieting of auxiliaries is presumably also an important factor. It may even be necessary to consider the design of the ship's hull and screws, and certainly the mounting and streamlining of hydrophones.

The only certain conclusion is that there is no one source of self-noise and that it is at present the factor which limits the performance of a listening system. Any development program must envisage an effort to reduce all sources of self-noise. This cannot be a minor part of the program, as it has in the past. Self-noise must be considered at all stages of the ship's construction. Ideally, the ship should be built around the listening system; in the past, the latter has been installed in the ship. The extent to which this ideal can be approached depends on the importance assigned to listening, and this may well vary from one type of ship to another.

### 15.3.6 Transmission Loss at Low Frequencies

The experiments on the transmission of audible sound, described in Chapter 3, are too recent and incomplete to have been assimilated into a definitive range-prediction scheme. The data for the frequency range 200 to 2,000 c can be schematically summarized as in Figure 7.

At ranges less than a few hundred yards, the transmission loss $H$ is variable because of the interference between direct and surface-reflected sound. This is indicated by the double hatching in the figure. Beyond this variable region, the transmission loss increases rapidly out to 1,000 or 2,000 yd. The frequency is a determining factor in this region, the higher frequencies suffering less loss than the lower frequencies. Downward refraction in the upper layers causes this loss to occur at shorter ranges, as discussed in Chapter 3. The single hatching on Figure 7 shows the region of rapidly increasing loss.

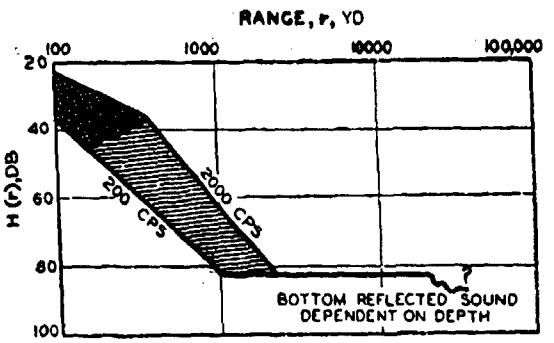


FIGURE 7. Schematic graph of transmission loss $H(r)$ for sonic sound. At ranges less than a few hundred yards, $H$ is variable; this is shown by means of the double hatching. Beyond this variable region, the transmission loss increases rapidly out to 1,000 or 2,000 yards; this region is indicated by the single hatching in the figure. The frequency is a determining factor in this region. Beyond this region, bottom-reflected sound is dominant, and $H$ remains constant out to 10,000 or 20,000 yards. (See Section 3.2.) The magnitude of $H$ and the range at which it begins depend on the depth of the ocean. At very long ranges the transmission loss must again increase, but there are very few data to indicate the rate of increase.

Beyond this region, bottom-reflected sound is dominant, and the transmission loss remains constant out to 10,000 or 20,000 yd. Possible reasons for this remarkable phenomenon have been discussed in Section 3.3, but there may be others as well. The magnitude of this loss and the range at which it begins both depend on the depth of water. A value of 80 to 85 db appears appropriate for 1,000-fathom water. This value appears to be relatively independent of thermal conditions, but increases slightly with the hydrophone depth. It is also subject to irregular fluctuations of considerable magnitude, but they do not appear to bear any systematic relation to the range.

At very long ranges, the transmission loss must again increase, but there is very little data to indicate the rate of increase.

The fact that the transmission loss of bottom-reflected sound is nearly independent of range has an important bearing on the maximum ranges obtained with sonic gear. If the available signal output is between 60 and 80 db, the maximum range is likely to be less than 1,000 yd and unlikely to be greater than 2,000 yd. Contact will not be established until the target becomes audible via direct sound. But if the available signal output is greater than 80 db, the bottom-reflected sound may become useful, and the range may suddenly increase to 10,000 or 20,000 yd.

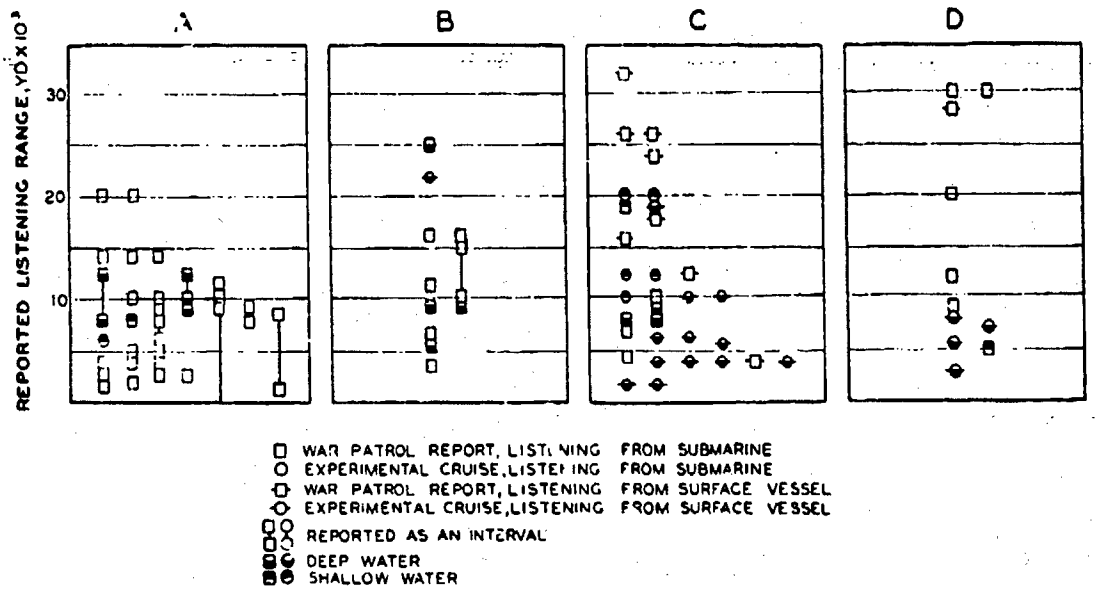


FIGURE 8. Reported sonic listening ranges. (A) Unidentified targets. Listening ships; submerged submarine. (B) Target: destroyer, unknown speed. Listening ship: submerged submarine or stationary surface vessel. (C) Targets: freighters, tankers, tugs, trawlers, transports, fishing vessels. Speed not known. Listening ship: submerged submarine or stationary surface vessel. (D) Targets: convoys, task forces. Listening ship: submerged submarine or stationary surface vessel.

This critical dependence on the available signal output undoubtedly explains the extreme variability of reported sonic listening ranges. These are shown on Figure 8. In evaluating these data, it should be noted that long ranges are more likely to be reported than are short ranges. It thus appears that the sonic listening gear in present use is capable of detecting targets at ranges in excess of 15,000 yd under favorable conditions. These are low self-noise and high actual output of the target.

Transmission of the higher audible frequencies, above 2,000 c, presumably behaves in a manner intermediate between that of frequencies below 2,000 c, and that of the supersonic frequencies (see Section 13.4). The effects of source directionality may increase, though this is doubtful in the case of ship sounds. It is therefore impossible to evaluate the importance of bottom reflection until further experiments have been performed.

## 15.4 SUPERSONIC LISTENING

### 15.4.1 Recognition

Supersonic sound is made audible by heterodyning, so that the loudspeaker of the listening system emits audible sound. The general principles of recognition are thus identical with those applying to audible sound. However, several quantitative differences exist.

In the first place, supersonic receivers usually have pass bands not more than 1 kc wide. The spectrum of the heterodyned output may thus be confined to the range 300 to 1,300 c, as compared to 100 to 10,000 c in sonic listening.

In the second place, a 1-kc band of one supersonic spectrum is very similar to a 1-kc band of another. There are no single-frequency peaks, and while most spectra slope 5 to 9 db per octave the change in spectrum level over a 1-kc band is negligible for many purposes. This applies to background noise as well as to the sound output of ships.

Thus, there will usually be no one frequency of the heterodyned sound that is more audible than another. There will be no tonal quality to distinguish the signal from the background.

In general, the recognition differential will be zero. This statement requires a slight modification, since supersonic sound from a ship's screw is usually rhythmically modulated in intensity. Recognition occurs when the maximum level of a rhythmic signal is equal to or possibly a few decibels less than the average level of nonrhythmic background. The maximum level of screw sounds is usually about

3 db above the average level. Since most measurements yield average values, they must be increased by about 3 db in calculating the available signal. This increase is sometimes loosely called a recognition differential.

An exception to these statements occurs when the target vessel is echo ranging. The pings will be heard as tonal pulses of sound which have a high recognition differential (see Chapter 9), as well as a high source level.

## 15.4.2 The Available Signal Level

These considerations just presented introduce some simplification into the calculation of ranges. The spectra of the signal and the background noise need not be considered in detail; it is sufficient to state the spectrum levels at the mid-point of the listening band.

With regard to background noise, the situation is similar to that of sonic listening. That is, if the listening station is quiet, the limiting factor will be ambient noise, whereas if listening is done from a noisy vessel, the noise of the listening vessel will predominate. In supersonic listening, however, when ambient noise is limiting, shrimp crackle becomes important. While the ordinary levels of ambient noise range from −78 to −53 db depending on sea state, if shrimp are present the ambient noise levels may be −49 to −39 db.

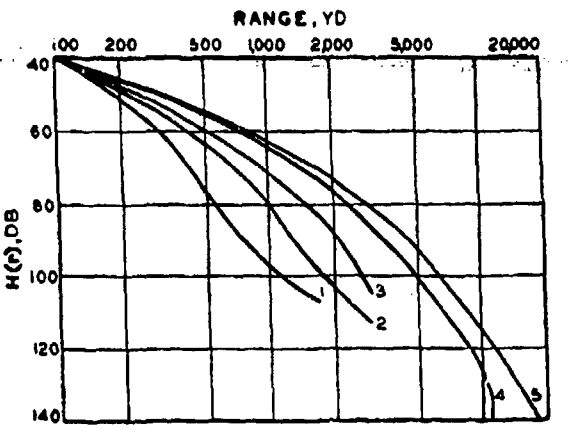


FIGURE 9. Transmission loss $H(r)$ at 24 kc for various thermal conditions. The curves are based on the anomaly curves of Figure 14 of Chapter 3, and the same numbering is used.

When used at supersonic frequencies, listening gear will discriminate against ambient noise. A directivity index $D$ of −23 db, (equal to that of standard echo-ranging transducers) is common.

## 15.4.3 The Transmission Loss

This has already been discussed in connection with maximum echo ranges and in Chapter 3. The graphs

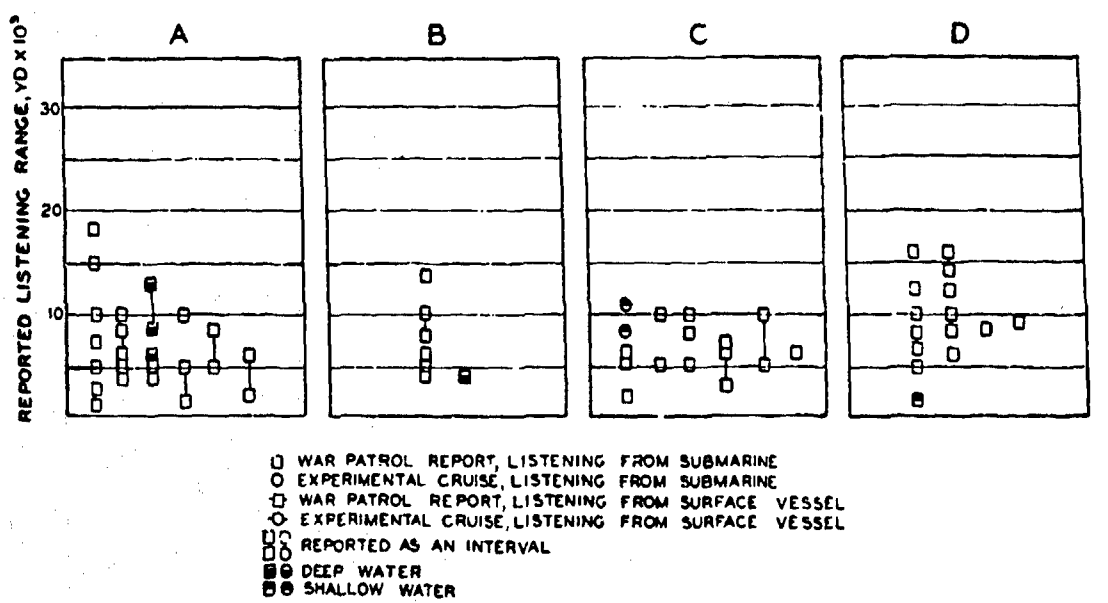


FIGURE 10. Reported supersonic listening ranges. (A) Same as Figure 8A. (B) Same as Figure 8B. (C) Same as Figure 8C. (D) Same as Figure 8D.

of Figure 9 should be compared with Figure 7, in order to contrast the transmission loss of the supersonic and sonic frequencies. Since there is no horizontal portion of the curve, the supersonic ranges should show less variation than do the sonic ranges. Because of this fact, also, there seems less probability of achieving great improvement in the performance of supersonic systems by a reduction in self-noise. However, this conclusion must be accepted with some caution. The source of the sound used in obtaining Figure 13 of Chapter 9 was an echo-ranging projector. This discriminates strongly against transmission via bottom reflection until relatively long ranges are reached. It is therefore possible that the transmission loss of supersonic ship sounds is not correctly given by this graph.

The possibility of using this bottom-reflected sound for detection by supersonic listening has not been explored. It would require the use of hydrophones that do not discriminate against sound rays that are inclined at large angles to the horizontal.

The reported ranges at which targets have been detected by supersonic listening gear are shown in Figure 10.

## LIST OF SYMBOLS USED

Meanings of symbols used consistently in several different sections are listed below. Definitions may be found in the sections indicated.

| | | Section |
|---|---|---|
| $a$ | Attenuation coefficient | 3.2.4 |
| $A$ | Transmission anomaly (db) | 1.3.3 |
| $b$ | Beam pattern function | 1.2.5 |
| $B$ | Beam pattern function (db) | 1.2.5 |
| $c$ | Velocity of sound in water | 2.1.2 |
| $D$ | Directivity index (db) | 7.4.3 |
| $D_2$ | Depth at which temperature 0.3 degrees F less than surface temperature first occurs | 2.1.5 |
| db | Decibel, measure of sound pressure level above unit pressure | 1.2.1 |
| $E$ | Sound level of echo (db) | 8.1.1 |
| $F$ | Energy flow (watts per yd$^2$) | 1.2.1 |
| $H$ | Transmission loss (db) | 1.3.2 |
| $I$ | Intensity (pressure$^2$) | 1.2.1 |
| $I_a$ | Intensity on acoustic axis | 1.2.5 |
| $I_1$ | Intensity at unit range | 1.2.3 |
| $J_v$ | Volume reverberation index | 5.3.4 |
| $J_K$ | Surface reverberation index | 5.3.4 |
| $L$ | Sound level (db) | 1.2.1 |
| $L_a$ | Source level on acoustic axis (db) | 1.2.5 |
| $L_1$ | Source level at unit range or 1 yard (db) | 1.2.3 |
| $M$ | Recognition differential (db) | 10.3.1 |
| $M_R$ | Recognition differential for reverberation-limited echoes (db) | 10.3.1 |
| $M_N$ | Recognition differential for noise-limited echoes (db) | 10.3.1 |
| $N$ | Noise level (db) | 9.1.3 |
| $N(f)$ | Noise spectrum level at $f$ | 9.1.3 |
| $p$ | Pressure (dynes per sq cm) | |
| $Q$ | Resonance parameter | 9.1.2 |
| $r$ | Range (yd) | |
| $r_3$ | Ping length (yd) | 11.3.2 |
| $r_{\text{lim}}$ | Range to shadow boundary | 3.2.3 |
| $r_{40}$ | Range at which received sound level is 40 db less than that received at 100 yd | 3.2.3 |
| $R(f)$ | Response spectrum level at $f$ | 9.1.1 |
| $RL$ | Reverberation level (db) | 5.3.4 |
| $S$ | Source level (db) | 8.1.1 |
| $T$ | Target strength (db) | 8.1.1 |
| $Z$ | Mechanical impedance | 7.1.1 |
| $\lambda$ | Wavelength | |
| $\mu$ | Reflection coefficient | |
| $\rho$ | Density | |
| $\tau$ | Area, cross section | |

# BIBLIOGRAPHY

Numbers such as Div. 6-540.4-M1 indicate that the document listed has been microfilmed and that its title appears in the microfilm index printed in a separate volume. For access to the index volume and to the microfilm, consult the Army or Navy agency listed on the reverse of the half-title page.


## Chapter 1

1. *Sonar Calibration Methods*, Summary Technical Report, NDRC Division 6, Volume 10.
2. *Sonar Operator's Handbook*, West Coast Sound School, San Diego, Calif., 1944 Edition.
3. *Acoustics*, Alexander Wood, Interscience Publishers, 1941.
4. *Acoustics*, Stewart and Lindsay, D. Van Nostrand Co., 1930.
5. *Theory of Propagation of Explosive Sound in Shallow Water*, Chaim L. Pekeris, OSRD 6545, NDRC 6.1-sr1131-1891, CUDWR, January 1945.
   Div. 6-510.12-M5

## Chapter 2

1. *The Oceans*, H. U. Sverdrup, M. W. Johnson, and Richard H. Fleming, Prentice-Hall, 1942.
   1a. *Ibid.*, p. 790.
2. *Measurements of the Horizontal Thermal Structure of the Ocean*, Norman J. Holter, Report S-17, USNRSL, Aug. 18, 1944.
   Div. 6-540.4-M1
3. *An Acoustic Interferometer for the Measurement of Sound Velocity in the Ocean*, Robert J. Urick, Report S-18, USNRSL, Sept. 18 1944.
   Div. 6-510.22-M6
4. *Calculation of Sound Ray Paths in Sea Water, Theory, Tables and Description of a Slide Rule for Computation of Limiting Echo Ranges and Construction of Sound Ray Diagrams from Bathythermograph Observations, with Examples*, Richard H. Fleming and Roger Revelle, UCDWR, Jan. 16, 1942.
   Div. 6-510.11-M3
5. *The Theory of Sound*, Lord Rayleigh, Macmillan Company, 1940.
   5a. *Ibid.*, Vol. 2, p. 131.
6. *The Sonic Ray Plotter*, Leonard I. Schiff, NDRC 6.1-sr30-1741, Service Project NS-140, Report U-246, Aug. 8, 1944
   Div. 6-510.11-M8

## Chapter 3

1. *Vibration and Sound*, Philip M. Morse, McGraw-Hill Book Co., 1936.
   1a. *Ibid.*, p. 248.
   1b. *Ibid.*, p. 304.
2. *Theory of Sound*, John William Strutt and Baron Rayleigh, Macmillan Company, London, 1937.
   2a. *Ibid.*, Vol. II, pp. 215, 217
   2b. *Ibid.*, Vol. II, p. 319.
3. *Lloyd Mirror Effect in a Variable Velocity Medium*, Richard R. Carhart, Report M-140, UCDWR, Oct. 23, 1943.
   Div. 6-510.111-M1
4. *Variation of the Sound Field Near the Surface in Deep Water*, H. T. O'Neill and T. F. Johnston, Report U-49, UCDWR, Mar. 16, 1943.
   Div. 6-510.11-M5
5. *Some Theoretical Studies of the Propagation of Sound in Shallow Water*, Glen D. Camp and Carl Eckart, NDRC 6.1-sr30-1208, Report U-102, UCDWR, Aug. 15, 1943.
   Div. 6-510.11-M7
6. *Acoustics*, Alexander Wood, Interscience Publishers, 1941.
   6a. *Ibid.*, pp. 200, 203.
7. *The Stability of Air Bubbles in the Sea and the Effect of Bubbles and Particles on the Extinction of Sound and Light in Sea Water*, Paul S. Epstein, NDRC C4-sr30-027, UCDWR, Sept. 1, 1941.
   Div. 6-540.21-M1
8. "Absorption of Supersonic Waves in Water and Aqueous Suspensions," G. K. Hartmann and Alfred B. Focke, *The Physical Review*, Vol. 57, Feb. 1, 1940, p. 221.
9. *Transmission of Explosive Impulses in the Sea*, T. F. Johnston and R. W. Raitt, NDRC C4-sr30-403, Report U-8, UCDWR, Dec. 2, 1942.
   Div. 6-510.23-M6
10. *Propagation of Sound in a Medium of Variable Velocity*, Chaim L. Pekeris, NDRC C4-sr20-001, NLL, Sept. 20, 1941.
    Div. 6-510.11-M2
11. *Theory of Diffraction of Sound in the Shadow Zone*, Chaim L. Pekeris, NDRC 6.1-sr20-846, CUDWR, May 5, 1943.
    Div. 6-510.11-M6
12. *The Attenuation of Sound in the Sea*, Carl F. Eckart, NDRC 6.1-sr30-1532, Report U-236, Service Project NS-140, UCDWR, July 6, 1944.
    Div. 6-510.22-M4
13. *Theory of Propagation of Explosive Sound in Shallow Water*, Chaim L. Pekeris, OSRD 6545, NDRC 6.1-sr1131-1801, CUDWR, January 1945.
    Div. 6-510.12-M5
14. *Transmission of 24-Kc Sound in Shallow Water*, Report M-368, Service Project NObs-2074, UCDWR, Nov. 20 1945.
    Div. 6-510.221-M4
15. *The Additive Effects of Wind Force, Thermal Gradient and Particle Size on the Transmission of 24-Kc Sound over Sand Bottoms in Shallow Water*, Report M-375, Service Project NObs-2074, UCDWR, Dec. 1, 1945.
    Div. 6-510.221-M5

16. *Transmission of Sound in the Sea*, E. B. Stephenson, S-1204, NRL, October 16, 1935.
Div. 6-510.22-M1

*Absorption Coefficients of Sound in Sea Water*, E. B. Stephenson, Report S-1466, NRL, Aug. 12, 1938.
Div. 6-510.222-M1

*Absorption Coefficients of Supersonic Sound in Open Sea Water*, E. B. Stephenson, Report S-1549, NRL, Aug. 2, 1939. Div. 6-510.222-M2

17. *Attenuation of Underwater Sound*, Frederick A. Everest and H. T. O'Neill, NDRC C4-sr30-494, UCDWR, Revised, July 30, 1942.
Div. 6-510.2-M1

18. *Fluctuation of Transmitted Sound in the Ocean*, Sonar Analysis Section, NDRC 6.1-sr1121-1883, Technical Memorandum 6, UCDWR, Jan. 17, 1945.
Div. 6-510.3-M4

19. *Ultrasonics and Their Scientific and Technical Applications*, Ludwig Bergmann, John Wiley and Sons, 1939.
19a. *Ibid.*, pp 128-130.

20. *Transmission of 2-Kc Sound from a Deep Projector*, Report M-408, Sonar Data Division, UCDWR, March 1946.

21. *Attenuation and Fluctuation Studies Based on Supersonic Bottom Echoes*, Report M-384, Service Project NObs-2074, UCDWR, Dec. 13, 1945.
Div. 6-510.221-M6

22. *Acoustic Properties of Gas Bubbles in a Liquid*, Part I, Lyman Spitzer Jr., OSRD 1705, NDRC 6.1-sr20-918, CUDWR, July 15, 1943.
Div. 6-540.22-M1

23. *Propagation of Sound Through a Liquid Containing Bubbles, Part II, Experimental Results and Theoretical Interpretation*, E. L. Carstensen and Leslie L. Foldy, OSRD 3872, NDRC 6.1-sr1130-1629, Service Project NS-141, USRL, June 23, 1944.
Div. 6-540.3-M4

## Chapter 4

1. *Military Oceanography*, Summary Technical Report, NDRC, Division 6, Volume 6A.

2. *Long Range Sound Transmission*, Maurice Ewing and J. Lamar Worzel, Interim Report 1, March 1, 1944, to January 20, 1945, WHOI, Aug. 25, 1945.
Div. 6-510.1-M4

3. *Oceanography for Meteorologists*, H. U. Sverdrup, Prentice-Hall, 1942.
3a. *Ibid.*, Chapter 4.
3b. *Ibid.*, Chapter 6, pp. 123, etc.

4. *The Oceans*, H. U. Sverdrup, M. W. Johnson, and Richard H. Fleming Prentice-Hall, 1942.
4a. *Ibid.*, Figures 210 and 212, pp. 748 and 753.

## Chapter 5

1. *Theory of Sound*, John William Strutt and Baron Rayleigh, Macmillan Company, 1937, Vol. II, p. 283.
1a. *Ibid.*, Vol. I, p. 41.

2. "On the Absorption of Sound Waves in Suspensions and Emulsions," Paul S. Epstein, *Theodore von Kármán Anniversary Volume*, CIT, May 11, 1941, pp. 162-168.

3. *The Stability of Air Bubbles in the Sea and the Effect of Bubbles and Particles on the Extinction of Sound and Light in Sea Water*, Paul S. Epstein, OSRD C4-sr30-027, UCDWR, Sept. 1, 1941.
Div. 6-540.21-M1

4. *Dissipation of Energy due to the Presence of Air Bubbles in the Sea*, F. H. Willis, OSRD C1 British 503. Comment, Conyers Herring, CUDWR—Special Studies.
Div. 6-540.2-M3

5. *Acoustic Properties of Gas Bubbles in a Liquid*, Lyman Spitzer, Jr., OSRD 1705, NDRC 6.1-sr20-918, CUDWR, July 15, 1943.
Div. 6-540.22-M1

6. *Propagation of Sound Through a Liquid Containing Bubbles, Part I, General Theory*, Leslie L. Foldy and E. L. Carstensen, OSRD 3601, NDRC 6.1-sr1130-1378, Service Project NS-141, USRL, Apr. 25, 1944.
Div. 6-540.22-M2

7. *Reflection and Scattering of Sound*, F. H. Willis, OSRD WA-02-10f, NDRC C4-brTS-501, British Internal Report 50, HMA/SEE, Fairlie Laboratory, Great Britain, Dec. 20, 1941.
Div. 6-530.1-M1

8. *The Discrimination of Transducers Against Reverberation*, OSRD 1761, NDRC 6.1-sr30-968, Report U-75, UCDWR, May 31, 1943.
Div. 6-520.1-M8

9. *The Detection of an Echo in the Presence of Reverberation*, Carl F. Eckart, OSRD 173, NDRC C4-sr30-175, UCDWR, May 12, 1942.
Div. 6-560.32-M1

10. *Reverberation Studies at 24 Kc*, OSRD 1098, NDRC C4-sr30-401, Report U-7, UCDWR, Nov. 23, 1942.
Div. 6-520-M2

11. *Frequency Characteristics of Echoes and Reverberation*, W. M. Rayton and Raymond C. Fisher, OSRD 4159, NDRC 6.1-sr30-1740, Service Project NS-140, Report U-244, UCDWR, Aug. 9, 1944.
Div. 6-520.3-M2

12. *The Attenuation of Sound in the Sea*, Carl F. Eckart, NDRC 6.1-sr30-1532, Service Project NS-140, Report U-236, UCDWR, July 6, 1944.
Div. 6-510.22-M4

13. *Stratification of Sound Scatterers in the Ocean*, George E. Duvall, Service Project NObs-2074, Report M-397, UCDWR, Feb 16, 1946.
Div. 6-520.22-M3

14. *Forward Scattering from the Deep Scattering Layer*, Richard R. Carhart, Service Project NObs-2074, Report M-398, UCDWR, Mar. 19, 1946.
Div. 6-520.22-M4

## Chapter 6

1. *Laboratory Studies of the Acoustic Properties of Wakes*, Parts I and II, Jeffries Wyman, Wendel Lehmann, and David Barnes, NDRC 6.1-sr31-1069, Service Project NS-141, Apr. 3, 1944.
Div. 6-540.3-M3

2. "On the Destructive Action of Cavitation," Kornfeld and Suvorav, *Journal of Physics of USSR*, Vol. 7, No. 3, 1944, pp. 171-181.

3. *Propagation of Sound Through a Liquid Containing Bubbles, Part I, General Theory*, Leslie L. Foldy, OSRD 3601, NDRC 6.1-sr1130-1378, Service Project NS-141, USRL, Apr. 25, 1944.
Div. 6-540.22-M2

*Part II, Experimental Results and Theoretical Interpretation*, E. L. Carstensen and Leslie L. Foldy, OSRD 3872, NDRC 6.1-sr1130-1629, Service Project NS-141, USRL, June 23, 1944.
Div. 6-540.3-M4

4. *Sound Transmission Through Destroyer Wakes*, OEMsr-30, Service Project NS-141, Report M-189, UCDWR, Mar. 8, 1944.
Div. 6-540.32-M3

5. *Echoes from Wakes*, Carl F. Eckart, NDRC C4-sr30-498, UCDWR, Aug. 29, 1942.
Div. 6-540.31-M1

6. *Acoustic Measurements of Surface Wakes in San Diego Harbor*, Richard R. Carhart and George E. Duvall, OSRD 1628, NDRC 6.1-sr30-961, Report C-62, UCDWR, May 8, 1943.
Div. 6-540.32-M1

## Chapter 7

1. "On the Effects of Magnetism upon the Dimensions of Iron and Steel," J. P. Joule, *The London, Edinburgh and Dublin Philosophical Magazine and Journal of Science*, Vol. 30, 1847, p. 76.

2. *Magnetostrictive Transducers*, Malcolm H. Hebb and Harvey Brooks, NDRC 6.1-sr287-898, HUSL, June 22, 1943.
Div. 6-612.1-M2

3. *Design and Construction of Magnetostriction Transducers*, Summary Technical Report, NDRC, Division 6, Volume 13.

4. *Sonar Operator's Handbook*, West Coast Sound School, San Diego, Calif., 1944 Edition

5. J. and P. Curie, *Comptes Rendus Academie Sci., Paris*, Vol. 91, 1880, p. 294 and Vol. 93, 1881, p. 1137.

6. "Uses and Possibilities of Piezoelectric Oscillators," A. Hund, *Proceedings of the Institute of Radio Engineers*, Vol. 14, 1926, p. 447.

7. *Design and Construction of Crystal Transducers*, Summary Technical Report, NDRC Division 6, Volume 12.

8. *A Practical Dictionary of Underwater Acoustical Devices* (Volume 1 and Supplementary Loose Leaf Sheets), OSRD 772, NDRC 6.1-sr20-889, CUDWR-USRL, July 27, 1943.
Div. 6-554-M28

9. *Vibration and Sound*, Philip M. Morse, McGraw-Hill Book Co., New York, 1936.

10. *Loudspeakers*, Norman W. McLachlan, Oxford, Clarenden Press, 1934.

## Chapter 8

1. *Reflections from Submarines at Close Ranges, Model Experiments Using Optical Method*, Service Project NS-222 and MIT Research Project DIC-6187, MIT, Apr. 8, 1944.
Div. 6-530.23-M2

2. *Studies of Optical Reflections from Submarine Models* (Part I), OSRD 3706, NDRC 6.1-sr1046-1053, Service Project NS-222, Research Project DIC-6187, MIT, Apr. 12, 1944.
Div. 6-530.23-M3

3. *Studies of Optical Reflections from Submarine Models* (Part II), OSRD 3706, NDRC 6.1-sr1046-1668, Service Project NS-222, Research Project DIC-6187, MIT, Aug. 15, 1944.
Div. 6-530.23-M4

4. *Some Measurements of the Directivity Patterns, Target Strengths, and Directivity Factors of Spheres, Discs, Triplanes, and Polyplanes*, C. J. Borbank and Raymond C. Fisher, File 02.133, UCDWR Report C-81, Calibration Group, UCDWR at the USNRSL, San Diego, California, Aug. 2, 1945.
Div. 6-633.2-M6

5. *Reflection of Light from a Submarine Model*, R. B. Tibbey, Report M-61, UCDWR, May 12, 1943.
Div. 6-530.23-M1

6. *Measurement of Reflections from Submarines Using Models and High Frequency Sound*, Joseph B. Keller, OSRD 4439, NDRC 6.1-sr1130-1834, Service Project NS-140, USRL, Sept. 27, 1944.
Div. 6-530.23-M5

7. *Physics of Sound in the Sea*, Summary Technical Report, NDRC Division 6, Volume 8.

## Chapter 9

1. *Computed Maximum Echo and Detection Ranges for Submarine Echo-Ranging Gear*, NDRC 6.1-sr1128, 1131-1688, CUDWR, July 1944.
Div. 6-570-M2

2. *Self-Noise of Sonar Gear*, OEMsr-1131, OEMsr-1483, and NObs-2083, Report C-2(6.1.332), SAG-WHOI, August 1, 1946.
Div. 6-580.32-M1

3. *Status Report on Task No. 5, Effect of Short Pulse Length and Receiver Bandwidth on Echo Ranging*, Robert W. Kirkland, Report 3510-RWK-HP, BTL, July 15, 1944.
Div. 6-632.03-M5

4. *Interim Report on Electronic Own Doppler Nullifier*, A. Wilson Nolle and W. A. Felsing, NDRC 6.1-sr287-719, HUSL, Mar. 24, 1943.
Div. 6-631.31-M5

5. *Dependence of Operational Efficacy of Echo-Ranging Gear on its Physical Characteristics*, Henry Primakoff and Martin J. Klein, Service Project NS-182, NDRC 6.1-sr1130-2141, CUDWR, USRL, Mar. 15, 1945.
Div. 6-551-M14

6. *A Survey of the Problem of Maximum Echo Ranges* (Preliminary Draft), Carl Eckart, NDRC 6.1-sr30-1315, Report U-130, UCDWR, Nov. 20, 1943.

## Chapter 11

1. *Bearing Deviation Indicator*, OSRD 6425, NDRC 6.1-sr287-2075, HUSL, Nov. 1, 1945.
Div. 6-631.4-M1

2. "FM Sonar Joins the Fleet," Lt. J. J. Crowley, USNR, BuShips *Electron*, NavShips 900,100, September 1945.

3 *Frequency Modulation Sonar*, Malcolm C. Henderson and Charles A. Hisserich, OEMsr-30, Report U-95, UCDWR, Sept. 4, 1943.
Div. 6-635.241-M3

4. *Frequency Modulation Echo-Ranging Systems, Calar, Pribar, and Subsight*, Malcolm C. Henderson, NDRC 6.1-sr30-308, Report U-12, UCDWR, Dec. 30, 1942.
Div. 6-635.2-M1

5. *Underwater Sound Equipment IV—Frequency Modulated Sonar Systems*, Summary Technical Report, NDRC Division 6, Volume 17.

6. *Instruction Book for QLA and QLA-1 Sonar Equipment*, Service Project NObs-2674, Report NavShips 900,790, UCDWR, Feb. 27, 1946.
Div. 6-635.3-M1

7. *Doppler Effect in FM Sonar*, Malcolm C. Henderson, OSRD 1955, NDRC 6.1-sr30-1115, Report U-107, UCDWR, Sept. 20, 1943.
Div. 6-635.12-M4

*Doppler Effect in Frequency Modulation Sonar, Mathematical Appendix*, Malcolm C. Henderson, OEMsr-30, Service Project NS-142, Report M-184, UCDWR, Feb. 8, 1944.
Div. 6-635.12-M5

8. *A Practical Dictionary of Underwater Acoustical Devices, Cards 120 and 121*, OSRD 772, USRL, July 27, 1943.
Div. 6-554-M28

9. *Status Report on Echoes from Small Objects*, Report M-388, Sonar Data Division, UCDWR, Feb. 14, 1946.

10. *Time Variation of Gain for QC Receivers* (Memorandum), J. Lewis Hathaway, HUSL, Dec. 8, 1942.

11. *Automatic Gain Control in Echo-Ranging Systems*, Frederick V. Hunt, NDRC 6.1-sr287-764, HUSL, Apr. 13, 1943.
Div. 6-631.13-M1

12. *Automatic Frequency Response Recorder*, Alfred K. Tatum, Report P35/671, NLL, Dec. 22, 1943.
Div. 6-553.5-M1

## Chapter 12

1. *Installation, Operation and Maintenance Instructions for Model JP-1 Sound Receiving Equipment, Topside Sonic Listening Equipment*, Service Project NS-114, Report D24,417, CUDWR-NLL, Sept. 1, 1943.
Div. 6-623.1-M1

2. *Noise Level Monitor and Cavitation Indicator*, William B. Snow, OSRD 4685 NDRC 6.1-sr1128-1930, Service Project NS-113, Report P55/1281, NLL, Jan. 31, 1945.
Div. 6-642.1-M3

3. *How to Operate the Noise Level Monitor and the Cavitation Indicator*, OEMsr-1128, Report P55/1191, CUDWR-NLL, Feb. 1, 1945.

4. *Underwater Sound Output of USS Timosa (SS 283)*, Report M-303, UCDWR, Mar. 5, 1945.
Div. 6-580.1-M11

5. *Survey of Underwater Sound. Sounds from Submarines*, Vern O. Knudsen, R. S. Alford, and J. W. Emling, 6.1-NDRC-1306, Report 2, Dec. 31, 1943.
Div. 6-580.1-M2

6. *The Acoustic Fields of Ships of Various Kinds as Determined on the Mark 2 Acoustic Range at Wolf Trap*, Report 700, NOL, Mar. 25, 1943.
Div. 6-580.2-M1

7. *Survey of Underwater Sounds. Sounds from Surface Ships*, M. T. Dow, J. W. Emling, and Vern O. Knudsen, OSRD 5424, NDRC 6.1-2124, Report 4 June 15, 1945.
Div. 6-580.2-M7

8. *Acoustic Measurements (75-150 cps) on Escort Vessels at Treasure Island, California*, Joseph Ashbrook, Report AAR-35, U. S. Navy Department, Bureau of Ordnance, Dec. 1, 1944.
Div. 6-580.2-M5

9. *The Sound Spectrograph, A Time-Frequency-Intensity Analyzer*, OEMsr-435, BTL, Oct. 1, 1943.
Div. 13-302.1-M2

10. *A Practical Dictionary of Underwater Acoustical Devices* (Volume I and Supplementary Loose Leaf Sheets), OSRD 772, NDRC 6.1-sr20-889, CUDWR—USRL, July 27, 1943
Div. 6-554-M28

## Chapter 13


1. *Sound Survey, San Francisco Harbor during November, 1942*, Report U-27, UCDWR, Feb. 3, 1943.
   Div. 6-580.33-M1
2. *Radio Engineers' Handbook*, F. E. Terman, McGraw-Hill Book Co., 1943.
   2a. *Ibid.*, p. 476.
3. *USS Shark—Noise vs Speed Tests*, William B. Snow and Henry B. Hoff, Report P32/P33/R812, NLL, Apr. 12, 1944.
   Div. 6-580.1-M5
4. *Sound Cavitation Tests on USS Spranger (SS 414)*, Laboratory Report M-283, UCDWR, Dec. 20, 1944.
   Div. 6-580.1-M9
5. *Survey of Underwater Sound, Ambient Noise*, Vern O. Knudsen, R. S. Alford, and J. W. Emling, 6.1-NDRC-1848, Report 3, Sept. 26, 1944.
   Div. 6-580.33-M2
6. *Self-Noise in Sonar Gear*, OEMsr-1131, OEMsr-1483, and NOrs-2083, Report C-2 (01.332), WHOI, Aug. 1, 1946.
   Div. 6-580.32-M1


## Chapter 14


1. "Auditory Patterns," Harvey Fletcher, *Reviews of Modern Physics*, Vol. 12, January 1940, p. 47.
2. "Differential Pitch Sensitivity of the Ear," E. G. Shower and R. Biddulph, *The Journal of the Acoustical Society of America*, Vol. III, 1931, pp. 275-287.
3. *Tone Duration as a Factor in Pitch Discrimination*, E. G. Wever, Report M-179, UCDWR, Feb. 16, 1944.
   Div. 6-560.1-M4
4. "Differential Intensity Sensitivity for Pure Tones," R. R. Riesz, *The Physical Review*, Ser. II, Vol. 31, 1928.
5. "Theory of Hearing: Vibration of Basilar Membrane; Fatigue Effect," G. V. Bekesy, *Physikalische Zeitschrift*, March 1929, p. 118.
6. *Hearing, Its Psychology and Physiology*, S. Smith Stevens and Hallowell Davis, John Wiley and Sons, 1938, p. 223.
7. *Speech and Hearing*, Harvey Fletcher, D. Van Nostrand Co., 1929.
8. "Loudness, Masking, and their Relation to the Hearing Process and the Problems of Noise Measurements," Harvey Fletcher, *The Journal of the Acoustical Society of America*, Vol. 9, 1938, p. 282.
9. *Masking Experiments, Part I*, NDRC 6.1-sr30-1751, Report U-229, Service Projects NO-163 and NS-164, UCDWR, June 28, 1944.
   Div. 6-560.21-M4
10. *Masking Experiments, Part II*, NDRC 6.1-sr30-1757, Report U-258, Service Projects NO-163 and NS-164, UCDWR, Sept. 15, 1944.
    Div. 6-560.21-M6


## Chapter 15


1. *Sonic Listening Aboard Submarines*, OSRD 5311, NDRC 6.1-sr1131-1885, Service Project NS-140, Sonar Analysis Section, CUDWR, February 1945.
   Div. 6-623.1-M8
2. *Basic Factors Affecting the Performance of Sonic Listening Gear on Submarines*, OSRD 5031, NDRC 6.1-sr1131-1888, Service Project NS-140, CUDWR, February, 1945.
   Div. 6-623.1-M9
3. *Comparative Tests on Submarine and Surface Craft Listening Equipments*, Donald P. Loye and Ralph C. Maninger, NDRC 6.1-sr20-1020, Service Project NS-113, Report D24 D38-391, NLL, Sept. 10, 1943.
   Div. 6-623-M4
4. *Maximum Listening Ranges of Underwater Sound Equipment*, Ralph C. Maninger, Report P33/R794, NLL, Mar. 13, 1944.
   Div. 6-570.22-M1
5. Addendum I to *Maximum Listening Ranges of Underwater Sound Equipment* (Report P33/R794), LeRoy A. Woodward, Report P33/R1008, NLL, July 1, 1944.
   Div. 6-570.22-M2
6. *A Study of Binaural Perception of the Direction of a Sound Source*, Irving Langmuir, Vincent J. Schaefer, and others, OSRD 4079, NDRC 6.1-sr323-1840, General Electric Company, June 30, 1944.
   Div. 6-560.1-M5
7. *Experimental Investigation of Factors Involved in Sonic Listening*, Ralph C. Maninger, NDRC 6.1-sr1128-1932, Report P33/1319, NLL, Feb. 28, 1945.
   Div. 6-621-M7
8. *Prediction of Sonic and Supersonic Listening Ranges*, NDRC 6.1-sr1131-1884, Service Project NS-140, CUDWR, December 1944.
   Div. 6-570.1-M6

## CONTRACT NUMBERS, CONTRACTORS, AND SUBJECT OF CONTRACTS

| *Contract Number* | *Name and Address of Contractor* | *Subject* |
|---|---|---|
| OEMsr-20 | The Trustees of Columbia University in the City of New York<br>New York, New York | Studies and experimental investigations in connection with and for the development of equipment and methods pertaining to submarine warfare. |
| OEMsr-1131 | The Trustees of Columbia University in the City of New York<br>New York, New York | Conduct studies and investigations in connection with the evaluation of the applicability of data, methods, devices, and systems pertaining to submarine and subsurface warfare. |
| OEMsr-30 | The Regents of the University of California<br>Berkeley, California | Maintain and operate certain laboratories and conduct studies and experimental investigations in connection with submarine and subsurface warfare. |
| OEMsr-31 | Woods Hole Oceanographic Institution<br>Woods Hole, Massachusetts | Studies and experimental investigations in connection with the structure of the superficial layer of the ocean and its effects on the transmission of sonic and supersonic vibrations. |
| OEMsr-287 | President and Fellows of Harvard College<br>Cambridge, Massachusetts | Studies and experimental investigations in connection with (i) the development of equipment and devices relating to subsurface warfare. |

## SERVICE PROJECT NUMBERS

The projects listed below were transmitted to the Executive Secretary, NDRC, from the War or Navy Department through either the War Department Liaison Officer for NDRC or the Office of Research and Inventions (formerly the Coordinator of Research and Development), Navy Department.

| *Service Project Number* | *Subject* |
|---|---|
| NO-222 | Acoustic reflection fields of submarines |
| NS-140 | Acoustic properties of the sea bottom |
| Ext. | |
| NS-140 | Range as function of oceanographic factors |
| NS-141 | Acoustic properties of wakes |

# INDEX

The subject indexes of all STR volumes are combined in a master index printed in a separate volume. For access to the index volume consult the Army or Navy Agency listed on the reverse of the half-title page.


Absorption of sound
  air bubbles, 55
  causes, 55-57
  definition, 9, 55
  ship wakes, 123-124, 125, 127-128
Acoustic projectors
  *see* Projectors, sonar
Acoustic shadow in ocean
  diffraction, 33
  ECR layer, 112-113
  formation, 83
  limiting range, 32
  scattering of sound, 33
  and intensity, 26-27
  theory, 16-17
ADP projectors (ammonium dihydrogen phosphate), 140-141, 148
Air bubbles in ocean
  as deceptive target, 174
  attenuation of sound, 57
  sound absorption, 57
  target area, 85-86
  wakes from ships, 122, 126-127
Airborne noise, 243
Ambient noise, 248-254
  biological noise, 250-254
  from harbors, 253
  general character, 249
  in echo ranging, 182-184
  sea noise, 249-250
  sonic listening, 273
  sources, 248
Ammonium dihydrogen phosphate projectors, 140-141, 148
Amplification ratio, 177
Amplifiers, response curves, 177
ARSB (anchored radio sono buoy), 223
Asdic projector, 139-141, 147
Attenuation of sound, 34-36, 55-60
  air bubbles, 57
  causes, 55-58
  coefficient, 9, 34-36, 57
  definition, 7
  depth of hydrophone, 34
  fresh water, 57
  minimal coefficient, 58-60
  recommendations, 57
  reverberation, 108
  scattering, 103
  thermal gradients, 58
  thermocline layer, 34
  transmission, 7, 9
  vertical pulsing, 59-60
  viscosity, 57-58
Auditory masking
  *see* Masking, auditory
Autocorrelation coefficient of signals, 63-64
AVC (automatic volume control) in sonar receivers, 220

Bathythermograph measurements
  description of instrument, 11-12
  isothermal layer, 13
  isotherms, 74
  positive and negative temperature gradients, 12
  temperature-depth graphs, 12-13
  thermocline layer, 13
BDI (bearing deviation indicator), 209-210
  TVG control, 210
Beam patterns of transducers
  *see* Directivity in sonic listening
Bearing deviation indication, 207-210
  definition of bearing deviation, 205
  devices, 207
  split transducer, 207
  standard BDI, 209-210
Bearing of target
  *see* Target bearing
Bell Telephone Laboratories, 239
Biological noise, 250-254
  fish choruses, 252-253
  shrimps, 251-252
  sources, 250
Bottom reverberation, ocean, 88-90, 109-112
  effects of refraction, 110-111
  reverberation levels, 111-112
  scattering coefficients, 90, 112
  transmission loss, 109-110
  types of sea bottom, 109
British Asdic projector, 139-140, 147
Bubbles in ocean
  as deceptive target, 174
  attenuation of sound, 57
  sound absorption, 57
  target area, 85-86
  wakes from ships, 122, 126-127
Buoy, anchored radio sono, 223

Capacitive rotation sonar, 212-213
  comparison with FM sonar, 218-219
Cavitation
  effect on projector power output, 148
  effect on wake echoes, 120-122
  from submarines, 231, 232
  from surface ships, 237
Circuit noise, 245-246
  hum, 246
  microphonies, 246
  sources, 245
  spectrum, 245
  thermal, 245
  tubes, 246
Circuits, electronic
  AVC sonar receivers, 220
  reverberation-controlled gain, 220
  time varied gain, 220
Cochlea of ear, 256
Compression wave, underwater explosions, 23
Convective overturn of ocean layers, 71
Cooling of ocean, 71, 76-77
  effective back radiation, 76
  evaporation, 77
  incoming radiation, 76
CR sonar (capacitive rotation), 212-213
  comparison with FM sonar, 218-219
Crystals, piezoelectric in projectors, 138-141
  quartz projectors, 139-140
  Rochelle salt and ADP projectors, 140-141
  theory, 138
  types, 138
Currents, effect on ocean temperature, 72, 78-79
  divergence and convergence of surface currents, 79
  drift currents, 78
  internal waves, 79
  permanent currents, 78-79
  tidal currents, 79

Density of sea water, 69
Depth determination of targets, 221
Diffraction of underwater sound, 33
Dipole effect in sound transmission, 24-25, 44-48
  refraction, 25, 46-48
  sonic frequencies, 45
  sound transmission, 45-46
Directivity in sonic listening, 141-146, 272-273
  beam pattern correction, 90
  directivity index, 146-147, 180, 229
  directivity patterns of transducers, 5-6, 143-146, 228-229
  probable bearing error, 273
  submarine sounds, 234-235
Distortion in signals, 60-62, 226
Domes, acoustic effect on projector, 150-152
Doppler effect, 193-195
  echo ranging, 194
  FM scanning sonar, 217-218

formula for doppler shift, 193
hydrophones, 179-180
own-doppler nullifier, 180
reverberation, 179
target doppler, 194
theory, 193-194
up-and down-doppler, 194
Double-source effect in sound transmission, 24-25, 44-48
refraction, 46-48
sonic frequencies, 45
sound transmission, 45-46
Drift currents, ocean, 78

Ear, human, 255-260
anatomy, 255-256
binaural effect, 259-260
masking, 258
psychological characteristics of sound, 258-260
sensitivity, 257
threshold of hearing, 258
Echo, 83-85, 165-174
*see also* Reverberation
energy flow, 83
envelopes of echoes, 165-167
formula for echo level, 84
from artificial targets, 170-174
from ocean bottom and surface, 24, 36
from small particles, 84-85
from wakes, 120-122, 130, 170
intensity, 83-84, 154, 158, 167-169
ping length, 165-169, 187-188, 197-198, 219-220
reverberation ratio, 219-220
scattering of sound, 83-84
target area and strength, 83, 84
theory, 59-60, 83-84
travel time, 87
Echo ranging
*see also* Hydrophones; Projectors, sonar
comparison with listening, 223
doppler effect, 194
general discussion, 133
noise background, 182-184, 189-191
range calculation, 189-191, 196-199, 267-268
reverberation, 192-193, 195-199, 219-220
target strength, 153-174
Echo ranging applications, 200-221
scanning sonar, 210-219
search operations, 200-204
small object detection, 219-220
target bearing, 204-210
target depth determination, 221
target detection, 201-203
Echo ranging signal, 148-150
frequency, 148-150
keying length and interval, 150
Echo recognition, 184-189
aural recognition, 195-196
definition of recognition, 184
effect of ping length, 187-188
effect of reverberation, 195-196
multiple pulses, 188
range recorder, 185
recognition differential, 184-185, 188-189, 195
recognition level, 186
recognition probability, 188-189
Echo repeater, 153
ECR ocean layer
acoustic shadow, 112-113
diurnal cycle, 101
reverberation, 108, 112-113
Electronic rotation sonar, 212-213
Energy of sound field, 1-2, 83
ER sonar (electronic rotation), 212-213
ERSB (expendable radio sono buoy), 223
Evaporation in ocean, 77
Explosions underwater
*see* Underwater explosions

FM scanning sonar, 214-219
application to fire control problems, 218
comparison with CR sonar, 218-219
doppler range error, 217-218
echo duration, 216
effective ping length, 216
principles of operation, 214-215
range and bearing indication, 216
target range and echo frequency, 215-220
Formulas
attenuation coefficient, 57
beam pattern of sound source, 6
directivity index of a projector, 146
doppler shift, 193
echo level, 84
echo ranging target strength, 153
echo recognition differential, 184
efficiency of a projector, 147
energy flow of echoes, 83
energy of sound field, 1-2, 4
inherent threshold of hydrophone, 181
intensity of bottom reflected sound, 49
intensity of volume reverberation, 87-88
mechanical impedance of projectors, 135
pressure in reflected sound wave, 45
radiation impedance of projectors, 135
Rayleigh formula, reverberation, 92
recognition differential for reverberation, 195
recognition level for noise and reverberation, 197
reverberation level, 90, 111
sound intensity, 2
sound level, 2
strength of wake, 125
target strength of sound scatterer, 84

Harvard Underwater Sound Laboratory, 209
Hearing process, 255-265
auditory masking, 260-265
binaural effects, 259-260
human ear, 255-260
psychological characteristics, 258-260
theory, 256-257
threshold of hearing, 258
Heating of ocean, 71, 76-77
effective back radiation, 76
incoming radiation, 76
negative gradients, 71
Helmholtz theory of hearing, 256
Hydrophones, 175-182
automatic volume control, 220
characteristics, 227
dependence of attenuation on depth, 34-36
dependence of transmission on depth, 31-32, 43, 51-52
directivity, 228-229
directivity index, 146, 180, 229
discrimination against noise, 180
doppler effect, 179-180
inherent threshold, 181
JK hydrophone, 230
JP hydrophone, 229
magnetostriction, 229, 232
multiple hydrophones, 205-207
noise from, 247
operation, 175-176
own-doppler nullifier, 180
response, 176-179, 227
reverberation, 179-180
self-noise, 246
specifications, 181-182, 266-267
spectrum level, 177-178
time varied gain, 220
tuning, 175, 179-180
use of multiple hydrophones, 203-207

Image effect in sound transmission, 24-25, 44-48
refraction, 25, 46-48
sonic frequencies, 44
Impedance of projectors, 135-136
mechanical impedance, 135
radiation impedance, 135-136
Intensity of sound
*see* Sound level

Invar for magnetostriction projectors, 137
Isothermal layer in the ocean, 16-17
  definition, 13
  effect on supersonic frequencies, 31
  formation, 80
Isotherms (temperature curves), 71

Japanese listening gear, 230
JP hydrophone, 229-230
  amplifier, 229
  directivity pattern, 229

Listening, 223-224, 227-230, 266-277
  *see also* Hearing process; Hydrophones
  applications, 223-224
  background noise, 243-254, 272-275
  basic factors, 224
  comparison with echo ranging, 223
  enemy listening gear, 230
  frequency range, 266
  maximum range, 266-272
  objectives of sound operator, 223
  sonic frequencies, 272-275
  supersonic frequencies, 275-277
Listening range equations, applications, 269-272
  choice of listening band, 270-271
  range prediction problem, 271-272
  reduction of noise background, 269-270
  reduction of sound output for defense, 269
Lloyd mirror effect in sound transmission, 24-25, 44-48
  refraction, 25, 46-48
  sonic frequencies, 44
  sound transmission, 45-46
Lobe suppression, directivity patterns, 145

Magnetostriction hydrophones, 229, 232
Magnetostriction projectors, 137-138
  maximum voltage, 148
  oscillator, 137
  polarizing current, 137-138
  production of sound waves, 138
  theory, 137-138
  use of nickel, 137
Masking, auditory, 260-261
  adjacent masking, 263-265
  by complex sound, 262-263
  by pure tone, 261-262
  definition, 258
  effect of receiver, 265
  probability of signal recognition, 260
  theory, 261
  threshold of masking, 260-261
  variable levels, 265
Massachusetts Institute of Technology, 159
Microphonics in circuits, 246
Monel for magnetostriction projectors, 137

Naval Research Laboratory, 148
Navy Radio and Sound Laboratory, 44
Negative gradients in the ocean
  cause, 71, 81
  definition, 13
  depth, 72
  effect on supersonic frequencies, 31
  geographical location, 78
  intensity of sound, 26
  limiting range, 32
Nickel for magnetostriction projectors, 137
NLM (noise level monitor), 232
Noise background, echo ranging, 182-184, 189-191
  ambient noise, 182-184
  effect on range calculation, 189-191
  equipment noise, 183-184
  general classification, 182-183
Noise background, listening, 243-254
  airborne, 242
  ambient noise, 248-249
  circuit noise, 245-246
  classification of noise, 243-245
  equipment noise, 246-248
  overall levels of background noise, 244-245
  reduction, 269-270
  sonic frequencies, 269-270, 272-275
Noise level monitor, 232

Ocean bottom
  echoes, 36
  effect on transmission, 40-41
  reflected sound, 36-37, 44, 48-50, 59
  reverberation, 109
Ocean depth
  effect on reverberation, 99-109
  effect on sound attenuation, 34
  effect on transmission, 30-32, 39-44
Ocean temperature
  convective overturn, 71
  isothermal layer, 13, 16-17, 31, 74, 80
  mixed layer, 34
  negative gradients, 71-72, 78, 81
  positive gradients, 71, 81
  stability, 69-71
  theory, 17, 21
  thermocline, 13, 16-17, 31, 34
Oceanography, 68-81
  acoustic properties, 6-7
  acoustic shadow, 16-17, 26-27, 32-33, 83, 112-113
  air bubbles, 57, 86
  currents, 72, 78-79
  density of sea water, 69
  geographical variations, 79-81
  recommendations for future research, 33-34
  salinity of sea water, 69
  temperature factors, 68-79
ODN (own-doppler nullifier), 180
Oscillograms
  reverberation, 91, 94, 98
  sound transmission underwater, 60, 226
Ossicles of ear, 256
Own-doppler nullifier, 180

PAL (phase-actuated locator), 207
Periodmeter, measurement of reverberation distortion, 95-97
Permendur for magnetostriction projectors, 137
Phase-actuated locators, 207
Piezoelectric projectors, 138-141, 147-148
  materials used, 138
  quartz projectors, 139-140
  Rochelle salt and ADP projectors, 140-141
  theory, 138-139
Ping length
  definition, 87-88
  effect on echoes, 165-169, 187-188, 197-198, 219-220
  effect on reverberation, 87-88, 92, 95, 219-220
  effect on wake echoes, 130
  FM scanning sonar, 216
  small object detection, 219-220
Pinna of ear, 255
Plan position indicator, 212-213
"Pokes" of sound, 23
Positive gradients in the ocean, 71, 81
PPI (plan position indicator), 212-213
Pressure level of sound, 1-2
Projectors, sonar, 135-152
  acoustic axis, 146
  basic principles, 135
  characteristics of standard projectors, 147
  directivity, 90, 141-146
  effect of cavitation, 148
  effect of domes, 150-152
  impedance, 135-136
  limitation of power output, 148
  magnetostriction projectors, 137-138, 148
  motor of projector, 136-137
  piezoelectric projectors, 138-141, 147-148
  QB projectors, 144, 147
  quartz, 139-140
  roll and pitch, 64-65
  rotating, 213-214

sound output, 147-148
spread source, 141-142
transmission from deep water, 43
transmission from shallow water, 30-32
voltage breakdown, 148
Psychological characteristics of hearing, 258-260
Pulsed scanning sonar
*see* Scanning sonar-pulsed transmission

QB and QC projectors, 144, 147
QGA projectors, 144, 147
Quartz projectors, 139-140

R sound rays, 27
Radiation impedance of projectors, 135-136
Radiation in the ocean, 76
back radiation, 76-77
incoming radiation, 76
Radio and Sound Laboratory, U. S. Navy, 44
Radio sono buoy, anchored, 223
Range calculation, echo ranging, 189-191, 196-199
comparison of noise and reverberation-limited ranges, 198-199
comparison with listening range, 267-268
general principles, 189-190, 196-198
maximum range 190-191, 198-199
noise-limited ranges, 189-191
parameters, 190, 197-198
ping length, 197-198
recognition level for noise and reverberation, 197
reverberation-limited ranges, 196-199
target speed and aspect, 164-165, 169, 197
Range calculation, listening, 266-272
available signal output, 267
comparison with echo ranging, 267-268
critical band spectrum levels, 268-269
equations and applications, 269-272
maximum range, 268
principles of range calculation, 267-268
recognition level, 267
Range indicator, sonar, 150
Range recorder, echo ranging, 185-186
Ranging on echoes
*see* Echo ranging
Rayleigh formula, reverberation, 85, 92
RCG (reverberation controlled gain), 220
Receivers for listening gear
*see* Hydrophones
Recognition level
listening, 267
noise and reverberation, 197
Recommendations for future research
attenuation coefficient, 57
low frequency transmission, 52
roll and pitch of projector, 64
scattering of sound, 33
thermal microstructure in the sea, 34
Reflection of sound
effective reflection coefficient, 49-50
formula for pressure, 45
from large sphere, 113-114
interference with direct signal, 24-25, 36-37
ocean bottom, 36-40, 45, 48-50, 59
reverberation, 108, 110-111, 113-114
surface reflection, 23-25, 45, 109-110
time delay of reflected pulse, 23-24
Refraction of sound, 10-21
bottom reverberation, 110-111
downward, effect on reverberation, 108
error in depth determination, 221
image effect, 25, 46-48
Snell's law, 14
sound ray diagrams, 15-16
temperature variations in the sea, 12-13
theory, 14-15
typical diagrams, 15-21
velocity of sound, 10-11, 14
Response curves of underwater sounds, 222-223
Reverberation, 82-114
amplitude of reverberation, 91-95
average reverberation curves, 104-106, 109
beam-pattern correction, 90
bottom reverberation, 88-90, 109-112
coherence of reverberation, 93-95
doppler effect, 180
effect of ping length, 87-88, 92, 95
effect of wind speed, 104-106
forward scattering from ECR layer, 112-113
general discussion, 82
hydrophones, 179-180
in deep water, 99-114
indices, 91
level, 90-92, 111-112
measurement of reverberation distortion, 95-97
oscillograms, 91, 94, 98
pitch, 82
Rayleigh formula, 85, 92
recognition, 195
recognition level, 197
reflected sound, 108, 110-111, 113-114
reverberation tail, 61, 112
scattering by single particles, 83-87
scattering coefficients, 90
small object detection, 219
spines of reverberation, 92
surface reverberation, 88-90, 106-107
theory, 87-98
volume reverberation, 87-88, 99-104, 107-109
wave form, 95-98
Reverberation, echo ranging, 195-199
echo recognition, 195-196
frequency, 192-193
maximum echo ranges, 196-199
ping length, 219-220
spectrum of reverberation, 192-193
Reverberation controlled gain (RCG), 220
Rochelle salt projectors, 140-141, 230

SC rays (sound channel), 27
Scanning sonar—continuous transmission
*see* FM scanning sonar
Scanning sonar-pulsed transmission, 210-214
CR and ER sonar, 212-213
echo duration, 211-212
objective, 210
plan position indicators, 212
principles of operation, 210-212
rotating projectors, 213-214
sector scan sonar, 213
Scattering of sound
acoustic shadow, 53
attenuation, 103
coefficients, 90, 102-103, 107, 112
definition, 55
echo formation theory, 83-84
echoes from small particles, 84-85
effect of frequency, 85-86
effective cross section, 84
intensity, 84
recommendations, 33
reverberations, 83-87, 90, 100-103
ship wakes, 123-125, 127-128
target area, 85-87
target strength, 84
theory, 33
transmission loss, 9
travel time, 62
Sea noise, 240-250
Sector scan sonar, 213
Shadow, acoustic
*see* Acoustic shadow
Ship sounds
*see* Surface ship sounds
Shock wave, 22
Shrimp noise, 251-252
Signal distortion, 60-62, 226
Signal fluctuation, 62-66
autocorrelation coefficient, 63-64
causes, 47-48, 64-66
deep projector, 44

Best Available Copy

definition, 60
direct sound and surface echo, 65
error in target strength measurement, 163-164
measurement, 62-63
roll and pitch of the projector, 64-65
transmission loss, 60-66
variance, 62
Signal variation
causes, 66-67
definition, 60
statistical treatment of data, 66-67
transmission loss, 60
Small object detection (SOD), 219-220
echo-reverberation ratio, 219-220
general principles, 219
ping length, 219-220
reverberation, 219
Snell's law of refraction, 14
Sonar devices
anchored radio sono buoy, 223
bearing deviation indicator, 209-210
expendable radio sono buoy, 223
noise level monitor, 232
own-doppler nullifier, 180
phase-actuated locator, 207
plan position indicator, 212-213
range indicator, 150
range recorder for echo ranging, 185-186
reverberation controlled gain, 220
small object detection, 219-220
vector bearing indicator, 207
Sonar projectors
*see* Projectors, sonar
Sonar systems
CR and ER scanning sonar, 212-213
FM scanning sonar, 214-219
scanning sonar-pulsed transmission, 210-214
Sonic frequency transmission, 44-51
7.5 kc sound, 52
22.5 kc sound, 50-51
comparison with supersonic, 44
effect of range, 50
experiments, 44-45
hydrophone depth, 51-52
ocean bottom reflection, 48-50
simultaneous transmission of frequencies, 50-51
sound paths, 48
surface image effect, 45-48
transmission loss, 274-275
Sonic listening, noise background, 272-275
ambient, 273
directivity, 272-273
equipment noise, 273
reduction, 269-270
sound output, 272
Sono buoy, radio, 223
Sound, psychological characteristics, 258-260
Sound, single-frequency components, 239-242
audibility, 239-240
time patterns, 240-242
Sound absorption
air bubbles, 55
causes, 55-57
definition, 9, 55
ship wakes, 123-125, 127-128
viscosity, 57-58
Sound attenuation
*see* Attenuation of sound
Sound channels
definition, 17
explosions in permanent channel, 27-29
Sound level, 1-2
direct sound, 25-27
echoes, 81, 154-158, 167-169
effect of frequency, 237
for typical ray diagrams, 17-20
formula, 2
overall level, 225
ray divergence and intensity, 17-19
scattered sound, 83
submarine sounds, 232-234
surface ships, 235
underwater explosions, 25-27
volume reverberation, 87-88
wakes, 127-128
Sound masking
*see* Masking, auditory
Sound measurement
*see* Underwater sound measurement
Sound peaks, 24
Sound pressure, 1-2
Sound ray diagrams, 15-21
crossing rays and sound channels, 17
isothermal layer and thermocline, 16-17, 31
limiting ray, 16
sharp downward refraction, 15-16
sound intensity, 17-21, 26
split-beam pattern, 16
Sound ray theory, 14-15, 32-35
attenuation coefficient, 34-36
diffraction, 33
formation of shadows, 16-17
instrument for plotting rays, 15
layer effect, 17, 21
limiting range, 32-33
rays in a composite gradient, 15
rays in a constant gradient, 14-15
scattering of sound, 33
Snell's law of refraction, 14
supersonic frequency transmission, 32-35
thermal microstructure in sea, 33
weak gradients, 34
Sound reflection
*see* Reflection of sound
Sound refraction
*see* Refraction of sound
Sound scattering
*see* Scattering of sound
Sound spectrum
*see* Spectrum of sound
Sound transmission, ocean
*see* Underwater sound transmission
Sound travel time patterns, 237-242
changes in spectrum, 239
perception of time patterns, 238
single-frequency components, 240-242
Sound underwater
*see* Underwater sound
Sound velocity, underwater
influencing factors, 10-11
measurement, 13
Specifications for hydrophones, 181-182
Spectrum of sound
circuit noise, 245
critical band level, 262-263, 268-269
energy level of pulse, 177-178
fish noise, 252
hydrophone level, 177-178
level, spectrum, 225
line spectrum, 226
reverberation, 192-193
sea noise, 249
spectrograph, 239
submarine sounds, 231, 233-234
surface ships, 235-236
Spines of reverberation, 92
Spool pulse, 37
Submarine sounds, 230-232, 247-248
directivity, 234-235
effect of speed, 248
measurement, 231-232
overall source levels, 232-234
propeller beats, 231, 238
sound spectra, 231, 233-234
sources, 231
Submarine wakes
*see* Wakes of ships
Submarines, target strength measurement, 165
Supersonic frequency transmission, 29-44
24 kc sound, 43-44
60 kc sound, 42-43
comparison of theory and experiment, 32-35
comparison with sonic, 44
deep water, 43-44
depth of thermocline, 32
echo ranging, 148-150
experiments, 29-30
influencing factors, 30-32
isothermal layer, 31

negative surface gradients, 31
ocean depth, 31-32, 39-40
range, 31
reflection from ocean bottom, 36-40
shallow water, 30-32, 40-42
Supersonic listening, 275-277
available signal level 276
listening gear, 230
recognition, 275-277
transmission loss, 276
Surface reverberation, 88-90, 106-107
beam-pattern correction, 90
dependence on wind speed, 107
effect of range, 89, 104
horizontally directed beam, 106-107
scattering coefficient, 90, 107
Surface ship sounds, 235-237
cavitation, 237
distribution of sound field, 237
measurement, 235
overall sound output, 235
propeller beats, 238
spectra of sounds, 235-237
Surface vessel wakes
*see* Wakes of ships

Target area, 83-87
effect on echoes, 83
non-spherical objects, 86
of bubbles, 85-86
small scatterers, 85
variation with sound wavelength, 84
Target aspect, 164-169
echo intensity, 167-169
effect on echo range calculation, 198
effect on echo shape, 165-167
effect on target strength, 164-165
measurement, 159
Target bearing, 204-210
bearing deviation, 205
crossing the target, 205
depth determination, 221
maintaining contact, 205
multiple hydrophones and split transducers, 205-207
Target depth determination, 221
Target detection, echo ranging, 201-204
single ping, 201-202
successive pings, 201-203
Target doppler, 194
Target search operations, 200-204
effect of motion of sonar and target, 202-204
objectives, 200-201
probability of target detection, 201-204
Target strength, echo ranging, 153-165
definition, 84, 153
function of frequency, 169
function of range and target speed, 160
function of target aspect, 164-165
general principles, 153-154
of spheres, 153-154
scattered sound, 84
submarines, 165
Target strength measurement, 158-164
acoustic experiments, 159-161
echo and source level, 84, 162-163
errors caused by fluctuation, 163-164
method, 158
optical experiments, 159-161
ships and submarines, 161-164
transmission loss, 163
triplane, 174
use of scaled models, 159-160
Targets, artificial
bubble targets, 174
echo repeater, 153
echoes, 170-174
Temperature factors, ocean, 68-79
afternoon effect, 75-76
diurnal temperature cycle, 74-76
heat budget of the ocean, 77
heating and cooling, 71, 76-77
mixing processes, 71-72, 77-78
rotation of the earth, 78
seasonal temperature changes, 74-75
stability of ocean layers, 69-71
stratification of the ocean, 69-71
thermal structure at great depths, 72-74
transport by currents, 72, 78-79
Temperature measuring instrument, ocean
Bathythermograph measurements
mal gradients
*see also* Negative gradients in the ocean
attenuation coefficient, 58
deep gradients, 41-42, 72-74
positive, 71, 81
recommendations for future research, 33-34
stability, 69, 71
transmission of sound, 55
weak gradients, 34
Thermocline layer
attenuation coefficient, 34
definition, 13
effect of depth on transmission, 32
sound ray diagrams, 16-17, 31
Thresholds
hearing, 258
hydrophone, 180-181
inherent threshold of sound, 227
masking, 260-261
Tidal currents, ocean, 79
Time patterns of sound, 237-242
changes in spectrum, 239
perception of time patterns, 238
single-frequency components, 240-242
Time-varied gain, 210, 220
Train length of sound pulses, 87
Transducers
*see* Hydrophones; Projectors, sonar
Transformer pulse, 37
Transmission loss, 7-8, 60-67
*see also* Scattering of sound
autocorrelation, 63-64
bottom reverberation, 109-110
bottom-reflected sound, 274-275
low frequencies, 274-275
signal distortion, 60-62
signal fluctuation, 60-66
signal variation, 60
supersonic listening, 275-277
target strength measurement, 163
temperature distribution, 29
variability with time, 60, 66-67
Transmission of sound in the sea
*see* Underwater sound transmission
Triplane, practice target, 170-174
TVG control (time-varied gain), 210, 220

Ultrasonic frequency transmission
*see* Supersonic frequency transmission
Underwater explosions, 22-29
compression wave, 23
explosion bubble and its oscillation, 22-23
intensity of direct sound, 25-27
permanent sound channel, 27-29
reflection of sound at surface, 23-25
refraction and image effect, 25
sound in the acoustic shadow, 27
summary of theory, 29
Underwater projectors
*see* Projectors, sonar
Underwater sound analysis, 223-241
general description of sounds, 224-225
listening to sounds, 223-224, 227-230
single-frequency components, 239-242
sounds of submarines, 230-232
sounds of surface ships, 235-237
time patterns and propeller beats, 237-242
Underwater sound measurement
calibration of measuring systems, 224
distortion, 226
inherent threshold, 226
measuring instruments, 224
oscillograms, 226
overall levels, 225
response curves, 224-225
spectrum level, 225
Underwater sound transmission, 6-9, 22-67
absorption of sound, 9

acoustic properties of the ocean, 6-7
attenuation of sound, 7, 9, 55-60
hydrophone depth, 31-32, 43, 51-52
ideal medium, 1-6
image effect, 45-46
ocean layer depth, 30, 39-40
order of arrival of sounds, 28-29
oscillograms, 60, 226
recommendations for low frequencies, 52
scattering of sound, 9
shallow water, 30-32, 40-42
sonic frequencies, 44-54
supersonic horizontal beams, 29-44
thermocline layer, 32
through surface vessel wakes, 128-129
transmission anomaly, 8-9
transmission loss, 7-8, 60-67
underwater explosions, 22-29
U. S. Navy Radio and Sound Laboratory, 42
University of California
ship wakes, 128
sonic frequency transmission, 44
supersonic frequency transmission, 29-30

Vector bearing indicator (VBI), 207
Velocity of underwater sound
influencing factors, 10-11
measurement, 13
Viscosity, sound absorption, 57-58
Volume reverberation, 99-104, 107-109
beam-pattern correction, 90
deep scattering layers, 100-102
dependence on frequency, 103-104
dependence on range, 89, 99, 104
dependence on wind speed, 107
ECR layer, 108
effect of attenuation, 108
intensity, 87-88
scattering coefficient, 90, 102-103
with horizontal beam, 104-109
with tilted beam, 99-104

Wakes of ships, 115-132
acoustic properties, 117-119
age of wakes, 128-130
bubbly wakes, 122, 126-127
cavitation, 120-122
echo formation, 120-122, 129, 170
measurement of sound intensity, 127
narrow wakes, 124-125
scattering and absorption of sound, 123-125, 127-128
screening action, 124-125
strength, 125-126, 128-132
temperature effects, 117
theory of acoustic properties, 119-128
transmission of sound through wakes, 128-129
wide wakes, 125-126
Woods Hole Oceanographic Institution
cavitation, effect on wake echoes, 122
variability of transmission loss, 22

X-cut quartz crystals, 139-140

Y-cut quartz crystals,, 138, 139

Z-cut quartz crystals, 139

UNCLASSIFIED

TITLE: Principles and Applications of Underwater Sound - Volume 7

ATI- 30820
REVISION (None)
ORIG. AGENCY NO. (None)
PUBLISHING AGENCY NO. (None)

AUTHOR(S): Eckart, Carl; Knudson, V. O.; Iselin, V. O.; and others
ORIGINATING AGENCY: Office of Scientific Research and Development, NDRC, Div 6
PUBLISHED BY: (Same)

| DATE | DOC. CLASS. | COUNTRY | LANGUAGE | PAGES | ILLUSTRATIONS |
|---|---|---|---|---|---|
| 1946 | [redacted] | U. S. | Eng. | 278 | photos, tables, diagrs, graphs |

ABSTRACT:
The purposes of the report are to discuss the factors which limit the performance of underwater sound apparatus, particularly those originating in the sea itself, and the manner in which the dynamic properties of the ocean influence the propagation of sound and cause it to differ from propagation in an ideal static medium. As an introduction, the generation and the transmission of sound in an ideal medium are reviewed. The refraction of sound, the transmission of sound in the sea, oceanography of sound conditions, echoes, scattering and reverberation, and wakes are also discussed. The problems of echo ranging are presented under the following titles: the acoustic output of sonars, target strength and echo level, maximum echo ranges when background noise or reverberation is limiting, and miscellaneous echo ranging applications. The section "Listening" gives the nature and method of measuring underwater sounds.

DISTRIBUTION: Copies of this report obtainable from Air Documents Division; Attn: MCIDXD

DIVISION: Electronics (3)
SECTION: Communications (1)

SUBJECT HEADINGS: Wave propagation, Sound (98030); Sonar (87473); Echo ranging (31434.5); Research - Summary reports (81658.95)

ATI SHEET NO.: R-3-1-29

Air Documents Division, Intelligence Department
Air Materiel Command

AIR TE[illegible] INDEX

Wright-Patterson Air Force Base
Dayton, Ohio